

## Durham E-Theses

---

### *High Arctic Paraglacial Coastal Evolution in Northern Billefjorden, Svalbard*

STRZELECKI, MATEUSZ,CZESLAW

#### How to cite:

---

STRZELECKI, MATEUSZ,CZESLAW (2012) *High Arctic Paraglacial Coastal Evolution in Northern Billefjorden, Svalbard*, Durham theses, Durham University. Available at Durham E-Theses Online:  
<http://etheses.dur.ac.uk/7363/>

#### Use policy

---

The full-text may be used and/or reproduced, and given to third parties in any format or medium, without prior permission or charge, for personal research or study, educational, or not-for-profit purposes provided that:

- a full bibliographic reference is made to the original source
- a [link](#) is made to the metadata record in Durham E-Theses
- the full-text is not changed in any way

The full-text must not be sold in any format or medium without the formal permission of the copyright holders.

Please consult the [full Durham E-Theses policy](#) for further details.

---



Academic Support Office, Durham University, University Office, Old Elvet, Durham DH1 3HP  
e-mail: [e-theses.admin@dur.ac.uk](mailto:e-theses.admin@dur.ac.uk) Tel: +44 0191 334 6107  
<http://etheses.dur.ac.uk>



Department of Geography

# High Arctic Paraglacial Coastal Evolution in Northern Billefjorden, Svalbard

Mateusz Czesław Benedykt Strzelecki

*Ustinov College*

Thesis submitted for the degree of Doctor of Philosophy

December 2012

The difficult is what takes a little time;  
the impossible is what takes a little longer.

*Fridtjof Nansen*

## **High Arctic Paraglacial Coastal Evolution in Northern Billefjorden, Svalbard**

In contrast to mid and low latitude coasts, relatively little is known regarding the potential impacts of climate and sea-level change on cold region coastal margins. This is an important area of research given the pace of recent climate change and future predictions. Svalbard provided a superb location to quantify how High Arctic coasts are responding to climate warming and the associated paraglacial landscape transformation. The geographical focus for the thesis is Petuniabukta and Adolfbukta, the northernmost bays of Billefjorden, central Spitsbergen. The study area has a sheltered location, a semi-arid, sub-polar climate, limited wave fetch and tidal range, and rapid retreat rate of all surrounding glaciers. Using a combination of geomorphological, sedimentological, remote sensing and dating methods, the thesis investigates the processes that control coastal evolution over annual, century and millennial timescales.

Interannual changes observed between 2008 and 2010 show that High Arctic gravel-barriers are resilient to the impact of local storms and the operation of sea-ice processes. The results of a Schmidt Hammer test demonstrate a significant reduction in rock resistance with decreasing distance from the modern shoreline. Shoreline changes since the end of the Little Ice Age (late 19<sup>th</sup>/early 20<sup>th</sup> century) reflect a dramatic increase in sediment supply associated with retreating local ice masses, a shortened winter sea-ice season and melting of permafrost. A new approach of dating of juvenile marine molluscs found in uplifted raised beaches enables the development of a new model of relative sea-level change in the study area.

The thesis demonstrates that existing models of paraglacial coastal evolution, developed on mainly temperate latitude coasts, are not applicable to the High Arctic. Whilst the fundamental importance of the sediment supply and relative sea-level is noted, in the High Arctic these processes are modified by climate-driven factors that influence sediment delivery from terrestrial sources, the extent of sea-ice, permafrost as well as river discharge and slope stability. A new model of paraglacial coastal evolution is proposed that captures these processes and recognises the importance of bedrock topography as a key control on landforms preservation.

# Table of contents

Title page	I
Abstract	III
Table of contents	IV
List of figures	XIII
List of tables	XIX
Norwegian topographic names	XX
Declaration	XXI
Statement of Copyright	XXI
Acknowledgements	XXII
Chapter I INTRODUCTION	I
1.1 Research rationale	2
1.2 Research aims and objectives	8
1.3 Research questions	9
1.4 Conceptual framework	9
1.4.1 Theories of cold landscape evolution	9
1.4.2 Coastal zone terminology	14
1.5 Research schedule	15
1.6 Chapter summary	17
Chapter 2 RESEARCH CONTEXT	18
2.1 Introduction	19
2.1.1 Processes operating on Arctic beaches	25
2.1.2 Processes operating on Arctic rock coasts	34

2.1.3 Existing conceptual models of Arctic coastal zone evolution	37
2.1.4 Recent developments in High Arctic coastal research with particular consideration of Svalbard	41
2.2 Chapter summary	45
 <b>Chapter 3: THE STUDY AREA</b>	 <b>47</b>
3.1 Introduction	48
3.2 Geology and landscape	48
3.3 The climate of Svalbard	55
3.3.1 Present-day meteorological conditions on Svalbard	58
3.3.2 Present-day glaciation of Svalbard	59
3.4 The study area	60
3.4.1 Overview	60
3.4.2 Geology and landscape	62
3.4.2.1. Bedrock geology	62
3.4.2.2. Glacial and periglacial geomorphology	63
3.4.3 Fjord processes	72
3.4.4 Local climate	75
3.5 Sediment supply pathways to the Petuniabukta coastal zone	77
3.6 Chapter summary	79

<b>Chapter 4 ANNUAL TIMESCALES: PROCESSES OPERATING ON THE PRESENT-DAY SEDIMENTARY COASTS</b>	<b>80</b>
<b>4.1 Introduction</b>	<b>81</b>
<b>4.2 Background - factors influencing the stability of Arctic barrier coasts</b>	<b>81</b>
<b>4.3 Methods</b>	<b>83</b>
<b>4.4 Results</b>	<b>88</b>
<b>4.4.1 Meteorological conditions 2008-2010</b>	<b>88</b>
4.4.1.1 Air temperature	88
4.4.1.2 Wind speed and direction	88
<b>4.4.2 Processes that control modern barrier coasts in Petuniabukta</b>	<b>91</b>
4.4.2.1 Ice pile-up and bulldozing	95
4.4.2.2 Icefoot	95
4.4.2.3 Pitted-beach	98
4.4.2.4 Ice-pushed micro-relief	98
4.4.2.5 Erratic boulders	101
4.4.2.6 Storm ridges blocking stream outlets	101
4.4.2.7 Rockfalls, debrisflows, mudflows, solifluction	104
4.4.2.8 Seaweed	104
4.4.2.9 Driftwood	107
4.4.2.10 Human activity	107
<b>4.4.3 Barrier profile changes 2008-2010</b>	<b>110</b>
4.4.3.1 Profile 1 – Southern Raudmosepynten	110
4.4.3.2 Profile 2 – Western Raudmosepynten	111
4.4.3.3 Profile 3 – Rock glacier coast	112

<b>4.4.3.4 Profile 4 – Barrier formed along the relict coastal landforms</b>	<b>113</b>
<b>4.4.3.5 Profile 5 – Barrier strongly modified by sea-ice processes</b>	<b>114</b>
<b>4.4.3.6 Profile 6 – Barrier supplied with debris Flows and formed along the anhydrite/gypsum rock cliffs</b>	<b>115</b>
<b>4.4.3.7 Profile 7 – Barrier blocking the Dynamiskbekken</b>	<b>116</b>
<b>4.4.3.8 Profile 8 – Wide barrier coast along the Skottehytta cliff</b>	<b>117</b>
<b>4.4.3.9 Profile 9 – Barrier blocking outlet of tundra creek</b>	<b>118</b>
<b>4.4.3.10 Profile 10 - Barrier formed along low, solifluction cliff</b>	<b>119</b>
<b>4.4.3.11 Profile 11 – Barrier formed along the spit-platform</b>	<b>120</b>
<b>4.4.3.12 Profile 12 – Narrow barrier exposed to long-fetch waves from Adolfbukta</b>	<b>121</b>
<b>4.4.3.13 Profile 13 – Narrow barrier formed along the snow-fed fan delta 1</b>	<b>122</b>
<b>4.4.3.14 Profile 14 – Barrier along snow-fed alluvial fan delta 2</b>	<b>123</b>
<b>4.4.3.15 Profile 15 Barrier along snow-fed alluvial fan delta 3</b>	<b>124</b>
<b>4.4.3.16 Profile 16 – A wide barrier before Elzaelva and the Ferdinandelva fan deltas</b>	<b>125</b>
<b>4.4.3.17 Profile 17 – Barrier along Ferdie Spit 3</b>	<b>126</b>



4.4.4 Surface sediments characteristics and local geomorphic controls	127
4.6 Chapter summary	129
 <b>Chapter 5 ANNUAL TIMESCALES: PROCESSES OPERATING ON THE PRESENT-DAY ROCKY COASTS</b>	<b>130</b>
5.1 Introduction	131
5.2 Background	131
5.2.1 The study site: Adolfbukta	132
5.3 Methods	134
5.4 Results	136
5.5 Chapter summary	138
 <b>Chapter 6 CENTURY TIMESCALES: THE POST-LITTLE ICE AGE EVOLUTION OF THE PETUNIABUKTA COAST</b>	<b>139</b>
6.1. Introduction	140
6.2 Background	140
6.3 Controls on non-glacial fed barrier systems	142
6.3.1 The Ebba spit-platform and the barrier coast in east Petuniabukta	142
6.3.2 Quantifying geomorphic change on non-glacial fed coasts: material and methods	145
6.3.2.1 Topographic survey	145
6.3.2.2 Sedimentological characteristics	147
6.3.2.2 Aerial photogrammetry	149

<b>6.4 Non-glacial fed barrier systems – results</b>	<b>150</b>
6.4.1 Post-Little Ice Age spit platform evolution – evidence from air photos	150
6.4.2 Beach ridge morpho-sedimentary changes	152
<b>6.5 Controls on glacial-fed barrier systems</b>	<b>155</b>
6.5.1 The barrier coast of north-western Petuniabukta	155
6.5.2 Quantifying geomorphic change along glacial-fed coastal system - material and methods	157
6.5.2.1 Geomorphological mapping and topographic survey	158
6.5.2.2 Aerial photogrammetric analysis and DTM production	158
6.5.2.3 Characteristics of surface sediment cover	162
6.5.2.4 Seabed bathymetry	162
<b>6.6 Glacial-fed barrier systems – results</b>	<b>163</b>
6.6.1 Post-Little Ice Age barrier coast evolution – evidence from air photos	164
6.6.2 The proglacial zone	164
6.6.3 Alluvial fans	166
6.6.4 Coastal and tidal landforms	173
6.6.5 Sediment characteristics of proglacial, alluvial and coastal landforms	189
6.6.6 Post-Little Ice Age surface elevation changes and sediment storage capacity	191
6.6.6.1 Calculation of surface elevation changes across the proglacial and the coastal zone	191

6.6.6.2 Changes in sediment transfer in NW Petuniabukta between 1990 and 2009	194
6.7 Chapter summary	198
 Chapter 7 MILLENIAL TIMESCALES: HOLOCENE RELATIVE SEA-LEVEL CHANGE AND COASTAL EVOLUTION IN PETUNIABUKTA	 199
7.1. Introduction	200
7.2 Background - the raised beaches and evidence for relative sea-level change	200
7.3 New dating campaign - material and methods	206
7.4 Radiocarbon dating results	208
7.4.1 Testing for reworking in the modern beach environment	208
7.4.2 Testing for reworking in a late Holocene beach and developing a chronology for the Holocene raised beaches in the Ebbadalen	210
7.5 Holocene relative sea-level changes in the Ebbadalen	211
7.6 Chapter summary	215
 Chapter 8 DISCUSSION – HIGH ARCTIC PARAGLACIAL COASTAL ZONE EVOLUTION OVER ANNUAL, CENTURY AND MILLENNIAL TIMESCALES	 216
8.1 Introduction	217

<b>8.2</b>	<b>ANNUAL TIMESCALES:</b> Processes controlling the evolution of Petuniabukta coast	<b>217</b>
	8.2.1 Gravel-dominated coasts	217
	8.2.2 Rocky coasts	223
<b>8. 2</b>	<b>CENTURY TIMESCALES:</b> The Post-Little Ice Age evolution of the Petuniabukta coast	<b>226</b>
	8.3.1 The post-LIA response of non-glacial -fed systems	226
	8.3.1.1 Climatic influence on sediment transfer in High Arctic settings	226
	8.3.1.2 Post-LIA coastal morphodynamics of Ebba spit-platform system	228
	8.3.2 The post-LIA response of glacial-fed systems	233
<b>8.4</b>	<b>MILLENNIAL TIMESCALES:</b> Mechanisms controlling Late Holocene relative sea-level change and coastal evolution in Petuniabukta	<b>245</b>
	8.4.1 Dating Arctic raised beaches with marine molluscs	245
	8.4.2 Implications for the former Svalbard-Barents Sea Ice Sheet	249
<b>8.5</b>	<b>A new model for paraglacial coastal evolution in the High Arctic</b>	<b>254</b>
<b>8.6</b>	<b>Future research</b>	<b>261</b>
<b>8.7</b>	<b>Chapter summary</b>	<b>265</b>

<b>Chapter 9</b>	<b>CONCLUSIONS</b>	<b>266</b>
<b>9.1</b>	<b>Introduction</b>	<b>267</b>
<b>9.2</b>	<b>What is the interannual morphological variability of the gravel-dominated barriers along Petuniabukta between 2008-2010?</b>	<b>268</b>
<b>9.3</b>	<b>What processes operate on recently deglaciated rocky coasts in the study area?</b>	<b>269</b>
<b>9.4</b>	<b>How did glacial and non-glacial-fed, gravel-dominated barriers in Petuniabukta respond to warmer, post-LIA conditions characterised by enhanced paraglacial processes?</b>	<b>270</b>
<b>9.5</b>	<b>How can we improve the accuracy of sea-level reconstructions and long-term coastal evolution studies in the High Arctic?</b>	<b>272</b>
<b>9.6</b>	<b>Developing a new conceptual model of paraglacial coastal evolution in the High Arctic</b>	<b>274</b>
<b>Chapter 10</b>	<b>BIBLIOGRAPHY</b>	<b>276</b>
<b>APPENDIX I</b>	<b>Coastal sections selected for analysis</b>	<b>304</b>
<b>APPENDIX II</b>	<b>Research initiatives and projects</b>	<b>325</b>
<b>APPENDIX III</b>	<b>Published academic papers</b>	<b>327</b>

# List of Figures

<b>Chapter 1</b>	<b>Page</b>
<i>Figure 1.1. Arctic sea ice minimum extent in September 1982 and 2008</i>	2
<i>Figure 1.2. Arctic coastal environments</i>	3
<i>Figure 1.3. The state of Arctic coasts in 2010</i>	5
<i>Figure 1.4. Svalbard Archipelago and present-day ocean circulation patterns in the European Arctic</i>	6
<i>Figure 1.5. Paraglacial landforms and processes</i>	7
<i>Figure 1.6. A model of the transition from glacial to paraglacial and periglacial environments</i>	11
<i>Figure 1.7. Sediment cascades within paraglacial landsystems</i>	13
<i>Figure 1.8. Coastal terminology applied to the description of gravel barriers</i>	14
<i>Figure 1.9. Temporal scales of coastal changes analysed during this PhD research</i>	15
 <b>Chapter 2</b>	
<i>Figure 2.1. The cyclone activity index (CAI) anomalies for the Arctic region</i>	20
<i>Figure 2.2. Subdivision of the coastal zone by types of ice formations and their effects on the coast and sea bed</i>	22
<i>Figure 2.3. Mechanism for the development of strudel scour depressions</i>	23
<i>Figure 2.4. Examples of an icefoot complex developed in Petuniabukta and Adventfjorden, Spitsbergen</i>	24
<i>Figure 2.5. Types of ice-pushed, ice-lifted and rafted coastal landforms</i>	27
<i>Figure 2.6. Typical polar beach</i>	29
<i>Figure 2.7. Model of the development of Arctic beach frost mounds</i>	31
<i>Figure 2.8. Driftwood as a geomorphic agent in polar coastal zone (examples from Petuniabukta and Adolfbukta, Spitsbergen)</i>	32
<i>Figure 2.9. Seaweed as a geomorphic factor in polar coastal zone (examples from Petuniabukta and Adolfbukta, Spitsbergen)</i>	33
<i>Figure 2.10. Examples of rocky coast environments from central Spitsbergen</i>	36
<i>Figure 2.11. Conceptual model of coastal evolution in the thermokarst topography of southern Canadian Beaufort Sea modified after RUZ et al. (1992)</i>	38
<i>Figure 2.12. Diagram of links between changes in climate, glacierization, sediment supply and RSL in two climate change scenarios: A warm summers, B warm and moist winters (after SYVITSKI and ANDREWS (1994)</i>	39
<i>Figure 2.13. Prediction of thermoabrasive and accumulation coast profile changes in the Eurasian Arctic (modified from PAVLIDIS et al. (2007)</i>	41
<i>Figure 2.14. High Arctic paraglacial coastal system formed in a recently deglaciated area – Josephbukta, Bellsund, Spitsbergen</i>	42
<i>Figure 2.15. A scenario of geo-ecological changes of Svalbard coasts under global warming</i>	44
 <b>Chapter 3</b>	
<i>Figure 3.1. Simplified geology map of Svalbard</i>	49
<i>Figure 3.2. Relative sea-level changes on Svalbard</i>	51
<i>Figure 3.3. Periglacial landforms on Svalbard</i>	52

<i>Figure 3.4. Svalbard coastal environments and classification</i>	54
<i>Figure 3.5. The North Atlantic Oscillation</i>	57
<i>Figure 3.6. Svalbard meteorological observations since 1912 based on monthly meteorological series homogenised by the Norwegian Meteorological Institute</i>	58
<i>Figure 3.7. Mean annual air temperature (°C) and mean annual precipitation (mm water equivalent (w.e.) for High Arctic meteorological stations in 2009</i>	59
<i>Figure 3.8. Present and former glaciations of Svalbard</i>	60
<i>Figure 3.9. Location of the study area</i>	61
<i>Figure 3.10. Geological sketch of the northern Billefjorden region</i>	62
<i>Figure 3.11. Model of Late Weichselian and Holocene glacial episodes in northern Billefjorden</i>	66
<i>Figure 3.12. Age correlation of marine and glacial sediments in Petuniabukta and Adolfbukta</i>	68
<i>Figure 3.13. Summary of glacier retreat rates since the beginning of 20<sup>th</sup> century</i>	69
<i>Figure 3.14. Major geomorphological features in the surroundings of Petuniabukta and Adolfbukta</i>	71
<i>Figure 3.15. Bathymetry of Petuniabukta based on sonar sounding carried out in 2009</i>	73
<i>Figure 3.16. Seafloor map of Adolfbukta and profiles across submarine landforms formed by Nordenskiöldbreen during post-LIA deglaciation</i>	74
<i>Figure 3.17. Climatic conditions in Petuniabukta and climate data recorded in weather stations located in coastal west Spitsbergen</i>	76
<i>Figure 3.18. Coastal division based on the dominant sediment supply sources along bays</i>	77
 <b>Chapter 4</b>	
<i>Figure 4.1. Location of 17 barrier profiles selected for analysis</i>	83
<i>Figure 4.2. Sea-ice conditions between 2008-2010 in Petuniabukta</i>	86
<i>Figure 4.3. Air temperature changes 2008-2010 recorded at Adam Mickiewicz University Polar Station</i>	89
<i>Figure 4.4. Wind conditions during 2008-2010 recorded at Adam Mickiewicz University Polar Station</i>	90
<i>Figure 4.5. The spatial distribution of processes operating on beaches within the study area between 2008 and 2010</i>	92
 <i>Figure 4.6. Location of the main ice pile-ups and ice bulldozing in Petuniabukta</i>	96
<i>Figure 4.7. Sections of the barrier with remnants of the icefoot</i>	97
<i>Figure 4.8. Sections of the barrier with a 'pitted-beach' micro-relief</i>	99
<i>Figure 4.9. Sections of the barrier with accumulations of ice-pushed landforms</i>	100
<i>Figure 4.10. Sections of the barrier with accumulations of erratics</i>	102
<i>Figure 4.11. Sections of the barrier with stream outlets blocked by storm-ridges</i>	103
<i>Figure 4.12. Sections of the barrier covered with rockfalls, debris flows and solifluction</i>	105
<i>Figure 4.13. Sections of the barrier with accumulations of seaweed</i>	106
<i>Figure 4.14. Sections of the barrier with accumulations of driftwood</i>	108
<i>Figure 4.15. Sections of the barrier affected by human-activity</i>	109
<i>Figure 4.16. Profile 1</i>	110
<i>Figure 4.17. Profile 2</i>	111
<i>Figure 4.18. Profile 3</i>	112

<i>Figure 4.19. Profile 4</i>	<i>113</i>
<i>Figure 4.20. Profile 5</i>	<i>114</i>
<i>Figure 4.21. Profile 6</i>	<i>115</i>
<i>Figure 4.22. Profile 7</i>	<i>116</i>
<i>Figure 4.23. Profile 8</i>	<i>117</i>
<i>Figure 4.24. Profile 9</i>	<i>118</i>
<i>Figure 4.25. Profile 10</i>	<i>119</i>
<i>Figure 4.26. Profile 11</i>	<i>120</i>
<i>Figure 4.27. Profile 12</i>	<i>121</i>
<i>Figure 4.28. Profile 13</i>	<i>122</i>
<i>Figure 4.29. Profile 14</i>	<i>123</i>
<i>Figure 4.30. Profile 15</i>	<i>124</i>
<i>Figure 4.31. Profile 16</i>	<i>125</i>
<i>Figure 4.32. Profile 17</i>	<i>126</i>

## **Chapter 5**

<i>Figure 5.1. Location of the Schmidt hammer rock test (SHRT) case study</i>	<i>133</i>
<i>Figure 5.2. Location and key findings of the SHRT in northern Adolfbukta</i>	<i>136</i>
<i>Figure 5.3. Mean R-values obtained during the SHRT</i>	<i>137</i>

## **Chapter 6**

<i>Figure 6.1. Location of study site: E5-E8 and sources of non-glacial sediment supply</i>	<i>143</i>
<i>Figure 6.2. The present-day gravel dominated barrier in Petuniabukta</i>	<i>144</i>
<i>Figure 6.3. Seasonal changes in the Petuniabukta coastal system</i>	<i>145</i>
<i>Figure 6.4. Orthophotomap of barrier coast and Ebba spit-platform in north-eastern Petuniabukta</i>	<i>146</i>
<i>Figure 6.5. Representative surface photographs of 24 beach ridges</i>	<i>148</i>
<i>Figure 6.6. The post-LIA progradation of the Ebba spit-platform</i>	<i>151</i>
<i>Figure 6.7. Glacial and coastal landscapes of NW Petuniabukta studied in this research</i>	<i>156</i>
<i>Figure 6.8. DGPS measurement of ground control points</i>	<i>158</i>
<i>Figure 6.9. Examples of aerial imagery used in the study</i>	<i>160</i>
<i>Figure 6.10. DTMs of the study area produced of aerial images from 2009 and 1990</i>	<i>161</i>
<i>Figure 6.11. Mosaic composed in LPS ERDAS software based on orthophotos from 2009 NPI aerial imagery</i>	<i>162</i>
<i>Figure 6.12. Three phases of post-LIA landscape change on the NW coast of Petuniabukta</i>	<i>163</i>
<i>Figure 6.13. Post-LIA geomorphic changes in the proglacial zone of Ferdinandbreen</i>	<i>165</i>
<i>Figure 6.14. Post-LIA changes of the Old Ferdie Fans 1 and 2</i>	<i>169</i>
<i>Figure 6.15. Main features of the Old Ferdie Fans landscape</i>	<i>170</i>
<i>Figure 6.16. Post-LIA changes of the modern Ferdie Fans 3 and 4</i>	<i>171</i>
<i>Figure 6.17. Main features of the Ferdie Fans landscape</i>	<i>172</i>
<i>Figure 6.18. Post-LIA changes of the barrier coast formed along the Ferdie Fans</i>	<i>179</i>
<i>Figure 6.19. Main features of the gravel-dominated Ferdie Barrier Spits</i>	<i>180</i>
<i>Figure 6.20. Post-LIA changes of the Elzaelva delta</i>	<i>181</i>



<i>Figure 6.21. Main features formed along the eroded coast between the Elzaelva delta and the FF4 fan delta</i>	<i>182</i>
<i>Figure 6.22. The Ferdie Spits and direction of formation of main recurved beaches</i>	<i>183</i>
<i>Figure 6.23. Post-LIA changes of the (fetch-limited) Ferdie Barrier islands</i>	<i>184</i>
<i>Figure 6.24. Main features of the (fetch-limited) Ferdie Barrier Islands</i>	<i>185</i>
<i>Figure 6.25. Post-LIA changes of the largest tidal island surface in the Petuniabukta tidal flat</i>	<i>186</i>
<i>Figure 6.26. Main features of the Petuniabukta tidal flat</i>	<i>187</i>
<i>Figure 6.27. Approximate shift in the position of tidal flat step that occurred between 1961-2009</i>	<i>188</i>
<i>Figure 6.28. Representative sediment surfaces in proglacial, alluvial and coastal zones and histograms summarizing size distribution analysis carried out in Wolman_Jack software.</i>	<i>190</i>
<i>Figure 6.29. DTM differencing of 1990 and 2009 models</i>	<i>192</i>
<i>Figure 6.30. Method of GIS construction undertaken in advance of sediment storage and erosion calculations</i>	<i>193</i>
 <b>Chapter 7</b>	
<i>Figure 7.1. Examples of raised beaches in High Arctic settings</i>	<i>201</i>
<i>Figure 7.2. Oblique air photograph of the raised beaches in section E6 at the entrance to Ebbadalen Petuniabukta</i>	<i>201</i>
<i>Figure 7.3. The stratigraphy of the Billefjorden raised beaches</i>	<i>202</i>
<i>Figure 7.4. Geomorphological map of the raised beaches and associated landforms located to the south of the Ebba River, Petuniabukta, based on field observations and air photographs</i>	<i>203</i>
<i>Figure 7.5. The present-day beach environment, south of the Ebba River</i>	<i>205</i>
<i>Figure 7.6. Shallow excavation into the crest of a late Holocene beach crest with two valves of a once articulated specimen of Astarte borealis</i>	<i>207</i>
<i>Figure 7.7. The marine bomb spike curve of Kalish et al. (2001) based on radiocarbon dates from known-age cod otoliths from the Barents Sea region</i>	<i>210</i>
<i>Figure 7.8. Relative sea-level graph based on Astarte borealis from the Ebbadalen beaches</i>	<i>212</i>
<i>Figure 7.9. a) Relative sea-level data from Billefjorden; b) Billefjorden and associated place names mentioned in the text</i>	<i>213</i>
 <b>Chapter 8</b>	
<i>Figure 8.1. The present-day state of Petuniabukta barrier coast</i>	<i>220</i>
<i>Figure 8.2. Scenarios of interannual High Arctic coastal change</i>	<i>221</i>
<i>Figure 8.3. Coastal areas of Spitsbergen investigated in previous studies vs. this study</i>	<i>235</i>
<i>Figure 8.4. Simplified water surface circulation in the study area and the functioning of the Ekman spiral in NW Petuniabukta</i>	<i>238</i>
<i>Figure 8.5. Scenarios of High Arctic coastal change over century-timescales. Note the emphasis on climate as a key driver</i>	<i>243</i>
<i>Figure 8.6. A comparison of the relative sea-level records developed from this study, based on marine shells (Astarte borealis) and a record from southern Edgeøya based on driftwood (BONDEVIK et al. 1995)</i>	<i>247</i>
<i>Figure 8.7. Estimated frequency of beach ridges deposited during the last ca. 6000 cal. yr BP based on the chronology provided by samples of Astarte borealis</i>	<i>248</i>
<i>Figure 8.8. Relative sea-level data from central and eastern Svalbard and reconstructed Svalbard–Barents Sea Ice Sheet domes and ice flows</i>	<i>251</i>
<i>Figure 8.9. Scenarios of High Arctic coastal change over millennial –timescales</i>	<i>252</i>
<i>Figure 8.10. Cycle of formation, destruction and re-formation of paraglacial barrier systems according to BOYD et al. (1987)</i>	<i>255</i>

<i>Figure 8.11. Major controls on mid-latitude paraglacial coastal progradation or recession: the rate and direction of sea-level change and the availability of sediments. After CARTER et al. (1987)</i>	256
<i>Figure 8.12. Key differences between mid-latitude and High Arctic paraglacial coastal evolution</i>	258
<i>Figure 8.13. Late Holocene evolution of High Arctic paraglacial coastal system at the entrance to Ebbadalen, Eastern Petuniabukta coast</i>	259

## **Appendix I**

<i>Figure A.1. Coastal sections studied during this research project</i>	306
<i>Figure A.1.1. Petuniabukta coast section E1</i>	307
<i>Figure A.1.2. Petuniabukta coast section E2</i>	308
<i>Figure A.1.3. Petuniabukta coast section E3</i>	309
<i>Figure A.1.4. Petuniabukta coast section E4</i>	310
<i>Figure A.1.5. Petuniabukta coast section E5</i>	311
<i>Figure A.1.6. Petuniabukta coast section E6</i>	312
<i>Figure A.1.7. Petuniabukta coast section E7</i>	313
<i>Figure A.1.8. Petuniabukta coast section E8</i>	314
<i>Figure A.1.9. Petuniabukta coast section N1</i>	315
<i>Figure A.1.10. Petuniabukta coast section N2</i>	316
<i>Figure A.1.11. Petuniabukta coast section N3</i>	317
<i>Figure A.1.12. Petuniabukta coast section W1</i>	319
<i>Figure A.1.13. Petuniabukta coast section W2</i>	320
<i>Figure A.1.14. Petuniabukta coast section W3</i>	321
<i>Figure A.1.15. Petuniabukta coast section W4</i>	322
<i>Figure A.1.16. Adolfbukta coast section A1</i>	323

# List of Tables

<b>Chapter 3</b>	<b>Page</b>
<i>Table 3.1. Key environmental studies in the northern Billefjorden region</i>	<b>63</b>
<b>Chapter 4</b>	
<i>Table 4.1. Barrier profiles studied for morphological changes (2008-2010)</i>	<b>84</b>
<i>Table 4.2. The Douglas Sea Scale</i>	<b>87</b>
<i>Table 4.3. Sea-ice conditions in Petuniabukta (2008 and 2010)</i>	<b>89</b>
<i>Table 4.4. Geomorphic features associated with local geomorphic processes</i>	<b>92</b>
<i>Table 4.5. Summary of the sedimentological properties of the Petuniabukta barriers and morphological changes observed (2008-2010)</i>	<b>127</b>
<b>Chapter 5</b>	
<i>Table 5.1. Schmidt Hammer Rock Tests summary</i>	<b>135</b>
<b>Chapter 6</b>	
<i>Table 6.1. Post-LIA changes (length/area) of three spits formed in the mouth of Ebbaelva</i>	<b>151</b>
<i>Table 6.2. Sedimentological characteristics of surface sediments collected from the seaward slopes of five spits in the Ebbaelva mouth</i>	<b>153</b>
<i>Table 6.3. Characteristics of fine sediments collected from beach ridge swales</i>	<b>154</b>
<i>Table 6.4. Post-LIA changes (length/area) of the Ferdie barrier spits</i>	<b>173</b>
<i>Table 6.5. Volumes of sediments stored and eroded from selected landforms in NW Petuniabukta</i>	<b>195</b>
<b>Chapter 7</b>	
<i>Table 7.1. Radiocarbon dates from this study</i>	<b>209</b>
<b>Chapter 8</b>	
<i>Table 8.1. Comparison of coastal change rates and glacier retreat rates between central, western and southern Spitsbergen</i>	<b>234</b>
<b>Appendix I</b>	
<i>Table A1 – Research plan</i>	<b>305</b>
<b>Appendix II</b>	
<i>Table A2. Research initiatives and projects that have evolved from this PhD research</i>	<b>325</b>



***Norwegian topographic names:***

bekken – stream

breen – glacier

elva – river

fjorden – fjord

kammen – crest

oya – island

vatne – lake

bukta – bay

dalen – valley

fjellet – peak

fonna – ice-field

odden – cape

pynten – cape

# Declaration

*I confirm that no part of the material presented in this thesis has previously been submitted by me or any other person for a degree in this or any other institution. In all cases, where relevant, material from the work of others has been acknowledged. The copyright of this thesis rests with the author. No quotation from it should be published without prior written consent and information derived from it should be acknowledged.*

*©Mateusz Strzelecki, Durham, December 2012*

## Statement of copyright

*The copyright of this thesis rests with the author. No quotation from it should be published without prior written consent and information derived from it should be acknowledged.*

Signed:

A handwritten signature in blue ink, appearing to read 'Mateusz Strzelecki', with a stylized, flowing script.

Dated: 20.12.2012

# Acknowledgements:

Firstly, I would like to thank my supervisors Professor Antony Long and Dr Jerry Lloyd. Not only for being the single most important driving force to complete this thesis but also for teaching me how to be a better researcher and better man. Antony's vision, devotion to Quaternary science and great personality has shaped me as a person and helped me to understand that in both 'normal' and 'scientific' life we are not walking so far to relax, but to wrestle with our weaknesses and to explore new solutions and new paths.

Jerry is the most modest and hard-working researcher I know and I am really grateful for his kindness and patience and providing constant support and advice throughout my thesis.

This thesis is a culmination of number of years of travel, work, places and meeting amazing people. It has ended and started on Svalbard.

In summer 2007 I participated in my first scientific conference, which took place in Svalbard. This was probably that kind of moment in life which has changed the rest of it. I have met Dr Ian Evans and his wife Marta, who, when asked where is the best place to study Geography answered without any doubt: 'DURHAM – it's obvious.' ... That was the first time I heard about this fascinating medieval town in the NE England. Ian and Marta helped me a lot with fulfilling all application procedures to Durham University and were always very supportive during those 4 years I've spent in the UK. So, first of all I would like to thank them for placing Durham on the map of my life.

During the same meeting I've also met Prof Olav Slaymaker – his talk had influenced the way I understand the paraglacial landscape change in the cold regions and draw my attention on the processes controlling sediment budgets in Arctic coastal zone. Motivated by my Polish supervisor and mentor Professor Andrzej Kostrzewski I have applied and received my first research grant funded by Polish Ministry of Science and High Education (Award no. N306 284335) which allowed me to carry out the research on Svalbard in years 2008-2011. I'm grateful for his protection and supporting me with all needed things to receive funding and various scholarships over last 5 years.

Finally, on 28<sup>th</sup> September 2008 I entered the doors of the Department of Geography and started new academic life as a member of the Ustinov College which became my home for almost 4 years. It would not be possible without a support I received from my parents Anna and Edward and my parents in law Krzysztof and

Katarzyna, who helped me when it was the most needed. I am grateful to my parents who believed in me and thought me that if a man works hard and prays even harder can move mountains. I am also grateful to my younger brother Paweł, who took care of my parents when I was abroad and had always time for me and my troubles. Thanks also to my brother in law Błażej, who helped Marta while I was away.

Living and studying in Durham was a fascinating experience mainly because of friends I've met there who shared with all ups and downs of a PhD-student life. I would like to particularly mention my Departmental colleagues: Tim, Vicky, Tasha, Steven, Matt, Chris, Rachel, Joy, Emma, Ed, Ladan, Anne, Rob, Michele, Milo Diana and Tom. I would like to also mention my flatmates Eun Young, Dawid, Marta who became one of our best friends. I will also never forget great time and discussions with Hassan.

This research would not be completed without help from great team of technicians from our Department: Neil, Frank, Grzegorz, Mervyn, Sam, Jane and Chris Orton. Thanks also to John Thompson for patience and support in dealing with postgraduate teaching and his respect and knowledge on Polish history.

Durham was a special experience also thanks to the support I have received from great group of academics, who always have time to explain me in detail many geomorphological processes and relationships. I would like to thank: Mike Bentley for fruitful discussions and great sea-level fieldwork on Iceland as well as 'future' Antarctic plans, Dave Evans, for helping me understand glacial landscapes and work on map of the Hørbyebreen, Dave Roberts for showing me fascinating world of glacial tills, Chris Stokes for his sense of humour and knowledge of ice streams, Colm O'Cofaigh for explaining the processes in glaciomarginal environments, Jeff Warburton for insight into peat erosion and river transport, Jim Innes for support in lab, David Milledge for teaching my GIS and photogrammetric analyses, Sarah Woodroffe for teaching me about salt marshes, Mike Lim for common work on COROCO project, Nick Rosser for great time and explaining the functioning of landslides and rockfalls.

This PhD was made possible by financial support from Crescendum Est Polonia Foundation, Adam Mickiewicz University Foundation, Ministry of Science and Higher Education, NERC Radiocarbon Facility (award number 1520.0910) Ustinov College Travel Bursary, National Science Foundation, World Meteorological Organisation, IASC, Norwegian Polar Institute, European Commission and EU ESF funds.

I am also very grateful to German Academic Exchange Service who funded my research fellowship at Alfred Wegener Institute in Potsdam, where I wrote couple of



thesis chapters as well as to Research Council of Norway for funding my post-doctoral position at University Centre in Svalbard, where I could focus on the final parts of this work in a really friendly but also mysterious atmosphere of High Arctic polar night.

Over those four years I have met number of great teachers, mentors, researchers and friends from around the world and I would like to thank in particular: Prof. Antoni, Lewkowicz, Prof. Piotr Migoń, Prof. Jacek Jania, Prof. Piotr Głowacki, Prof. Achim Beylich, Prof. Scott Lamoureux, Prof. Ole Humlum, Prof. Hanne Christiansen, Prof. Collin Balantyne, Prof. Dennis Mercier, Prof. Daniel Germain, Dr Armelle Decaulne, Prof. Alan Trenhaile, Harald Aas, Dr Paul Overduin, Karoline Baelum.

My colleagues from APECS: Jenny, Hugues, Jose, Ben, Kim, Daniela, Alexey, Billy, Mike – thanks for shaping the future of polar research during the IPY and forever.

My friends from AMUPS and other Polish Polar Stations: Kuba, Tomek, Agata, Krzychu, Marlena, Adam, Staszek, Monika, Evert, Ola, Iza, Beata, Piotr, Uwe, Jacek, Darek.

My best friends from Poland: Nati, Darek, Piotr, Anka, Filip

My geography teachers: prof. Krystyna Adamczak (primary school) and prof. Dorota Indrzejczak (Kędzia) from high school – who shaped my fascination in physical geography and interests in landscape change studies.

I would not get to the Arctic without a support from Professor Grzegorz Rachlewicz, who became my mentor and advisor and taught me how to be a good head of the family and head of the research team. Many improvements to this work were triggered by challenging discussions with Dr Witek Szczuciński, who changed my understanding of fjord systems and introduced to the fascinating world of tsunami research and proving that it is possible to be an excellent researcher and even better father.

Finally I am grateful for patience, support, trust and love I have received from my beloved wife Marta. This thesis is also your great effort and I will do my best to pay off all the time and nerves you lost because of my laziness and egoism. Thank you for taking care of our little Rita and keeping us as a couple for all those years. I love you.

*For Marta my beloved wife  
and Rita my little pearl*

# Chapter I: Introduction

## 1.1 Research rationale

The tremendous research efforts undertaken during the 4<sup>th</sup> International Polar Year 2007 – 2008 have revealed that, currently, the Arctic is experiencing the largest and most rapid increases in air and sea temperatures on Earth (IPCC 2007). Some of the most visible changes are those connected with marine environments, which are experiencing a rapid reduction of the sea ice extent and thickness (COMISO *et al.* 2008, WANG and OVERLAND 2009, KWOK and ROTHROCK 2009). Sea ice loss (Figure 1.1.) is however, only one measure of the rapid changes that are already affecting physical and ecological processes operating in Arctic regions.

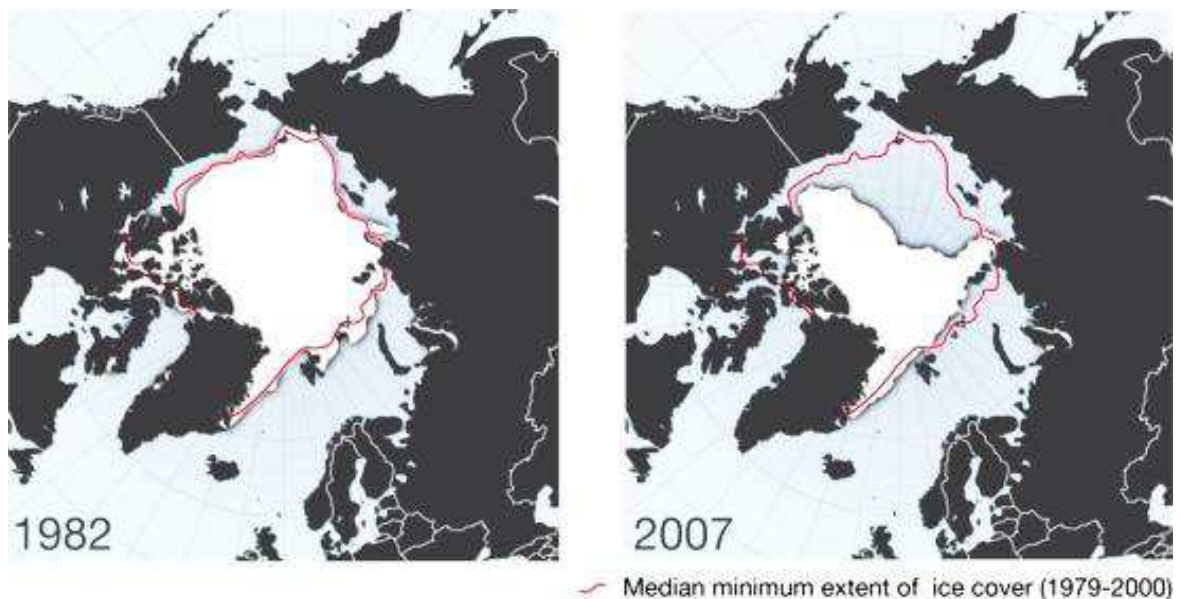


Figure 1.1. Arctic sea ice minimum extent in September 1982 and 2008. (Source: <http://maps.grida.no>, based on Fetterer and Knowles (2002), updated in 2004. Sea ice index. Boulder, CO: National Snow and Ice Data Center). The ice extent was 7.5 million km<sup>2</sup> in 1982, 5.6 million km<sup>2</sup> in 2005 and only 4.3 million km<sup>2</sup> in 2007. The retreat of the ice cover was particularly pronounced along the Eurasian Arctic coast.

Other rapid changes include increased permafrost thawing (LAWRENCE *et al.* 2008, ROMANOVSKY *et al.* 2010), rapid ice mass loss from glaciers (ARENDR *et al.* 2002; HAGEN *et al.* 2003; DYURGEROV and MCCABE 2006; BASSFORD *et al.* 2006; OERLEMANS 2007; NUTH *et al.* 2010) and the Greenland Ice Sheet (RIGNOT *et al.* 2008; PRITCHARD *et al.* 2009), accelerated fluvial discharge, river erosion and transport (SYVITSKI 2002; GORDEEV 2006; COSTARD *et al.* 2007; OVEREEM and SYVITSKI 2010), the geomorphic transformation of deglaciated areas (GLASSER and HAMBREY 2003; LØNNE and LYSÅ 2005; RACHLEWICZ 2009), rapid changes to lacustrine systems (Smith *et al.* 2005), and the shift of boreal forests into tundra (LIESS *et al.* 2010). Many of these changes are occurring faster than predicted in former studies (e.g. STROEVE *et al.* 2007; ROWLAND *et al.* 2010; RIGNOT *et al.* 2011).

These processes directly and indirectly change the nature of the Arctic coastal zone (Figure 1.2.). Of particular interest is the response of Arctic coastal systems to increased sediment and nutrient supply from land, as well as increasing open-water conditions that is leading to accelerated shoreline erosion and sediment transport.

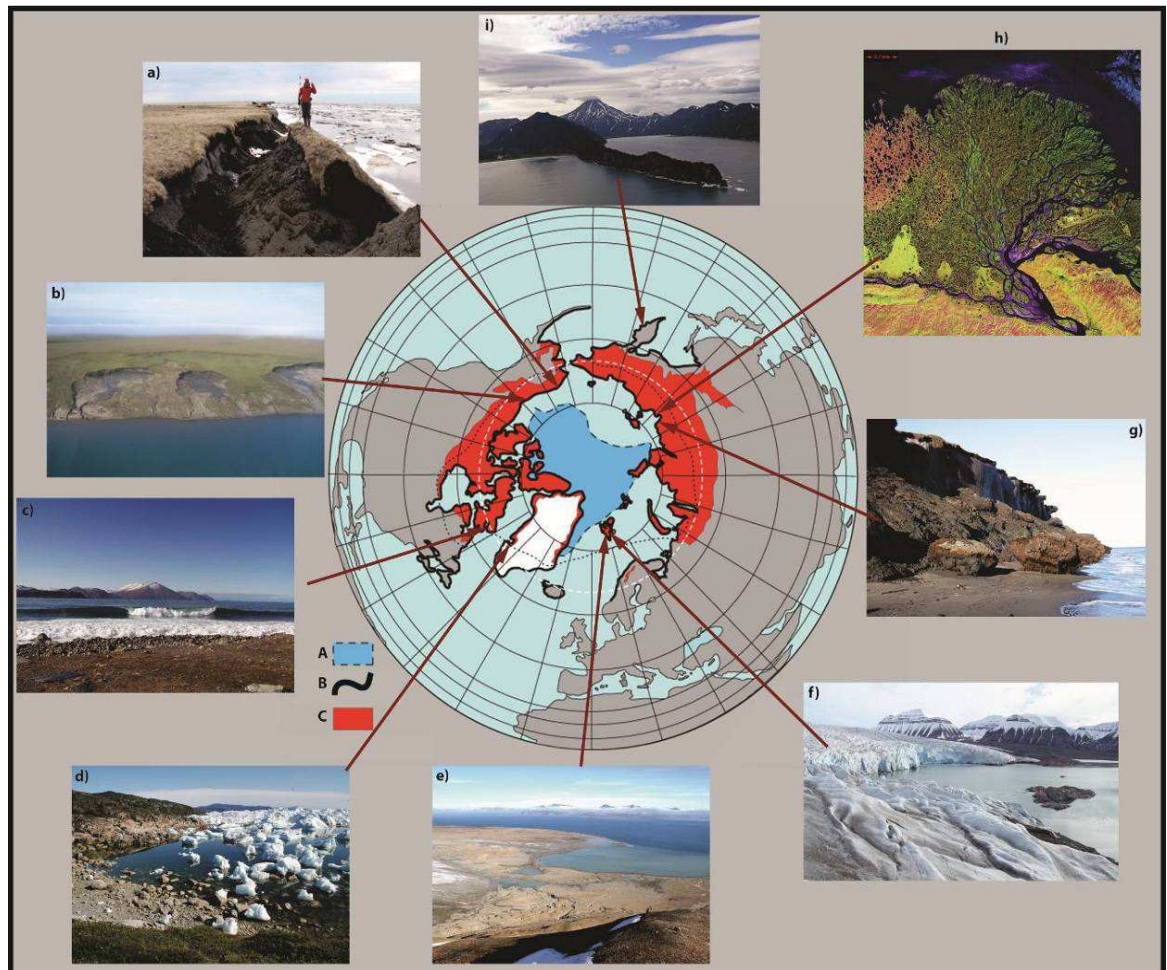


Figure 1.2. Arctic coastal environments. A - sea-ice minimum extent in 2007; B - cold region coasts in the northern hemisphere according to BYRNE AND DIONNE (2002); C – zone of continuous permafrost; Examples of coastal types: a) rapidly eroding coastline Drew Point, northern Alaska. Photo by ROBERT ANDERSON INSTAAR; b) Hershel Island coast fed by retrogressive thaw slumps. Photo by HUGUES LANTUIT AWI; c) gravel-beach Baffin Island Canadian Arctic Archipelago Photo: <http://arctickingdom.com>; d) rocky coastline affected by waves driven by ice-berg roll events in Illulissat Icefjord; e) paraglacial coast exposed after the retreat of Renardbreen, Recherchefjorden, Svalbard; Photo by PIOTR ZAGÓRSKI f) ice-cliffed coast formed by tide-water Nordenskiöldbreen, Svalbard; g) thermoabrasion coast in Muostakh Island, Laptev Sea, Siberia Photo by VOLKER RACHOLD; h) Lena Delta Photo Google Earth; i) Rock coast in Gulf Viljuchinsky, Kamchatka Peninsula, Pacific ocean Photo: [skyscrapercity.com](http://skyscrapercity.com)

The recently published ‘The State of Arctic Coast 2010 Report’ (FORBES *et al.* 2011) suggests that the circumpolar coastal zone is the key interface in the entire Arctic characterised by the most rapid and severe environmental changes which have serious implications for communities living on coastal resources. Despite the potential significance

of these changes, relatively little is known of the physical processes that control high latitude coasts or how they might change in the future.

It is also important to note that many of the existing ideas regarding the functioning of polar coasts are based on limited observations that provide an inadequate base from which to predict the future. Not only is the number of academic papers on high latitude coastal environments lower than from temperate and tropical regions, but also their descriptive nature often means that they cannot be used for numerical modelling. This situation has persisted for several decades and is highlighted by the remark from TRENHAILE (1983, 77 p.) that *'there is a lack of even basic agreement on the efficiency of coastal processes in the high latitudes'*. Almost twenty years later, BYRNE and DIONNE (2002) in their review of the state of high latitude coastal geomorphology, noted that polar coastlines, that account for at least 30% of the World coasts, were still very neglected. LANTUIT *et al.* (2010) indicated that only 1% of Arctic coastlines have been investigated in sufficient detail to allow quantitative description of processes operating on them.

The most recent advances in high latitude coastal geomorphology pertain to the ice-rich permafrost coasts of Siberia and Alaska (ROMANOVSKII *et al.* 2004; RACHOLD *et al.* 2005; SOLOMON 2005; ARÉ *et al.* 2008; LANTUIT *et al.* 2009). In contrast, much less work has been done on the rocky, sheltered coastlines of Arctic archipelagos such as Svalbard, Franz Joseph Land, the Canadian Arctic Archipelago or Greenland, whose melting ice masses contribute the greatest to present-day sea level rise (Figure 1.3.). One of the key messages stemming from recent papers reviewing developments in Arctic coastal studies is the need for long-term coastal change monitoring and the selection of core indicators that could be used in a unified way under the umbrella of a circumpolar observation network (e.g. JOHN and SUGDEN 1975; FORBES and TAYLOR 1994; TRENHAILE 1997; BYRNE and DIONNE 2002; URDEA 2007; LANTUIT *et al.* 2011; FORBES *et al.* 2011). Thus, although knowledge of the response of the coastal zone to climate change is fundamental to understanding how polar landscapes will adjust to global warming, we still lack the observational base to quantify the rate and scale of coastal change for vast areas of the Arctic. At the heart of this problem lies a mismatch between old concepts based on short field observations and the need for longer-term studies that link Arctic coastal evolution with changes to the Arctic landscape on seasonal, decadal, century and millennial timescales. This is a particular case in the High Arctic where the impact of past and



present climate changes on the factors that control coastal evolution is poorly understood.

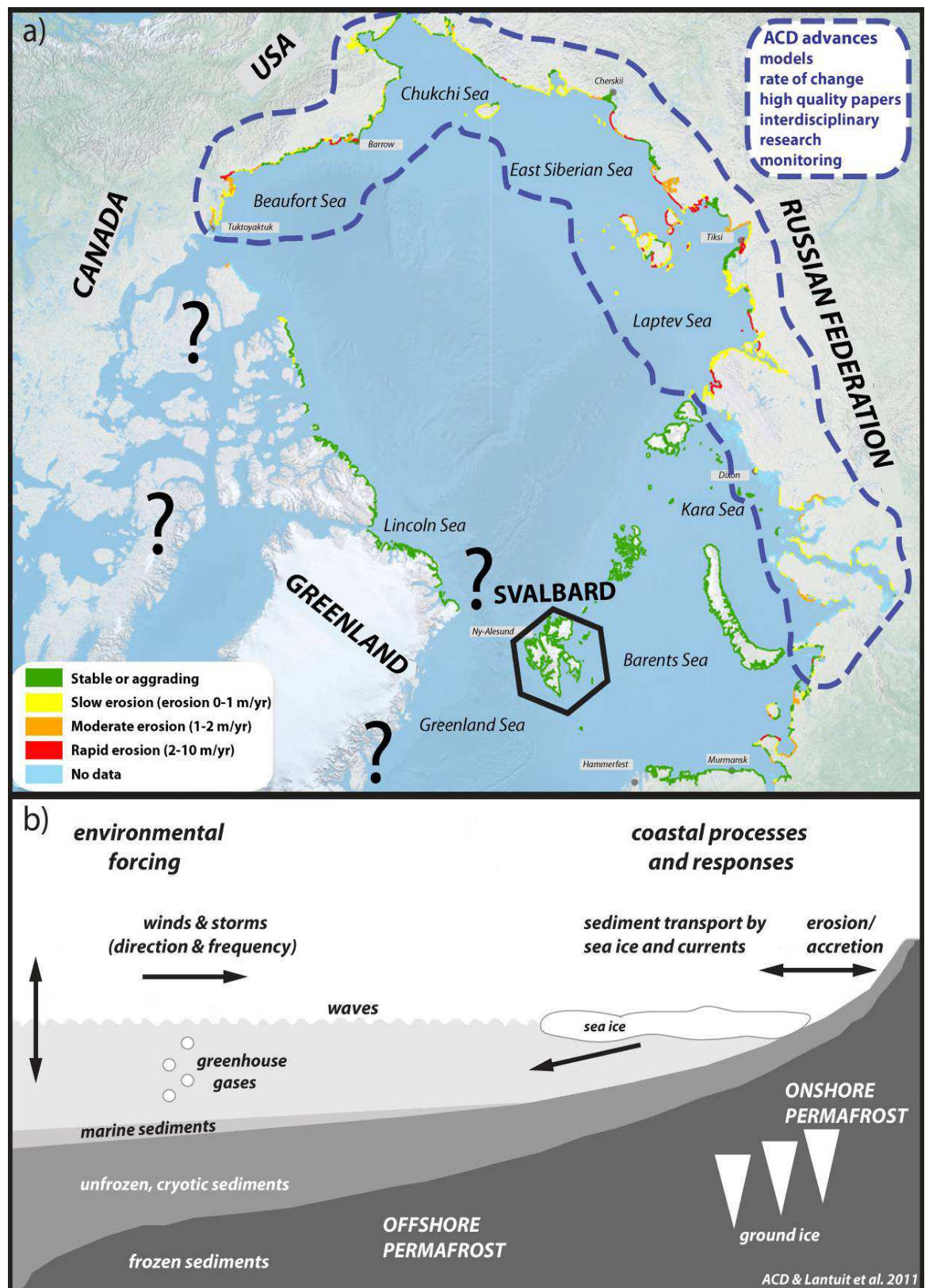


Figure 1.3. The state of Arctic coasts 2010: a) The base map is a circum-Arctic depiction of coastal erosion rates by LANTUIT et al. (2011). For vast areas of High Arctic (e.g. CCA, Greenland) the state of the coastal environment is largely unknown. The Svalbard Archipelago (in a black polygon) is one of the key areas to

make further progress in Arctic coastal studies; b) Characteristic processes operating along ice-rich permafrost Arctic coasts (modified after LANTUIT *et al.* (2011)).

Due to its location at the boundary between oceanic and atmospheric fronts (Figure 1.4.), the Svalbard archipelago is well-placed to study the High Arctic sensitivity to climate change (D'ANDREA *et al.* 2012). The Svalbard region has, therefore, been an area of many scientific studies including: palaeo-climate reconstructions (e.g. Isaksson *et al.* 2005); the extent of the last glaciation (e.g. MANGERUD *et al.* 1998; SVENDSEN *et al.* 2004); Holocene sea level changes (e.g. FORMAN *et al.* 2004); modern and relict glacial systems (e.g. BOULTON 1972; LØNNE and LYSÅ 2005; NUTH *et al.* 2010); periglacial permafrost processes and mechanisms (e.g. HUMLUM *et al.* 2003), and; ocean water interaction and mixing (e.g. HALD *et al.* 2004; ŚLUBOWSKA-WOLDENGEN *et al.* 2007; MAJEWSKI *et al.* 2009).

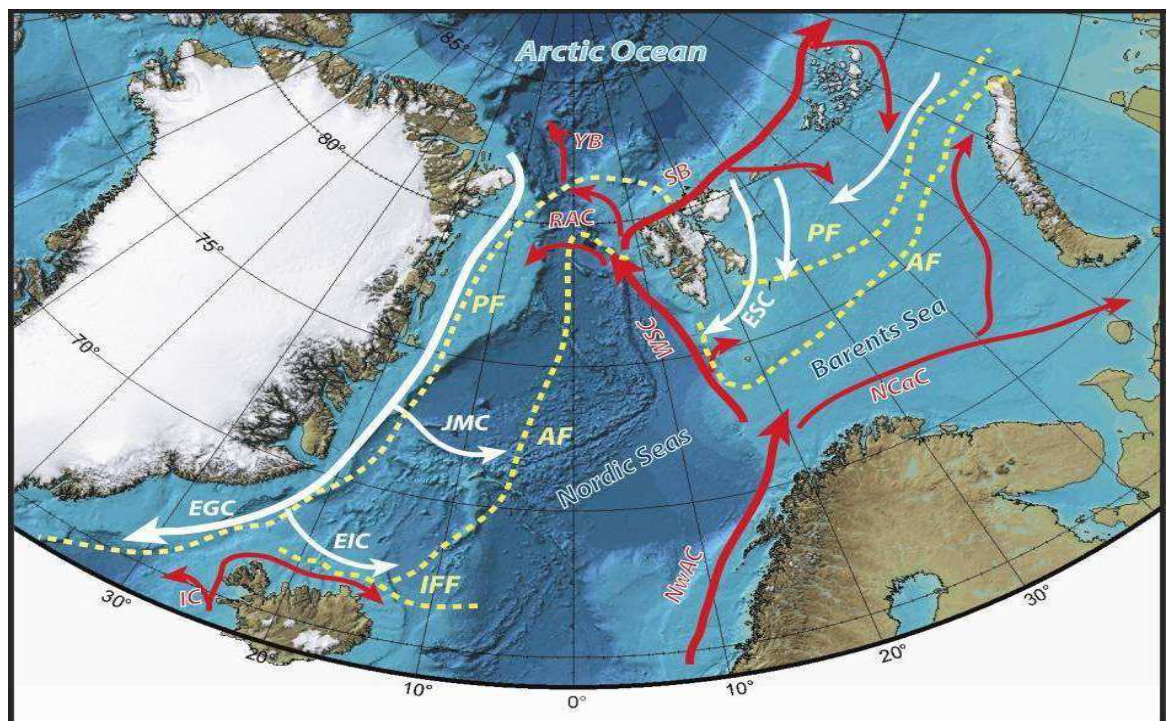


Figure 1.4. The Svalbard archipelago and the present-day ocean circulation in the European Arctic sector (modified from ŚLUBOWSKA-WOLDENGEN *et al.* (2008)). **LEGEND:** Atmospheric Fronts: AF - Arctic Front, IFF - Faroe Island Front; Ocean Waters: Red arrows - Atlantic Water, White arrows - Polar Water; Warm Ocean Currents: WSC - West Spitsbergen Current, YB - Yermak Branch, SB - Svalbard Branch, RAC - Return Atlantic Current, NCaC - North Cape Current, NwAC - Norwegian Atlantic Current; IC - Irminger Current; Cold Ocean Currents: EGC - East Greenland Current, EIC - East Iceland Current, ESC - East Spitsbergen Current, JMC - Jan Mayen Current

Despite the research which has been undertaken in Svalbard, there has been little study of coastal processes and environments. During the last century, the landscapes of Svalbard have experienced a major change from glacial towards paraglacial domains as a consequence of widespread glacier retreat and the extensive reworking of glacial sediments by non-glacial subaerial processes (MERCIER and LAFFLY 2005; MERCIER *et al.*



2009; RACHLEWICZ 2010). According to LAFFLY and MERCIER (2002), in recent decades paraglacial processes (Figure 1.5.) have become the most effective geomorphological processes on Svalbard, reducing the impact of glacial processes to a secondary role in landscape change.

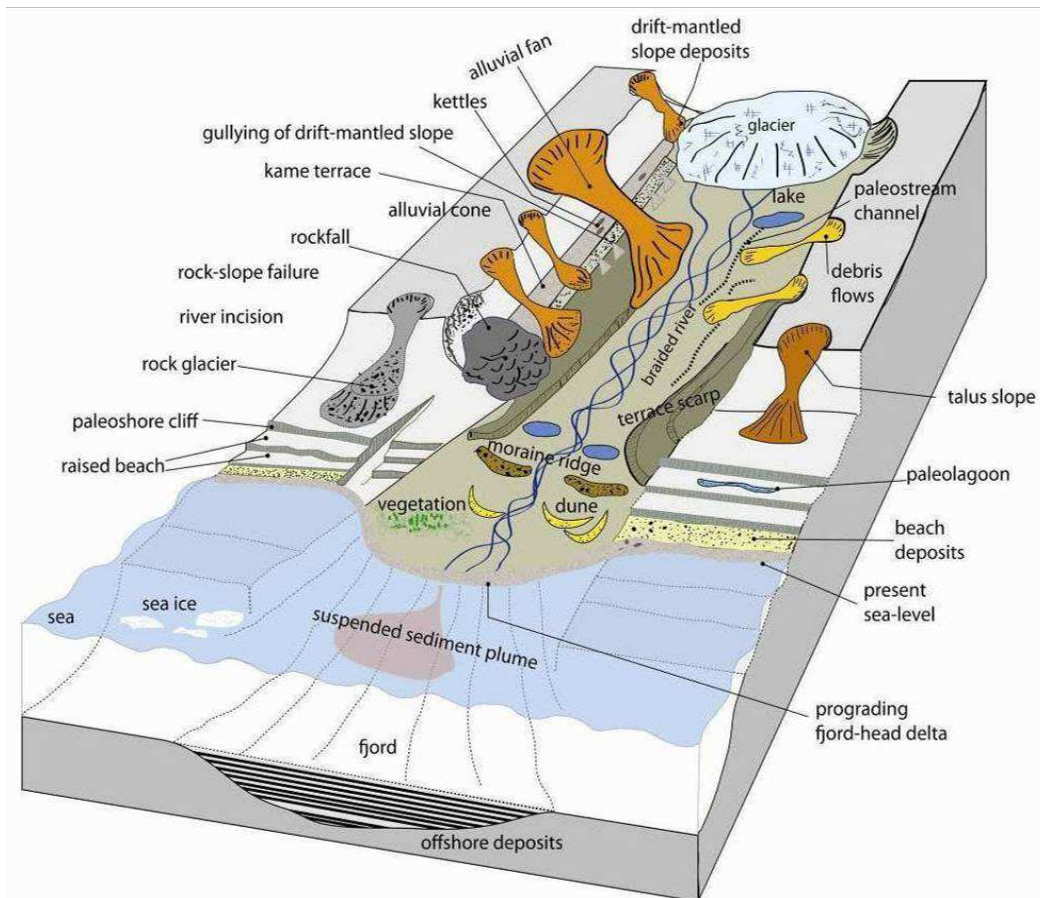


Figure 1.5. Paraglacial landforms and processes (after MERCIER (2007)).

In Svalbard, climate models predict an increase in air temperature of between 3 and 8°C by the end of this century and an increase in precipitation of c. 12% (FØRLAND *et al.* 2009). Without a proper understanding of past coastal behaviour, models of future change provide unrealistic scenarios of cold region coastal evolution. In polar regions, the legacy of Quaternary climatic, tectonic and geomorphic processes remains fresh in modern landscapes (HEWITT 2002). Therefore, understanding the present-day state of the Svalbard coastal zone must be informed by a longer-term knowledge of coastal zone development since the Last Glacial Maximum (LGM) and especially during the late Holocene.

This thesis addresses this theme by investigating the mechanisms that control the functioning of the High Arctic coastal zone of central Spitsbergen (the main island of the Svalbard archipelago) over a range of timescales from the late Holocene to the present.

The geomorphological diversity of the study area enables investigation of processes that have received little attention previously in Svalbard, notably the functioning of depositional and rocky coasts in sheltered fjord-headed bays with limited open-water periods.

To address the thesis aim, I present the results of three field seasons of fieldwork (winter and summer observations) during which I collected extensive field data regarding the nature of the coastal zone and the processes that control present-day (micro-scale) coastal morphodynamics. I combine these with laboratory analysis of sediments, as well as remote sensing techniques to reconstruct patterns and processes that operated in coastal zone during the last century, since the end of the Little Ice Age (LIA). Finally, by the application of radiocarbon dating of marine shells found in raised beaches I develop a new record of relative sea-level change in central Spitsbergen during the Late Holocene and consider the implications for the wider deglacial history of Svalbard.

## **1.2 Research aims and objectives**

The overall aim of this project is: *to develop a comprehensive description and process-based understanding of coastal changes in central Spitsbergen in response to recent climate change and to identify possible linkages between coastal morphodynamics and paraglacial activity in adjacent deglaciaded landscapes during the late Holocene.*

To achieve these aims, I identify the following research objectives:

- to characterise the landforms and processes operating on the modern depositional and rocky coasts of central Spitsbergen;
- to use archival data, photogrammetric analysis of aerial images and GIS techniques to quantify the post-Little Ice Age adjustment of coastal zone to landscape change during the last century;
- to reconstruct late Holocene coastal morphodynamics and decipher the relative importance of terrestrial and marine processes in controlling landform change;
- informed by the above, to establish a new model of paraglacial coastal zone evolution for High Arctic coasts.

### 1.3 Research questions

Previous studies carried out mainly along the western coast of Spitsbergen document significant changes in sediment flux and coastal response since the end of the Little Ice Age (e.g. HÉQUETTE and RUZ 1986; MERCIER and LAFFLY 2005; ZAGÓRSKI *et al.* 2012). The scale of changes observed along coasts of Kongsfjorden, Bellsund, Hornsund and Sørkapp are large, but the response of coastlines in the protected interior of Svalbard, such as in Billefjorden, inner Petuniabukta (the field area of this thesis) that experience reduced wave fetch, low rates of precipitation and extended sea-ice cover, has received limited study.

The present research seeks to answer the following research questions:

- 1) What is the interannual morphological variability of the gravel-dominated barriers along Petuniabukta between 2008-2010?*
- 2) What processes operate on recently deglaciated rocky coasts in the study area?*
- 3) How did glacial and non-glacial-fed, gravel-dominated barriers in Petuniabukta respond to warmer, post-LIA conditions characterised by enhanced paraglacial processes?*
- 4) How can we improve the accuracy of sea-level reconstructions and long-term coastal evolution studies in the High Arctic?*
- 5) Can answers to questions 1-4 above enable the formulation of a new conceptual model of paraglacial coastal evolution in the High Arctic?*

### 1.4 Conceptual framework

#### 1.4.1 Theories of cold landscape evolution

At the beginning of the 21<sup>st</sup> Century, periglacial scientists started to challenge the longstanding theoretical concepts of landscape evolution in cold environments (HALL *et al.* 2002; ANDRÉ, 2003; THORN, 2004). ANDRÉ (1999) argued that understanding of periglacial environments was hidden in a 'smokescreen' of traditional theories that were dominated by climate-driven geomorphic processes involving frost, snow and ice, and which were disconnected from the complex processes that operate in periglacial domains. More recently ANDRÉ (2009) distinguished five stages in the history of periglacial geomorphology tantamount to the development of a theoretical framework and approach to cold region (and coastal) landscape evolution:

1940 – 1960:	<i>the classic climatic geomorphology period;</i>
1960 - 1980:	<i>the 'freeze-thaw dogma' period;</i>

1980 - 1990:            *the anti-freeze-thaw dogma and search for new approach period;*  
1990 - 2000:           *the redefining of cold-region geomorphology;*  
2000 – present:        *the paraglacial period, challenging the effects of global change on cold region landscape evolution.*

In parallel, EVANS (2005) clarified the *glacial landsystem* concept, highlighting the need to treat glacial landscapes as dynamic systems controlled by the superimposition of depositional and erosional features of different age and different significance for further earth surface evolution. This prepared the ground for further unification of geomorphological research in Arctic regions, illustrated recently by the appearance of research projects that seek to link glacial and permafrost environments (e.g. HARRIS and MURTON, 2005).

More recently, BERTHLING and ETZELMÜLLER (2011, 380 p.) introduced the *cryo-conditioning* concept that links landform and landscape evolution in cold regions and was defined as an “*interaction of cryotic surface and subsurface thermal regimes and geomorphic processes*”. The fundamental premis of this theory is that periglacial, glacial and so called ‘azonal’ processes are conditioned by the cryotic superficial and underground thermal regime. This new contribution to the debate on the genesis and future of cold landscapes creates the chance to unify concepts of glacial, periglacial and paraglacial geomorphology under the banner of *cryogeomorphology*.

As explained by SLAYMAKER and KELLY (2007), the key word which enabled the ongoing consolidation in cold region geomorphology is *transience*. This implies that the aim of modern cold region geomorphology is to understand the nature of transition from glacial to non-glacial landscapes with a concurrent consideration of periglacial and paraglacial stages of this transformation.

The *paraglaciati*on concept was first introduced by RYDER (1971a, b) during her study of British Columbia alluvial fans that formed following deglaciation in the early Holocene. Although MERCIER (2008) states that the term was known since the 1960s (GODDARD 1965) and that the first ‘paraglacial’ approach to studying post-LIA readjustment was applied over century ago by SURELL (1841), the proper conceptualisation of the term first appeared in CHURCH and RYDER (1972, 3059 p.) where the phrase *paraglacial* was defined as the ‘*non-glacial processes directly conditioned by glaciation*’.

Subsequently, mainly North American geomorphologists (e.g. RHINE and SMITH, 1988; CHURCH and SLAYMAKER, 1989) began to apply this term to describe periods of landscape recovery following glaciation that are characterised by high rates of sediment delivery from proglacial zones and valley slopes into fluvial, aeolian and coastal systems, often developing in periglacial realm (Figure 1.6.).

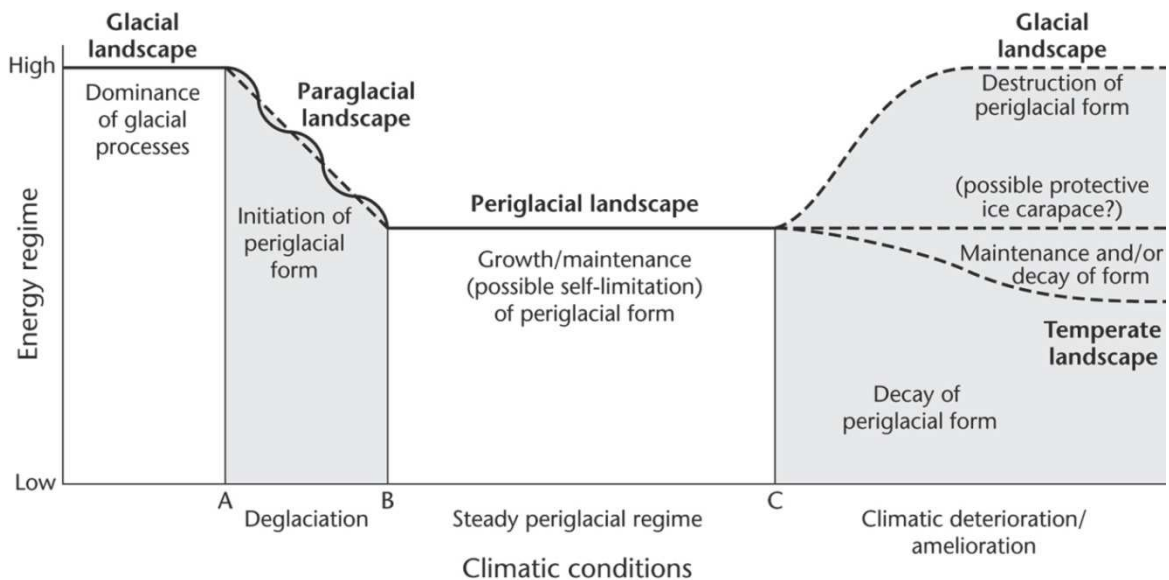


Figure 1.6. Model of transition from glacial through paraglacial into periglacial environment (after SLAYMAKER 2011 modified after THORN and LOEWENHERZ, 1987)

CHURCH and SLAYMAKER (1989) suggested a modification of the paraglacial concept and its extension into the postglacial (mainly Holocene) era, arguing that the reworking of glacial sediments may be reactivated long after deglaciation. A further development was the HARBOR and WARBURTON (1993) sediment-budget model that showed that similar sediment yields can occur at different times after deglaciation in small, medium and large catchments. Both papers applied the cascade of sediment 'wave model' to explain the release of glacial sediment from storage systems. BENN and EVANS (1998, 2010) criticised the attribution of distinct *paraglacial processes* since, they argued, these processes do not differ in nature from 'normal' subaerial processes. Instead, these authors suggested that the term 'paraglacial' should retain its original temporal meaning a '*period of rapid environmental readjustment following glacier retreat*'.

In a global review of the concept, BALLANTYNE (2002, 1938 p.) broadened the paraglacial definition to '*non-glacial earth surface processes, sediment accumulations, landforms, land systems and landscapes that are directly conditioned by glaciation and deglaciation*'. He based his discussion on glacial sediment release from storage and the re-entrainment of already reworked glacial sediments on the sediment exhaustion model proposed by CRUDEN and HU (1993).

BALLANTYNE (2005) identified six paraglacial landsystems (glacier forelands, rock slopes, drift-mantled slopes, fluvial, lacustrine and coastal systems) (Figure 1.7.) and this classification formed a framework for a complex analysis of present-day and former evolution of recently deglaciated areas. Paraglacial mobilisation of sediment, which is normally at its maximum just after deglaciation, varies in different geomorphic settings. For example, a reduction of moraine gradients takes approximately 1000 years, whereas the formation and stabilisation of alluvial fans may take > 6000 years (BALLANTYNE, 2002). BALLANTYNE (2002) explained that, depending on the particular geosystem under study, the relaxation to 'equilibrium' state of sediment transport may involve a time period even longer than that of most interglacials.

However, such a broad definition of the concept invited criticism and most recently SLAYMAKER (2009) rejected both the spatial and temporal dimensions of the theory, instead suggesting that paraglaciation should be considered as the rate and trajectory of Holocene modification of glaciated landforms and landscapes. In this approach, geomorphologists should use '*paraglacial thinking*' while '*focusing attention on the ways in which glaciated landscapes respond to non-glacial conditions (80 p.)*' rather than simply describing numerous types of processes, landforms or landsystems.

HEWITT (2002) used the term '*palimpsest*' to describe the transitional and overlapping behaviour of cold region landscapes as they transform from their relict to present form. The term is suitable for many polar regions where the effects of former glaciations are still visible amongst recently formed non-glacial landforms or sediment assemblages controlled mainly by permafrost, fluvial and aeolian activity.

Working in Svalbard, where paraglacial landscape transformation is modified by permafrost and frost activity, MERCIER (2008, 225 p.) used the term '*paraperiglaciation*' to define '*earth surface processes, sediment accumulations, landforms, landsystems and landscapes that are directly conditioned by permafrost thaw-degradation*'. This term might be used to explain the rate and trajectory of non-glacial, frozen ground landscape adjustments to climate shifts. The concept is important because it links glaciated, deglaciated and non-glaciated parts of cold regions, emphasising their particular sensitivity to climate change. MERCIER (2008) suggested the existence of subsequent *paraglacial and paraperiglacial crises*, the first occurring after glaciation and the latter after a period of periglacial landscape modification. According to MERCIER (2008) the Quaternary era, with long glaciations and short interglacials, meant that paraglacial and paraperiglacial crises never fully ended due to exhaustion of glacial sediments or the full dominance of non-

glacial/non-permafrost processes, instead being abruptly over-ridden by the next glaciation.

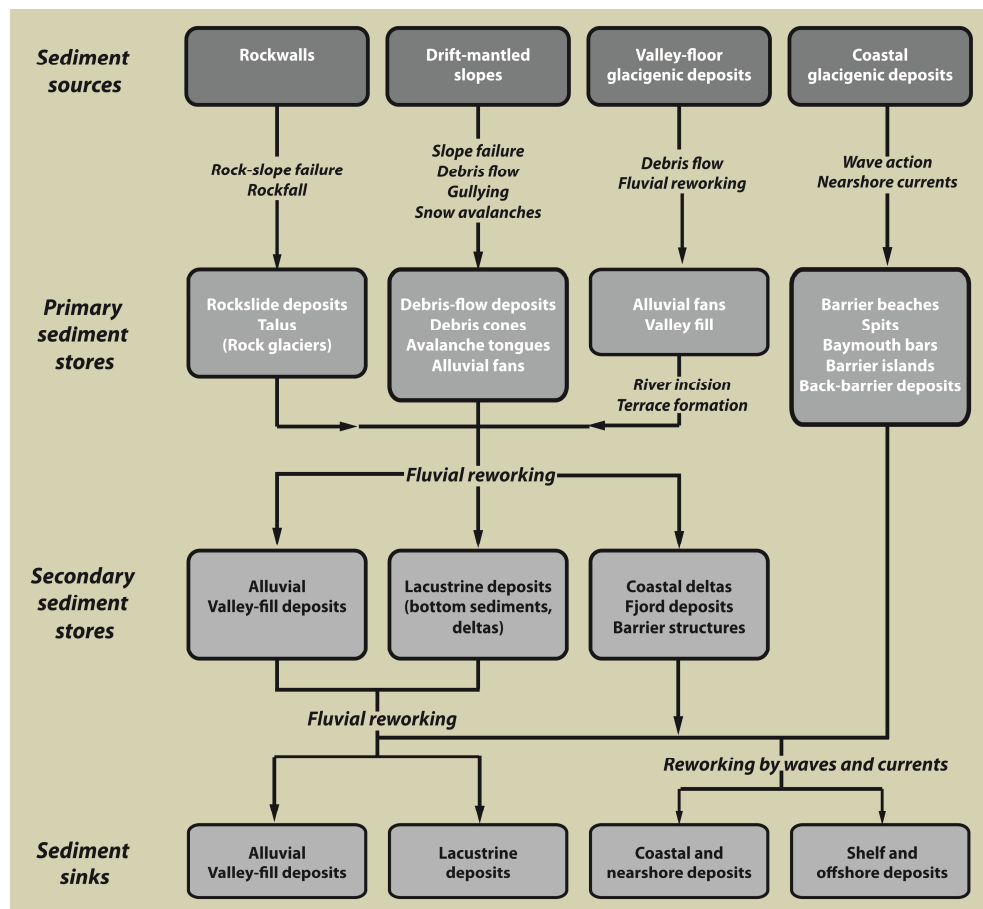


Figure 1.7. Sediment cascades within paraglacial landsystems, modified after BALLANTYNE (2002, 2005)

In this thesis, I use the term ‘paraglacial’ following the most recent views of SLAYMAKER (2009, 2011), treating it as a state of transitional landscape that evolves concurrently with deglaciation (ice-sheet covered landscapes) or the retreat of glaciers (glacierised landscapes), and which is characterised by intensified sediment supply from proglacial zones and valley systems and enhanced transport to coastal and marine sediment sinks.

### 1.4.2 Coastal zone terminology

To date, no conceptual framework exists to describe the High Arctic coastal zone. Therefore, in this thesis I use the coastal zone definition of CARTER (1988, 1 p.) as '*the space in which terrestrial environments influence marine environments and vice versa. The coastal zone is of variable width and may also change in time*'.

I also follow the definition of paraglacial coasts proposed by FORBES and SYVITSKI (1994, 376 p.) who defined them '*to be those on or adjacent to formerly ice-covered terrain, where glacially excavated landforms or glacial sediments have a recognizable influence on the character and evolution of the coast and nearshore deposits*'.

Several recent studies in coastal geomorphology adopt the tripartite classification of gravel beaches developed by JENNINGS and SHULMEISTER (2002) that divides them into: pure gravel beach, composite sand and gravel beach, mixed sand and gravel beach. However, in this thesis I use the term 'gravel barrier' to describe both coarse-grained beaches and barriers. This follows the suggestion made by ORFORD *et al.* (2005) to use term 'barrier' as a collective term covering gravel barriers and beaches, noting that all coastal barriers include a beach component (Figure 1.8.).

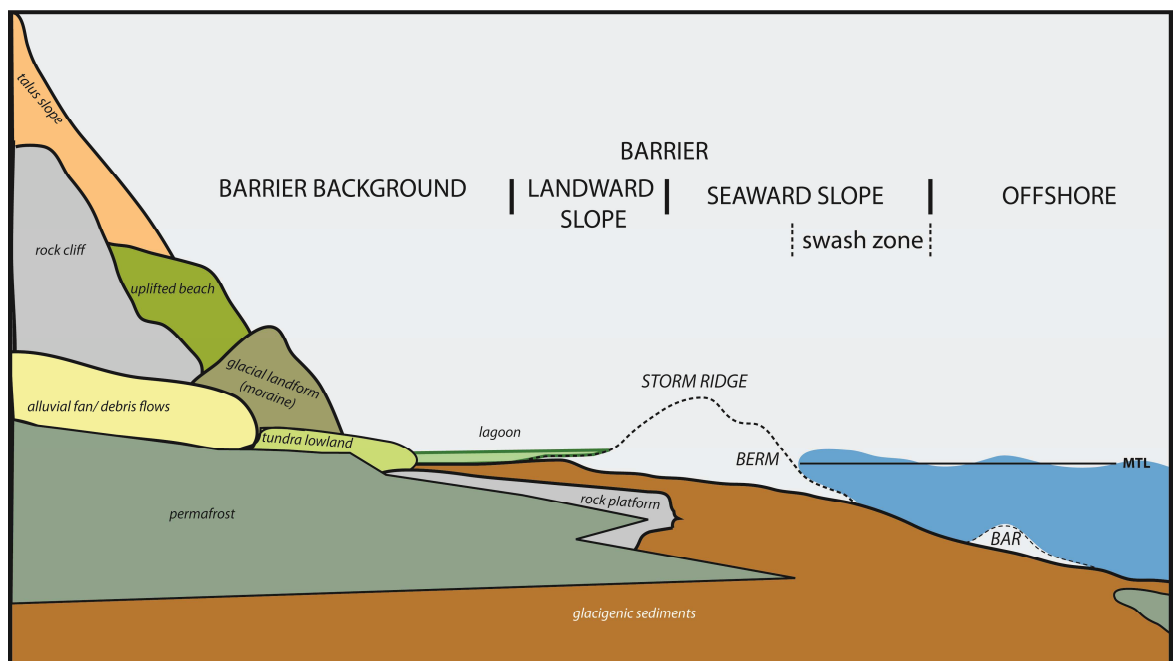


Figure 1.8. Coastal terminology applied to the description of gravel barrier environment.



## 1.5 Research schedule

The research detailed in this thesis forms part of a longer programme of work in Petuniabukta area that, for the author, commenced in 2005 when I worked as a Master's student examining the physical processes operating in the study area under the supervision of Professor Andrzej Kostrzewski. This experience provided an excellent introduction to previous research in the area, as well as to the particular logistical challenges of undertaking research in the High Arctic. It provided the basis for the formulation of the current PhD thesis.

The use of methods was designed to enable a comprehensive analysis of the interaction between sediment supply, sea-level change and coastal evolution in three temporal scales (Figure 1.9.):

- annual changes during the period 2008 – 2010;
- century changes, with a particular focus on post-LIA landscape transition between 1900 – 2009;
- millennial changes, taking into consideration the Late Holocene sea-level and coastal evolution history of the study area.



*Figure 1.9. Temporal scales of coastal change analysed during this PhD research.*

Field research detailed in this thesis was undertaken during the Arctic summers of 2008, 2009 and 2010. In addition, winter field observations were completed in 2009. Processing and correction of DGPS data was undertaken with Miss Samantha Waugh (Durham University). Photogrammetric analysis of aerial images and GIS processing were completed at the GIS Laboratory (Durham University) under the supervision of Dr David Milledge, with sonar data processed by Professor Alfred Stach at the Faculty of Geographical and Geological Sciences at AMU in Poznań. AMS radiocarbon dating of collected shells was conducted by National Environmental Research Council Radiocarbon Facility (award number 1520.0910) with support from by Dr Charlotte Bryant (SUERC, Glasgow University).

A programme of work is provided in Table AI (Appendix I) which details when different stages of the research detailed in this thesis were completed.

## 1.6 Chapter summary

This chapter provides the underpinning rationale for research into the High Arctic coastal zone in Svalbard and explains the research motivations of this PhD project. This chapter summarises the key theoretical concepts used in description of cold region environmental change and defines the coastal zone terminology used. Finally, the Chapter outlines the research methods and timetable of research used.

To answer the key research questions of this PhD project, the thesis is structured in the following manner:

*Chapter 2* reviews previous research on cold region coastal geomorphology with a particular emphasis on the characteristic processes and landforms in Arctic settings.

*Chapter 3* introduces the study area, including its geology, climate and coastal geomorphology.

*Chapter 4* details patterns of recent morphosedimentological changes of gravel-dominated formed in Petuniabukta between 2008 and 2010.

*Chapter 5* details rock resistance characteristics of modern rocky coastal landscapes in Adolfbukta.

*Chapter 6* details coastal zone response to post-Little Ice Age landscape transformation focusing on two types of sediment supply systems: non-glacial fed barrier system and glacial-fed barrier systems.

*Chapter 7* presents the results of investigations into the late Holocene sea-level history of the study area.

*Chapter 8* integrates the results of Chapters 4-7 to examine the controls of coastal evolution on annual, century and millennial timescales. It critically reflects on previous research and proposes a new model of paraglacial coastal evolution over different timescales.

*Chapter 9* presents a summary of the main findings of the thesis, assesses limitations to the work and identifies future research directions.

# Chapter 2:

# Research Context

## 2.1 Introduction

Cold region coasts (Figure 1.2.) are defined as *'those areas where frost and ice processes are active during a period of the year which is sufficient to have a significant, if not permanent, impact on the near terrestrial, coastal and marine environments'* (BYRNE and DIONNE 2002 p. 141). Several authors (e.g. FORBES and TAYLOR 1994; TRENHAILE 1997) noticed that many cold coast landforms (cliffs, beaches, barriers, dunes, spits, embayments, lagoons) and processes (tides, currents, waves) are similar to those from lower latitudes and that their distinction lies in the effects of permafrost, ground ice, frost action, sea ice, snow cover, isostasy, glacial history (sediment supply and topography) on coastal morphodynamics. According to KELLETAT (1989) the concept of 'zonality' in Arctic coastal geomorphology is arguably the most applicable among all types of World coasts as several processes operating on them are restricted only to circumpolar regions.

The duration of open-water conditions is crucial in determining the influence of azonal processes operating on cold coasts. In DAVIES's (1980) major World wave environment classification the majority of the Arctic coastline is included in 'protected sea' environments, apart from the east coast of Labrador, the south eastern coast of Greenland and the coasts of Iceland. Davies's (1980) classified most of the Arctic to the zone of semi-diurnal micro-tides with tidal range < 2 m (excluding Hudson Strait and Hudson Bay with tidal range > 6m). In general, Arctic coasts are described as ice-dominated, low-energy environments with storm-waves being the dominant influence on sediment budgets and morphology (OWENS and HARPER 1983). In certain High Arctic locations, the open water period lasts only up to 2.5 months, but even in areas where open water conditions exists for longer, the wave fetch is often still reduced due to the presence of an icefoot and/or movement of pack ice (FRENCH 1997).

What is more, the wave fetch along Arctic coasts is often limited by shoreline configuration, especially in the narrow fjords of Alaska, the Canadian Arctic, Svalbard or Greenland. In many cases the protective role of ice and the reduced space for wave action results in limited beach morphological modification and sediment reworking. Such conditions, together with limited longshore drift, lead to the development of narrow beaches with poorly sorted and rounded sediments delivered mainly from local, terrestrial sources. For these reasons, several authors (e.g., HARRY *et al.* 1983; OWENS and HARPER 1983; TRENHAILE 1997) have emphasised that, along these coasts, the role of storm surges is often much more significant than in the lower latitudes. For instance, HUME and SCHALK (1967) calculated that a storm event at Barrow, Alaska in October

1963 moved a volume of sediments that is transported under normal wave conditions in approximately 20 years. MCCANN (1972) reported that one storm event which entered Resolute Bay (Cornwallis Island) in 1968-1970 led to major beach erosion and the lowering of beach profiles by more than 0.5 m. According to OWENS *et al.* (1981), Arctic coastal processes are therefore characterised by aperiodic pulses of high-wave energy. However, this situation is likely to change in the future with more frequent episodes of high rates of erosion and storm flooding. This is because since the second half of the 20<sup>th</sup> century there has been an increase in the number, intensity and duration of cyclones entering the Arctic (Figure 2.1.), particularly in summer (ZHANG *et al.* 2004).

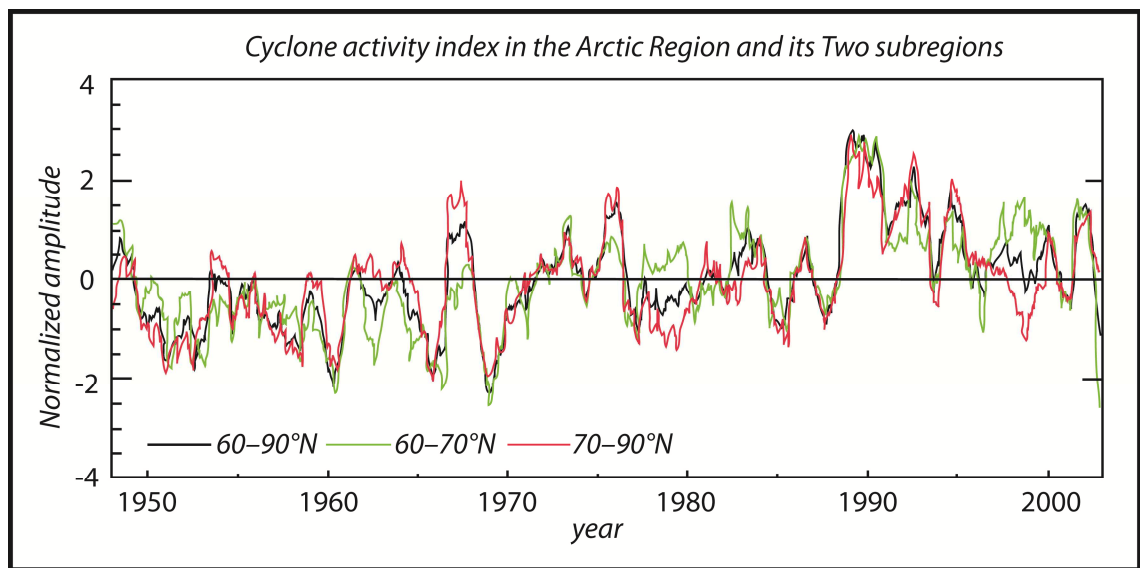


Figure 2.1. The cyclone activity index (CAI) anomalies for the Arctic region (60–90°N) and its two subregions, the Arctic Ocean (70–90°N) and the Arctic marginal zone (60–70°N) modified after ZHANG *et al.* 2004.

Storm surges are extremely threatening for low-lying coastal plains in Siberia and Alaska where they can extend several kilometres inland. For instance, ZENKOVITCH (1985) reported a storm surge (no information about the wave height is given) that ran ca. 30 km inland in the mouth of Indigirka River, whilst PISARIC *et al.* (2011) proved that recent storm surges that inundated the Mackenzie Delta caused erosion and led to probably irreversible changes in delta ecology by intrusion of salt water.

In fjord-settings, where constraining topography can amplify wave heights, coastal zone morphology can be seriously modified by extreme waves (tsunami) resulting from landslides or ice-berg roll. Although the devastating effect of tsunami waves induced by landslides have been documented along Arctic coasts (e.g. 1958 Lituya Bay tsunami (MILLER, 1960) or Disko Bugt 2000 tsunami (DAHL-JENSEN *et al.* 2004)) little is known

about the frequency and formative role of these types of extreme events along circumpolar coasts.

The main factor which modifies the wave action in Arctic coastal morphodynamics is ice. OWENS and HARPER (1983) distinguished five major sources of ice in the Arctic coastal zone: I) grounded floes; II) frozen wave swash and snow in the littoral zone; III) freezing of the sea surface; IV) the presence of a frost table or permafrost in the littoral zone, and; V) glaciers or ice caps that extend into the coastal zone. Each of the above has indirect (protection from wave, tides and currents) and direct (geomorphic) impacts on high latitude coasts resulting from six main processes: ice rafting, ice push, ice override, ice bound, ice burying and ice melt. These processes are particularly effective during the periods of freeze-up and break-up.

Ice rafting is an important process for sediment transport along Arctic coasts. Ice rafts can contain a wide range of sediments which get entrained in various phases of ice formation, often from different sections of coast (Figure 2.2.). Apart for the most obvious sources, which are the deposition of aeolian sediments on the ice surface and mass movement from unconsolidated cliffs, OSTERKAMP and GOSINK (1984) distinguished several processes of sediment entrainment into ice. According to these authors, coarse-grained sediment entrainment occurs: I) by anchor ice, with subsequent flotation and incorporation in the overlying ice cover; II) by discharge of sediment-laden anchor ice from rivers; III) by ice gouging at the sea bed; IV) by seabed freezing and subsequent flotation. In contrast, fine-grained sediments tend to be trapped by: I) frazil ice during initial ice cover formation under conditions of high turbulence; II) entrainment and deposition under the ice cover by frazil ice formed in leads or in a broken ice cover; III) 'katabatic' flow of dense, cold brine, formed nearshore under the ice and draining downslope (offshore) where suspension of sediments and frazil ice formation could occur; IV) anchor ice formation of very short duration and with subsequent flotation; V) trapping in frazil ice when sea water is forced, or filtered, through it.

According to OGORODOV (2003) the Arctic coastal zone can be divided into six zones based on the type of ice and its effect on the coastal geomorphology (Figure 2.2.). The most seaward zone from the coast (Zone 6) is characterised by the occurrence of polynas and moving drift ice. New ice originating from this zone is often pushed on the fast ice edge to form ice hummocks and pile-ups. Ice-gouging landforms that occur here are generally the deepest. Zone 5, called 'the belt of hummocking', is characterised by the strongest stresses and deformation of drift ice. Erosion of the sea floor by ice scouring is

at a maximum here. Zone 4 is divided into two subzones: subzone (d) which is characterised by a relatively smooth sea floor with single hummocky ridges and reduced effect of ice on morphology, and subzone (c) which is severely affected by ice movements where multiple ridges of hummocks and grounded hummocks form on submarine bars.

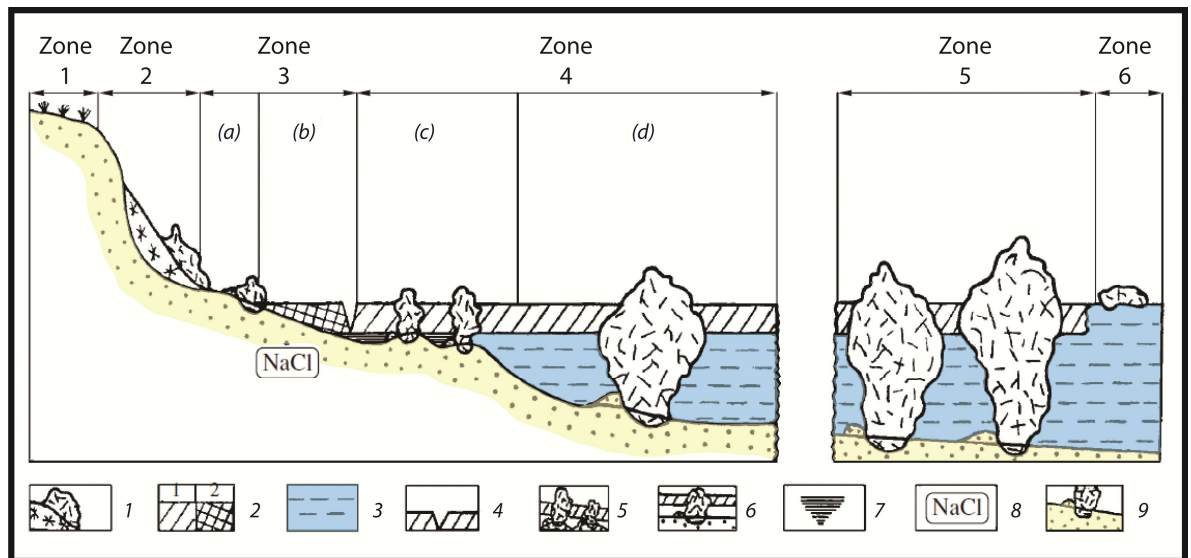


Figure 2.2. Subdivision of the coastal zone by types of ice formations and their effects on the coast and sea bed (after OGORODOV (2003)) 1 - Banks of firn, heapings and ice overthrusts; 2- Fast ice (1-floating, 2 - frozen to the bed); 3 - Water under fast ice; 4- Tidal crack; 5 -near-coast grounded hummocks and hummocks on submarine bars and shallows; 6 - grounded hummocks and belts of hummocking in the fast ice near edge zone.

Zone 3 is a border zone between sea and land and extends from the base of the coastal cliffs to the marine limit of fast ice, often marked by a crevasse zone. OGORODOV (2003) distinguishes two subzones here; subzone (b) where fast ice freezes to the seabed and subzone (a), which is affected by ice floes thrown by waves and tides onshore.

The mean tidal range along the majority of the Arctic Ocean is less than 2 m and, thus, tide action plays a less significant role compared to that seen on meso and macro-tidal, temperate latitude coasts. The formation of a characteristic polar coastal zone landform – the boulder barricade - is associated by ROSEN (1979) with water level fluctuations in the nearshore zone. Where the tidal range is larger (e.g. Hudson Strait) the role of tides in shore morphology is more profound, mainly due to movement of fragments of sea ice for further distances and the creation of larger erosional and depositional landforms (BYRNE and DIONNE 2002).

Zone 3 is characterised by the most effective transformation of relief by a combination of ice push, override and scouring, as well as gouging. It is important to note that the existence of permafrost or a seasonal frozen layer in the beach and cliffs is able



to inhibit ice-induced erosion of the coast. In the case of Arctic deltas, an additional subzone of Zone 3 can be distinguished - the strudel zone (Figure 2.3.). The characteristic processes occurring in strudel zone is an excavation of deep craters or channels in a seafloor by flood waters, which due to ice blocking of river outlets is forced to flow over the fast ice and drain through ice fissures with velocities high enough to scour the seabed (FORBES and TAYLOR 1994). In Zone 2, coastal cliffs and the upper parts of the beach provide the dominant processes including the formation of ridges composed of ice and unsorted sediments as well as processes related to degradation of permafrost, which is intensified during open water periods. In coastal lowlands, this zone may be affected by storm surges during the summer and ice override (hundreds of meters inland) during cold months. Finally, Zone 1 extends from the top of cliff landward to beyond the immediate reach of sea ice.

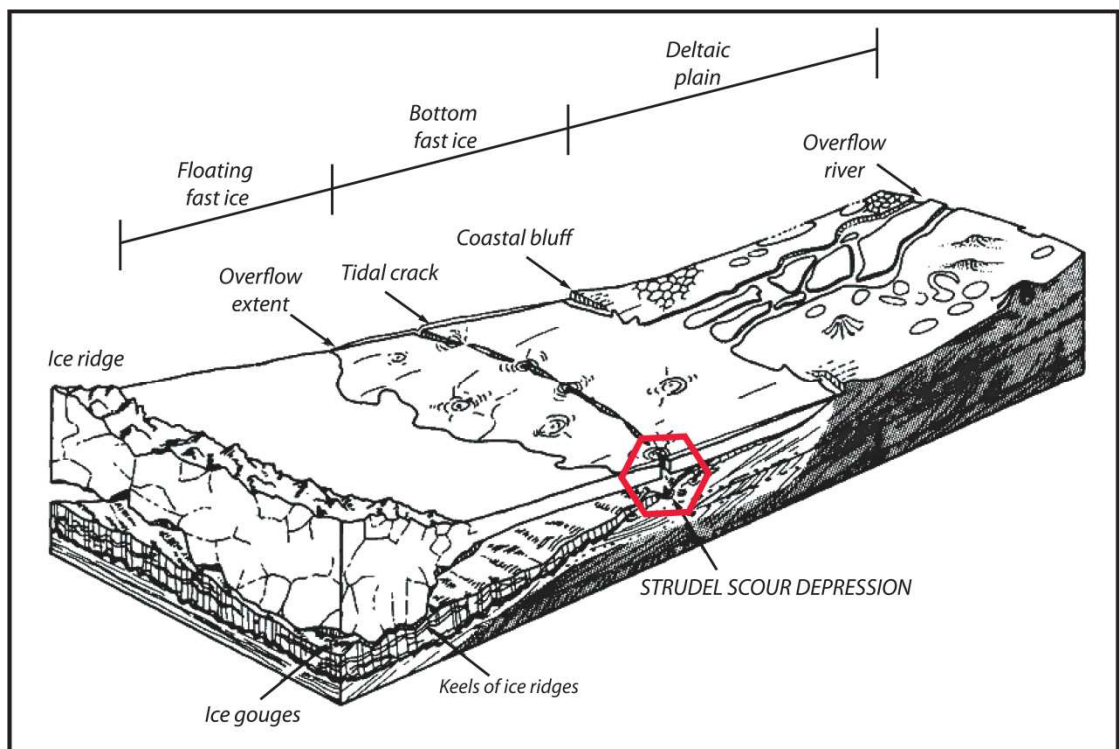


Figure 2.3. Mechanism of development of strudel scour depression after BARNES et al. (1988)

Among various forms of ice activity along polar shores the most characteristic one is an icefoot which occupies mainly Zones 3 and Zone 2 in the OGORODOV (2003) classification. The icefoot is formed along both beaches and rocky Arctic coasts by the freezing of ice lumps that are pushed onshore and mixed with snow, sea water spray, and ice from fresh water draining from the land (Figure 2.4.). The icefoot complex is probably the most widely described feature in cold region coastal geomorphological studies and over the years an expanded typology has developed. As noted by JOHN and SUGDEN

(1975), probably every part of polar coast has its own specific icefoot developing under characteristic sea ice conditions, wave climate, tidal range and shore configuration.



Figure 2.4. Examples of icefoot complex developed in Petuniabukta and Adventfjorden, Spitsbergen.

Various authors (e.g. WRIGHT AND PRIESTLEY 1922; JOYCE 1950; REX 1964; MOORE 1968; GREENE 1970) distinguished at least eight main types of icefoot:

- *tidal platform icefoot* – a solid, formed by sea ice moving on steeply sloping as tide rises and falls;
- *storm icefoot* – a thick, continuous, formed by spray above the high water mark;
- *drift icefoot* – thick, formed by snow and the freezing of sea water;
- *pressure icefoot* – formed by slabs of sea ice pushed onshore;
- *stranded floe icefoot* – formed by fragments of brash ice mixed with bergy bits stranded on shore;
- *false icefoot* – formed by freezing snow above the high water mark;
- *wash-and-strain icefoot* – formed by the freezing of sea water in pebbly beach sediments;
- *kaimoo (gravel-sand-icefoot)* – multilayered ramparts of ice and sediments formed by freezing of swash and wind-blown sediments mainly along microtidal basins.

Based on the observations in St. Lawrence Estuary, DIONNE (1988) identified two major types of icefoot regarding their location in the intertidal zone:

- *ice terraces which are fixed to the upper part of the coast (mostly to the base of the cliff);*
- *ice platforms which often carpet the whole intertidal zone.*

The geomorphic role of the icefoot is complex. DIONNE (1973) demonstrated that, for most of the time, an icefoot reduces the effects of wave erosion and plays the protective role, but that under certain conditions the icefoot can act as an erosive agent. NIELSEN (1979), for instance, detected that often during melting period an icefoot removes fragments of rocks from the cliff wall. This explains the common occurrence of heaps of angular rocks on arctic beach surfaces adjacent to cliffs.

In the intertidal zone, where fragments of a decaying icefoot that was formerly frozen to the seabed start to float, they may erode and transport whole blocks of seafloor sediment or even sizeable boulders (TRENHAILE 1997). Moreover, when the icefoot is not fully frozen to sea bed, waves and tides can penetrate this free space, alternating between eroding it and filling with sediments. During spring break-up, blocks of icefoot scour the shore and sea bed leaving elongated marks and flutes. Overall, icefoot-derived micro-relief is quickly washed out during first days of open water conditions.

### **2.1.1 Processes operating on Arctic beaches**

Arctic barriers have been described in many sites (e.g. REX 1964; HUME and Schalk 1964*a, b*, 1967, 1976; ZENKOVITCH 1967; KING and BUCKLEY 1968; MCCANN and OWENS 1969; GREEN 1970; OWENS and MCCANN 1970; MCCANN and TAYLOR 1975; ROSEN 1978; TAYLOR 1978; REINSON and ROSEN 1982; SEMPELS 1987; REIMNITZ *et al.* 1990; BARNES *et al.* 1993; CAMPEAU and HÉQUETTE 1995). Typically, cold region barriers are narrow (a function of the typically low tidal range) and consist of poorly sorted coarse sand, gravel and cobbles delivered to the beach system from local sources by glacial or snow fed streams, slope processes and wind or sediments transported by sea ice.

NICHOLS (1961) classified polar beaches as those showing one or more of the following features:

- *the beach may rest on ice (ice floes, icefoot or buried glacial ice)*
- *the beach may be pitted as a result of melting ice (ice floes, icefoot or buried glacial ice)*
- *the beach morphology may be dominated by ice-pushed, ice-lifted and ice-deposited ridges (Figure 2.5.)*

- *the beach may be truncated and terminate abruptly due to the presence of ice or snowdrift ice slabs at the moment of their formation*
- *the beach sediments may be transported by ice-rafting*
- *the beach gravel may be poorly rounded*
- *the beach environments may be modified by the operation of frost, gelifraction, solifluction and other periglacial processes, including those leading to the formation of patterned ground*
- *bedrock sections of coast may be striated by drift ice action*
- *beach ridges may be eroded by meltwaters streams*
- *beaches may be associated with ice-contact features (proglacial deltas, esker-like features) and glaciomarine deposits*
- *beach ridges (mainly uplifted) may contain highly polished ventifacts.*

The mosaic of factors including sea-ice rafting, frost sorting, periglacial nature of fluvial activity and slope processes and proximity of glacial systems unite to create the complex polar beach sedimentology.

Although sediments composing High Arctic beaches encompass a whole range of particle sizes from boulders (boulder beaches and boulder barricades) to fine sands, the majority of them represent gravel or mixed sand-gravel dominated environments. There are several explanations for gravel domination of polar coasts. The most obvious is the inheritance of glacial sediments from glaciers or the active supply of coarse material from tide-water glaciers.

The second reason is the delivery of fluvially-transported coarse-grained sediments to the coastal zone. However, if glacier rivers braid through long valleys and extensive outwash plains, or meander through gently sloping tundra plains (e.g. rivers of Alaskan North Slope or Chukotka Peninsula), their transport capacity of gravel is reduced. Therefore, the lead role here is played by short, steep mountain streams and creeks that carry large loads of gravel and pebbles, often fed by snow patches and glaciarets rather than by glaciers (SYVITSKI 1987).

A third source of gravel is associated with primary sedimentation from adjacent cliffs, which is particularly important in coastal sections with exposed, ice-rich permafrost bluffs. Another reason for the abundance of coarser sediments along Arctic coasts is the effective rock weathering in polar climates and the production of significant amounts of debris by frost-related rock disintegration processes. Ice-rafting of gravel and pebbles may

also occur but its role is minor in comparison with the above mentioned sources (FORBES and TAYLOR 1994).

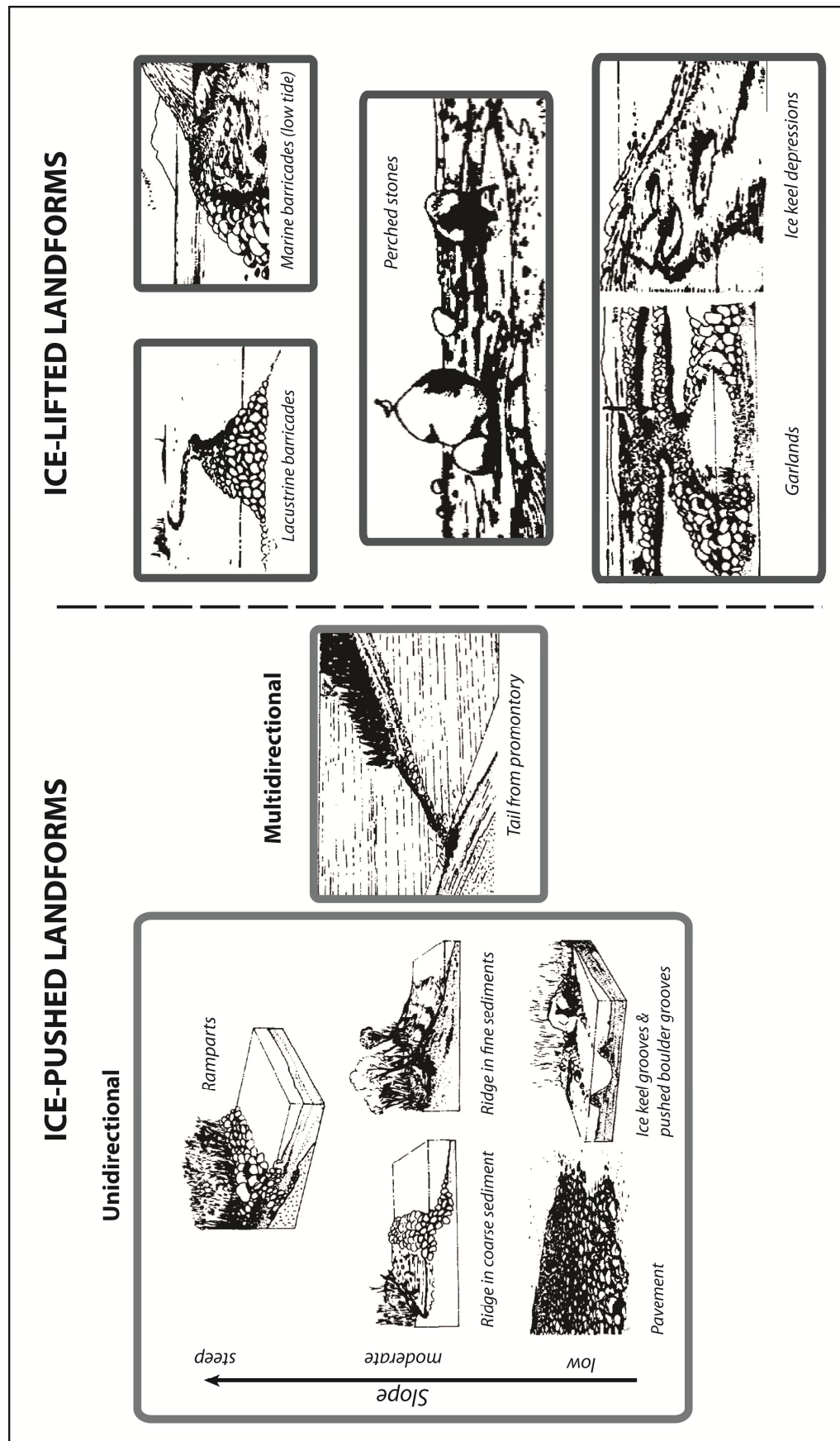


Figure 2.5. Types of ice-pushed, ice-lifted and ice-rafted coastal landforms according to GILBERT (1990)

REIMNITZ and MAURER (1979b) suggested that wind-winnowing of beach surfaces can also be important, noting that this is active most of the year as opposed to wave action which can be less pervasive. Observations from Egg Island in Prudhoe Bay show that during one winter season, wind removed approximately 300 tonnes of sand from a 1.2 km<sup>2</sup> barrier island, suggest that deflation may be a significant mechanism leading to the coarsening of beach surfaces in the Arctic regions (REIMNITZ and MAURER 1979b).

Several authors (e.g. HANSOM and KIRK 1989; CAMPEAU and HÉQUETTE 1995) have previously addressed the seasonal cycle of polar beach development (Figure 2.6.). Thus, TAYLOR and MCCANN (1983) divide the polar coastal year into four periods. The first is *freeze-up*, which starts in the autumn with the development of a narrow intertidal icefoot made of mixed ice slush and frozen swash, spray and sea water in shore sediments. The second - *complete ice cover in the coastal zone* - develops during the winter months and is modified practically only by tide movement of ice attached to the land. The third - *break-up* - is characterised by relatively rapid melting of snow and the continual development of series of large tidal cracks in ice cover that leads to fragmentation and subsequent melting of ice across the intertidal zone. A characteristic break between the sea ice cover and the icefoot complex, which outlasts the first phase of melting, is formed. The fourth - *open water* – is a period of wave domination that erases the effects of sea-ice depending on the length of ice free conditions as well as the frequency and magnitude of storms that reach the shore.

Observations of Northern Alaska coast led SHORT and WISEMAN (1974) to identify seven stages of barrier freezing: (I) solidification of the upper beach face, (II) the formation of snow cover, (III) the deposition of ice cakes on the beach surface, (IV) filling the lagoon by ice slush, (V) deposition of ice slush berms on the beach face, (VI) formation of interbedded layers of ice and sediments, and finally (VII) the formation of icefoot.

Surprisingly, only a few observations to date exist regarding the role of permafrost on High Arctic beach morphology and coastal evolution (e.g. MCCANN and HANNELL 1971; HANSELL *et al.* 1985). In many High Arctic fjords, coastal permafrost is relatively young since it could only develop only after deglaciation, and is often divided by taliks. Therefore, the influence of permafrost on coastal development is less clear than along the ice-rich permafrost coasts of Siberia and Alaska where older permafrost has controlled coastal evolution for several hundred thousand years (WETTERICH *et al.* 2008, 2009; SCHIRRMESTER *et al.* 2010; KIENAST *et al.* 2011).



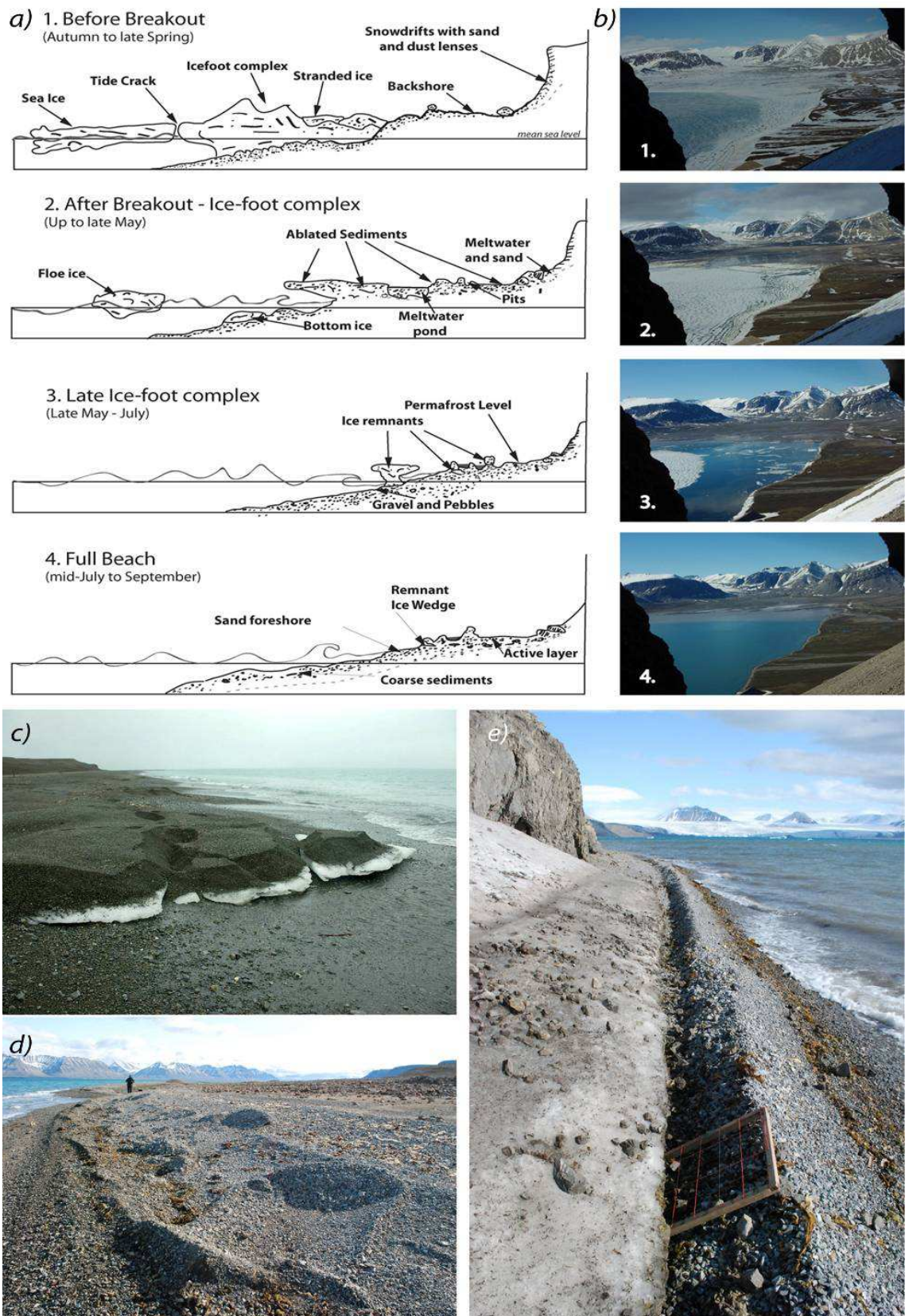


Figure 2.6. Polar beach a) 1-4 Seasonal changes in polar beach morphology (sketches modified after HANSOM AND KIRK (1989)) linked with the operation of sea-ice, nival and permafrost related processes; b) Examples of different stages of beach evolution from Petuniabukta (time-lapse images from Wordiekammen massif in years 2009-2010): 1- before breakout, 2- after breakout, 3- late ice-foot, 4 – full beach c) characteristic high Arctic beach micro-relief modified by sea-ice processes – pitted beach with mixed sand-gravel sediments overwashed on melting ice floes, d) – ice-pushed ridges, e) – storm ridge developing along the crest of icefoot and supplied by rockfalls sliding down steep icefoot slope.

Nevertheless, permafrost and permafrost-related processes may affect polar beach sediment budgets and is the second most important agent in modification of micro-relief, after sea-ice (TRENHAILE 1997). The presence of permafrost is effective in protecting beach sediments from erosion. COX and MONDE (1985) calculated that under the same wave conditions, a frozen gravel berm erodes up to 10 times more slowly than an unfrozen gravel berm.

Although the spatial distribution of coastal permafrost and its transition to submarine permafrost under the High Arctic fjords seafloor is largely unexplored, several studies exist that detail the thermal state of beach and intertidal zone. MCCANN and HANNELL (1971) carried out the first monitoring of active layer development across the High Arctic intertidal zone in Cornwallis and Devon Islands. Between 1967 and 1969, they observed that in several profiles the depth of the active layer increased slowly toward the low water mark, but it was not significantly deeper than the active layer above high water mark.

A characteristic permafrost-related landform that develops along Arctic depositional coasts are seasonal frost mounds that form in beach and barrier sediments. CAMPEAU and HÉQUETTE (1995) developed a conceptual model of seasonal frost mound (Figure 2.7.) development in Arctic beaches based on three years of monitoring (1991-1993) of the coastal zone in the Tuktoyaktuk Peninsula (Beaufort coast of Northwestern Territories). Their work illustrates the complex interplay between types of sediment cover, the duration of sea-ice conditions, and the frequency of storms able to saturate beach sediments with sea-water.

URDEA (2007) reported the development of 10 m wide and 3 m high ice blisters of a similar nature to frost mounds described by CAMPEAU and HÉQUETTE (1995) along the southern coast of Isfjorden, Svalbard. CAMPEAU and HÉQUETTE (1995) support the views of several other studies along Arctic coasts (e.g. REIMNITZ and MAURER 1979a; OWENS and HARPER 1983; PISARIC *et al.* 2011) that the two main features of polar coastal zone morphology are the development of landforms formed by ice and permafrost, and the catastrophic role of low-frequency, high magnitude events that occur during open-water conditions.

Other factors that influence Arctic beach micro-relief include the role of driftwood, seaweed and polar animals. Driftwood accumulations are widespread across many Arctic beaches. Studies on driftwood provenance and age have been used to infer changes in sea-ice conditions and sea-level fluctuations over Holocene timescales (e.g. SALVIGSEN



1978; HÄGGBLOM 1982; DYKE and MORRIS 1990; EGGERTSSON and LAEYENDECKER 1995; DYKE *et al.* 1997; BENNIKE 2004; FUNDER *et al.* 2011), but no study has focused on the geomorphic role of driftwood in the contemporary polar coastal zone.

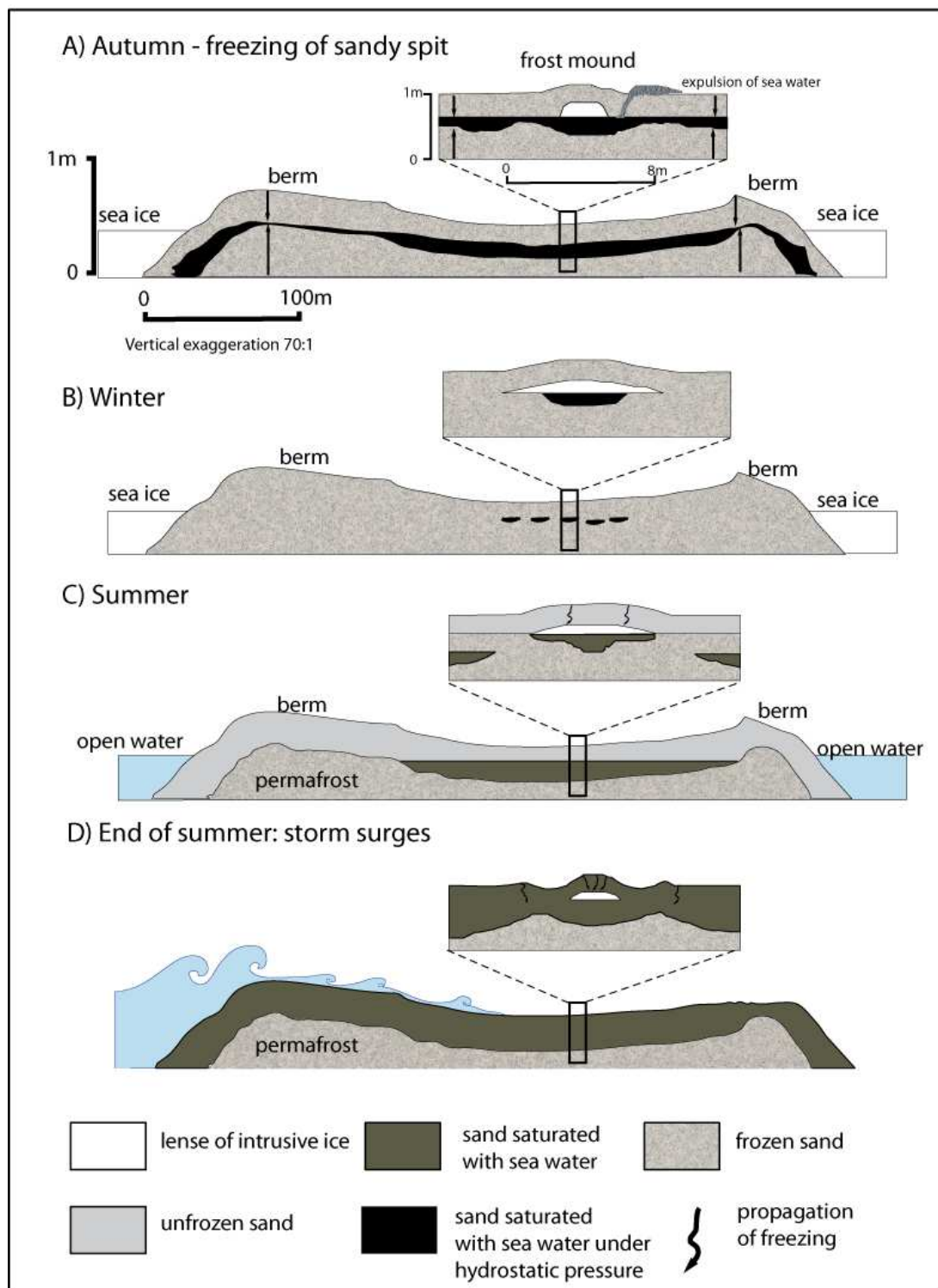


Figure 2.7. Conceptual model of development of Arctic beach frost mounds by CAMPEAU and HÉQUETTE (1995).

Along the Spitsbergen coast, driftwood that becomes incorporated in beach sediments plays an important role in beach micro-relief leading to the formation of

characteristic ridges and mounds with wooden chunks acting as landform backbones (Figure 2.8.).



*Figure 2.8. Driftwood as a geomorphic agent in polar coastal zone (examples from Petuniabukta and Adolfbukta: a) Trunks incorporated in gravel barrier; b) Trunks and kelp blocking snow-melt streams; c) Trunk accumulation blocking gravel along rocky coasts; d) Trunks incorporated in upper tidal flat sediments, often stopping fine sediments transported by wind from the surrounding outwash plain.*

Driftwood may serve as a local sediment storage and carrier as sand, gravel and small pebbles often get stuck in trunk cracks or in-between fragments of the remaining root system or bark. In tropical regions, EMERY (1955) claimed that driftwood is a chief rafting agent for large boulders; in high latitudes where ice plays the most significant role in sediment rafting the role of driftwood is undoubtedly of secondary importance relative to other processes but locally it may come into prominence. According to WALKER and BARRIE (2004) and EAMER and WALKER (2010) large woody debris is a significant agent in British Colombia beach sedimentology and acts as a buffer reducing erosion of coastal landforms. Trunks trap considerable amounts of windblown sand in the backshore, altering beach sediment budgets and initiating dune formation. In polar regions, the configuration of driftwood in relation to shoreline is also important as trunks parallel to shore can be pushed by sea-ice and act as a bulldozer, smoothing the beach surface, whereas trunks perpendicular to shore erode the beach surface and lead to the creation of grooves and plough marks.



Another geomorphic factor which until today has not gained interest of cold region coastal geomorphologists is the accumulation of seaweed on beach surfaces (Figure 2.9).

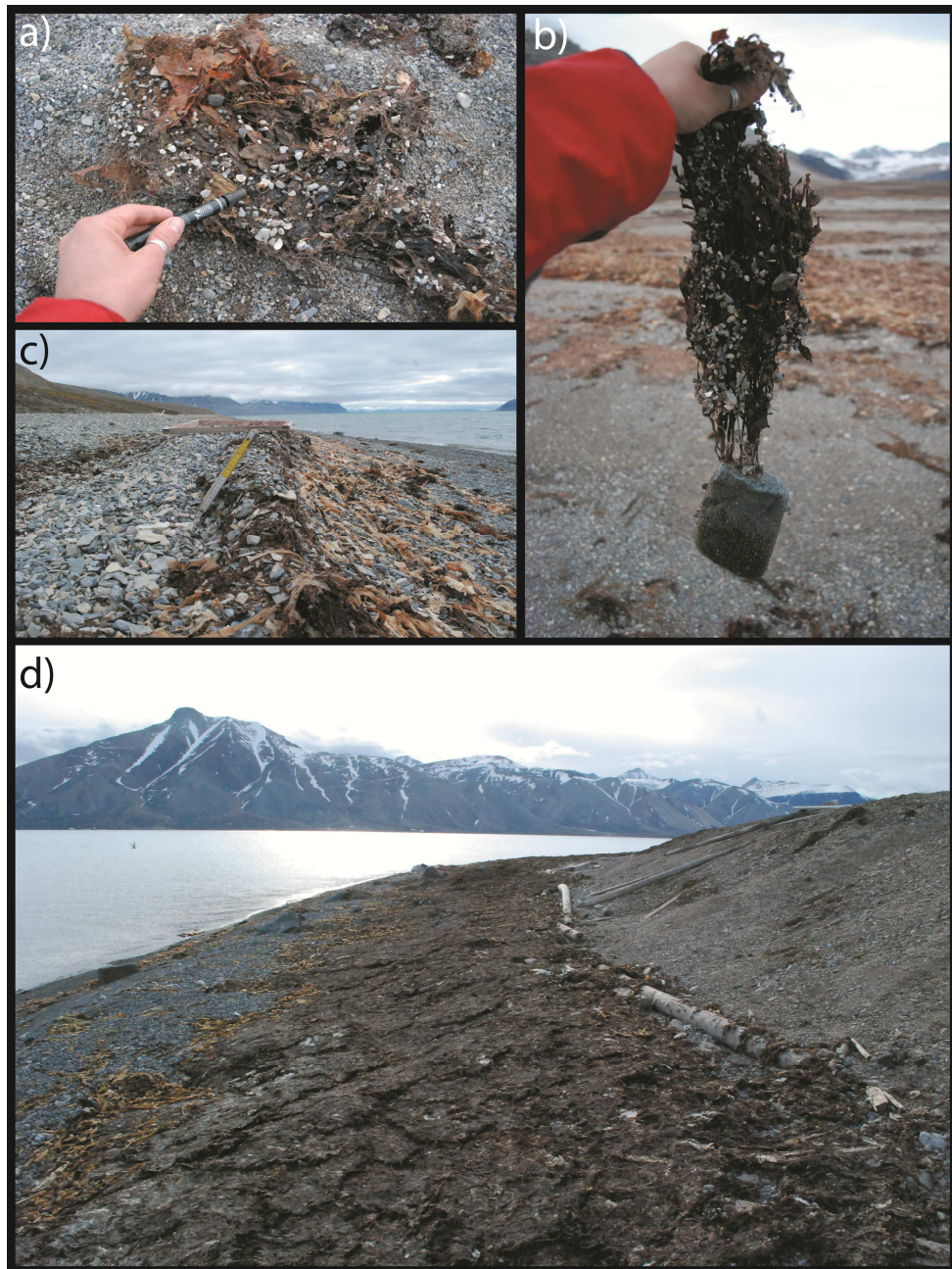


*Figure 2.9. Seaweed as a geomorphic factor in polar coastal zone (examples from Petuniabukta and Adolfbukta): a) fragment of seaweed trapping sand and gravel; b) kelp fixed to 0.6 kg pebble washed on shore after storm; c) Storm ridge formed by mixing of coarse sediments with seaweed; d) dried out seaweed mattress protecting upper beach from deflation and often cushioning the erosive effects of sea-ice movements.*

An early study which tested kelp efficiency in redistribution of sediments along High Arctic coast was carried out by GILBERT (1984) on Baffin Island. He demonstrated that the buoyancy of algae enable it to carry pebbles and cobbles over significant distances. Even if algae are too light to float a pebble, they facilitate dragging of stones by waves and tidal

currents. In addition, DIONNE (1965) claimed that marine algae may play an important role in stone entrainment into sea ice as they provide a larger surface around the stone to which ice can be attached. Field observations along Spitsbergen beaches suggests that kelp can not only trap and carry appreciable amount of sand and gravel but often constitutes an important part of beach ridge structure (Figure 2.9. c).

It is also notable that the Arctic coastal zone is a main breeding and migration area for many animals (i.e. bird colonies, marine mammals, polar bears, reindeers, rodents) and their activity may also affect the functioning of polar coasts. A classic example is the geomorphic effect of geese grazing on Arctic tidal flats leading to the bioturbation and erosion of surface sediments (BYRNE and DIONNE 2002).

Little is known about the impact of massive bird colonies (e.g. little auks, gulls, puffins) that occupy Svalbard beaches, talus slopes and rocky cliffs and platforms on rock weathering. The impact of large marine mammals such as seals, which can swallow several kilograms of beach pebbles to be used as gastroliths (NORDØY 1995), on the nearshore and beach micro-relief has been also little studied.

## **2.1.2 Processes operating on Arctic rock coasts**

Although up to 35% of Arctic coastlines are rock-dominated (FORBES *et al.* 2011), only few studies on the controls on cold rocky coasts evolution have been undertaken (e.g. JAHN 1961; NIELSEN 1979; TRENHAILE 1983; TRENHAILE and MERCAN 1984; DIONNE and BRODEUR 1988; FOURNIER and ALLARD 1992; ØDEGÅRD and SOLLID 1993; ØDEGÅRD *et al.* 1995; LUNDBERG and LAURITZEN 2002; WAGENSTEEN *et al.* 2007). Furthermore, the geomorphology of cold region rocky coasts (Figure 2.10.) is marked by significant regional contrasts. On the one hand, during the last three decades several geomorphological studies along Atlantic Canada's rocky shorelines have made fundamental advances in our understanding of ice and frost action on the morphology of intertidal zones as well as the influence of 'freezing–thawing and wetting-drying' on shore platforms and cliff relief (e.g. DIONNE and BRODEUR 1988; DIONNE 1989; TRENHAILE and MERCAN 1984; TRENHAILE *et al.* 1998; TRENHAILE 2001; TRENHAILE *et al.* 2006; PORTER and TRENHAILE 2007; PORTER *et al.* 2010). However, relatively few studies have tested the efficiency of those processes in polar settings.

One of the most controversial questions in cold region coastal geomorphology is determining the relative significance of littoral processes versus frost weathering in

controlling rocky cliff and shore platform morphology. The classic example of this debate is the origin of extensive coastal plains called strandflats which has been a regular topic for discussion in the geomorphological literature for almost a century (e.g. NANSEN 1922; DAHL 1946; WERENSKIOLD 1952; MOIGN 1974; GUILCHER *et al.* 1986; HOLTEDAHL 1998). Although during the years several mechanisms have been proposed to control strandflat formation including frost action, shore ice action, glacier action and wave action there is no clear agreement on the dominant factor sculpting strandflat relief (TRENHAILE 1997).

Another controversy is associated with different views on the efficiency of periglacial shoreline evolution, with theories about the slow environmental adjustments (ZENKOVICH 1967) and, on the other hand, rapid modern shore development (JAHN 1961).

A comprehensive review of the rock coast environment evolution in high latitudes is provided by TRENHAILE (1997). He highlighted the role of frost weathering in preparation of rock surfaces for erosion and the contentious significance of icefoot, sea ice, wave action and tidal range in further cliff-platform system development. In addition, his review illustrated strong regional discrepancies in cold climate rock coasts studies, with major advances achieved in upper mid-latitudes and subarctic or subantarctic locations rather than in polar latitudes.

A notable exception to the lack of research in High Arctic regions is that undertaken on Svalbard. JAHN'S (1961) concluded that annual limestone cliff retreat at Veslebogen in Hornsund (south-west Spitsbergen) ranges between 0.025 – 0.05 m per year, leading him to conclude that littoral processes operating in the periglacial zone are highly effective and that frost weathering in the coastal zone is much more intensive than in non-coastal settings.

SALVIGSEN and ELGERSMA (1985) observed the development of coastal karst characteristic of carbonate and evaporite outcrops in central and eastern Spitsbergen, hypothesising that the evolution of dolina relief in Vardeborgsletta, which is often mantled in marine and glacial deposits, is strongly linked with sea-level change. Karstic processes in rocky coasts were likely to have initiated during periods of high relative sea-level when frozen rocks thawed and were subsequently emerged due to glacioisostatic land uplift.

Cliff temperature investigations in Kongsfjorden and Liefdefjorden (northern Spitsbergen) highlight the importance of the duration of snow insulation, frequent subzero temperature oscillations and the formation of segregation ice in rock cracks as critical controls on rock disintegration (ØDEGÅRD *et al.* 1993, 1995).



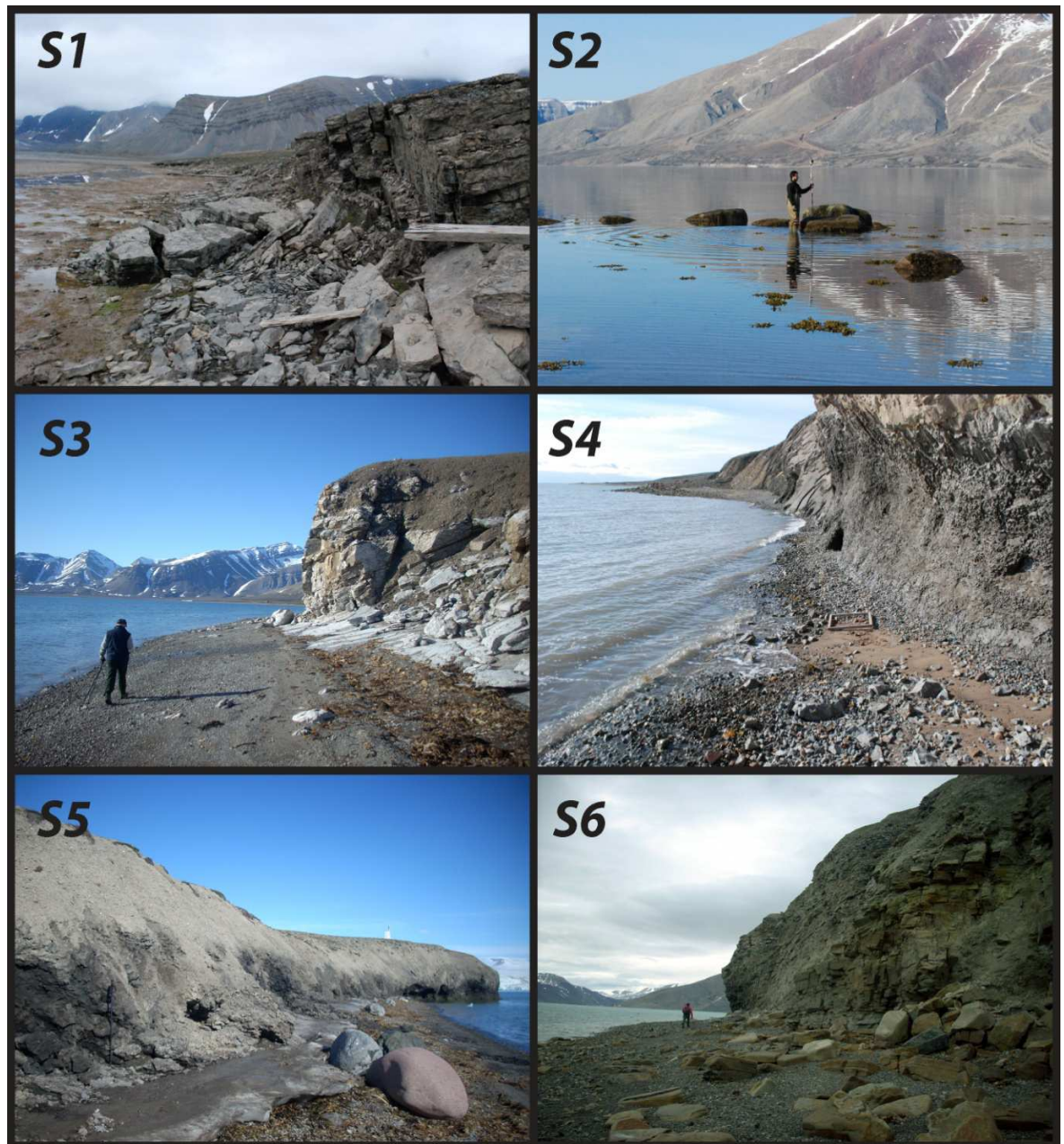


Figure 2.10. Examples of rocky coasts from central Spitsbergen: S1 relict, heavily fractured sandstone cliff cut off from wave action due to progradation of tidal flat; S2 – Skerry Islands composed of erratic boulders deposited by glaciers during the last glacial advance; S3–anhydrite cliffs and platforms formed in a micro-tidal fjord; S4 – weathered rock cliffs exposed to the combined action of sea-ice and waves, S5 – heavily weathered dolomitic breccias cliff covered with uplifted marine sediments, S6 – drift-mantled sandstone cliffs.

WAGENSTEEN *et al.* (2007) noted the severity of periglacial weathering along Arctic shorelines in comparison with rates observed on inland rock surfaces. Their analysis used digital photogrammetry to identify cliff retreat in Kongsfjorden at rates of  $0.0027\text{--}0.0031\text{ m yr}^{-1}$ . This is significantly higher than previous estimates ( $0.00007\text{--}0.0005\text{ m yr}^{-1}$ ) based on more inland locations (e.g. RAPP 1960; ANDRÉ 1997). This research reinforced the views of others (e.g. WILLIAMS 1949; CORBEL 1959; SUNAMURA 1992) that heat and moisture transfers strongly influence the rates of rockwall retreat and, in

particular, emphasised that ‘coastal’ effects involving *freeze-thaw-drying-wetting* cycles can greatly amplify rock weathering. Interestingly, similar ‘coastal amplification’ of weathering along polar shorelines was previously postulated by JAHN (1961), but the concept has never been adequately tested and clarified.

### 2.1.3 Existing conceptual models of Arctic coastal zone evolution

To my knowledge only *one (sensu stricto)* conceptual model of Arctic coastal evolution and two coastal evolution predictions have been proposed in academic literature on the subject. RUZ et al. (1992) created a conceptual model to explain coastal zone evolution in a transgressed thermokarst landscape based on observations along Canadian Beaufort Sea (Figure 2.11). The RUZ et al. (1992) model is applicable to ‘ice-rich’ permafrost coastlines characteristic for Siberia, N Alaska and NW Canada. SYVITSKI and ANDREWS (1994) developed a model that analysed sedimentation and coastal processes under various climate scenarios for fjord coastal environments of Eastern Canadian Arctic (Figure 2.12). More recently, PAVILIDIS *et al.* (2007) compiled several observational datasets from the Eurasian Arctic and proposed a general forecast of Arctic coastal evolution in the 21<sup>st</sup> century for both ice-rich permafrost and ‘fjord’ coastal environments (Figure 2.13). Each of these models is described in more detail below.

#### ***Conceptual model of coastal evolution in thermokarst topography by RUZ et al. (1992)***

The dominant features of the thermokarst landscape of Arctic coastal lowlands are retrogressive thaw slumps, ice wedges, thermal gullies and thaw lakes (Figure 2.11.). Degradation of permafrost in these landforms leads to the release of significant amounts of unconsolidated sediments to rivers and seas. RUZ et al. (1992) noticed the dual significance of such a landscape on development of coasts: In stage 1, rising sea-level exerts high pressure on ice-rich permafrost coast and easily erodes land leading to drainage of thermokarstic lakes by breaching of banks and the creation of embayments. In stage 2 a characteristic headland and spit morphology is developed. As the headlands erode the spits tend to expand and close former lake basins. In stage 3 the erosion of headlands continues and leads to cutting of migrating spits. Some of the spits erode, some stay active as long as sediment supply from longshore drift balance the wave erosion – the isolated barrier islands are formed. Barrier islands migrate landward as a result of storm-induced washovers. In stage 4, the barrier degrades. On a short term, this is controlled by storms, but over long-time scales the dominant mechanism of barrier erosion and

landward migration is controlled by sea-level rise. The factor which locally can disturb this process-form continuum is the pre-existing landscape. If the thaw lakes are deep enough they create a sink for sediments released from migrating barriers.

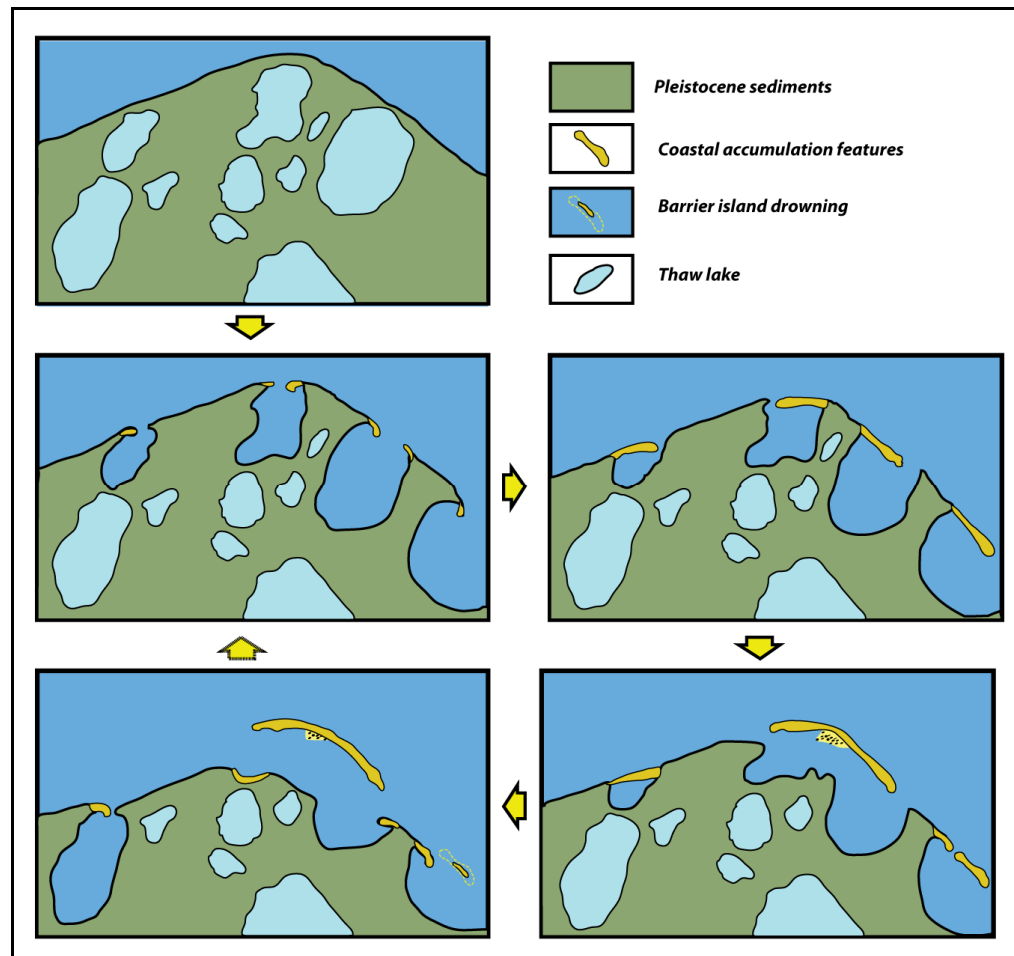


Figure 2.11. Conceptual model of coastal evolution in the thermokarst topography of southern Canadian Beaufort Sea modified after RUZ et al. (1992)

***Conceptual model of the adjustment of Arctic coastal processes to climate change by SYVITSKI and ANDREWS (1994).***

The SYVITSKI and ANDREWS (1994) conceptual model was an important attempt to predict the functioning of the eastern Canadian Arctic coastal zone in warmer summers and warmer and moister winters (Figure 2.12.). This model was applied to two contrasting zones of relative sea-level change: Zone I (inner fjords and coasts of Baffin Island and Labrador Peninsula) - representing the area of continuous isostatic recovery, and Zone II (outer coasts of Baffin Island and Labrador Peninsula) - representing a region of continuous submergence (and forebulge collapse). According to their model, in the next two centuries changes in RSL will be of secondary importance in terms of controlling the functioning of the coastal zone when compared to increased sediment supply to the coast from deglaciated catchments.



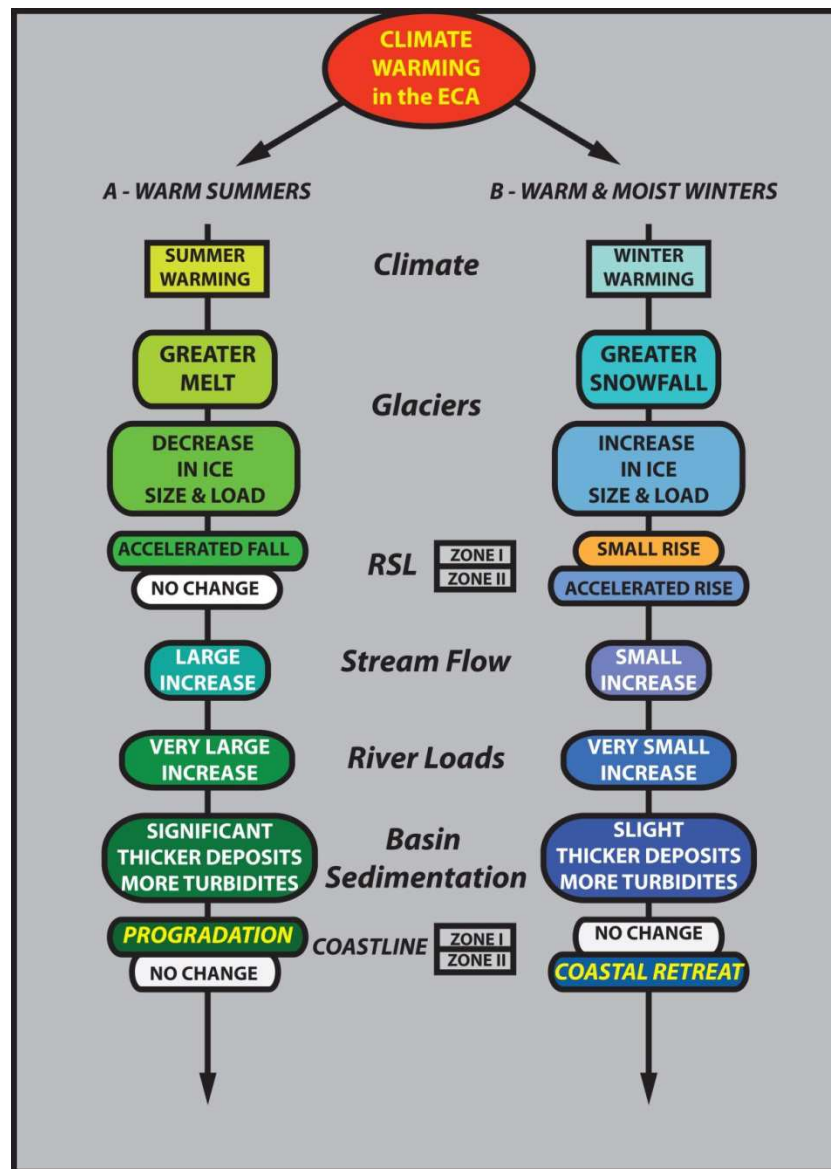


Figure 2.12. Diagram of links between changes in climate, glacierization, sediment supply and RSL in two climate change scenarios: A warm summers, B warm and moist winters (after SYVITSKI and ANDREWS (1994))

Every change in river (and permafrost) hydrology predicted in this model causes a serious change to the coastal environment. For instance, in the case of warmer summers (more intensified change in hydrology and accelerated RSL fall) the coastlines in Zone I are predicted to prograde into the marine environment due to more turbid river plumes that will spread out from the coast. In the case of warm and moist winters, the coasts of Zone I are expected to stay unchanged as sediment delivery will counterbalance change in sea-level. However the model emphasises that the number of turbid currents affecting the coast will decrease as more sediment will be trapped in proglacial outwash plains. Submerging coasts (Zone II) are rather more sensitive to the scenario of warmer and moister winters when a lack of sufficient sediment supply will result in coastal retreat.

***Prediction of the evolution of the coastal zone in the 21st century in Eurasian part of Arctic by PAVLIDIS et al. (2007).***

The key conclusion of this work is that sea-level will potentially be of secondary importance to sediment supply in controlling the future dynamic of Arctic coastlines. This matters because many of the existing conceptual models of paraglacial coastal evolution (e.g. ORFORD *et al.* 1991) argue that sea-level is a controlling variable in many instances. PAVLIDIS *et al.* (2007) forecast the evolution of Arctic thermoabrasive and accumulative coasts (Figure 2.13.) under warming temperature and rising sea-level conditions based on numerical modelling of shore profiles of known parameters including morphodynamics, sediment lithology and hydrodynamics of surrounding basins. Their most important predictions are:

- a) The most prominent coastal changes will occur in the East Siberian Sea with the up to 4-fold growth of thermoabrasion rates that will significantly affect patterns of coastal sedimentation.
- b) The Laptev Sea coast will be affected by the extension of ice-free period (from 2 to 3 months) which will allow longer wave activity leading to increased erosion. Here, the intensity of the wave impact will cause a 1.5- to 2-fold intensification of the coastal thermoabrasion.
- c) Coastal evolution along the Kara Sea is expected to become more rapid due to an increase in water heating, more intensive penetration of the Atlantic water masses to the basin and prolonged open water conditions (at least 4 months), which will combine to increase wave impact and activate more coastal processes.
- d) No dramatic consequences are predicted for Arctic depositional coasts (e.g. the barrier islands of Chukchi Sea) as their development will keep pace with sea level rise. However, if rates of sea level rise reach the level known from Holocene climate optimum (when these landforms were formed) then these barriers will quickly disappear.
- e) Pechora Sea coasts will be affected by the inflow of the warm Atlantic waters leading to increased open water conditions. Changes will occur particularly along southern coasts undergoing slow tectonic subsidence. Thermoabrasion and abrasion will proceed under stronger wave influence which increases the annual coast retreat up 4 meters.
- f) The coasts of Norway and the Barents seas are predicted to experience the smallest modification. The prediction for this region (Svalbard, Franz Joseph Land, Novaya Zemlya) supports the SYVITSKI and ANDREWS model (1994) – attributing the dominant role to changes in hydrological processes. According to PAVLIDIS *et al.* (2007) even here, where the predicted climate warming will result in the up to a 50% increase in glacial runoff during the current century, the supply of terrigenous sediments will not seriously affect the coastal zone as they will be deposited off the coast in relatively deep basins. It is noteworthy that the inflow of

warm Atlantic waters is predicted to push the position of floating ice northwards, clearing the western coast of Novaya Zemlya and opening the Sedov Trench for longer periods.

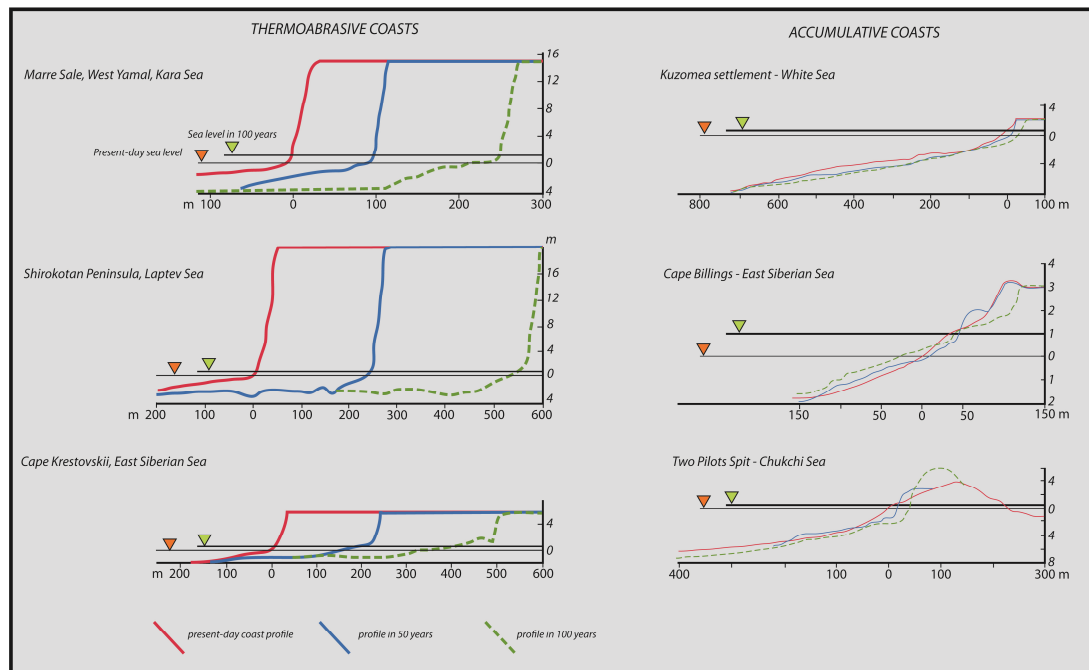


Figure 2.13. Prediction of thermoabrasive and accumulation coast profile changes in the Eurasian Arctic (modified from PAVLIDIS *et al.* (2007))

#### 2.1.4 Recent developments in High Arctic coastal research with particular consideration of Svalbard

To date, coastal research in Svalbard has been strongly linked with the application of the ‘paraglaciation’ theory in cold region geomorphological studies. As noted in Chapter I, during the 20<sup>th</sup> century the Svalbard landscape has experienced a significant shift from glacial-dominated into the non-glacial dominated environment (MERCIER 2000). This process is associated with the rapid retreat of glaciers since the termination of the Little Ice Age (LIA), which on Svalbard occurred around AD 1900 (SZCZUCIŃSKI *et al.* 2009). The recent deglaciation exposed vast glacier forelands and valley slopes providing favourable conditions for paraglacial metamorphosis of glacial landforms (LØNNE and LYSÅ 2005; ETIENNE *et al.* 2008; RACHLEWICZ 2010; EWERTOWSKI *et al.* 2012).

In several fjords the climate-driven transformation of glacier systems from marine-terminated into land-terminated type led to the formation of entirely new coastlines composed of unstable glacial sediments prone to abrupt modification by marine processes (Figure 2.14.). In addition, the warming of climate and the occurrence of more extreme precipitation events observed in the last century, destabilised and reactivated sediment delivery to the coast from numerous periglacial landforms including debris

flows, slush avalanche lobes and solifluction tongues (JAHN 1967; ÅKERMANN 1984; ANDRÉ 1990; MERCIER *et al.* 2009). These processes have influenced the evolution of Svalbard coastal zone by providing huge amounts of unconsolidated sediments, which have been used to accumulate new coastal landforms such as spits, tombolos, lagoons, barriers, deltas and tidal flats (e.g. MOIGN and GUILCHER 1967; KLEMSDAL 1986; HÉQUETTE and RUZ 1990; KOWALSKA and SROKA 2008).

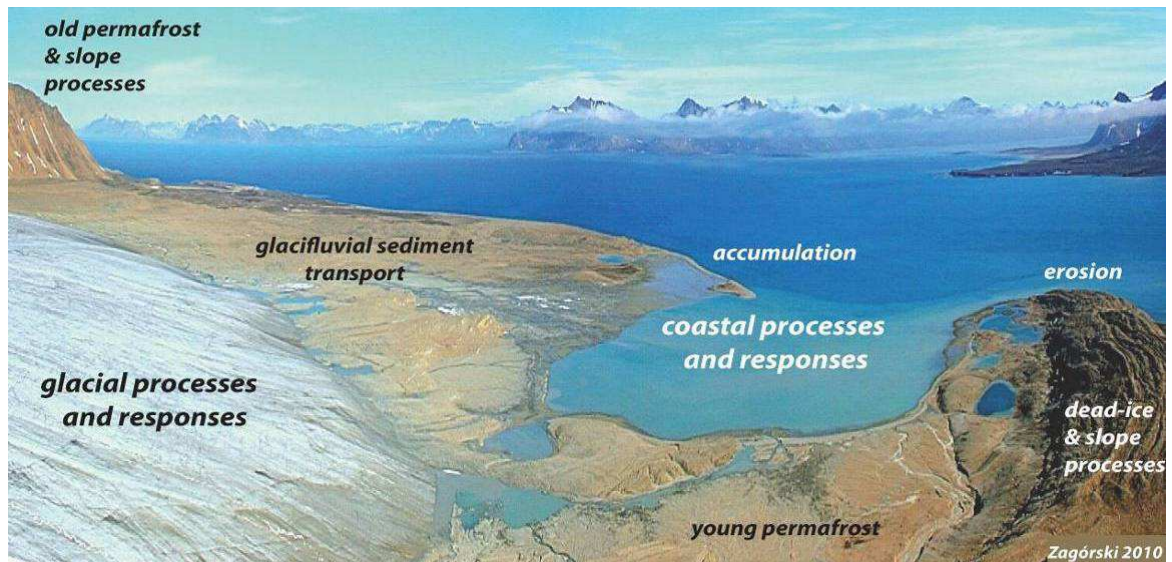


Figure 2.14. The complexity of High Arctic paraglacial coastal system formed in deglaciaded area – Josephbukta, Bellsund, Spitsbergen. Photo by ZAGÓRSKI (2010)

MERCIER and LAFFLY (2005) linked periods of intensified sediment supply, associated with the post-Little Ice Age (LIA) retreat of Pedersenbreen, Austre, Midre and Vestre Lovénbreen with coastal progradation. In the last 30 years, the mean annual coastal progradation along the studied section of Kongsfjorden was 3 m, although in coastal sections where glaciofluvial sediment delivery was reduced, shoreline recession was observed. Their study demonstrated the sensitivity of High Arctic coasts to mechanisms controlling the supply of sediments from deglaciaded catchments and confirmed earlier observations from Atlantic Canada made by FORBES and TAYLOR (1987) who recorded onshore migration of gravel barriers during periods of sediment shortage and spit extension after an increase in sediment input.

Earlier works in Kongsfjorden by HÉQUETTE (1991) and HÉQUETTE and RUZ (1990) suggested that under certain conditions High Arctic coasts can transform very rapidly. Their study on coastal margins of glaciofluvial outwash plains in northwest Spitsbergen (Brøgger Peninsula) documented a whole mosaic of abrupt changes in coastal morphology during the short Arctic summer with co-existing episodes of erosion and deposition, the formation of new and cannibalisation of old barriers, deposition of micro deltas, landward

and seaward migration of coastlines that depended on the rate of glaciofluvial activity in the surrounding and the ability of storm waves to overwash barrier crests.

The strong link between glaciofluvial sediment input and coastal evolution has been also observed in Calypsostranda by ZAGÓRSKI (2011). His study suggests that during 1936-2007, the shift in direction of sediment delivery from the retreating Renardbreen resulted in the cessation of sandur seaward progradation and, as a consequence of expanded open water conditions, over 100 m coastal erosion. In southern Spitsbergen (Sørkappland) ZIAJA *et al.* (2009) found an evidence of a even more dramatic coastal change in the form of ca. 200-460 m shoreline retreat between 1936-2005 which led to the destruction of Davislaguna lake.

Based on several environmental monitoring case studies on Strokdammane Plain (west Spitsbergen), ÅKERMAN (2008) designed a conceptual model of geo-ecological changes in Svalbard coastal zone under global warming conditions (Figure 2.15.). ÅKERMAN predicts that a more prolonged duration of open waters will be critical to the future impacts of coastal and near-coastal processes and environments. He argues that Svalbard coastal geoecosystems will change rather abruptly. According to his scenario the coastal landscape will be transformed by more frequent storms abrading unprotected shores

already destabilised by thawing permafrost and spring floodings of coastal lowlands related to the formation of high and wide barrier systems that will block stream outlets.

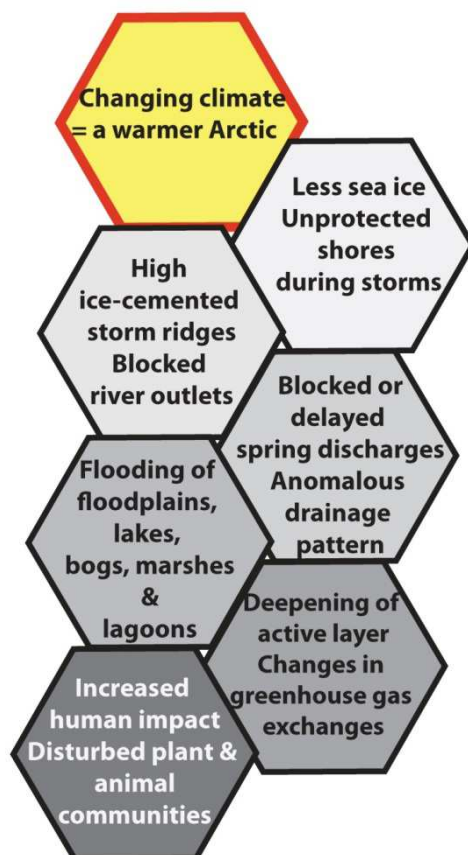


Figure 2.15. Scenario of geoecological changes of Svalbard coasts under global warming conditions (modified after ÅKERMAN 2008)

ZIAJA *et al.* (2009) documented a whole cycle of coastal landscape transition related to the post-LIA deglaciation of Humbergbukta in SE Sørkapp, which highlighted the role of changes in High Arctic coastal zone as a stimulator of polar life expansion. The retreat of Hambergbreen and other surrounding glaciers lead to formation of new coastlines

which quickly become transformed by coastal processes, but also exposed new areas for plant succession and animal colonisation.

More recently, based on study of post-LIA geosuccession in Recherfjorden region, ZAGÓRSKI *et al.* (2012a) developed a concept of direct and indirect glacial influence on High Arctic coastal evolution, which differentiates coasts formed after retreat of tide-water glaciers from coasts formed due to intensification of sediment delivery from valley-glacier systems.

One of the detailed examples of application of coastal landforms in palaeogeographical reconstruction is a study by LØNNE and NEMEC (2004) on High Arctic coastal fan delta in Advenfjorden (Spitsbergen). By precise sedimentological analysis of fan depositional structures, they demonstrated the importance of fan deltas as a proxy record of deglaciation history and environmental change in a High Arctic terrain. The sediments of a small fan system developing at the foot of Hiorthfjellet records the interplay between terrestrial and marine processes adjusting to shifts in sediment delivery from retreating glacier as well as fluctuations of a sea-level. Their work is probably the first to focus on coastal landforms developing in an inner section of a fjord system (Isfjorden) characterised by a relatively dry polar climate and limited fetch, in contrast to the maritime often stormy climate of the western coast where the majority of previous Svalbard coastal studies were carried out.

In Andréeland (NW Spitsbergen), BRÜCKNER *et al.* (2002) and BRÜCKNER and SCHELLMANN (2003) postulated that uplifted beach ridges may help us decipher the glacio-isostatic and palaeo-oceanographic changes. They based their hypothesis on the assumption that conditions favourable for formation of beach ridges reflect the existence of ice-free conditions associated with the retreat of glacier systems and open-water summer season with wave and current activity.

To sum up, it is noteworthy that the majority of previous studies describing the adjustment of coastal zone to paraglacial landscape transformation have been in western and southern Spitsbergen directly influenced by the West Spitsbergen Current and exposed to storm waves originating from the Greenland and Barents Seas (e.g. MOIGN and HÉQUETTE 1985; HÉQUETTE and RUZ 1986; HÉQUETTE 1992; MARSZ 1996; MERCIER and LAFFLY 2005; ZIAJA *et al.* 2009; ZAGÓRSKI *et al.* 2012a, b). On the contrary, little is known about the coastal behaviour in inner fjord environments of Spitsbergen, characterised by sheltered location, prolonged sea-ice conditions, low tidal range and ephemeral pulses of sediment delivery from landforms developing in semi-arid, polar desert climate.

## 2.2 Chapter summary

The key issues that arise from this review of literature on Arctic coastal zone studies are:

- 1.) The Arctic coastal zone is particularly vulnerable to climate change because it acts as a buffer between rapidly changing polar landscapes and oceans with lengthening ice-free conditions and increasing storminess. Although a number of research programs have been completed in the last five decades, Arctic coastal research has generally been neglected. The most recent research has shed new light on Arctic coastal change, with an emphasis on the ice-rich permafrost coasts of Siberia, Alaska and Canada.

*Mindful of the limited understanding of geomorphological processes operating on High Arctic coasts, this thesis describes in detail the mechanisms that control the evolution of Svalbard coastal zone, focusing on processes operating in both accumulating and rocky coast sections.*

- 2.) Previous coastal studies in Svalbard have concentrated mainly along the western and southern coasts of Spitsbergen, in contrast to sheltered, low energy coastal environments that are characteristic for inner parts of fjords. Studies of the coastal response to glacier retreat conducted along western and south-western Spitsbergen record rapid coastal progradation and the development of new coastal landforms. However, the rate of similar landscape changes observed in inner-fjord settings is not known.

*This thesis presents the first study of a central Spitsbergen coast to the post-LIA deglaciation and compares the rates and types of processes that shape the coastal zone in inner-fjord setting with those observed along more oceanic settings of western and south-western Spitsbergen.*

- 3.) There are very few data on the seasonal changes of coastal zone on Svalbard and its adjustment to increasing ice-free periods.

*To gain a better understanding of small-scale / ephemeral changes of High Arctic coastal microrelief, this thesis presents the results of three years of field-based*



*observations of gravel-dominated barriers in northern Billefjorden and describes the geomorphic role of factors that include : sea-ice, icefoot, snow-patches, accumulations of erratic boulders, debrisflows, driftwood, seaweed and human activity.*

- 4.) Previous studies conducted along rocky coastal sections have hypothesised about the existence of ‘coastal amplification’ of rock weathering in High Arctic settings; however this concept has not been tested using modern geomorphological methodologies.

*This thesis presents the results of the first application of Schmidt hammer rock tests in Arctic settings to characterise rock resistance variability across a recently deglaciated rocky coastal zone.*

- 5.) The application of the “paraglacial concept” in High Arctic coastal studies provides an opportunity to integrate research dealing with climate change and that on sediment transport to Arctic coastal systems.

*This thesis proposes a new conceptual models of coastal zone development in High Arctic conditions in seasonal, century and millennial timescales.*



# Chapter 3:

## The Study Area

### 3.1 Introduction

Svalbard (Norwegian Svalbarð 'cold shore') is a High Arctic archipelago which lies between 74° - 81° North and 10° - 35° East (Figure 1.4). The total land area of 62 248 km<sup>2</sup> is divided between several main islands: Spitsbergen (the biggest island - 38 612 km<sup>2</sup>), Nordaustlandet (14 443 km<sup>2</sup>), Edgeøya (5 230 km<sup>2</sup>), Barentsøya (1 321 km<sup>2</sup>), Kvitøya (682 km<sup>2</sup>), Prins Karls Forland (615 km<sup>2</sup>), Kongsøya, 191 km<sup>2</sup>), Bjørnøya (178 km<sup>2</sup>), Svenskøya (137 km<sup>2</sup>), Wilhelmøya (120 km<sup>2</sup>) and hundreds of smaller islands (together, 621 km<sup>2</sup>). Located on the boundary between Norwegian Sea, the Barents Sea and the Arctic Ocean, Svalbard is one of the key areas to study the sensitivity of the Arctic to climate change. The sharp environmental gradients induced by climatic and oceanographic processes operating around Svalbard intensify the interactions between cryosphere, atmosphere and hydrosphere.

### 3.2 Geology and Landscape

Svalbard geology is very complex and its rocks cover more than 400 million years. JOHNSEN *et al.* (2000) identified five major geological provinces spanning from Precambrian to Tertiary strata, which are covered by Quaternary deposits in glacial valleys and on some of the mountainous plateaus (Figure 3.1.).

According to Springer's *Encyclopedia of World's Coastal Landforms* (2010, p. 581) 'the characteristic element of Svalbard geology is the Hecla Hoek Complex, found in the northern part of the Nordaustlandet, in the northeast and along the western coast of Spitsbergen, on PrinsKarls Forland. This complex consists of Pre-Cambrian metamorphic rocks with some Cambrian and Ordovician sedimentary formations that were metamorphosed during the Caledonian orogeny (late Silurian – early Devonian) and vary from marbles and schists, quartzites and limestone/marble to highly metamorphosed gneisses and migmatites. The Svalbard geology is renowned for its huge variety of sedimentary rock units. The Devonian found in the central and northern parts of Spitsbergen rocks are represented by shales and sandstones. Carboniferous and Permian rocks in the southern parts of Nordaustlandet, in the north-eastern and central parts of Spitsbergen and in small areas in the western parts of Spitsbergen, from west of Ny-Ålesund in the north to the area of Hornsund in the south, consist mainly of continental sandstones, beneath limestone and chert with seams of coal. Triassic rocks constitute the central parts of southern Spitsbergen, south from Isfjorden, and include clay, shale, siltstone, and sandstone which are overlaid by Jurassic shale and conglomerates.

Cretaceous rocks are represented by sandstones and shales which are often covered by Tertiary shales and seams of coal.'

The Svalbard bedrock geology experienced intensive folding, thrusting and faulting during the Caledonian Orogeny. Later on, during the Tertiary, the opening of the North Atlantic Ocean caused further faulting and flexuring of the Svalbard bedrock which afterwards was sculptured by Quaternary glaciations.

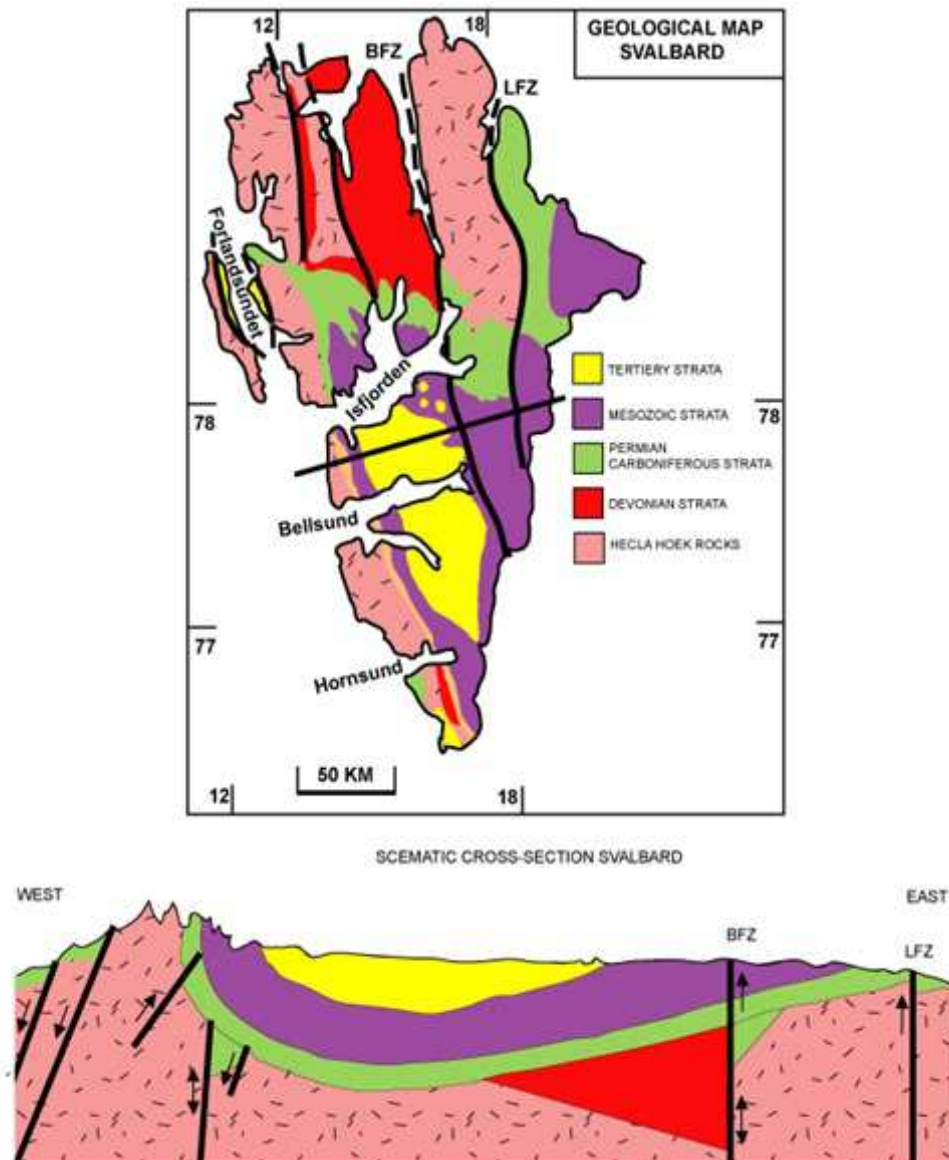


Figure 3.1. Simplified geology map of Svalbard after SVALEX Project, Arild Andresen (2006), BFZ – Billefjorden Fault Zone, LFZ – Lomfjorden Fault Zone. 1. PINK - Metamorphic rocks of Precambrian to early Silurian age reworked during the Caledonian orogeny, characteristic for the western coast and on the north-eastern part of Spitsbergen and Nordaustlandet – famous Hecla Hoek complex. 2. RED - The Devonian cover rocks on northern Spitsbergen – Old Red Sandstone. 3. The central basin in the central parts of Spitsbergen with Early/mid-Carboniferous rift deposits, Mid-Carboniferous- Permian shelf carbonates (GREEN) and Mesozoic siliclastic deposits (PURPLE). 4. The platform areas on the eastern parts of Spitsbergen and on Barentsøya and Edgeøya. 5. YELLOW - The Tertiary fold-belt along the west coast of Spitsbergen.

The landscape of Svalbard is dominated by mountains, wide glacial valleys and fjords systems, all shaped by repeated Quaternary glaciations. During last 150 000 years Svalbard was covered by several large ice-sheets (MANGERUD *et al.* 1998), which probably over-rode the whole archipelago at the LGM and extended onto the shelf areas west of Svalbard (Figure 3.8.b). LØNNE and LYSÅ (2005) observed that although in many places the landforms and sediment records in glacial valleys, fjords and shelf morphology suggest the development of large warm-base ice masses inundating the landscape. The geomorphic signature of Quaternary glaciations along some sections of shallower shelves, coastal lowlands or mountain plateaus are less clear and suggests spatial and temporal variability in glacial activity during the last glaciation. LØNNE and LYSÅ (2005) proposed that deglaciation progressed differently on Svalbard than in lower latitudes, emphasising the rapidity of fluvial and periglacial reworking of a thin glacial sediment cover throughout the Holocene.

The history of glacial unloading and isostatic rebound on Svalbard is inferred by the pattern of relative sea-level change reconstructed on the basis of the elevation of raised beaches located in ice-free areas (Figure 3.2.) (e.g. LANDVIK *et al.* 1987; STANKOWSKI *et al.* 1989; FORMAN 1990; SALVIGSEN *et al.* 1991; ZIAJA and SALVIGSEN 1995; BRÜCKNER *et al.* 2002). In general, during the Holocene, sea-level was continuously falling (Figure 3.2.a), however in some of the western and northern sites, evidence for mid-Holocene transgression is recorded (FORMAN *et al.* 2004). Investigations of the spatial variability in postglacial emergence (Figure 3.2.b) suggest thicker ice over the central sector of the Barents Sea (INGÓLFSSON 2011). The pattern of Holocene isostatic loading and unloading by ice, and the associated rebound of glaciers, especially during the Neoglacial and Little Ice Age (LIA) (1890-1900 AD) is uncertain. However, tide gauge data from Barentsburg (Figure 3.2.c) and Ny-Alesund (Figure 3.2.d) show that along the western coast of Spitsbergen, sea-level continues to fall, meaning that this part of Svalbard has not yet reached isostatic equilibrium.

The glacial influence on the Svalbard landscape was reduced during the early- to mid-Holocene when climate warming meant that glaciers were probably smaller than present. A sediment record from Linnévatnet suggests the existence of totally ice-free conditions in the valleys of central Spitsbergen before the Neoglacial (SNYDER *et al.* 2000). The presence of *Mytilus Edulis* around the northern coast of Svalbard between 9400 – 5300 cal. yr BP (SALVIGSEN 2002) and to 3500 cal. yr BP in the inner fjords (SALVIGSEN *et al.* 1992) suggests that the surrounding seas also were also warmer in the first half of

Holocene. Approximately 4000 years ago, the Neoglacial cooling led to glacier readvance (BAETEN *et al.* 2010). Svalbard glaciers reached their Holocene maximum extent at the end of the Little Ice Age, most likely the coldest part of the entire Holocene (BRADLEY 2000).

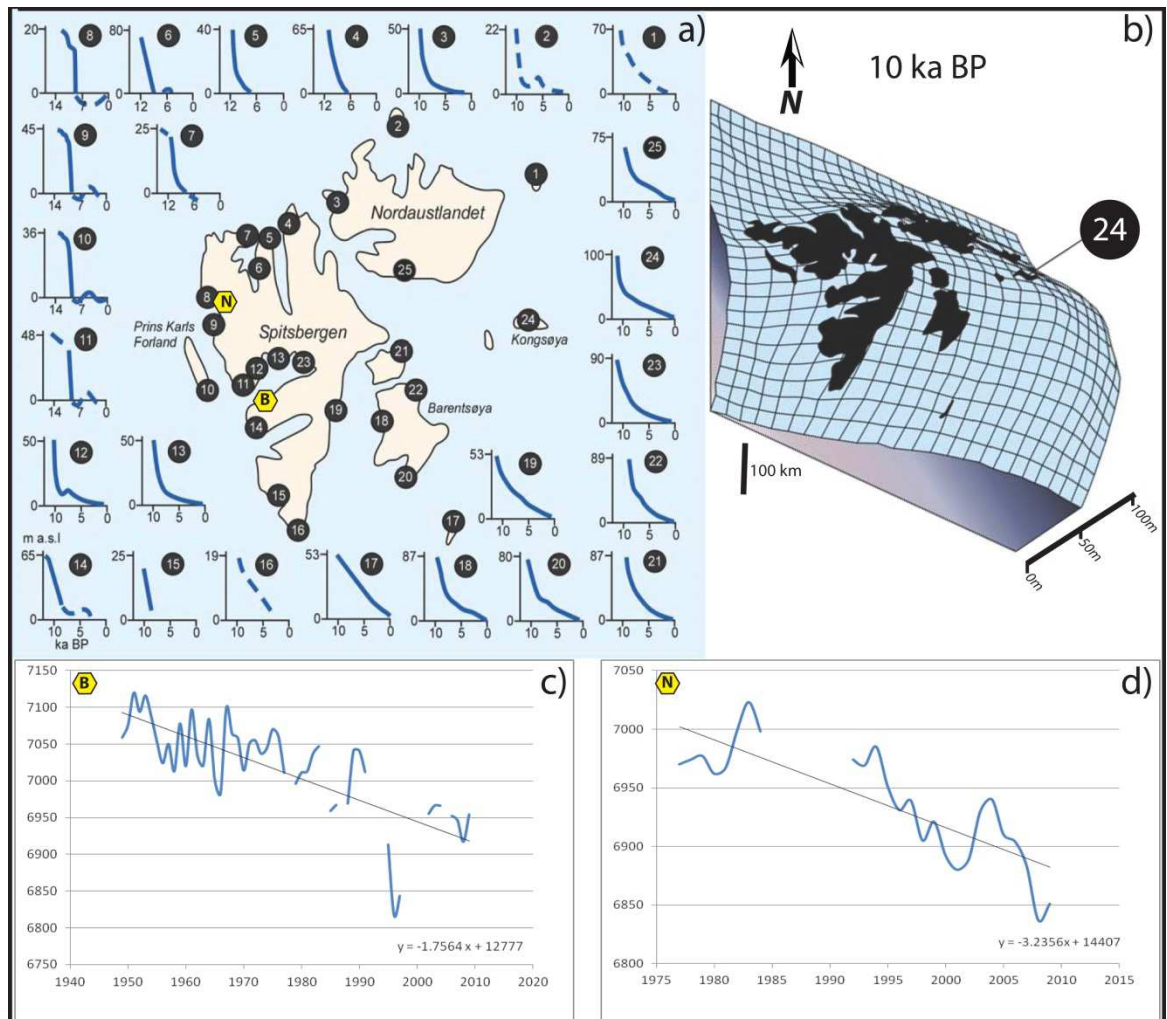


**Figure 3.2.** Relative sea-level change on Svalbard a) Relative sea-level curves from Svalbard showing how the crust has rebounded after glacier retreat (modified after FORMAN *et al.* (2004)) b) Isostatic depression caused by the Svalbard–Barents Sea ice sheet inferred by the pattern of postglacial raised beaches (modified after BONDEVIK (1996)). Black dot no. 24 indicates the highest elevation of the post-glacial marine limit recorded on Kongsøya established by SALVIGSEN (1981). c) GIA-corrected rate of the 20<sup>th</sup> century sea-level change from a tide gauge in Barentsburg (yellow polygon B), where in the last 70 years sea level has been falling approximately -1.76 mm per year. d) GIA-corrected rate of the 20<sup>th</sup> century sea-level change from a tide gauge in Ny Alesund (yellow polygon N), where in the last 40 years sea level has been falling approximately -3.24 mm per year; Data from: Permanent Service for Mean Sea Level (PSMSL) carried out by NERC funded National Oceanography Centre in Liverpool. [http://www.psmsl.org/about\\_us/](http://www.psmsl.org/about_us/)

In areas not covered by glaciers, the geomorphology is dominated by permafrost and periglacial processes (ÅKERMAN 1987) with many examples of rock glacier, ice wedges, pingo systems, and patterned ground (Figure 3.3.).



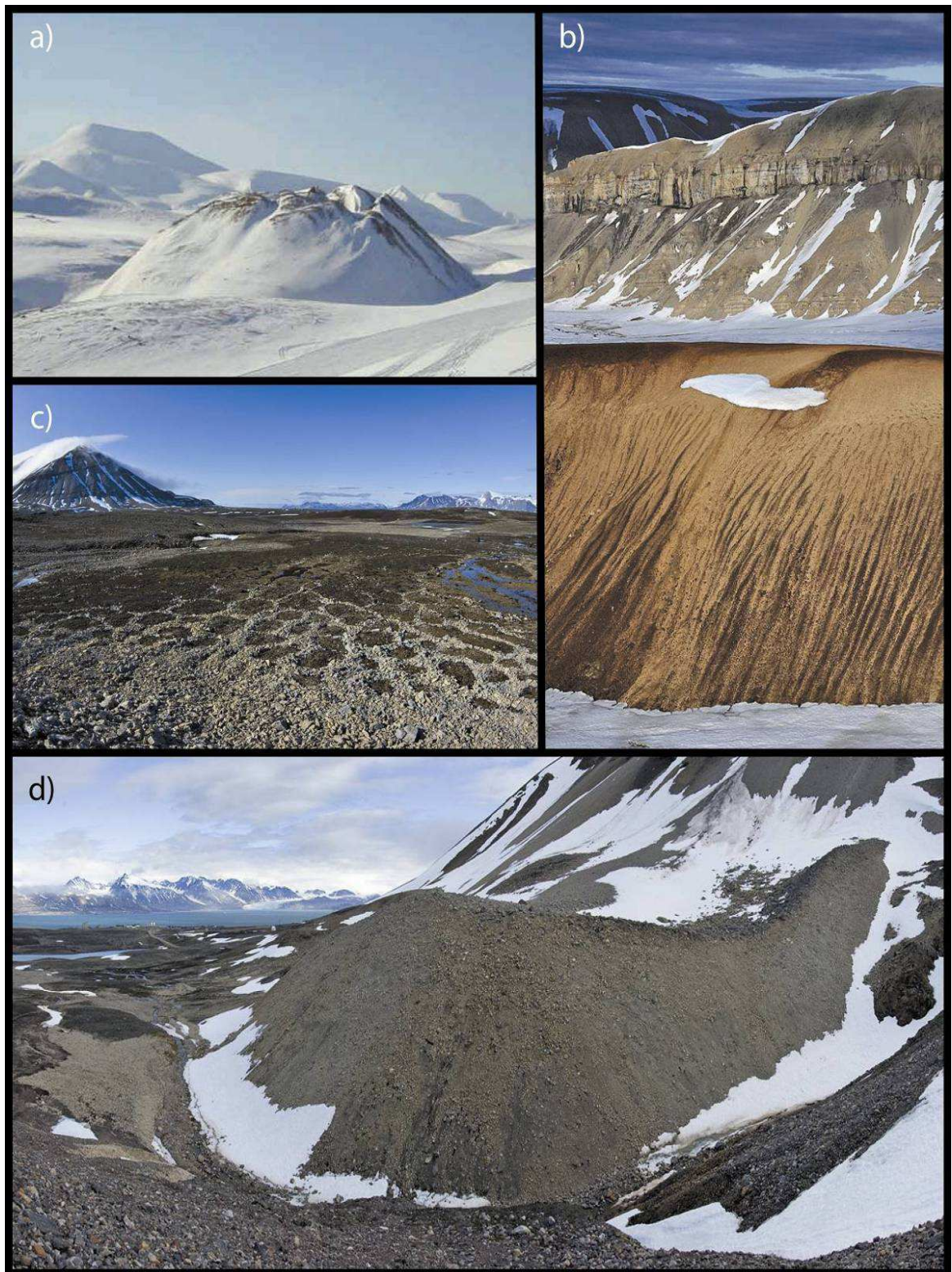


Figure 3.3. Periglacial landforms on Svalbard a) Pingo in Eskerdalen photo by: HANNE CHRISTIANSEN, source: <http://europlanet.dlr.de/node/index.php?id=491>; b) Stone stripes on slopes in Ny Friesland, photo by MICHEAL HAMBREY c) Stone circles in Brøggerdalen, photo by JÜRGEN ALEAN; d) Small rock glacier in Brøggerdalen, photo BY JÜRGEN ALEAN, source: [www.glaciers-online.net](http://www.glaciers-online.net)

Frozen ground conditions are extensive and vary from thick and continuous permafrost in the mountain ranges (more than 450 m thick) to relatively thin and recently developed permafrost in glacial valleys (HUMMUM *et al.* 2003). Discontinuous and thin

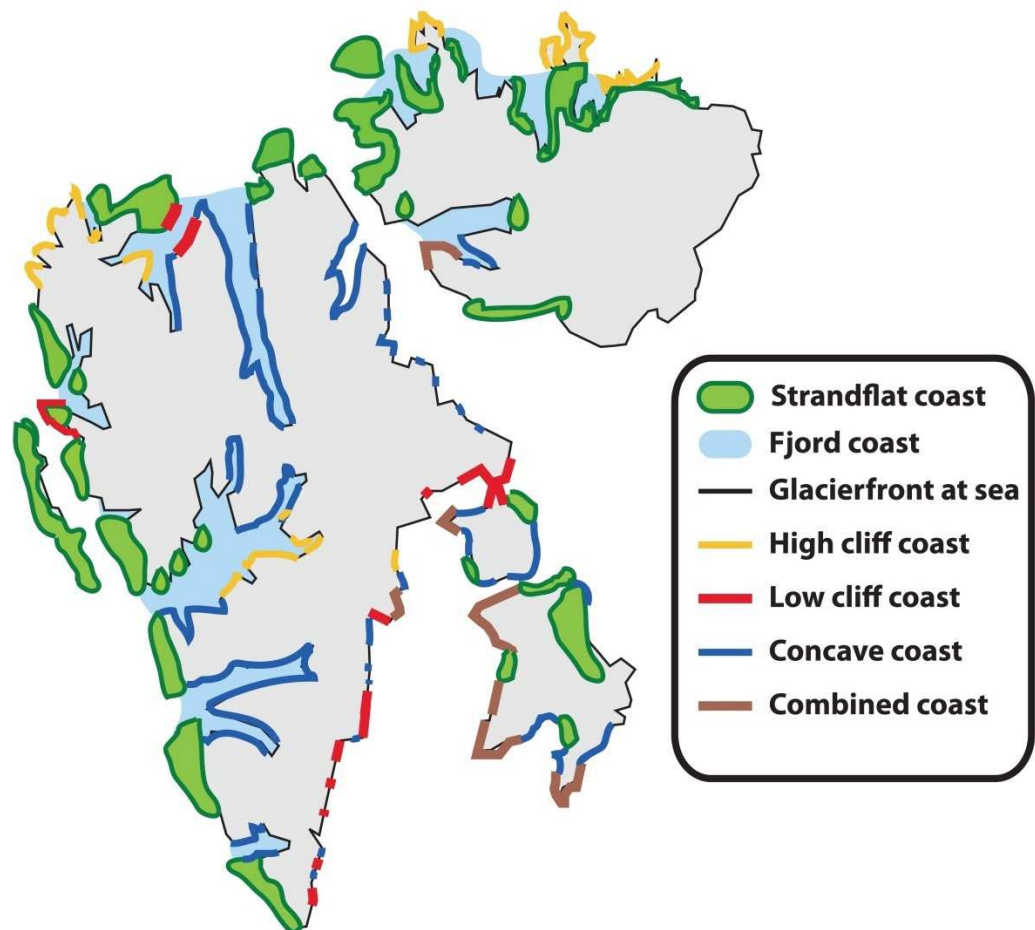
permafrost (or even non-frozen ground) occurs in the coastal and seabed area of the fjords (HUMMUM *et al.* 2003). Thinning of permafrost in coastal and seabed areas is probably related to glacio-isostatic rebound and RSL fall since the LGM (BERTHLING and ETZELMÜLLER 2007), although the thawing impact of warmer sea waters and longer periods of open water conditions in the fjords may also be important.

A characteristic element of the Svalbard scenery are wide (up to 12 km) gently sloping, undulating coastal lowlands called strandflats, usually located at the entrance of major fjords and formed by the interplay of extensive frost weathering, sea ice scouring and glacier erosion during glacials, as well as fluvial action and sea abrasion during interglacials (TRENHAILE 1997).

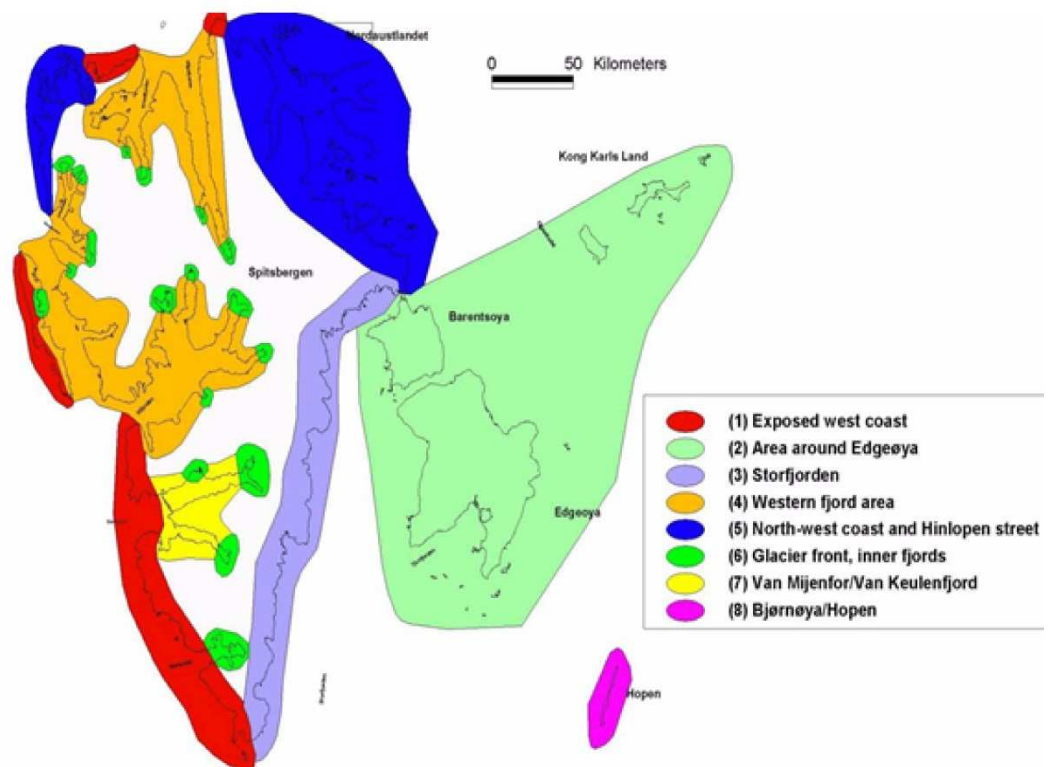
Coastal depositional landforms in Svalbard include alluvial fan-deltas, beaches, pocket beaches, barriers, barrier islands and spits separating coastal lagoons (KLEMSDAL 1986). KLEMSDAL (2010) proposed a division of coastal landforms in Svalbard into five main types: strandflat, fjord, cliff, composite cliff, and concave slope (Figure 3.4.a). However, some of those terms are very roughly explained and unsupported with clear examples. In connection with an oil spill protection program in the Barents Sea, ETZELMÜLLER *et al.* (2003) carried out geomorphological mapping of Svalbard coasts. Their GIS analyses led to the subdivision of Svalbard into 8 coastal regions (Figure 3.4.b):

- (1) *Wave exposed areas along the west- and north coast of Spitsbergen.* The area is dominated by rocky shore (> 30%), barriers and lagoons, indicating active marine transport processes along the coast. Calving glaciers and rock cliffs (< 15%) are seldom.
- (2) *Moderate wave exposed area at Barentsøya, Edgeøya and Kong Karls Land.* The coast is moderately exposed to waves because of shore ice during most of the year, and active erosion in bedrock is supposed to be low.
- (3) *Coast dominated by calving glaciers - the Storfjorden area.* Glacier fronts and wide sediment beaches, showing lower wave action and sediment supply by the glaciers, dominate this area. Rocky shores and rock cliffs are more seldom.
- (4) *Coast dominated by rock cliffs with beach sediments - the western fjord areas.* Rock cliffs behind beach sediments, indicating active coastal erosion in bedrock, dominate the area. The grain size of the beach is often more sandy, reflecting the dominance of Mesozoic and Tertiary sedimentary bedrock in the area.





a)



b)

Figure 3.4. a) Diversity of Svalbard coastal environments (map modified after KLEMSDAL (2010)). b) Different coastal regions on Svalbard, based on GIS analyses by ETZELMÜLLER et al. (2003)



- (5) *Coast dominated by rock cliffs and rocky shore with low amount of beach sediments – the northwest coast of Spitsbergen/Hinlopenstretet.* This area is dominated by metamorphic rocks and sea ice exposition towards north and northeast. The grain size is coarser, and the amount of unconsolidated sediments in the shore zone is low. Rocky shore and rock cliffs dominate.
- (6) *The inner fjord areas.* These contain an abundance of deltas and sand-rich sediments. They have the highest abundance of clayey beaches and tidal flats and the shoreline is more unstable due to rapid changes in sediment supply. Wide beaches dominate; cliffs are infrequent and rocky shores are absent.
- (7) *Coasts dominated by unconsolidated sediments - Van Mijenfjorden/Van Keulenfjord.* These fjord areas are unique by being dominated by beaches of unconsolidated sediment, with 20% of the area consisting of sediment cliffs, and sandy to gravelly grain sizes in the remaining shore zone. Sea ice cover is longer than in other fjord areas, helping to protect the shores.
- (8) *Coasts dominated by high rock cliffs - the islands of Bjørnøya and Hopen.* These islands are almost totally dominated by high rock cliffs, with 70% of the shore area. Sediment beaches are seldom.'

### 3.3 The climate of Svalbard

Due to the confluence of major North Atlantic air masses and ocean currents occurring in the proximity of Svalbard (Figure 1.4), the climate across the archipelago is complex. The western and southern coastal margins are influenced by both warm ( $>3^{\circ}\text{C}$ ) and highly saline ( $>35\text{‰}$ ) Atlantic Water (West Spitsbergen Current flowing along western coast) and cool ( $0\text{--}4^{\circ}\text{C}$ ) and relatively saline ( $34.6\text{--}34.9\text{‰}$ ) Arctic Water and cold ( $-1 - 3^{\circ}\text{C}$ ) and less saline ( $34.4\text{‰}$ ) Polar Water (East Spitsbergen Current transporting a mixture of Arctic and Polar water masses along eastern coast). These ocean currents are accompanied with air masses of different temperatures (Swift 1986). Throughout the Holocene the interplay between the inflow of Atlantic and Arctic and Polar Waters has caused shifts in the state of regional climate and the functioning of glacial systems (i.e. HALD *et al.* 2001, 2004, 2007; ŚLUBOWSKA *et al.* 2005; ŚLUBOWSKA-WOLDENGEN *et al.* 2007, 2008; MAJEWSKI *et al.* 2009).

According to WADHAMS (1981), land-fast ice bounds Svalbard fjords in November until June, but in general the state of sea-ice cover (thickness, timing) differs from season to season and between fjords (GERLAND and HALL 2006). Thermal differences between

ocean currents determine the distribution of pack-ice, which is much denser along the eastern coast of Spitsbergen. BENESTAD *et al.* (2002) associates the high sensitivity of the Svalbard climate with sea-ice extent, which profoundly impacts heat and moisture exchange between the atmosphere and ocean (e.g. KOENIGK *et al.* 2009). The complex state of the Svalbard climate is also related to the proximity of the main North Atlantic cyclone track, which according to DICKSON *et al.* (2000) is the primary route of water vapour to the Arctic.

Another driving mechanism responsible for the diversity of the Svalbard climate is the Arctic Oscillation, with its major component the North Atlantic Oscillation NAO (SERREZE *et al.* 2000) - the strongest pattern of atmospheric circulation variability in the Northern Hemisphere. Positive NAO conditions (Figure 3.5.a) deliver increased winter precipitation and above-normal air temperatures in Northern Europe, and lower air temperatures in eastern Canada and western Greenland (HURRELL *et al.* 2003). In the negative phase of the NAO (Figure 3.5.b), weakening of the Icelandic Low and Azores High leads to the delivery of cold and dry air masses to Northern Europe and above-normal, milder temperatures in eastern Canada and western Greenland (HURRELL *et al.* 2003).

Although HUMLUM (2005) claimed that our understanding of Arctic climate responses to NAO variability observed during the 20<sup>th</sup> century (Figure 3.5.c) is still relatively poor, there is good evidence for a correlation between the NAO index and winter moisture distribution across the region. For example, HURRELL *et al.* (2003) stated that the NAO in many cases determines the Arctic winter conditions, specifically the number of snow-free days and the start of snow-melt and duration of snowfall seasons.

From a Svalbard perspective, the state of the NAO is important because it influences the number of storms (moisture transport) entering the North Atlantic and air temperatures that affect glacier advance/retreat and sea-ice cover. According to various studies (WANG *et al.* 2004; LIU *et al.* 2004; YAMAMOTO *et al.* 2006) during a positive NAO, air and ocean temperatures in the proximity of Svalbard are warmer, leading to reduced sea ice cover. Thus, the rapid reduction of sea-ice extent observed over the Barents Sea in the last 40 years may be linked to a persistent positive NAO index observed since the late 1970s. With the continuation of present trends in sea-ice loss, KOENIGK *et al.* (2009) predict that the Barents Sea will be the first Arctic region without winter sea ice. After the end of a persistent negative NAO phase which lasted during the 1960s, SERREZE *et al.* (1997) observed an increase in the number and intensity of storms

north of 60°N. ROGERS and MOSLEY-THOMPSON (1995) counted many more cyclones intruding northern high latitudes since the beginning of the positive NAO phase in the 1980s.

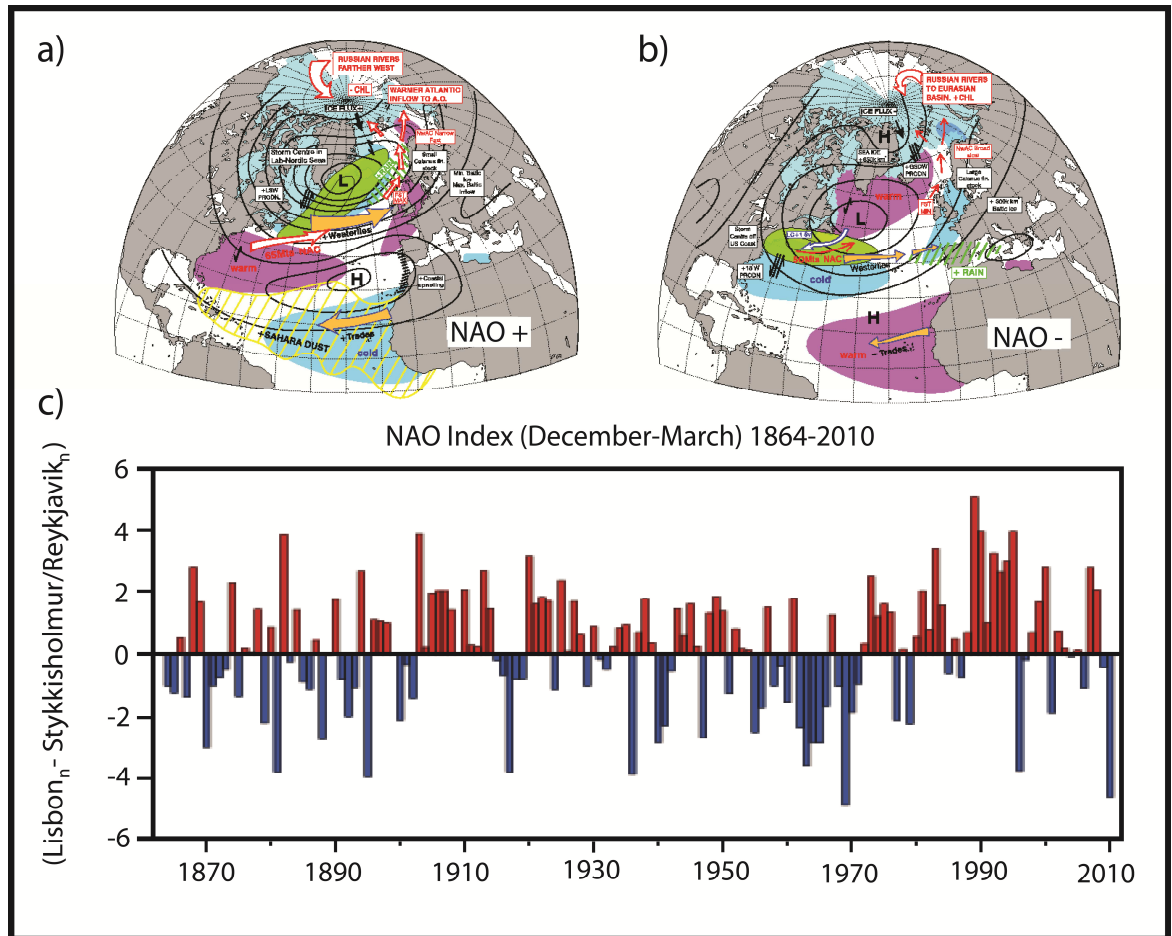


Figure 3.5. Northern Hemisphere during a positive (a) and negative (b) NAO phase. Both images from <http://www1.secam.ex.ac.uk/nao-images.dhtml?#naoplus>; c) NAO winter index between 1864-2010, which displays the greatest interannual and interdecadal variability (Hurrell 1995), calculated as the annual winter (December through March) deviance from the average difference in atmospheric pressure at sea level at Lisbon (Portugal) and Stykkisholmur (Iceland) normalised relative to the period 1864– 1983. Diagram courtesy of HURRELL (National Center for Atmospheric Research): <http://www.cgd.ucar.edu/cas/jhurrell/nao.stat.winter.html>

The increase in the number of cyclones passing into the High Arctic has been confined mainly to the summer months (SERREZE *et al.* 2000), which together with reduced sea-ice cover typical for this part of the year may have a profound effect on the functioning of the coastal systems. Since about 2000, the NAO index has weakened (according to NOAA winter 2009/2010 was characterised probably by the lowest NAO values ever recorded).

The relation between AO-NAO indexes and the 20<sup>th</sup> century air temperature changes from Svalbard is uncertain, but there are three phases of air temperature and NAO index change to analyse in more detail (Figure 3.6.):

Phase 1 - Temperature rise between 1915-1930, with almost 6°C rise between 1917 and 1922. The NAO index was positive between 1900 – 1930;

Phase 2 - Temperature fall between 1957 -1968, with *ca.* 4 °C cooling (HUMLUM 2003). There was a period of negative NAO from the early 1940s to the early 1970s.

Phase 3 – Temperature rise since 1976, which intensified since the late 1990s and persists to the present. The NAO index was generally positive over the last 30 years, although a weakening of index began at the start of the 21<sup>st</sup> century.

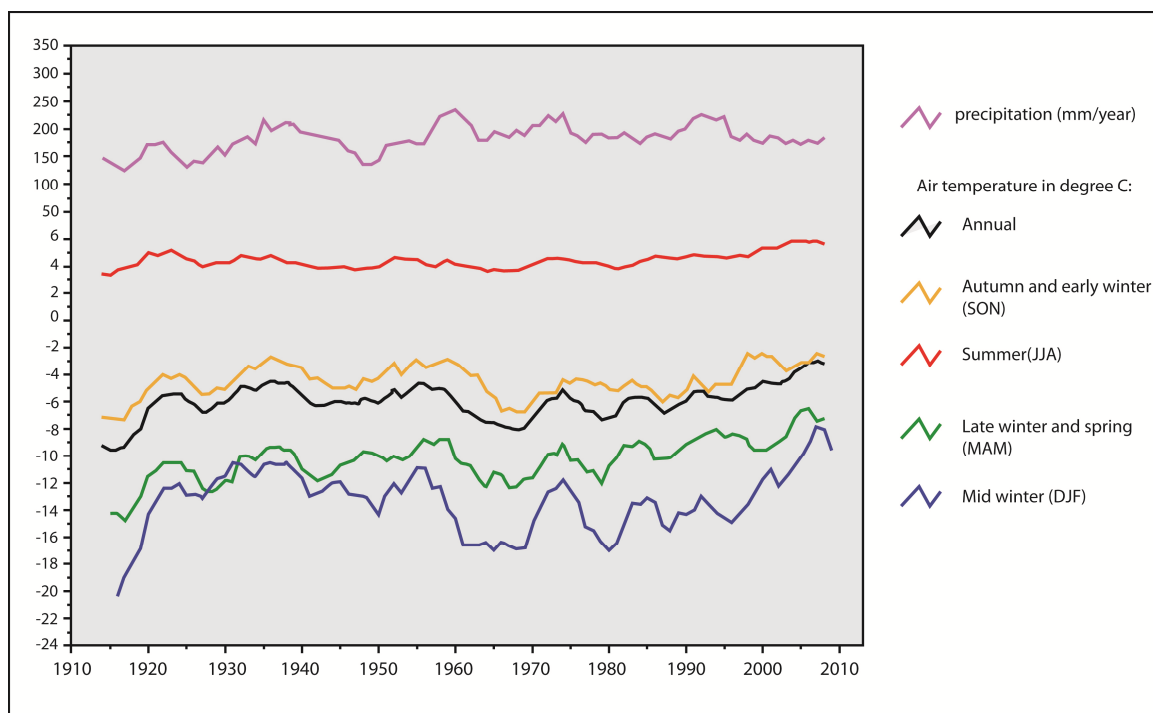


Figure 3.6. Svalbard meteorological observations since 1912 based on monthly meteorological series homogenised by the [Norwegian Meteorological Institute](#). The lines depict running 5-yr means. Modified from the [climate4you.com](#). website by OLE HUMLUM.

### 3.3.1 Present-day meteorological conditions on Svalbard

The mean annual air temperature on Svalbard is about –6°C at sea level and approximately –15°C in the mountains. Figure 3.7. shows that Svalbard is characterised by relatively milder temperatures compared to other High Arctic regions of an equivalent latitude (e.g. Greenland, Siberian and Canadian islands). This reflects the moderating influence of the West Spitsbergen Current.

The mean annual precipitation, with snow as a dominant component, is much higher along the western coast of Svalbard than in central and north-eastern parts. With *ca.* 400-600 mm precipitation along the coastal margins and only about 200 mm in the interior, many parts of the islands are semi-arid environments (RACHLEWICZ 2009). The

strong variability of precipitation is also reflected in the height of the equilibrium line altitude (ELA), which falls from *ca.* 800 m in the north-east (the driest part ) to *ca.* 200 m along the western coast (the moistest part). Svalbard climate is also known for strong winds (the main wind direction across the archipelago is from SSE to NNW) that are responsible for rapid re-distribution of snow cover during winter months and fogs that develop mainly along the coast during Arctic summers.

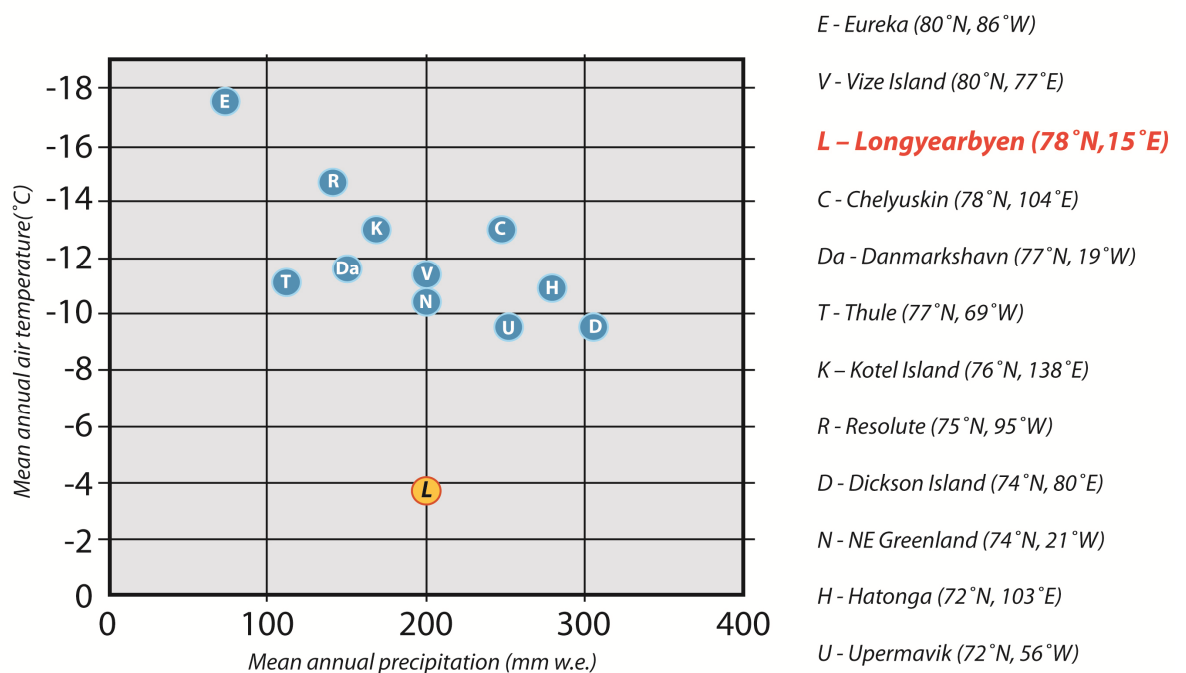


Figure 3.7. Mean annual air temperature and mean annual precipitation for High Arctic meteorological stations in 2009, showing that Svalbard (Longyearbyen) is significantly warmer (modified after ECKERSTORFER and CHRISTIANSEN (2011)).

### 3.3.2 Present-day glaciation of Svalbard

Currently 60% of Svalbard is glaciated - 36 502 km<sup>2</sup> (Figure 3.8.a). The largest European glacier, Austfonna, has an area of 8 412 km<sup>2</sup> and is located on Nordaustlandet (NE Svalbard). Most Svalbard glaciers are polythermal, characterised by low velocity ice flow with the glacier bed interacting with underlying frozen ground (JANIA *et al.* 2005; NUTH *et al.* 2010).

Many Svalbard glaciers are surging types (SUND *et al.* 2009) and are characterised by pulsating (50-100 years interval) rapid advances of several kilometres i.e. one of the Austfonna glaciers, the 30 km-wide Bråsvellbreen surged more than 20 km between 1936 and 1938 (SCHYTT 1969). This is probably the largest glacier surge ever recorded. Analysis made by BŁASZCZYK *et al.* (2009) shows that 163 Svalbard glaciers are tidewater

and their calving cliffs comprise 860 km of archipelago's coastline (ca. 20% of the total coastline length).

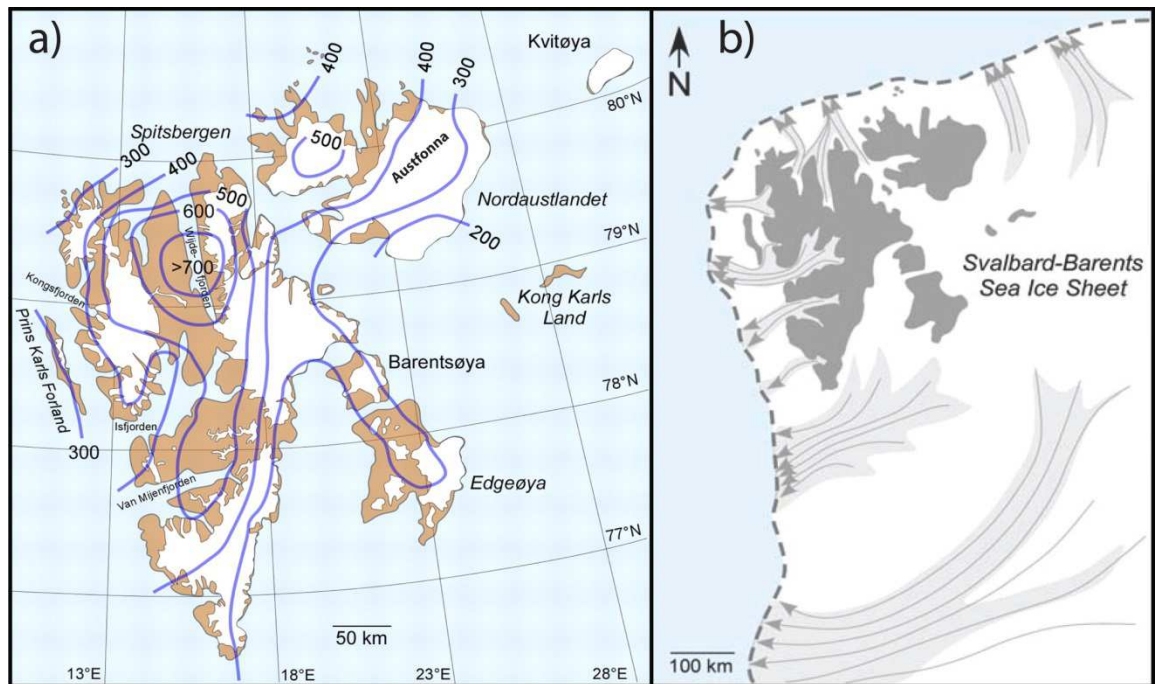


Figure 3.8. Present and former glaciations of Svalbard modified after INGÓLFSSON (2011): a) Present-day glaciations of Svalbard Archipelago with distribution pattern of ELA given as 100m contour intervals modified after HAGEN *et al.* (2003); b) Reconstruction of the Svalbard-Barents Sea Ice Sheet modified after OTTESEN *et al.* (2005).

According to NUTH *et al.* (2010), the geodetic mass balance of Svalbard is the most negative in the entire Arctic, with a mass loss that is double that of the Canadian Arctic, and four times bigger than that of the Russian Arctic. Their study showed that in last 40 years Svalbard (excluding the Austfonna and Kvitøya ice caps) ice volumes decreased on average  $9.71 \pm 0.55 \text{ km}^3$  per year, contributing to a global sea level rise of 0.026 mm per year sea level equivalent (4% of the global contribution from smaller glaciers and ice caps).

### 3.4 The Study Area

#### 3.4.1 Overview

Two bays, Petuniabukta and the neighbouring Adolfbukta, located in central part of Spitsbergen Island, were chosen for detailed investigation in this PhD. Those two small fjord-headed bays (submerged parts of hanging valleys) are the northernmost branches of Billefjorden, the centre branch of Isfjorden and the largest fjord system of Spitsbergen (Figure 3.9.). The northern Billefjorden was selected for PhD project to improve our understanding of the coastal evolution in sheltered and low-energy environments on the



contrary to previous studies that concentrated on the western and south-western coasts of Spitsbergen affected by storm-waves.

A state-of-the-art review of glacial sediment fluxes and relief changes in the north Billefjorden region was published by RACHLEWICZ (2009). This provides a comprehensive overview of the area's geology, climate, hydrology and geomorphology. Therefore, here I only briefly summarise the core facts regarding the physical geography of the study area, with an emphasis on those elements that directly influence the coastal zone.

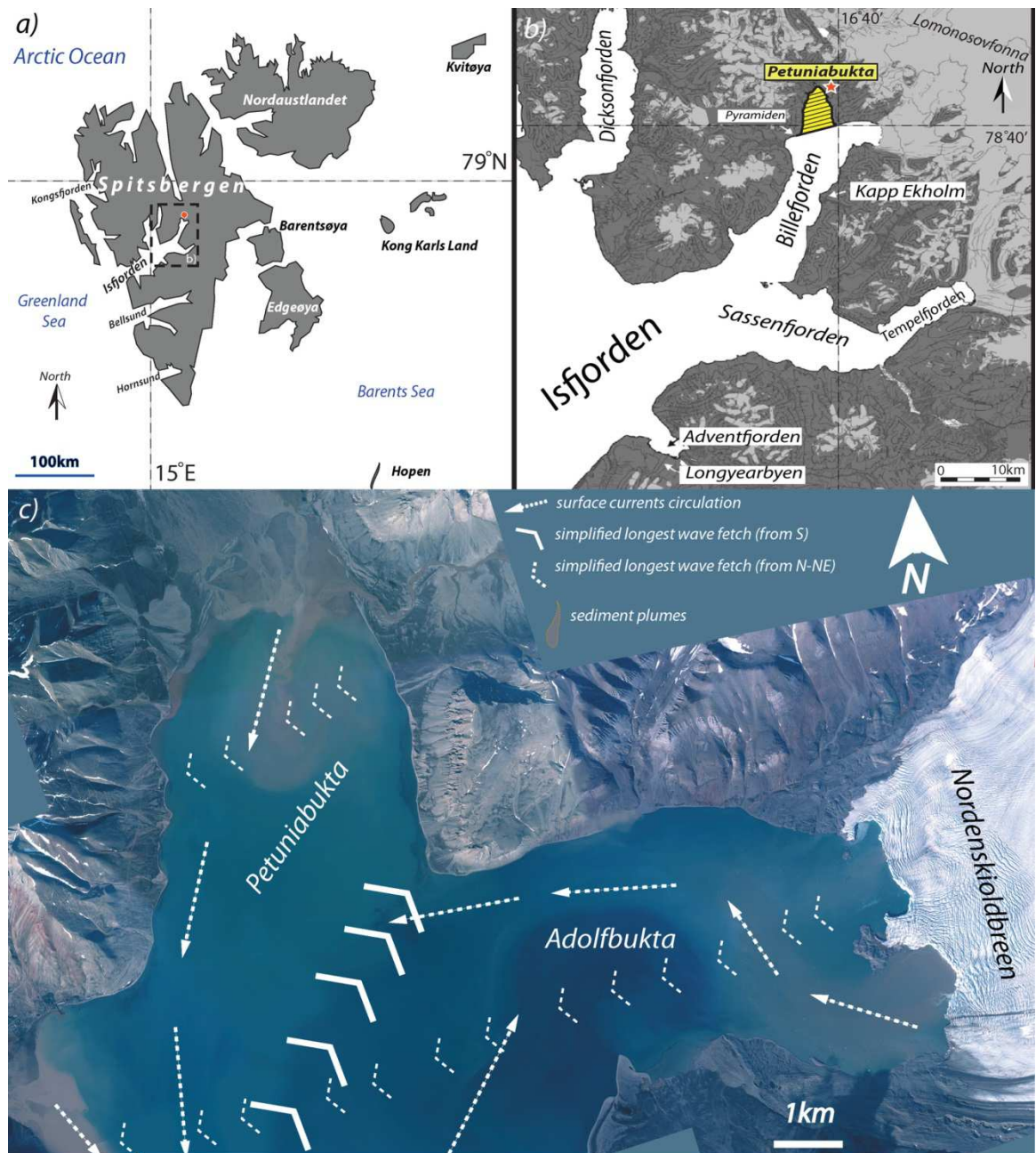


Figure 3.9. Location of the PhD study area: a) Northern Billefjorden. b) An overview map of Isfjorden system and its major tributaries. Light grey represents glacier coverage and the yellow shows the location of Petuniabukta. Map modified after BAETEN et al. (2010). c) Simplified water surface circulation and directions of longest wave-fetch in Petuniabukta and Adolfbukta.

### 3.4.2 Geology and landscape

#### 3.4.2.1. Bedrock geology

The study area geology (Figure 3.10.) is one of the most diverse in the Svalbard Archipelago due to disturbance of geological units associated with the N-S trending Billefjorden Fault Zone (BFZ) and the related Billefjorden Trough (DALLMANN *et al.* 2004).

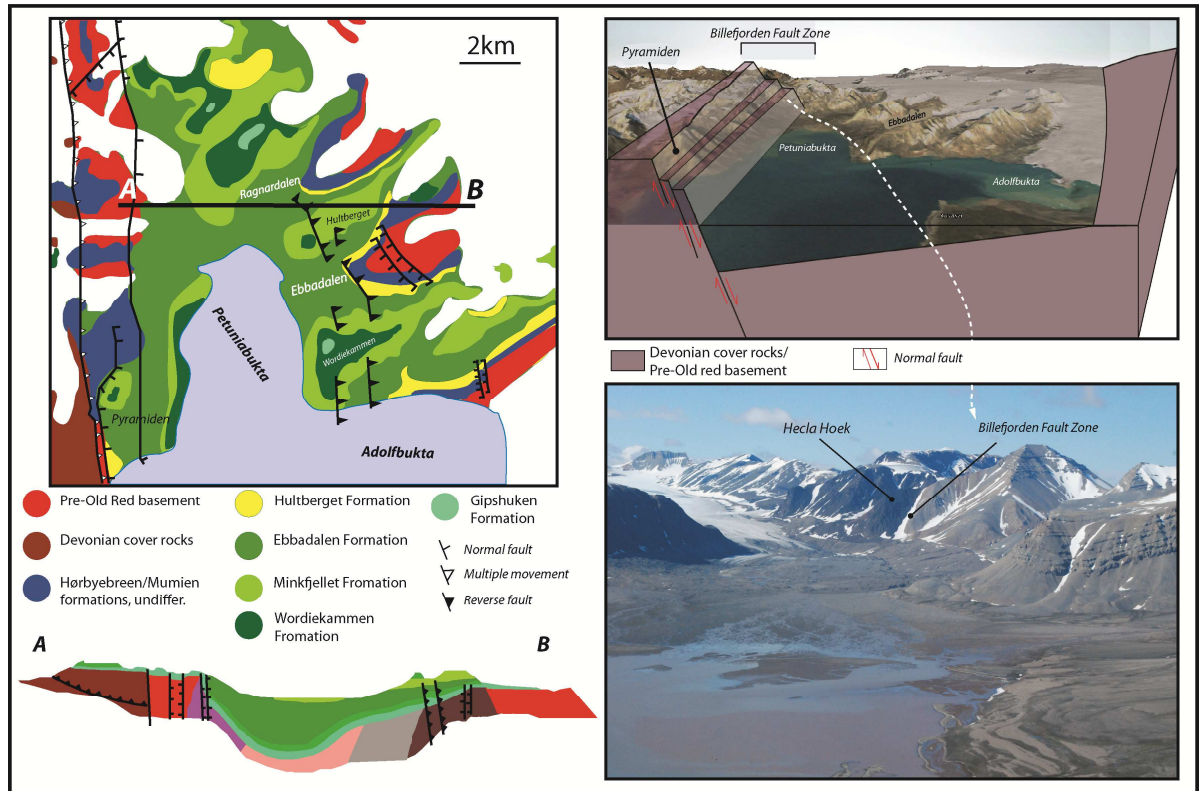


Figure 3.10. Geological sketch map of the northern Billefjorden region. Most of the area is composed of Carboniferous and Permian sedimentary rocks. The Nordenskiöldbreen in Adolfbukta is underlined by crystalline rocks. Image in upper right corner presents schematic geological model of the Billefjorden trough. Both map and model modified after SVALEX Project resources (<http://svalex.net>).

The oldest structural unit of region consists of various crystalline (intrusive e.g. gabbro and metamorphic gneisses, amphibolites and schists) Precambrian rocks, often called the Hecla Hoek Succession (or Pre-Old Red rocks). The Devonian sedimentary rocks, represented mainly by sandstones and mudstones, are the dominant geological unit west of the fault. Due-east of the fault, the prevailing rocks are from Carboniferous-Permian units composed of various sedimentary rocks: conglomerates, sandstones, mudstones, limestones, coal (exploited until 1998), gypsum, anhydrites and dolomites.

The youngest geological unit, mainly covering the coastal zone, valley floors and proglacial zones is of Quaternary age and constitutes various sediments including



glacimarine muds, beach sands and gravels, intertidal deposits, glacial and glacialfluvial terrestrial deposits and sedimentary covers on slopes.

### 3.4.2.2. Glacial and periglacial geomorphology

The geomorphology of the surroundings of Petuniabukta and Adolfbukta is characterised by a diversity of glacial and periglacial landforms that is typical of deglaciated High Arctic settings and which have been extensively studied during last century (Table 3.1.).

SLATER (1925)	Glacial deposits and landforms (Nordenskiöldbreen, Ebbabreen, Svenbreen)
BOULTON (1976)	Nordenskiöldbreen frontal margin
PULINA (1982)	Karst-related phenomena in the surrounding of Bertilbreen
KŁYSZ (1983)	Main geomorphological features of Ebbadalen
KŁYSZ (1985)	Glacial landforms in Ebbabreen foreland
KARCZEWSKI et al. (1987)	Development of the marginal zone of Hørbyebreen and Petuniabukta tidal flat
KŁYSZ et al. (1988)	Late Quaternary glacial episodes and sea-level changes in N Billefjorden
RYGIELSKI (1988)	Geomorphology of anhydrite/gypsum rocks of the surrounding of Petuniabukta;
KŁYSZ et al. (1989)	Late Pleistocene and Holocene relief modelling of Ebbadalen and surrounding of Nordenskiöldbreen
RACHLEWICZ (1989)	Structure of braided river bars in Hørbyebreen outwash plain
KARCZEWSKI (1989)	The marginal zone of Hørbyebreen
BORÓWKA (1989)	Development and relief of Petuniabukta tidal flat;
KOSTRZEWSKI et al. (1989)	Rate of denudation of glaciated (Ebbaelva) and non-glaciated (Dynamiskbekken) catchments
STANKOWSKI et al. (1989)	General morphogenesis of Hørbyebreen and Ebbabreen valley systems
KARCZEWSKI and KŁYSZ (1994)	Glacial depositional landforms in the Svenbreen system
SAMOŁYK (2002)	Glaciofluvial transport and sediments in Ragnarbreen valley
KOSTRZEWSKI and ZWOLIŃSKI (2003)	Sedimentary environment of talus slopes
RACHLEWICZ (2003)	Geomorphology of Ebbabreen marginal zone
RACHLEWICZ <i>and</i> SZCZUCIŃSKI (2003)	Uplifted marine terraces in central Spitsbergen
PALUSZKIEWICZ (2003)	Aeolian transport in Ebbabreen valley
GIBAS et al. (2005)	Ebbabreen and Hørbyebreen marginal zones
KASPRZAK <i>and</i> EWERTOWSKI (2007)	Ragnarbreen ice-cored moraines
RACHLEWICZ et al. (2007)	Post-LIA glacier retreat
BUCHWAŁ (2008)	Human impact on mountain slopes
ZWOLIŃSKI et al. (2008)	Development and matter fluxes in tundra lakes

MAKOWSKA (2008)	Dynamics of glacialfluvial transport of Ebbaelva;
MAŁECKI (2009)	Post-LIA deglaciation in the surrounding of Petuniabukta
RACHLEWICZ (2009)	Floods and their impact on relief of the surrounding of N Billefjorden
STRZELECKI (2009)	The dynamics of suspended and solute sediment transport of Bertrambreen stream
SZCZUCIŃSKI et al. (2009)	Influence of post-LIA glacier retreat on sediment accumulation rates in Billefjorden
SZCZUCIŃSKA and MAZUREK (2009), SZCZUCIŃSKA (2011)	Functioning of Petuniabukta springs and seeps
CZAJKA (2010)	Deglaciation rates since the second half of 20 <sup>th</sup> century
RACHLEWICZ (2010)	Paraglacial modification of glacial and valley sediments
SZUMAN and KASPRZAK (2010)	Hørbyebreen moraine development
STRZELECKI (2011)	Rock surface resistance variability across rocky coastal zone in Adolfbukta
EWERTOWSKI et al. (2012)	Geomorphology and sedimentology of Ragnarbreen foreland
EVANS et al. (2012)	Hørbyebreen ( landforms of polythermal glacial landsystem)
MAZUREK et al. (2012)	Variability of water chemistry in tundra lakes
LONG et al. (2012)	Holocene RSL changes in Petuniabukta

*Table 3.1. Key environmental studies in the northern Billefjorden region*

During the LGM, Billefjorden supported a fast-flowing ice stream that drained the Svalbard-Barents Sea Ice Sheet (SBSIS) and which ultimately deposited extensive glacimarine sediments on continental slope west from Svalbard (INGÓLFSSON, 2011). It is widely accepted that the largest fjord system of Spitsbergen (Isfjorden), together with its tributaries, underwent a stepwise deglaciation between *ca.* 14,100 – 11,200 cal. yr BP (e.g. ELVERHØI *et al.* 1995; SVENDSEN *et al.* 1996; MANGERUD *et al.* 1998).

Recently, BAETEN *et al.* (2010) and FORWICK and VORREN (2011) used high resolution seismic data to reveal that deglaciation was interrupted by a couple of significant still-stands and readvances. The latest model of deglaciation of Isfjorden proposed by FORWICK and VORREN (2011) suggests that the ice front retreated only up to the mouth of the Billefjorden during the Allerød. This was followed by a *ca.* 25 km readvance in the Younger Dryas (YD). These findings are important for several reasons. First, as with MANGERUD and SVENDSEN (1990), they question the interpretation of BOULTON (1979) of much greater ice retreat into inner Billefjorden (based on 13,362-12,320 cal. yr BP shells in a glacial diamict at Kapp Ekholm, located *ca.* 4 km from the entrance to Adolfbukta). Secondly, the scale of the subsequent readvance may explain the retarded isostatic uplift during the YD (as seen by FORMAN *et al.* (1987) on Bröggerhalvöya). A similar slow RSL fall during this time is described by LANDVIK *et al.*

(1987) in the Ytterdalen area. LANDVIK *et al.* (1987) record is also in contradiction with onshore record (moraines of Scottbreen) presented by MANGERUD and LANDVIK (2007) which suggests very small or no glacier advance during the Younger Dryas.

A second study using swath bathymetry and gravity core data (BAETEN *et al.* 2010) focused on the deglaciation of Adolfbukta, which could act as a representative scenario for northern Billefjorden (Figure 3.11.). Their reconstruction comprises the following periods and events:

- A - Subglacial conditions before 11,230 cal. yr BP when Petuniabukta, Mimerbukta and Adolfbukta were covered by ice-streams. Subglacial erosion led to the formation of glacial lineaments found in the central parts of the fjords.
- B - Rapid deglaciation 11,230 – 11,200 cal. yr BP. Rapid retreat is inferred from about 30 recessional moraines found between the axis of Billefjorden and the central part of Adolfbukta which suggests frontal recession of *ca.* 170m a<sup>-1</sup> for about 30 years.
- C – A period of diminished glacial activity 11,200 - 7930 cal. yr BP that coincided with early Holocene warming. At this time Nordenskiöldbreen was a tide-water glacier but was probably smaller than present. The neighbouring Pollockbreen was probably fully melted or at least retreated several hundred meters north and the exposed valley was filled with unstable deposits that were a source of sediment plumes formed by glacier rivers reached the fjord. The warm climate restricted sea-ice formation and may have encouraged the formation of wide beaches in Petuniabukta and Adolfbukta.
- D – Increased glacier activity 7930 - 5470 cal. yr BP caused by regional climate cooling. Nordenskiöldbreen grew and started to produce significant amounts of icebergs. Sea-ice conditions became harsher.
- E – A second period of increased glacier activity 5470 - 3230 cal. yr BP Nordenskiöldbreen continued to grow with intensified calving.
- F – The Holocene glacial maximum period 3230 cal. yr BP – AD 1900. During this climate cooling Nordenskiöldbreen began its biggest readvance during the Holocene. The period is characterised by very harsh sea-ice conditions which bounded surrounding fjords, often for the entire year.
- G – A period of post-LIA retreat AD 1900 – present. After reaching the Holocene maximum extent, Nordenskiöldbreen started a retreat that has persisted to present (see Figure 3.13. for post-LIA glacier retreat rates).

# **Conceptual model of Adolfbukta glacial history during the Late Weichselian and the Holocene modified after Baeten et al. (2010)**

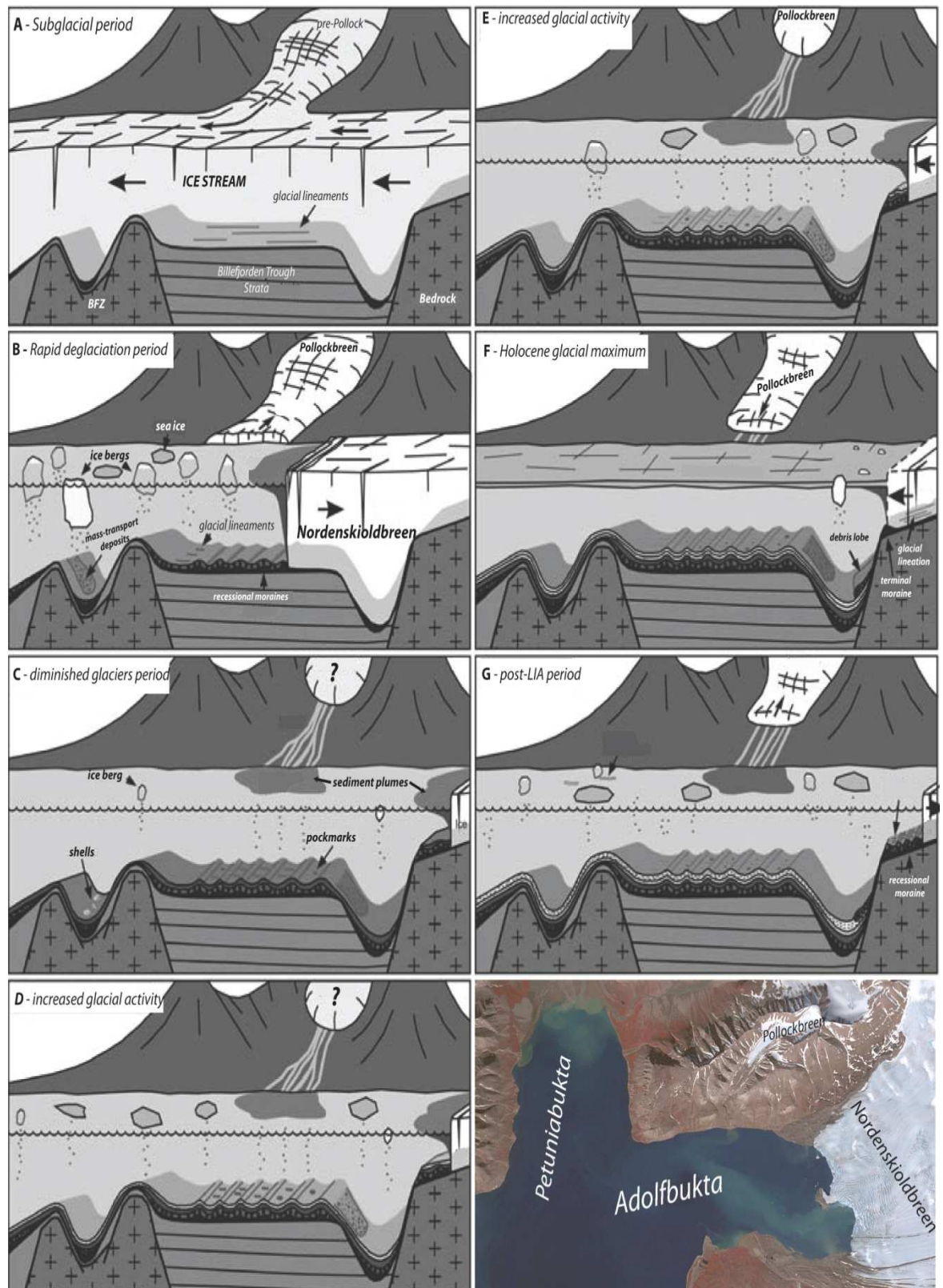


Figure 3.11. Model of Late Weichselian and Holocene glacial episodes in northern Billefjorden adapted after BAETEN et al. (2010).

The most famous onshore record of regional glacial history is known from Kapp Ekholm, where four main glacial/deglacial cycles are found; one Late Saalian, and three in

the Weichselian (MANGERUD and SVENDSEN 1992; MANGERUD *et al.* 1998). In Petuniabukta, however, glaciations curves have also been established for Hørbyedalen and Ebbadalen.

According to KARCZEWSKI and RYGIELSKI (1989) four till layers found in the exposure located at the foot of Gizehfjellet suggests that Hørbyebreen advanced during the early 'Billefjorden Stage' (30,578 – 31,139 cal. yr BP). This was followed by significant retreat and marine transgression around 25,096 cal. yr BP. The next glacier advance culminated around 11,000 cal. yr BP (the young Billefjorden Stage in Kapp Ekholm). These authors suggest that during the Holocene, Hørbyebreen experienced a third advance which started around 1000 cal. yr BP and culminated during the LIA. In Ebbadalen, KŁYSZ *et al.* (1989) and STANKOWSKI *et al.* (1989) proposed evidence for five glacial episodes - two Weichselian and three of Holocene age (Figure 3.12.) although it must be noted that age constraints on these episodes is limited.

Currently, the study area has a smaller degree of glaciation than the rest of the archipelago because of its near-continental climate. The Petuniabukta drainage area (*ca.* 170 km<sup>2</sup>) is glaciated by *ca.* 33% (with the largest Ebbabreen covering 22.8 km<sup>2</sup>). The Adolfbukta catchment (drainage area 265 km<sup>2</sup>) is dominated by Nordenskiöldbreen which covers *ca.* 80% of the basin (212 km<sup>2</sup>), whilst other glaciers in the catchment (Pollockbreen, Matthewbreen and Geritbreen) together cover just *ca.* 6 km<sup>2</sup>.

Present-day glaciers have retreated since the end-of the LIA (which occurred at the turn of 19<sup>th</sup> and 20<sup>th</sup> century) when the majority of them were probably at their Holocene maximum. Several authors (RACHLEWICZ *et al.* 2007; MAŁECKI 2009; CZAJKA 2010) studied post-LIA glacier retreat in the Petuniabukta region and show large variability in retreat rates (Figure 3.13.). For instance, Ragnarbreen retreated about 1500 m between 1900 – 2008 whereas, at the same time, the cold-based Bertrammbreen located on the Sporehogda massif retreated only about 200 m. Overall, the glaciated area in Petuniabukta decreased by almost 30% from 79 km<sup>2</sup> in 1900 to 56 km<sup>2</sup> in 2008 (MAŁECKI 2009).

The post-LIA retreat rates range from 1 to 52 m/year for land-terminating glaciers and 35 m/year for the marine-terminating Nordenskiöldbreen. Small valley glaciers (Bertil, Elsa, Ferdinand, Sven and Pollockbreen) whose axis lengths were reduced by 30-69%, appear more sensitive to current climate warming. In the case of larger glaciers i.e. Hørbyebreen, Ebbabreen and Ragnarbreen, axis length reductions were smaller (10-20%) (MAŁECKI 2009). According to MAŁECKI (2009), the mean annual retreat rate between 1900 - 1960 was 7.5 m for glaciers that still occupied the valley floors.



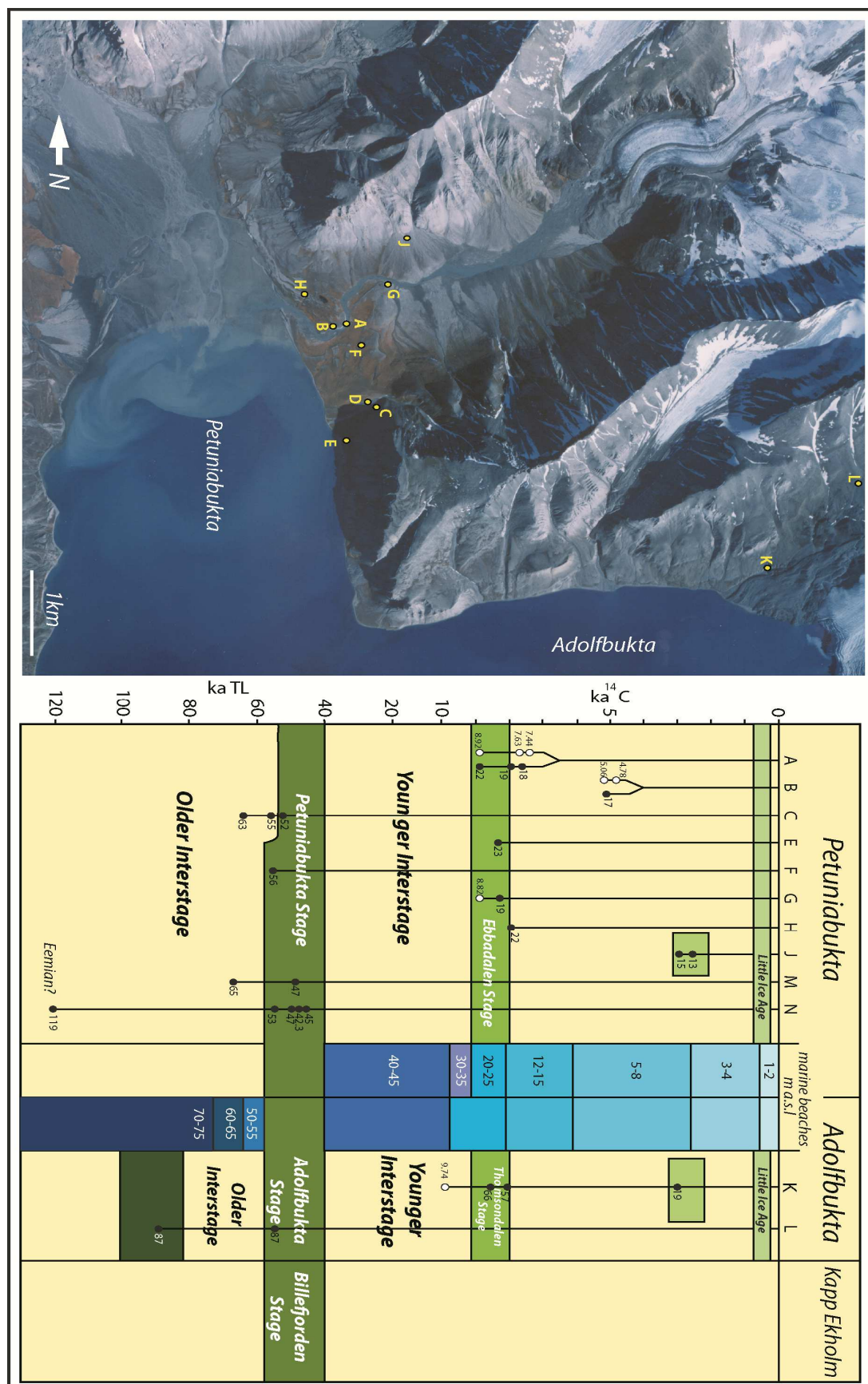


Figure 3.12. Age correlation of marine and glacial sediments in Petuniabukta and Adolfbukta based on KŁYSZ et al. (1989). Letters on the map indicate exposure sites from where samples were taken. Black dots on a graph indicate sediments dated by the thermoluminescence method, white dots indicated radiocarbon dated marine shells.

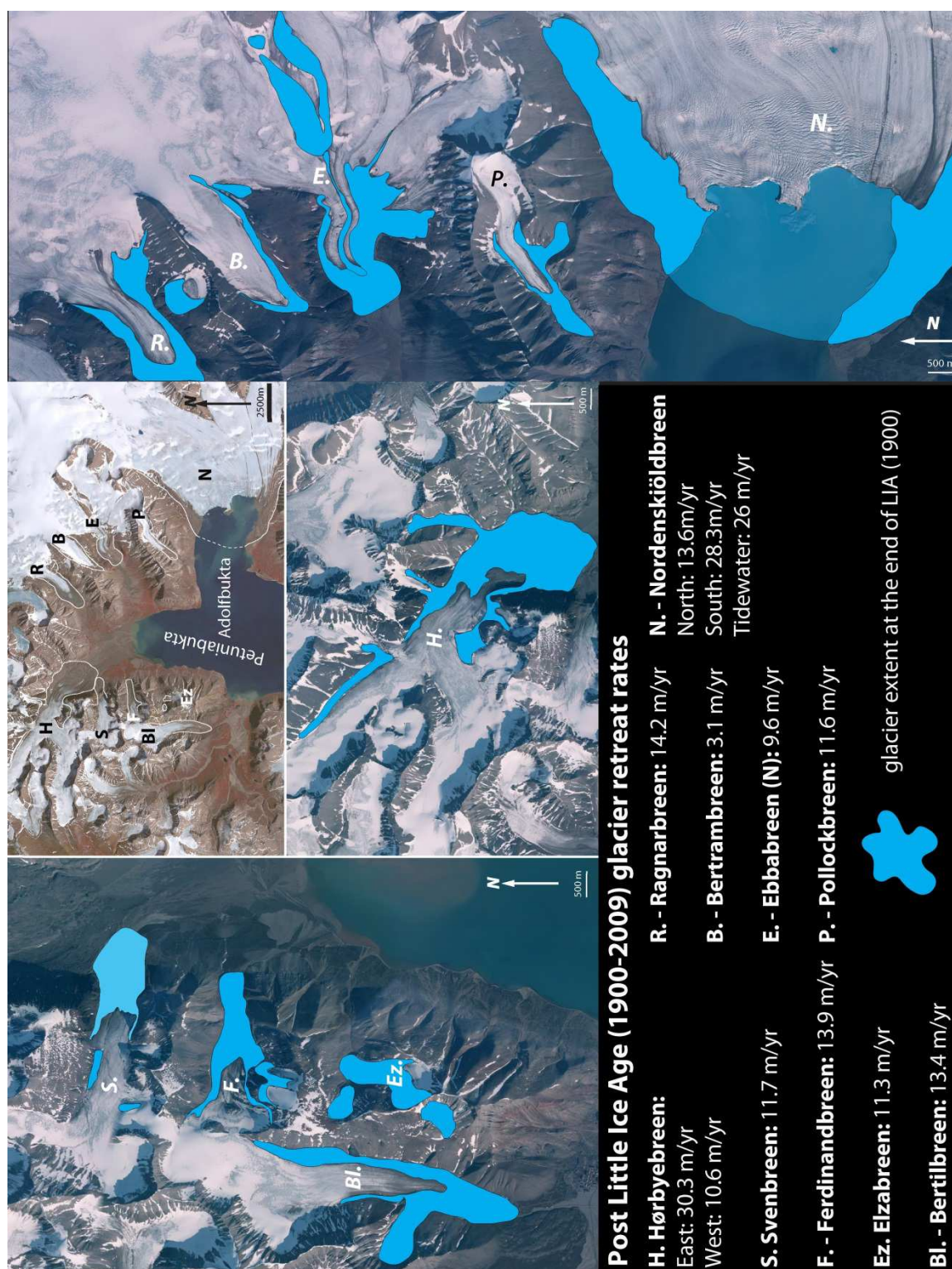


Figure 3.13. Summary of glacier retreat rates since the beginning of the 20<sup>th</sup> century based on the most recent glacier front extent delimited using aerial images taken by Norwegian Polar Institute in the summer of 2009 (source: this study).

An important geological imprint on the study area's relief is the relatively low resistance of the sedimentary rocks that comprise the majority of mountain massifs, which are very prone to frost weathering. The mountains surrounding the bays are characterised by flat-topped peaks and much gentler slopes than those known from



western Spitsbergen (whose name literally means ‘pointed mountain’). On the other hand, frost shattering has led to the formation of unstable talus slopes made of coarse, sharp-edged debris which are a characteristic landscape element along the southeast coast of Petuniabukta (Figure 3.14.a). During the Holocene valley slopes were extensively remodelled by periglacial (frost sorting, solifluction, rock creep) and paraglacial (gulling, slumping) processes that modified or removed traces of former glacial activity.

The Ebbadalen (Figure 3.14.d) is an excellent example of the paraglacial transformation of a glacial landscape that has occurred in many valleys of Svalbard, with fluvial and slope processes reducing the geomorphological role of glacial processes to a secondary role. Glacial landforms are now either covered by extensive alluvial fans (>10 m thick) which formed during the Holocene and overlie the lower parts of valley slopes and valley floor or are almost completely eroded by the braided (proglacial zone) and meandering (from the middle part of the valley) Ebbaelva. In addition, numerous erratic boulders that are spread across the valleys and flat mountain peaks are actively being reshaped by aeolian weathering.

The largest fluvial feature in the study site is an extensive outwash plain formed by glacier rivers that drain Hørbyebreen and Ragnarbreen and which combine into a vast tidal flat in the north of Petuniabukta (Figure 3.14.b). The Hørbyebreen-Ragnarbreen outwash-tidal flat system is the biggest secondary sediment storage of study area. In the case of Ragnarbreen, part of the sediment is stored in a proglacial lake that developed in last 50 years (presently over 1000 m long, 400 m wide) (EWERTOWSKI *et al.* 2012). This accumulation of glaciofluvial and marine sediments constitutes the most important source of aeolian sediments transported during dust storms which are the dominant sediment supplier to the fjord in the autumn months, following the freeze-up of rivers and streams. In some locations (e.g. Wordiekammen, Løvehovden) chemical weathering of limestone, anhydrite/gypsum and dolomite outcrops have formed karstic features including collapsed caverns and dolinas/sink-holes (Figure 3.14.g). Some miniature karstic landforms are common along the anhydrite/gypsum rocky section of the Petuniabukta coast. The most geomorphologically active parts of the study area are the proglacial zones that surround the present glaciers. Of the seven glaciers surrounding Petuniabukta, the most important for coastal sediment supply is the marginal zone of Hørbyebreen (Figure 3.14.e) which is the largest land terminating glacier in the study area and which probably underwent a surge in the first half of 20<sup>th</sup> century (KARCZEWSKI 1989).

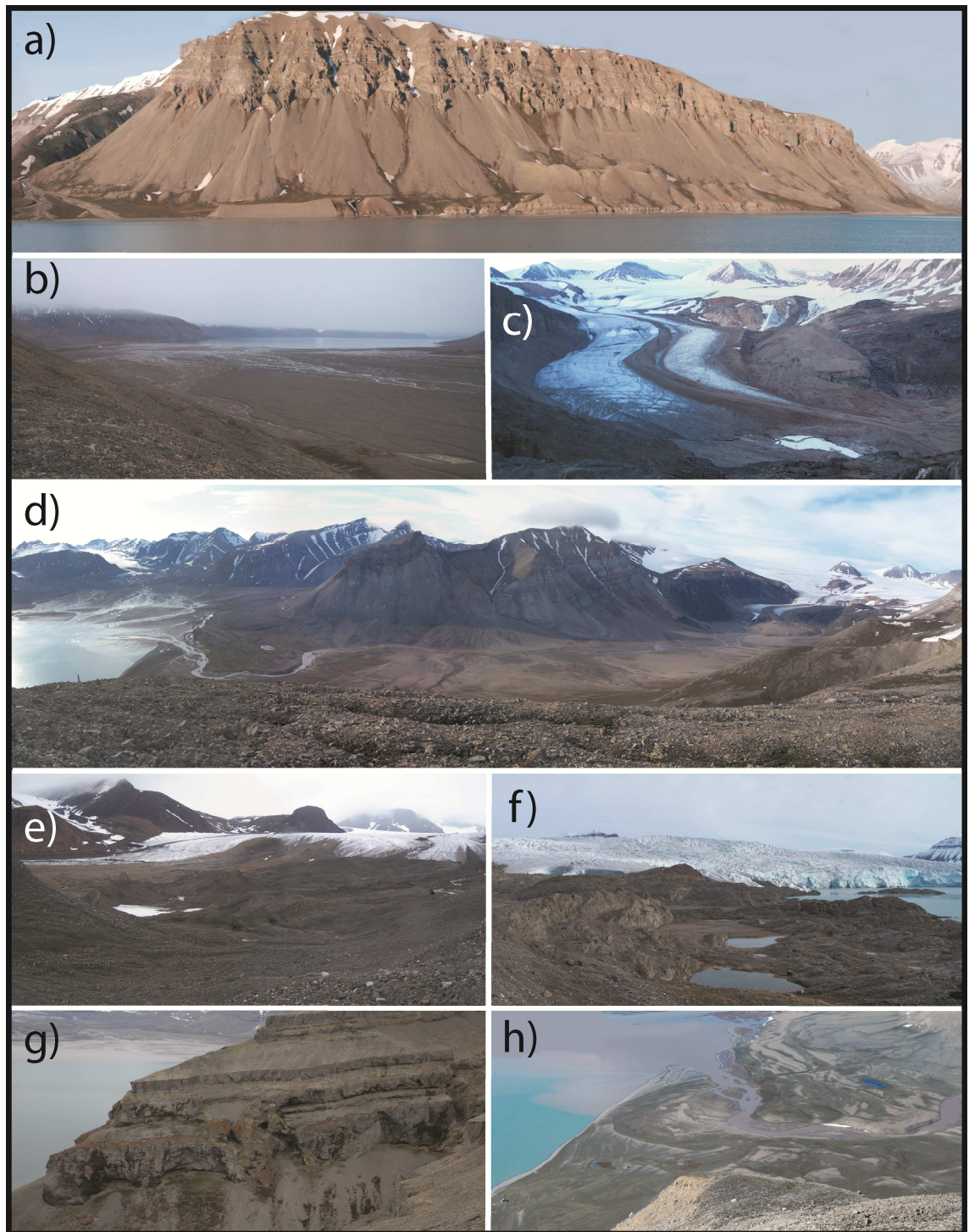


Figure 3.14. Major geomorphological features in the surroundings of Petuniabukta and Adolfbukta. a) Talus slopes on the western slopes of the Wordiekammen massif; b) Hørbyebreen outwash plain; c) Ebbabreen with well-defined medial moraine and debris covered snout; d) overview of Ebbadalen; e) Ice-cored moraines and eskers in front of Hørbyebreen; f) Metamorphic roches moutonnées, Nordeskioldbreen; g) Karstic sinkhole and small collapsed caverns in the upper part of Wordiekammen massif h) Coastal lowland with Ebba River cut through uplifted marine deposits. Photographs by Tom Wawrzyniak 2008-2010.

Landform assemblages seen in the foreland of Hørbyebreen are typical for many Svalbard polythermal glaciers characterised by well-developed subglacial bedforms (flutings, eskers) lying up-valley from controlled moraines (*sensu* EVANS 2009) or ice-

cored moraines, pitted with kettle holes, hollows and debris flows. The Hørbyebreen moraine arc is composed of frontal moraine ridges (up to 25 m high) and lateral moraines (up to 150 m high), and is subject to intensive down-wasting, enhanced by melting of ice-cores (EVANS *et al.* 2012). This hummocky terrain is heavily cut by numerous melt-water streams that carry sediments to an extensive outwash plain that grades into a gently sloping tidal flat. As reported by RACHLEWICZ (2009), mass movements on the slopes of ice-cored moraines is the most effective process around other neighbouring glaciers, although the sediments derived from erosion and mass wasting must pass through more intermediate storage systems before reaching the fjord.

In the case of second largest glacier - Ebbabreen (Figure 3.14.c) - large parts of the LIA moraine belts have already been eroded by a system of braided river channels, which forms an extensive backwater in the middle of Ebbadalen. In the case of small, cold-based glaciers such as Elzabreen, Ferdinandbreen and Svenbreen (western coast of Petuniabukta) or Bertrambreen, sediment delivery to the coastal zone is limited by either geological thresholds (e.g. the bedrock steps in Bertrambreen, Svenbreen) or by the rapid rate of retreat and a reduction in sediment production. Sediments in source-to-sink cascade systems developed in other small valley glaciers in the vicinity (i.e. Bertilbreen (draining to Mimerbukta) and Pollockbreen (draining to Adolfbukta) can reach the coast relatively easily via steep slopes and short distances to the fjord.

The Adolfbukta landscape is dominated by the tide-water glacier of Nordenskiöldbreen, which has an area of 212 km<sup>2</sup> and constitutes approximately 60% of the glaciated area in the region (MAŁECKI 2009). In northern Adolfbukta, recently exposed roches moutonnées cut in resistant metamorphic outcrops are covered with a thin surficial layer of glaciﬂuvial sediments.

### 3.4.3 Fjord processes

Petuniabukta consists of two basins: a deeper basin along the eastern coast (maximum depth *ca.* 60 m) and a western basin (maximum depth *ca.* 50 m) divided by a bedrock ridge that causes a shallowing in the central part of the bay (Figure 3.15.). Both bays are semidiurnal microtidal environments with a maximum tide range of 1.5 m, a low-energy wave climate, and are characterised by lengthy periods of sea ice cover forming during the fall.

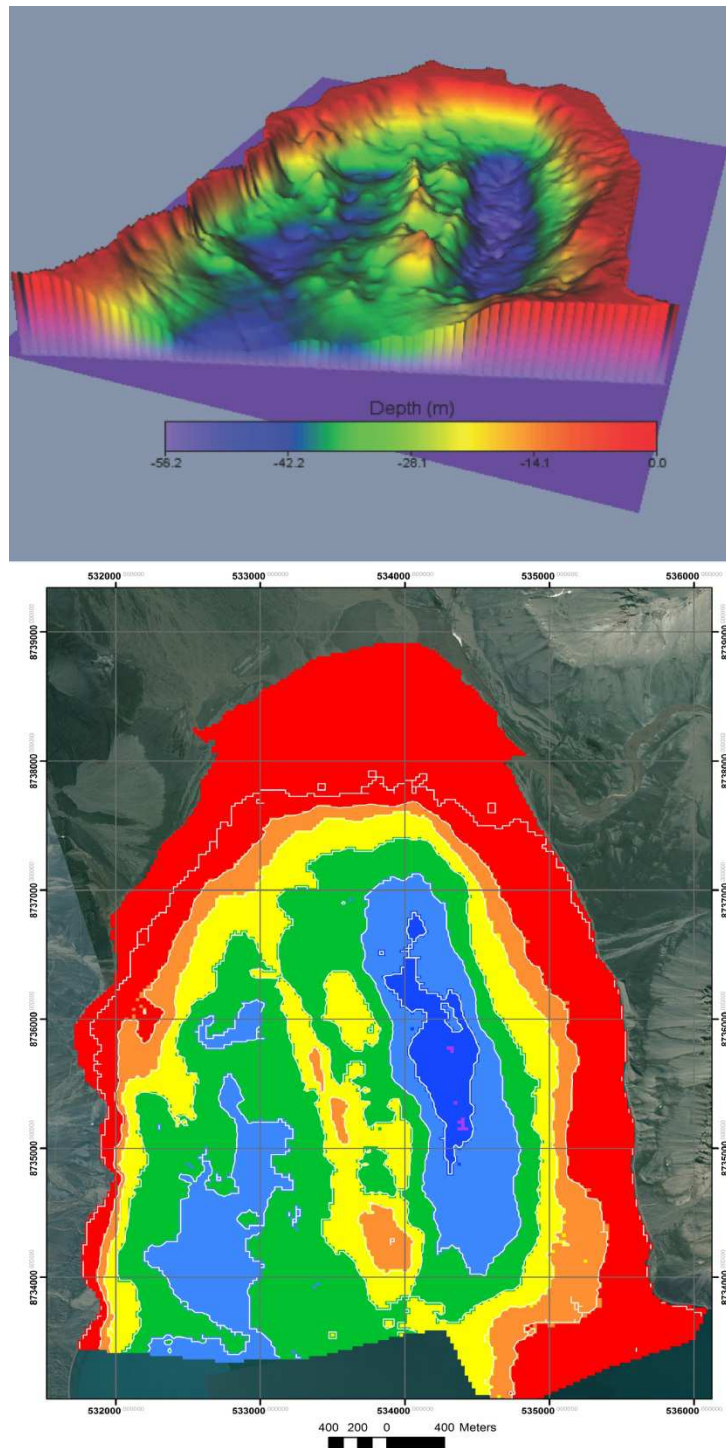


*Figure 3.15. Bathymetry of Petuniabukta based on sonar sounding carried out during 2009 fieldwork. Note the two basins divided by a longitudinal ridge that is probably of tectonic origin. Note a striking difference in shallowness of nearshore zone along the eastern and western coasts of the bay. The sharp transition from shallow to deep water observed along the western coast is associated with the disturbance of bedrock by the tectonic fault (Billefjorden fault).*

After break-up (normally May/June), floating sea ice is rapidly removed from bays. Under appropriate wind conditions, sea ice can be cleared in only a matter of hours. During the summer, the coastlines (especially in Adolfbukta) are affected by floes and



growlers of debris-rich glacier ice which are sourced by calving from the Nordenskiöldbreen.

The bay bathymetry was surveyed by SZCZUCIŃSKI (2004) and repeated in more detail again during this study. Sonar sounding carried out during the summer 2009 revealed that the eastern basin is characterised by a gentle morphology, whereas the seafloor along the mid-bay ridge and western basin has a more varied relief. An important morphological change occurs in the northern part of the bay where the tidal flat ends with a very sharp, steep step. The adjacent Adolfbukta was recently surveyed using a Kongsberg Maritime Simrad EM 300 multibeam echo sounder by researchers from Trømso University (BAETEN *et al.* 2010), revealing a whole mosaic of glacial landforms including glacial lineations and recessional moraines (Figure 3.16.).

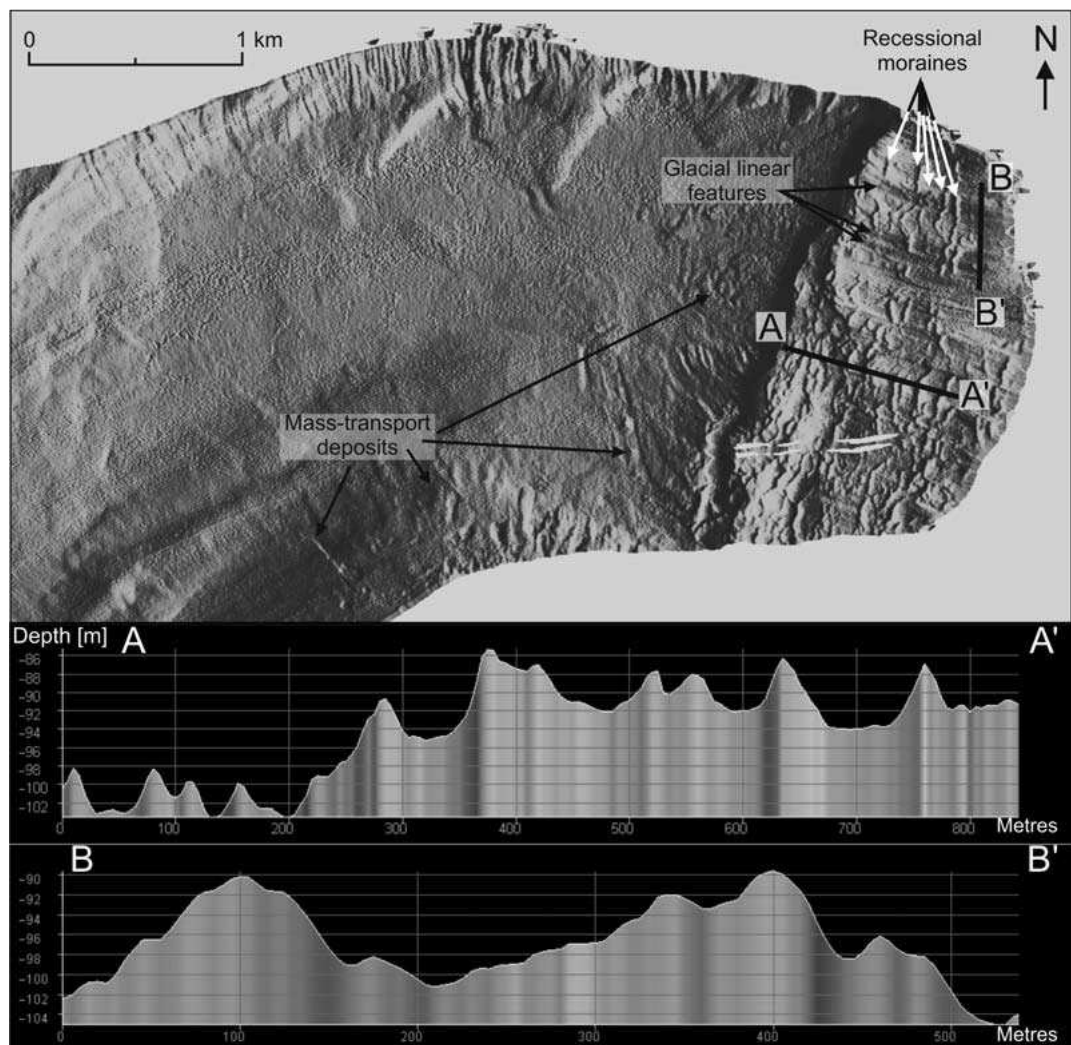


Figure 3.16. Seafloor map of Adolfbukta and profiles across submarine landforms left by Nordenskiöldbreen during post-LIA deglaciation. Profile A–A' crosses moraines; profile B–B' crosses glacial linear features. Source: BAETEN *et al.* (2010).

Adolfbukta is much deeper than Petuniabukta and also can be divided into two parts: a shallower (up to 100 m depth) part (crystalline rock terrace) extending

approximately 2 km from the present-day front of Nordenskiöldbreen, and second deeper area over 200 m water depth (the deepest basin of Billefjorden).

Wave action in both bays is limited by the narrow entrance to the fjord and restricted to the ice-free summer months. The surrounding topography influences local winds that exert a strong influence on wave activity (Figure 3.9.c). Thus, the only direction allowing development of significantly long-fetch waves is from the south or south-west. During the fieldwork in northern Adolfbukta occasional high waves were observed, caused by calving and ice-berg roll in Adolfbukta. The biggest icebergs observed in Adolfbukta 2008-2010 summer seasons were approximately 10 to 15 m long.

The influence of freshwater influx on surface circulation is characteristic for fjord environments (GILBERT 1983; SYVITSKI *et al.* 1987; ZAJĄCZKOWSKI *et al.* 2004). Major glacial rivers in Petuniabukta and subglacial or englacial channels of Nordenskiöldbreen deliver significant amounts of suspended sediments via sediment plumes that gradually depositing the sediment load across the fjord bottom through flocculation. A detailed description of processes controlling rates of sedimentation in both bays is provided by SZCZUCIŃSKI *et al.* (2009).

#### 3.4.4 Local climate

At the head of Billefjorden, average annual precipitation is typically less than 200 mm, and the mean annual air temperature is *ca.*  $-6.5^{\circ}\text{C}$  with air temperatures above  $0^{\circ}\text{C}$  between June and the middle of September (HANSEN-BAUER *et al.* 1990). The warmest months are July and August with a maximum annual temperature of  $5-6^{\circ}\text{C}$ , but in the last decade this has reached as high as  $7^{\circ}\text{C}$  (RACHLEWICZ, 2003). In comparison with the Svalbard Lufthavn station, located in Adventfjorden (central Billefjorden), winter temperatures are *ca.*  $3.3^{\circ}\text{C}$  lower and summer temperature are up to  $1.3^{\circ}\text{C}$  higher (RACHLEWICZ and STYSZYŃSKA 2007). RACHLEWICZ (2009) applied MARSZ'S (1995) oceanity index and classified the study area as belonging to the zone of sub-oceanity conditions characterised by higher amounts of mixed and solid precipitation than along the western and south-western coast of Spitsbergen (Figure 3.17.).

Frozen ground conditions are extensive in Spitsbergen valley systems, with older permafrost in mountain massifs and younger permafrost underneath valley floors following deglaciation. As noted by RACHLEWICZ (2009), one of the zones of potential discontinuity or even absence of frozen ground are the snouts and proglacial zones of polythermal glaciers (e.g. Hørbyebreen in northern Petuniabukta). The active layer

thickness at the end of summer season varies between 0.9 – 1.2 m, however GIBAS *et al.* (2005) detected deeper thawing (up to 2.5 m) using DC resistivity surveys on the Hørbyebreen and Ebbabreen outwash plains and moraine belts.

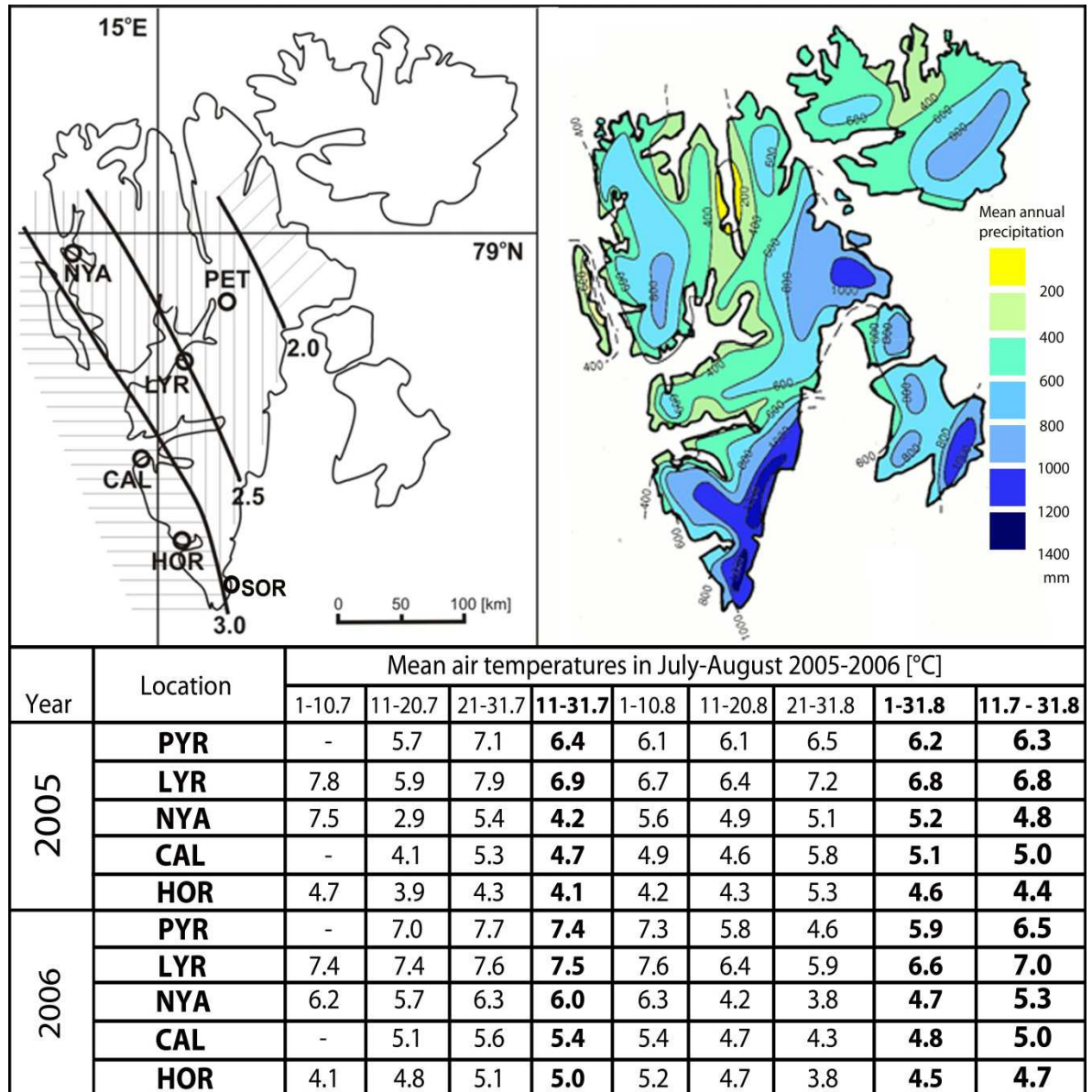


Figure 3.17. Climatic conditions in Petuniabukta against a background of climate conditions recorded in weather stations located along western coast of Spitsbergen. a) Climatic oceanicity zones of Spitsbergen modified after RACHLEWICZ (2009), based on MARSZ (1995) oceanicity index distribution. Circles indicate the location of former coastal studies on Spitsbergen discussed in this study: PET- Petuniabukta, Billefjorden (this study), LYR – Longyearbyen, Adventfjorden (LØNNE and NEMEC 2004), NYA – NyÅlesund, Kongsfjorden (MOIGN and HÉQUETTE 1985; HÉQUETTE 1992; MERCIER and LAFFLY 2005), CAL – Calypsostranda, Bellsund (ZAGÓRSKI 2011; ZAGÓRSKI *et al.* 2012), HOR - Hornsund (MARSZ 1996), SOR – Sørkappland, open coast of Barents Sea (ZIAJA *et al.* 2009), horizontal lines – oceanic conditions, vertical lines – sub-oceanic conditions, oblique lines – continental conditions; c) Mean annual precipitation [mm] on Svalbard based on HAGEN *et al.* 1993; d) 10-day mean air temperatures between July-August 2005-2006 in study area (PET), LYR – Central Spitsbergen, NYA – NW Spitsbergen, CAL – SW Spitsbergen, HOR – SW Spitsbergen based on PRZYBYLAK *et al.* (2006, 2007) modified after MAŁECKI (2009).

A detailed study of the active layer in summer was conducted along the eastern coast of Petuniabukta in years 2000 -2003 (RACHLEWICZ and SZCZUCIŃSKI 2008). Their



study indicated that, in comparison with sites located along western of Spitsbergen, the active layer here is influenced less by precipitation and more strongly by air temperature. During days with temperature above freezing, the depth of the permafrost table was lowered about 1 cm per day. Snow cover is typically thin, reaching *ca.* 0.3 m on the ice-bounded fjord and 0.6-0.9 m in the valleys, although wind action accumulates 1-2 m deep snowdrifts at the bottom of cliffs.

### 3.5. Sediment supply pathways to the Petuniabukta coastal zone

From the perspective of sediment type and sediment supply to the coastal zone, I have divided the study into the following zones (Figure 3.18.):

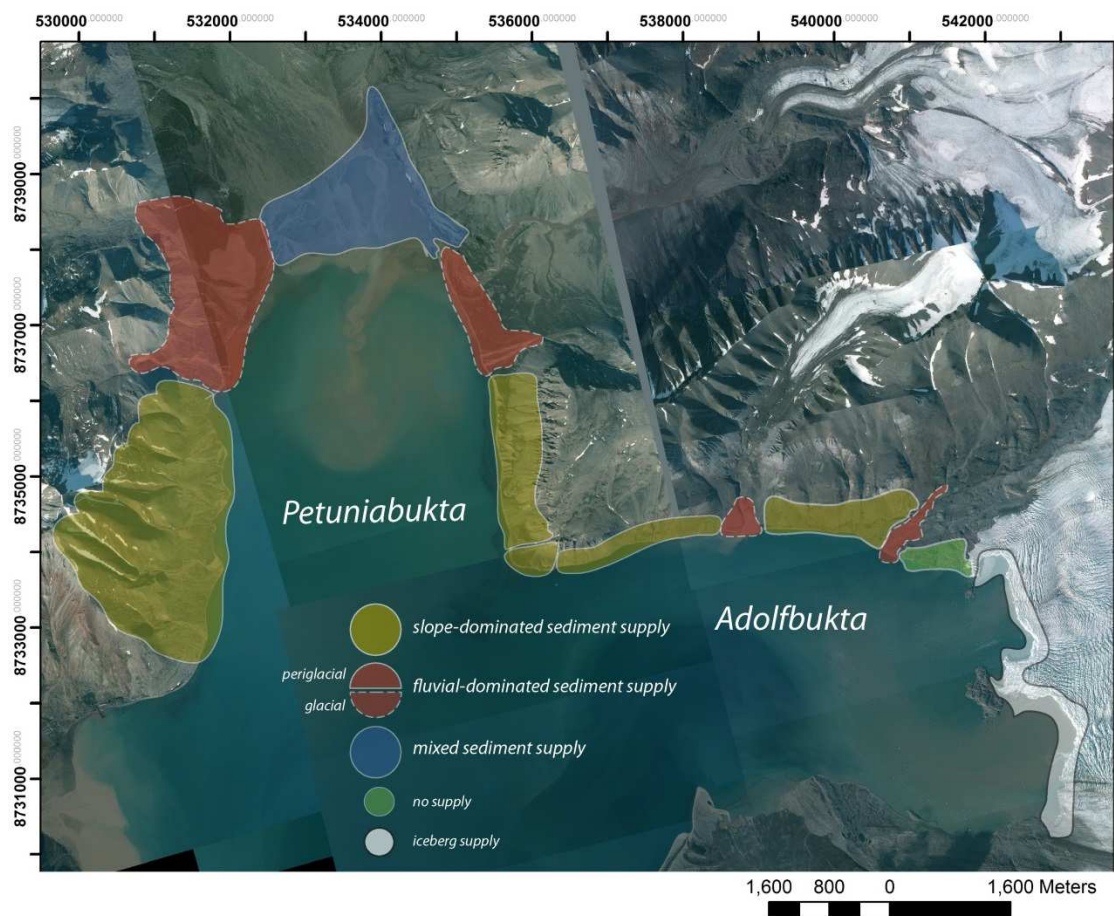


Figure 3.18. Coastal division based on the dominant sediment supply sources along bays.

- i) A slope-dominated sediment supply zone, characteristic for northern Adolfbukta and south western Petuniabukta.
- ii) A fluvial-dominated sediment supply zone which can be further divided into:
  - A periglacial-fluvial dominated subzone (eastern Petuniabukta)
  - A glaciofluvial dominated subzone (western Petuniabukta)

iii) A mixed-type characteristic for the whole northern coast where sediments are delivered by rivers (Svenelva, Hørbyeelva, Ragnarelva and Ebbaelva) but also from the reworking of modern and uplifted marine deposits by tides in the Ebbaelva estuary and adjacent tidal flat).

In addition a “no sediment delivery” zone can be identified, characteristic of the area covered by roches moutonnées in northern Adolfbukta and the area adjacent to Nordenskiöldbreen.

### 3.6 Chapter summary

This chapter has detailed the background information regarding the physical setting of the study area and introduced the coastal sites located in the Petuniabukta region chosen for further analysis. The key points are:

- The Svalbard bedrock geology is complex and records several phases of folding, thrusting and faulting. This makes the bedrock weak in places and liable to weathering and erosion.
- At the Last Glacial Maximum, the former Svalbard-Barents Sea Ice Sheet covered the entire archipelago, with a major ice streams draining the fjord system. The history of glacial unloading and isostatic rebound can be inferred by the pattern of relative sea-level change reconstructed on the basis of elevation of raised beaches.
- In areas not covered by glaciers, the Svalbard geomorphology is dominated by permafrost and periglacial processes with abundant rock glaciers, ice wedges, pingo systems, and patterned ground. Frozen ground conditions are extensive and vary from thick and continuous permafrost in the mountain ranges to relatively thin and recently developed permafrost in glacial valleys.
- Coastal depositional landforms in Svalbard include alluvial fan-deltas, beaches, pocket beaches, barriers, barrier islands and spits that separate coastal lagoons.
- The mean annual air temperature on Svalbard is about  $-6^{\circ}\text{C}$  at sea level and approximately  $-15^{\circ}\text{C}$  in the mountains. Svalbard is characterised by relatively milder temperatures compared to other High Arctic regions of an equivalent latitude because of the moderating influence of the West Spitsbergen Current.
- Twentieth century climate data indicate that Svalbard is sensitive to the North Atlantic Oscillation which influences temperatures as well as storminess and sea-ice extent.
- The main study area of the thesis is introduced. Located at the head of Billefjorden, the field area includes the coastlines that abut the inner part of Petuniabukta and the neighbouring Adolfbukta, located in central Spitsbergen.
- A detailed introduction to the coastal sections selected for analysis over seasonal (2008-2010), decadal (1900-2009) and millennial (Late Holocene) timescales is provided.

The results of fieldwork carried out along those coasts will be described over next four chapters (Chapters 4-7) and interpreted in Chapter 8.

# **Chapter 4:**

## **ANNUAL TIMESCALES**

### **Processes operating on the present-day sedimentary coasts**

## 4.1 Introduction

Chapter I identified five research questions to be answered during this PhD project. This chapter addresses the first of these, specifically:

*What is the interannual morphological variability of the gravel-dominated barriers along Petuniabukta between 2008 and 2010?*

To answer this question the following objectives were addressed:

- I) to identify the processes that control the modern barrier micro-relief in Petuniabukta, and;
- II) to describe the interannual changes of barrier profile between 2008 and 2010.

## 4.2 Background – factors influencing the stability of Arctic barrier coasts

Studies along Arctic coastal barriers thrived five decades ago and led to detailed descriptions of seasonal micro-relief changes and advances in terminology (e.g. REX 1964; HUME and SCHALK 1964, 1967a,b; ZENKOVICH 1967; KING and BUCKLEY 1968; MCCANN and OWENS 1969; GREEN 1970; OWENS and MCCANN 1970; MCCANN and TAYLOR 1975; DIONNE 1976; ROSEN 1978; TAYLOR 1978, REINSON and ROSEN 1982). The textbook depiction of polar depositional coasts known from this literature is of a narrow barrier composed of poorly sorted and gravel-dominated sediments that is sculptured by sea-ice, nival and periglacial processes, and reshaped in ice-free months by limited wave action, tidal action and permafrost thawing (FORBES and TAYLOR 1994; TRENHAILE 1997). However, the scale of changes which have recently impacted polar coastal environments calls into question the applicability of these previous studies which, for the most part, were carried out in the coldest decades of the 20<sup>th</sup> century (BYRNE and DIONNE 2002). Thus, it is highly probable that the image of a protected, low-energy environment ascribed to Arctic barriers results rather from the severity of cold weather conditions encountered by researchers at the time of observations (1960's-1970's) than their real morphodynamics.

HARRY *et al.* (1983) claimed that the fact that many Arctic coastal studies were carried out in ice-limited fetch conditions has distorted our understanding of polar coasts which for many years has become deeply-ingrained in conventional wisdom as a low-energy environment. Their study along Sachs Harbor Spit on Banks Island (CAA) suggested a rapid adjustment of Arctic beach to the release of unconsolidated sediments and storm events in the form of dynamic landform adjustment and high coastal erosion

rates. HÉQUETTE and RUZ (1991) also documented a dynamic interplay between sediment release from ice-rich bluffs and the migration of mixed sand-gravel spits and barrier islands along coasts of Yukon, enhanced by storm overwashing. At Point Barrow (Alaska), HUME and SCHALK (1967) recorded a removal of the equivalent of two decades of normal beach sediment transport during one storm. As noted in Chapter 2, low-frequency high magnitude storms in favourable conditions (lack of sea-ice protection) can lead to catastrophic erosion and storm surge encroachment across significant distances (e.g. MCCANN 1972; REIMNITZ and MAURER 1979).

Recent studies on the impacts of storm surges on Arctic coasts have revealed more complex responses. PISARIC *et al.* (2011) and KOKELJ *et al.* (2012) emphasised the long-lasting and often irreversible effects of extreme storms on the functioning of deltaic shorelines in the Mackenzie Delta. Conversely, in one of the most comprehensive studies of Arctic barrier morphodynamics carried out on Cornwallis Island, ST. HILLAIRE-GRAVEL *et al.* (2011) demonstrate considerable resilience of polar gravel-dominated barriers to storm events and the ephemeral character of storms on coastal morphology. This difference in views is most likely related to contrasts in the range of wave exposure of the studied coastlines to storm waves. The Mackenzie Delta represents an open-sea site, whereas Cornwallis Island is located in a more sheltered setting.

In Kongsfjorden, NW Spitsbergen, HÉQUETTE and RUZ (1990) investigated the annual (summer 1983) and interannual (1983-1985) morphological changes of a gravel-dominated barrier formed along the outwash plains of Midre- and Vestre- Lovénbreen. During the summer, the barrier experienced a cycle of micro-relief changes of amplitudes that range between 0.1 – 0.3 m. The main process observed in this study, which is characterised by a barrier coast that is breached by glacial-fed rivers, is the formation of a *ca.* 0.2 m high gravel-bar, that due to increased sediment supply from glacial-fed rivers, migrates across the intertidal zone and increase in elevation by up to *ca.* 0.5 m, often evolving into the swash bars. These features are then reworked by waves and longshore currents to supply gravel-dominated barriers that then move seaward. In the subsequent open-water season, freshly formed barriers were observed to be eroded by glaciofluvial streams with eroded sediments forming microdeltas. One of the key findings of their study is the strongly interannual irregularity in barrier evolution with phases of seaward and landward migration controlled by glaciofluvial processes that supply sediments from proglacial zones and from erosion of former coastal landforms.

### 4.3 Methods

Fieldwork was completed during three summer seasons (July-August 2008 and 2010) and one winter fieldwork (April 2009). A combination of methods has been used, including DGPS barrier profiling, geomorphological mapping of barrier micro-relief, time-lapse camera observations of coastal state and analysis of local weather and sea-ice conditions. Seventeen barrier profiles were selected for change analysis. Eleven profiles were chosen along the eastern coast and six profiles along the western coast (Figure 4.1.).

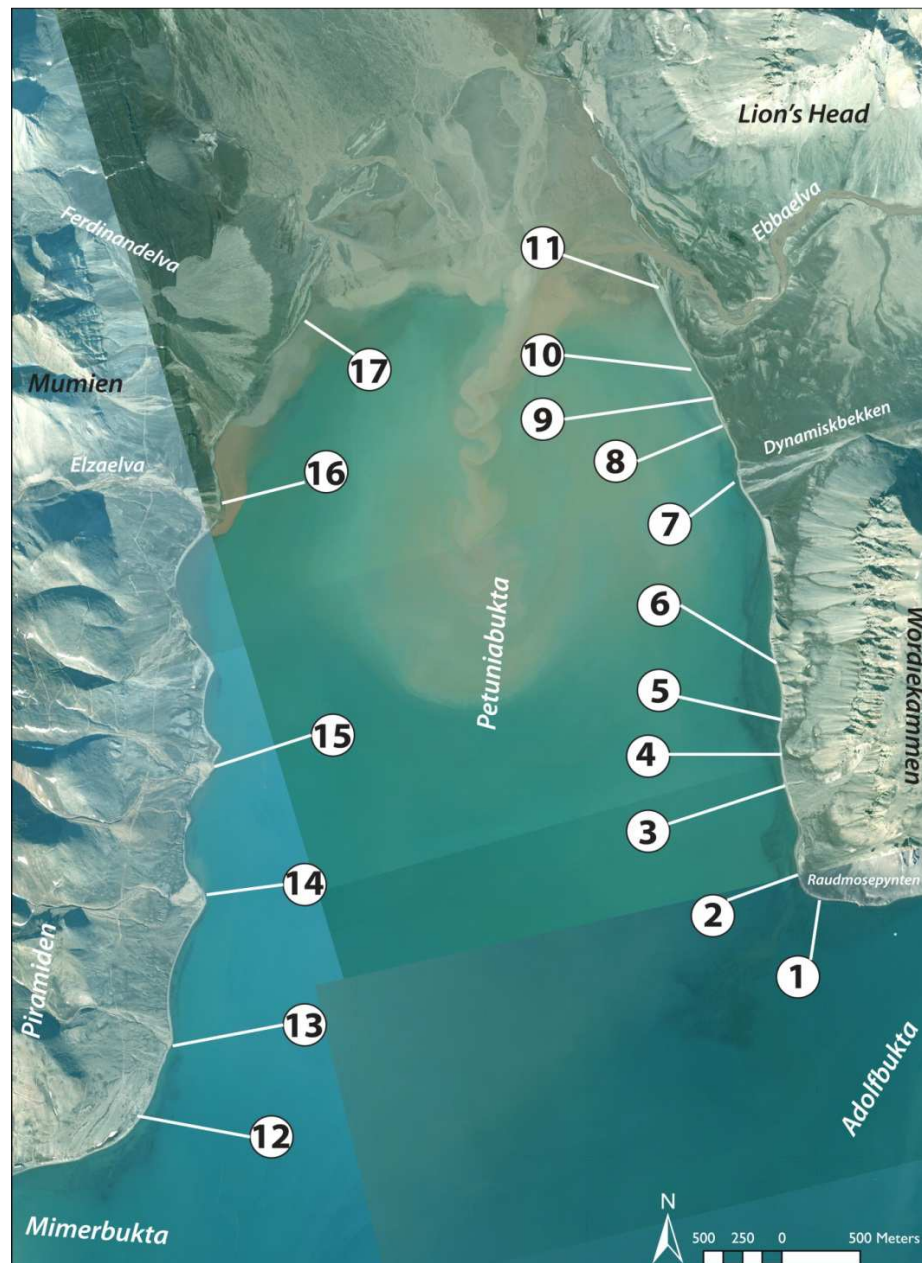


Figure 4.1. Location of 17 barrier profiles selected for the case study.

The main criteria for selecting each barrier profile were the type of landform located in the barrier background and the main source of sediment supply. Table 4.1 presents the background information of each of the chosen sites.



Profile	Coastal section	Barrier width [m]	Landform and sediment supply	Date of DGPS survey
Profile 1	E1: Raudmosepynten Coast	23 m	Cliff in uplifted marine terrace composed of fine sand, mud and shell detritus	25.07.2008-2010
Profile 2	E1: Raudmosepynten Coast	28 m	Low-lying uplifted relict barrier plain with series of lagoon	25.07.2008-2010
Profile 3	E2: Rock glacier coast	7 m	Cliff formed in rock glacier slope with thermokarst	25.07.2008-2010
Profile 4	E2: Rock glacier coast	31 m	Relict barrier and lagoon blocking rock glacier	25.07.2008-2010
Profile 5	E2: Rock glacier coast	38 m	Solifluction slope with rockfalls from talus slopes	25.07.2008-2010
Profile 6	E3: Anhydrite/gypsum cliff and shore platform coast	6 m	Rocky cliff and shore platform supplied by debris flows from uplifted beaches and talus slope	25.07.2008-2010
Profile 7	E5: Dynamiskbekken delta coast	40 m	Delta formed by snow-fed Dynamiskbekken and uplifted palaeo-spit	20 <sup>th</sup> of July 2008-2010
Profile 8	E6: Skottehytta coast	45 m	Solifluction cliff formed in uplifted marine terrace	23.07.2008 26.07.2009 29.07.2010
Profile 9	E6: Skottehytta coast	42 m	Coastal lowland with abandoned tundra lake creek	23.07.2008 26.07.2009 29.07.2010
Profile 10	E6: Skottehytta coast	26 m	Low solifluction cliff	23.07.2008 26.07.2009 29.07.2010
Profile 11	E8: East Petunia spit platform coast	186 m	Spit-platform with 24 gravel-dominated beach ridge	23.07.2008 26.07.2009 29.07.2010
Profile 12	W1: Snow-fed alluvial fan coast 1	22 m	Low cliff formed in diamicton and uplifted marine deposits	20.07.2008 23.07.2009 23.07.2010
Profile 13	W1: Snow-fed alluvial fan coast 1	23 m	Alluvial fan delta formed by snow-fed streams draining the Piramiden massif	20.07.2008 23.07.2009 23.07.2010
Profile 14	W1: Snow-fed alluvial fan coast 1	37 m	Alluvial fan delta formed by snow-fed streams draining the Piramiden massif	20.07.2008 23.07.2009 23.07.2010
Profile 15	W3: Alluvial fan coast 2	47 m	Alluvial fan delta formed by snow-fed streams that drain the Piramiden massif, debris flows from limestone cliff	20.07.2008 23.07.2009 23.07.2010
Profile 16	W3: Alluvial fan coast 2	52 m	Coastal lowland with incised uplifted beaches	20.07.2008 23.07.2009 23.07.2010
Profile 17	W4: Ferdinandbreen alluvial fans coast	20 m (the width of spit)	Ferdie Fan 3 and system of spits divided by shallow lagoons	22.07.2008 26.07.2009 30.07.2010

*Table 4.1. Barrier profiles selected for study of morphological changes in years 2008-2010. All coastal sections selected for this study are described in detail in Appendix 1.*

Barrier profiling was completed using two Leica DGPS systems: A500 in 2008 and 2009 and a Leica 1200 in 2010, which provided horizontal and vertical accuracy of 0.02 m. Profiling was undertaken during the low tide to enable mapping of the longest possible profile, which often reached the lower part of the intertidal zone. Point measurements

were taken every 2 seconds. The starting point of each of the profiles was marked with a 15 cm steel nail that was relocated each field season. All measurements were tied to a bench mark established by geodetic survey in 2008.

During barrier mapping, attention was paid to the local geomorphic factors influencing the barrier micro-relief. Table 4.4 details the features observed during both fieldwork and from time-lapse imagery taken between 2009 and 2010 from a camera installed on the coastal cliffs above beach profile 6.

In addition to profiling, a simple sedimentological study was completed. In each profile site an ash spatula was used to collect a 2 cm-thick surface layer of fine sediments from the middle of the swash zone. Samples were returned to Durham and dried for a week in an oven at +40°C and then sieved in a fume cupboard using a 2 mm sieve installed on a *Fritsch Vibratory Sieve Shaker Analysette 3* to determine the proportion of sand present in the swash zone surface. All samples were weighed on a Sartorius analytical balance. To determine pebble shape, a random sample of 50 pebbles was collected from approximately 1 m<sup>2</sup> from the surface of swash zone and storm ridge which were not buried in finer sediments. Pebbles were measured for their *a*, *b* and *c* -axes with a vernier calliper and classified in shape classes according to ZINGG classification (ZINGG 1935). Pebble roundness was determined in the field using roundness categories proposed by BENN (2006). The time-lapse images were taken using DigiSnap system designed by Harbotronics (Pentax SLR camera in a rugged box) from a cave on the western slope of Wordiekammen. Images were taken between 27 August 2009 – 11 July 2010 every 6 hours covering the surface of the bay and coastal sections E4-E8, N1-N3 and part of W4 (see Figure 2.6.)

These observations were complemented by meteorological observations based on a portable weather station (Davis Vantage Pro) which was deployed during the summer months close to the Skottehytta cabin in coastal section E6, 50 m from the coast of Petuniabukta, 5 m a.s.l. and 2 m above ground covered with tundra vegetation. The instrument recorded air temperature and humidity, barometric pressure, wind speed and direction, precipitation, incoming shortwave and UV radiation. Meteorological monitoring was conducted around Petuniabukta by Adam Mickiewicz University Polar Station (AMUPS) (along the eastern coast of Petuniabukta – limited to summer months (JAS) and a Czech Republic scientific consortium working on the project INGO - LA 341 (2007 - 2010): *'Biological and climate diversity of the central part of the Svalbard Arctic archipelago'* (along the western coast of Petuniabukta – full year).

In addition to weather and sea state observations, sea-ice conditions in central Spitsbergen were analysed for the 2008-2010 period using ice charts of Svalbard provided by the Polar View Earth Observation ([www.polarview.org](http://www.polarview.org)). Attention was paid on the timing of the appearance/disappearance of fast ice cover (sea ice that has fastened to the coast and extends out from land into sea) and drift ice (sea ice that floats on the surface of the water) in the fjord. Figure 4.42 provides information on the first and last day of the presence of fast conditions in Billefjorden area in 2008, 2009 and 2010. Table 4.3 summarises the data on ice and open-water conditions observed between 2008 and 2010.

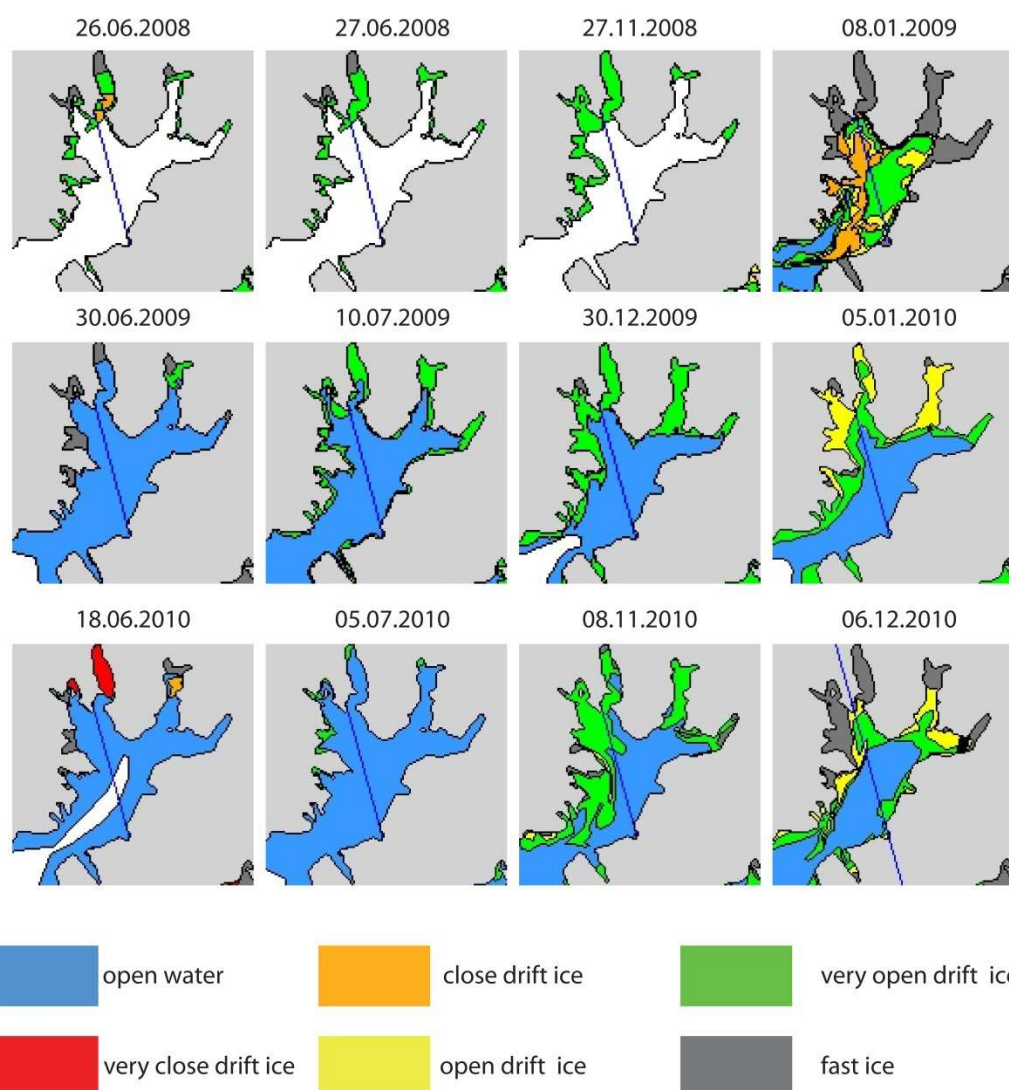


Figure 4.2. Last and first days of the formation of fast ice and filling of the fjord with very loose drift ice between 2008 and 2010 (Source: Polar View Earth Observation ([www.polarview.met.no](http://www.polarview.met.no))).

Year	Last day of fast ice	Last day of very loose drift ice filling full fjord	First day of drift ice	First day of fast ice bay	ice-free days
2008	26.06.2008	27.06.2008	27.11.2008	08.01.2009	154
2009	30.06.2009	10.07.2009	30.12.2009	05.01.2010	174
2010	18.06.2010	05.07.2010	08.11.2010	06.12.2010	127

Table 4.2. Sea-ice conditions in Petuniabukta during 2008 and 2010 based on Polar View ice charts ([www.polarview.met.no](http://www.polarview.met.no)) presented in Figure 4.4.

Weather measurements were also supplemented with observations of the state of sea using the Douglas Sea Scale (Table 4.2.). The highest state of sea recorded in Petuniabukta was 4 (Moderate) and occurred on July the 20<sup>th</sup> 2009 and August 15<sup>th</sup> 2010. For most of the open water season Petuniabukta remained smooth (state 2) with slight conditions (state 3) occurring only under stronger winds descending from glacier valleys.

State of the sea	Wave height (m)	Description	Swell
0	0	Calm (glassy)	No swell
1	0.0 – 0.1	Calm (rippled)	Very low (short and low wave)
2	0.1 – 0.5	Smooth (wavelets)	Low (long and low wave)
3	0.5 – 1.25	Slight	Light (short and moderate wave)
4	1.25 – 2.5	Moderate	Moderate (average and moderate wave)
5	2.5 – 4.0	Rough	Moderate rough (long and moderate wave)
6	4.0 – 6.0	Very rough	Rough (short and heavy wave)
7	6 – 9	High	High (average and heavy wave)
8	9 – 14	Very high	Very high (long and heavy wave)
9	over 14	Phenomenal	Confused (wave length and height indefinable)

*Table 4.3. Douglas Sea Scale source: Met Office UK: [library.metoffice.gov.uk](http://library.metoffice.gov.uk)*

## 4.4 Results

### 4.4.1 Meteorological conditions 2008-2010

#### 4.4.1.1 Air temperature

During the first year of this project, in the period between mid-July 2008 mid-August 2009, the mean air temperature at Czech station in north-western Petuniabukta (marine terrace 15 m a.s.l.) was  $-4.5^{\circ}\text{C}$ . The lowest air temperature was  $-32.6^{\circ}\text{C}$  (January 12, 2009) and the maximum was  $16.2^{\circ}\text{C}$  (28<sup>th</sup> July of 2009). During the second year (beginning of July 2009 – end of June 2010) the mean temperature was  $-3.6^{\circ}\text{C}$ , and the lowest temperature was  $-27.8^{\circ}\text{C}$  (5<sup>th</sup> of March 2010). The mean global shortwave radiation was  $85.9\text{ W/m}^2$  in 2008-2009 and  $95.1\text{ W/m}^2$  in 2009 – 2010. The daily maximum global radiation intensity was observed on the 28<sup>th</sup> June 2010 and reached  $369\text{ W/m}^2$ . Temperature measurements at AMUPS between 2008 and 2010 period are summarised in Figure 4.3.

#### 4.4.1.2 Wind speed and direction

Wind conditions in the study area are strongly influenced by surrounding orography and the presence of a large ice-plateau in the NE (Lomonosovfonna). In 2008-2010 the prevailing winds (with mean speed  $3.9\text{ m s}^{-1}$ ) along the north-western coast of Petuniabukta were from the S-SSE (34%), and the second dominant wind direction (18%) was from the NE (katabatic winds coming from Ragnarbreen valley, one of the outlet glaciers draining the ice field). The latter were stronger than those from the southern directions and occasionally exceeded  $20\text{ m s}^{-1}$ .

Similar orographic forcing was recorded along the eastern coast of Petuniabukta at Skottehytta station (marine terrace 5 m a.s.l.). Here, the second predominant winds after S (45%) are those blowing from a NE direction (25%) direction coming down the Ebbabreen valley system (Figure 4.3.). It is important to note that the summers of 2008 and 2009 were calmer (average wind speed  $2.7\text{ m s}^{-1}$  and  $2.0\text{ m s}^{-1}$ ) than the summer of 2010, with mean wind speed reaching about  $4\text{ m s}^{-1}$  (the strongest gusts reached  $19.2\text{ m s}^{-1}$ ). The summer 2010 was the only season with waves observed higher than 1 m and stormy conditions on the bay lasting longer than 5 hours.

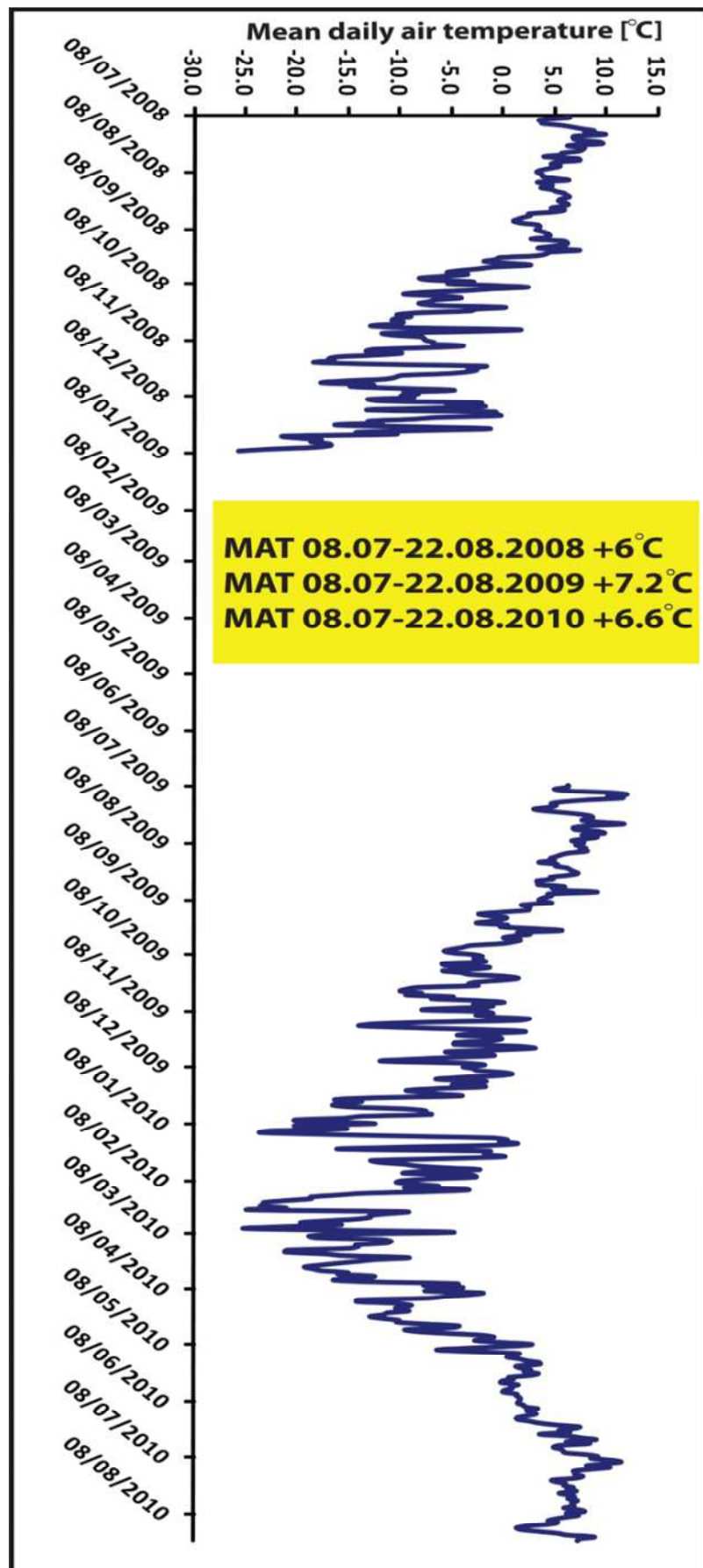


Figure 4.3. Air temperature changes during 2008-2010 recorded at Adam Mickiewicz University Polar Station.



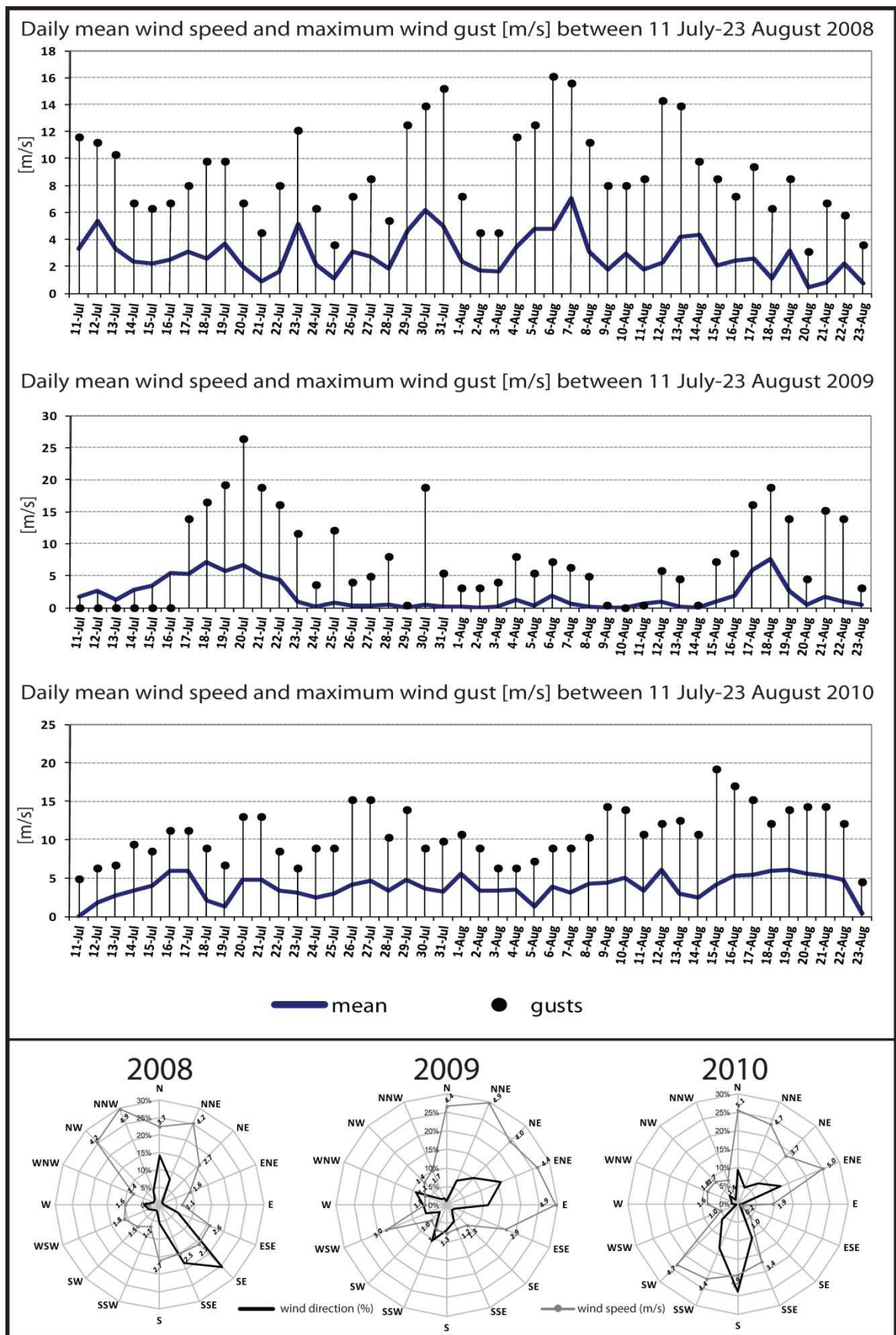


Figure 4.4. Upper: daily mean wind speed and maximum wind gusts, 11 July and 23 August (2008, 2009 and 2010). Lower: wind direction and average wind speed between 8 July - 29 August 2008; 7 July - 3 September 2009, 11 July - 23 August 2010

#### **4.4.2 Processes that control the modern barrier coast in the Petuniabukta**

This section starts with a qualitative description of coastal landforms and processes observed during fieldwork. It is followed by a quantitative analysis of beach profile change based on survey data. Figure 4.5. summarises the results of the mapping of features that control barrier micro-relief (2008-2010). There is a clear distinction between the eastern and western coast of Petuniabukta in terms of the diversity of coastal landforms and processes that operate.

The eastern coast of Petuniabukta is characterised by a greater diversity in the geomorphology of barrier background (number of various landform and potential sediment sources) and more numerous instances of coastal processes related to the presence of sea-ice and snow-cover. Barriers formed along east Petuniabukta (in the southern and central parts) border on the steep slopes of the Wordiekammen massif that supplies the coast with coarse debris via rockfalls, debris flows and mudflows from series of talus slopes, two rock glaciers, and a 1000 m-long section of rock cliffs that is covered by uplifted beaches. The important factor controlling the accumulation of barriers along this part of Petuniabukta coast is a submerged rocky shore platform that extends along the coast almost up to the entrance to the Ebbadalen. This rocky bench locally extends up to 250 m seaward and significantly shallows the nearshore zone. One of the characteristic features observed on the surface of this shore platform are accumulations of boulders (erratics and material from rockfalls) that lead to the breakage, piling up and anchoring of sea-ice or icefoot cover. In the summer months, accumulations of boulders often act as anchors for seaweed and driftwood that gets blocked between these large boulders. In open-water summer conditions this platform forces waves to break further from the shore and reduces the sediment transport capacity of the longshore current. For these reasons, the rocky platform exerts an important control on the piling-up of ice floes in the winter season and on longshore sediment transport during the summer season.

The thickness of barrier deposits on the shore platform along the section of anhydrite/gypsum cliffs (the central part of the east coast) is reduced and ranges between 5 cm and 40 cm. As well as limited sediment availability, the occurrence of frequent rockfalls from the anhydrite/gypsum cliff often leads to the disruption of barrier formation and hinders longshore drift of material that is delivered to the coast from erosion of the Raudmosepynten cliffs or rock glaciers located to the south.

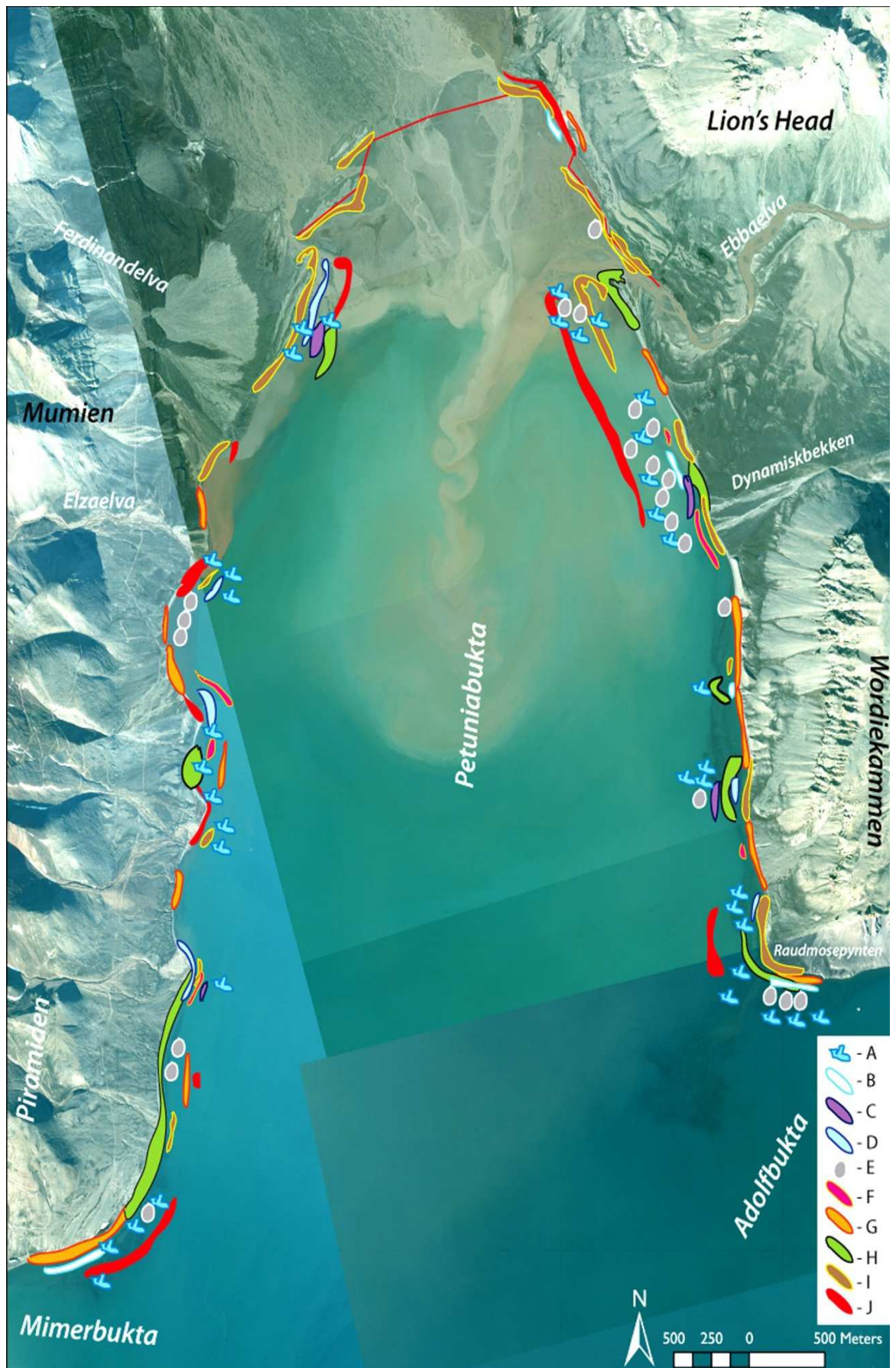


Figure 4.5. The spatial distribuion of processes operating on beaches within the study area between 2008 and 2010. For the description of A-J factors please refer to Table 4.4.

Type of feature	Observation:
A - ice-pile up and bulldozing (winter conditions)	Location of zones of ice piling-up along the bay
B - remnants of ice-floes and icefoot	Sections of coast with remnants of sea-ice, the icefoot remaining during the summer months
C - ice-melted landforms	Presence and preservation of 'pitted-beach' surface in the summer months (open water conditions): kettle holes, meltwater ponds etc.
D - ice-pushed landforms	Preservation of ice-pushed ridges on the surface of barrier in summer months (open water conditions)
E - erratics	Erratics left by SBSIS along the fjord which are present in/on the barrier surface
F - blocked stream outlets	Presence of storm-ridges blocking outlets of snow-fed streams and glacier rivers
G - rockfalls, debrisflows, solifluction	Occurrence of rockfalls, debris flows and slumping of tundra blocks due to solifluction that reaches the barrier surface
H - seaweed accumulations	Presence and thickness of seaweed accumulations (mattress) on the surface of the barrier
I - driftwood accumulations	Presence and number of driftwood in barrier deposits and surface
J - traces of human activity (garbage and tracks of boats or heavy machines)	Presence and preservation of human activity (mining, tourism and research) that impacted the barrier morphology

*Table 4.4. Features that influence the coastal microrelief in the thesis study area.*

The eastern barrier forms along the entrance to the Ebbadalen where the main factors controlling barrier micro-relief and sediment supply are the snow-fed stream Dynamiskbekken, solifluction of the low cliffs formed in uplifted marine deposits, and the ebb-tide delta formed on the prograding tidal flat by Ebbaelva. The coast is restricted by a belt of skerry islands formed by large erratic boulders (probably remnants of Ebbabreen moraine left after last deglaciation) that break waves in the summer months and trap sea-ice during the winter. This section of the coast is also heavily modified by human activities linked with the operation of the research station, tourists and mining exploration (which ended in late 1990's).

Intensified human activity led to:

- high concentrations of garbage (ropes, nets, glass, various plastic materials, rusty wires or parts of machine) on the surface and within barrier deposits;
- the displacement of driftwood previously embedded in barrier deposits;
- the formation of series of grooves across the beach related to the dragging of trunks from the Ebba spit-platform and Dynamiskbekken delta to the surrounding of Skottehytta base camp;
- and disturbance of the barrier surface by the landing of boats.

The barrier formed along the western coast of Petuniabukta borders a wide coastal lowland that separates the coastal zone from the direct influence of debris flows and rockfalls from the adjacent mountains. Apart from the surface of alluvial fans and the channels of glacial rivers / snow-fed streams, the lowlands are covered with tundra. The steep nearshore bedrock topography quickly deepens and the piling up of ice-floes was observed only along the submerged parts of river deltas and the tidal flat step. Accumulations of driftwood were also observed along the shallower sections of the coast associated with alluvial fan deltas and the prograding tidal flat.

The longest section of coastline covered with a thick (10-45 cm) layer of seaweed is located in the southern part of the western barrier where the coast is impacted by long waves driven by winds that descend the Nordenskiöldbreen in Adolfbukta. On several occasions it was observed that larger waves cast seaweed over the storm ridge where it accumulated a relatively thick seaweed mattress covering the landward slope of the barrier. The central part the western barrier is ruptured by a *ca.* 600 m long section of limestone cliff that is fringed by a narrow rocky platform. This is the only section where thickness of barrier sediments decreases below 50 cm. In contrast to the straight coast formed in the eastern part of Petuniabukta, the western coast is indented with alluvial fan deltas and bedrock outcrops which cause the characteristic headland-bay shape of the coast.



#### 4.4.2.1 Ice pile-up and bulldozing

In Petuniabukta ice pile-up was concentrated mainly along the eastern coast where slabs of ice crumble on accumulations of erratics or rock blocks (Figure 4.6.). Pile-ups on the east coast are concentrated *ca.* 20-200 m from the coast, whereas pile-ups along the western coast were often pushed up onto the barrier. Smaller pile-ups were found along the border of the prograding tidal flat and ebb-tide delta formed by Ebbaelva. Field observations (April 2009) show that average ice slab pile-up along the coast was *ca.* 25-40 cm thick and that the sea-ice that piled-up along the alluvial fan deltas or tidal flat margin contained more sediments frozen to their base than ice-floes (30-50 cm thick) that accumulated in pile-ups formed on boulders and shore-platforms.

#### 4.4.2.2 Icefoot

Remnants of icefoot were observed each summer along short sections of the eastern and western coast (Figure 4.7.). The icefoot formed along the Raudmosepynten (E coast), in three consecutive seasons, covered the barrier until the second week of July. The icefoot represented the 'stranded floe' type that is formed by fragments of ice slabs stranded on shore and anchored to erratic boulders at the base of the cliff, and was up to 1.5 m thick.

At over 100 m long and 3 m thick, an icefoot was observed each summer at the entrance to Mimerbutka (SW coast) that resembled the 'ice platform' described in the St Lawrence Estuary by DIONNE (1988) and covering the major part of the intertidal zone. The icefoot was usually covered by frozen snowpatches that were dissected by mudflows and debris flows from the slopes of Piramiden Mountain. In 2008 and 2009, a small 'pressure' icefoot (30 m long, 2 m thick), formed by slabs of sea ice, was observed along the anhydrite cliffs in the central part of the east coast until the second week of July. Following the melt of the icefoot, the shore platform here was covered with large accumulations of coarse rock fragments with several blocks larger than 1 m in diameter. The most persistent icefoot was observed in NE Petuniabukta, where it developed along a relict, frost-shattered limestone cliff and was covered by a snowpatch over 2 m thick. In 2008, the icefoot survived until the third week of July. In 2009, it remained there the whole summer season and in 2010 it melted in the last week of July. A smaller icefoot seen on the gravel barriers north from the Dynamiskbekken delta in July 2008 and 2009 was composed of frozen snow and resembled a 'false icefoot' (DIONNE 1973).

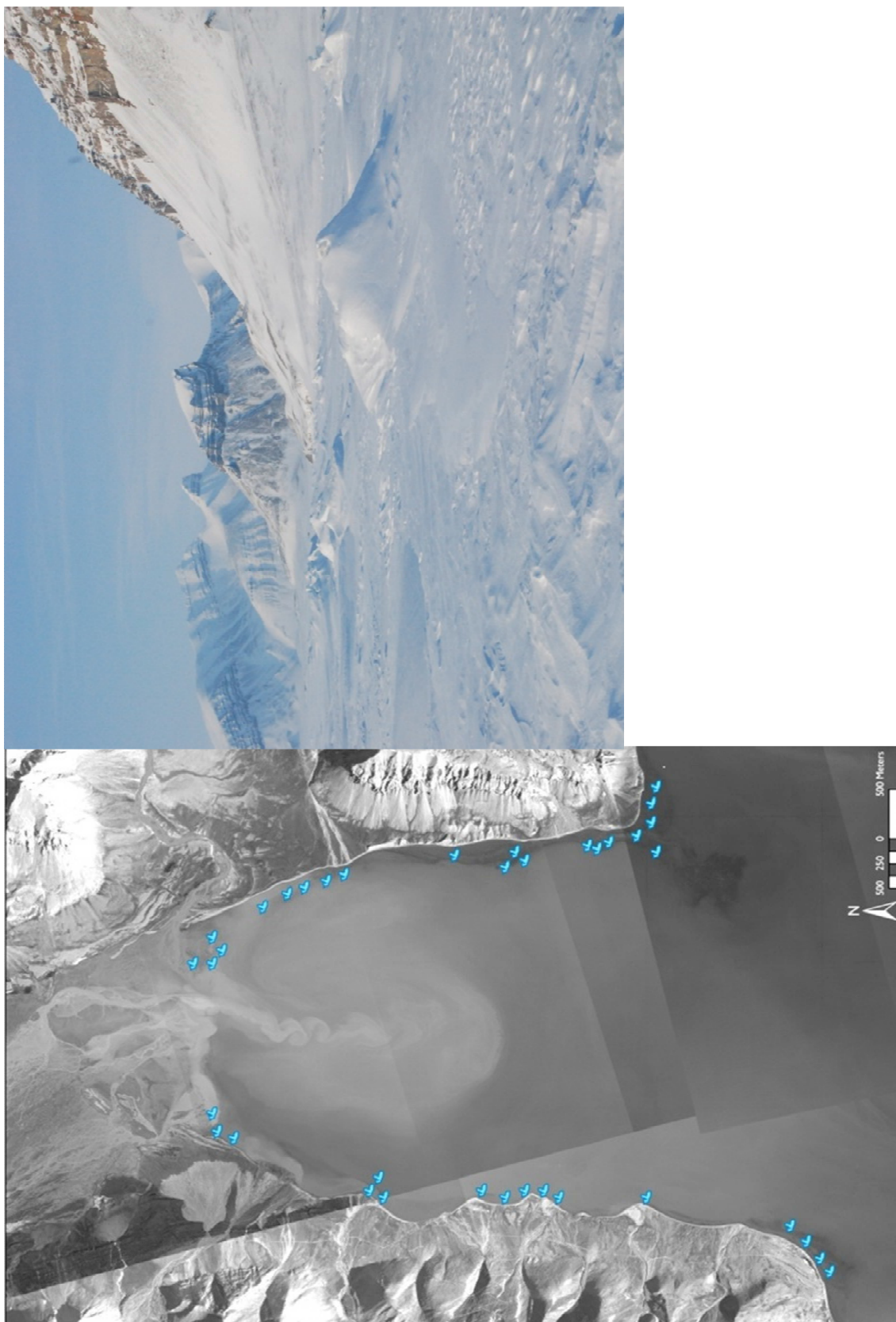


*Figure 4.6. Location of main accumulations of ice pile-ups and ice bulldozing along the coasts of Petuniabukta*





*Figure 4.7. Sections of the barrier with the long-lasting remnants of an icefoot.*

#### **4.4.2.3 Pitted-beach**

Pitted-beach micro-relief forms when fragments of ice floes, icefoot or growlers which have been previously covered with sediments (either thrown by waves or from terrestrial sources i.e. landslides, slumping, debrisflows, and mudflows) start to melt and collapse leaving pits and hollows of various size and depths (e.g. NICHOLS 1961, 1968). In Petuniabukta a well-developed 'pitted beach' occurs only in one site along the eastern coast (section E2). Over a 100 m distance, the barrier is patterned with dozens of melt-out pits, elongated hollows mixed with post-kaimoo hillocks (hillocks formed after the melt out of ice from multi-layered ramparts of ice and sediments formed by freezing of swash and wind-blown sediments) and ice-pushed ridges (Figure 4.8.). It is important to note that the pitted surface is present only above the modern storm ridge and occupies the landward slope of the barrier. Small (20-50 m) zones of pitted beach micro-relief were found in just two sites along the western barrier (sections W1 and W4) and on the eastern barrier north from Dynamiskbekken delta (section E5). However, in contrast to section E2, pitted micro-relief along those three sites was formed on a seaward slope of the barrier and disappeared after just few days of wave operation.

#### **4.4.2.4 Ice-pushed micro-relief**

Ice pushed ridges are formed by waves pushing grounded sea-ice slabs up the seaward slope of barrier during the ice breakup period (ROSEN 1978). Ice-pushed ridges and mounds are often accompanied by long, shallow trenches gouged by moving ice blocks (ARÉ et al. 2008) and kaimoo formed due to mixing of barrier, slope and aeolian sediments with stranded ice floes. In Petuniabukta, the ice-pushed features are found in the same sites where the 'pitted-beach' micro-relief is formed and where major accumulations of ice-piling up occur (Figure 4.9.). As with the 'pitted' features, the majority of ice-pushed ridges were washed away by waves by the second week of July and were preserved only on landward slope of the 'pitted' barrier from the E2 section. An exception to this pattern was the well-preserved mounds and ridges that were occasionally seen along the Petuniabukta barrier in late July and early August 2009 and 2010. Those features comprised coarse gravel and cobbles mixed with seaweed and fragments of driftwood.



*Figure 4.8. Sections of the barrier with 'pitted-beach' micro-relief.*



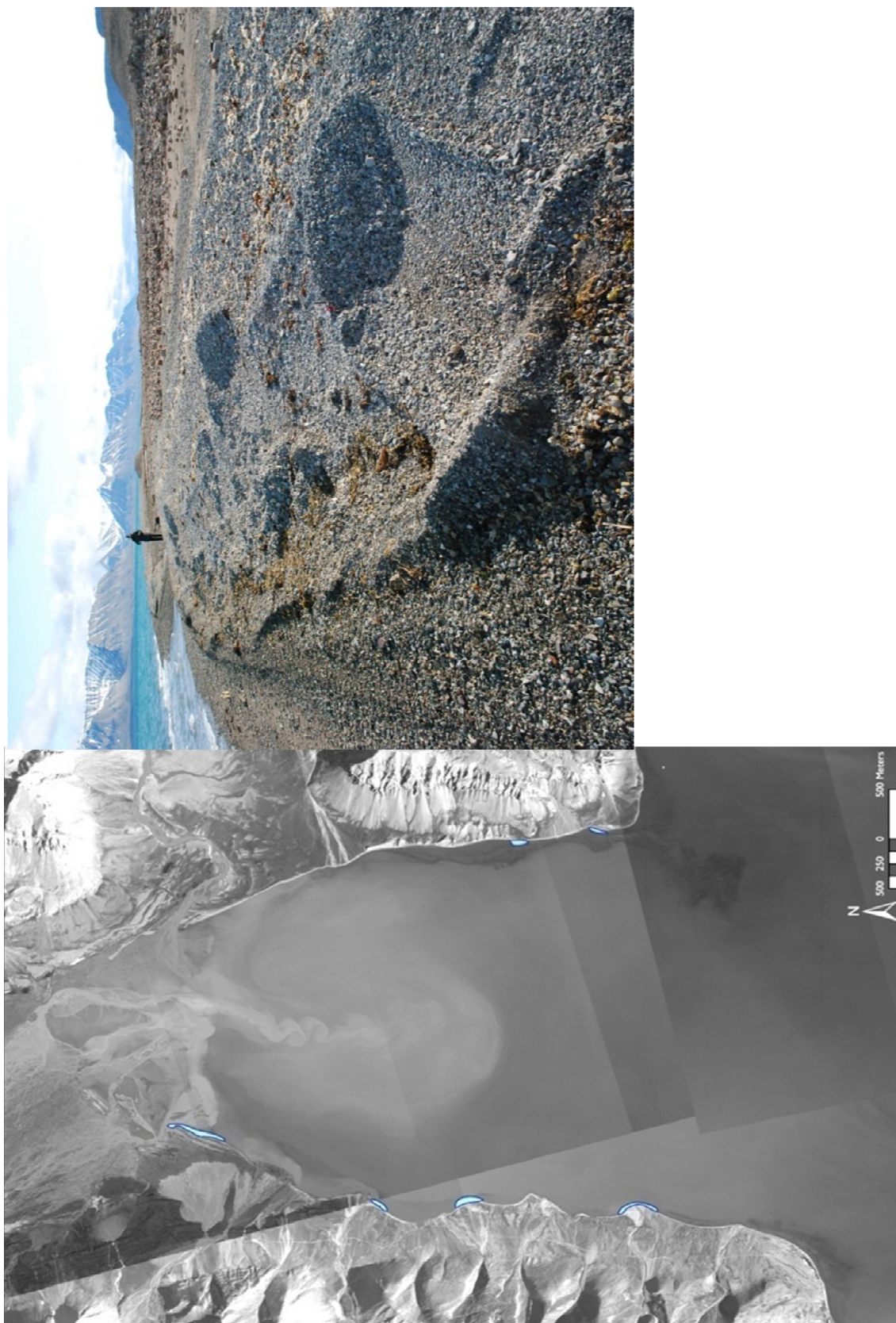


*Figure 4.9. Sections of the barrier with accumulations of ice-pushed landforms.*

#### **4.4.2.5 Erratic boulders**

There are two types of erratic boulder accumulations found along the coast of Petuniabukta (Figure 4.10.). The first type comprises small groups of erratic boulders (1-6 boulders) embedded in barrier deposits or lying on barrier surfaces. These types were observed at seven sites and, as noted above, play an important role in anchoring the icefoot during winter months as well as seaweed and driftwood during the open-water season. Boulders also act as natural barricades for debris or mudflows flowing from adjacent slopes. Space between them is frequently filled with material delivered by ice floes that melted on top of them.

The second type of boulder accumulation is located in the intertidal zone in NE Petuniabukta (coastal section E7) where boulders group into 'skerry islands' composed of 3-25 large boulders and comprise a *ca.* 1600 m long belt between Dynamiskbekken and the tidal flat. These boulders break waves during the open-water season.

#### **4.4.2.6 Storm ridges blocking stream outlets**

Blocking of snow-fed streams outlets and small river channels by gravel-dominated storm ridges is one of the common features found along Spitsbergen coasts (Figure 4.11.). ÅKERMAN (2008) claims that the blocking of streams and the delaying of spring discharges is one of the crucial controls of anomalous drainage patterns and floodings of coastal lowlands observed along Kapp Linné (central Spitsbergen). Between 1975-2005 he observed an increase in size of storm ridges along the coast and linked their formation to the occurrence of strong autumn and winter storms that impact on coasts that are less frequently protected by sea ice than previously.

In Petuniabukta, most small snow-fed streams were blocked by storm ridges throughout the summer. Among seven streams mapped along the coast, only three managed to breach the barrier in 2009 and in 2010. The main channels of larger streams or rivers such as Dynamiskbekken, four streams from the alluvial fan deltas along the western coast, as well as Elzaelva and Ferdinandelva, regularly breached their barriers during peak summer discharges. Once discharge fell and streams started to dry out, waves quickly built storm ridges that were sufficiently high and wide to block the streams before the freeze-up period.

A common feature observed were ponds filled with fine (sandy-muddy) sediments (up to 45 cm thick) that accumulate throughout the whole summer discharge period behind the

storm ridges when streams are percolating through the barrier to the fjord. In the consecutive years when streams managed to break the storm ridge during spring melt and peak summer discharge the ponds were often washed out, leading to the occurrence of small, local sediment plumes in the nearshore waters.

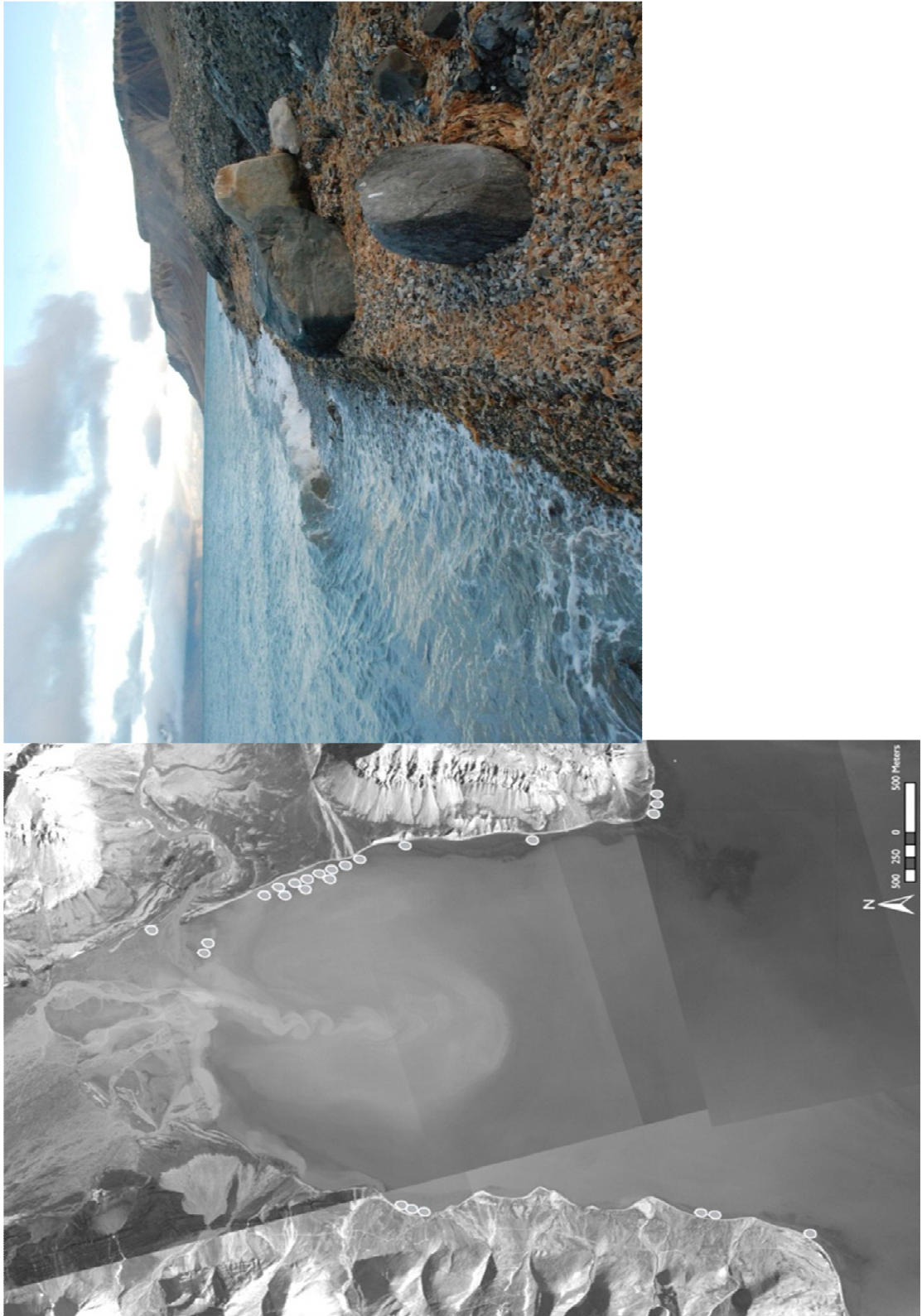


*Figure 4.10. Sections of the barrier with accumulations of erratics.*



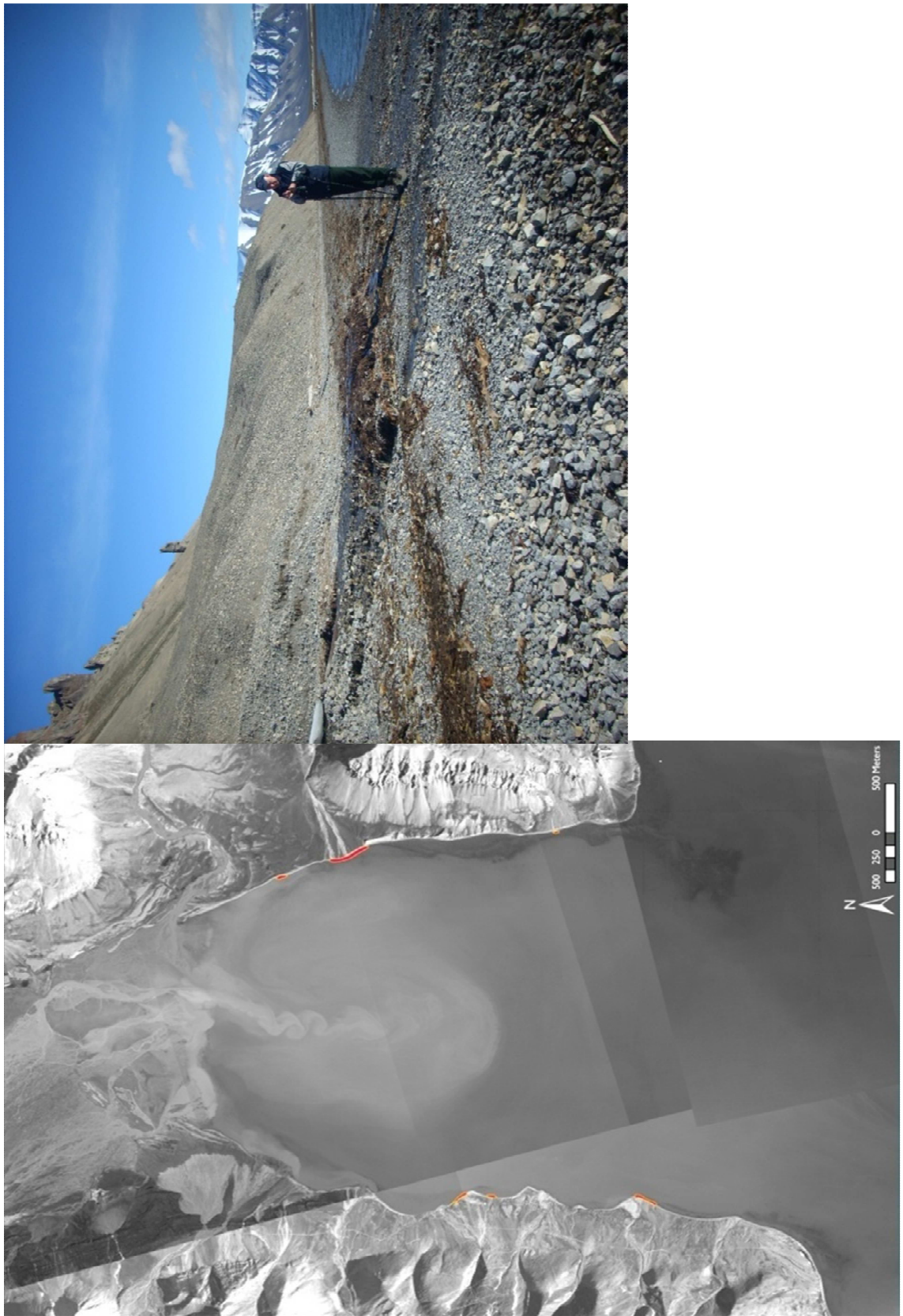


*Figure 4.11. Sections of the barrier with stream outlets blocked by storm-ridges.*

#### 4.4.2.7 Rockfalls, debrisflows, mudflows, solifluction

Debrisflows are the most common means of coarse sediment delivery from mountains slopes and uplifted beaches to the Petuniabukta barrier coast (Figure 4.12.). Along the eastern coast, where the coast borders on rocky cliffs, rock glaciers and talus slopes of Wordiekammen, the barrier is additionally supplied with boulders and rock blocks delivered by occasional rock falls and rock avalanches (section E3). Smaller rockfalls were observed in 2009 from the limestone cliff along the western coast (section W2).

Melting of snow patches and rare summer rainfall events lead to the formation of small mudflows that can cover the rock cliffs and barrier surface with thin layer of fine sediments that are easily reworked by waves. In coastal sections W3 and E6, solifluction of low unconsolidated cliffs delivered blocks of tundra and fine slope sediments or reworked marine deposits, to the surface of barrier.

#### 4.4.2.8 Seaweed

Major accumulations of seaweed (kelp) covered barriers along the Raudmosepynten and accumulate around Ebba spit-platform and Ferdie Spits (Figure 4.13.).

The longest section of barrier covered with a seaweed mattress is on the western coast (W1 and W2) where long, high waves originating in Adolfbukta throw seaweed over the storm ridge where it mixes with barrier sediments and dries out to form a stiff mattress. Seaweed strengthens ice-pushed ridges and increase barrier resistance to wave erosion.

In all the sections of Petuniabukta that are characterised by huge accumulations of *Ulva lactuca* beach berms were wider, higher and more stable than along seaweed-free sections of coast. Seaweed mixed with finer sediments forms a very thick (several centimetres), elastic layer which may protect beach sediments from washing out by waves. The rinsing of beach sediments by meltwaters from ice-floes is significantly reduced along shores covered by fresh seaweed mattress. After drying out, multilayered seaweed mattress may reduce the effects of ice-push and pile-up on shore. The influence of seaweed accumulations or lichen covers on degree of rock shores weathering and disintegration remains unknown.

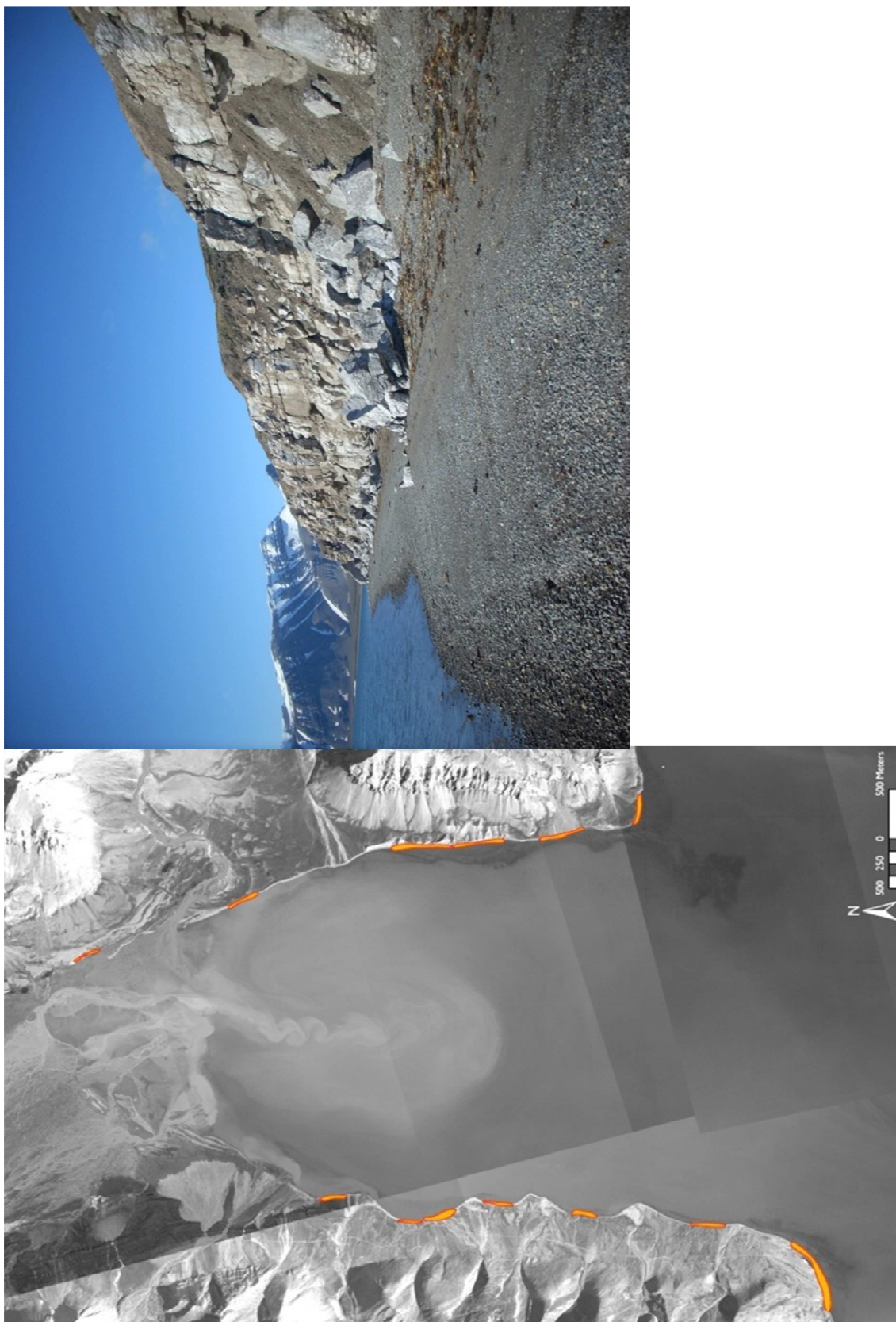


*Figure 4.12. Sections of the barrier covered with rockfalls, debris flows and affected by solifluction.*



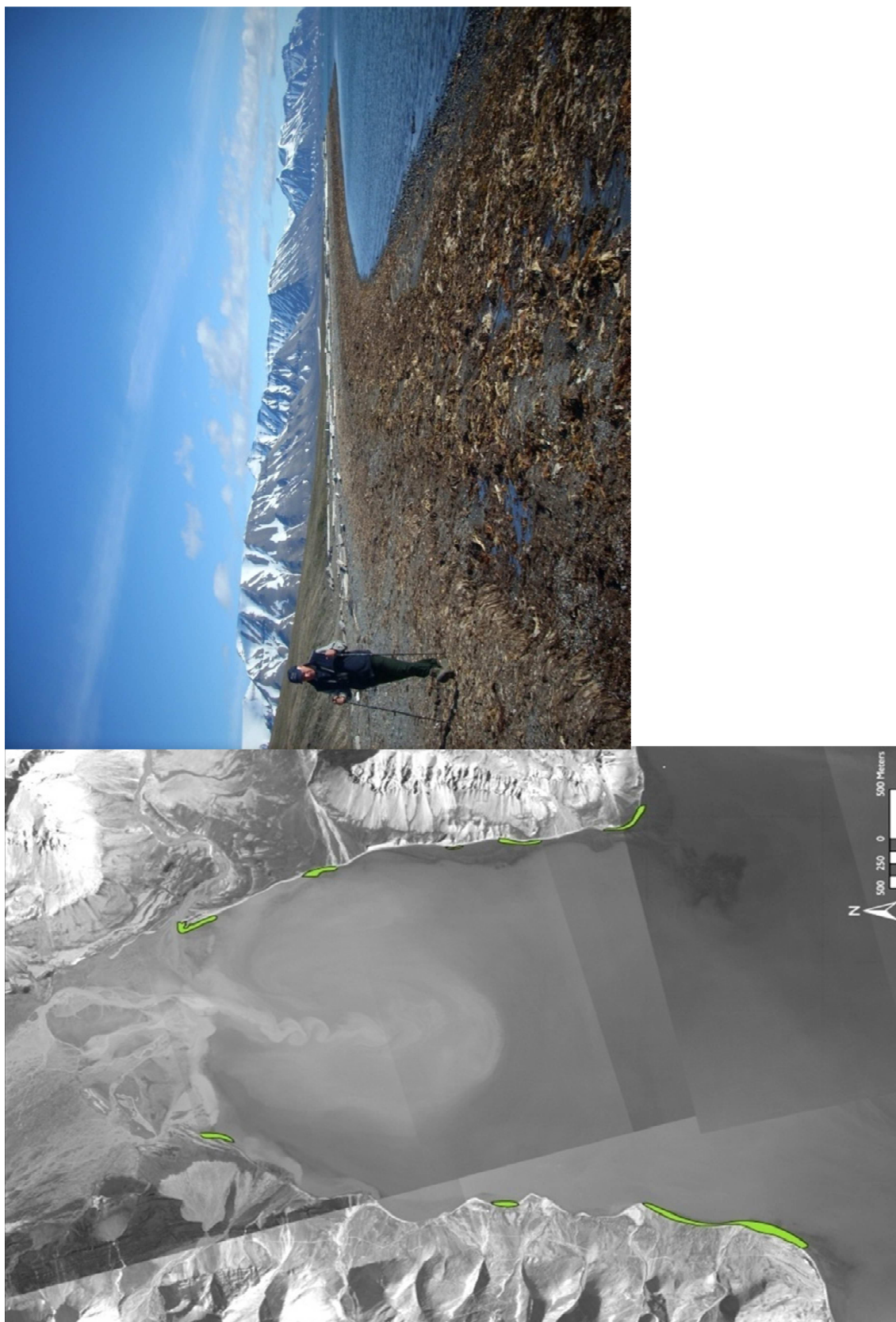


*Figure 4.13. Sections of the barrier with accumulations of seaweed.*

#### **4.4.2.9 Driftwood**

The Petuniabukta coasts are heaped with driftwood (Figure 4.14.) that constitutes an important control on barrier micro-relief by damming debris flows and mudflows, forming straight and robust axes of storm ridges encased with barrier deposits and damming stream outlets to hamper sediment transport down or along the barrier. The abundance of driftwood reflects the trapping of wood drifting in Billefjorden-Isfjorden basin (the northernmost, sheltered bay of Billefjorden) as well as local human activity (the construction of wood cabins and establishment of settlements at Brucebyen and Piramiden) that required the import of large quantities of driftwood as basic construction and fuel. Huge concentrations of driftwood occur in the area surrounding the Ebba spit platform and the western Raudmosepynten in east Petuniabukta, and also associated with the lagoons and barriers formed between the Elzaelva fan delta and the Ferdie Spit along the west coast.

#### **4.4.2.10 Human activity**

The history of human activity in Petuniabukta region goes back to the late 19<sup>th</sup> century and is related to mining exploration and establishment of two settlements, the wooden-built Brucebyen (abandoned in early 20th century) and the third largest town of Svalbard, Piramiden, that operated between the 1960s and the late 1990's. Since 1984, the eastern coast of Petuniabukta has also been home for several research expeditions organised by Adam Mickiewicz University in Poznan and more recently by the University Centre in Svalbard.

The picturesque landscape and interesting history of human activity in the Petuniabukta region bring numerous tourist trips both in summer and winter seasons. Due to human activity in the area, the barriers of Petuniabukta are littered and trampled, in places supporting heavy machinery. In northern Petuniabukta (N1-N3) the most significant human transformation of coastal landscape is the old road used by Russians since the 1960's which crosses the northern tidal flat, small barrier islands and the gravel barrier north from the Ebba mouth. This area is also littered by rusted mining and drilling equipment and huge amounts of plastic garbage including fishing nets, broken buoys and bags that are incorporated into the barriers and tidal flat (Figure 4.15.). The western shoreline of Petuniabukta is littered with a huge amount of metal cables and wires. The barrier and cliff coast here borders remnants of mine waste dumps, slag heaps and piles of

debris removed from Piramiden slopes during construction of a road that crosses the coastal lowlands. Coal, slag, broken glass, fragments of wood, metals and plastic are commonly incorporated into the barrier deposits down the entire western coast.

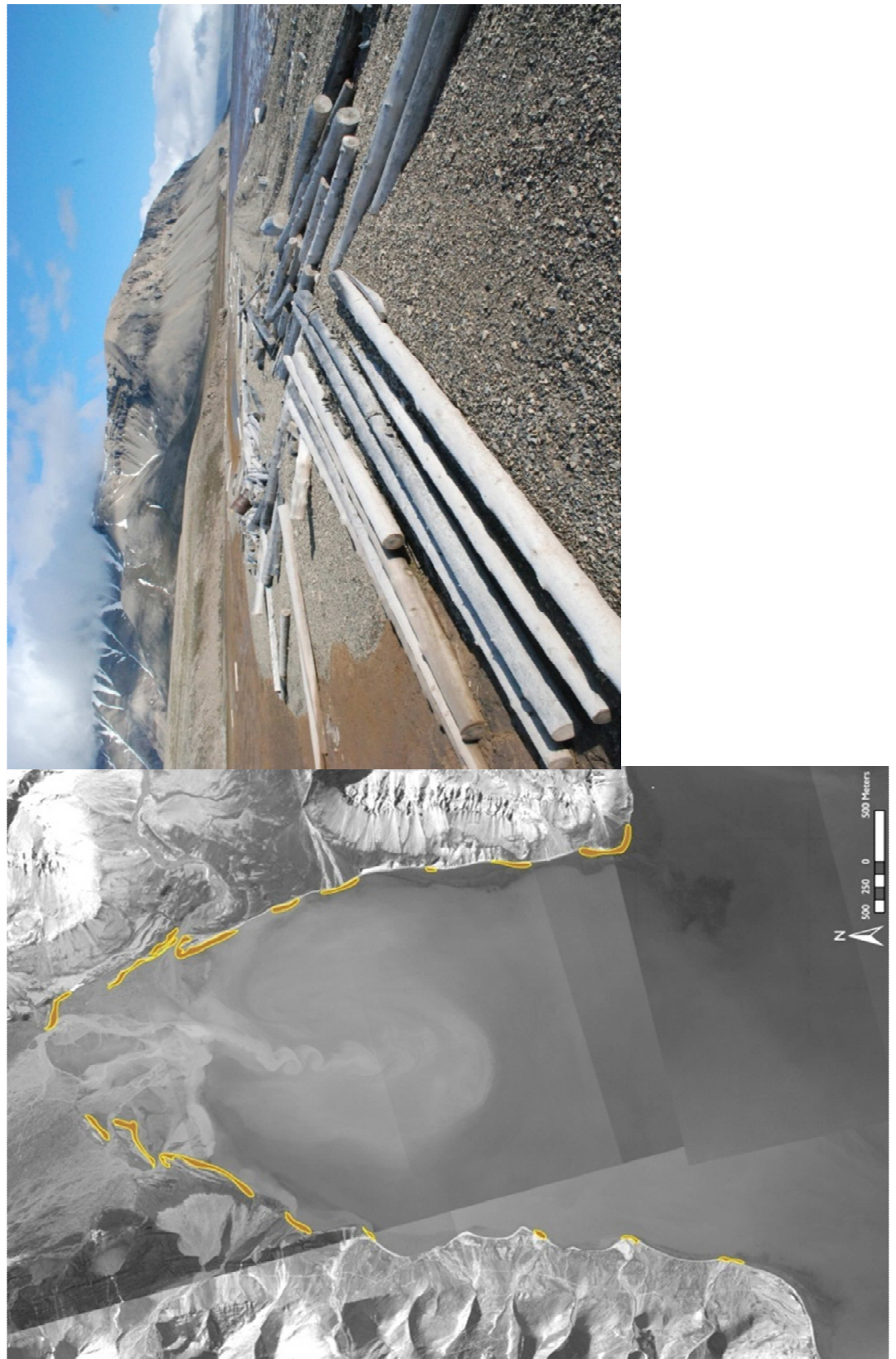


*Figure 4.14. Sections of the barrier with large accumulations of driftwood.*



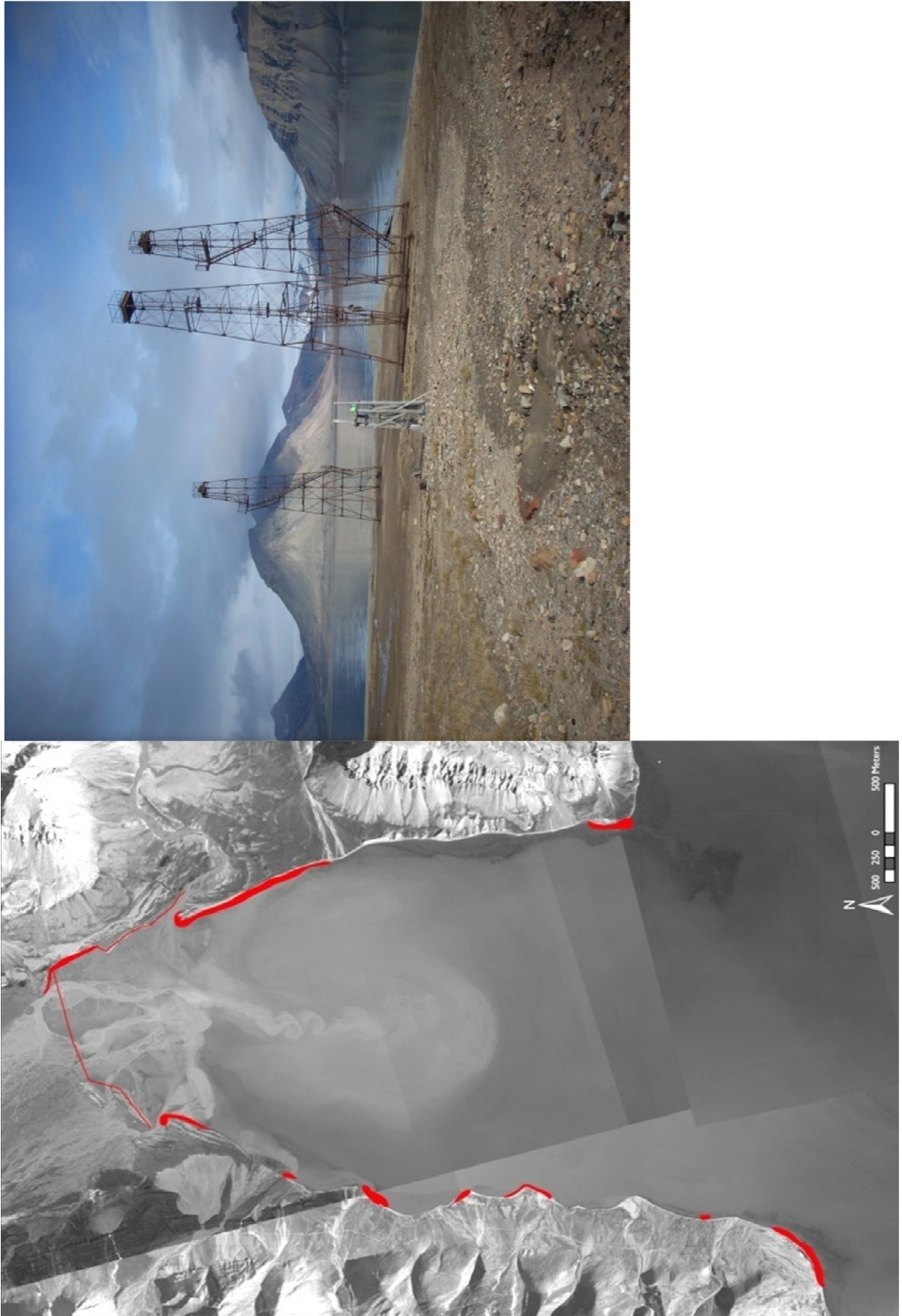


*Figure 4.15. Sections of the barrier affected by human-activity.*

#### 4.4.3 Barrier profile changes 2008-2010

##### 4.4.3.1 Profile I – southern Raudmosepynten (Figure 4.16.)

Profile I extends across the barrier formed at the base of a low (2.5 m) unconsolidated cliff that is eroded in the uplifted beach/lagoon deposits rich in shell detritus (Figure 4.16.). The barrier here is subject to long-fetch waves from the Billefjorden and those originating in inner Adolfbukta. In winter, the area around the cape is packed with stranded ice floes and the cliff walls are covered with up to 3 m thick snow patches. The gravel-dominated barrier is often covered with 0.1-0.2 m thick seaweed mattress anchored to numerous erratic boulders scattered over the barrier surface. Dry seaweed mixed with mudflows from the low cliff creates a stiff crust that encases almost the entire landward slope of the barrier and the base of the cliff.

Between 2008 and 2010, the barrier profile has gently flattened and lowered *ca.* 0.15 m. The storm ridge retreated *ca.* 0.4 m and lowered *ca.* 0.45 m. These changes are related to the erosion of a section of seaweed mattress that in 2008-2009 was incorporated in the ridge. Material released from the storm ridge was redistributed along the swash zone. The high concentration of ice-push and ice-melted features observed along the 2009 profile was attributed with the late disappearance of drift ice that often grounded on shore.

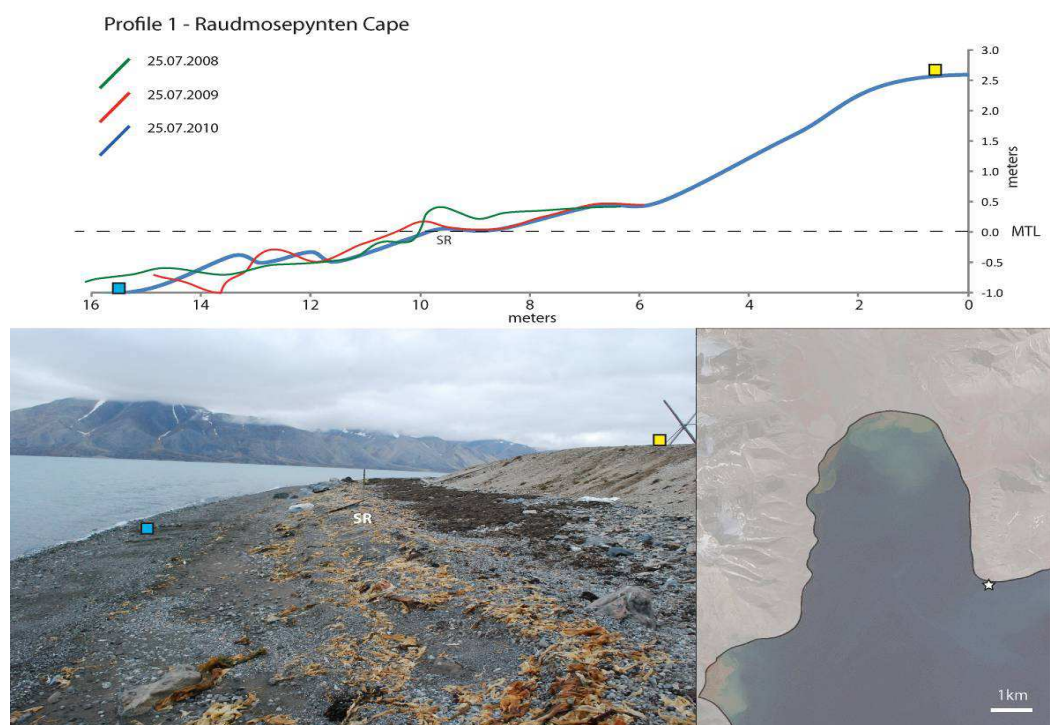


Figure 4.16. Profile I. Upper part: Barrier profile changes observed in 2008-2010. Lower part: photograph of the barrier and location of site along the coast of Petuniabukta.

#### 4.4.3.2 Profile 2 – Western Raudmosepynten (Figure 4.17.)

Profile 2 extended across a gravel-dominated barrier developed on a low step eroded in uplifted lagoon deposits (Figure 4.17.). This is the only section of the eastern coast where well-developed overwash fans were observed on the seaward slope of the barrier. The barrier surface supports less seaweed than in Profile 1, although more fragments of driftwood were incorporated in barrier sediments. As with Profile 1, between 2008 and 2010 the barrier surface has flattened and the storm ridge has lowered by *ca.* 0.1 m. The storm ridge migrated inland *ca.* 1.1 m between July 2008 and July 2009 and then migrated seawards by *ca.* 0.4 m by July 2010. The thickness of the gravel layer on the relict lagoon surface increased *ca.* 0.3 m, most likely due to the redistribution of material accumulated behind the storm ridge in 2009 and washed onto the lagoon in summer 2010. The large ridge (berm) present in 2009 was established on boulders plastered with seaweed and was removed by July 2010. By the time of profiling, the surface of the swash zone was already reshaped by wave action.

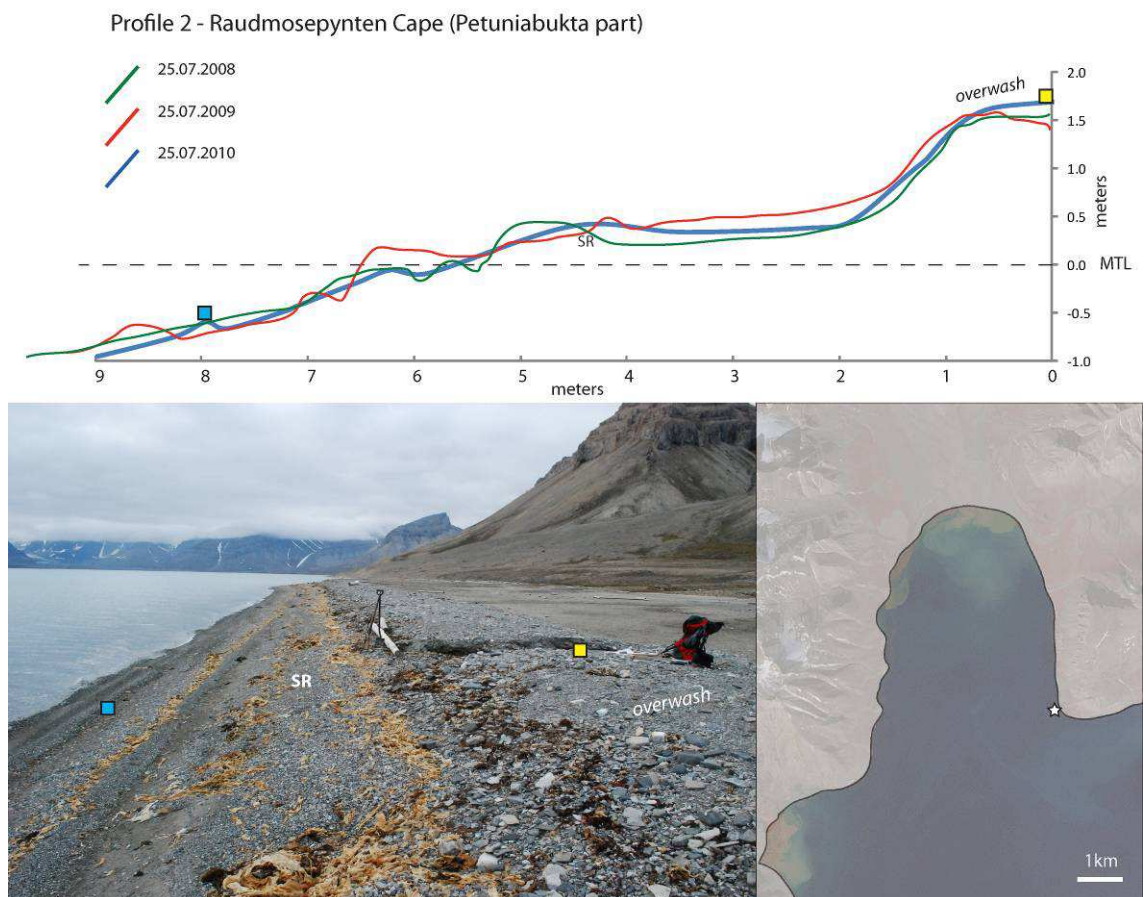


Figure 4.17. Profile 2. Upper part: Barrier profile changes observed between 2008 and 2010. Lower part: photograph of the barrier and location of site along the coast of Petuniabukta.



#### 4.4.3.3 Profile 3 – Rock glacier coast (Figure 4.18.)

Profile 3 is located beneath the steep scree slopes below a rock glacier (Figure 4.18.). The major change observed between 2008 and 2009 related to a small landslide that occurred in 2009 and which formed a debris pile at the cliff base. The material from the ridge was then distributed across the barrier and significantly smoothed the barrier surface. By July 2010, no clear outline of the storm ridge was present along the barrier profile, although fragments of seaweed, litter and driftwood thrown on the cliff slope suggest that the modern storm ridge was at the cliff toe. Micro-relief changes along the seaward slope of the barrier ranged between 0.1 – 0.5 m and were related to the formation of several small gravel-dominated berms on sandy surfaces that migrated up and down the swash zone throughout the open-water season.

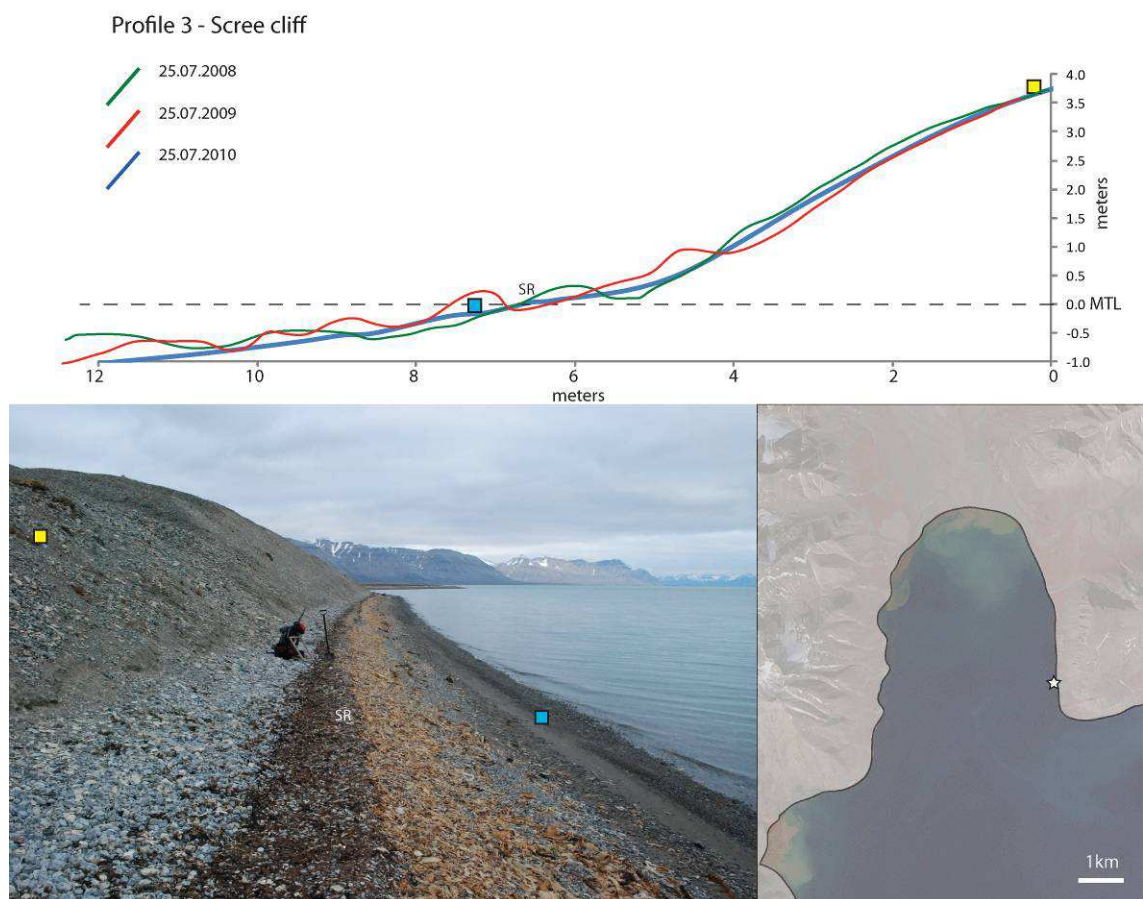


Figure 4.18. Profile 3. Upper part: Barrier profile changes observed between 2008 and 2010. Lower part: photograph of the barrier and location of site along the coast of Petuniabukta.

#### 4.4.3.4 Profile 4 – Barrier formed along the relict coastal landforms (Figure 4.19.)

Profile 4 extends across a barrier formed by a series of high and wide storm ridges that separate a former lagoon/coastal pond formed between a rock glacier front and the coastal barrier (Figure 4.19.). Currently, the lagoon is vegetated and filled with both barrier gravels and finer slope deposits. Driftwood occurs in and spreads over the surface of the storm ridges. The older ridges contain coarser pebbles than the material found in the most recent ridges. The active storm ridge is formed on the seaward slopes of the large, older barrier complex. Between 2008 and 2010, the location of the modern storm ridge has remained stable although the feature has significantly decreased in height. There was no well-developed storm ridge in July 2009 and that surveyed in summer 2010 was *ca.* 0.5 m lower than the ridge from 2008. In the same period the swash zone was eroded and lowered up to 0.65 m, leading to a steepening of the seaward slope of the barrier.

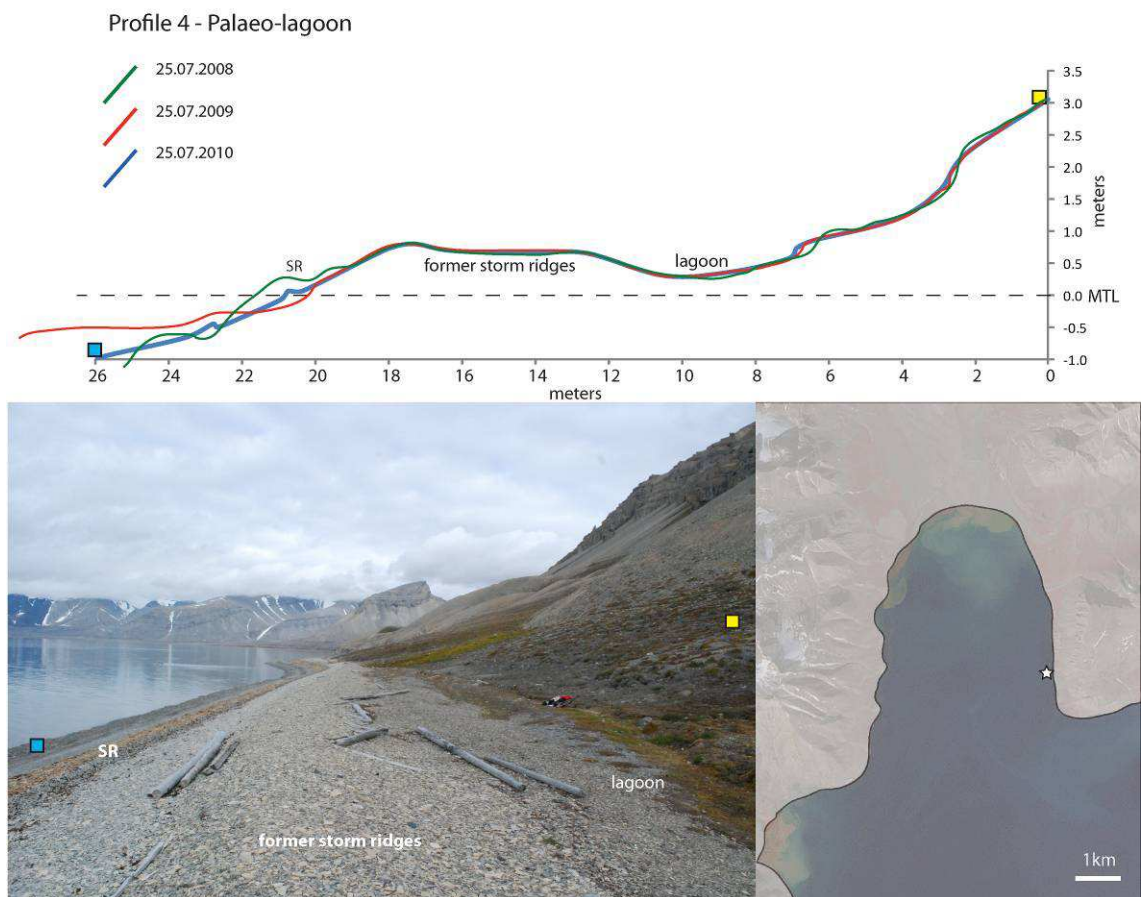


Figure 4.19. Profile 4. Upper part: Barrier profile changes observed between 2008 and 2010. Lower part: photograph of the barrier and location of site along the coast of Petuniabukta.

#### 4.4.3.5 Profile 5 – Barrier strongly modified by sea-ice processes (Figure 4.20.)

The site was selected due to the varied barrier micro-relief observed that is linked with the intensive operation of sea-ice processes. The area is characterised by one of the biggest concentrations of sea-ice pile-ups and large accumulations of driftwood and seaweed (Figure 4.20.). These conditions are probably linked to the change in the submarine topography that occurs between coastal sections E2 and E3. The submerged shore platform along the coast narrows to *ca.* 100-150 m and allows waves to break closer to the shore as well as development of longshore current in the deeper nearshore water.

In section E3, the submerged shore platform widens and this causes refraction of longshore current and waves, causing the large amount of material (sea-ice, driftwood, seaweed, sediments) to be thrown onshore. Profile changes observed in years 2008-2010 ranged between *ca.* 0.1 m over the surface of a kaimoo hillock to *ca.* 1 m over the surface of storm ridge and were mainly related mainly to melting of sea-ice underneath the barrier surface sediments and to ice bulldozing action. The storm ridge migrated *ca.* 1.5 m seaward between 2008 and 2009 and returned to the same position as in 2008 by the end of July 2010.

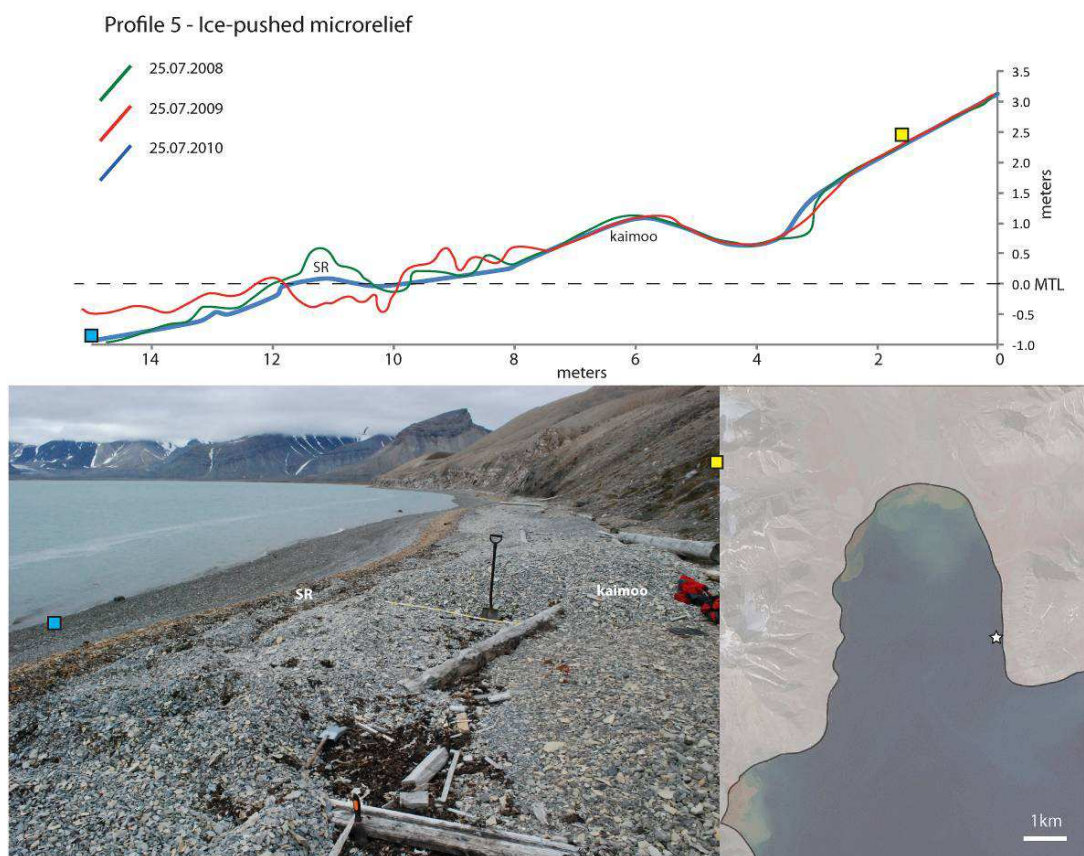


Figure 4.20. Profile 5. Upper part: Barrier profile changes observed between 2008 and 2010. Lower part: photograph of the barrier and location of site along the coast of Petuniabukta.



#### 4.4.3.6 Profile 6 – Barrier supplied with debris flows and formed along the anhydrite/gypsum rock cliffs (Figure 4.21.).

Profile 6 borders on anhydrite/gypsum cliffs (Figure 4.21.). There was only a small surface change (ca. 0.1 – 0.3 m) observed along the profile between 2008 and 2010 that was related to the local redistribution of debris delivered to the surface of a barrier in early July 2008. Although the storm ridge lowered (ca. 0.2 m) and decreased in width (ca. 0.9 m), it has remained in a stable position during three consecutive years.

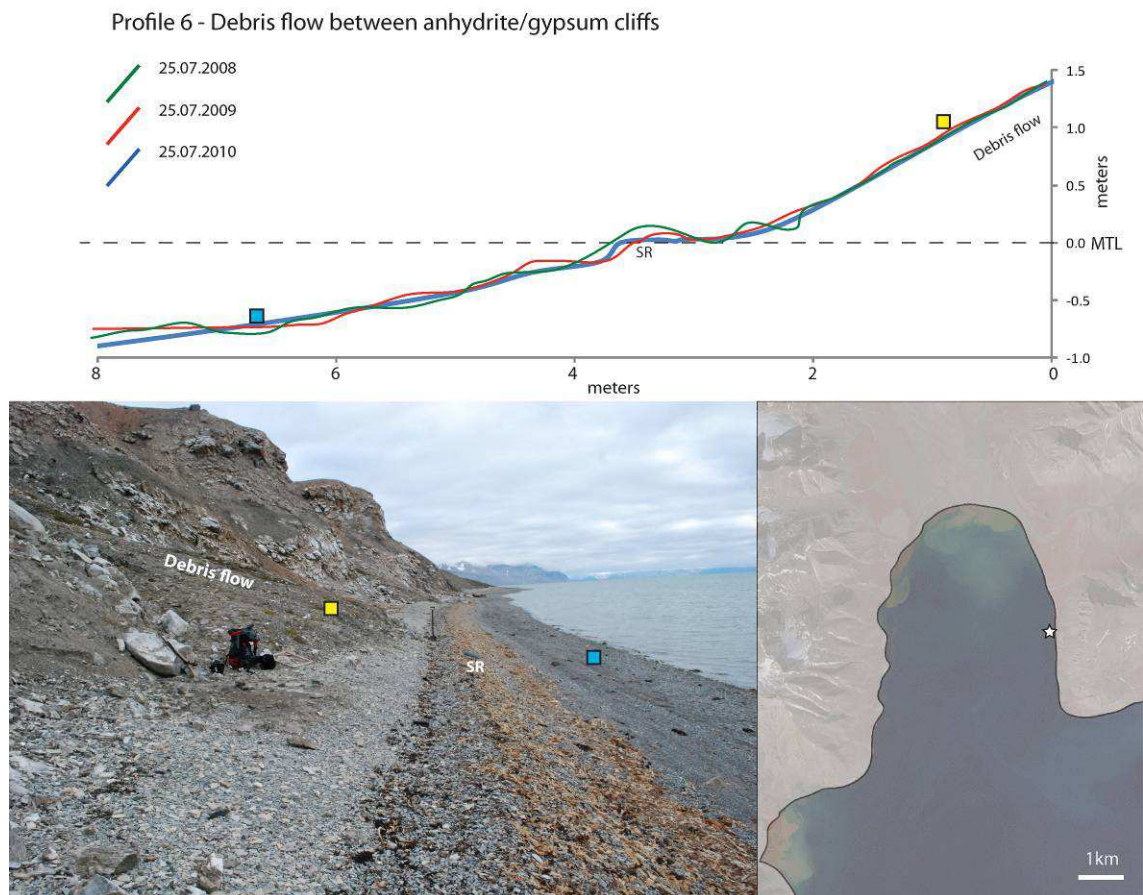


Figure 4.21. Profile 6. Upper part: Barrier profile changes observed between 2008 and 2010. Lower part: photograph of the barrier and location of site along the coast of Petuniabukta.

#### 4.4.3.7 Profile 7 – Barrier blocking the Dynamiskbekken outlet (Figure 4.22.)

Profile 7 is located at the Dynamiskbekken fan delta, where the barrier blocks an active outlet from the alluvial fan (Figure 4.22.). A storm ridge on this section is *ca.* 2.5 m wide and extends to *ca.* 0.6 – 0.8 m above MTL, providing a strong barrier for debris flows and streams that discharge from the fan in summer months. The storm ridge was breached by Dynamiskbekken in summer 2009 and this explains the significant lowering (*ca.* 0.45 m) of the ridge crest and the accumulation of several mounds across the swash zone composed of finer gravel and sand that was previously stored in the back of a barrier. Between 2008 and 2010 the storm ridge moved seaward *ca.* 1.3 m and, because of the removal of a *ca.* 0.4 m-thick layer of sediments from the swash zone, became steeper. This section of the barrier is also characterised by the frequent occurrence of ice floes buried in the barrier sediments, so the measured surface changes may also be related to melting of ice during first 2-3 weeks of July and associated formation of shallow hollows and pits.

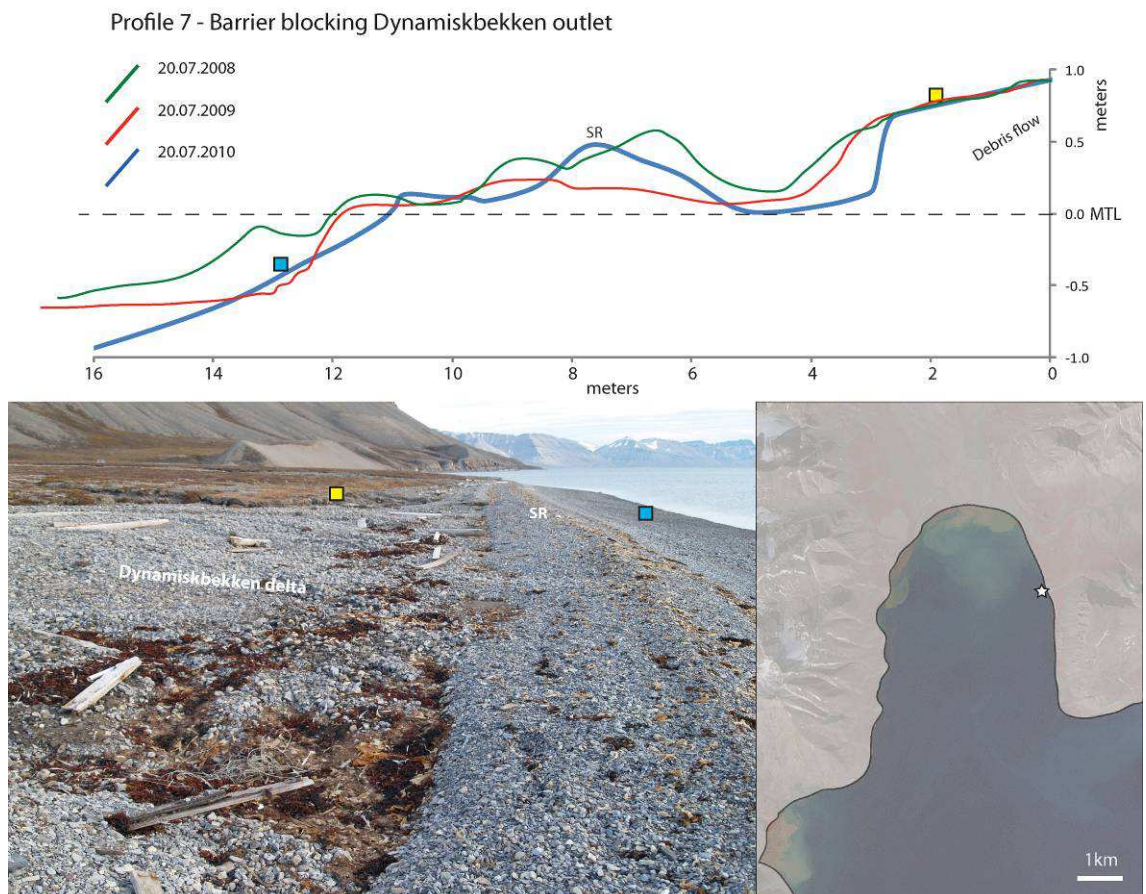


Figure 4.22. Profile 7. Upper part: Barrier profile changes observed between 2008 and 2010. Lower part: photograph of the barrier and location of site along the coast of Petuniabukta.

#### 4.4.3.8 Profile 8 - Wide barrier coast along the Skottehytta cliff (Figure 4.23.)

Three profiles are measured downdrift (north) of the Dynamiskbekken delta in section E6. The first of these extends across the barrier that has formed along a low cliff that is cut in uplifted beaches (Figure 4.23.). The barrier coast here comprises two elements: a wide relict storm ridge covered with tundra at the base of a solifluction cliff, and a massive modern storm ridge that is adjacent to a wide, low-angled swash zone. The storm ridge remained stable during the observation period and the 2010 ridge lowered (*ca.* 0.4 m). Micro-relief changes observed along the slope of the cliff and the seaward slope of the barrier were associated with frequent shore-landing of boats and trampling of the cliff by people. The vegetated top of the cliff was relatively stable and slumps, 0.4 m long and 0.3 wide, were restricted to trampled paths. The characteristic feature observed along the barrier swash zone was a *ca.* 0.5 m deep hollow formed behind the erratic boulder that was gradually infilled with sediments during the summer months. The formation of the hollow was linked with the melting of icefoot remnants anchored to the boulder that was covered with gravel and sand during the first weeks of open water conditions in the bay.

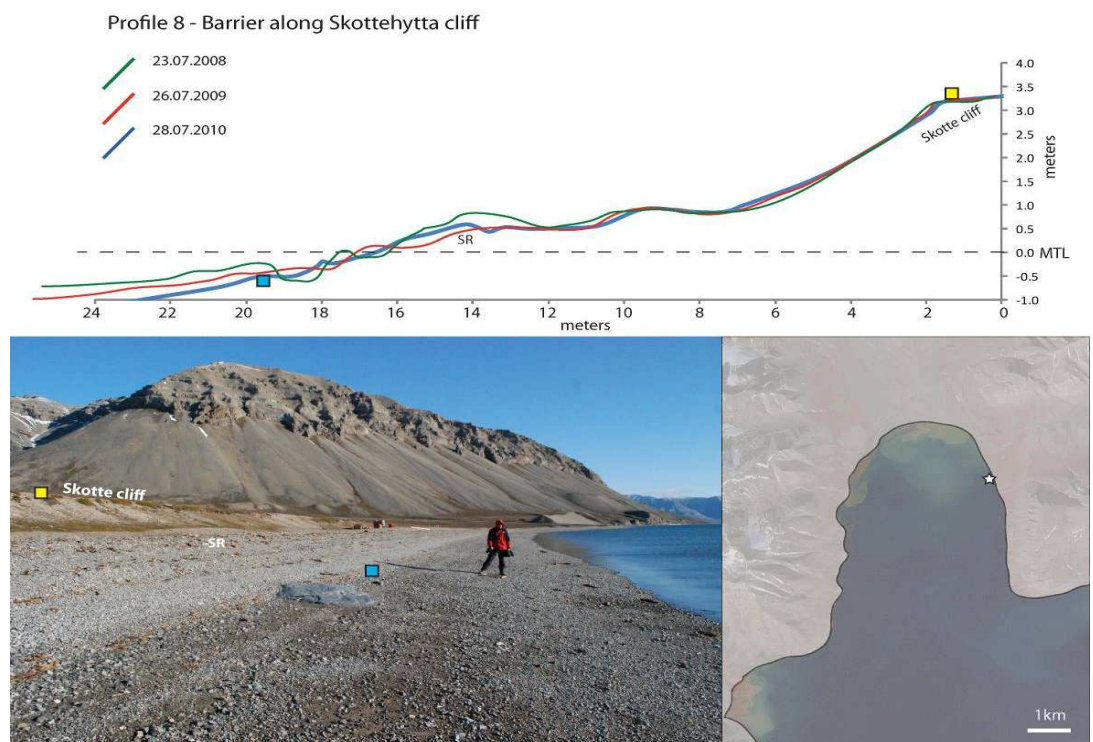


Figure 4.23. Profile 8. Upper part: Barrier profile changes observed between 2008 and 2010. Lower part: photograph of the barrier and location of site along the coast of Petuniabukta.



#### 4.4.3.9 Profile 9 – Barrier blocking outlet of tundra lakes creek (Figure 4.24.)

Profile 9, also in section E6, occurs where the barrier blocks a small creek that drains three tundra lakes that have developed on uplifted marine terraces (Figure 4.24.). The barrier comprises four *ca.* 2 m-wide ridges that have accumulated up to 0.7 m MTL (above mean tide level). The modern storm ridge remained stable between 2008 and 2010 and, as with Profiles 7 and 8 lowered (by *ca.* 0.3 m) in summer 2009. Although the barrier was not breached during the observation period, the small pond behind the barrier was frequently flooded by seepage through the gravel-dominated barrier at high tide. During the 3-years period of observation, the seaward slope of the barrier steepened and the morphology of the barrier surface became smoother.

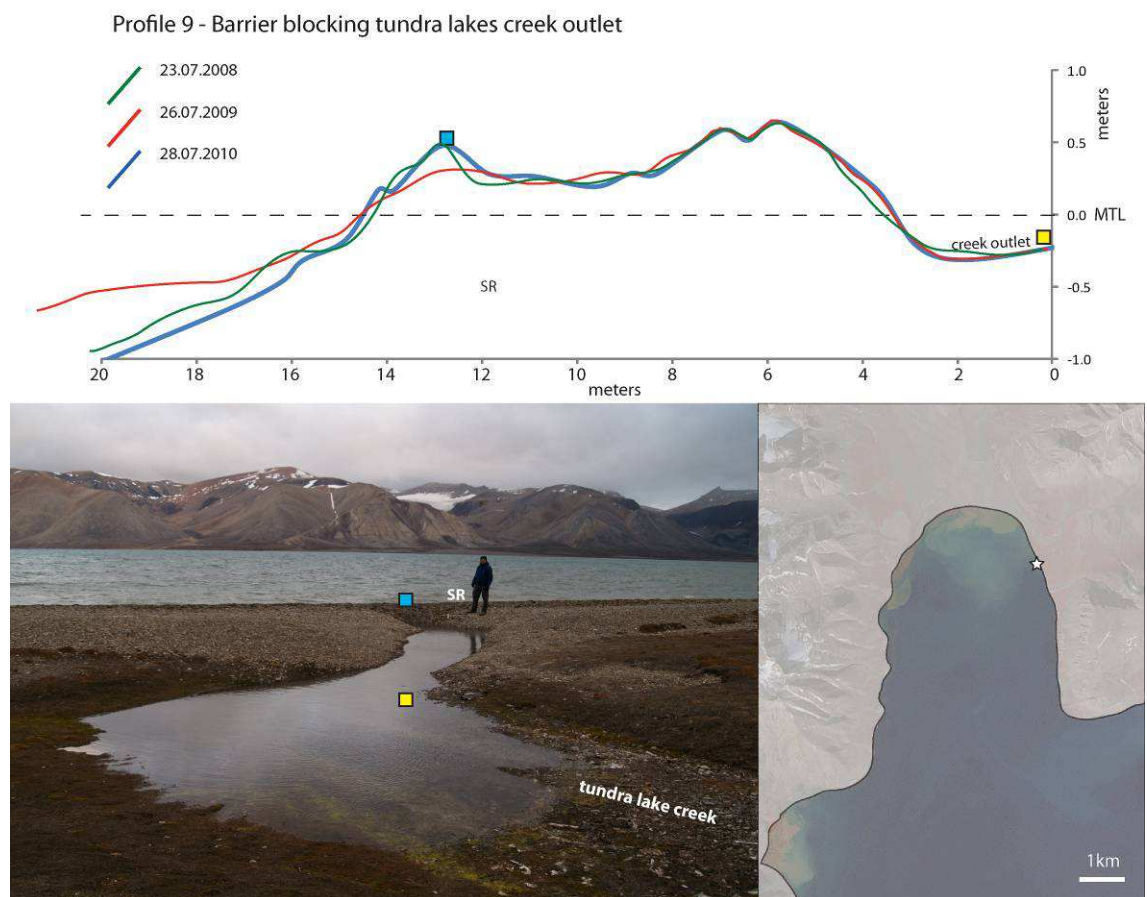


Figure 4.24. Profile 9. Upper part: Barrier profile changes observed between 2008 and 2010. Lower part: photograph of the barrier and location of site along the coast of Petuniabukta.

#### 4.4.3.10 Profile 10 – Barrier formed along low, solifluction cliff (Figure 4.25.)

Profile 10 is located along a coastal section where the barrier is supplied with slumping of tundra blocks from a small active cliff that is eroding into a low-lying (*ca.* 1.2 m MTL) raised beach (Figure 4.25.). The average recession of the cliff wall observed between 2008 and 2010 along a 200 m section was less than  $0.1 \text{ m yr}^{-1}$ , although local slumps produced small (*ca.* 0.4 m) stretches of accelerated retreat in the cliff edge. The material accumulated at the base of the cliff was fine (sand, mud with occasional pebbles) and was a subject of intensive deflation. Storm ridge construction was strengthened by seaweed insets. This was particularly prominent in 2008, when the ridge lowered to *ca.* 0.7 m MTL. Between 2008 and 2010, the storm ridge migrated *ca.* 0.6 m inland and developed a smoother seaward slope.

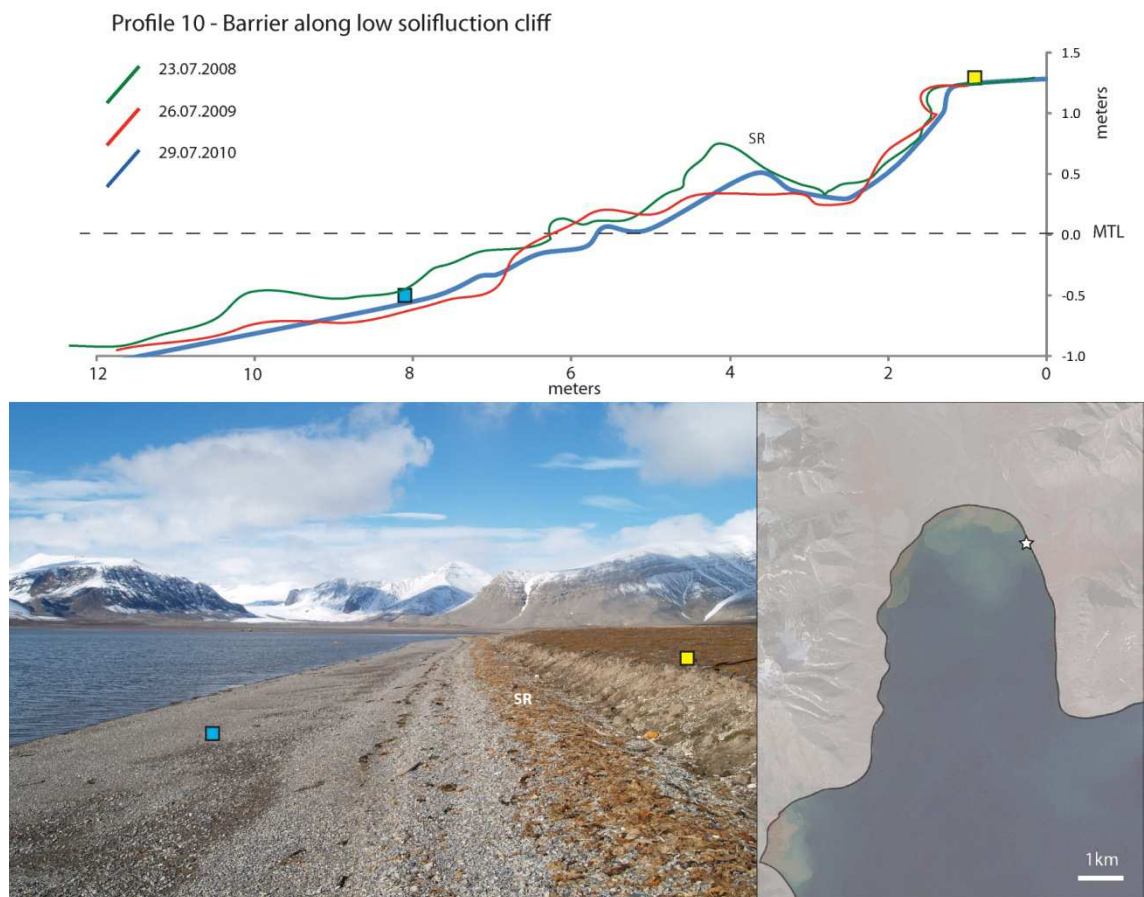


Figure 4.25. Profile 10. Upper part: Barrier profile changes observed between 2008 and 2010. Lower part: photograph of the barrier and location of site along the coast of Petuniabukta.

#### 4.4.3.11 Profile 11 – Barrier formed along the spit-platform (Figure 4.26.)

Profile 11 extends across the most recent gravel ridges of the Ebba spit-platform. Between 2008 and 2010, the storm ridge retreated *ca.* 1.1 m landward and became steeper (Figure 4.26.). The landward shift of the storm ridge in summer 2010 was associated with storm-weather conditions with wind gusts exceeding  $19 \text{ m s}^{-1}$ . In the course of three years the amount of seaweed and sand incorporated in the gravel- barrier storm ridge increased.

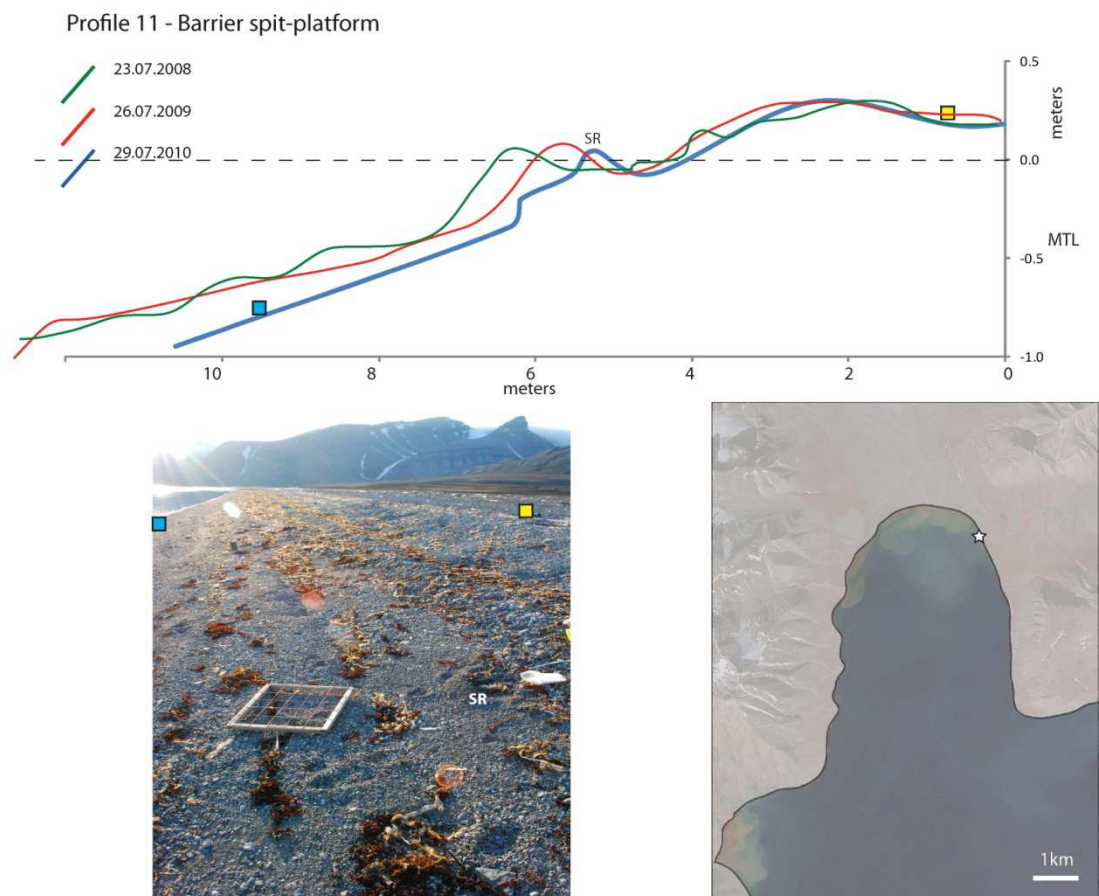


Figure 4.26. Profile 11. Upper part: Barrier profile changes observed between 2008 and 2010. Lower part: photograph of the barrier and location of site along the coast of Petuniabukta.



#### 4.4.3.12 Profile 12 – Narrow barrier exposed to long-fetch waves from Adolfbukta (Figure 4.27.)

Profile 12 extends across a narrow barrier that is washed by waves generated by strong winds that descend from the Nordenskiöldbreen (Figure 4.27.). The barrier is formed along a small cliff that is eroded in a strongly lithified diamicton that is covered by uplifted Holocene marine sediments and comprises a mixture of coarse gravel and seaweed. The barrier in this section experienced the largest profile change in the entire study. Between 2008 and 2010 the swash zone was lowered by *ca.* 1 m. The well-developed storm ridge that was present in summer 2008 and 2009 disappeared during first two storms that occurred on the 16<sup>th</sup> and 17<sup>th</sup> of July 2010.

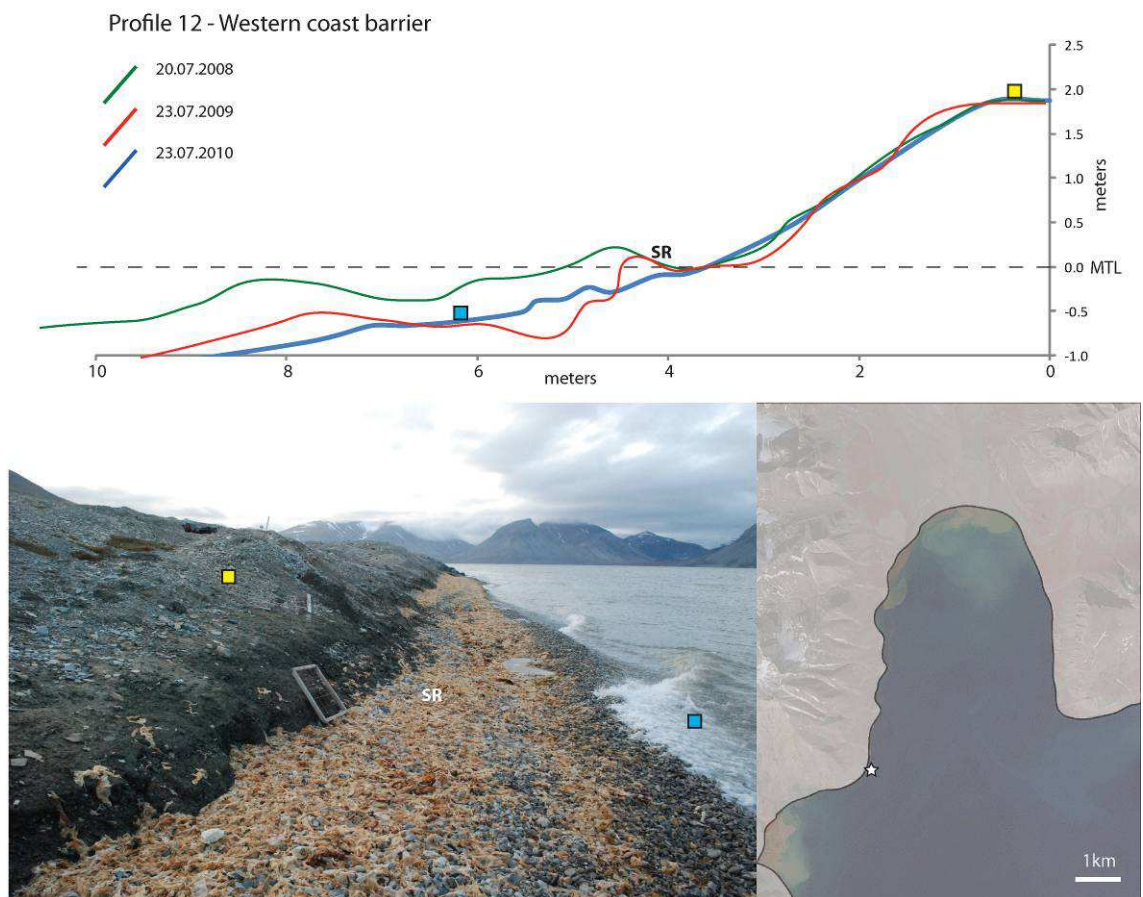


Figure 4.27. Profile 12. Upper part: Barrier profile changes observed between 2008 and 2010. Lower part: photograph of the barrier and location of site along the coast of Petuniabukta.

#### 4.4.3.13 Profile 13 – Narrow barrier formed along the snow-fed fan delta (Figure 4.28.)

Profile 13 is located along a small cliff that is eroded into an alluvial fan delta that is fed by snow-melt streams which drain the eastern slopes of Mount Piramiden (Figure 4.28.). The storm ridge comprises a gravel-dominated ridge that overlies a belt of boulders eroded from the seaward margin of the alluvial fan. The surface of the barrier is frequently flooded during stormy conditions that coincide with high tides. Between 2008 and 2010 the storm ridge retreated inland *ca.* 1.2 m and lowered *ca.* 0.3 m. The storm ridge blocked the snow-melt streams in the summer of 2008. As well as changes to the storm ridge, the surveys show a *ca.* 0.4 m lowering of the swash zone between 2009 and 2010.

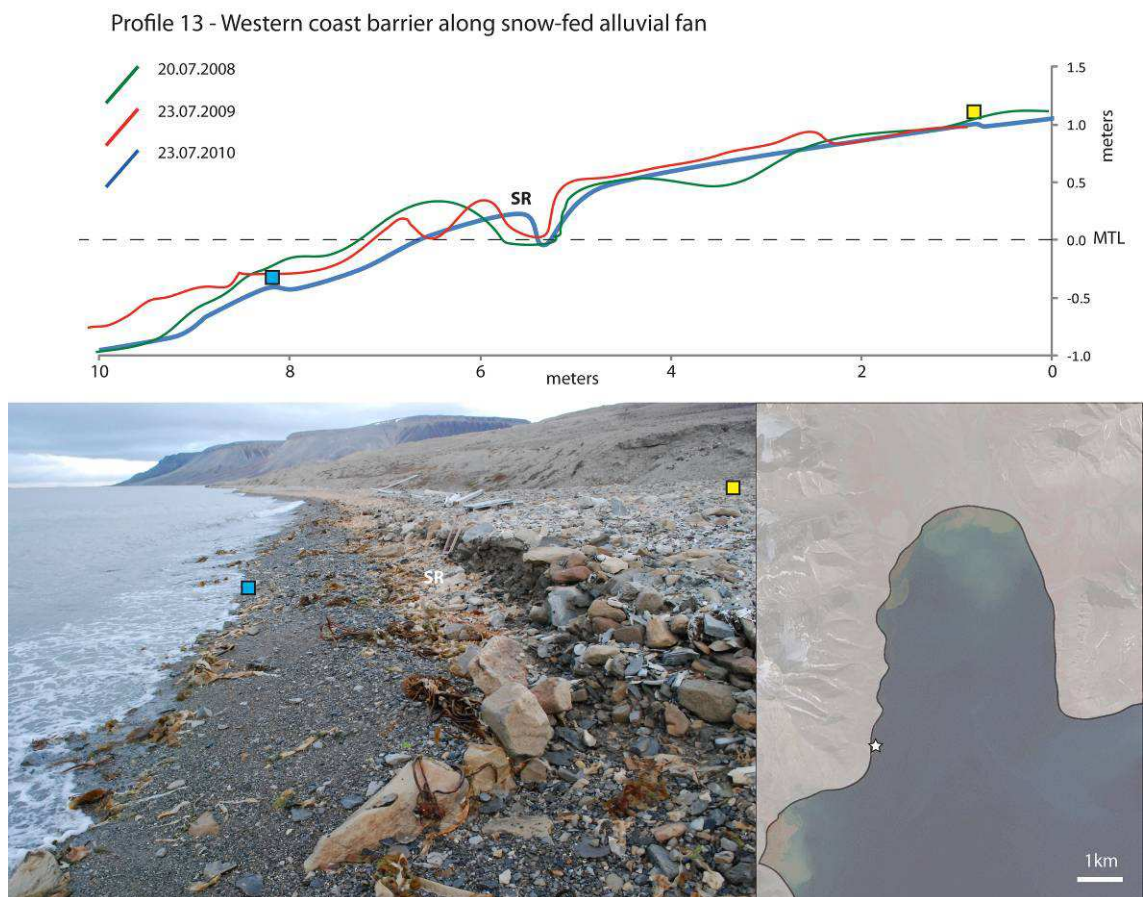


Figure 4.28. Profile 13. Upper part: Barrier profile changes observed between 2008 and 2010. Lower part: photograph of the barrier and location of site along the coast of Petuniabukta.

#### 4.4.3.14 Profile 14 – Barrier along snow-fed alluvial fan delta 2 (Figure 4.29.)

Profile 14 extends across a barrier that blocks the outlets of snow-fed streams that are building a fan delta (Figure 4.29.). This section of coast is rich in ice-push ridges and kaimoo hillocks. The barrier has a well-developed 2 m-wide storm ridge and swash zone composed of fine gravels and sand. Between 2008 and 2010 the position of the storm ridge has not changed significantly although the crest of the ridge has lowered by *ca.* 0.2 m. The wave erosion of ice-pushed ridges and the melting of ice-floes buried in the barrier caused the micro-relief present along the seaward slope of the barrier. In 2008 and 2010, ice-pushed ridges survived in the upper swash zone until the end of July. The surface changes of the seaward slope ranged between 0.1 and 0.5 m.

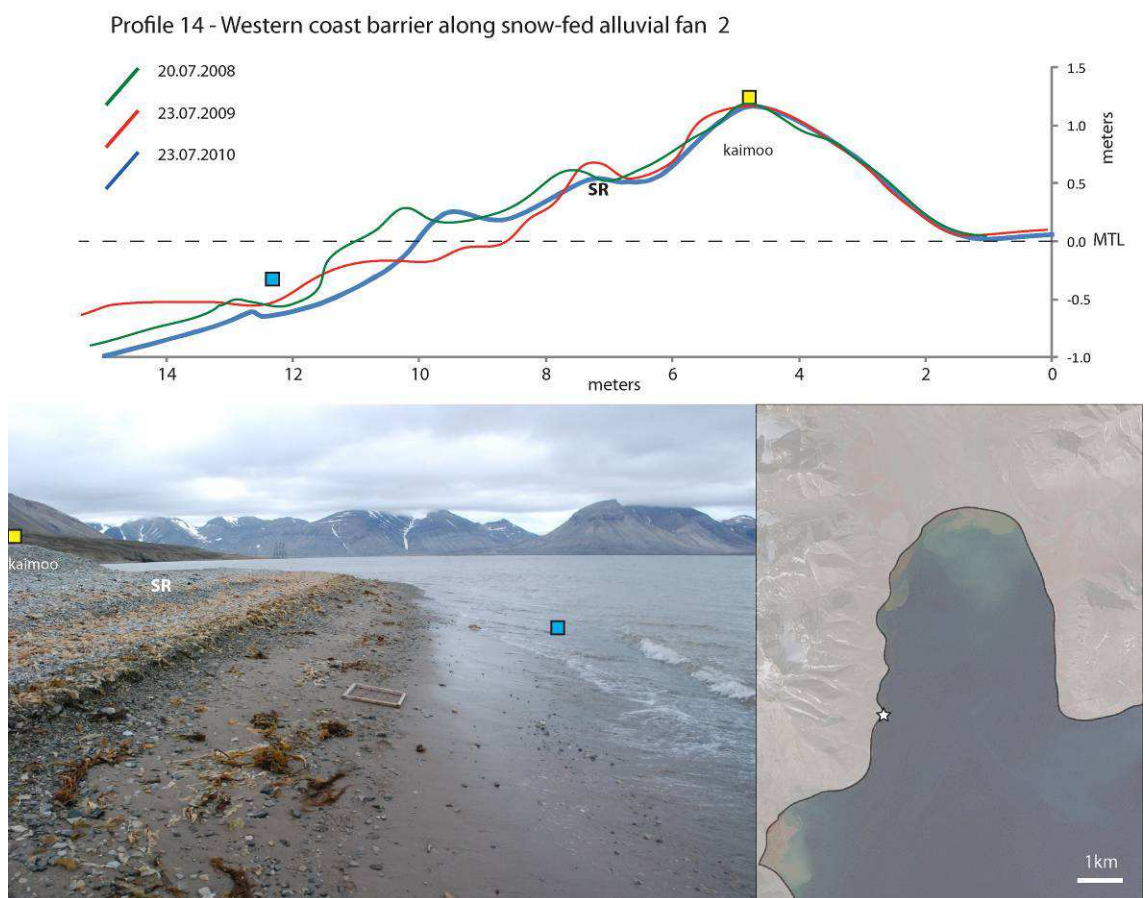


Figure 4.29. Profile 14. Upper part: Barrier profile changes observed between 2008 and 2010. Lower part: photograph of the barrier and location of site along the coast of Petuniabukta.



#### 4.4.3.15 Profile 15 Barrier along snow-fed alluvial fan delta 3 (Figure 4.30.)

Profile 15 crosses a beach formed adjacent to another alluvial fan delta that is supplied by snow-fed streams which flow down the eastern slopes of Mount Piramiden (Figure 4.30.). The fan supplies significant amounts of fine gravel and sandy sediments to the coast. The barrier was breached by streams in the early part of the summers of 2008 and 2009 when the storm ridge comprised mixed sand and gravel. A *ca.* 2 m wide and 0.45 m MTL high storm ridge was formed mainly by gravel and seaweed in 2010 and was of a sufficient size to block the stream outlets until the middle of August of that year. Between 2008 and 2010 the storm ridge widened *ca.* 0.9 m and prograded seaward *ca.* 0.8 m. During the observation period the surface elevation of the swash zone increased *ca.* 0.15 m.

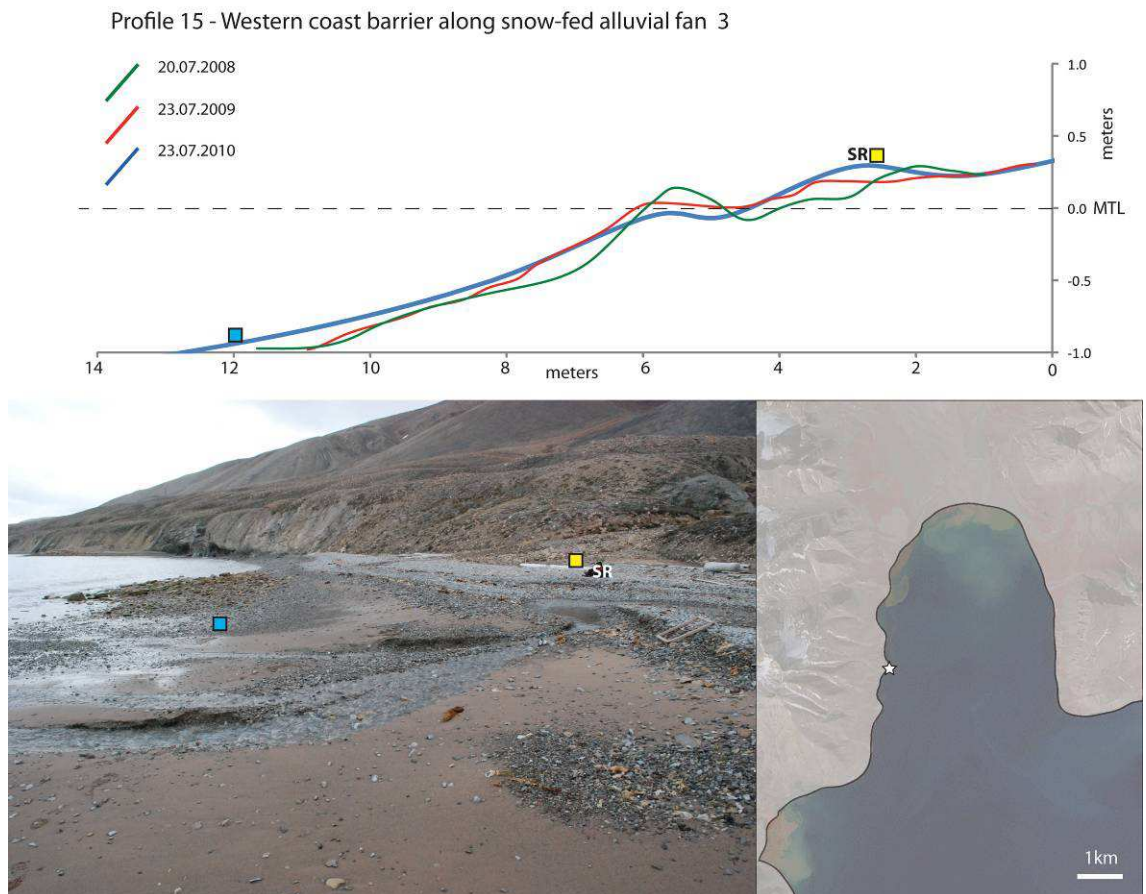


Figure 4.30. Profile 15. Upper part: Barrier profile changes observed between 2008 and 2010. Lower part: photograph of the barrier and location of site along the coast of Petuniabukta.

#### 4.4.3.16 Profile 16 – A wide barrier before Elzaelva and the Ferdinandelva fan deltas (Figure 4.31.)

This is one of the widest parts of the western coast (*ca.* 55 m) where the barrier has formed along low solifluction cliffs (Figure 4.31.). The barrier has a wide and gentle seaward slope and is composed predominantly of fine gravels and sand. Between 2008 and 2010 the seaward slope of the barrier increased by an average of 0.15 m. However, the storm ridge has migrated landward (*ca.* 0.9 m) and lowered *ca.* 0.1 m. This is the first section of the barrier where the storm ridge was devoid of seaweed. The development of a *ca.* 0.8 m high and (up to) 3 m-wide storm ridge is partly enabled by long trunks of driftwood that are incorporated within the barrier beach at this profile.

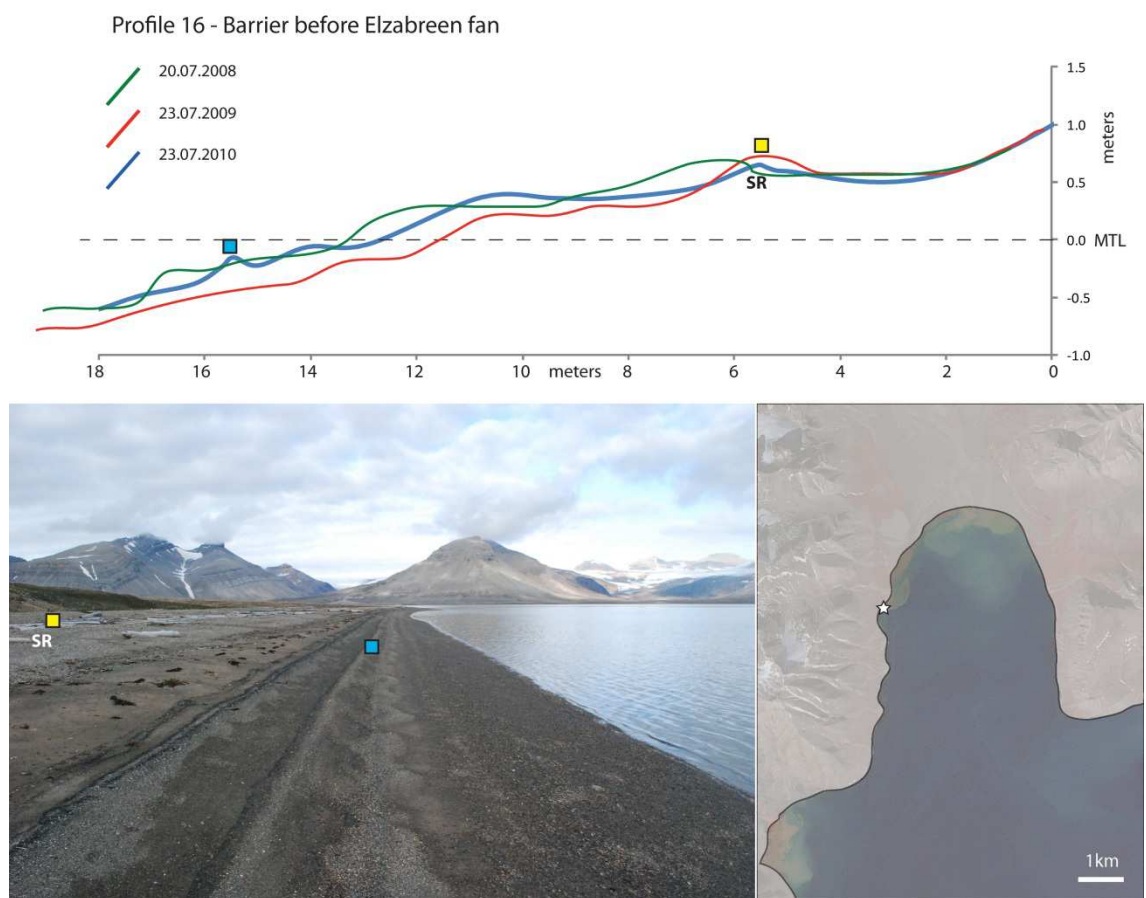


Figure 4.31. Profile 16. Upper part: Barrier profile changes observed between 2008 and 2010. Lower part: photograph of the barrier and location of site along the coast of Petuniabukta.



#### 4.4.3.17 Profile 17 – Barrier along Ferdie Spit 3 (Figure 4.32.)

Profile 17 crosses three spits formed along the Ferdie Fan 3 (Figure 4.32.). The changes observed along the surface of Ferdie Spits 1 and 2 (ca. 0.1 to 0.2 m) were related to the periglacial sorting of surface sediments and a redistribution of sandy deposits by strong winds blowing from the surrounding glacier valleys. The surface of the modern barrier forming the Ferdie Spit 3 is dotted with driftwood and litter, and was previously covered with ice-push and ice-melt features until at least the third week of July. The most significant morphological changes observed between 2008 and 2010 occurred along the barrier seaward slope which has steepened and lowered by ca. 0.3 m. The lowering of the barrier slope applied not only to the zone composed of gravel and sand, but also the muddy zone where the barrier merges with the prograding tidal flat, which has lowered ca. 0.05-0.1 m.

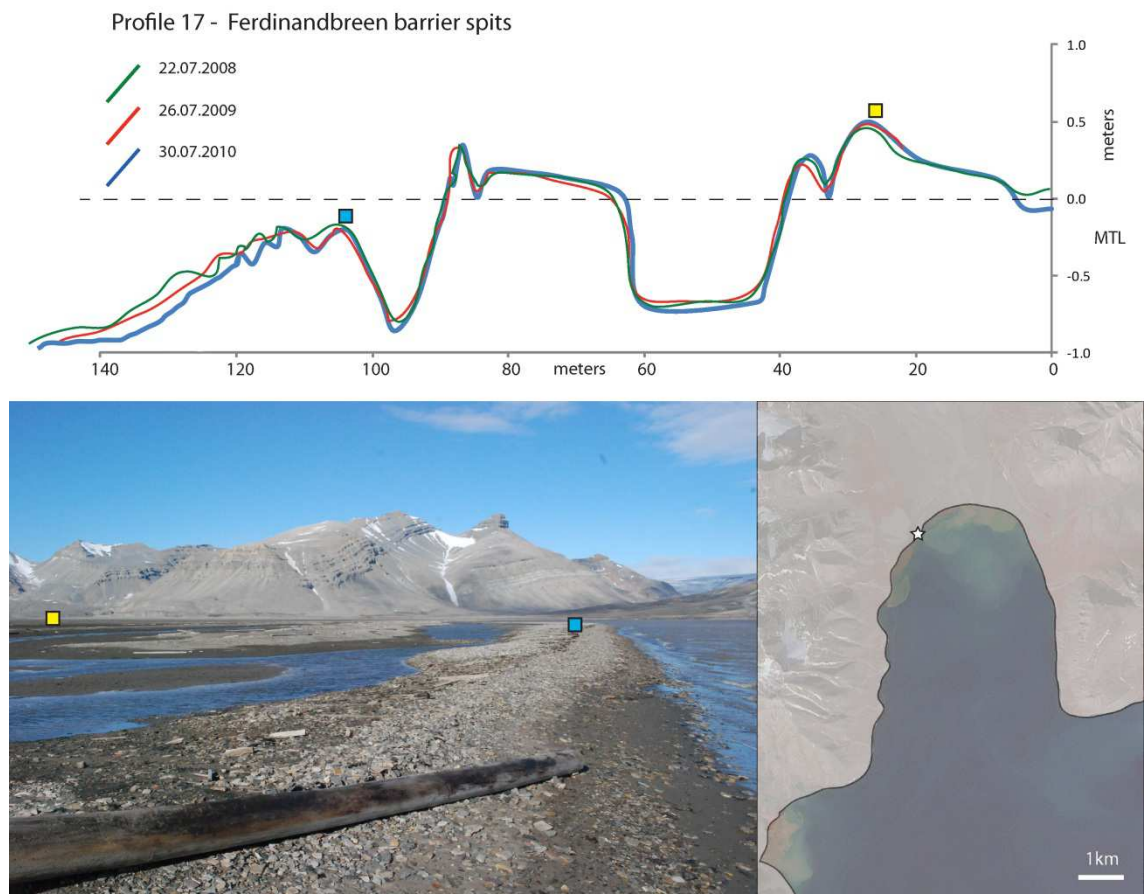


Figure 4.32. Profile 17. Upper part: Barrier profile changes observed between 2008 and 2010. Lower part: photograph of the barrier and location of site along the coast of Petuniabukta.

#### 4.4.4 Surface sediments characteristics and local geomorphic controls on barrier morphology

In addition to surveying 17 beach profiles, surficial samples were collected from the barriers studied to characterise their surficial grain size characteristics. The results are presented in Table 4.5.

Profile	Proportion of sand/gravel in the swash zone (%) + occurrence of boulders (B) and mud (M)			Dominant pebble shape in the storm ridge (ZINGG (1935) classification) + clast roundness category (after BENN 2007)		Morphological changes of the barrier: - landward/seaward migration of storm ridge LM/SM or stable ST - decrease/rise of storm ridge height DH/RH - erosion/accumulation of swash zone ES/AS		
1	40/60	B		DISCS	<i>sub-rounded</i>	ST	DH	AS
2	35/65	B	M	DISCS	<i>sub-rounded</i>	LM	DH	ES
3	20/80	B		RODS	<i>sub-angular</i>	SM	DH	ES
4	25/75	B		DISCS	<i>sub-rounded</i>	ST	DH	ES
5	45/55	B		DISCS	<i>sub-rounded</i>	ST	DH	ES
6	20/80	B	M	RODS	<i>sub-angular</i>	SM	DH	ES
7	48/52	B	M	RODS	<i>sub-angular</i>	SM	DH	ES
8	46/54	B		DISCS	<i>sub-rounded</i>	ST	DH	ES
9	48/52			DISCS	<i>sub-rounded</i>	ST	RH	ES
10	55/45	B	M	DISCS	<i>rounded</i>	LM	DH	ES
11	52/48	B	M	DISCS	<i>rounded</i>	LM	DH	ES
12	5/95	B		DISCS	<i>sub-rounded</i>	LM	DH	ES
13	7/93	B		RODS	<i>sub-angular</i>	LM	DH	ES
14	73/27	B	M	RODS	<i>sub-rounded</i>	LM	DH	ES
15	65/35	B	M	RODS	<i>sub-angular</i>	SM	RH	AS
16	62/38		M	DISCS	<i>sub-rounded</i>	LM	DH	AS
17	52/35		M	BLADES	<i>sub-rounded</i>	LM	DH	ES

Table 4.5. Summary of sedimentological properties of Petuniabukta barriers and morphological changes observed between 2008 and 2010.

The most important finding stemming from sedimentological survey is the tendency for the seaward migration of storm ridges composed of subangular, rod-shaped pebbles that are delivered to the barriers by debris flows and rockfalls (Profile 3, 6 and 7). One of the barriers supplied with subangular and rod-shaped pebbles by an ephemeral snow-melt stream (Profile 15) also migrated seaward in the period of observation. This suggests that on the inter-annual timescale the Petuniabukta barrier coast can prograde only when it receives significant amount of fresh and coarse sediments from the terrestrial sources.

The erosion and associated lowering of many of the seaward slopes of Petuniabukta barrier coast that occurred during summer 2010 were also independent of sediment cover properties. A reasonable explanation of this process can be seen in the sea-ice cover dynamics (Figure 4.4.). The summer of 2010 was characterised by the earliest disappearance of fast ice cover in Petuniabukta from among three analysed years and this allowed the longer operation of wave action on the barrier seaward slope. The landward migration of storm ridge was more frequent along the western coast. This may imply increased exposure to waves triggered by strong glacier winds and the greater depth of nearshore zone allowing larger waves to approach and break closer to the barrier face. These changes are discussed in more detail in Chapter 8.

## 4.6 Chapter summary

This Chapter has presented a qualitative description of coastal processes operating in the study area, as well as the results of repeat levelling surveys completed over the course of three years at 17 profiles. The main findings are:

- Ongoing climate warming on Svalbard reduces sea-ice cover, increases permafrost thaw, glaciofluvial and slope sediment supply, and increases storm activity. These processes should, in combination, lead to rapid coastal change.
- This study has shown that the barriers that currently form along the sheltered coasts of Petuniabukta are, over annual timescales, characterised by rather small and irregular morphological changes that are controlled by episodic sediment supply from terrestrial sources (glacier rivers, snow-fed streams, rockfalls, debrisflows) or by the occurrence and displacement of seaweed and driftwood accumulations.
- The impact of sea-ice geomorphic processes were short-lived and only preserved in coastal sections that are exposed to a particular combination of seabed topography, wave activity, and zone of concentrated piling up of sea-ice.
- The morphological changes of barrier profiles observed during three summer seasons (2008-2010) ranged between 0.1- 0.9 m (vertical) and 0.1-1.2 m (horizontal). The most common process observed along the barriers between summer 2008 and summer 2010 was the slight decrease in storm ridge height and a steepening of the seaward slope associated with the erosion of swash zone. This latter process occurred regardless of barrier location and physical properties of sediments covering the barrier surface.
- The earlier disappearance of fast ice cover in early summer 2010, which extended open-water conditions, is likely responsible for the enhanced seaward slope erosion.

The following Chapter adds to our understanding of the modern coastal zone in the study area through investigations of rock resistance variability across the recently deglaciated rock coast in neighbouring Adolfbukta.

# **Chapter 5:**

## **ANNUAL TIMESCALES**

### **Processes operating on the present-day rocky coasts**



## 5.1 Introduction

This chapter addresses the second of the research questions defined in Chapter I, namely:

*What processes operate on recently deglaciated rocky coasts in the study area?*

To answer this question the following objective was addressed:

to examine the hypothesis of “coastal amplification” of weathering rates on the rocky coasts of Spitsbergen by measurements of rock resistance variability across a recently deglaciated rocky coastal zone using Schmidt Hammer Rock Tests (SHRT).

The results of this aspect of the research presented here are published in Strzelecki (2011) - Appendix III.

## 5.2 Background

One of the most controversial problems of cold region coastal geomorphology is the determining of the relative significance of littoral processes and frost weathering in controlling rocky cliff and shore platform morphology. Indeed, until the beginning of the 21<sup>st</sup> century, world-leading coastal geomorphologists often claimed that it was impossible to obtain a clear agreement on the efficiency of coastal processes in the high latitudes (TRENHAILE 1983; BYRNE and DIONNE 2002).

As discussed in Chapter 2, the major focus of recent Arctic coastal research initiatives under the umbrella of Arctic Coastal Dynamics (ACD) group has been on understanding and modelling ice-rich permafrost coastlines, particularly in Alaska, western Canada, and the Laptev Sea regions, which are characterised by some of the most rapid erosion rates in the World (LANTUIT *et al.* 2011). In contrast, the role of ice, snow and frost action on rocky cliffs and shore platforms, specifically in sheltered fjords of polar archipelagos, remains poorly understood.

Furthermore, the geomorphology of cold region rocky coasts is marked by significant regional contrasts. During the last three decades several geomorphological studies along Atlantic Canada's rocky shorelines (e.g. DIONNE and BRODEUR 1988; DIONNE 1989; TRENHAILE and MERCAN 1984; TRENHAILE *et al.* 1998; TRENHAILE 2001; TRENHAILE *et al.* 2006; PORTER and TRENHAILE 2007; PORTER *et al.* 2010) have enabled fundamental advances in our understanding of ice and frost action on the morphology of intertidal

zones as well as 'freezing–thawing and wetting–drying' influence on shore platform and cliff relief. Relatively few investigations, however, have tested the efficiency of those processes in polar settings.

In the early 1990's, ØDEGÅRD and SOLLID (1993) and ØDEGÅRD *et al.* (1995) investigated the rocky cliffs of northern Spitsbergen (Kongsfjorden and Liefdefjorden) in an effort to understand the thermal regime in frozen rocks beneath a melting snow cover. Their observations identified four periods of differing thermal impacts on coastal cliff breakdown, and postulated processes of thermal stresses that were related to sub-zero temperature oscillations. They argued that the formation of segregation ice in fractured rock is one of the leading mechanisms controlling rock coastal morphology in polar environments. The only Arctic Coastal Dynamics project carried out on a High Arctic rocky coastal zone was a study by WAGENSTEEN *et al.* (2007) in Kongsfjorden. Using detailed photogrammetric survey these authors demonstrated that rockwall retreat rates in polar coastal settings are higher relative to the more inland locations studied by RAPP (1960) and ANDRÉ (1997). Interestingly, a similar 'coastal amplification' of weathering rates along polar shorelines has previously been proposed by JAHN (1961), but the concept has yet to be rigorously tested.

### **5.2.1 The study site: Adolfbukta**

Research was undertaken in the coastal section AI, on the recently exposed rocky forefield of Nordenskiöldbreen, along the northern shores of Adolfbukta (Figure 5.1.). After spring/summer break-up, floating sea ice in Adolfbukta is normally rapidly removed from the basin under appropriate wind conditions. During the summer, the coastline is influenced by debris-rich growlers which are sourced by calving from Nordenskiöldbreen. Wave energy is limited by a shallow fjord sill (less than 50 m) and narrow entrance and is restricted to the ice-free summer months, mainly at high tides and under rare storm events.

Since the end of the LIA, Nordenskiöldbreen has retreated *ca.* 3.5 km (Figure 5.1. C) exposing *ca.* 17 km<sup>2</sup> of unstable para-periglacial landscape (following the definition of MERCIER (2008)) (RACHLEWICZ 2010). The major bedrock units exposed by post-LIA retreat of Nordenskiöldbreen consist of resistant Precambrian metamorphic rocks (Smutsbreen Unit), which includes plagiogneisses, garnet-biotite schists, amphibolites, quartzites and marbles.

In this study, I selected an area of *ca.* 1 km<sup>2</sup> zone, encompassing plagiogneiss roche moutonnées and plunging cliffs, between the present-day shoreline, ice-cliff and LIA moraine belt (Figure 5.1. C)

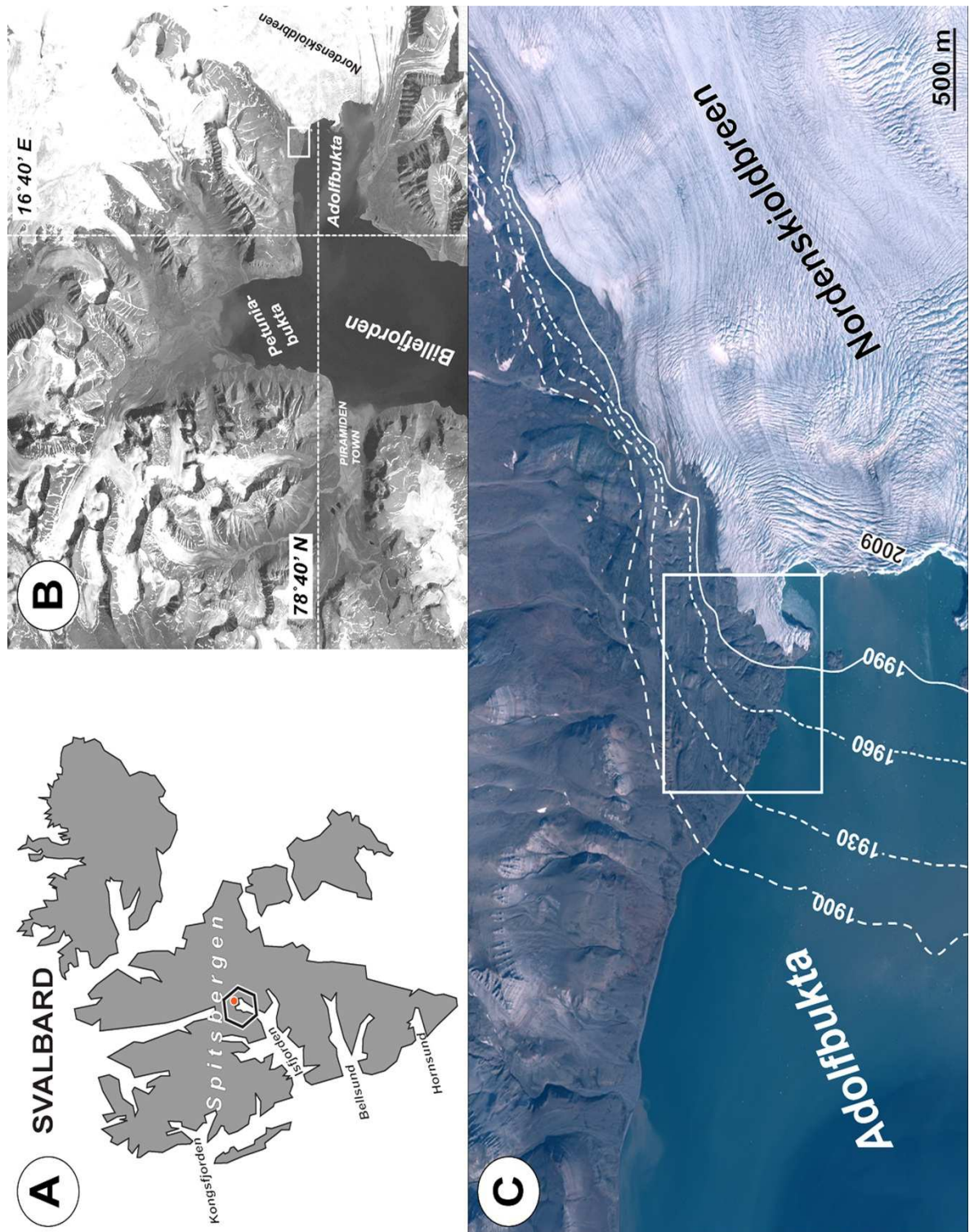


Figure 5.1. Location of the Schmidt hammer rock tests case study. **A.** Svalbard Archipelago, map shows main fjords along the western coast of Spitsbergen Island. Dot in a polygon marks location of study area. **B.** coastal section A2 **C.** Part of an orthophotomap based on Norwegian Polar Institute aerial photographs taken in 2009. The image shows the current front of Nordenskiöldbreen, the dashed lines indicate positions in 1900–1930–1960–1990. The white square marks the selected roche moutonnée field where SHRTs were carried out in 2009–2010 and is enlarged in Figure 5.2.A.

### 5.3 Methods

Schmidt hammer tests have been used in weathering and dating investigations of glacier forelands and mountainous areas since the 1960's (GOUDIE 2006), although more recently this inexpensive tool has thrown new light on hard rock coastal geomorphology (e.g. TRENHAILE *et al.* 1998; STEPHENSON and KIRK 2000a, b; DICKSON *et al.* 2004; THORNTON and STEPHENSON 2006; CRUSLOCK *et al.* 2010; CHELLI *et al.* 2010; KENNEDY *et al.* 2010).

In a pilot study, 725 Schmidt hammer readings were taken following the methodology of Day and Goudie (1977) and Selby (1980), using a classic Proceq N-type tool which provides an arbitrary measure of rock resistance shown on a scale from 10-100 (rebound values - R). During measurements 25 hits were made at points randomly selected from each of the 29 sites (white squares on Figure 5.2.A). According to NIEDZIELSKI *et al.* (2009) this number of readings provides accurate mean Schmidt hammer test values in the majority of lithologies. Only on several inaccessible surfaces located on the higher parts of cliffs was the number of hits reduced to ten. Each site consisted of a *ca.* 10×10 cm area of exposed gneissic bedrock.

The sampling strategy took into consideration distance of the rock surface from the present-day shoreline, and from the current glacier front position (Figure 5.2.A). The starting point of each of the five profile lines was a rock surface at mean sea-level, approximately 0.5 m (Profile A: S1-S5), 200 m (Profile B: S6-S11), 400 m (Profile C: S12-S17), 600 m (Profile D: S18-S23) and 800 m (Profile E: S24-S29) from the present ice cliff position. From each of the starting points, the profiles continued inland every 150 m, parallel with the Nordenskiöldbreen front.

To test if there is any vertical difference in rock resistance up the cliff wall, additional SHRT were taken on the top of the cliffs above the starting points (5 to 15 m a.s.l) in Profiles B – E. Prior to statistical analysis, all anomalous R-values were removed on the basis of Chauvenet's criterion, recommended in the interpretation of SHRT by GÖKTAN and AYDAY (1993). Chauvenet's criterion is a statistical approach for removing outliers from a set of 'n' data points. In this approach, all data points of a set of n observation which lie within a "maximum deviation" are assumed to be probable. Those that fall outside this maximum can be rejected.

To test the significance of differences between R-values measured along coastal and more inland roche moutonnée surfaces, a Cochran and Cox test was applied. Kruskal-Wallis and Dunn's tests were run to compare the R-values variations between zones I, II and III.

## 5.4 Results

Table 5.1. summarises the SHRT results and presents the mean R-values calculated for each tested rock surface.

Site	Mean R-value	Margin of error (95%CI)	Median	Mode	Min	Max	Skewness	Distance from the shoreline (m)	Distance from the glacier front (m)	Height above sea-level (m)	Age of exposure from beneath glacier ice
S1	51	1.17	51	multimodal	45	57	-0.19	0	0.5	0	2008-2009
S2	68	0.58	68	68	65	70	-0.01	150	0.5	23	2008-2009
S3	67	0.68	67.5	69	64.5	69	-0.58	300	0.5	42	2008-2009
S4	68	0.5	68	69	66	70	-0.12	450	0.5	37	2008-2009
S5	68	0.79	69	70	64	70	-0.59	600	0.5	72	2008-2009
S6	57	0.83	57	57	54	61	0.65	0	200	0	1960-1990
S7	65	0.87	66	66	62	68	-0.20	1	200	28	1960-1990
S8	69	0.58	69	70	66.5	71	-0.03	150	200	37	1960-1990
S9	72	0.28	72	73	71	73	-0.62	300	200	33	1960-1990
S10	65	0.47	65	65	63	67	-0.29	450	200	63	1930-1960
S11	62	0.67	62	63	59	64	-0.35	600	200	96	1930-1960
S12	62	0.48	62	61	61	64	0.83	0	400	0	1930-1960
S13	69	0.74	69	70	66	72	-0.20	1	400	13	1930-1960
S14	68	0.79	69	70	64	70	-0.59	150	400	20	1930-1960
S15	68	0.74	68	70	64	70	-0.46	300	400	52	1930-1960
S16	73	0.35	73	73	71	74	-0.68	450	400	78	1900-1930
S17	60	0.88	60	58	55	63	-0.37	600	400	81	1900-1930
S18	59	1.05	59	multimodal	54	64	0.24	0	600	0	1930-1960
S19	63	1.04	63	multimodal	60	68	0.26	1	600	14	1930-1960
S20	68	0.82	69	70	64	70	-0.91	150	600	20	1930-1960
S21	73	0.4	73	73	71	74	-0.45	300	600	40	1930-1960
S22	65	0.56	65	65	62	67	-0.48	450	600	90	1900-1930
S23	63	0.55	63	63	60	65	-0.59	600	600	164	1900-1930
S24	58	0.91	58	58	54	62	-0.08	0	800	0	1900-1930
S25	59	1.16	59	multimodal	54	65	0.14	1	800	14	1900-1930
S26	65	0.73	65	63	62	68	0.19	150	800	17	1900-1930
S27	65	0.7	66	66	62	68	-0.60	300	800	14	1900-1930
S28	70	0.38	70	70	68	71	-0.24	450	800	27	1900-1930
S29	73	0.26	73	73	72	74	-0.30	600	800	40	1900-1930

Table 5.1. Schmidt Hammer Rock Tests summary. Statistical parameters (mean, margin of error – 95% confidence interval, median, mode, max, min and skewness) for each of the test sites and topographical information regarding their distance from ice front, present shoreline and approximate time of the post-LIA deglaciation. Sites in grey shading were the starting points of each of the five profiles.



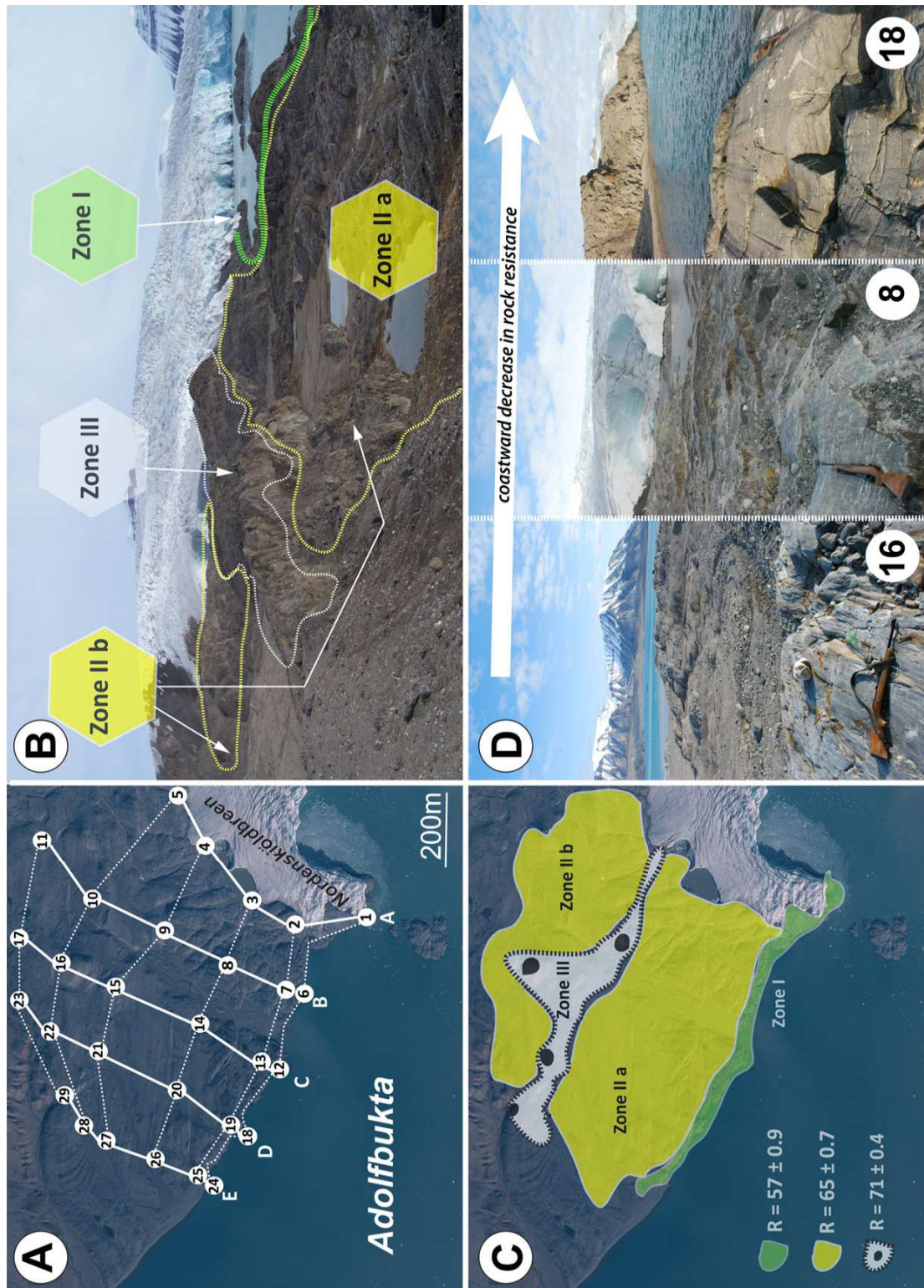


Figure 5.2. Location and key findings of SHRT in northern Adolfbukta. **A.** SHRT sites and profiles – white dots with numbers 1–29 indicate locations of rock surfaces hit. Letters A–E mark the starting point of each profile. **B.** Zones of similar rock resistance. **C.** Rock resistance variability: Zone I – the coastal zone with lowest rock resistance, Zone II – interior forefield of medium rock resistance, and Zone III – peaks of roches moutonnées of highest rock resistance. **D.** Examples of rock surfaces from different resistance zones, a riffle indicates the direction of ice flow, white arrow indicates the general trend of lowering rock resistance. Left image: example from Zone III – peaks of roches moutonnées – highest rock resistance, smooth surfaces, no snow cover; Middle image: example from Zone II – forefield interior – medium rock resistance, debris cover, thick winter snow cover; Right image: example from Zone I – coastal strip – lowest rock resistance, occasional snowdrifts, wave and tide action. Numbers in white dots (bottom right corner) indicate location of given SHRT site shown on Figure 5.2.A.

From the results in Table 5.1. the following zones of rock resistance can be clearly distinguished (presented on Figure 5.2. B and C):

Zone I – the coastal: strip covering the lower part of plunging cliffs affected by sea ice movement, wave action and sea spray (Sites S1, S6, S12, S18 and S24), with mean R-values of  $57 \pm 0.89$  – (green zone on Figure 5.2. B, C)

Zone II – area of intermediate rock resistance with mean R-values of  $65 \pm 0.7$  - (yellow zone on figure 5.2 B, C). This zone can be subdivided into areas regarding the distance from the shoreline:

- a) a strip of roches moutonnées between the top of the cliffs and Zone III (Sites S2, S3, S7, S8, S13, S14, S19, S20, S25, S26, S27), with mean R-values of  $66 \pm 0.83$ ;
- b) a strip of roches moutonnées adjacent to Nordenskiöldbreen lateral moraines (Sites S5, S11, S17, S23), with slightly lower mean R-values equal  $64 \pm 0.65$ .

Zone III – summits of roches moutonnées – characterised by the highest rock resistance, with mean R-values of  $71 \pm 0.42$  – (white zone on Figure 5.2.B, C)

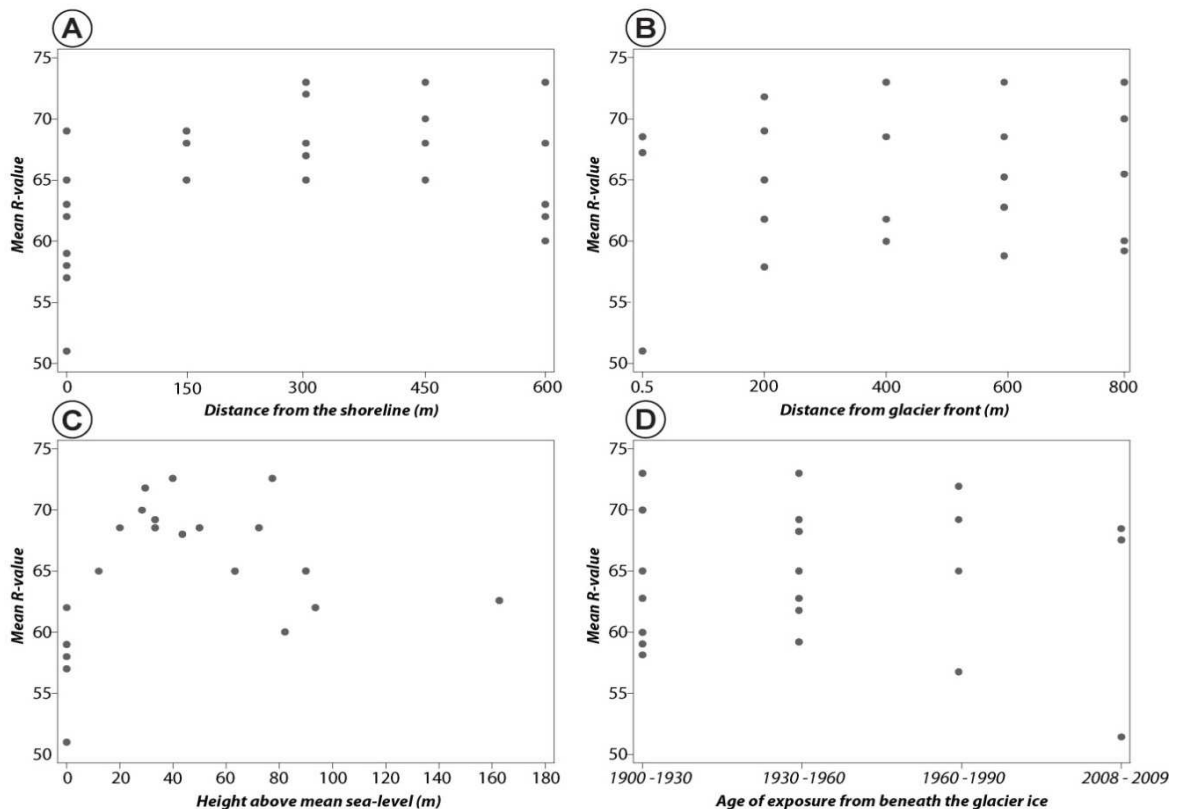


Figure 5.3. Mean R-values obtained during SHRT. **A.** SHRT run along the coast and more inland locations with a statistically significant trend of seaward rock resistance weakening. **B.** SHRT run along lines perpendicular to glacier front – no significant relationship found. **C.** SHRT run across roches moutonnées of different height above mean sea-level – no significant relationship found. **D.** SHRT run across zones exposed by retreating Nordenskiöldbreen since the end of LIA – no significant relationship found.

In general, all results of SHRT taken along the present-day shoreline of Adolfbukta were about 5 units lower compared to R-values on the upper parts of the plunging cliffs, and often over 10 units lower than those from summits of roches moutonnées and more inland sites. In all cases Cochran and Cox tests confirmed differences in R-values between coastal (lower resistance) and inland sites (higher resistance). Regression analysis shows that the R-values from rocks located along the coast were significantly lower than those obtained along inland roches moutonnées (Figure 5.3.A). No trends exist across profiles perpendicular to glacier front (Figure 5.3.B-D).

## 5.5 Chapter summary

- The recently deglaciated rocky coastal zone in Adolfbukta provides an interesting study area to examine the processes operating on present-day High Arctic rock coast and to test the hypothesised ‘amplification’ of rock weathering in polar coastal environments.
- The results of the Schmidt Hammer Rock Tests applied to the rock surfaces of the roches moutonnées that border the northern shores of Adolfbukta indicate a clear relationship between the distance from the shoreline and rock resistance.
- Among all tested sites, the rock surfaces influenced by coastal processes were less resistant than those located further inland.

Chapter 8 discusses the possible mechanisms responsible for the rock weakening observed.

The following chapter returns to the coastal barrier environment and considers the response of Petuniabukta barriers over century timescales, with a focus on the post-Little Ice Age landscape change.

# Chapter 6:

## CENTURY TIMESCALES

### The Post-Little Ice Age evolution of the Petuniabukta coast

## 6.1. Introduction

This chapter addresses the third question defined in Chapter I of this thesis:

*How did glacial and non-glacial-fed, gravel-dominated barriers in Petuniabukta respond to warmer, post-LIA conditions characterised by enhanced paraglacial processes?*

To answer this question the following objectives are addressed:

- I) to quantify the rates of coastal zone change in a non-glacial and glacial-fed barrier systems following the end of the LIA;
- II) to identify the processes responsible for causing coastal zone changes;
- III) to examine how these High Arctic coasts responded to enhanced paraglacial processes following the end of the LIA.

## 6.2 Background

As discussed in Chapter 2, the 20<sup>th</sup> century climate warming has had a profound effect on the Svalbard landscape, forcing a paraglacial transition (*sensu* SLAYMAKER 2009, 2011) from a glacial-dominated to a non-glacial environment. This change is well-documented in slope, valley floor and glacier foreland systems, where glacial landforms are denudated by fluvial, aeolian or mass-wasting processes, often accelerated by permafrost degradation (e.g. ÅKERMAN 1980; KIDA 1986; LØNNE and LYSÅ 2005; LUKAS *et al.* 2005; ETZELMÜLLER and HAGEN 2005; SCHOMAKER and KJÆR 2008; MERCIER *et al.* 2009; IRVINE-FLYNN *et al.* 2010, 2011). In contrast, the response of the Svalbard coastal zone to this paraglacial transition is little known.

Thus far, coastal studies have focused mainly on the western coasts of Spitsbergen (e.g. ZAGÓRSKI *et al.* 2012a, b; MERCIER and LAFFLY 2005). In southern Bellsund, for example, between 1936 and 2007, the accelerated sediment delivery from the retreating Scottbreen, and erosion of uplifted marine terraces, led to over 60 m coastal progradation (ZAGÓRSKI 2011). In Josephbukta, the retreat of Renardbreen and Recherchebreen during the 20th century led to the formation of more than 20 km of new shoreline and the development of new coastal landforms including a *ca.* 700 m long spit (ZAGÓRSKI *et al.* 2012a). MERCIER and LAFFLY (2005) observed a strong relationship between coastal progradation (*ca.* 3 m yr<sup>-1</sup> in the last 30 years) and accelerated sediment supply associated with the post-LIA retreat of surrounding glaciers in Kongsfjorden. Observations from Bellsund and Kongsfjorden also showed that once glaciofluvial



sediment delivery is reduced, shorelines quickly start to erode. Several reports from the Brögger Peninsula document changes to beach micro-relief caused by shifts in glaciofluvial transport during the short Arctic summer months (e.g. MOIGN and GUILCHER 1965; MOIGN and HÉQUETTE 1985; HÉQUETTE and RUZ 1986, 1990).

In Isbjørnhamna (Hornsund, SW Spitsbergen), ZAGÓRSKI *et al.* (2012b) studied coastal changes between 1960 and 2011 and observed a dominance of coastal erosion over accumulation that started in the 1970's and continues to the present. They associated this process with the retreat of a previously marine-terminating (tide-water) glacier (Hansbreen) that retreated on-land and exposed an unstable paraglacial coastline that is easily reached by waves and which has eroded by up to 46 m (at an average rate of *ca.* 0.9 m yr<sup>-1</sup>). In SE Spitsbergen (Sørkappland), ZIAJA *et al.* (2009) found evidence of an even more dramatic coastal change in the form of *ca.* 200 to 460 m shoreline retreat between 1936 and 2005 which led to the destruction of Davislaguna lake.

These examples show that Svalbard coasts, generally considered as low energy systems, can transform quite rapidly under certain conditions. These studies are all located in western and southern parts of Spitsbergen, directly influenced by the West Spitsbergen Current and exposed to storm waves formed in the Greenland and Barents Seas. In contrast, little is known about the coastal behaviour in inner-fjord environments of Spitsbergen (e.g. the Petuniabukta study area), that are characterised by sheltered locations, prolonged sea-ice conditions, low tidal ranges, and ephemeral pulses of sediment delivery from landforms that develop in a semi-arid, polar desert climate. The evolution of those coasts is strongly influenced by sediment delivery from talus slopes and snow-fed mountain streams forming coarse-grained alluvial fan deltas (MÖLLER *et al.* 1995; LØNNE and NEMEC 2004). This is in marked contrast to glacier-dominated systems, known from the previous studies referred to above.

As noted by LØNNE and NEMEC (2004), sediment supply from High Arctic alluvial fans to the coast is controlled by a 'unique combination' of environmental conditions. These include ephemeral runoff, dependent mainly on air temperatures and precipitation, and high topographic relief which shortens the pathway of coarse clastic sediments released from ice, snowdrifts or permafrost to the coast.

The sensitivity of alluvial fans to changes in climatic conditions is known also from other morphoclimatic zones (e.g. NEMEC and STEEL 1988; RACHOCKI and CHURCH 1990; COLELLA and PRIOR 1990; MARZO and PUIGDEFÀBREGAS 1993; HARVEY *et al.* 2005). Alluvial fans are sensitive to both temperature and humidity changes and may respond to these by

changes in the form of streamflows, mudflows and debris flows. On Svalbard, these landforms respond to warmer and cooler conditions by varying the supply of sediment to the coast in response to changes in run-off and snowpatch development, as well as changes in frost heave and vegetation extent.

Therefore, in this chapter I firstly aim to address the limited research to date on non-glacial-fed High Arctic coastal systems through a detailed study of post-LIA Ebba spit-platform development in NE Petuniabukta. Then I focus attention on a glacial-fed coastal zone formed after the termination of the LIA in NW Petuniabukta to compare the rate of coastal zone changes in central Spitsbergen with previous studies completed along the western coast described above.

### **6.3 Controls on non-glacial fed barrier systems**

#### **6.3.1 The Ebba spit-platform and barrier coast in east Petuniabukta**

The steep valley slopes of Ebbadalen support extensive alluvial fans. The largest fan system in NE Petuniabukta is formed by Dynamiskbekken (coastal sections E5-E8, Figure 6.1.-2) which is fed sediment and water by melting snow-patches and permafrost in the Wordiekammen massif (Figure 6.1.-1). In the summer months, this fan delivers sediment to the coast which is then transported along-shore (Figure 6.1.-4) towards the Ebbaelva mouth where it is deposited in a gravel-dominated spit (Figure 6.1.-7). The abundance of sand and fine gravel in several sections of the barrier may also be associated with the erosion and redistribution of the (mainly) Holocene raised beaches that lie south of the stream fan-delta (Figure 6.1.-3).

The modern barrier has an active storm ridge crest to the south of the mouth of the Ebbaelva at *ca.* 0.75 to 0.25 m above mean tide level, and is part of a larger spit system separated by shallow lagoons that are inundated during high tides. The current beach comprises varying quantities of fine gravel and sand, with seaweed and abundant driftwood. Typically, the beach comprises finer, often sandy sediments in the lower parts with a distinct break in beach slope that separates sandy from gravelly parts higher up (Figure 6.2.), suggesting a classification of the modern beach within the “composite gravel beach type” proposed by JENNINGS AND SCHULMEISTER (2002, p. 211). The beach resembles the fair-weather Arctic beaches described by MASON (2010) with no evidence for significant overwash or overtopping features. As discussed in Chapter 4, the morphological effects of ice-push, ice pile-up and ice melting on the beach are ephemeral and destroyed in the first few days of open water conditions each year (Figure 6.3.).

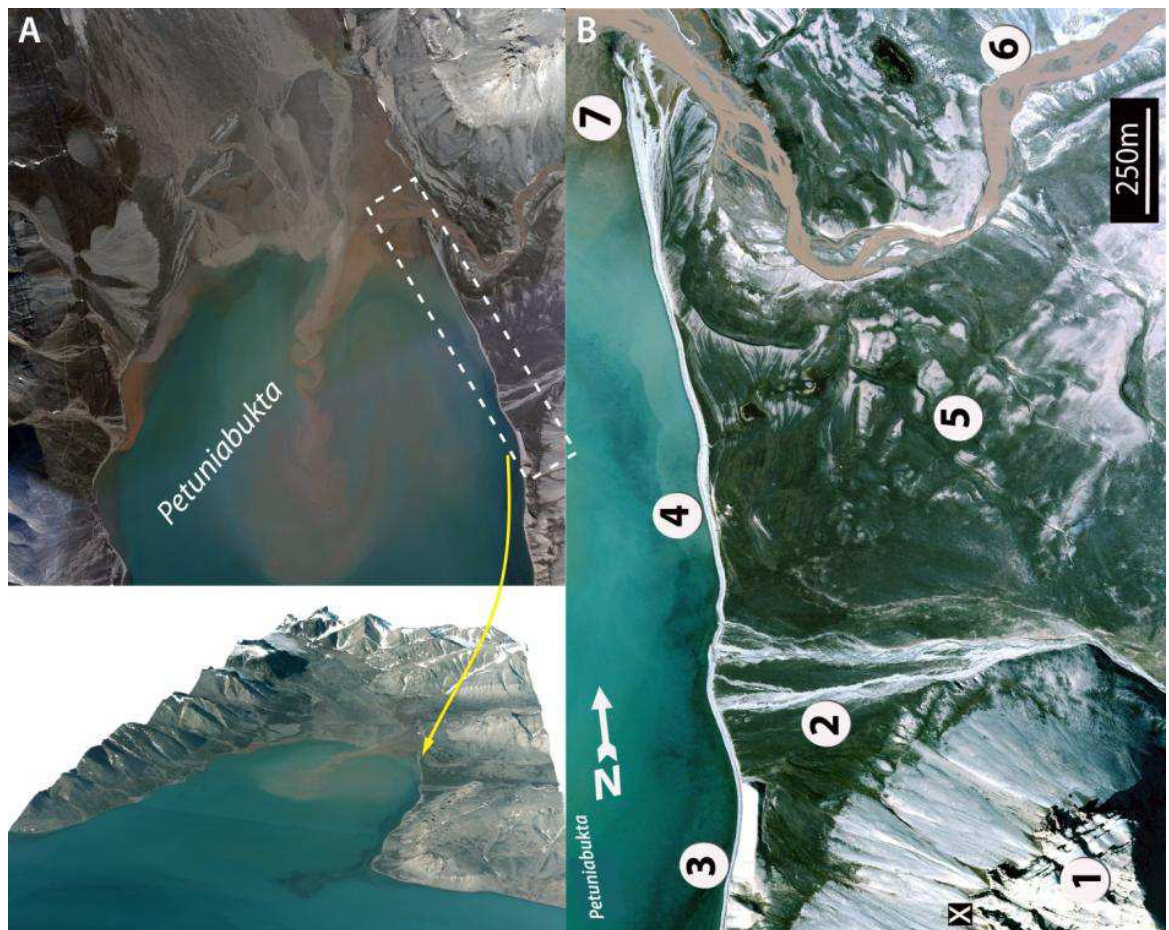


Figure 6.1. A Location of study site: E5-E8, B Sources of non-glacial sediment supply : 1 – Wordiekammen massif with extensive talus slopes, black square with cross on eastern slope of Wordiekammen indicates location of time-lapse camera, which took the images in Figure 6.3., 2 – The Dynamiskbekken alluvial fan and delta, 3 – uplifted palaeospit, 4 – low unconsolidated cliff eroded in raised marine terrace, 5 – flights of raised beaches, 6 – Ebbaelva incising into raised beaches, 7 – Ebba spit-platform with five spits, separated by shallow lagoons.

The new RSL change reconstruction presented in Chapter 7 indicates that the highest Holocene beaches (ca. 40-45 m a.s.l.) along the eastern coast of Petuniabukta formed shortly after local deglaciation at ca. 10,000 cal. yr BP. Later, RSL fell from this level to reach within a meter of present sea-level by ca. 3000 cal. yr BP. The absence of any sea-level data points younger than ca. 3000 cal. yr BP, together with the downward trend in mid and late Holocene RSL, suggests that RSL fell below present and rose again in the last two millennia.

The late Holocene RSL rise likely caused an increase in sediment supply from coastal erosion and the potential formation of an extensive beach-ridge plain (e.g. ST-HILLAIRE-GRAVEL *et al.* 2010). Harsh sea-ice conditions and limited longshore transport have probably attenuated this process in Petuniabukta leading to the development of a narrow barrier (6 to 15 m) which, only in the mouth of the Ebbaelva, developed into an 80 to 100 m wide barrier-plain (Figure 6.4.).



The present-day Ebba spit-platform (ESP) is tipped with five finger-like spits. In the widest section of the platform, 24 narrow ( $<1$  m) and low ( $<0.5$  m) beach ridges can be distinguished, which are separated from the uplifted late Holocene marine terrace (1.24 m MTL) by a low cliff.

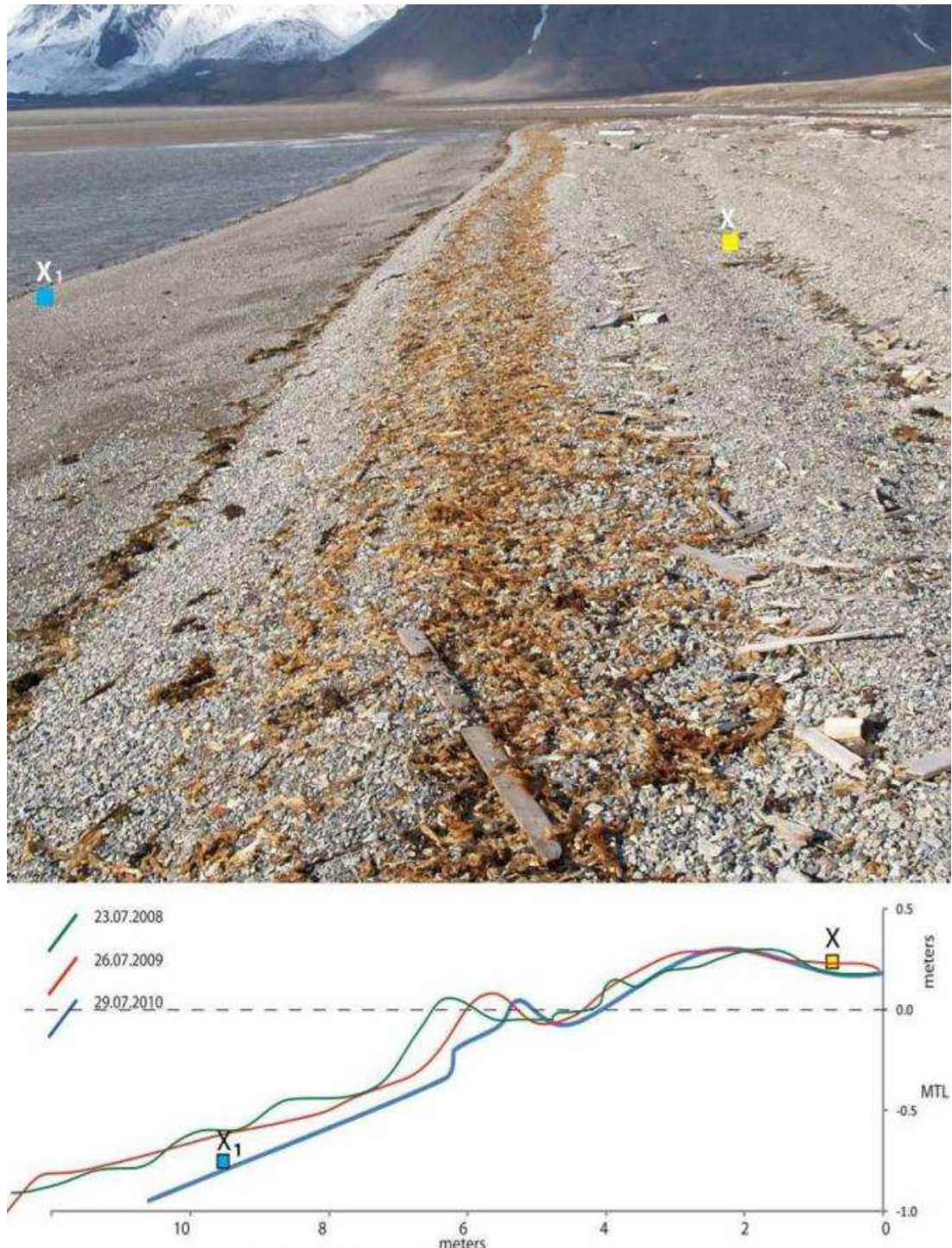


Figure 6.2. Present-day gravel dominated barrier in Petuniabukta. Note the abundant accumulation of seaweed and driftwood mixed with coarse gravel in a storm-ridge and a zone of finer (fine gravel, sandy) sediments in the upper swash zone. A DGPS survey along the barrier carried out in July 2008, 2009, 2010 indicates small-scale variations in barrier morphology between and a ca. 1 m landward shift of storm ridge in the summer of 2010 associated with storm-weather conditions with wind gusts that exceeded  $19 \text{ m s}^{-1}$ .

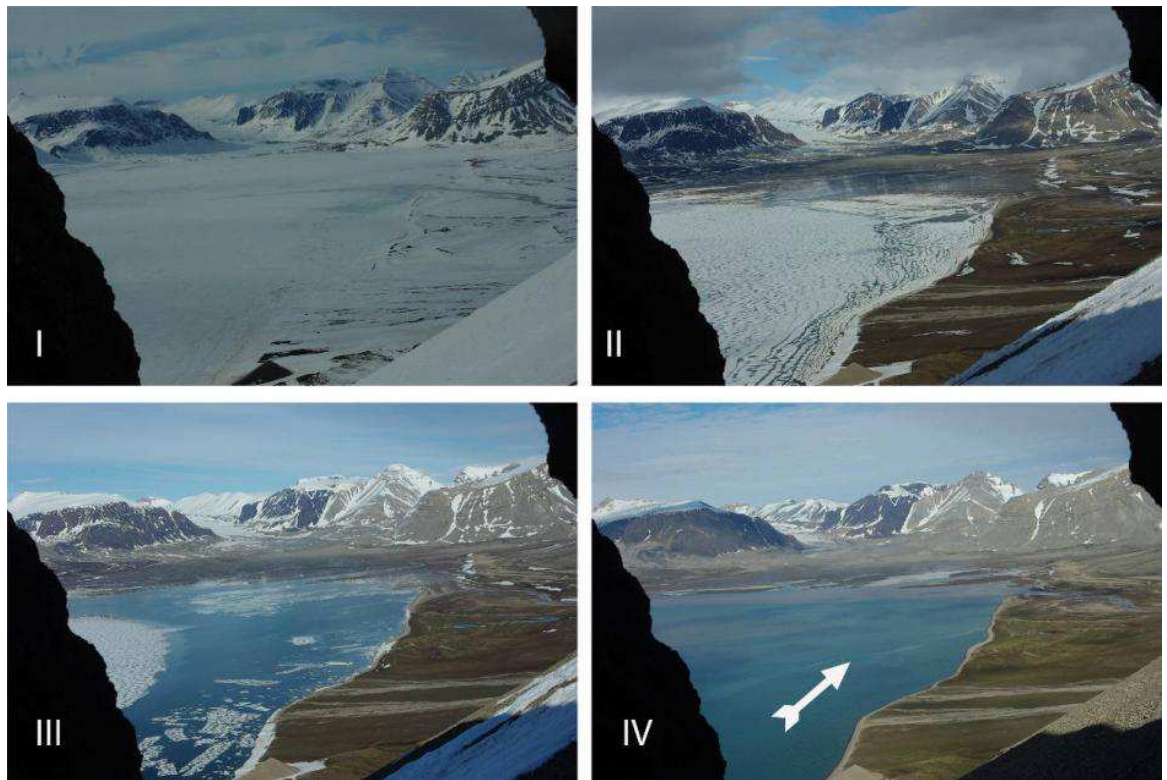


Figure 6.3. Seasonal changes in Petuniabukta coastal system (images taken by a time-lapse camera installed on Wordiekammen. I – Before breakout (Autumn to late Spring), II – After breakout – (up to late May), III – Late ice-foot complex (Late May-June), IV – Full beach (July-September). The arrow denotes north.

### 6.3.2 Quantifying geomorphic change on non-glacial fed coasts: material and methods

#### 6.3.2.1 Topographic surveying

A DGPS survey across the Ebba spit-platform was conducted in the widest part with the best preserved beach ridges (Figure 6.4.a). All surveys were tied back to a benchmark established during the 2008 expedition, so their elevation indicates height above mean tide level in meters. DGPS measurements were also used to mark the location of several reference markers (2 x 3 m white geofiber rectangles) placed in advance of Norwegian Polar Institute aerial photography flights carried out in the summer of 2009. Rectangles were placed on stable natural points for ground control such as rocky outcrops and boulders to improve the precision of the constructed orthophotomaps and Digital Elevation Models (DEM).



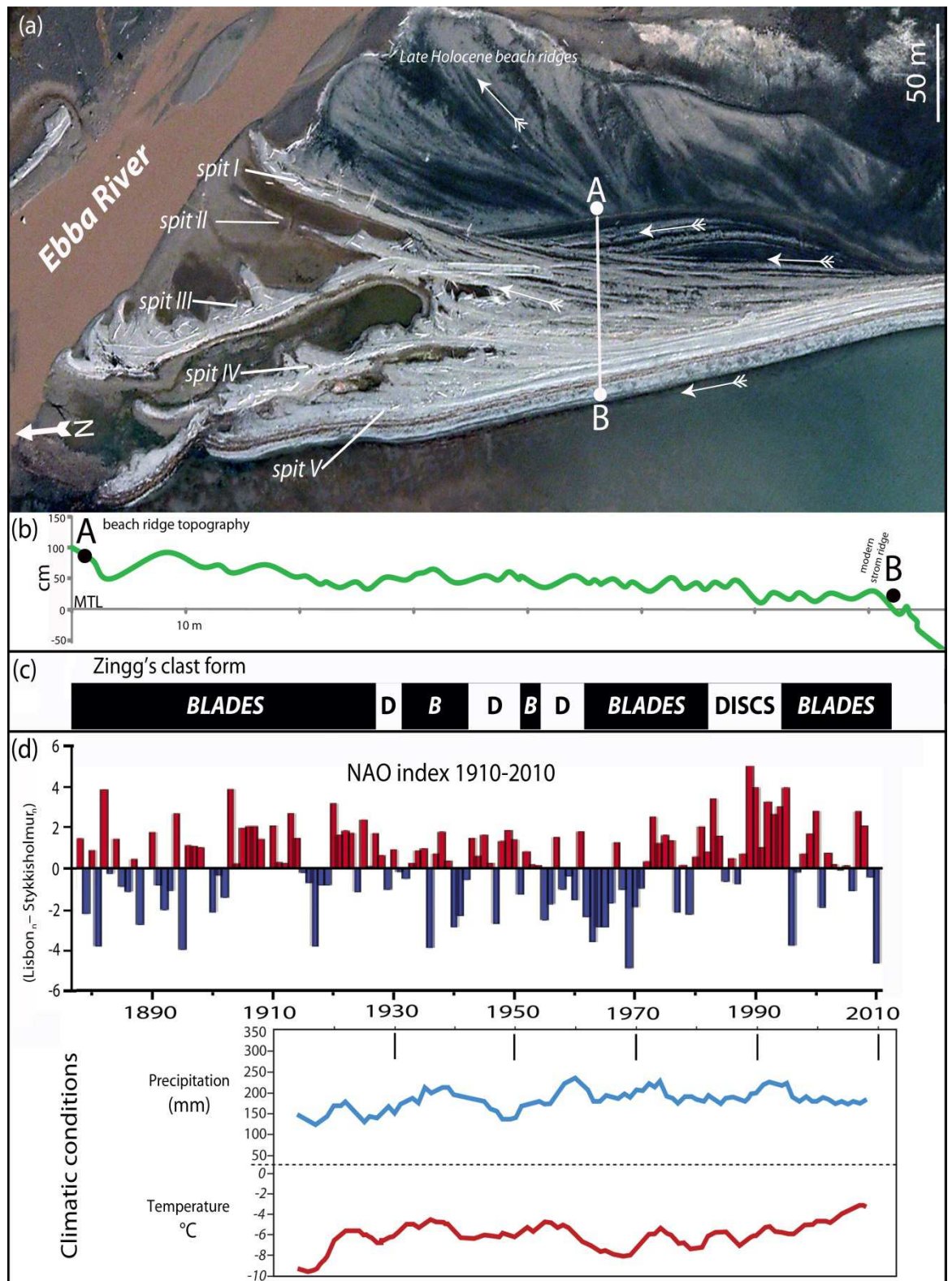


Figure 6.4. (a) Orthophotomap of barrier coast and Ebba spit-platform in north-eastern Petuniabukta. Five spits are marked including spits I, II, III that were analysed in geographic information system software; white arrows indicate the dominant direction of beach ridge progradation; (b) Ebba spit-platform topography along A-B transect based on DGPS survey (summer 2009); (c) Classification of clast form composing beach ridge crests based on ZINGG (1935); (d) Upper diagram: NAO winter index between 1910 and 2010, (HURRELL 1995). Lower diagram: Svalbard precipitation and air temperature record since 1912 based on a 5-year running mean of monthly meteorological series homogenised by the Norwegian Meteorological Institute. Modified after: [www.climate4you.com](http://www.climate4you.com) website by Prof. OLE HUMLUM.

### 6.3.2.2 Sedimentological characteristics

The surface of each of the 24 ridges was photographed using Nikon D80 Digital SLR camera from a constant height of 1.5 m. On the crest of each ridge a 50 x 50 cm wooden grid was placed for scale (Figure 6.5.). To determine clast size, digital images were processed in Wolman\_Jack software - a graphic user interface programmed in the MATLAB environment by Dr PATRICE CARBONNEAU (Durham University), which calculates grain size distribution based on b-axis measurements. In addition, 50 pebbles were randomly collected from each ridge crest for *a-b-c* axes measurements. Each pebble was measured in the field using a vernier calliper in order to determine their form (blades, discs, spheres, rods) using ZINGG's classification (ZINGG 1935).

The shape of pebbles composing the beach ridge may yield information on environmental conditions in which they were deposited (e.g. BARTRUM 1947; VAN ANDEL *et al.* 1954; BLUCK 1967, 1969; CARR *et al.* 1970; ORFORD 1975; MATTHEWS 1983, GALE 1990; HOWARD 1992; SUTHERLAND and LEE 1994; PYÖKÄRI 1997, 1999). In general, disc-shaped clasts are typical for beach gravels and are transported further up a beachface than rods and spheres, which tend to accumulate downslope (BLUCK 1967; ANTHONY 2008). The blades, which in this study are also found in the upper part of the beach profile, are considered to be freshly formed and associated with brief remodelling in fluvial transport (HOWARD 1992). According to HOWARD (1992), the abundance of blades is an indicator of sediment maturity with the greatest number of blades in fluvial systems, smaller in the coastal zone and the lowest in the subtidal environment. It is hypothesised that the dominant form of clasts found in the 24 ridges studied should provide an indirect measure of the intensity of wave action.

Information on movement, depositional processes and provenance of finer coastal sediments can be obtained from studies of their magnetic properties (LARIO *et al.* 2001; HOUNSLOW and MORTON 2004; BOOTH *et al.* 2005; ROTMAN *et al.* 2008; CIOPPA *et al.* 2010; GAWALI *et al.* 2010). To this end, I analysed the size distribution and magnetic susceptibility (MS) of fine sediments from the 24 beach ridge swales described above. Samples (*ca.* 0.5 kg) were dried and sieved in a fume cupboard using a 2 mm sieve installed on *Fritsch Vibratory Sieve Shaker* Analysette 3. Later, each sample of fine sediments (<2 mm) was divided in a riffle-box and *ca.* 12 g of sample was ball-milled in a Fritsch pulverisette. After ball-milling, the homogenous powder was packed in 10 cc pots and analysed in a Bartington Instruments Ltd MS2B Dual Frequency Sensor, which measures susceptibility at low frequency (470 Hz) and high frequency (4700 Hz).



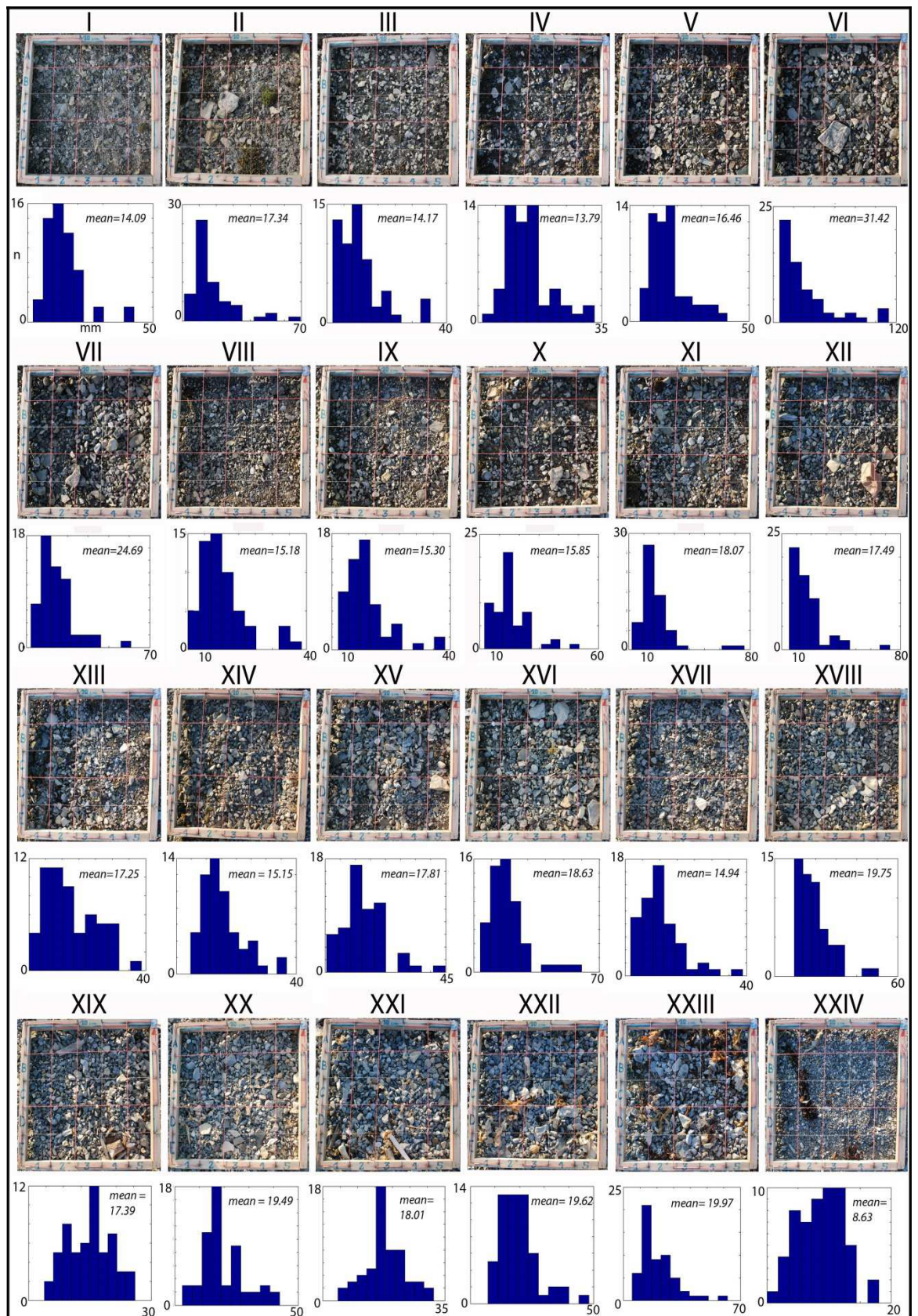


Figure 6.5. Representative surface photographs of 24 beach ridges (I-XXIV) photographed in summer 2009 and histograms summarising size distribution analysis carried out in Wolman\_Jack software. Mean size is presented in mm.

The average of five measurements was calculated and expressed as mass specific values in  $10^{-6} \text{ m}^3 \text{ kg}^{-1}$ . In addition to morphosedimentological analysis of coarse and fine sediments composing 24 beach ridges, *ca.* 2 kg samples of surface sediments were collected from the middle of the seaward slope of each of spits formed since the termination of the LIA (Figure 6.4.a). Finally, the morphological and sedimentological characteristics of beach ridges were compared with Svalbard weather data and the NAO index from 1912-2010 to check if the observed shifts in climatic conditions were recorded in beach ridge morphology and sedimentology (Figure 6.4.d).

### 6.3.2.2 Aerial photogrammetry

Aerial images taken by the Norwegian Polar Institute (NPI) in 1936, 1961, 1990 and 2009 were compared to determine the course of post-LIA Ebba spit-platform evolution. The basis for comparison was an orthophotomap created in the Leica Photogrammetry Suite 2010 from digital aerial images taken in 2009 which were calibrated using ground control points measured with DGPS during the 2010 summer fieldwork. Images from 1961 and 1990 were imported to ArcGIS 9 software, overlaid on the 2009 orthophotomap and georectified using a third order polynomial transformation with a total root mean square error of less than 0.5 m.

Shorelines of 1961, 1990 and 2009 were delimited using the middle of the first, fully emerged ridge visible on the image. This procedure was undertaken to minimise the error stemming from different phases of tidal cycle captured on individual photographs. Because it was impossible to distinguish if the visible forms comprise ephemeral gravel berms or storm ridges, and knowing that currently the distance between those shoreface elements is *ca.* 2 m, changes in shoreline position that were smaller than 2.5 m were not considered.

Unfortunately, the image from 1936 could not be used in quantitative analysis executed in ArcGIS software, because of its low resolution and angle of photography (it is an oblique image). However, based on the configuration of visible coastal landforms and other orientation points such as wooden huts built on uplifted marine terraces, an approximate outline of the contemporary Ebba spit-platform was established (Figure 6.6.).

## 6.4 Non-glacial fed barrier systems - results

### 6.4.1 Post-Little Ice Age spit platform evolution – evidence from air photos

Between 1936 and 2009 the Ebba spit platform prograded and developed three new spits (Figure 6.6.). It was assumed that spits I and II (see Figure 6.4.a) adjacent to the uplifted marine terrace were also formed after the end of the LIA, but the lack of imagery covering the first decades of the 20<sup>th</sup> century precludes quantitative description of the rate of change and time of accumulation. Analysis of aerial photographs from 1961, 1990 and 2009 enabled identification of the following coastal changes.

Between 1961 and 1990 the Ebba spit platform along transect A - B on Figure 6.4.a prograded 28 meters (*ca.* 1 m yr<sup>-1</sup>) seaward. Between 1990 and 2009 the rate of progradation dropped to 0.4 m yr<sup>-1</sup> and the platform increased in width by *ca.* 8 meters.

The Ebba spit platform doubled in area between 1961 and 1990, expanding from 14,320 m<sup>2</sup> to 24,100 m<sup>2</sup> (Figure 6.6.). In the next 19 years, the area of platform expanded to 29,840 m<sup>2</sup>. The increase in platform extent is related to the development of three new spits which grew out from the widest part of the platform during the last 70 years. The first spit (spit III), which formed between 1936 and 1961, was 140 m long and covered 2,848 m<sup>2</sup> (Table 6.1.). In the following 29 years this spit platform extended 1.9 m yr<sup>-1</sup> northward and was 196 m long in 1990. During this period the spit area grew by 615 m<sup>2</sup>. Between 1990 and 2009, the spit migration towards the mouth of the Ebbaelva ceased and a loss of 449 m<sup>2</sup> was observed due to erosion. The formation of spit IV must have begun before 1961 (Figure 6.6.) as the beginning of the landform was already jutting out of the barrier plain in 1961 and covered 611 m<sup>2</sup>. The northward growth of the spit between 1961 and 1990 amounted to 149 m (5.1 m yr<sup>-1</sup>). Between 1990 and 2009, the spit extended northward *ca.* 20 m and migration into the mouth of Ebbaelva stopped. However, the expansion of the spit continued as the tip started to branch. The new tip of the spit prograded *ca.* 70 m north-west from the 1990s end of spit. Figure 6.4.a shows that barriers were shifting across the platform relatively often.

The Late Holocene beaches visible on the surface of the marine terrace between the Ebbaelva and the analysed Ebba spit-platform were drifting mainly towards the NE. Similarly, the axes of two old spits (spit I and II formed before 1936) and adjoining the marine terrace also are oriented in a north-easterly direction.



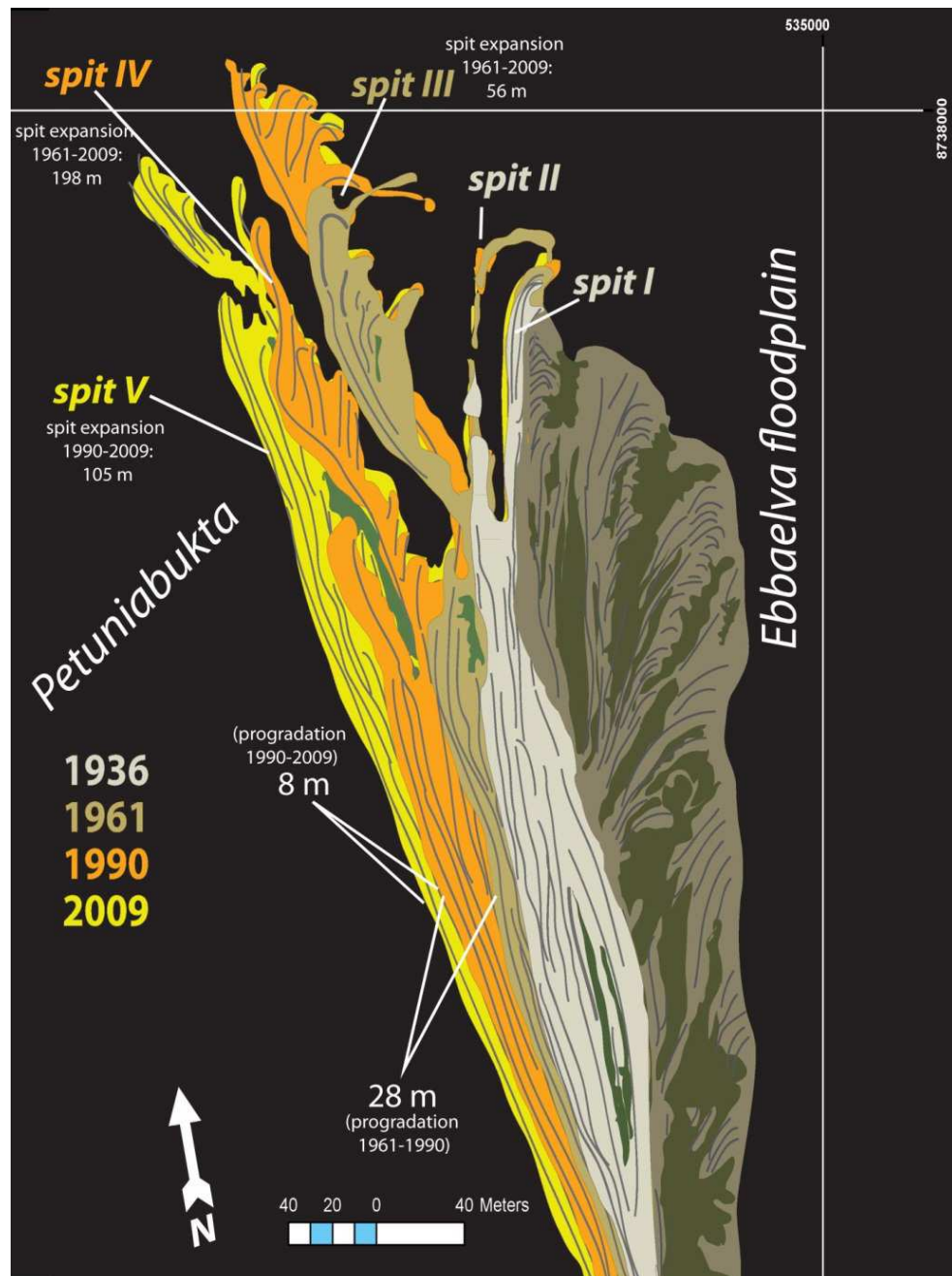


Figure 6.6. The post-LIA progradation of Ebba spit-platform based on digital photogrammetric analysis of images taken by Norwegian Polar Institute in years 1961-2009. The location of the 1936 shoreline and Ebba spit-platform extent is approximate and based on visual interpretation of an oblique photograph. The map presents Ebba spit-platform extension and morphology in 1936, 1961, 1990 overlaid on the spit-platform as visible on a 2009 image.

Spit	1961		1990		2009		Rate of spit growth [m yr <sup>-1</sup> ]		
	axis length [m]	area [sq km]	axis length [m]	area [sq km]	axis length [m]	area [sq km]	1961-1990	1990-2009	1961-2009
Spit III	140	0.0028	196	0.0035	196	0.0030	1.9	x	x
Spit IV	52	0.0006	201	0.0033	250	0.0037	5.1	2.6	4.1
Spit V	X	x	67	0.0009	172	0.0041	x	5.5	x

Table 6.1. Post-LIA changes (length/area) of three spits formed in the mouth of Ebbaelva. x – landform did not exist in this period, no rate calculated.

The first five beach ridges that formed below the late Holocene terrace are oriented NNW. The following eight beach ridges that supplied the pre-1936 spits returned to a NNE direction. Another shift occurred at a time of the formation of spit III (1961-1990), when the axes of ridges were oriented again towards the NNW. Spit IV developed almost perpendicularly to spit III (also NNW), but the second branch diverged from the 1990s tip of the spit in a more westward direction. Beach ridges and spit V formed during last 20 years and are oriented almost exactly northward.

In comparison with the extension of spit III and IV, the formation of the most recent spit was faster (*ca.* 5.5 m yr<sup>-1</sup>). Between 1990 and 2009, the spit V extended 105 m and expanded by 3138 m<sup>2</sup>. The further extension of the youngest spit was probably impeded once the barrier reached the westward branch of spit IV. This led also to the closure of a lagoon between the two spits. As observed during the 2010 fieldwork, the gap between spit V and the west tip of spit IV has continued to decrease and in future years the continued westward migration of the spit is expected.

#### **6.4.2 Beach ridge morpho-sedimentary changes**

DGPS topographic surveys indicate that the mean slope of the spit-platform formed until 1961 was *ca.* 10‰ (1 cm per 1 m). The slope of the platform section that formed during the next 30 years rose to 11 ‰ (1961-1990) and increased to 16 ‰ for the section formed between 1990 and 2009. The thirteen beach ridges that formed before 1961 were also wider (mean width between ridges 2.8 m) and have gentler slopes than that of the younger ridges. The mean height of beach ridge crests above MTL was approximately 60 cm. The eight ridges formed between 1961 and 1990 were much more closely spaced. These ridges were thus narrower (mean width 2.2m) and have steeper seaward slopes than those formed in the first half of the 20<sup>th</sup> century. By 1990 the height of crest of beach ridges above MTL had dropped to *ca.* 30 cm from 48 cm, which is typical for the 1961-1990 period, and in the last 20 years the distance between consecutive storm ridges has been growing.

In summary, beach ridge crest height has been gradually decreasing through the 20<sup>th</sup> century, while the spacing between ridges has been more variable. The spacing decreased from 1961 to 1990 and has been increasing again since 1990.

In terms of clast morphology, the surface of the beach ridges (Figure 6.5.) are dominated by blade-shaped pebbles (18 ridges: I-VI, VIII, IX, XII, XIV-XVII, XXII-XXIV). Discs dominate in a few ridges formed around the 1960s (VII, X, XI) and three ridges that

accumulated at the beginning of the 1990s (XIX-XXI). No correlation between change in clast form and size exists. Mean *b*-axis size ranged between 17.8 mm for clasts building ridges formed before 1961, through to 17.6 mm for clasts in ridges of 1961-1990 period and 19.2 mm on the surface of beach ridges accumulated in the last two decades (ridges XXI-XIII). Of the 24 beach ridges studied, only the 2009 storm ridge was composed of granule size clasts, which were approximately half the size of the clasts in the remaining three ridges deposited between 1990 and 2009 (Figure 6.5.). The trend to finer sediment sizes is also recorded in the five spits (Figure 6.4.a) that project from the platform (Table 6.2.).

Spit:	% Gravel	% Sand	% Mud	Mean	Sorting	Skewness	Kurtosis
Spit I	62.6	36.2	1.2	-1.35	1.6	0.31	0.84
Spit II	42.1	54.8	3	-0.53	2.06	-0.06	0.78
Spit III	48.9	50.5	0.5	-1.12	1.35	-0.13	0.86
Spit IV	36.5	63.1	0.4	-0.23	1.40	0.01	0.23
Spit V	27.4	72.5	0.1	-0.01	1.73	-0.17	0.90

*Table 6.2. Sedimentological characteristics of surface sediments composing the seaward slopes of 5 spits in the Ebbaelva mouth. For location of spits and sampling points see Figure 6.4.*

The middle of the seaward slope of spit I, adjacent to the uplifted marine terrace, is for the most part composed of gravel. The *b*-axis from clasts forming the spit crest is 21.1 mm. In spit II and spit III (1961) the percentage of gravel remains above 40% and the mean size of *b*-axis of clasts in the crest was 17.9 mm for the former and 17.2 mm for the latter.

A significant decrease in the amount of gravel sediments occurred between 1990 and 2009. From this, it follows that the mosaic of poorly sorted sediments in spit IV (1990) and spit V (2009) was dominated by sand (63-72 %). However, the mean size of clast *b*-axes stayed above 17 mm in the crest of spit IV and even increased to 22.4 mm in the most recently accumulated spit. The image of the spit V surface analysed for its pebble size distribution was taken shortly after a storm event on the 15<sup>th</sup> of August 2010, which had thrown larger clasts onto the beach ridge surface.

The sedimentological analysis of the fine sediment comprising the matrix that fills the spaces between pebbles in beach ridge swales (Table 6.3.) reveals substantial changes in magnetic susceptibility (mass specific MS values in  $10^{-6} \text{ m}^3 \text{ kg}^{-1}$ ) whenever the sand incorporated into the beach ridge coarsens (see swales X, XI, XV, XXIV and modern swash). In swales formed before 1961 and composed of very fine sands, MS ranged from

19 to 26, whereas in swales filled with coarse and very coarse sand, MS decreased to 5-7. Similarly, MS of fine sandy deposits in swales from the 1961-1990 period fluctuated between 22 and 30 and experienced a sharp drop to 6 when material composing contemporary beach turned to very coarse sand. The first two swales between beach ridges formed in 1990-2009 period had MS *ca.* 16 which dropped to 12 in swale XXIII and reached *ca.* 8 in the last swale, again filled with coarse sands. The MS of sediments covering the middle of the modern swash zone was characterised by the lowest value in the whole transect (1.5).

Beach ridge swale	Sediment name	Mean $\phi$	Sorting	Skewness	Kurtosis	Magnetic Susceptibility $10^{-6} \text{ m}^3 \text{ kg}^{-1}$
<b>pre-1961 swales</b>						
I	Very Coarse Silty Very Fine Sand	4.0	1.8	0.4	1.4	21.8
II	Very Coarse Silty Very Fine Sand	3.9	1.7	0.4	1.5	25.7
III	Very Coarse Silty Very Fine Sand	3.7	2.1	0.3	1.6	21.4
IV	Very Coarse Silty Very Fine Sand	3.6	2.1	0.3	1.7	19.5
V	Very Coarse Silty Very Fine Sand	4.0	1.8	0.4	1.5	23.7
VI	Very Coarse Silty Very Fine Sand	3.8	2.3	0.2	1.6	18.6
VII	Very Coarse Silty Very Fine Sand	4.0	1.7	0.3	1.5	25.5
VIII	Very Coarse Silty Very Fine Sand	3.8	1.7	0.4	1.5	21.2
IX	Very Coarse Silty Very Fine Sand	3.7	1.9	0.2	1.6	24.4
X	Poorly Sorted Very Coarse Sand	0.1	1.4	0.7	2.5	6.8
XI	Poorly Sorted Coarse Sand	0.4	1.2	0.3	1.7	4.9
XII	Very Coarse Silty Very Fine Sand	3.4	2.0	0.1	1.6	20.1
<b>1961-1990 swales</b>						
XIII	Very Coarse Silty Very Fine Sand	3.5	1.9	0.2	1.7	23.8
XIV	Very Coarse Silty Fine Sand	3.4	1.7	0.2	1.7	23.0
XV	Poorly Sorted Very Coarse Sand	-0.01	1.2	0.5	1.9	5.7
XVI	Very Coarse Silty Very Fine Sand	3.4	1.8	0.2	1.4	30.5
XVII	Very Coarse Silty Very Fine Sand	3.4	1.8	0.2	1.6	27.3
XVIII	Very Coarse Silty Fine Sand	3.6	1.8	0.3	1.3	29.4
XIX	Very Coarse Silty Very Fine Sand	3.7	2.4	0.1	1.5	26.0
XX	Very Fine Sandy Very Coarse Silt	5.0	2.7	0.3	1.1	22.0
<b>1990-2009 swales</b>						
XXI	Very Coarse Silty Very Coarse Sand	1.9	2.7	0.6	0.9	16.5
XXII	Very Fine Sandy Very Coarse Silt	4.9	2.3	0.4	1.1	16.0
XXIII	Coarse Silt	7.0	2.4	0.2	1.0	12.0
XXIV	Poorly Sorted Very Coarse Sand	0.6	1.7	0.6	1.7	7.5
swash zone	Moderately Sorted Very Coarse Sand	-0.3	0.7	0.5	1.5	1.5

Table 6.3. Characteristics of fine sediments collected from beach ridge swales including logarithmic Folk and Ward (1957) graphical measures and corresponding magnetic susceptibility.

## 6.5 Controls on glacial-fed barrier systems

### 6.5.1 The barrier coast of north-western Petuniabukta

Since the end of the LIA, all glaciers in NW Petuniabukta experienced rapid retreat ( $12\text{--}15\text{ m yr}^{-1}$ ) exposing *ca.*  $17\text{ km}^2$  of deglaciated terrain (Figure 3.13.). These rates are within the range for glaciers in other parts of Spitsbergen, excluding large fast flowing glaciers (RACHLEWICZ *et al.* 2007).

Recent glacier retreat has exposed valley systems that are filled with fresh, unstable glacial sediments that are available for reworking by proglacial meltwater streams and modification by paraglacial slope processes (mainly slumping, gully and debris flows). This paraglacial sediment cascade is augmented by the melting of ice-cored glacial landforms (controlled ridges, eskers, lateral moraines) that also contribute high rates of sediment flux to proglacial rivers. In the study area, the most direct expression of this sediment flux is the accumulation of large alluvial fans at the entrance to Ferdinanddalen and Elzadalen and the massive sandur system that stores sediment released from the decaying Svenbreen, Hørbyebreen and Ragnarbreen (Figure 6.7.). The coastal zone adjacent to these alluvial fans is a gravel-dominated barrier comprised of elongated spits and barrier islands, together with an extensive tidal flat.

This section details the main patterns of coastal landscape changes that occurred in the study area since the end of the LIA, with a particular focus on the second half of the 20<sup>th</sup> century.

*Figure 6.7. (next page). Main features of the glacial and coastal landscape in NW Petuniabukta investigated in this case study. Retreating glaciers: H. Hørbyebreen; R. – Ragnarbreen; S. – Svenbreen; F., – Ferdinandbreen; E. – Elzabreen; see Section 3.2.3 for retreat rates.*

*SHR –outwash plain developed by glacier rivers draining Svenbreen, Hørbyebreen (the main sediment source) and Ragnarbreen.*

*Relict coastal landforms: OFF 1 – Old Ferdie Fan 1, OFF 2 – Old Ferdie Fan 2 – abandoned and incised alluvial fans previously supplied by Ferdinandelva; FOS – Ferdie Old Spits – uplifted relict spits developed along alluvial fans fed by Ferdinandelva;*

*FBI – Ferdie Barrier Islands – uplifted barrier islands*

*Modern coastal landforms: FF3 – Ferdie Fan 3 and FF4 Ferdie Fan 4 – modern alluvial fans supplied by Ferdinandelva; FF4 develops a fan delta prograding into Petuniabukta;*

*SSF – small fans fed by snow-melt streams draining slopes of surrounding mountains;*

*EF – alluvial fan delta developed by Elzaelva;*

*FS1 – Ferdie Spit 1, FS2 – Ferdie Spit 2, FS3 – Ferdie Spit 3 –spits formed along FFs since the end of LIA;*

*L. – section of eroded barrier coast with a lagoon developing in the backshore area.*



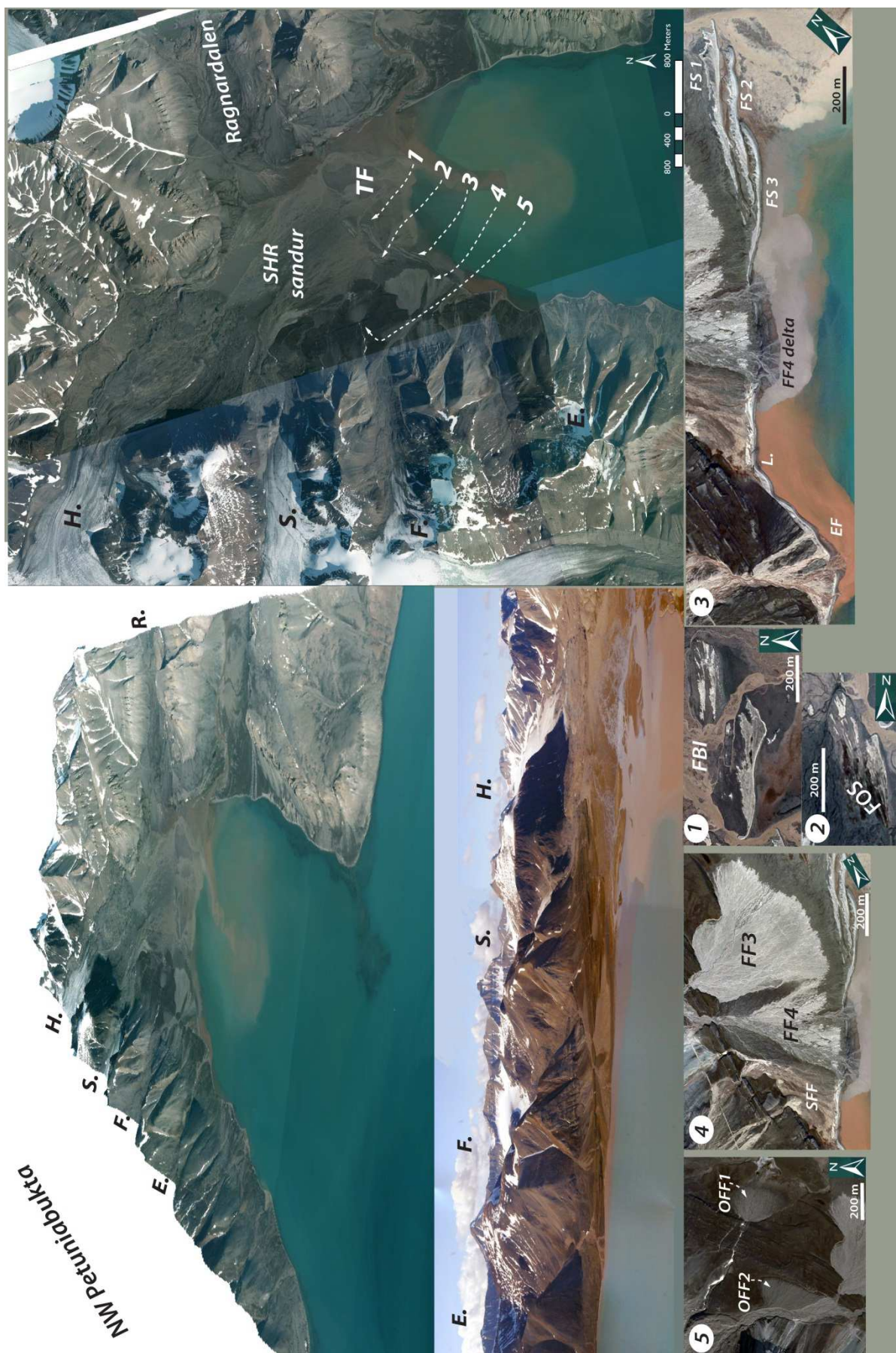


Figure 6.7.

### **6.5.2 Quantifying geomorphic change along glacial-fed coastal system - material and methods**

I used a combined geomorphological field observations, differential GPS (DGPS) survey, aerial photogrammetric analysis, digital elevation modelling (DEM) in a geographic information system (GIS) and sedimentological analysis of alluvial fan and coastal barrier surface deposits. Field observations were carried out in three summer seasons between 2008 and 2010.

#### **6.5.2.1 Geomorphological mapping and topographic survey**

In 2008 and 2009 geomorphological mapping was carried out during each summer field season. This was combined with field sketches and interpretation from aerial photos and old maps (ground-truthed in the field) to produce geomorphological maps. I collected and analysed the following maps of the central Spitsbergen region:

- Dunér and Nordenskiöld map from 1867 compiled principally during the Swedish Expedition in 1861-4;
- Cambridge University map of West Spitsbergen by HARLAND (1949) based on topographical surveys carried out during Cambridge Expeditions in 1949, 1938 and 1930;
- KARCZEWSKI *et al.* (1990) geomorphological map of Petuniabukta region, 1: 40,000;
- DALLMAN *et al.* (2004) geological map of Billefjorden, 1: 50,000.

I also examined sketches and notes taken during early expeditions to the central part of Spitsbergen and published by WALTON (1922), SLATER (1925), JACKSON (1931), BALCHIN (1941) and FEYLING-HANSEN (1955).

DGPS was used to precisely measure the altitude of stable surfaces on bedrock or large boulders (Figure 6.8.) for orthorectification of images and DTM production. Over 50 points from stable surfaces were complemented by DGPS measurements of several reference markers (2 x 3 m white geofiber rectangles) placed in advance of the Norwegian Polar Institute aerial photography flights carried out in summer 2009 as part of this PhD project. Rectangles were placed on stable natural points for ground control, such as rocky outcrops and boulders to improve the precision of the constructed orthophotos and DTMs (Figure 6.10.).





*Figure 6.8. DGPS measurement of ground control points. The images show an example of a geofiber rectangle placed on boulder in the Petuniabukta tidal flat and on a temporary benchmark at the entrance to Adolfbukta.*

#### **6.5.2.2 Aerial photogrammetric analysis and DTM production**

A selection of representative sites in NW Petuniabukta including alluvial fan deltas, coastal barriers, barrier islands and proglacial landforms were investigated for patterns of multidecadal change using information from aerial imagery spanning the period 1936-2009 taken by Norwegian Polar Institute and historical maps. The following images were used :

- One oblique 1936 NPI image of the Ebbadalen;
- Twelve 1961 NPI aerial images lines: S61\_2964-2969, S61\_3099-3104;
- Fifteen 1990 NPI aerial images lines: S90 1706-1711, S90 1760-61, S90 1796-1807;
- Twenty-eight digital 2009 NPI aerial lines: s2009\_13822\_00001-00008, 00027-00034, s2009\_13833\_00477-00485, 00491-493.

The 2009 aerial photographs were also used to produce a set of DTMs which serve as a basis for morphometric analysis of landscape changes. Ground-truthing was carried out on the majority of sites using DGPS surveys, ground (oblique) photography and surface sediment sampling of selected landforms.

Aerial images taken in 1960-1 and 2009 were transferred to a Leica Photogrammetric Suite 2010 (LPS) where they were viewed directly on screen. The LPS enables very good zooming which was helpful in the interpretation of mapped landforms and comparison of landscape change visible on sets of images taken in different years. Prior to image analysis, photographs from 1960-1 were scanned to a high resolution (>600dpi) on a photogrammetric scanner. Due to the poor quality of some of the photographs, copies of 1990 images were excluded from analysis in LPS. All images, from 1961 and 1990 were imported to ArcGIS 9 software and overlaid on the 2009 orthophoto for determination of landscape evolution from 1961-1990 and 1990-2009 (Figure 6.9.).

Selected images from 1961 and 1990 were georectified using a third order polynomial transformation with a total root mean square (horizontal) error of less than 0.5 m. Delimitation of shorelines and barrier extent for 1961, 1990 and 2009 were estimated using the middle of the first, fully emerged storm ridge visible on the image to minimise the error stemming from different phases of the tidal cycle captured on individual photographs. In general, shoreline changes smaller than 2.5 m were ignored because it was impossible to distinguish if the emerging forms comprised ephemeral gravel berms or storm ridges. The survey error cited was also based on the observations of the present-day shoreface, where the distance between these shoreline elements is *ca.* 2 m. Measurements of landforms length (spits, barriers, barrier islands) were carried along the main axis of the fully emerged storm ridge visible on the image.

DTMs based on 2009 images were automatically produced in the LPS (Figure 6.10.). The LPS software uses the bundle block adjustment, with least squares estimation, to establish the relationship between the positions of a set of photographs and a ground coordinate system, based on the interior and exterior parameters input into the software and the location of ground control points. As aerial images from summer 2009 (27 July and 11 August) were taken by NPI with an UltraCam Xp Large Format Digital Aerial Camera manufactured by Vexcel, the interior parameters were already inserted in image files so only exterior parameters had to be manually entered into the software. Each set of photographs was then processed as for a digital camera. The projection used was UTM, with the spheroid WGS 84 for zone 33N. For each of the 2009 images used for DTM creation, at least five ground control points were collected using DGPS. Five DTMs were generated from the 2009 images with ground resolutions ranging from 1 to 20 m. Due to the series of software failures associated with high numbers of processing

operations the DTMs of 1, 5, 8 and 10 m resolution were produced only for limited areas. A DTM of 20 m resolution covers the whole study area and is suitable for comparison with the DTM produced by NPI from the set of 1990 images obtained for this project (Figure 6.10.).

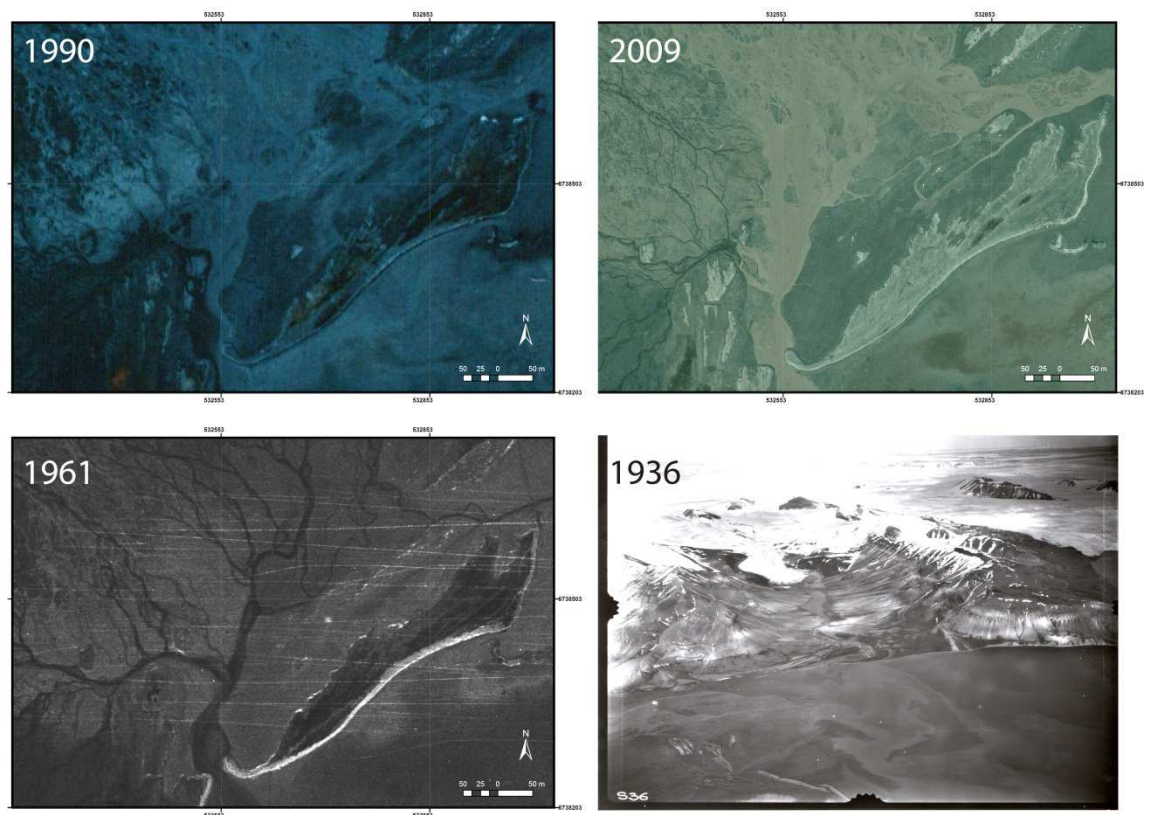


Figure 6.9. Examples of aerial imagery used in the study. Barrier island formed in NW Petuniabukta on aerial images from 1936 (oblique), 1961, 1990 and 2009.

Differencing of the 2009 and 1990 DTMs was done for the NW part of Petuniabukta by subtracting two DTMs in ArcGIS software. Estimation of surface elevation changes is an extremely useful method for landscape evolution studies and allows identification of zones of surface erosion and surface aggradation. In high latitudes this technique has been commonly applied to measure surface elevation changes of glaciers (e.g. WANGENSTEEN *et al.* 2006; MUSKETT *et al.* 2009; BARRAND *et al.* 2010) and proglacial landforms (e.g. IRVINE-FLYNN *et al.* 2010, SCHOMACKER and KJÆR 2007, 2008; BENNETT and EVANS 2012).

In this study, the subtracting of DTMs was carried out to investigate surface elevation change in the proglacial zone of Ferdinandbreen, Svenbreen and Hørbyebreen and to estimate the amount of sediment removed by paraglacial processes (fluvial, slope, aeolian activity) towards the coastal zone. DTMs were also used to generate 2009 orthophotos. Orthophotos were generated by resampling the aerial photographs using the 20 m DTM



at the resolution of the original photographs (0.5 m). The forward projection was applied to generate orthophotos, meaning that pixels from the original photos were projected on the DTM to ascribe spatial map coordinates and, in the next step, pixels with new 'spatial information' were projected onto the orthophoto.

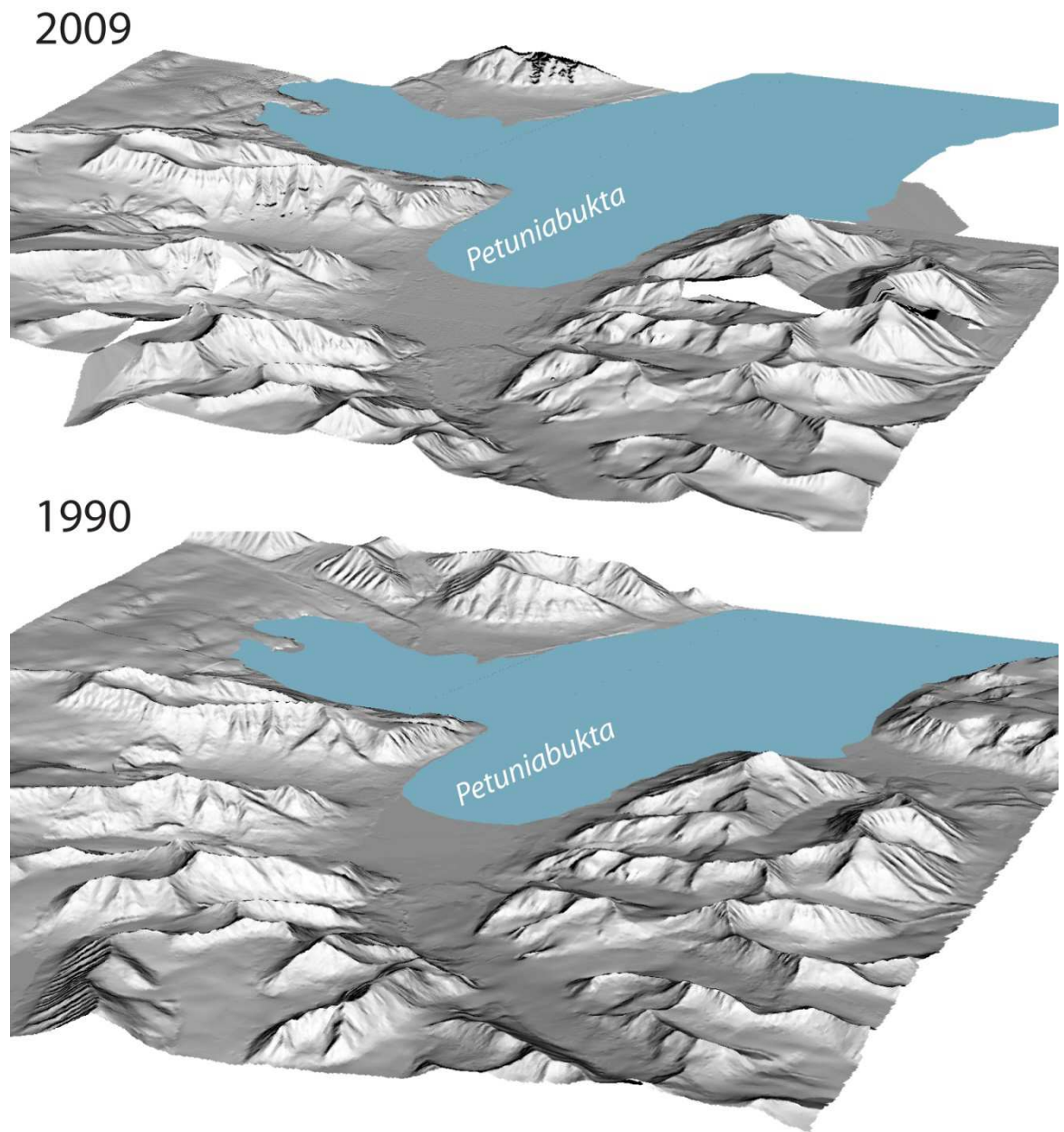


*Figure 6.10. DTMs of the study area produced of aerial images from 2009 (upper) and 1990 (lower)*

Orthophotos were subsequently reprocessed in LPS to generate a seamless radiometrically balanced mosaic covering the whole study area. The mosaic from 2009 orthophotos served as a basis for all geomorphological maps and 1961-1990-2009 image comparison (Figure 6.11.).

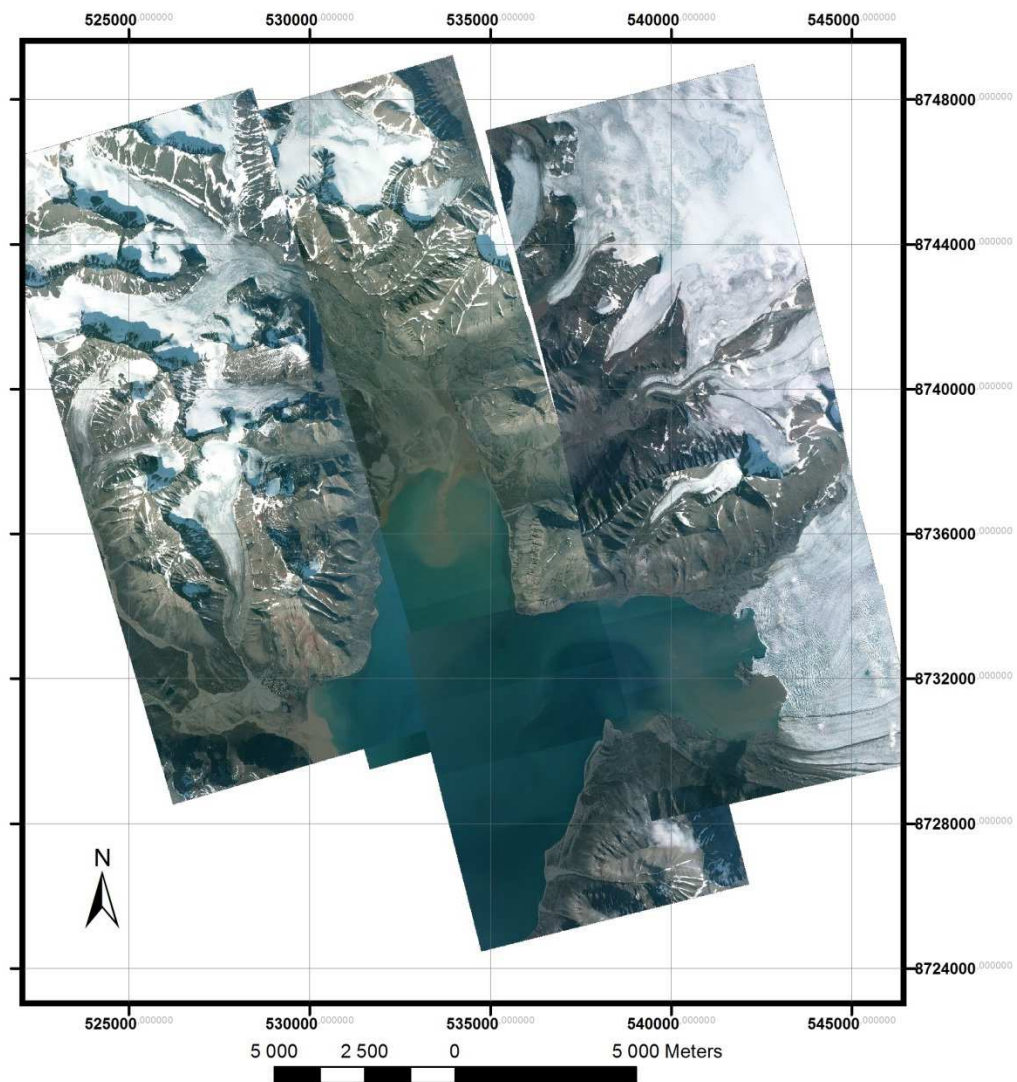


Figure 6.11. Mosaic composed in LPS ERDAS software based on orthophotos from 2009 NPI aerial imagery.

#### 6.5.2.3 Characterisation of surface sediment cover

A basic sedimentological study was carried out to characterise the surface sediments that cover the landforms chosen for analysis using digital images and calculations in Wolman\_Jack software to provide a basic estimate of sediment size and shape of selected landforms (Figure 6.7.).

#### 6.5.2.4 Seabed bathymetry

60,000 sonar soundings (Eagle FishElite 480 sonar) were carried out across Petuniabukta to map the seabed morphology. Sonar measurements were later combined with barrier profiling to describe the relationship between barrier and nearshore morphology. On the basis of sounding the new map and DTM of Petuniabukta seabed has been created (Figure 3.15.).



## 6.6 Glacial-fed barrier systems – results

The results of post-LIA landscape change analysis are presented in three parts focusing on the proglacial zone, the alluvial fan zone and coastal/tidal zone (Figure 6.12.).

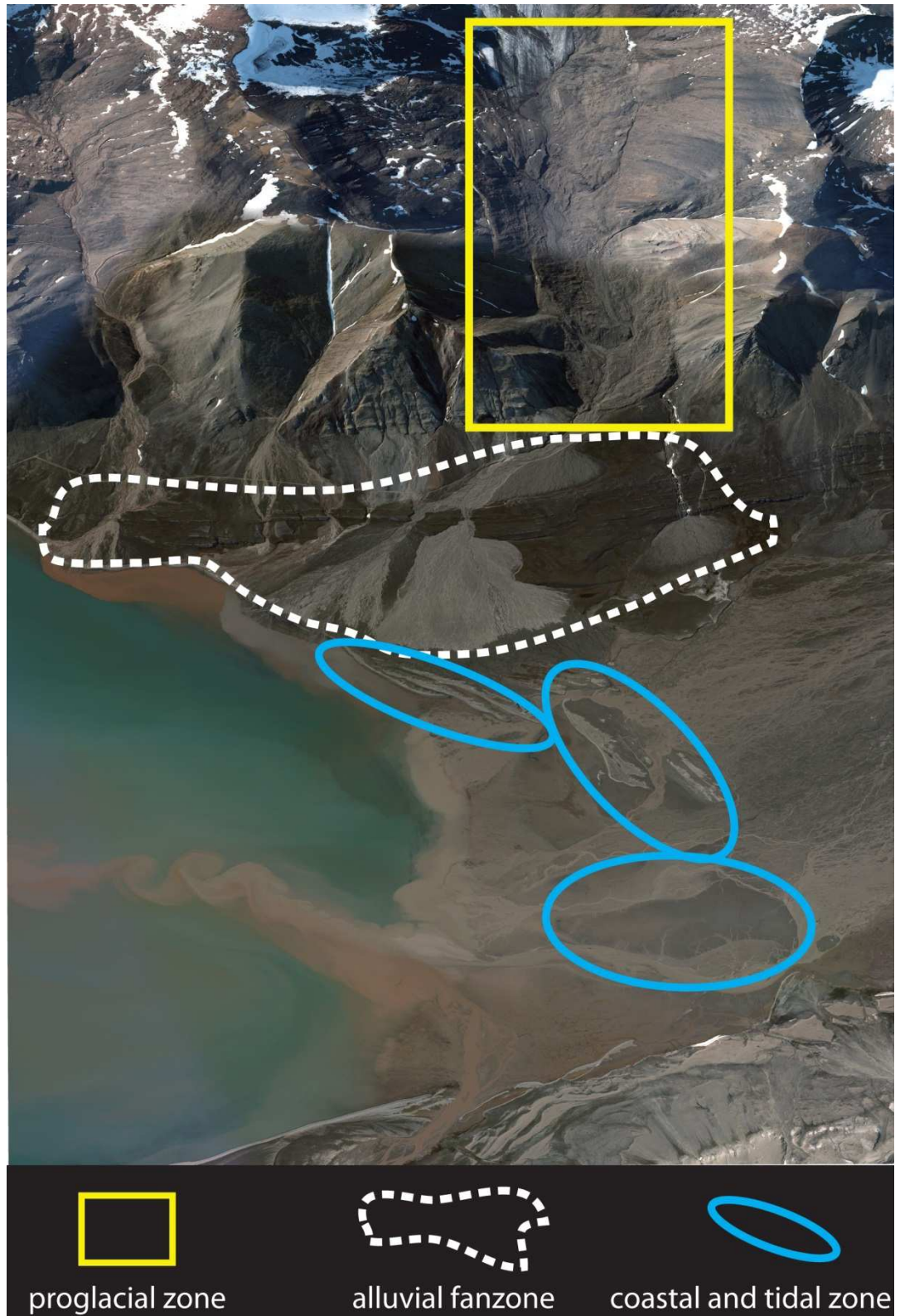


*Figure 6.12. Three elements of landscape change since the end of the LIA along the NW coast of Petuniabukta.*

## 6.6.1 Post-Little Ice Age barrier coast evolution – evidence from air photos

### 6.6.2 The proglacial zone

Recent studies have examined the processes that control the development of the proglacial and ice-marginal zones of Hørbyebreen (RACHLEWICZ 2009; SZUMAN and KASPRZAK 2010; EVANS *et al.* 2012) and Ragnarbreen (EWERTOWSKI *et al.* 2010; 2012). Therefore, the main focus of this study was on the proglacial zone of Ferdinandbreen. This glacier supplies sediments to the section of the coast in Petuniabukta that has changed in the most significant way since the end of LIA.

The post-LIA retreat of Ferdinandbreen has exposed *ca.* 1.6 km<sup>2</sup> of glacier valley between the LIA ice-cored frontal moraine arc and the ice margin. During this period, Ferdinandbreen retreated *ca.* 1500 m and lost over 60% of its area. Mass loss was particularly intensive from 1960 to 1990 period when Ferdinandbreen was losing *ca.* 0.02 km<sup>2</sup> per year and retreated *ca.* 28 m annually. Although the annual recession slowed down to *ca.* 6 m yr<sup>-1</sup> between 1990 and 2009, the glacier is still one of the fastest retreating in the Petuniabukta catchment.

Between 1961 and 2009 the snout of glacier has been transformed into a debris covered glacier (*sensu* LAMBRECHT *et al.* 2011) with a small lake dividing clean ice from a debris-covered part (Figure 6.13.). Presently, the main supraglacial channels drain into the lake before they form the proglacial stream that flows in the middle of a valley and cuts through ice-cored landforms. Until 1990, Ferdinandelva was partly blocked by *ca.* 250 m-long ice-cored ridge, exposed following retreat after 1961. This forced the stream to shift northwards before it incised through the main LIA moraine.

Due to the rapid glacier front recession, the length of the main proglacial channel (between snout and the gorge in the LIA frontal moraine) has increased from *ca.* 460 m in 1961 to over 1600 m in 2009 (Figure 6.13.). This is a significant factor controlling glaciofluvial sediment supply to alluvial fans and the coastal zone downstream. From 1960 to 1990, when sediment ‘evacuation’ was near the post-LIA maximum, the proglacial streams had a relatively short distance to cover before reaching the alluvial fans. Between 1990 and 2009 the potential for sediment interception and storage in the small proglacial lake and along elongated braided channel increased. This has had a direct influence on the development of alluvial fans and sediment delivery to the barrier coast, as explained below.





Figure 6.13. Post-LIA geomorphic changes in the proglacial zone of Ferdinandbreen.



### 6.6.3 Alluvial fans

- Old Ferdie Fan 1

Changes to this fan are linked to changes in the Ferdinandbreen proglacial drainage network and cessation of proglacial outflow through one of the gorges in the moraine belt (MG1 on Figure 6.14.). As marked on Figure 6.16., the LIA moraine belt is incised in two places. The present gorge MG2, located in the middle of moraine (Figure 6.15.), has been active since at least 1961 and drains proglacial waters in the direction of two alluvial fans (Ferdie Fan 3 and 4).

Another gorge (MG1), is located in the northern part of a morainic arc, adjacent to the mountain slope. MG1 is currently cut off from the proglacial river and hangs *ca.* 20 m above the bottom of the present glacier valley. The channel that once originated from the gorge is active only during spring-melt periods, when it drains meltwaters from *ca.* 2-3 m deep snowpatches formed in a bedrock ravine, before it spreads across the first alluvial fan formed along the coastal plain (OFF1).

The channel incision in limestone bedrock has created a system of small waterfalls, with well-shaped evorsion hollows (pot-holes) suggesting that it was formerly occupied by a significant stream (Figure 6.15.). Remnants of glacial sediment covering banks of the bedrock channel suggest that this channel was active during the LIA, when the glacier snout formerly extended out of the valley (see Figure 6.9.a, taken in 1930) and supplied the growth of *ca.* 100,000 m<sup>2</sup> alluvial fan (OFF1).

Once the glacier started to retreat from its LIA maximum, the proglacial drainage network shifted towards the modern gorge. As a result, the glaciofluvial sediment supply to alluvial fan OFF1 ceased and fan development became limited to modification of a few channels fed by ephemeral snowpatch melt. Today, scarce tussocks of tundra cover the majority of the dried-out fan channels (Figure 6.15.).

- Old Ferdie Fan 2

The evolution of OFF2 is linked to falling Holocene relative sea-level (RSL). The fan that formerly covered *ca.* 0.16 km<sup>2</sup> between Ferdinandbreen's LIA frontal moraine and bedrock outcrops emerging through the coastal plain (Figure 6.14.) has been significantly incised by Ferdinandelva and, up to the present, has lost *ca.* 40% of its (Holocene) maximum area. The abandoned fan surface spreads between *ca.* 61 m above MTL (proximal) and 34 m MTL (distal margin). Based on the RSL reconstruction presented in Chapter 8, this suggests the fan was at sea level at the start of the Holocene and its formation began just after the retreat of the Late Weichselian ice from Petuniabukta.

The incision of the fan by Ferdinandelva progressed with rapid RSL fall. The present day river channel runs from *ca.* 59 m MTL at the gorge in the LIA moraine to *ca.* 31 m MTL where it enters two gorges incised in bedrock outcrop (G1 and G2, Figure 6.16.). The volume of sediments that had to be eroded by Ferdinandelva and washed away from the OFF2 towards Ferdie Fan 3 and Ferdie Fan 4 is estimated to be *ca.* 210 000 m<sup>3</sup>.

The most important changes that occurred since the end of the LIA are the enlargement of a ravine in OFF2. It seems that this was produced mainly by lateral erosion of the incised fan deposits and a shift of the main channel of Ferdinandelva towards gorge G2. This shift happened after 1961, at which date the gorge was still covered by former fan deposits (Figure 6.14.). The area eroded from OFF2 between 1961 and 2009 was *ca.* 23,000 m<sup>2</sup>, including 13,000 m<sup>2</sup> of OFF2 that blocked access to the bedrock gorge G2.

It is important to note that erosion of OFF2 towards the bedrock gorge G2 took place mainly between 1961 and 1990 when the modern river valley widened *ca.* 20,000 m<sup>2</sup> (Figure 6.14.), whereas between 1990 and 2009 river eroded only 3000 m<sup>2</sup> of OFF2. Subsequent to fan erosion, Ferdinandelva was adjusting channels to the new proglacial zone exposed by the retreating glacier. This has caused the main channel (Figure 6.15.) to avulse from the first bedrock gorge towards the second, southern gorge.

Currently the outflow through the first gorge, G1, is active only during the period of highest springmelt and summer discharge. The above-mentioned drainage shift initiated the phase of intensive growth of Ferdie Fan 4 and gradual suppression of the enlargement of Ferdie Fan 3 (Figure 6.16.).

- Ferdie Fan 3

This is the largest fan system along the NW coast of Petuniabukta and fills the area between the modern barrier coast and the bedrock threshold (Figure 6.16.). The active fan is bordered by remnants of a relict fan that covered *ca.* 800,000 m<sup>2</sup> and has been incised *ca.* 2 to 4 m during the lowering of Ferdinandelva base-level (Figure 6.17.). The relict fan developed on the surface of older beach deposits. This explains the large accumulations of shells and fragments of whale bones seen in exposed cliff walls (Figure 6.17.). A fragment of the distal margin of an relict fan is located *ca.* 5 m MTL and suggests that the intensified surface erosion and the accumulation of the modern fan began at *ca.* 4000 cal yr BP.

As in the modern system, the relict fan was bordered by gravel-dominated barriers (FOS) whose remnants have a surface elevation of *ca.* 1.5 m MTL. The active fan can be divided into two zones:

- A stable zone that covers *ca.* 310,000 m<sup>2</sup> and extends from the gorge G1 (*ca.* 29 m MTL) to the dry edge (distal margin) of the fan located *ca.* 2 m MTL. The fan surface is covered with hundreds of partly vegetated dry and abandoned braided-channels (Figure 6.17.). Between 2005 and 2010, summer discharge was focused in a single channel that drained to the tidal flat creek between remnants of Ferdie Old Spits (FOS), Ferdie Spit I (FSI) and Ferdie Barrier Island I (FBII);
- An active zone penetrating into lagoons formed behind a gravel-dominated barrier and moistened by seepage of sea water through the barrier during high tide.

A comparison of the FF3 stable surface changes inferred from aerial images indicates that in the last 20 years the fan expanded just 10,000 m<sup>2</sup>. This means that sediment accumulation was significantly higher from 1961 to 1990, when the fan expanded from 220 000 m<sup>2</sup> to 300,000 m<sup>2</sup>. It is possible to explain this change by the opening of the second gorge (G2) and the drying up of two main channels that supplied the fan with sediments between 1961 and 1990 (Figure 6.16.).

#### • Ferdie Fan 4

This is the youngest fan among the analysed alluvial systems and has experienced rapid growth after 1961. FF4 is currently the main pathway for sediment transport from the deglaciating Ferdinandsbreen valley towards the coast (Figure 6.16.). Before the activation of the new Ferdinandsbreen channel (which eroded its way to the coast through G2) the FF4 surface was faintly incised by dozens of ephemeral snowmelt streams that drain from the slopes of the Mumien massif. These streams drain through another four bedrock gorges (G3-G6) and feed the small fan system (56,000 m<sup>2</sup>) that currently adjoins FF4 from the southwest. FF4 is divided from FF3 by remnants of an old fan surface that, like OFF2, has been incised by Ferdinandsbreen during the Late Holocene. It is very likely that with current rates of erosion of the former fan surface (*ca.* 1.2 m per year) the modern fans (FF3, FF4 and snowmelt fans) will merge by the end of 21<sup>st</sup> century.

Between 1990 and 2009, FF4 grew by *ca.* 50,000 m<sup>2</sup> and currently covers 180,000 m<sup>2</sup>. This includes 2400 m<sup>2</sup> that formed after breaching of the coastal barrier and the accumulation of the fan delta in Petuniabukta (Figure 6.16.). The breaching of the coastal barrier by FF4 channels was one of the most important processes leading to the shoreline change in NW Petuniabukta during the post LIA period.

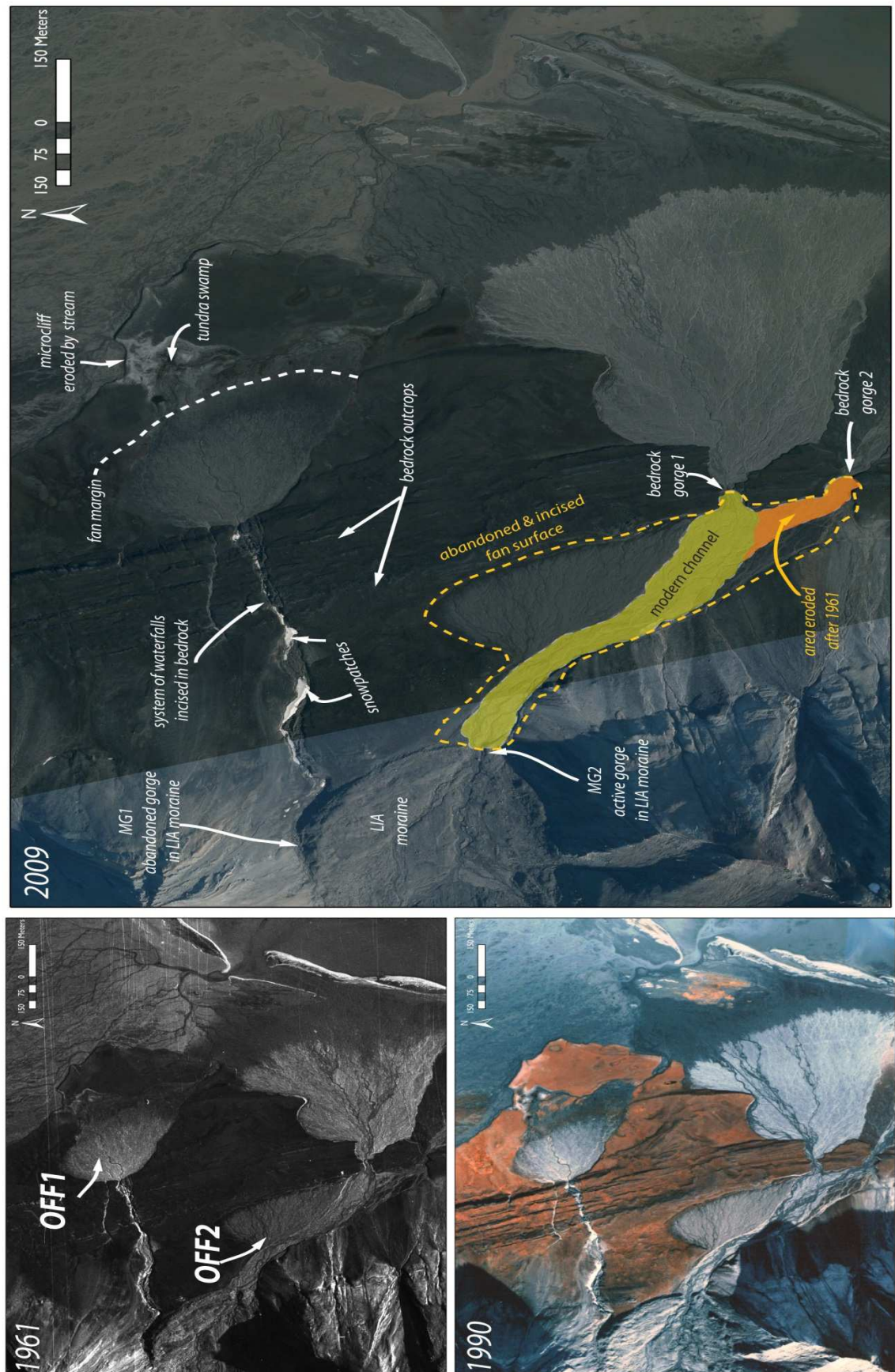


Figure 6.14. Post-LIA changes of Old Ferdie Fans 1 and 2.



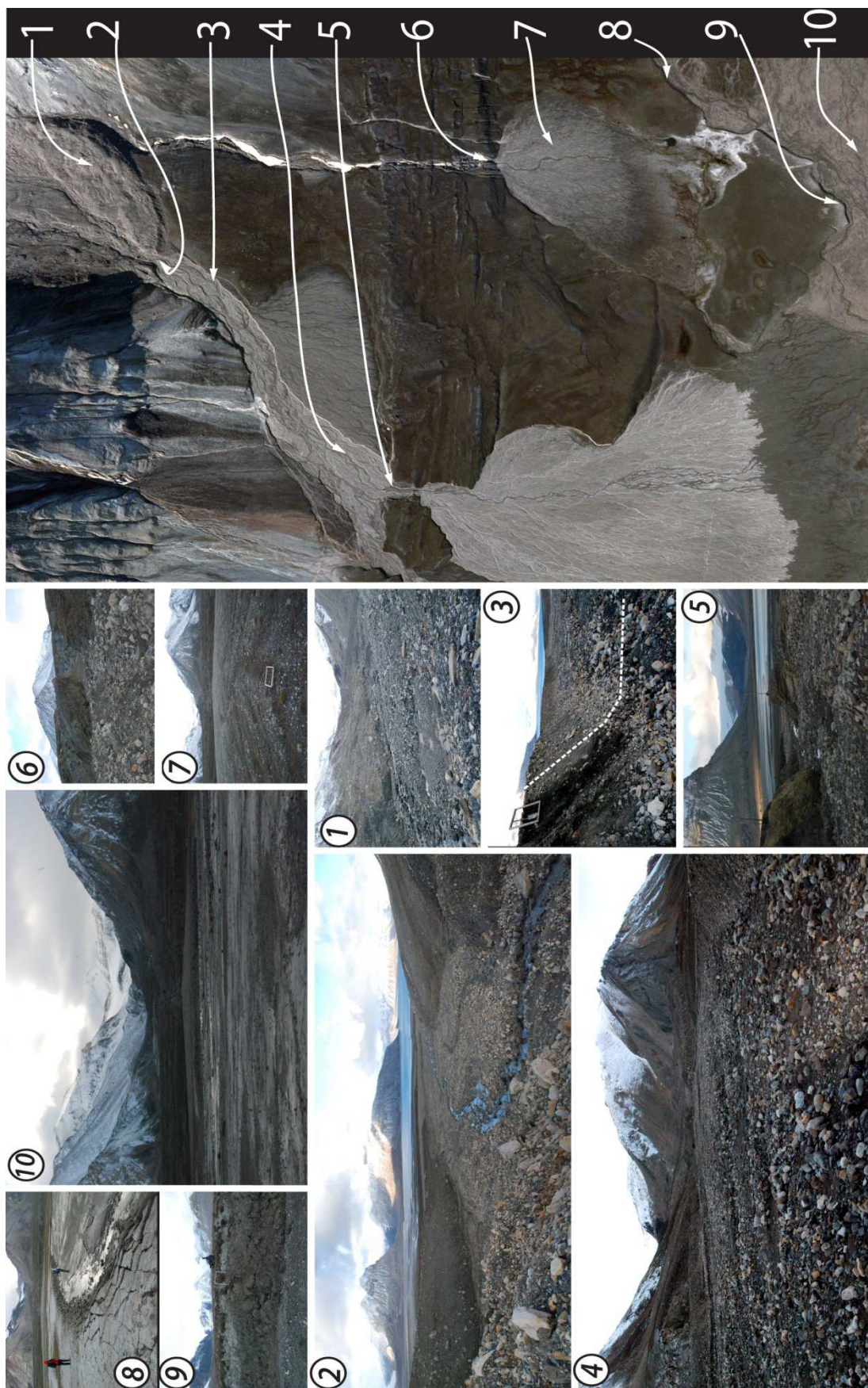


Figure 6.15. Main features of Old Ferdie Fans: 1- LIA moraine; 2 - MG2 gorge; 3 - incised surface of relict fan; 4 - modern river valley incised by Ferdinandelva in relict fan surface; 5 -GI; 6 - cascade formed in bedrock by stream supplying OFFI; 7 - dry, vegetated channels of OFFI; 8 and 9 - the distal margin of OFFI; 10 - braided channels on an outwash plain that is OFFI deposits.



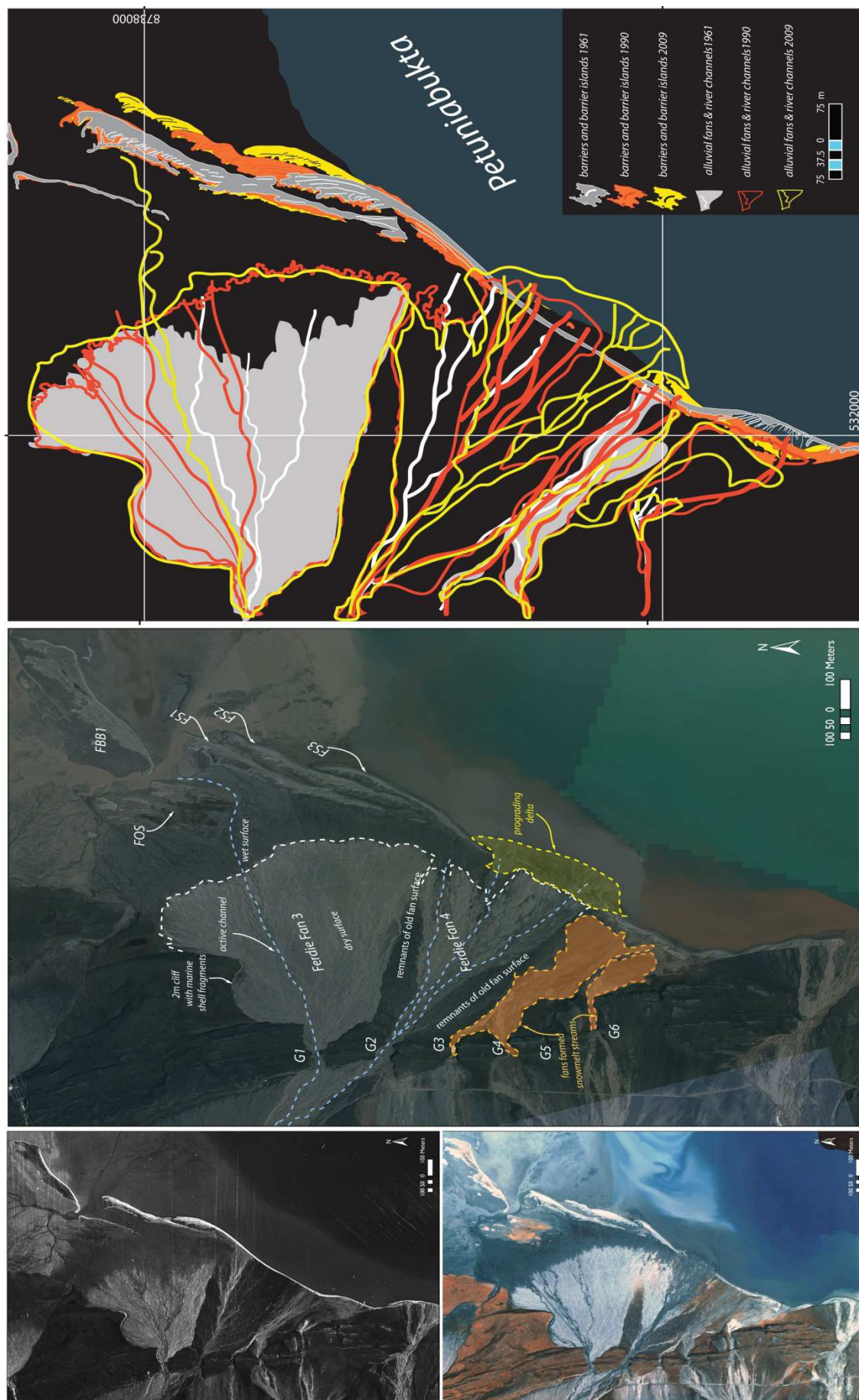
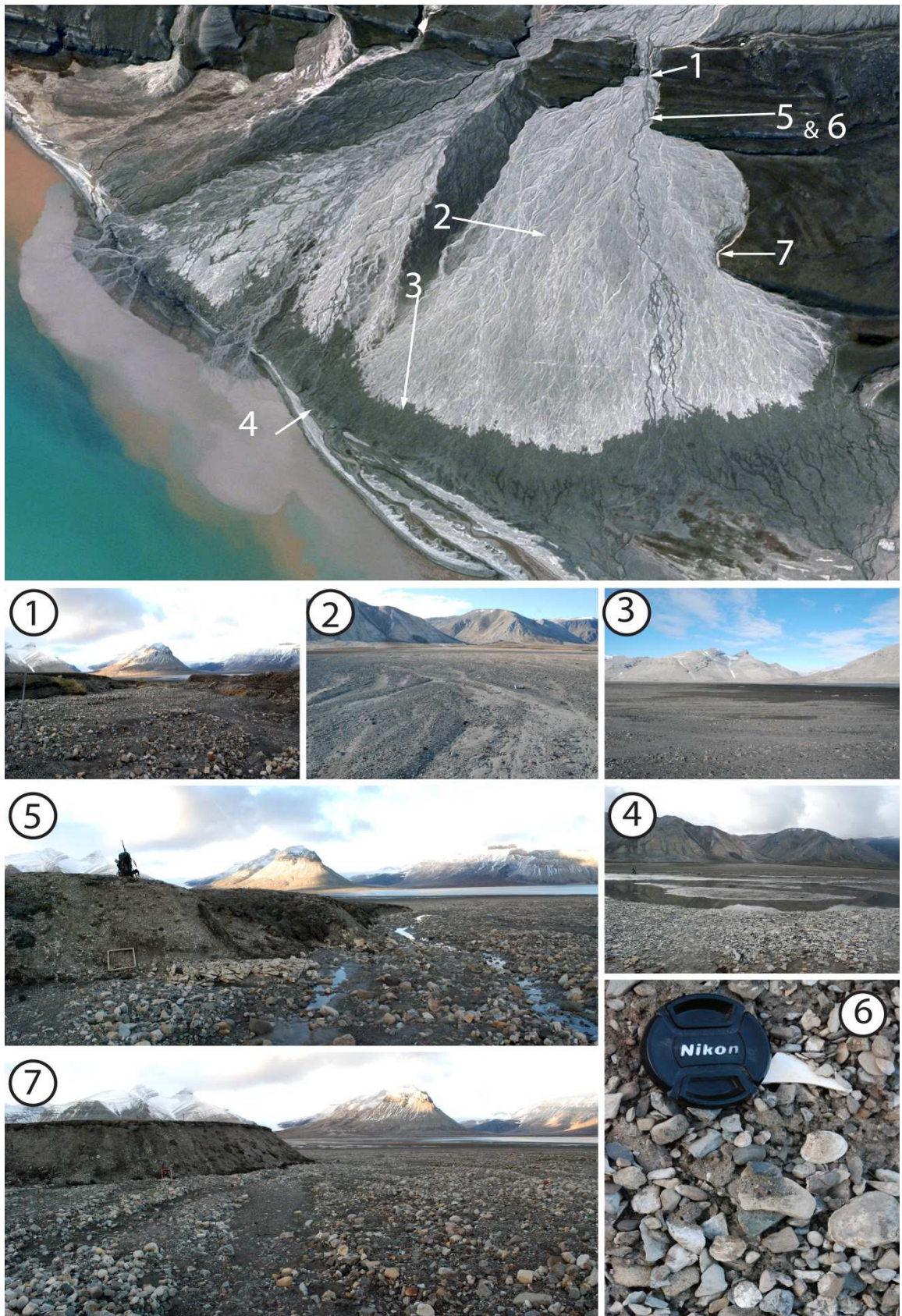


Figure 6.16. Post-LIA changes of modern Ferdie Fans 3 and 4.





*Figure 6.17. Main features of Ferdie Fans: 1 - G1; 2 - dry channels on surface of FF3; 3 - transition zone between dry and wet zones of FF3; 4 - gravel-dominated barrier blocking growth of FF3; 5 - cliff formed after incision of relict fan during the development of FF3; 6 - surface of a cliff wall with fragments of shells and whalebones ca. 26 m MTL; 7 – cliff wall (ca. 3.5 m high) formed by incision of relict fan surface by streams supplying prograding FF3.*

## 6.6.4 Coastal and tidal landforms

### • Ferdie Barrier Spits

The formation of new barrier spits along FF3 are the biggest change on the NW Petuniabukta since the end of the LIA (Figure 6.18.). The evolution of three spits (FS1, FS2, FS3) and small lagoons have had a profound effect on the evolution of FF3 by blocking its seaward progradation (Figure 6.18.). Table 6.4 summarises shoreline changes that occurred along the seaward margin of FF3 between 1936 and 2009.

Spit	1936	1961		1990		2009		rate of spit expansion [m yr <sup>-1</sup> ]		
		axis length [m]	area [sq m]	axis length [m]	area [sq m]	axis length [m]	area [sq m]	1961- 1990	1990- 2009	1961- 2009
FS1	present	679	210,000	696	18,000	735	17,000	0.6	2.1	1.2
FS2	embryo formed	270	10,000	431	13,600	557	13,000	5.6	6.6	6
FS3	x	x	x	315	7100	502	10,000	x	9.8	9.8

Table 6.4. Post-LIA changes (length/area) changes to the Ferdie barrier spits. x – landform did not exist in this period so no rate calculated.

Analysis of photographs taken by R.M. Jackson in 1930 and an oblique aerial image taken by NPI in 1936 suggest that the main body of FS1 had already formed by the 1930s, but did not block the outflow of FF3 channels to Petuniabukta. Between 1961 and 2009 the spit system has extended northwards *ca.* 56 m and its northernmost tip has recently reached the main tidal channel in the western part of Petuniabukta tidal flat (Figure 6.19.). Interestingly, the rate of spit expansion was slower from 1961 to 1990 (0.6 m yr<sup>-1</sup>), when the landform was still exposed to the operation of waves and longshore drift, than between 1990 and 2009 (2.1 m yr<sup>-1</sup>) when the spit was cut off from sediment supply from longshore drift and was becoming more protected from waves by the development of adjacent FS2. Perhaps the more rapid expansion of FS1 from 1990 to 2009 is a side effect of the formation of FS2. One explanation for landform elongation is spit erosion (area loss between 1961 and 2009 *ca.* 4000 m<sup>2</sup>) and reworking of released sediments by tidal currents flowing into a small lagoon between FS1 and FS2 during the high tide and additionally amplified by high discharge from channels draining Sven-Hørbye-Ragnar outwash plain system. A similar pattern is seen with the second spit, where expansion was slightly faster from 1990 to 2009 compared with 1961 to 1990 period. The total extension of this spit between 1961 and 2009 towards the tidal flat was *ca.* 287 m. Using archival maps and photographs it was hard to determine the exact time of spit inception,

although it can be assumed that FS2 started to form in the first decades of the 20<sup>th</sup> century as the well-established spit embryo is clearly visible on aerial image from 1936.

FS2 was the main barrier system that developed along the western coast of Petuniabukta and constituted its northernmost shoreline until at least 1961. During the 1960s the coastline had a rather straight edge and the main sediment supply to the barrier was from Elzaelva and ephemeral snowmelt streams from the Mumien massif. Sometime between 1961 and 1990 the situation changed significantly. The spit was cut off from the main barrier that was breached by one of the channels of Ferdinandelva that shifted towards the new gorge (G2) and eroded its way to the coast through the remnants of the old fan (Figure 6.19.). By 1990, Ferdinandelva had formed a small delta along the distal margin of FF4 that provided material for development of the third spit (FS3), which started to grow along FS2.

Another important process that occurred to the south of the Ferdie Spits was the erosion of 6000 m<sup>2</sup> of a low-lying (*ca.* 0.3 m MTL) relict barrier-platform located between the Elzaelva delta and the FF4 fan delta (Figure 6.20.). The erosion that in some places reached *ca.* 50 m inland (for 1961-2009 period) led to the removal of *ca.* 1800 m<sup>3</sup> of sediment that will have been redistributed along the modern barrier and FS3.

Reduction of the distance to the modern coast enabled several small snowmelt streams to incise through the weakened barrier and open two new connections between the relict lagoon and the fjord, thus supplying the coast with fine alluvial sediments. Up to this point these sediments would have accumulated behind the barrier (Figure 6.21.). However, these outlets are ephemeral features that are easily blocked by storm ridges, as has been documented during geomorphological mapping after a few stormy days in summer 2009 and 2010.

This emphasises that the delivery of sediment to the coast through breached barriers had a significant influence on sediment availability in NW Petuniabukta, which hitherto was controlled by small snowmelt streams and glaciofluvial discharges from the rapidly decaying Elzabreen. Therefore, even though FS2 was partially cut off from longshore drift by 1990, the landform was still able to grow and indeed extended another 126 m by 2009. Presumably, the downstream end of the spit was still receiving sediment via longshore drift of material carried beyond the tip of the newly forming FS3. The reduction of spit area observed between 1990 and 2009 suggests that the landform elongation was partly a product of spit reworking.

The youngest spit, FS3, was fed sediment from the FF4 fan delta. The barrier that started to develop in 1990 from the base of FS2 grew *ca.* 187 m in 19 years and increased in size to *ca.* 30,000 m<sup>2</sup>. This growth is the fastest among the three spits, emphasising the importance of the activation of sediment supply from FF4 and smaller suppliers such as snowmelt streams in last two decades.

Remotely-sensed and field-based geomorphological mapping indicates that, at least until 2010, the growth of spits occurred by the formation of recurved hooks (laterals) around the spit terminus that overlapped one another (Figure 6.22.). This mechanism led to the northward elongation and simultaneous landward bending of the spit (towards FS2). Between 1990 and 2009, *ca.* 19-23 recurves grew around the terminus of FS3 with widths that ranged from 1 to 4 m (Figure 6.19.). The same process occurred during the evolution of FS2, this time composed of *ca.* 36 recurves. FS2 was developing parallel to the original spit planform until at least 1961 and then started to gently shift towards the center of tidal flat (Figure 6.22.). FS1 has a similar construction showing that, as long as the spit extended by leaning against the margin of FF3, it managed to parallel the original planform. However, once the spit reached the deeper water of the tidal flat, the spit terminus began to bend. Although the degree of FS1 surface reworking (mainly by niveoaeolian processes) hampers the precise identification of all recurves accreted along the spit, at least 50 of them were counted on aerial images and ground-truthed in the field.

Figure 6.22. shows that the Ferdie spits gradually shift their axes from the NNE (FS1) towards the NE (FS3). Interestingly, the axes of relict Ferdie Old Spits run almost straight on to the N, suggesting that the lateral migration of modern barrier spits was linked with refraction of waves and longshore current in shallow waters at the shifting boundary between FF3 distal margin and prograding tidal flat.

- Ferdie (fetch-limited) Barrier Islands

Two small islands located in western part of Petuniabukta tidal flat are probably the most enigmatic landforms in the study area both in terms of their origin and spatial configuration (Figure 6.23.). Their morphological features identified from remote-sensed and field-based mapping, notably their small size (300-600 m long, 30-70 m wide), low elevation (< 1m), narrow inlets, location in a low-energy bay, and sparse vegetation cover suggest that they can be described as fetch-limited barrier islands *sensu* COOPER *et al.* (2007). The processes of formation of fetch-limited barrier islands (FLBI) have not previously been described in High Arctic settings, but it might be assumed that several



factors (sea-ice, snow cover, episodic sediment supply from glacierised and non-glacierised catchments, rapid RSL changes and accumulations of driftwood) were significant to their formation. The planform of Ferdie Barrier Islands has not been significantly modified during the last 50 years (Figure 6.23.). The inspection of series of images shown in Figure 6.5 taken between 1936 and 2009 allows one to surmise that the islands have been stable since the end of the LIA and remain unchanged even during events that led to the formation of Ferdie Barrier Spits and other large shoreline changes in NW Petuniabukta. According to PILKEY *et al.* (2009) the lack of larger changes and the associated high preservation potential of these landforms is one of the key attributes of FLBI. The only observable change that occurred was the gradual erosion of the small island to the south of FLBIs (yellow patch in Figure 6.23.) most likely due to washing out by wave action during spring tides, amplified by summer floods running over the outwash plain.

More important changes have affected the tidal flat surface and channel network around the FLBIs. Even though channels flowing around the islands frequently migrated and eroded new creeks in the tidal flat, the shape of the islands has remained stable. Symptomatic of their high preservation potential is the stabilization of a recurved hook in the tidal inlet between Ferdie Old Spits and FBII that stayed unchanged despite enlargement of the main tidal channel (Figure 6.23.). The likely explanation of this process is the location of the landforms above modern sea-level (*ca.* +0.7-1.3 m MTL). Uplift of those landforms was previously suggested by BORÓWKA (1989) who described the barrier islands as “dead” landforms indicating RSL fall in the area. Raising of the landforms may help also to explain their strange spatial configuration (WSW-ENE), tilted from the dominant direction of modern coastline (SSW-NNE). Most likely, is that at the time of barrier island formation the deeper water conditions and different configuration of the bay modified the surface circulation patten across the fjord.

Currently, the Ferdie Barrier Islands are reached from the south by low waves only during the spring tides or occasional storms, and the majority of surface changes are linked to subaerial processes dominated by aeolian deposition (Figure 6.23.). Winds deflate dust from abandoned channels of the Sven-Hørbye-Ragnar outwash plain, and relict alluvial fans, and cover the formerly gravel-dominated surface of FLBIs with a blanket of fine sand and silt.

There are four main factors influencing the extent of aeolian deposition over Ferdie Barrier Islands. First, they are the first landforms that lie parallel to the route of

autumn dust storms originating in the Sven-Hørbye-Ragnarbrei outwash plain. Secondly, they protrude above the surface of the tidal flat causing airflow perturbation and consequent deposition of aeolian sediments. These sediments can be easily trapped on the often damp surface of the FLBs. Thirdly, the surface of FLBs is covered with tundra vegetation which not only stabilises the landforms but also facilitates accelerated capture of aeolian deposits. Finally, the large accumulations of driftwood that girdle the FLBs and are embedded in their surface to produce a stable backbone for microdunes. The majority of these driftwood trunks are also partially embedded in tidal sediments and remain stable even when flooded by waves.

- Tidal flat

Analysis of post-LIA geomorphic changes that occurred across the Petuniabukta tidal flat was limited due to lack of information about the exact time of photographs from 1961 and 1990. This precluded determination of the tide level and caused problems with the accurate distinction between the flooded and dry surfaces of the tidal flat on the black and white images taken in 1961. Taking into account these limitations, only the most visible tidal island was analysed (Figure 6.25.). It should, however, be noted that in the present tidal flat system there are four bigger islands.

The largest tidal island currently covers *ca.* 230,000 m<sup>2</sup> and is surrounded by Hørbye-Ragnarelva channels. If one assumes that the older images were taken in the similar phase of tide, then the estimated island area loss since 1961 amounts to *ca.* 90,000 m<sup>2</sup>, including a 20,000 m<sup>2</sup> reduction since 1990. Inspection of time-lapse images of tidal flat taken in summer 2009 from the Løvehovden (Figure 6.26.) to some extent supports calculations made in ArcGIS. Time-lapse photos revealed that the surface of the tidal island was partly emerged even during the highest tides of the summer season, and fully emerged for most of the summer season. This suggests that the surface visible on the 2009 NPI aerial image is close to its maximum extent. Therefore, the differences in tidal island coverage between 1961, 1990 and 2009 are likely associated with subaerial erosional processes rather than by surface inundation by tidal waves. Since 1961 the largest change took place in the northern part of the tidal island which has been eroded by the main channel of Hørbye-Ragnarelva. Erosion led to the separation of two small islets and widening of the main tidal channel in eastern section of tidal flat.

The final feature selected for geomorphic change analysis was the seaward margin of the tidal flat. The tidal flat is the natural trap for sediments delivered by adjacent glacier rivers and streams and, as a result of continued sediment supply, has accumulated a

prograding delta that ends in the steep *ca.* 15° step (SZCZUCIŃSKI and ZAJĄCZKOWSKI 2012). A recent study of sediment accumulation rates in Billefjorden (SZCZUCIŃSKI *et al.* 2009) suggests that the post-LIA transfer of sediment released from decaying glaciers to the bay is almost 4 times higher than during the LIA and the rest of Holocene. They concluded that sedimentation from suspension takes place mostly within the first 100 m from the mouths of glacier rivers and tidal flat channels (Figure 6.27.).

Examination of the NPI aerial images from Petuniabukta allowed only limited comparison of changes in the position of the tidal flat step between 1961 and 2009 as the feature was obscured by sediment plumes from Ebbaelva and tidal channels. Therefore, the ArcGIS calculations of tidal step position shift were referenced to the new DTM of the Petuniabukta seabed based on sonar soundings from 2009. Two general tendencies were observed: a significant seaward progradation ranging between 40 and 140 m of the central sector of the tidal flat supplied by the main tidal channels and relative stability along the flanks merging with Ebbaelva ebb-tide delta to the east and Ferdinandelva and Elzaelva fan deltas to the west.

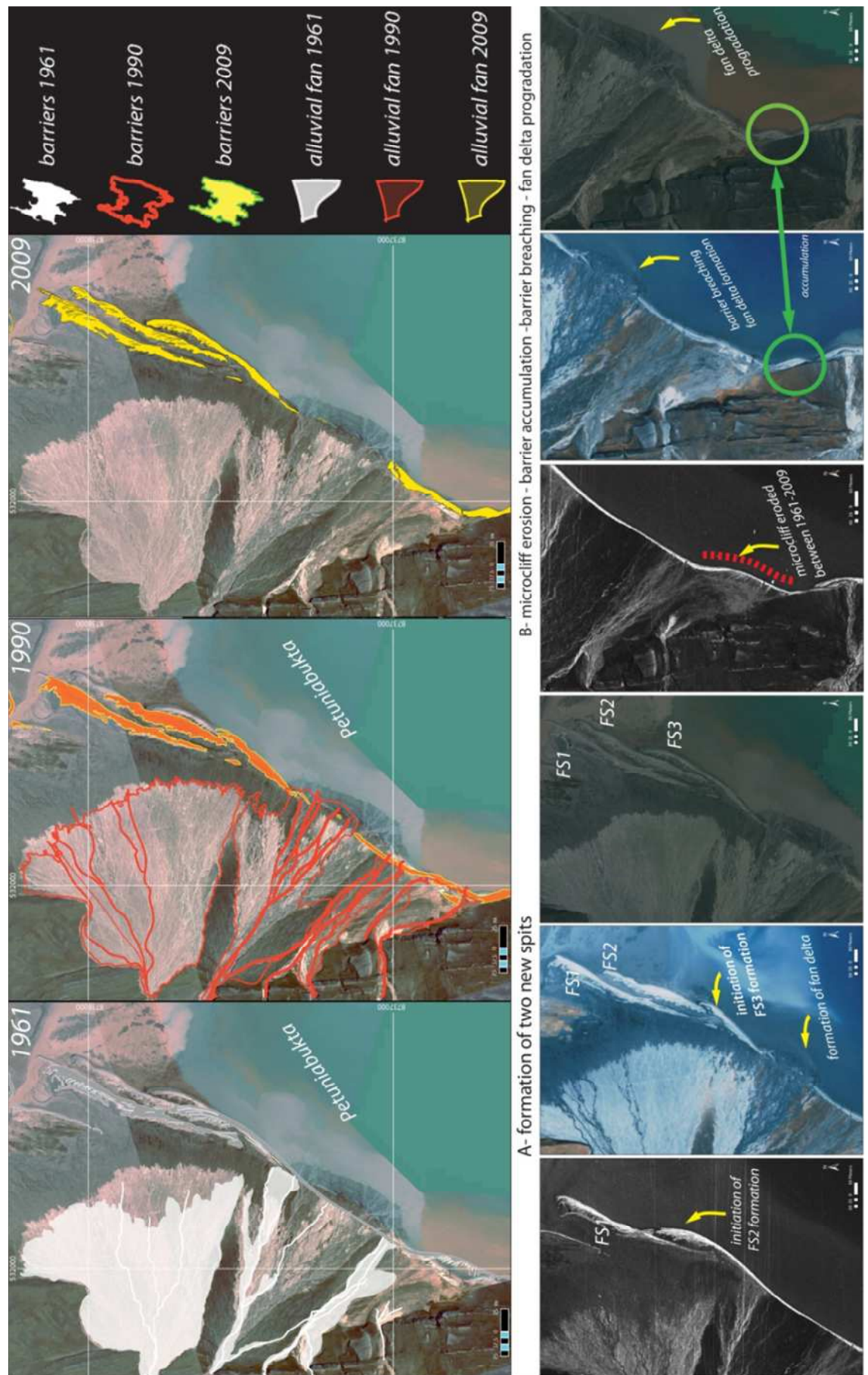
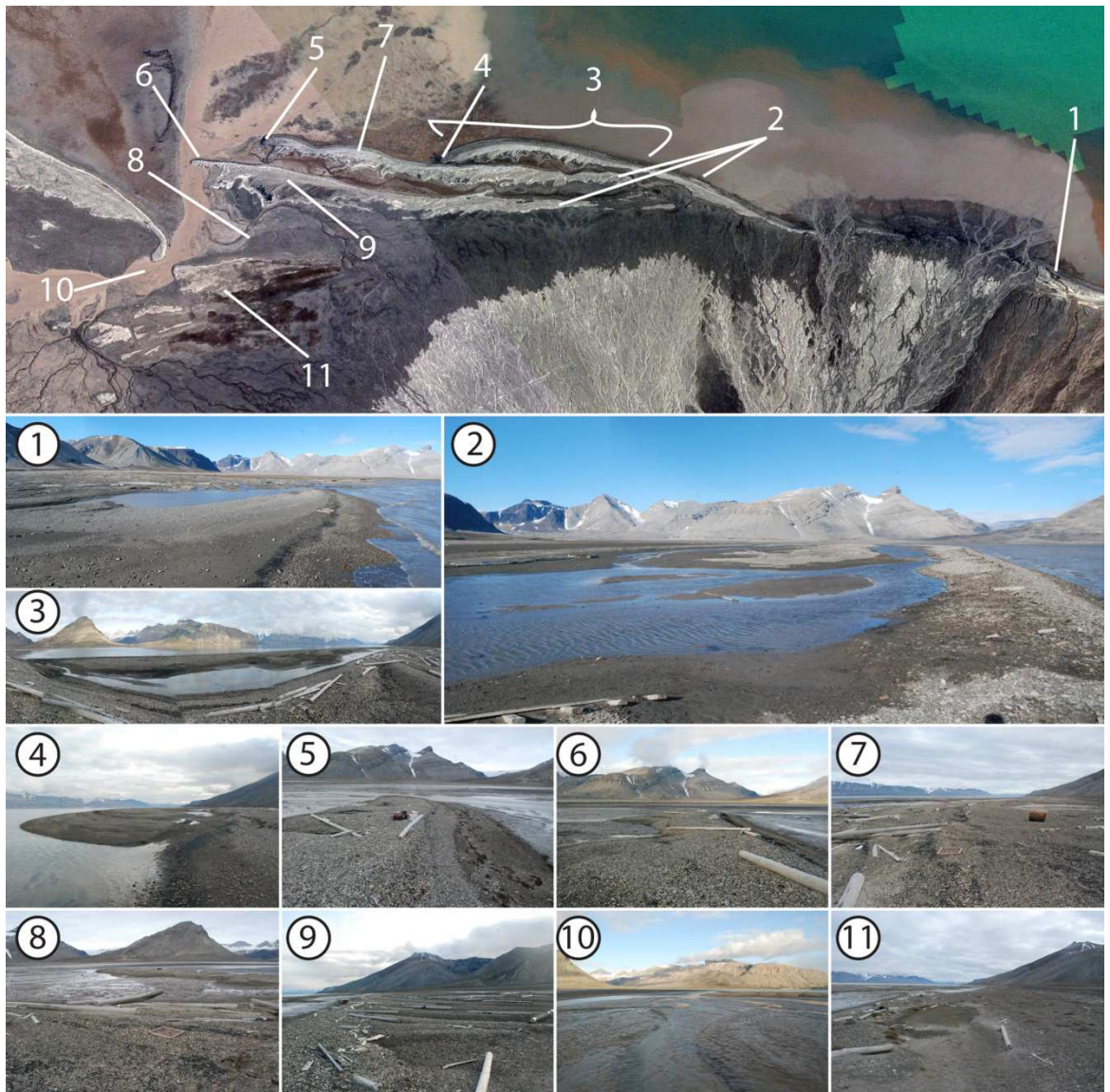


Figure 6.18. Post-LIA changes to the barrier coast formed along the Ferdie Fans.





*Figure 6.19. Main features of the gravel-dominated Ferdie Barrier Spits: 1- barrier breached by the main channel of Ferdinandelva draining FF4 and supplying growth of fan delta; 2 - three spits and associated lagoons at high tide; 3 - Ferdie Barrier Spit 3; 4, 5, 6 - terminus of Ferdie Barrier Spit 3, 2, 1; 7 - surface of FBS2; 8 - lagoon between FBS1 and Ferdie Old Spits; 9 - central part of FBS1; 10 - main tidal channel dividing Ferdie Barrier Spit 1 from Ferdie Barrier Island 1; 11 - surface of Old Ferdie Spits modified by aeolian process.*



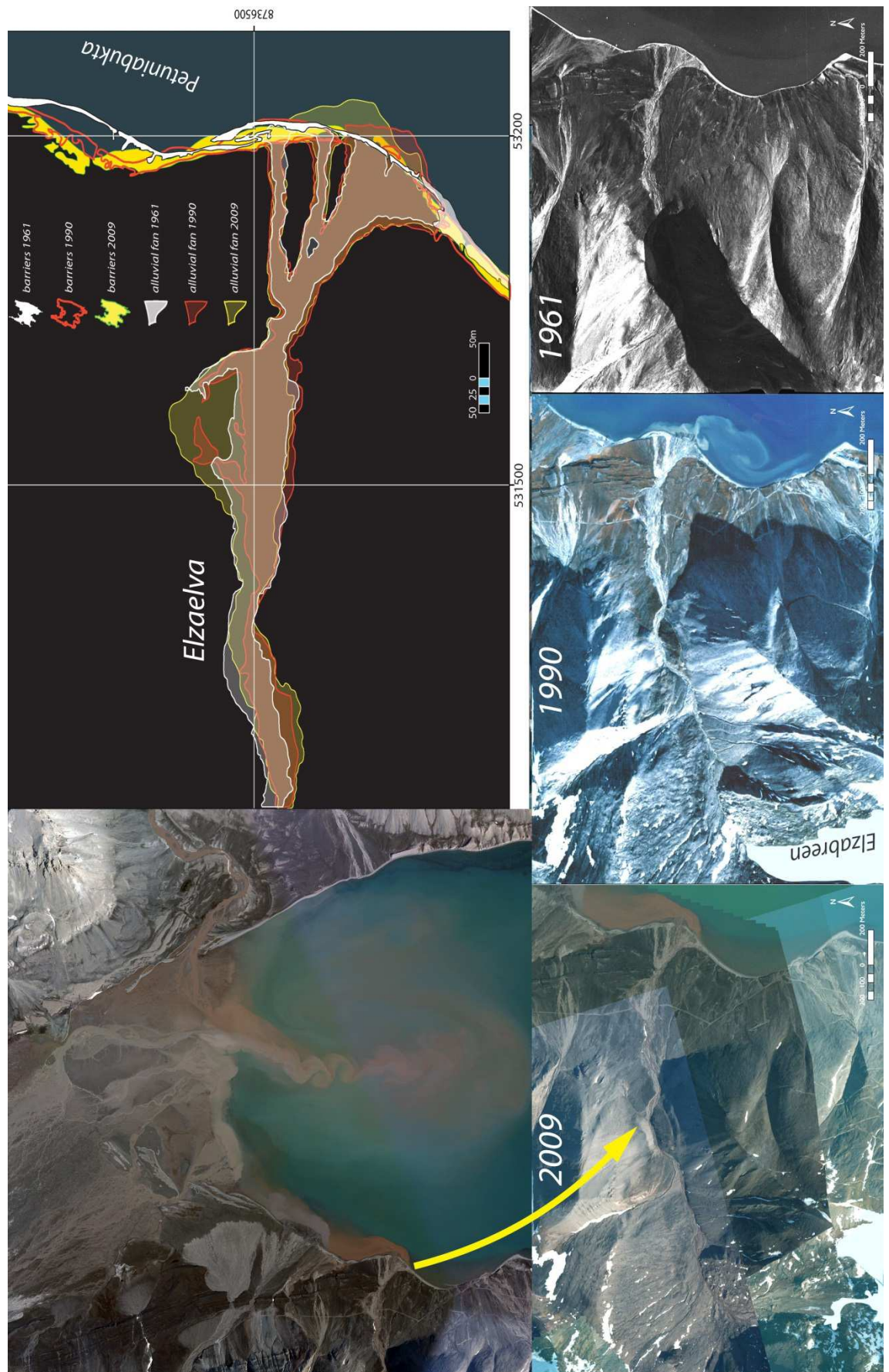


Figure 6.20. Post-LIA changes of Elzaelva delta.



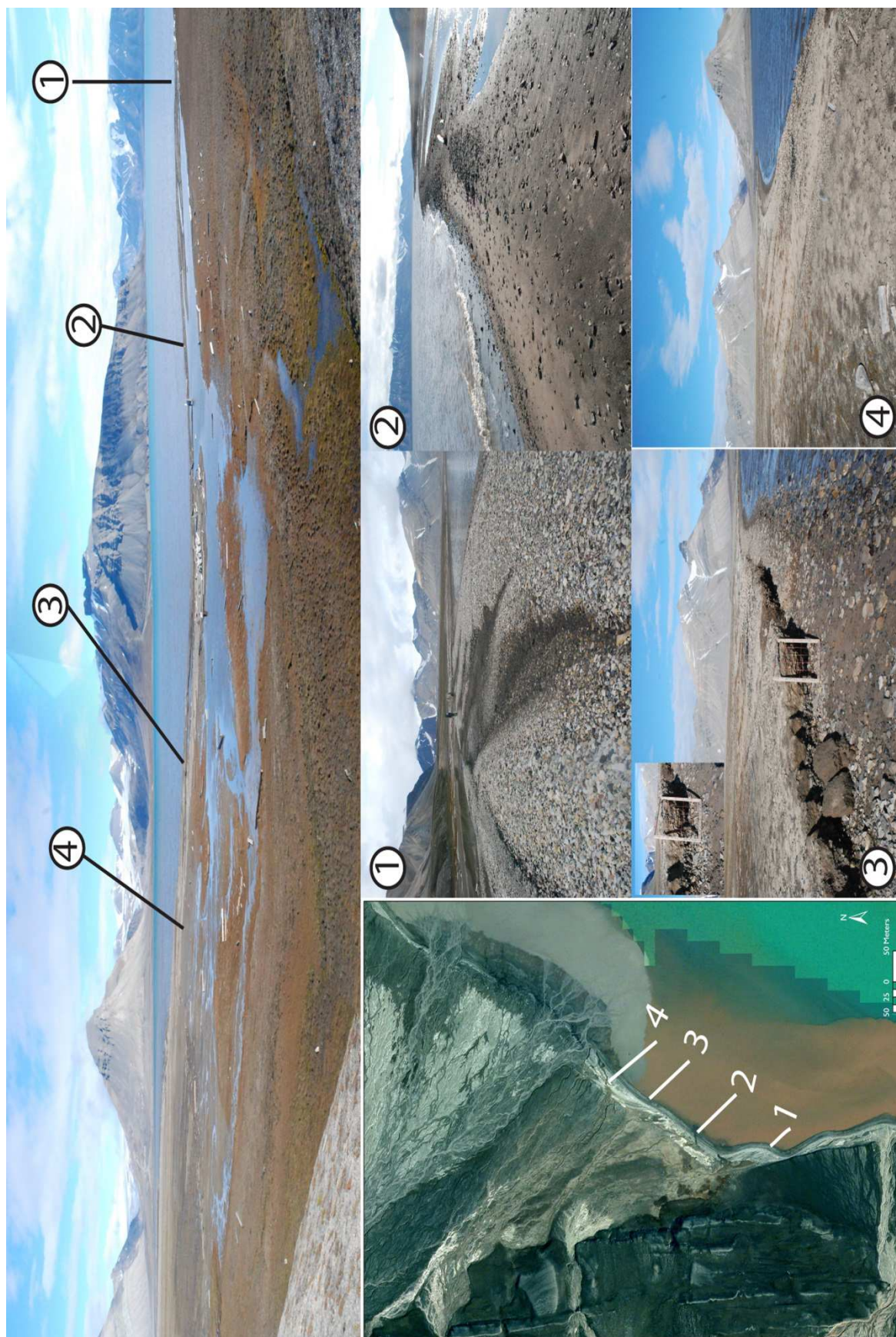


Figure 6.21. Main features formed along eroded coast between Elzaelva delta and FF4 fan delta: 1- uplifted storm ridges and lagoon; 2 - link between lagoon and fjord formed due to erosion and overwash of gravel-dominated barrier; 3 - surface modification to uplifted barrier-platform; 4 - surface of relict barrier-platform modified by aeolian processes.



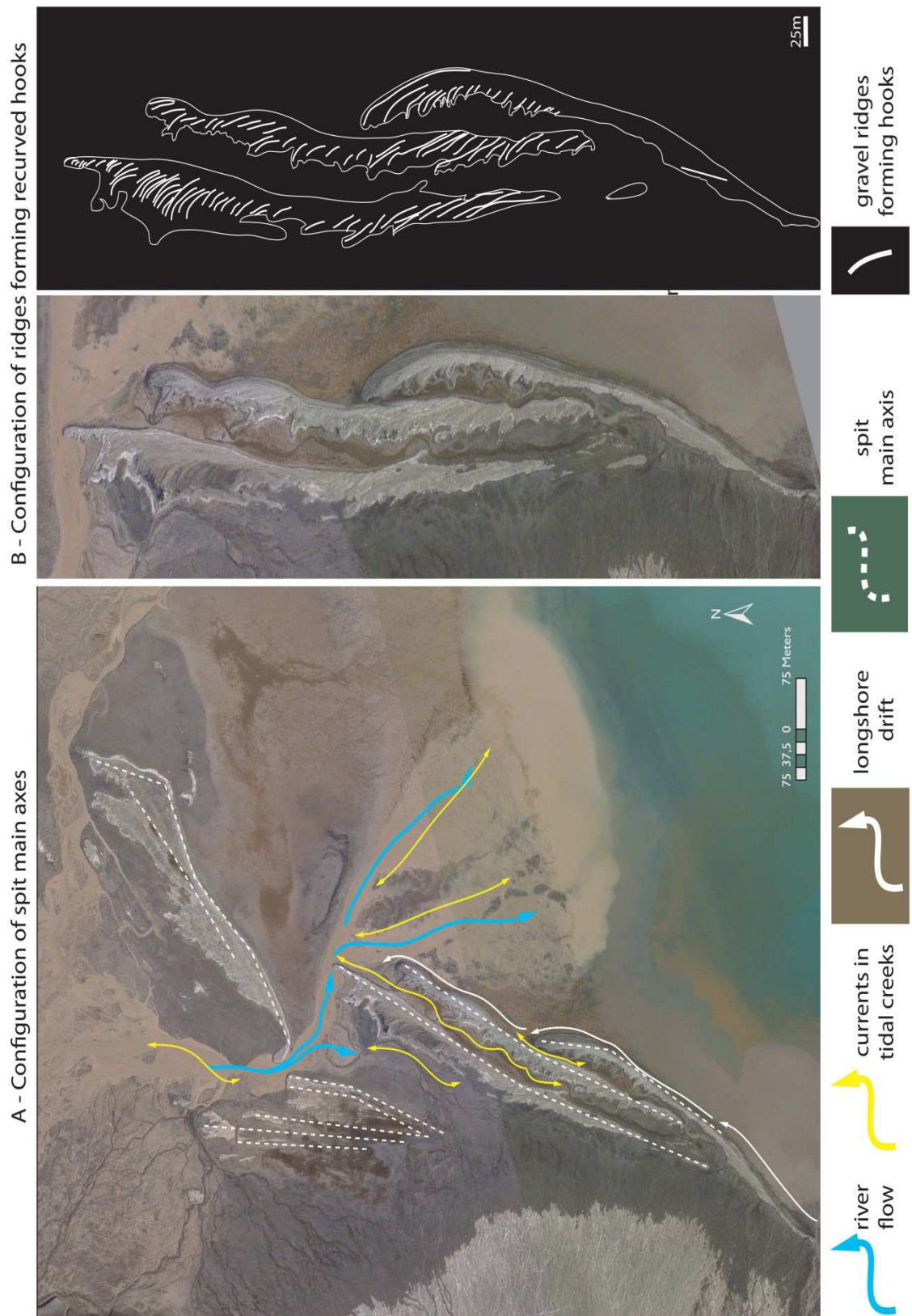


Figure 6.22. Controls on Ferdie Spits configuration and the orientation of the main recurved hooks



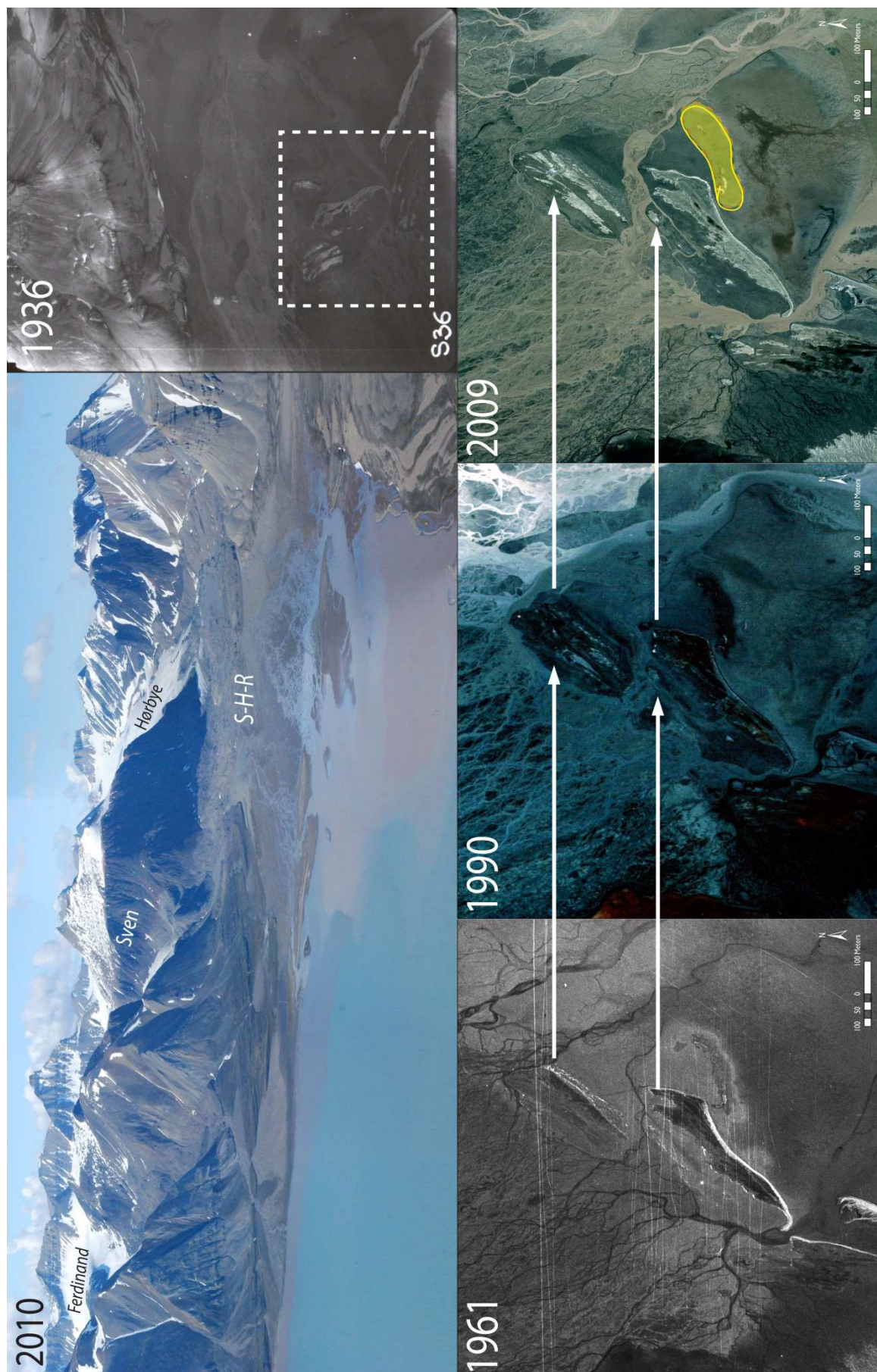


Figure 6.23. Post-LIA changes of (fetch-limited) Ferdie Barrier Islands.





Figure 6.24. Main features of (fetch-limited) Ferdie Barrier Islands: 1- recurved hook in tidal inlet; 2 -deflated surface of gravel-dominated barrier island; 3 - tundra in central part of barrier island; 4 - barrier island surface covered with aeolian deposits; 5 - aeolian deposits trapped by driftwood; 6 - driftwood embedded in tidal deposits; 7 - belt of driftwood accumulated around the seaward margin of barrier island.



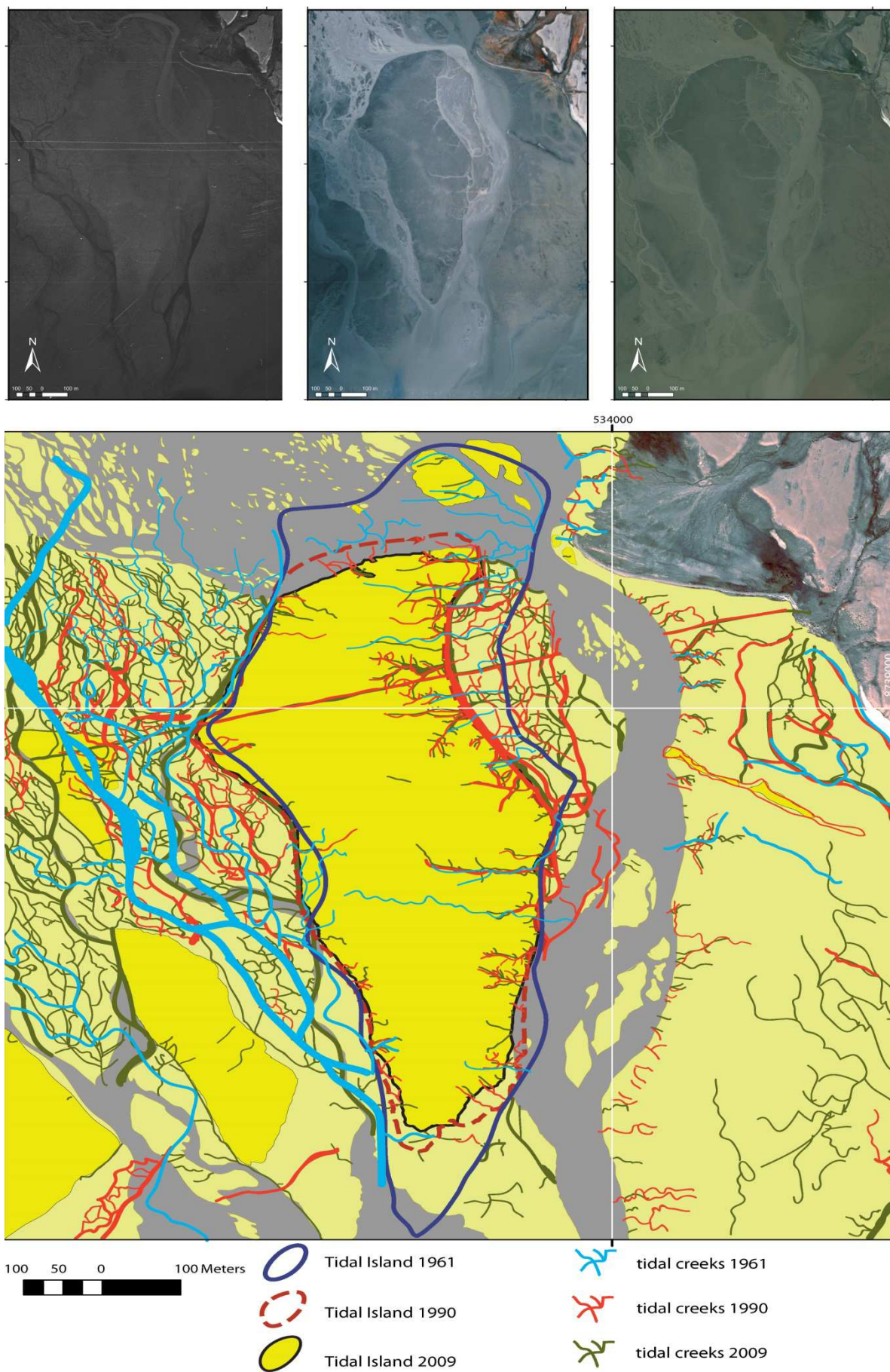
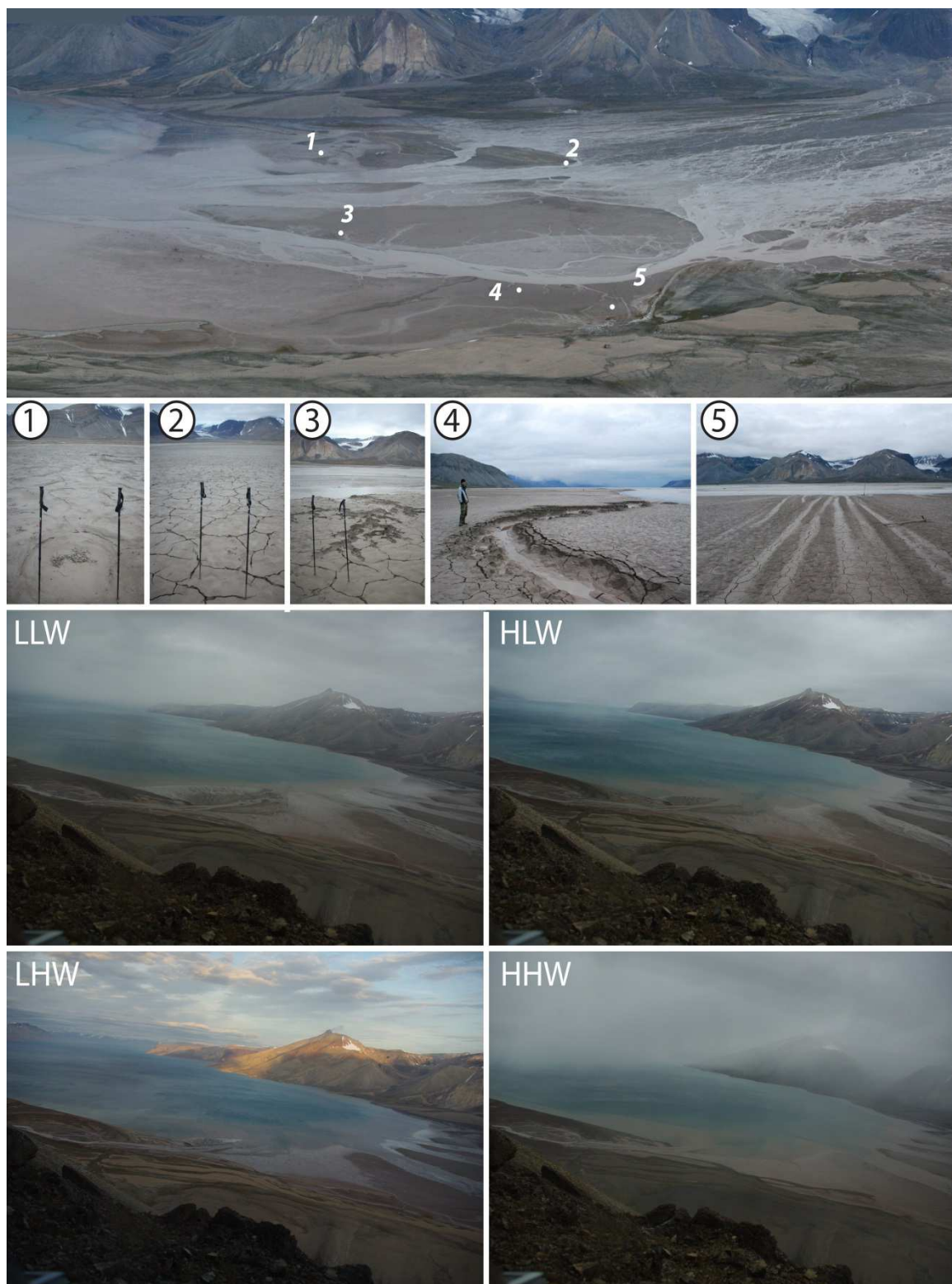


Figure 6.25. Post-LIA changes of the largest tidal island surface in the Petuniabukta tidal flat.



*Figure 6.26. Main features of the Petuniabukta tidal flat: 1 - mud polygons; 2 - mud cracks; 3 - small tidal creek; 4 - large tidal creek; 5 - old trails left by vehicles.*



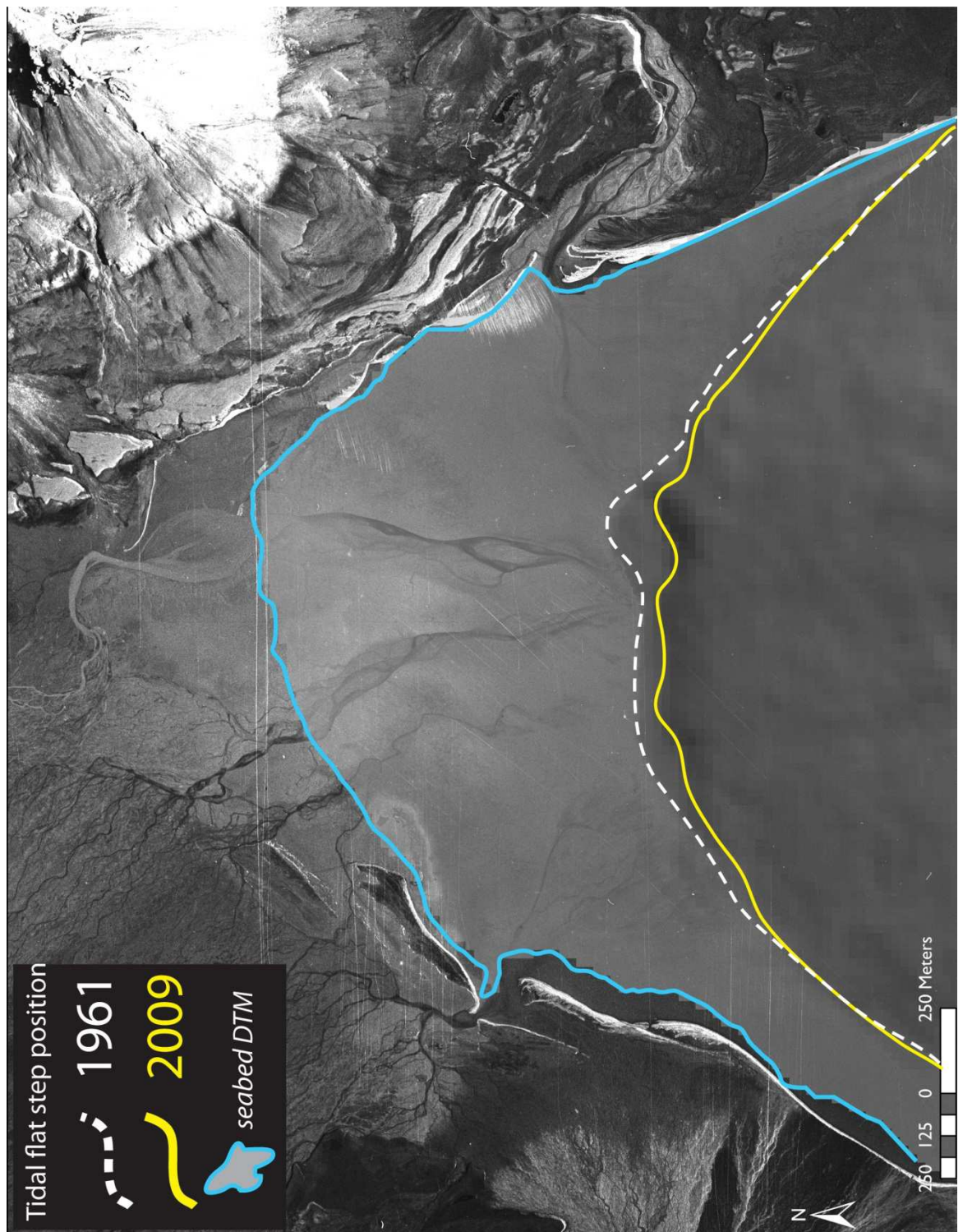


Figure 6.27. Approximate shift in the position of tidal flat step that occurred between 1961 and 2009 due to the increased post-LIA glaciofluvial sediment delivery to the fjord.

### 6.6.5 Sediment characteristics of proglacial, alluvial and coastal landforms

In general, the study area can be divided into two zones on the basis of the dominant grain size. The first zone is characterised by very coarse gravel. These sediments characterise areas located behind a line of bedrock gorges, on moraines (Figure 6.28. – Site 1), in the modern Ferdinandelva valley where OFF2 deposits are incised (Site 4), and on the relict surface of OFF2 (Site 3). The majority of pebbles were graded as angular or subangular (roundness categories after BENN (2007)) and they were rather poorly sorted. Alluvial landforms located to the east of bedrock gorges were covered mainly by coarse and medium gravels (OFF1 – Site 2, FF4 – Site 7), although some accumulations of very coarse gravel mixed with cobbles were mapped in the upper part of FF3 (Site 5), and on small fans fed by ephemeric snow-fed streams that drain the Mumien massif (Site 8). Very coarse gravel in short, snow-fed streams to the south of coastal zone supplied by Ferdie Fans may help explain the accumulation of large, subangular clasts in the modern barrier between the Elzaelva delta and the FF4 fan delta (Site 9). In comparison with that section of the barrier, three Ferdie Spits that formed after the FF4 fan delta are composed of finer, subrounded and better sorted pebbles (Sites 10-12). Such a pattern can be interpreted as a result of lateral grading controlled by selective action of longshore drift moving finer grains further because they are easier to mobilise and transport (BIRD 2008). On the other hand, in the case of the NW coast of Petuniabukta another factor is the breaching of the barrier by Ferdinandelva and the accumulation of the FF4 fan delta (Site 13). Progradation of the FF4 delta not only disturbed the alongshore transport of coarser material from the south (supplied by the Elzaelva fan and the snow-fed barrier section), but also provided an outlet for pulses of sorted and finer sediments from FF4, that were redistributed along the spits.

Probably the most valuable information gained from this study is the observed coarsening of surface deposits that cover modern landforms compared to relict landforms. This is particularly visible in the case of alluvial fans surfaces with OFF1 covered by medium gravels, incised OFF2 covered by coarse gravel, and modern fans and the river valley covered by very coarse gravels and cobbles. This pattern suggests higher energy in the post-LIA sediment transport system. This post-LIA delivery of coarser gravels to the coast is recorded in the surface sedimentology of coastal landforms. Thus, spits formed after the termination of the LIA (Ferdie Spit 2 and Ferdie Spit 3) are covered by coarser gravels than Ferdie Spit 1, Old Ferdie Spits (Site 17) and Ferdie Barrier Islands (Site 18).

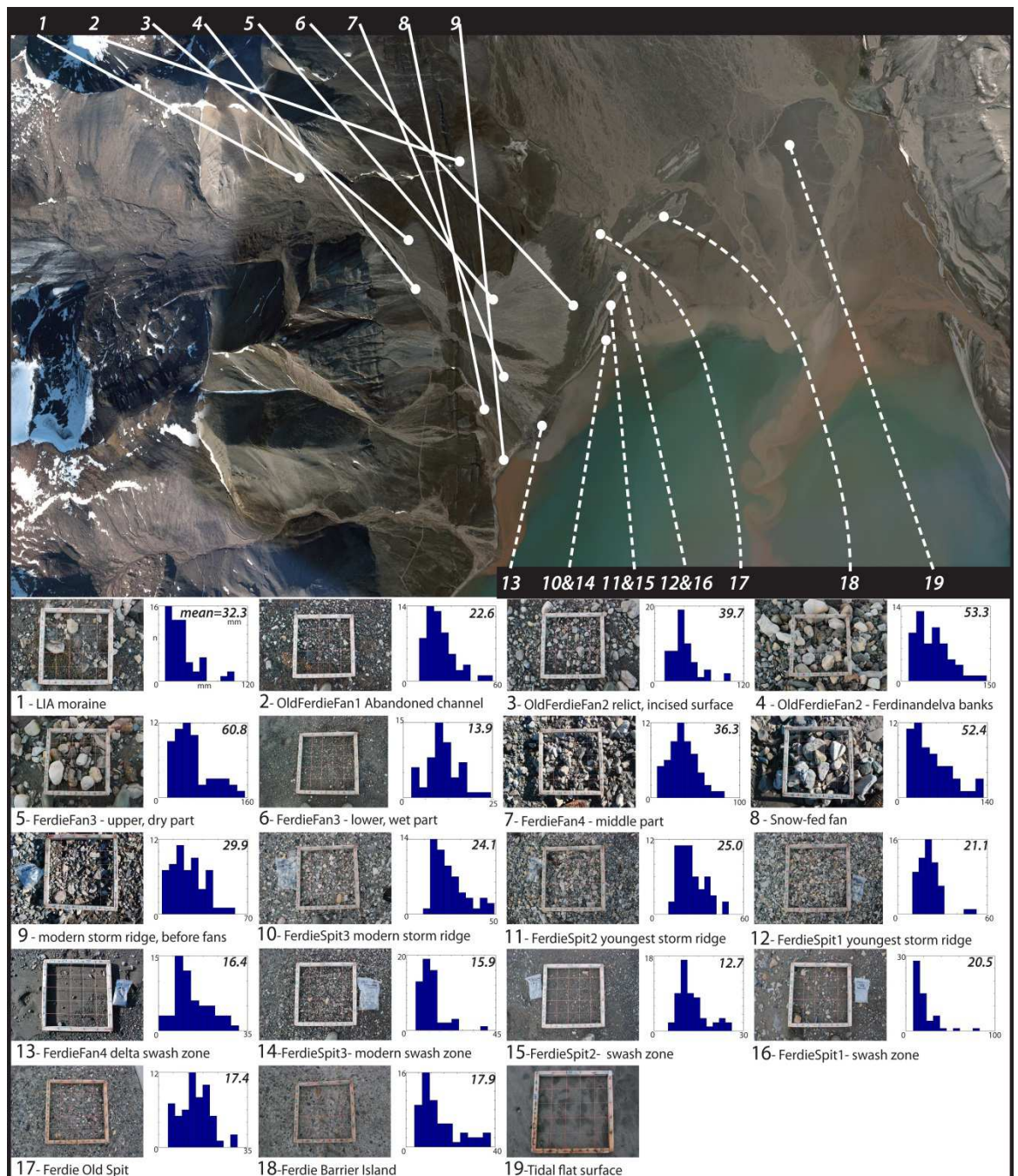


Figure 6.28. Digital images of the representative sediment surfaces in proglacial, alluvial and coastal zones and histograms summarising size distribution analysis carried out in Wolman\_Jack software.



### 6.6.6 Post-Little Ice Age surface elevation changes and sediment storage capacity

Previous studies on the post-LIA Svalbard coastal zone changes have focused on the rate of shoreline progradation and erosion (MERCIER and LAFFLY 2005; ZIAJA *et al.* 2011; ZAGÓRSKI 2011; ZAGÓRSKI *et al.* 2012). In this study I sought to estimate the vertical relief changes associated with sediment erosion and deposition since the LIA. To do this I used the 20 m resolution DTM from 2009 and 20 m resolution DTM from 1990 from the Norwegian Polar Institute to calculate the vertical surface change by subtracting the 1990 model from the 2009 model in ArcGIS software (Figure 6.29.).

#### 6.6.6.1 Calculation of surface elevation changes across the proglacial and the coastal zone

To calculate surface elevation changes observed across the proglacial and the coastal zone of NW Petuniabukta the following assumptions were made:

- 1.) Having just two DTMs from 1990 and 2009, it was possible to study surface elevation changes only for a short phase of post-LIA period (19 years). This period was characterised by a rapid (ca. 4 °C) temperature rise (see Figure 6.4.d) and a rapid increase in retreat rates of all Petuniabukta glaciers apart from Ferdinandbreen and Svenbreen (RACHLEWICZ *et al.* 2007; MALECKI 2009). I hypothesised that such conditions significantly increased sediment availability and the efficiency of sediment release and transport processes from deglaciated areas towards the coastal zone.*
- 2.) To check the vertical accuracy of surface elevation change, a vertical elevation error resulting from a potential mismatch of models during the overlying process was estimated. To do so 54,000 points lying along the contour lines on the 1990 DTM were selected from stable surfaces i.e. rocky outcrops, edges of rockwalls, coastal lowlands with bedrock outcrops avoiding unstable glacial and glaciofluvial landforms. Points were then re-measured on the 2009 DTM and the resulting elevation difference was plotted with height above sea-level and slope inclination ascribed to each point (Figure 6.30. B). Error analysis showed that the DTMs were matched closely and that the calculated surface elevation differences were not related to slope inclination or height a.s.l with both values close to 0 m (Figure 6.30. C). To estimate the vertical error range between models, the root mean squared error (RMSE) was calculated. As the RMSE increases exponentially with the slope inclination (Figure 6.30. C) it was assumed that detailed calculations of sediment volume change should be limited only to low-inclined areas distant from steep-sided mountain slopes (Figure 6.30. D).*
- 3.) It was assumed that the mean annual downwasting rate of ice-cored areas is ca. 0.9 m following the measurements made by SCHOMAKER and KJÆR (2008), across the ice-marginal zone of Holmströmbreen, which is a glacier located in central Spitsbergen that supplies an extensive outwash plain that merges into the muddy tidal flat of Ekmanfjorden. I treated*

surface elevation change values observed in these areas as a sum of dead-ice melting and sediment removal.

- 4.) Finally, it was assumed that the ice-marginal and proglacial zones acts as the largest sediment supplier to the NW coast of Petuniabukta, and the sediment removal from these environments is recorded in accumulation of material in outwash plains and alluvial fans.

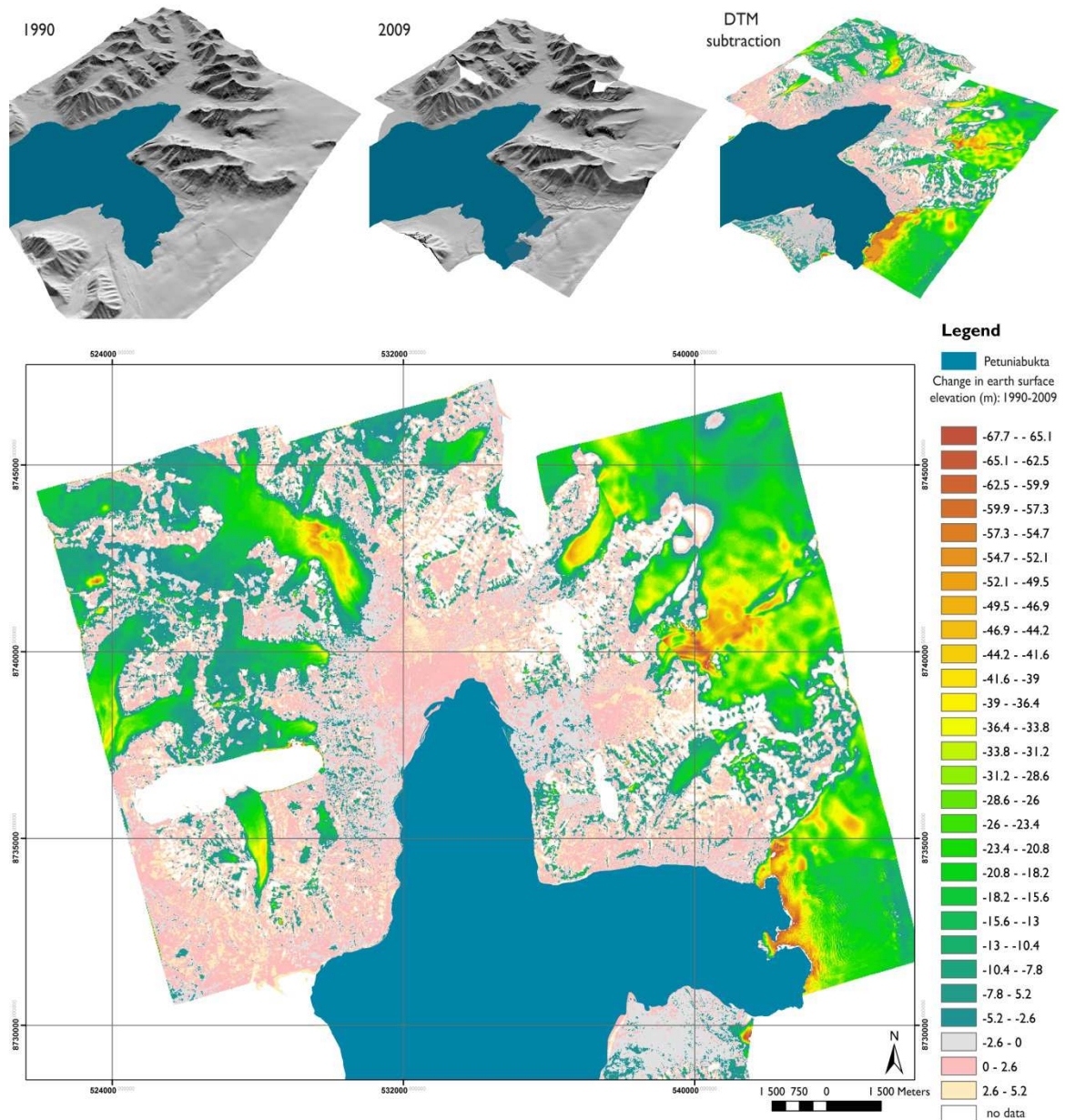


Figure 6.29. DTM differencing of 1990 and 2009 models. The map summarises surface elevation changes (m) that occurred between 1990 and 2009 in Petuniabukta region.

Figure 6.30. (next page). Method of GIS construction undertaken in advance of sediment storage and erosion calculations. A - analysis of orthophotomap and DTMs. B - overlying the slope inclination map on the DTM, C - calculations of vertical error between model and resulting map of mean RMSE of vertical elevation change overlaid on DTM with a map of slope inclination, D - separation of outwash plains and alluvial fans areas used for sediment volume calculations, E - map of surface elevation changes between 1990-2009 resulting from DTMs subtraction and applied to estimate the volume of sediments accumulated and eroded from selected landforms.



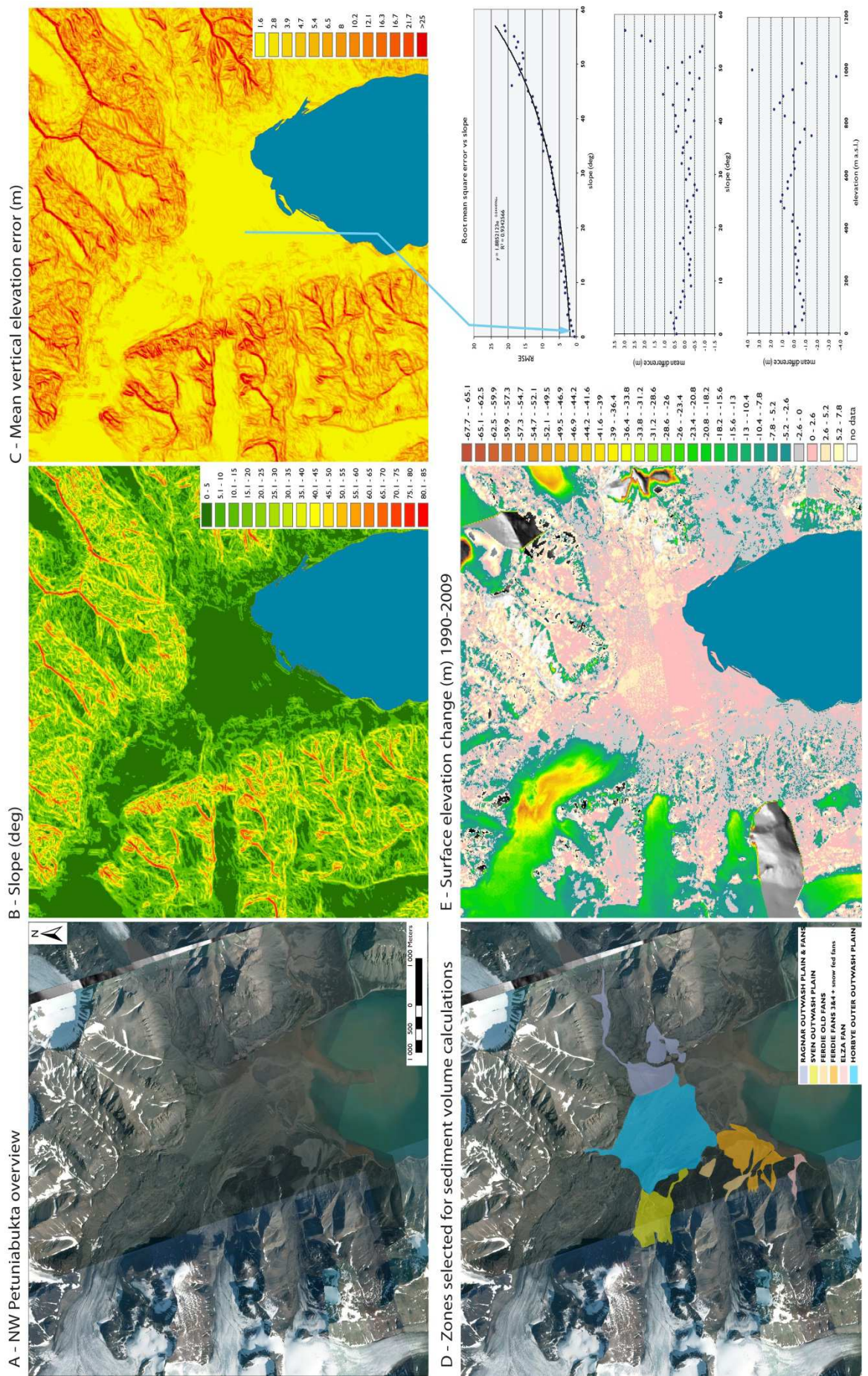


Figure 6.30.

#### 6.6.6.2. Changes in sediment transfer in NW Petuniabukta between 1990 and 2009

Between 1990 and 2009, recession of Petuniabukta glaciers exposed *ca.* 5 km<sup>2</sup> of land that was covered by fresh, unconsolidated material which was easy to transport and further modify by paraglacial processes that included fluvial, mass-wasting and wind action. Amongst the glaciers supplying sediments to the NW coast of Petuniabukta the largest area that was exposed was in front of Hørbyebreen (*ca.* 2.5 km<sup>2</sup>). Retreat of small valley glaciers along the western coast exposed in total *ca.* 0.66 km<sup>2</sup>: Elzabreen (*ca.* 0.28 km<sup>2</sup>), Svenbreen (*ca.* 0.22 km<sup>2</sup>) and Ferdinandbreen (*ca.* 0.16 km<sup>2</sup>). The retreat of Ragnarbreen, which supplies sediments to the tidal flat via an outwash plain that is linked with the Hørbyebreen outwash plain, exposed *ca.* 0.6 km<sup>2</sup> of new land. The role of Ragnarbreen in sediment delivery to the coast is limited by a proglacial lake that acts as a sediment trap for sediments released from the glacier and ice-marginal zone (EWERTOWSKI *et al.* 2012). The retreat of small glaciers (Elza, Ferdinand, and Sven) led to the lengthenning of their rivers (815 m, 105 m, 95 m respectively). Since 1990, these glaciers were already hidden deep in their valleys (Elza, Ferdinand) and behind a bedrock sill (Sven) that significantly focused sediment transfer from freshly exposed proglacial areas towards the coast (Figure 6.30. A).

The largest surface lowering, excluding that resulting from ice thickness changes of retreating glaciers fronts (over 60 m  $\pm$  1.6 m), occurred in the ice-marginal zones of glaciers: up to 50 m  $\pm$  8 m (Hørbye); up to 39 m  $\pm$  10.2 m (Sven); up to 35 m  $\pm$  4.7 m (Ferdinand), up to 24 m  $\pm$  2.8 m (Elza) and up to 55 m  $\pm$  3.9 m (Ragnar) (Figure 6.30. E). Such large decreases of surface elevation cannot be associated solely with sediment erosion and redistribution and likely records the decay of dead- ice in ice-cored landforms. Dead-ice melting is a characteristic process controlling surface lowering over ice-cored landforms (moraines, eskers, kames) in ice-marginal and proglacial areas (SCHOMACKER 2008). Using SCHOMACKER and KJÆR'S (2008) calculations of downwasting rates of ice-cored moraine surface, the estimated surface lowering related to decay of dead-ice is *ca.* 17m over the 19 years of analysis. In support of this assumption are slower lowering rates observed over the Hørbye frontal moraine, which according to a DC resistivity survey by GIBAS *et al.* (2005) is devoid of ice, compared with faster lowering of the frontal moraine of Ebbabreen, which is ice-cored. Thus, the maximum surface lowering of moraines in front of Ebbabreen was *ca.* 28 m  $\pm$  5.4 m, whereas remnants of Hørbyebreen frontal moraine lowered up to 13 m  $\pm$  3.9 m.

Taking into consideration the seven assumptions described above, an attempt was made to calculate the volume of sediments accumulated and eroded in 19 years over the outwash plains and fans formed by Hørbyebreen, Ragnarbreen, Svenbreen, Ferdinandbreen and Elzabreen (Table 6.5.). This shows that the alluvial fans and outwash plains of NW Petuniabukta acted as an effective trap for sediment released from decaying ice-marginal and proglacial landforms. During 19 years, the majority of landforms gained more sediments than they lost due to erosion.

Landform	Area [m <sup>2</sup> ]	Accumulation [m <sup>3</sup> ]	Erosion [m <sup>3</sup> ]	Net change [m <sup>3</sup> ]
Ragnarbreen outwash plain and fans	1,308,222	2,391,380	-352,242	2,039,138
Svenbreen outwash plain	917,943	423,800	-1,148,086	-724,286
Ferdinandbreen Old Fans land 2	237,374	240,466	-105 560	134,906
Ferdinandbreen Fans 3 and 4 and modern snow fed fans	1,049,210	955,383	-411 710	543,673
Elzabreen Fan	132,464	21,450	-196,253	-174,803
Hørbyebreen (outer) outwash plain	3,824,847	6,133,192	-87,109	6,046,083
Tidal flat	1,839,156	2,396,362	-112,061	2,284,300
<b>Total:</b>	<b>9,309,216</b>	<b>12,562,033</b>	<b>-2,533,230</b>	<b>9,028,803</b>

*Table 6.5. Volumes of sediments stored and eroded from selected landforms in NW Petuniabukta.*

Erosion dominated the sediment budgets of only two landforms - the outwash plain of Svenbreen and the fan formed by Elzaelva. In the case of the former, this may be related to the presence of dead-ice in the remnants of the frontal moraine and eskers eroded by Svenelva. Melting of dead-ice may have caused the loss of up to 603,309 m<sup>3</sup> of landform volume that would significantly reduce the amount of eroded sediments (to *ca.* 544,777 m<sup>3</sup>). Regarding the latter, this relates mainly to the remnants of old features (relict fans, uplifted beaches) that form islands that divide braided streams of the glacier river. It is important to note that the area of the Elzaelva fan and the river channel has been commonly washed out and incised by snow-melt streams with reduced glaciofluvial sediment supply from the decaying Elzabreen (*ca.* 46 m yr<sup>-1</sup> of glacier front retreat over 1990-2009 period), and this may explain the process of sediment loss. It was also observed between 2005 and 2010 that fragments of uplifted beaches located in the Elzaelva fan delta area were subject to wave erosion.

Between 1990 and 2009 the modern and relict alluvial fans supplied from Ferdinandbreen were the biggest sediment storage systems along the western coast of Petuniabukta. Interestingly, sediment accumulation dominated the areas abandoned by



Ferdinandelva channels (Old Ferdie Fan 1, relict surface of Old Ferdie Fan 2 and dry parts of Ferdie Fan 3) suggesting a significant role of sediment influx from snow-melt streams, slope movements (solifluction) or aeolian deposition. Conversely, in those parts of fans where the modern Ferdinandelva was active, erosion was dominant. Sediment evacuation was controlled by fluvial lateral erosion and surface incision of the margins of Old Ferdie Fans 2 and upper parts of Ferdie Fans 3 and 4, adjacent to bedrock gorges. According to the DTM subtraction a relatively large surface lowering occurred over small snow-fed fans (orange fans on Figure 6.16.) that accumulated between the relict lagoon and the prograding Ferdie Fan 4 delta. The erosion of the barrier and opening of outlets linking the lagoon with Petuniabukta that occurred between 1990 and 2009 may have led to increased erosion from fan aprons and the back of the barrier, but it is also probable that the results are biased by the presence of a steep rockwall that may have distorted the elevation change calculations processed in ArcGIS.

Certainly, the largest sediment storage system in the analysed area was the outer outwash plain of Hørbyebreen (terminology after RACHLEWICZ (2009) in which over 60% of sediments accumulated between 1990 and 2009. Sediment loss was observed only along:

- the sandur margins which border on remnants of the ice-cored western lateral moraine of Hørbyebreen;
- a retreating cliff formed in uplifted marine sediments (NW margin);
- the eroding slopes of the Hørbyebreen LIA frontal moraine (N margin);
- the eroding slopes of old rock glacierised moraine of Late Weichselian age (NE margin).

The second largest sediment storage was found in the Ragnarelva outwash plain and alluvial fans formed on southern slopes of Ragnardalen (Lion's Head Mountain) that supplies sediments to outwash plain and directly to tidal flat during snow-melt flood events.

Since the formation of a proglacial lake in the late 1980s, the sediment supply from Ragnarbreen's ice margin has been significantly reduced. The surface analysis changes suggest that the major source of sediments accumulated in the outwash plain comes from three sources:

- erosion and redistribution of sediments accumulated in the Ragnarbreen LIA frontal moraine;

- lateral erosion of river banks in the central sector of Ragnardalen;
- incision of river channel close to the proximal sector of Ragnar outwash plain.

One of the largest surface changes in the entire area occurred over fans that accumulated on slopes of Lion's Head Mountain. During 19 years, these gained *ca.* 1,400,000 m<sup>3</sup> of sediments derived mainly from ephemeral snow-fed streams, debris flows, slush avalanches and solifluction.

The last consideration is the upper part of the tidal flat. The lower part of tidal flat was fully flooded in 1990 and it was partly flooded in 2009, so it was assumed that the elevation difference over this area was unsuitable for further calculations. Therefore, only that sector of the tidal flat adjacent to the Hørbyebreen outwash plain to the north, and limited to the southern extent of main tidal islands to the south, was considered in calculations.

Interestingly, the amount of sediments stored in the upper part of tidal flat (2,396,362 m<sup>3</sup>) was about the same as the total amount of sediments eroded from the rest of the analysed landforms (2,300,969 m<sup>3</sup>). This shows that the tidal flat is a very effective sediment trap for sediments. The further progradation of the tidal flat is expected to facilitate the development of the barrier coast in NW Petuniabukta by providing the stable submarine platform for future spits and barrier islands.

## 6.7 Chapter summary

This chapter provided a new insight into the functioning of High Arctic paraglacial coastal environments characterised by sheltered fjord settings and supplied by sediments derived from glacial (glacierised catchments) and non-glacial (snow-fed streams and talus slopes) sources. In such low energy environments one might expect the limited modification of coastal landforms. However, information derived from aerial photogrammetric analysis, geomorphological mapping and sedimentological tests shows that the post-LIA behaviour of the Petuniabukta coastal zone are responsive to climatic and geomorphic changes that occurred during the last century.

The key findings of this Chapter are:

- Since the end of the LIA there has been widespread retreat of glaciers in the study area, as well as an overall warming of air temperatures. These changes have led to significant release and transport of sediment to the coastal zone.
- Using a combination of air photographs, DTMs and ground-based field mapping, I reconstruct post-LIA changes in non-glacial and glacial-fed fed barrier systems in Petuniabukta.
- The Ebba spit-platform and several glacial-fed fans provide excellent examples of how post LIA sediment delivery has influenced coastline development.
- Coastal landform change are closely linked to changes in nearshore sea bed bathymetry, itself a function of sediment delivery to the coastal zone. Progradation of tidal flats over the study period provide the depositional platform on which coastal features have developed.
- Comparison of DTMs developed for different periods of the 20<sup>th</sup> century show that there has been significant landscape change in the deglaciated hinterland. Overall, there is a 9 million m<sup>3</sup> increase in sediment deposition within the study area over the period of study. The main depositional area is the Hørbyebeen outwash plain.

Chapter 8 compares the results detailed in this Chapter with patterns of coastal and catchment change over shorter (annual) and longer (millennial) time scales to explore further the post-LIA evolution of non-glacial and glacial-fed barrier coasts in Petuniabukta.

## **Chapter 7:**

### **MILLENIAL TIMESCALES**

#### **Holocene relative sea-level change and coastal evolution in Petuniabukta**

## 7.1. Introduction

In this Chapter I address the fourth research question detailed in the Introduction to this thesis, namely:

*How can we improve the accuracy of sea-level reconstructions and long-term coastal evolution studies in the High Arctic?*

To answer this question the following objectives were addressed:

- I) to review previous RSL research in Svalbard and determine how improvements in reconstruction might be achieved;
- II) to develop a new method of sampling marine shells from raised beaches;
- III) to discuss the nature of Holocene RSL changes and beach ridge formation in Petuniabukta and to compare the results with those obtained from driftwood;

In Chapter 8 I use the new RSL record developed in this thesis to test different models of the configuration of the Late Weichselian Svalbard-Barents Sea Ice Sheet and reflect on the interaction of RSL and sediment supply in controlling patterns of coastal development in the Petuniabukta study area. The results of this aspect of the thesis are published in LONG *et al.* (2012) – Appendix III.

## 7.2 Background - the raised beaches and evidence for relative sea-level change in Petuniabukta

Arctic relative sea-level (RSL) change research is inherently linked with studies of raised beaches which are a product of glacial unloading and isostatic rebound following the decay of ice sheets. Therefore, the reconstruction of the pattern of postglacial emergence of Arctic beaches is crucial in assessing the distribution of former ice-sheets, calculating past ice volumes, and deciphering deglaciation histories (FORMAN *et al.* 2004). The geomorphology and sedimentology of Arctic beaches also contain valuable information about glacio-isostatic adjustment (GIA), sea-ice extent, storminess as well as changes in sediment supply.

The coasts of Svalbard are rich in many of those spectacular landforms (Figure 7.1.) (e.g. BALCHIN 1941; FEYLING-HANSEN 1955; JAHN 1959; BIRKENMAJER 1960; STÄBLEIN 1978; KARCZEWSKI *et al.* 1981; LINDNER *et al.* 1992; SALVIGSEN *et al.* 1995; FORMAN *et al.* 1990, 2004; BONDEVIK *et al.* 1995; MÖLLER *et al.* 1995; ZIAJA and SALVIGSEN 1995; BRÜCKNER *et al.* 2002; BRÜCKNER and SCHELLMANN 2003; SALVIGSEN and HØGVARD 2006) and other High Arctic coasts (e.g. ANDREWS 1970; BLAKE 1975; DYKE *et al.* 1991; FLETCHER



*et al.* 1993; RASCH and NIELSEN 1995; MÖLLER *et al.* 2002; SANJAUME and TOLGENSBARK 2009; ST-HILLAIRE-GRAVEL *et al.* 2010; FUNDER *et al.* 2011). Flights of raised beaches are a significant element of the Petuniabukta coastal landscape and one of the best-preserved flights of raised beaches is located at the mouth of the Ebbadalen, in coastal section E6 studied in this thesis (Figure 7.2.).

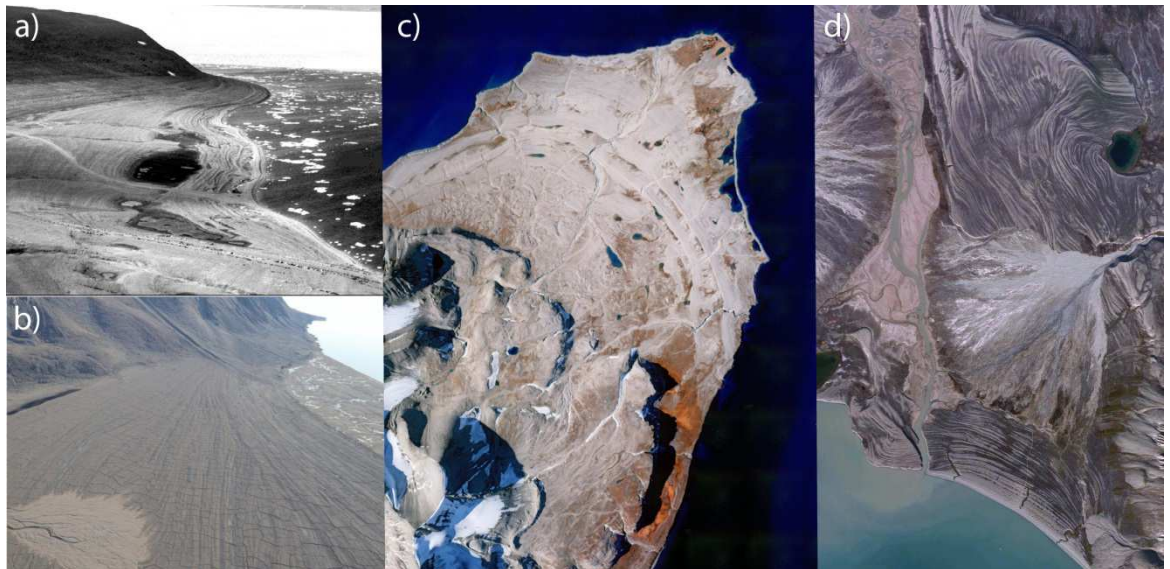


Figure 7.1. Examples of raised beaches in High Arctic settings: a) Sight Point, Cornwallis Island, Canadian Arctic Archipelago (CAA), modified after ST-HILLAIRE-GRAVEL *et al.* (2011); b) Raised beaches with ice wedges, Devon Island (CAA), image: Geological Survey of Denmark and Greenland; c) Kvadehuksletta and the outer parts of Brøggerhalvøya, W Spitsbergen, image: The Norwegian Polar Institute; d) Gipsdalen, image: The Norwegian Polar Institute.



Figure 7.2. Oblique air photograph showing the raised beaches in section E6 at the entrance to Ebbadalen, Petuniabukta. The AD 1936 shoreline is based on an air photograph taken by NPI. Three white dots along the coast indicate locations of contemporary shell samples. Letters (LH1-4, MH1-4) refer to locations that were dated using *Astarte borealis*. Note the difference in topography between the higher beaches (MH1-4), above c. 10 m asl, and beaches below this level. Modified after LONG *et al.* (2012).

It is noteworthy that northern Billefjorden featured in the first systematic analyses of raised shorelines and their associated shells in Svalbard (BALCHIN 1941; FEYLING-HANSEN 1955; FEYLING-HANSEN and OLSSON 1959; FEYLING-HANSEN 1965) (Figure 7.3.).

Isobase maps of Holocene shorelines, together with ice sheet modelling, suggest that a former centre of the Late Weichselian Svalbard-Barents Sea Ice Sheet (SBSIS) was located in the northern Barents Sea (e.g. BOULTON and RHODES 1974; BONDEVIK *et al.* 1995; LAMBECK 1995; FORMAN *et al.* 2004), although recent marine geophysical investigations provide evidence for a former ice dome located on easternmost Spitsbergen or southern Hinlopen Strait, at least 500 km west of its previously inferred position (DOWDESWELL *et al.* 2010).

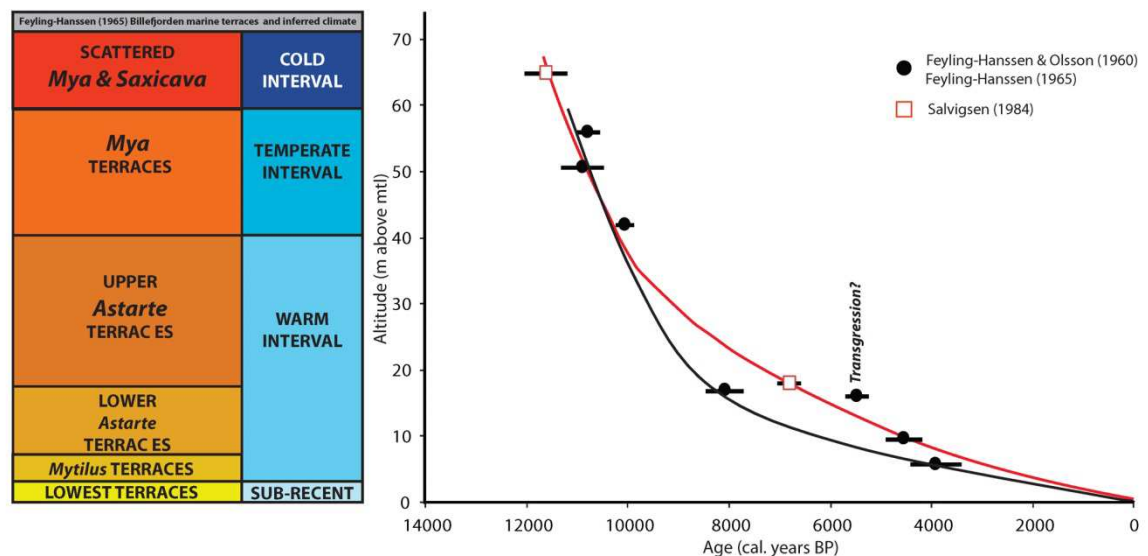


Figure 7.3. The stratigraphy of the Billefjorden raised beaches (Feyling-Hanssen and Olsson 1960; Feyling-Hanssen 1965). The figure shows the species of marine mollusca identified plotted against altitude, with the main terrace sequences proposed. The RSL graph is based on dates from Feyling-Hanssen (1965) with the original curve from Feyling-Hanssen and Olsson (1960). Shown for comparison is the RSL curve proposed by Salvigsen (1984). In both cases the radiocarbon dates are plotted with respect to mean tide level, but they have not been corrected for the difference in height between the present-day storm beach and mean tide.

The Ebbabreen was part of a large ice stream complex that drained the Late Weichselian ice sheet via Billefjorden into Isfjorden (LANDVIK *et al.* 1998). Retreat of the Ebbabreen and other tributary glaciers during the late glacial meant that by the start of the Holocene their termini were located inland of the present coast (BAETEN *et al.* 2010; FORWICK and VORREN 2010). Marine conditions at this time penetrated into the mouths of the tributary valleys, including the Ebbadalen and, as RSL fell rapidly, spectacular flights of raised beaches developed.

The beach ridges located in section E6 that are the focus of this study comprise a higher group of broad, straight beaches that trend into the former Ebbadalen, and a lower set that are made of many narrow, sinuous ridges (Figure 7.4.). The higher beaches (above ca. 11 m asl) are heavily modified by fluvial and aeolian processes, whilst those below are



exceptionally well preserved, although the River Ebba has eroded part of them. The current beaches formed along the E6 section comprises varying quantities of fine gravel and sand, with seaweed and abundant driftwood (Figure 7.5.). The morphological effects of ice-push, ice pile-up and ice melting on the beach are ephemeral and are destroyed in the first few days of open water conditions each year.

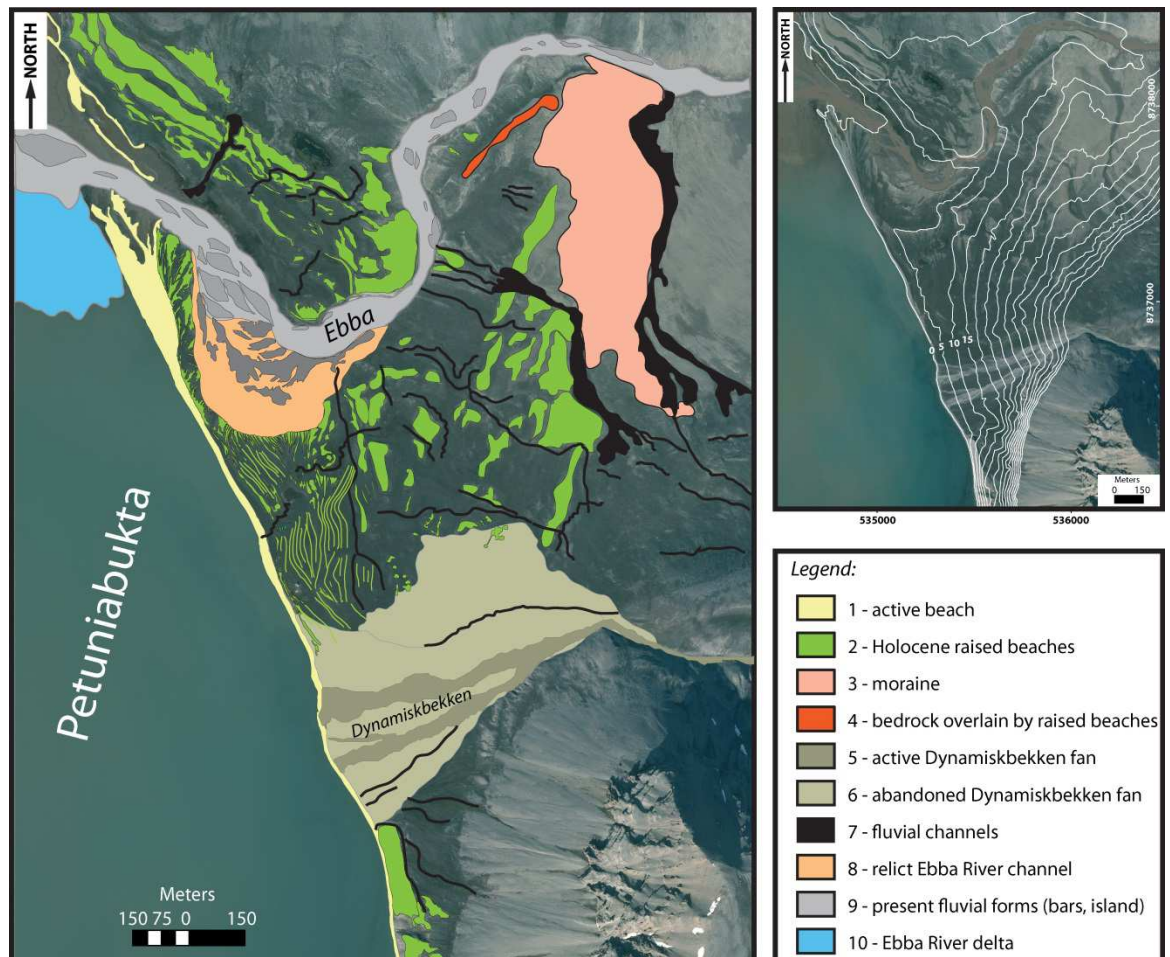


Figure 7.4. Geomorphological map of the raised beaches and associated landforms located to the south of the Ebba River, Petuniabukta, based on field observations and the interpretation of air photographs. Contours in the inset map are at 5 m intervals and are calculated from a digital elevation model.

The surface topography of the lower beach plain is characterised by low amplitude (<0.5 m) beach crests that are *ca.* 5 m in width. The beaches resemble the fair-weather beaches described by MASON (2010) with no evidence for significant overwash or overtopping features. There is, however, clear evidence for several periods of erosion when sections of the beach ridge plain were cannabilised to leave distinct scars that cross-cut older beaches (Figure 7.4.).

Sediment for longshore transport is provided mainly from an alluvial fan that crosses the coast at the south side of the Ebbadalen (the Dynamiskbekken fan), as well as from eroding cliffs of former raised beaches further to the south. Reworked marine

shells, dominated by the filter-feeder *Astarte borealis*, are abundant on the present-day beach, as elsewhere in the fjords of Spitsbergen (FEYLING-HANSEN 1955).

*Astarte* valves observed on the active shoreface are often broken or abraded, whilst better preserved specimens occur higher up the beach, some of which are still articulated and show minimal signs of reworking (e.g. little abrasion on the ventral edge and dorsal margin) (Figure 7.5.).

In the south of the study area, the coast is eroding and a 2 to 3 m high cliff cuts Holocene raised beaches. In the north, towards the Ebba river mouth, the shoreline switches to an aggradational landform, with many low relief beaches scattered with driftwood and seaweed that are prograding onto a tidal flat formed by sediment deposited from the Ebbaelva and the numerous meltwater channels that issue from the Hørbyebreen (Figure 7.2.).

The first RSL record from Billefjorden was proposed by FEYLING-HANSEN and OLSSON (1959) who used five radiocarbon dates on bulk shell samples to track RSL change (this curve was updated by FEYLING-HANSEN (1965) (Figure 7.3.). The oldest radiocarbon dates are associated with terraces rich in the remains of *Mya truncata* that were deposited when sea-level was above *ca.* 40 m asl. The fauna of these beaches indicate an early Holocene climate that was “slightly more favourable than today” (FEYLING-HANSEN and OLSSON 1959, p. 125). Between this level and 6 m asl are terraces rich in *Astarte borealis*, together with 39 new species of molluscs and cirripeds (mainly barnacles), seven of which are now extinct in Spitsbergen waters. During this interval, RSL fell and climate conditions were warmer than today (FEYLING-HANSEN and OLSSON 1959). Between 6 m and 3 m asl there are abundant remains of *Mytilus edulis*, whilst below this level the warm faunas, including *Mytilus edulis*, disappear. This latter change indicates a severe deterioration in climate (FEYLING-HANSEN and OLSSON 1959).

The FEYLING-HANSEN (1965) RSL record is similar to that published by SALVIGSEN (1984) from Petuniabukta, which includes inferred ages of four pumice levels and one other early Holocene radiocarbon date from a sample of *Larix* driftwood at *ca.* 65 m asl from Kapp Ekholm (Figure 7.1.). Although other Holocene radiocarbon dates have been collected since this time (e.g. STANKOWSKI *et al.* 1989; KŁYSZ *et al.* 1989; MANGERUD and SVENDSEN 1992), no significant revision to the FEYLING-HANSEN and OLSSON (1965) record has been attempted.

In a regional synthesis of RSL change in Svalbard, FORMAN *et al.* (2004) summarise the evidence from western and northern Spitsbergen for a mid Holocene transgression



between 6 and 4 k  $^{14}\text{C}$  BP but evidence for this, and for a second regression/transgression sequence in the late Holocene in Billefjorden is debated (e.g. SALVIGSEN 1984; FEYLING-HANSEN 1965; KŁYSZ *et al.* 1989).



Figure 7.5. The present-day beach environment in the south of the Ebba River. View looking north along the present beach towards the Ebba River mouth. Note the driftwood and seaweed on the present storm ridge crest with well-preserved, articulated *Astarte borealis* (lower inset) and samples of broken and abraded *Astarte borealis* from the present shore-face (upper inset). The small, juvenile samples of *Astarte borealis* were targeted for dating in the modern and Holocene beaches.



### 7.3 New dating campaign - material and methods

Shells are one of the commonly used materials to date staircases of Arctic raised beaches. If sampled from a section cut through a beach, one can relate the age and altitude of the sampled shell to a former beach crest. But accessing sections through an entire Holocene sequence is not always possible and shells are therefore often gathered from beach surfaces. These shells have been reworked and redeposited, typically by waves, frost heave, solifluction or stream erosion and have often been moved downslope from their original elevation (e.g. DONNER and JUNGNER 1975; MASON *et al.* 2010). Occasionally, it is possible to identify articulated pairs of shells, in their growth position in sub-littoral sands that are overlain by beach gravels (e.g. Brückner and Schellmann 2003). These are preferred for dating over other shell samples (mixed shells or paired shells collected from beach deposits) because the potential for their reworking is minimised. When RSL is falling quickly, such as during the early Holocene in Svalbard, problems with dating different shell fractions are reduced. However, when the rate of mid and late Holocene RSL change is slow, then the age and height uncertainties associated with dating different shell fractions will increase.

Because of these problems, in Svalbard and other High Arctic settings, researchers favour alternative material for dating, such as whale bone or driftwood (e.g. DYKE *et al.* 1991; BONDEVİK *et al.* 1995; FORMAN *et al.* 2004). This material has the advantage that it is washed onto the present-day storm beach and left either on the beach ridge surface or embedded within the beach deposits themselves. The dry, cold climate of the High Arctic means that such material can be well preserved and the often large samples make them ideal for radiocarbon dating (e.g. SALVIGSEN 1981; BONDEVİK *et al.* 1995). Alas, whalebone and driftwood are not always found in uplifted deposits. What is more, driftwood accumulations are commonly relocated by tourists and researchers using them as a main fuel source and construction material which can influence the accuracy of driftwood-based palaeo-shoreline reconstructions. This is the case of uplifted beaches in Petuniabukta which are almost devoid of whalebones and driftwood but rich in marine shells. However, it is important to bear in mind that the greater part of shells found in Petuniabukta, palaeo-beaches consists of broken shell detritus, often reworked by slope and aeolian processes or scattered by sea-birds.

Taking all of those issues into consideration, the target in this project was to collect well-preserved small, juvenile (< 10 mm diameter) specimens of articulated *Astarte borealis* that showed minimum signs of surface abrasion to minimise the effects of

reworking. Juvenile specimens were targeted because these are the most fragile specimens and least likely to survive significant reworking.

To achieve this series of shallow (<30 cm deep) pits (0.2 m<sup>2</sup>) were excavated into the surface of the present and Holocene beach ridges (Figure 7.6.). Next a penknife was used to carefully remove individual grains of gravel to extract suitable specimens of *Astarte borealis*. In the Holocene samples, the hinge ligament that connects the two valves had decomposed but once-articulated valves can still be identified as closed pairs.

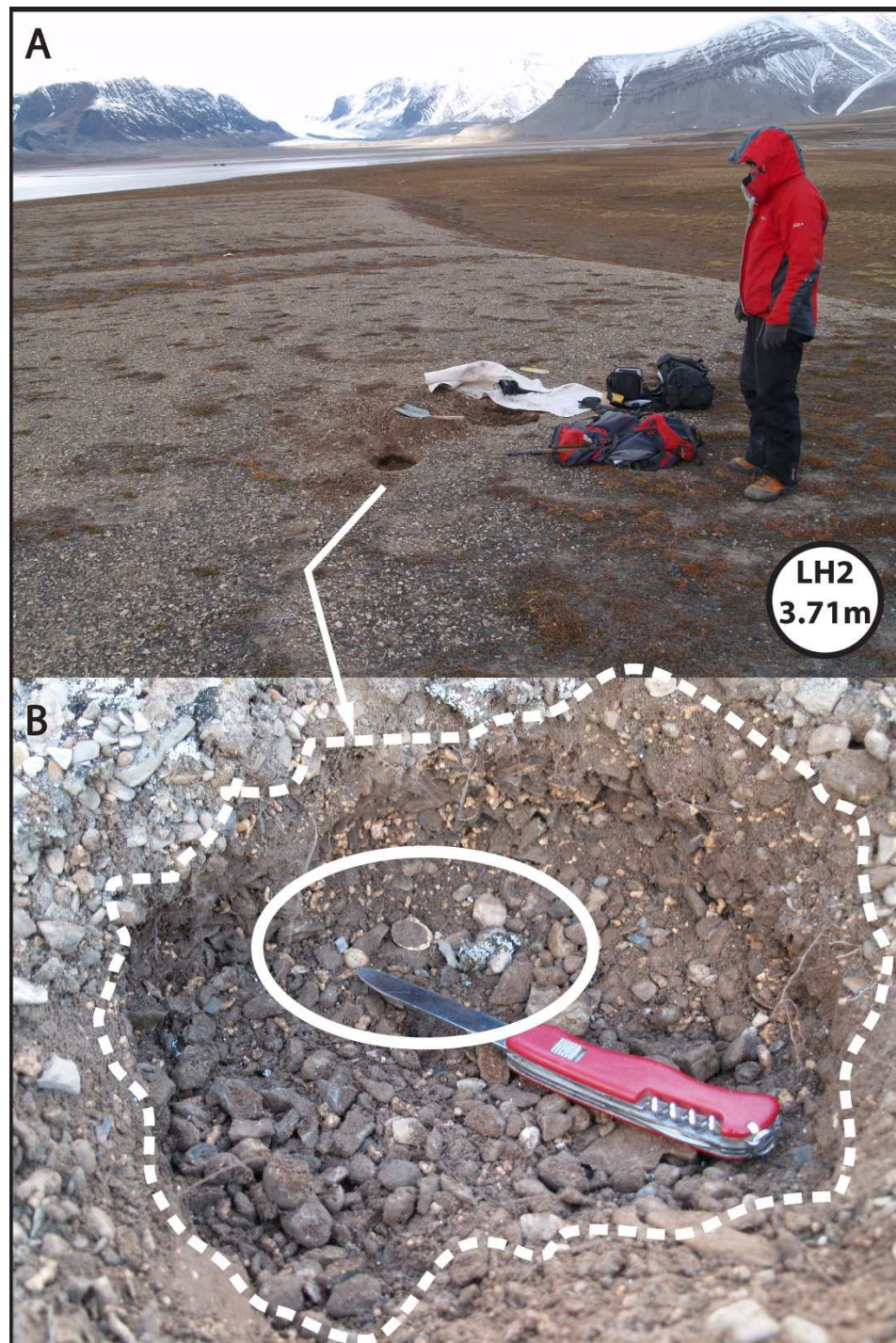


Figure 7.6. a) Shallow excavation into the crest of a late Holocene beach crest (LH-2) with two valves of a once articulated specimen of *Astarte borealis*; b) that were targeted for radiocarbon dating.

All elevations of samples were measured with respect to mean tide level (MTL). Sample collection took place in August 2010. The present storm beach in Petuniabukta has a maximum elevation of *ca.* 1.1 m above MTL. This value, therefore, was used to correct the altitude of beach ridges from which shells were dated from Billefjorden to MTL. A similar correction was applied to the data from other sites, using the values cited in the original publications.

Specimens of *Astarte borealis* were radiocarbon dated using the SUERC AMS facility in East Kilbride, Glasgow. Pretreatment involved removal of the outer 20% of the shells by controlled hydrolysis with dilute HCl. The samples were then rinsed in deionised water, dried and homogenised. A known weight of the pretreated sampled was hydrolysed to CO<sub>2</sub> using 85% orthophosphoric acid at 25°C. The CO<sub>2</sub> was converted to graphite by Fe/Zn reduction. All ages were calibrated using Calib 6.1.1 using the marine09 dataset (REIMER *et al.* 2009) and a  $\Delta R$  of  $100 \pm 39$  years based on four pre-bomb spike ages. Modern samples are reported using percent modern carbon and Holocene samples with a calibrated two standard error age range.

## 7.4 Radiocarbon dating results

### 7.4.1 Testing for reworking in the modern beach environment

Three pairs of juvenile *Astarte borealis* were dated to test whether the chosen sampling approach could avoid reworked material (Table 7.1., Ebba contemporary-1, Ebba contemporary-2 and Ebba contemporary-3). Each sample contains modern carbon indicating a post-1960 age. This shows that reworking of these types of small, delicate samples must be less than 50 years. The marine bomb spike curve of KALISH *et al.* (2001) was applied to determine a more precise age for these samples. Thermonuclear weapons testing in the 1950s and 1960s increased the atmospheric  $\Delta 14C$  signals from *ca.* 40 to 50‰ to 850-900‰ (LEVIN and KROMER 1997). This  $\Delta 14C$  spike was dampened in the marine realm by the dilution of bomb  $14C$  with non-bomb dissolved inorganic carbon (DIC) but still raised the DIC pool to *ca.* 200‰ by the end of the 1960s (HANSELL and CARLSON 2002). KALISH *et al.* (2001) dated archived pre- and post-bomb (1919-1992) cod otoliths of known age to define their marine bomb spike curve (Figure 7.7.). Their data show that the average pre-bomb (1950)  $\Delta 14C$  was 53.8‰ and increased to a peak of 134.2‰ in 1967. Between 1973 and 1992 the  $\Delta 14C$  declined linearly ( $n=5$ ,  $r^2=0.97$ ,  $p=0.002$ ) at the rate of 3.1‰ per year.

Lacking data regarding the DIC composition of the waters of Petuniabukta the assumption was made that the cod otolith bomb spike is applicable to the samples collected here. Support for this assertion is provided by KALISH et al. (2001) who note that pre-bomb spike  $^{14}\text{C}$  measurements from shells and seawater DIC from several locations in the Barents, Norwegian and Greenland seas provide independent validation of the otolith data, although it is recognised that the DIC of the fjord waters of Petuniabukta may differ from the Barents Sea because of freshwater dilution as well as potential influences from the local carbonate geology.

Sample code	Code	$^{14}\text{C}$ age $\pm 1$ SD	Calibrated age range $\pm 2$ SD	% Absolute modern $\pm 1$ SD	Altitude above MTL in meters	Carbon content % weight	$\delta^{13}\text{C}$ vPDB‰ $\pm 1$ SD
Ebba CT-1	SUERC-33584	modern		102.19 $\pm$ 4.74	0.8	10.4	1.3
Ebba CT-2	SUERC-33585	modern		102.74 $\pm$ 4.74	0.8	11.0	1.7
Ebba CT-3	SUERC-33586	modern		103.60 $\pm$ 4.81	0.8	9.8	0.9
Ebba LH-1	SUERC-35206	3411 $\pm$ 37	2995-3317		1.24	10.3	2.2
Ebba LH-2-1	SUERC-33587	4314 $\pm$ 37			3.71	10.3	1.4
Ebba LH-2-2	SUERC-33588	4382 $\pm$ 38			3.71	10.5	2.0
Ebba LH-2-3	SUERC-33589	4188 $\pm$ 37			3.71	9.7	3.0
	Pooled mean of LH-2 samples		4127-4416		3.71		
Ebba LH-3	SUERC-35209	4545 $\pm$ 37	4451-4797		5.01	11.4	1.9
Ebba LH-4	SUERC-35209	4930 $\pm$ 37	4957-5281		5.97	11.6	3.1
Ebba MH-1	SUERC-35210	6397 $\pm$ 38	6626-6898		11.73	12.0	2.2
Ebba MH-2	SUERC-35212	7292 $\pm$ 39	7558-7781		16.26	11.7	2.7
Ebba MH-3	SUERC-35213	8248 $\pm$ 39	8471-8850		20.5	11.8	2.1
Ebba MH-4	SUERC-35214	9125 $\pm$ 39	9536-9900		27.9	11.3	2.2

Table 7.1. Radiocarbon dates from this study

Noting these caveats, the three samples have two potential ages, one on the rising limb of the bomb spike at *ca.* 1962 and a second from between *ca.* 1999 and 2003. Due to the excellent shell preservation, the chance that all three samples are from the 1960s is remote and it is more likely that they represent younger ages. By assuming a constant decline in  $^{14}\text{C}$  of 3.1‰ pa since 1992 (see above) an estimation can be made that these samples lived between *ca.* 1999 and 2003 (Figure 7.7.).

The exact age of the samples is not known, but *Astarte borealis* is relatively short-lived (<10 years) and all collected samples were of juvenile specimens. Moreover, since it is possible that the decline in  $\Delta 14C$  occurred at a slower rate than assumed the dated specimens likely died within a decade (or less) of the date of sample collection.

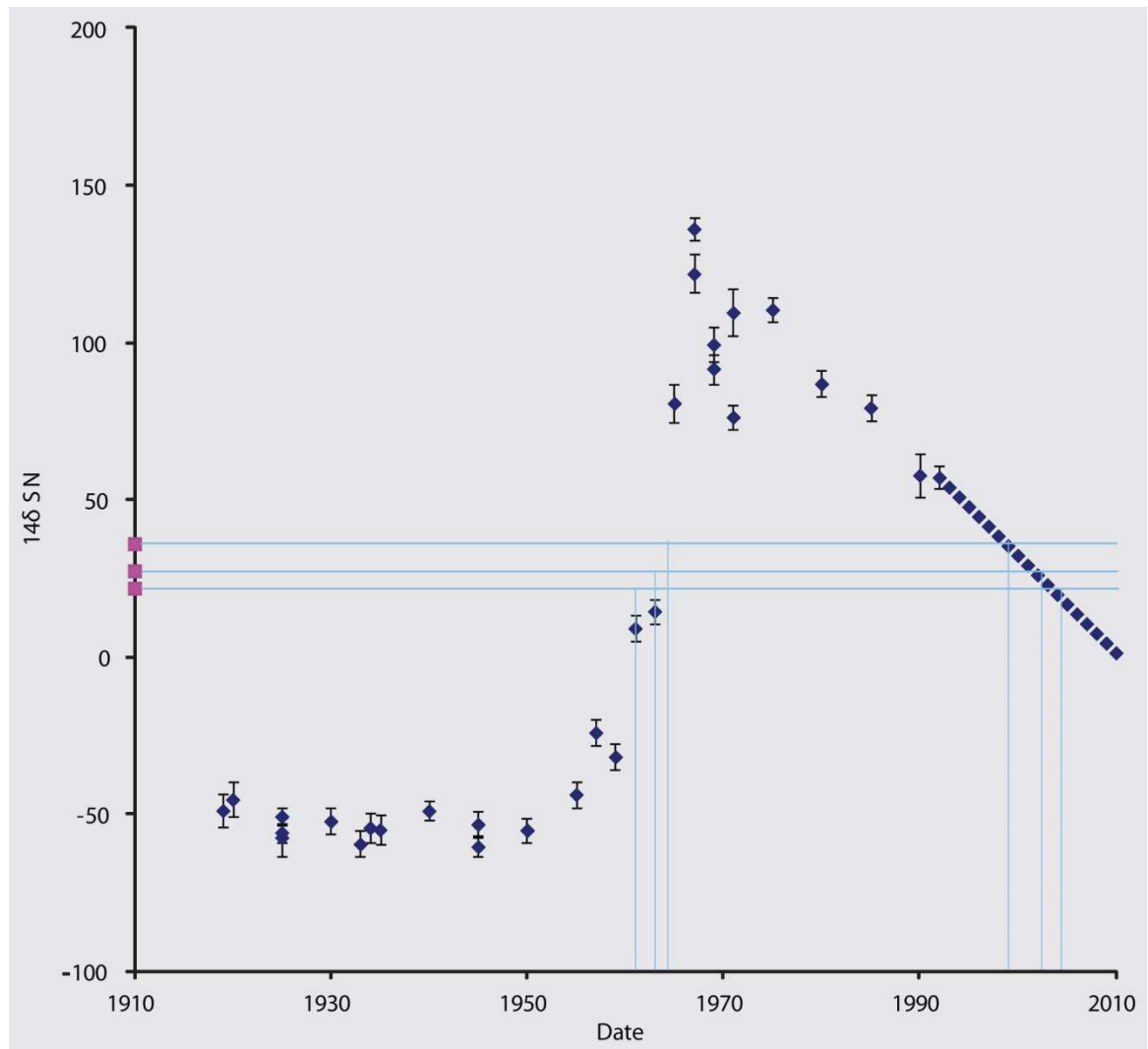


Figure 7.7. The marine bomb spike curve of KALISH et al. (2001) based on radiocarbon dates from known-age cod otoliths from the Barents Sea region. Samples (CT-1, CT-2 and CT-3) are plotted for comparison and have  $\pm 1$  SD  $\Delta 14C$  values of between 4.74 and 4.81 (which is smaller than the symbol). The youngest sample dated is from 1992 and the trend in  $\Delta 14C$  is extrapolated downwards at a rate of 3.1‰ per year to estimate the possible age of the samples (either ca. 1962 or, more likely, between 1999 and 2003).

#### 7.4.2 Testing for reworking in a late Holocene beach and developing a chronology for the Holocene raised beaches in the Ebbadalen

Having established that careful sample collection can reduce the risk of contamination by older, reworked shells, the next step was to date three samples of paired, juvenile *Astarte borealis* collected from a shallow excavation made into the crest of a late Holocene beach (LH-2, 3.71 m MTL). The age ranges of the samples (Table 8.1.)



indicate a close agreement and all three samples overlap in age at the two sigma calibrated age range. Although the sample size is small ( $n = 3$ ), these results indicate that age-mixing of paired specimens of *Astarte borealis* in late Holocene beaches is small.

In the next step, a further seven samples of paired, juvenile specimens of *Astarte borealis* were excavated from shallow pits in beach crests at elevations between 1.24 m (LH-1) and 27.9 m (MH-4), spanning the equivalent of the Lowest terraces, *Mytilus* terraces and the Lower and Upper *Astarte* terraces of FEYLING-HANSEN (1955). The results of this dating campaign show that all of obtained radiocarbon dates are in height and age sequence with no reversals (Table 7.1.).

Based on these results, it can be concluded that the approach developed here avoids the potential of dating reworked shells which is one of the challenges in existing shell-dating strategies. Also, because the original specimens died shortly before incorporation in the beach, and because they were deposited in the beach crest, they provide excellent indicators of former relative sea level.

## 7.5 Holocene relative sea-level changes in the Ebbadalen

The beach ridges dated in the Ebbadalen show that RSL fell from *ca.* 27 m asl at 9.7 k cal. yr BP to reach close to present sea level by 3.1 k cal. yr BP (Figure 7.8). The trend in the data are well approximated by a second order polynomial ( $y = 4E-07x^2 - 0.0008x$ ,  $R^2 = 0.99$ ). This pattern is typical of RSL records from near-field sites that record initially rapid glacio-isostatic rebound that decreases through time, to be replaced by RSL rise and glacio-isostatic subsidence associated with the collapse of one or more peripheral forebulges (e.g. FORMAN *et al.*, 2004). As noted above, it is also possible that some of the late Holocene RSL rise may also record the effects of local reloading of the Earth's crust due to a late Holocene increase in ice cover in Spitsbergen (FEYLING-HANSEN 1955).

The highest Holocene beach deposits are at *ca.* 40-45 m asl and mantle a ridge of glacial diamict that slopes downhill to the east towards the Ebbaelva (Figure 7.2., 7.4.). Parts of this ridge are strewn with large blocks of bedrock erratics (1-2 m in diameter) and its surface has been modified by fluvial and aeolian processes. Exposures through the lower level of this ridge in the valley floor reveal numerous articulated samples of *Mya truncata* preserved within a coarse diamict, suggesting deposition in a sediment-rich, ice proximal position.

Previously dated samples of these shells yield dates of  $8920 \pm 50$  (Gd-3180) (9638-9356 cal. yr BP) and  $8820 \pm 160$  BP (Gd-2395) (9813-8972 cal. yr BP) (KŁYSZ *et al.* (1988). These ages are similar to that from the highest specimen of *Astarte borealis* at 27.9 m asl, dated to  $9125 \pm 39$  (9900-9536 cal. yr BP). This supports the interpretation of KŁYSZ *et al.* (1988) that this ridge is an ice contact feature that marks a temporary ice margin position during the early Holocene retreat of the then tide-water Ebbabreen. The Holocene marine limit in the study area is marked by a small number of recurved beaches on the upper surface of the ice contact ridge described above. RSL fell from this level at an initially rapid rate of 30 to 15 m k/yr (Figure 7.8.).

During this initial interval, the recurved beach form was replaced by straighter, wider and longer ridges that extended into the Ebbadalen (Figure 7.4.). This style of beach deposition continued as RSL continued to fall at a progressively slower rate of *ca.* 6-7 m k/yr, reaching *ca.* 11 m by *ca.* 6800 cal. yr BP (Figure 7.8.). A marked change in beach ridge style occurred between *ca.* 6800 and 5100 cal. yr BP, with a switch to the development of many thin, long and narrow beaches. These accumulated until *ca.* 3000 cal. yr BP as RSL fell at a rate of *ca.* 2.5 m k/yr.

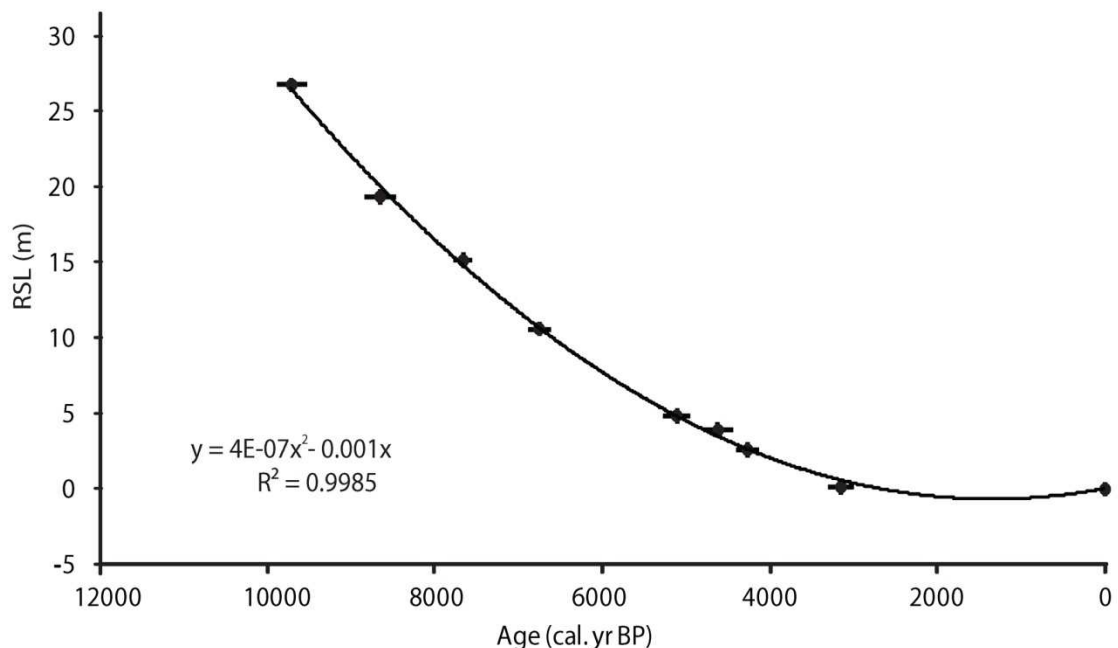


Figure 7.8. Relative sea-level graph based on *Astarte borealis* from the Ebbadalen beaches. The altitudes of the original samples (Table 7.1.) have been corrected by subtracting the height difference between the present storm beach crest and mean tide level. The age uncertainties are equal to the two sigma calibrated age range of the samples and the height uncertainty reflects the observed variability in the height of the current storm beach. The solid line is a second order polynomial that is forced through present mean tide level. The absence of data in the last 3000 cal. yr BP should be noted and trends in RSL during this period are therefore speculative.

Dates from the new dating campaign were compared with those from FEYLING-HANSEN (1965) and other published dates from shells and driftwood from Billefjorden (Figure 7.9.a). The four oldest sea-level index points from the study area plot above samples of *Astarte borealis* collected in this study. They show that RSL fell rapidly from *ca.* 65 m asl at 11,600 cal. yr BP to *ca.* 30 m asl by 10,000 cal. yr BP.

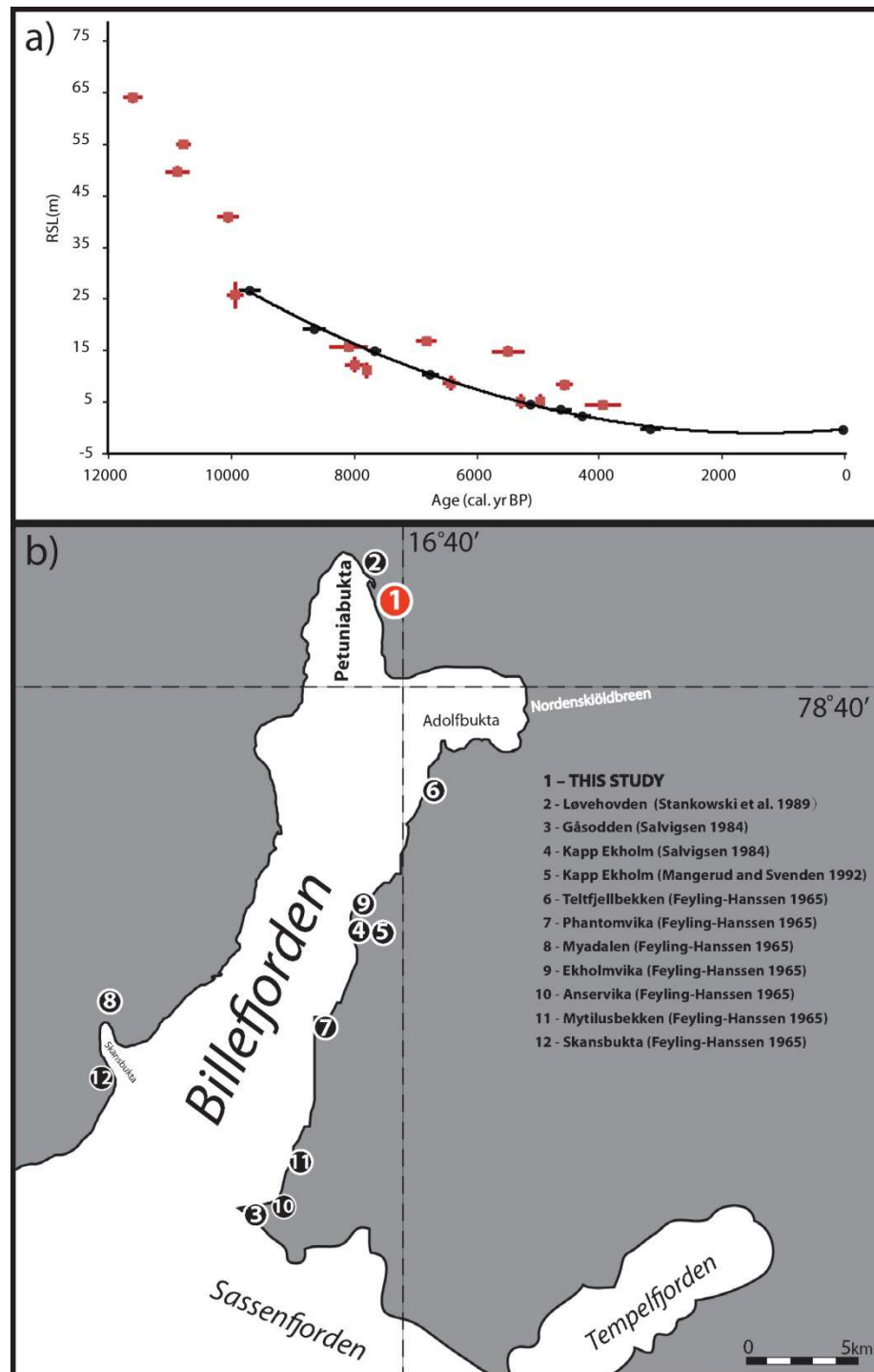


Figure 7.9. a) Relative sea-level data from Billefjorden – black points indicate radiocarbon dates from current study, red points indicate previously published dates; b) Sites along Billefjorden where previous sea-level studies were carried out in relation to current study.

Below this level, the new *Astarte borealis* samples provide a significantly tighter age/altitude distribution compared to the other index points, indeed in three instances the vertical offset between the *Astarte borealis* data and the other samples is 5 m or more, and the age differences exceed 1 k cal yr. The scatter in these data is too large to reflect real changes in RSL and must instead be due to local processes controlling the elevation of these samples. The outliers are all from sites in the outer part of Billefjorden where it joins with Sassenfjorden (Figure 7.9.b) and it is probable that some of the height difference can be explained by the fact that the beaches here formed under a higher storm wave run-up compared to the more protected parts of Billefjorden.

The youngest radiocarbon date from this study is very close to present-day sea-level, at only 1.24 m above mean tide level, or 0.74 cm above the present storm beach. A sample of *Astarte borealis* from this beach is dated to 3317-2995 cal. yr BP (Table 7.1.). The trend in the mid Holocene RSL data suggests that RSL may have fallen below present during the late Holocene before rising to the present. Unfortunately, it was not possible to date this phase with any greater precision. However, a clear change in the topography of the Ebba beaches at this time, with a marked distinction between more vegetated beaches close to LH-I and the less vegetated beaches to its seaward edge, together with the undulating and cross-cutting nature of these younger shorelines compared to the late Holocene complex (Figure 7.2., 7.4.) suggests that lateral erosion, if not RSL rise, has characterised the recent past. Elsewhere in Billefjorden, FEYLING-HANSEN (1955) noted that at Brucebyen, Kapp Napier and Skansbukta, the lowermost beach ridges increase in elevation towards the present storm ridge by about 0.5 m, suggesting a recent rise in sea level that correlates with a glacier readvance about 2500 years ago. In Adventfjorden, late Holocene erosion of a large fan delta is associated with sea level stabilising close to present (LØNNE and NEMEC 2004). Similarly, in northwest Spitsbergen FORMAN (1990) suggests RSL rose in the last two millennia.

## 7.6 Chapter summary

The focus of this Chapter has been on reviewing evidence for RSL change in the study area and developing a new method of sea-level reconstruction that over-comes the traditional limitations of reworking that has caused problems in previous studies in Svalbard and elsewhere. The key conclusions are:

The raised beaches of the Svalbard archipelago provide a spectacular record of glacio-isostatic rebound, RSL change and variations in sediment supply. Prior to this study, the most reliable dating control for these beaches has been provided by driftwood and whalebone, whereas shell-based approaches have been criticised because of difficulties in reconstructing both a precise age and former elevation of sea-level.

This study focused on the careful collection and dating of delicate juvenile specimens of the marine bivalve *Astarte borealis* that are cast up onto the beach and incorporated in the upper beach levels as articulated specimens.

Three specimens collected from the present-day beach crest contain modern carbon, indicating a minimum age of c. 50-60 years. Comparing the results with a previously dated cod otolith record from known-age samples collected from the Barents Sea indicates that the specimens were likely deposited after 1999.

Three formerly articulated specimens of *Astarte borealis* were collected from a late Holocene beach by shallow excavation of the gravel beach crest. The results from the three specimens overlapped at the two sigma calibrated age range and confirm that reworking within a single beach is not a problem.

A further set of single samples of *Astarte borealis* were collected from seven other beaches extending from close to present sea-level to a maximum altitude of c. 28 m a.s.l. These samples range in age across much of the Holocene and can be used to develop a new RSL curve from the study area.

The results of this study are interpreted and discussed with regard to coastal evolution, RSL change and ice sheet history in Chapter 8.



# **Chapter 8:**

## **DISCUSSION**

**High Arctic paraglacial  
coastal zone evolution  
over annual , century and  
millennial timescales**

## 8.1 Introduction

This Chapter integrates the results presented earlier in this thesis to evaluate existing models of paraglacial coastal evolution in the High Arctic over a range of timescales. It adopts a chronological approach, dealing with annual, post-LIA and then late Holocene timescales, before drawing the evidence together into a new model of coastal development in the study area (and potentially elsewhere in the High Arctic).

## 8.2 ANNUAL TIMESCALES: PROCESSES CONTROLLING THE EVOLUTION OF PETUNIABUKTA COAST

### 8.2.1 Gravel-dominated coasts

In general terms, the controls on High Arctic gravel barriers geomorphology are similar to those found in lower latitudes: (I) the sediment source, sediment availability and rate of sediment supply; (II) the rate and direction of sea-level change; (III) the bedrock topography and configuration, and ; (IV) the (storm-) wave climate and surface waters circulation pattern (e.g. ORFORD *et al.* 2002). The unique, additional control on High Arctic gravel barriers is the operation of frost and ice related processes that can provide protection to wave action (FORBES and TAYLOR 1994). As discussed in Chapter 3 and 4, the sea-ice activity is responsible for the development of typical microrelief composed of the mosaic of accumulative (e.g. ice-push ridges, ice-shove mounds, ice-melt mounds, kaimoo hillocks) and erosive (e.g. ice grooves, scour marks, ice melt hollows) features (e.g. OWENS and MCCANN 1970; TAYLOR and MCCANN 1983; REMINITZ *et al.* 1990; URDEA 2007).

According to ST-HILLAIRE-GRAVEL *et al.* (2011) the processes and timescales at which Arctic gravel coasts evolve and their thresholds of stability are still poorly understood. Their study, carried out along the coasts of Resolute Bay, demonstrated that despite the recent prolongation of open-water conditions and increased occurrence of storms, the morphology of the gravel barriers in that location has remained relatively resilient to storm-wave action. They also showed that after several storm events that hit the coasts of Cornwallis Island in July 2007, the majority of barrier profiles recovered to their pre-storm profile in about a month's time. Their work is important because it suggests that High Arctic barriers can, under certain circumstances, be remarkably resilient, at least over annual timescales.

The research presented in this thesis on the coastal barriers of Petuniabukta casts new light on the evolution of these High Arctic systems over annual timescales in several ways.

First, the long-lasting effect of sea-ice processes on coastal geomorphology has been documented previously along Arctic coasts that are exposed to the operation of long-fetch winds and waves or tides, which are strong enough to move and push sea-ice floes up to several hundreds meters inland (e.g. the Alaskan Beaufort Sea coastline investigated by HUME and SHALK (1964), SHORT (1976) and REIMNITZ *et al.* (1990). In Petuniabukta, observations show that barrier microrelief related to sea-ice is an ephemeral feature, disappearing within a few days of open-water wave action. The only barrier sections where the ice-related landforms were preserved for >3 years are located in a very specific sites that are characterised by the disturbance of surface water circulation and high concentrations of sea-ice pile-up and breakage (e.g. Profile 5 on the east coast (Figure 4.18.), Profile 14 on the west coast (Figure 4.27.)). These sections of barrier usually form along shallow nearshore zones associated with the progradation of submarine slopes of fan deltas or the existence of rocky shore platforms and islands made of erratic boulders that accentuate ice pile-up and disturbance of near-shore currents.

The observations from Petuniabukta are important for studies that seek to interpret ice-related micro-relief preserved in relict beaches as evidence for the intensity of palaeo-sea ice activity. For example, in a study of a recent transgression on the coasts of Melville Island (CAA), LAJEUNESSE and HANSON (2008) suggested that increased ice-push processes observed along the coast were related to climate warming that has decreased the duration of the fast ice season and increased the intensity and duration of ice-floe movement in the intertidal zone. As a result, larger and more numerous ice-push ridges are formed. However, at several of the sites in Petuniabukta the 'ice-related' microrelief was found above the barrier storm ridge, extending across the landward slope of the barriers and former storm ridges currently beyond the direct reach of contemporary coastal processes. This suggests that the preservation of sea-ice features in former (uplifted) barriers may be a function of near shore zone topography and site exposure to waves/currents (Figure 8.1.) and may not be a reliable indicator of the existence of harsh sea-ice conditions in the past.

Indeed, although it is widely accepted that the occurrence or absence of (storm) beach ridges is as signal of sea-ice conditions (BRÜCKNER and SCHELLMAN 2003; ST-HILLAIRE-GRAVEL *et al.* 2010; FUNDER *et al.* 2011) the degree of sea-ice features preservation in barrier beaches is potentially an unreliable proxy of the intensity of ice-processes. This undermines the view of MASON (2010) who sought to infer palaeo-sea ice extent from the preservation of ice-push features. Moreover, the observations made

during this PhD suggest that, in Petuniabukta at least, the preservation of ice-push or ice-melt features in the morphology of relict (uplifted) barriers is more likely an indicator of the primary depositional setting of the beach, and also the intensity of periglacial sorting and the reworking of sediments, rather than providing a reliable measure of past sea-ice conditions.

A second observation from this thesis is that the Petunibukta barrier beaches only prograded in coastal sections that were directly affected by the delivery of coarse debris from adjacent slopes or snow-melt streams. This pattern is similar to that described from Kongsfjorden by HÉQUETTE and RUZ (1990), where the seaward migration of barriers between 1983 and 1985 was controlled by glaciofluvial sediment supply or the delivery of material from the erosion of older storm ridges by meltwater streams. A contrast with the rapidly changing Kongsfjorden barrier coast is that in Petuniabukta, the reworking and longshore transport of freshly delivered sediments has been significantly slower and less effective.

A third important observation is that the landward migration of storm ridges was much more frequent along the western coast of the study area compared to the east (Figure 8.1. D). Along the latter, barrier development was influenced by the stronger and higher waves that are able to drive the landward rollover of barrier crests. These conditions are, in turn, caused by the tectonically disturbed bedrock topography (Billefjorden Fault Zone) which means that the western nearshore zone is deeper than along the eastern coast, which has a shallow submarine rock platform (Figure 8.1. A). In addition, the western coast is also exposed to higher waves formed by strong eastern glacier winds that blow from Adolfbukta, Ebbadalen and Ragnardalen (Figure 8.1. C).

An important observation made during the 2008-2010 period was the general lowering of the storm ridge height that occurred over ridges that migrated both landward and seaward, or those that remained static. This crest lowering suggests that overwashing was an important process operating in this interval. According to ORFORD *et al.* (1991) the balance between overtopping and overwashing is most commonly altered by sea-level change with overtopping increasing during periods of sea-level rise. Conversely, the inland migration of many storm ridges that occurred in 2010 may be linked with the overlapping effect of earlier disappearance of fast ice from the bay and occurrence of longer periods of stormy weather than in the preceeding summers of 2008 and 2009. These factors also help explain the widespread erosion of the seaward slopes of the Petuniabukta barriers.

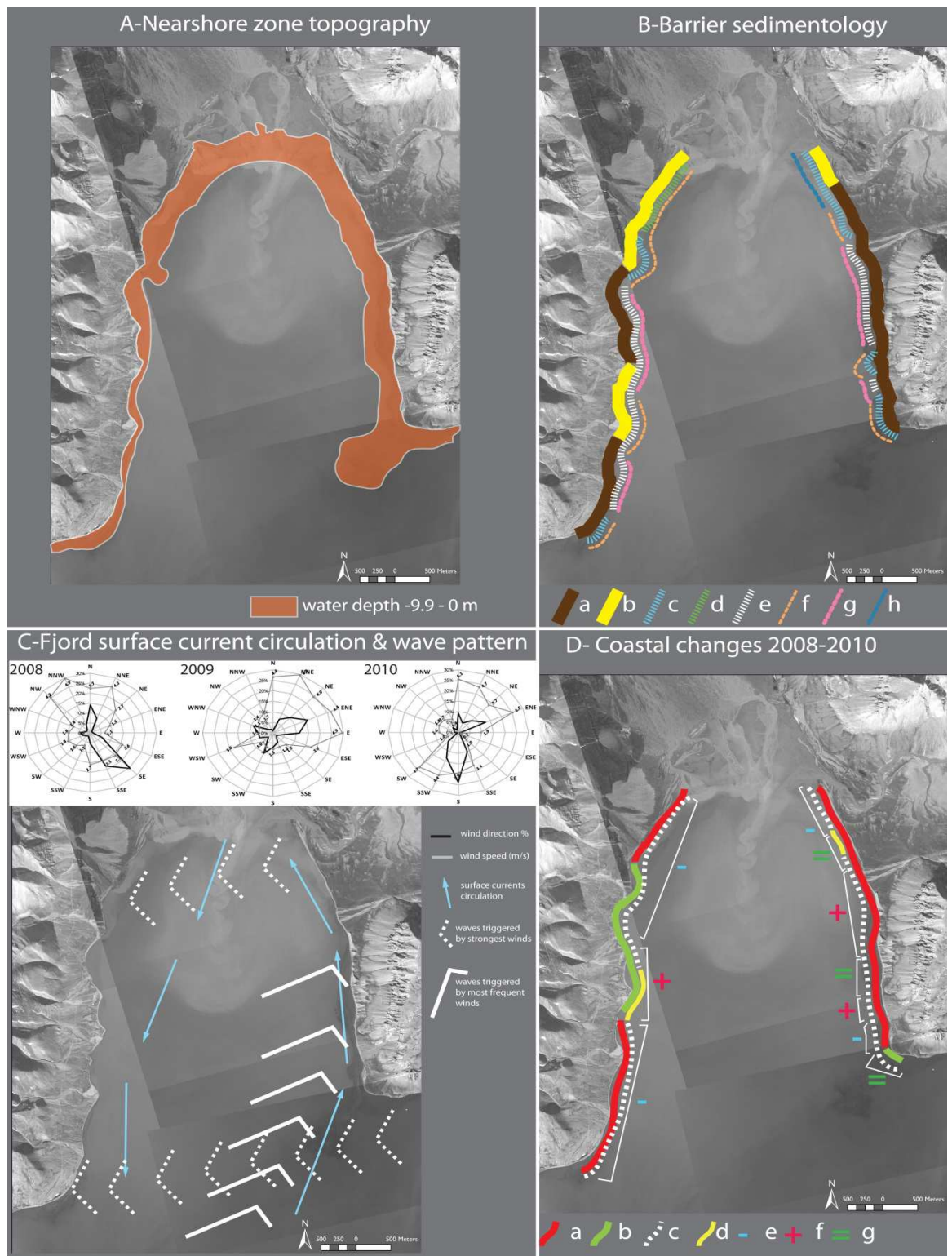


**Figure 8.1.** The present-day condition of the Petuniabukta barrier coast. **A** – difference in the nearshore topography between eastern (wide shallow platform ) and western (narrow shallow zone); **B** – Sedimentological properties of barrier surface sediments: a) swash zone surface dominated by gravel; b) swash zone surface dominated sand; c) Storm ridge pebbles dominated by disc-shaped clasts; d) Storm ridge pebbles dominated by blade-shaped clasts; e) Storm ridge pebbles dominated by rod-shaped clasts; f) Storm ridge pebbles dominated by sub-rounded clasts; g) Storm ridge pebbles dominated by sub-angular clasts; h) Storm ridge pebbles dominated by rounded clasts; **C** - Simplified surface currents circulation and directions of longest wave-fetch in Petuniabukta triggered by dominant and strongest winds observed between 2008 and 2010; **D**- Morphological changes of barrier observed between 2008 and 2010: a) Accumulation of swash zone; b) Erosion of swash zone; c) decrease in storm ridge height; d) rise of storm ridge height; e) landward migration of storm ridge over 3 years ; f) seaward migration of storm ridge over 3 years ; g) stable position of storm ridge over 3 years.



The short-term (2008-2010) lowering of crest elevation and shoreface profile are opposite to the trend of barrier evolution that has prevailed since the end of LIA, as discussed below. Thus, the interannual change in the barrier along Profile 11 indicates *ca.* 1.1 m landward migration of the contemporary storm ridge. The modern barrier is formed here along a spit-platform composed of gravel-dominated storm ridges that, between 1961 and 2009, migrated 28 m seaward (*ca.* 0.6 m yr<sup>-1</sup>). So, for the last half of the 20<sup>th</sup> century, shoreline progradation has dominated over decadal timescales, suggesting that there was a surplus of sediment in this period and perhaps also that RSL was falling in the post LIA period following local isostatic readjustment to rapid ice unloading.

Figure 8.2. summarises the potential scenarios of interannual coastal changes in the study area based on the observations carried out during this thesis. This illustrates the primacy of sediment supply and ice cover as two key controls on interannual changes in coastal geomorphology.

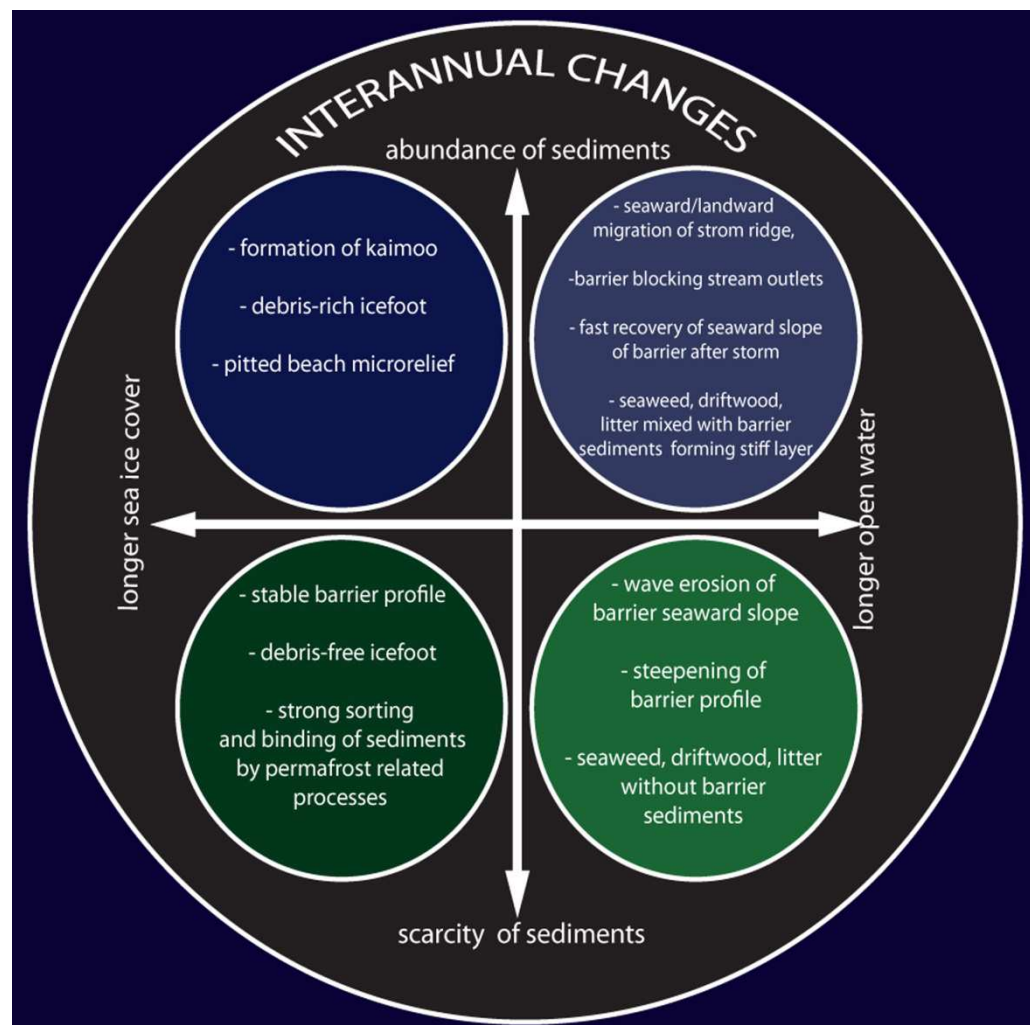


Figure 8.2. Scenarios of interannual High Arctic coastal change.

When sediment supply is high and the open water season long, then progradation of coastal landforms can occur and increases a degree of landform resilience. The extent of this resilience depends, in part, on whether terrestrial processes, such as snow-melt event, breach barriers or bury them at their landward limit by down-slope sediment movement. Conversely, high sediment supply with cold, ice-bound coasts leads to stable coasts, with sea ice-related processes shaping micro-relief on the barrier surfaces.

When sediment supply is low and the open water season long, then coastal erosion occurs and barriers will retreat via overtopping and overwashing, as well as occasional breaching under storm events. If sediment supply is low, and the open water season is short, then the coastline will be relatively stable and there will be low rates of coastal change. This model ignores relative sea-level changes because variations in sea-level operate over longer timescales than interannual intervals.

This above discussion raises an important question regarding the process of preservation of storm ridges and their palaeoenvironmental significance. Specifically, are the relict storm ridges observed in the coast plains of Petuniabukta formed over centuries or do they record occasional extreme events in climate and (associated) sediment supply that recur once per decade, century, millennium? Or, do they represent a mixture of superimposed ridges that reflects the operation of local coastal processes and climate change? In sections 8.3 and 8.4 the century and millennial coastal changes and paleoenvironmental significance of preserved storm ridges will be examined in more detail.

### 8.2.2 Rocky coasts

The short-term observations of beach profile changes provide an insight into the functioning of the unconsolidated coastline of Petuniabukta. In contrast, the Schmidt Hammer Rock tests inform understanding of the how the hard rock coasts of the study area develop over multi-decadal timescales. Taking advantage of the recently deglaciated terrain in Adolfbukta, the results of the SHRTs detailed in Chapter 5 indicate a clear relationship between the distance from the shoreline and rock resistance. Among all the test sites, the rock surfaces influenced by coastal processes were less resistant than those located further inland. This implies that weathering of the rock surfaces over decadal timescales does occur in this environment.

Interestingly, the rock surfaces on plunging cliffs in the study area do not contain any striae or evidence of glacial abrasion, whereas the roches moutonnées are covered with glacial striations and cracks. However, none of the latter surficial modifications reduced rock resistance of the inland roches moutonnées. It seems, therefore, that glacial erosion of the roche moutonnée surfaces exposed fresh, non-weathered rock, which was barely modified by para-periglacial processes. In contrast, rock surfaces deglaciated in the same period, but located within the zone of coastal influence, have experienced enhanced weathering.

The lower resistance of coastal rock surfaces in relation to inland outcrops may relate to the low-energy fjord environment. Thus, weak wave activity in such a sheltered fjord as Adolfbukta is unable to erode and remove rock weakened by intertidal wetting-drying and frost shattering. This may be responsible for preservation of a surficial weathered layer in the coastal zone. Moreover, the continuous and intensive operation of para-periglacial processes since the end of the LIA has led to the removal of unstable and weak rock surfaces from the Nordenskiöldbreen foreland, exhuming hard resistant outcrops. A similar pattern is reported by BLANCO-CHAO *et al.* (2007) during their study of shore platform evolution in a para-periglacial environment of northern Galicia, Spain. In their survey, SHRT indicated lower rock strength along platforms which were continuously influenced by tidally-induced weathering, whereas more resistant rocks occur in areas where weathered material was removed by abrasion. The Galician example highlights the significance that inherited factors, such as glacial deposits and former shoreline configuration, may have on rocky shoreline evolution.

Another factor that affects the degree of rock weathering is the extent of snow cover and its impact on rock thermal regime (e.g. ØDEGÅRD and SOLLID 1993). Field observations in winter revealed that the lower parts of the coastal cliffs in the study area are protected by up to 2 meter-thick snowdrifts, and an even deeper snow cover infills hollows between roches moutonnées in Zones II and IV (Figure 5.2.). However, snow cover along the cliffs is typically uneven, with frequent snow-free rock surfaces and rock bulges. The coastal cliff in Adolfbukta is south-facing and, therefore, these protruding rock surfaces warm-up strongly during the polar spring and summer, and snow cover melts or sublimates. After sunset, or during the polar day when the rockwall is in shadow, the surface temperature can cool rapidly, which can lead to freezing of water in rock cracks or crevices. These strong thermal stresses promote accelerated rock disintegration.

A study by HALL (1993) on Livingstone Island (Antarctica), emphasised that prolonged wetting of a rock surfaces by melting snowpatches enhances weathering, especially on leeward slopes. Differences in snow cover thickness and duration may also reduce rock resistance in roches moutonnées located far from the coast yet affected by late-lying snow cover. The only parts of the study area devoid of snow cover or glaciofluvial action were the summits of roches moutonnées and the tops of plunging cliffs, which may imply more stable moisture conditions, and less effective chemical weathering in those zones (e.g. BALLANTYNE *et al.* 1989). The upper parts of the cliffs, however, were often covered with bird guano (a layer up to 2 cm thick) and this likely led to enhanced chemical weathering and a slightly weaker resistance (the mean R-value for sites 7, 13, 19 and 25 are  $64 \pm 0.95$ , compared to more inland sites (e.g. 9, 15, 21 and 27) that have an equivalent value of  $67 \pm 0.53$ ).

Rock surfaces in Zones II and IV (Figure 5.2.) were also subject to lichen colonisation and there is also evidence of meltwater overwashing (old stream channels and accumulations of vegetated glaciofluvial sediments). Generally, even though the range of subaerial processes that may affect rock weathering are greater in more inland sites, the results of SHRT indicated that rock surfaces there are more resistant than rockwalls near the sea. This suggests the operation of processes, or the existence of specific conditions, responsible for the weakening of rock strength in the lower parts of the coastal cliffs. This implies a 'coastal amplification' of rock weathering associated with tidal wetting and drying, salt weathering, direct wave action or sea ice erosion. However, the influence of topographic factors (e.g. slope height, angle and aspect), and differences in rock stress release following deglacial unloading, cannot be excluded.

The survey design also allowed testing of the potential usefulness of SHRT in relative-dating of the Nordenskiöldbreen rocky forefield. While the zonation in rock resistance between coastal and inland sites was quite clear, no clear relationship existed between sites proximal to and distant from the glacier. For instance, profile A (S1-S5) extends across outcrops exposed from Nordenskiöldbreen during 2008-2009 but this surface demonstrated only slightly lower resistance than bedrock exposed during earlier stages of post-LIA deglaciation (Figure 5.2.D). Regression analysis showed no significant differences in R-values for sites close to the glacier front in comparison with more distant sites. This suggests that SHRT-dating of Nordenskiöldbreen foreland should be carried out with care and only with other, independent dating methods.

The work discussed here highlights the need for a greater understanding of the processes that control polar rocky coastal zones. It is noteworthy that the study site is characterised by a relatively dry polar climate and limited fetch, in contrast to the maritime (often stormy) climate of the western coast where the majority of previous rocky coastal studies were completed (JAHN 1961; MOIGN 1976; GUILCHER *et al.* 1986; ØDEGÅRD and SOLLID 1993; ØDEGÅRD *et al.* 1995; MIGOÑ 1997; WAGENSTEEN *et al.* 2007).



## **8.3 CENTURY TIMESCALES: THE POST-LITTLE ICE AGE EVOLUTION OF THE PETUNIABUKTA COAST**

### **8.3.1 The post-LIA evolution of non-glacial-fed coastal systems**

The first part of Chapter 6 focused on barriers developed in a sheltered bay characterised by limited wave action where sediments are supplied by non-glaciated, mainly snow-fed streams, together with the deposition from talus slopes in the form of debris flows. In such an environment, one might expect limited coastal zone change. However, the history of the post-LIA barrier and Ebba spit-platform evolution derived from aerial photogrammetry analysis and the analysis of sediments composing the ridges and swales has revealed a rather different picture of an actively transforming and dynamic system.

#### **8.3.1.1 Climatic influence on sediment transfer in High Arctic settings**

The study period (1936-2009) coincides with a particular phase of climatic change on Svalbard marked by two episodes of warming that coincide with positive NAO phases (Figure 6.4.). The first warming phase took place between 1900 and the 1930s and the second, that started in mid-1970s, saw an accelerated temperature rise in 1990s that has persisted until the present. As a result of the 20<sup>th</sup> century air temperature warming, Svalbard experienced rapid glacier retreat and an associated release of glacial sediment for paraglacial transport.

The phase of cooler air temperatures seen in the 1960s is probably linked to the occurrence of negative NAO phase at this time (Figure 6.4.). Negative NAO also resulted in a significant increase of precipitation, which culminated around 1960.

From a perspective of sediment delivery to the coast, this is an important factor because geomorphic activity in High Arctic settings is strongly controlled by the impact of precipitation on slope stability, solifluction processes, frost weathering and active layer development (HUMMUM 2002). As noted by LØNNE and NEMEC (2004) the High Arctic slope and fan sedimentation system is dependent on the combination of air temperature and precipitation changes.

Although the amount of snow precipitation determines the magnitude of important geomorphological processes such as snowmelt floodings (RACHLEWICZ 2009), erosion of plateau edges by cornice falls (ECKERSTORFER *et al.* 2012), debris flows (DECAULNE *et al.* 2005) or the development of avalanche-derived rock glaciers (HUMMUM *et al.* 2007) all leading to the entrainment, reworking and transporting debris from

mountain slopes and valleys towards the coast, but it is the air temperature that most commonly control the frequency of those events.

For instance, the typical weather for the occurrence of snow avalanches in central Spitsbergen are wet, warm and windy conditions associated with the low-pressure systems coming from the North Atlantic (ECKERSTORFER and CHRISTIANSEN 2011). According to those authors many of snow avalanches observed on Svalbard are triggered by air temperature fluctuations causing cooling or warming of upper snow-layers occurring after the additional snow loading. Another factor initiating snow avalanches in Spitsbergen are ephemeric rainfall or mixed snowfall with rainfall characteristic for mid-winter or spring period. It is then highly probable that during the first three decades of warming observed in the 20<sup>th</sup> century on Svalbard (1900-1930) the slope remodelling and debris transport could be to a large degree dominated by avalanches and snow-melt floods. I base this assumption on the fact that most of the warming observed within that period fell on winter period (see blue and green lines on Figure 3.6.) and predominance of positive NAO index associated with influx of warmer and moister air masses over Svalbard. The geomorphic effects of snow-melt floods or avalanches on slopes might be reinforced by summer rainfall events.

Sparse rainfall events occurring during short High Arctic summers are one of the triggers of the highest floods occurring in ablation season leading to peak sediment transport. Study of flood-types in central Spitsbergen carried out by RACHLEWICZ (2009) indicated that due to the very fast reaction of river systems to rainfall, the concentration of the drainage from extensive areas and thermal influences on snow cover and ice the rainfall-generated floods are very effectively remodelling glaciated and non-glaciated sections of the valleys. The study by RACHLEWICZ (2009) suggest also that intensive precipitation (rainfall) occurring usually after the arrival of föhn phenomena is responsible for the prolongation of the high river discharges initially triggered by increased ablation induced by warm air mass accompanying those warm winds.

According to JAHN (1967) the increase in precipitation observed in the middle of the 20<sup>th</sup> century on Svalbard initiated new slope processes and also reactivated the movement of relict solifluction lobes. It is reasonable to hypothesise that a combination of these processes may have significantly accelerated the delivery of sediment to the coastal zone. ÅCKERMAN'S (1984) analysis of debris flow occurrence in central Spitsbergen talus slopes also linked their development with 'wet conditions' related to enhanced precipitation. His study on the spatial distribution of debris flows suggests that, in the

inner part of the island, their formation is much more common on east and north facing slopes and/or in narrow valleys. This explains the huge accumulation of debris flows on the slopes of Dynamiskbekken valley (located on the northern slope of Wordiekammen), which additionally supplies the fan system with coarse clastic sediments (Figure 6.4.b). It is probable that occasional slush avalanches and debris flows occurred in Dynamiskbekken valley during the last century. Indeed, field observations show several old fan-like debris covers and boulder tongues overlaying the tundra in the middle part of the stream that resemble talus and block debris covers described after massive slush avalanche in Steinvikdalen (CZEPPE 1966; JAHN 1967).

It is noteworthy then that during the 1950-1970 period, several catastrophic slush avalanches and debris-flows were documented in central Spitsbergen that transported significant amount of coarse sediments and which were related to extreme meteorological and hydrological events (e.g. major rainfalls or spring snowmelts) (CZEPPE 1966; JAHN 1967, 1976; LARSSON 1982). One of the most tragic of these, the '1953 event' which demolished Longyearbyen hospital and killed three inhabitants, is a good example of the magnitude of those processes (ÁNDRE 1989).

#### **8.3.1.2. Post-LIA coastal morphodynamics of Ebba spit-platform system**

Many of the spits and the Ebba spit-platform evolution in Petuniabukta developed during a period of high sediment availability in both coastal and terrestrial environments that started after the end of the LIA. An important question to address is what effect did these specific conditions have on the coastal morphodynamics in Petuniabukta? The answer has two aspects; the first relates to the operation of marine processes and the second to the operation of terrestrially-based processes.

Since the end of LIA, the Ebba spit-platform in Petuniabukta has significantly expanded with the formation of three spits (III-V) which each extended alongshore *ca.* 200 m. These landforms are not only larger than spit I and II, formed before 1961, but their axes are also tilted towards the NW. One likely explanation for this process is the shallowing of the nearshore zone in NE Petuniabukta that was related to increased post-LIA sediment accumulation rates. Support for this hypothesis can be found in SZCZUCIŃSKI *et al.*'s (2009) analysis of LIA and post-LIA seabed sediment accumulation rate (SAR) in Petuniabukta. Their research highlighted that SAR in the fjord has rapidly increased since the end of the LIA reaching probably the highest rates in the last two millennia, and second, that sedimentation from suspension takes place mostly within the first 100 m of

the mouth of the Ebbaelva and main tidal flat channels. It seems likely that the increased accumulation of fine (muddy and sandy) sediments in the Ebbaelva area and progradation of the tidal flat created favourable conditions for the development of the submarine platform that, in turn, facilitated the dynamic growth of subaerial spits in the mouth of Ebbaelva and the concurrent seaward migration of the barriers. The progressive orientation of the axes of spits III-V towards NW may also be explained by this phenomenon.

The relationship between subaerial coarse clastic barrier development and subaqueous platform accretion is well-documented by SHAW and FORBES (1992) in Newfoundland. Their study suggests that, during the Holocene, the prerequisite for beach-ridge formation was the previous accumulation of large, fine sediment submarine platforms. The coastal margin topography and relative sea-level changes were clearly also important as a longer-term parameter that controls water depth and accommodation space, but sediment availability in the nearshore zone was crucial for paraglacial barrier coast development. Similar conditions are known from the Dungeness foreland in southern England (LONG *et al.* 2006). Similar processes, but at a decadal time-scale, have operated in Petuniabukta since the end of the LIA, when intensified sediment accumulation concentrated in intertidal and river mouth zones of the fjord prepared the ground for Ebba spit-platform development.

The difference in size and orientation between the pre-1961 spits (I and II) and post-1961 spits (III-V) may represent two phases of the post-LIA Ebba spit-platform evolution:

- i) an initial phase took place during the first half of the 20<sup>th</sup> century when large amounts of sediment released by post-LIA glacial retreat delivered large volumes of sediment to the coastal, forming a subaqueous platform and enabling the growth of the ebb-tide delta. At the same time, coarse sediment delivered from the Dynamiskbekken fan to the coast initiated the seaward migration of the Ebba spit-platform and the development of two gravel-dominated spits. However, due either to the lack of accommodation space or sufficient sediment supply, these spits could not expand into the mouth of the Ebbaelva;
- ii) the Ebba spit-platform entered the second phase of its post-LIA evolution, which started in the middle of the 20<sup>th</sup> century, with existing accommodation space for the accumulation of new depositional features. The start of this phase coincided with a

period of increased debris flow activity (as seen elsewhere in Svalbard – see above) triggered by the increase in precipitation associated with the negative NAO phase (1950-1970s). It is possible, therefore, that the role of sediment delivery from terrestrial sources (e.g. fan, talus slopes, catastrophic debris flows) dominated the spit and Ebba spit-platform evolution between 1961 and 2009.

Spits formed in the pre-1961 period are composed mainly of gravel from the landward part of the Ebba spit-platform, comprising wider beach ridges with gentler slopes than ridges formed from the second half of 20<sup>th</sup> century. The dominance of blade-shaped clasts in pre-1961 beach-ridges may suggest the constant delivery of freshly formed clasts from the fan. At the end of this period, however, there were changes either in wave activity/sea-ice conditions, or in the source of sediment supply, as the beach-ridges became dominated by disc-shaped clasts. The large accumulation of discs in the beach-ridges could reflect increased clast modification by waves or reactivation of relict channels in the fan system that extended the fluvial reshaping of clasts before reaching the coast. The second hypothesis is potentially compatible with numerous slush avalanches that occurred in central Spitsbergen at this time that could have supplied the beach ridges with disc-shaped pebbles. The sudden drop in magnetic susceptibility noted in sediments from the final stage of the pre-1961 period (swales X-XI) also implies a change in sediment source.

The composition and size of spit III suggests that an alternative sediment source was delivering abundant, albeit finer sediment to the system. This shift coincides with a significant cooling of climate on Svalbard that occurred during 1960s. The reduction in height of the beach-ridges formed between the 1960s and 1980s is probably also an expression of more severe sea ice conditions of that period, as discussed by ZINGER (2006). Such conditions would have precluded the deposition of the large spit III. However, it is possible that increased precipitation at the same time as temperature cooling resulted in increased snow accumulation in the Dynamiskbekken valley. Therefore, although the discharge season was shortened, snow-melt floods could likely still deliver significant amounts of sediment to the coast. Snowy conditions were favourable for slush avalanches and other nivation processes reactivating and rejuvenating debris tongues, as described from the nival cirque on Arieammen slopes during the snowy year of 1958 (JAHN 1967).



The prominence of fine sediments in spit III may record the washing out of fines from the fan by rainfall events which coincided with a negative NAO phase. However, the further fining of spit deposits observed in spit IV and spit V, which formed during a period of warming on Svalbard, requires a slightly different explanation. This change in spit sediment composition from gravel-dominated to sand-dominated may be a result of the previously mentioned shallowing of the nearshore zone associated with tidal flat progradation and Ebbaelva ebb-tide delta formation. An increase in finer sediments together with less severe sea-ice conditions coincided with the expansion of the Ebba spit-platform which between 1990 and 2009 migrated seaward over 40 m. The increase in availability of sandy deposits for the development of spit IV and V is also an outcome of the increasing significance of sediment delivery through alongshore transport from the erosion of the palaeo-spit as fan-fed sediment supply fell. My own field observations of Dynamiskbekken fan sediment delivery to the coast from 2005 to 2010 suggests that, in recent years, the supply of coarse sediments has reduced to extreme spring snow-melt discharges only. Reports on the Dynamiskbekken sediment supply from the late 1980s indicate that the stream was able to flow along the whole distance of the fan and discharge directly to the bay (KOSTRZEWSKI *et al.* 1989), suggesting that the fall in sediment delivery probably began in the 1990s and intensified in first decade of the 21<sup>st</sup> century.

One of the other factors that modified the delivery of fine sediments to the coast is the blocking of Dynamiskbekken outlets. In the last five years, the majority of fan channels were blocked by a prominent storm ridge that led to the formation of several deep hollows (several meters wide and up to 0.5 m deep) that became filled with muddy and sandy sediments in the back of the barrier.

As noted by ZENKOVICH (1967) the topography of beach ridge plains depends on the unequal strength of wave activity, the position of the sea-level and an uneven supply of sediments. Therefore, the difference in the grain size characteristics of spits III-V (48% of gravel in spit III, 36% of gravel in spit IV and 27% of gravel in spit V) also explains the change in Ebba spit-platform topography that divides beach ridges formed between 1961 and 1990 from those deposited between 1990 and 2009 (Table 6.2.). It is likely that production of wider ridges resulted from increased open-water conditions in the Isfjorden-Billefjorden system, such that although locally sea-ice conditions in Petuniabukta remained harsh, the fetch of the larger waves entering the bay from a S-SE direction increased longshore transport. This effect could be responsible for the drop of magnetic

susceptibility in the fine sediments that accumulated in beach-ridge swales deposited between 1990-2009 (Table 6.3.). The deposits characterised by such a low MS (<10) are found in the barrier coast developed at the entrance to Petuniabukta, so their entrainment into a most recent beach ridges and spit system must be related to enhanced longshore sediment transport.

It is possible that during the last decade the above processes may also explain the general decrease in clasts size seen in the modern beach ridge (ridge XXIV on Figure 6.5.). Following the possible cutting-off of coarse sediment supply through the blocking of Dynamiskbekken fan channels, the barrier would have lost its local source of coarser clasts. Thus, the modern barrier and spit are composed of sediments that, during longshore transport, experience significant sorting, as is typical for coarse-grained, drift-aligned beaches (ORFORD *et al.* 1991).

In the coming years, I expect further increase in sediment supply from both shoreface sources (i.e. erosion of the barriers of S Petuniabukta) and also erosion and cannabalisation of the palaeo-spit. Occasional fluxes of coarser debris from the fan will be important if spring-melt and summer floods manage to (occasionally) breach the barrier that currently blocks cross-shore stream discharge. The longer-term evolution of spits and barrier platform in E Petuniabukta will also depend on the continued paraglacial transformation of the adjacent glacier-forelands. With the maintenance of the current rate of glacier retreat, the distance between snouts of Hørbyebreen and Ebbabreen will continue to grow. This will increase the sediment storage capacity in extensive outwash and valley systems and delay the delivery of material to the coastal zone. Such processes may influence the behaviour of the barrier system as seaward progradation depends on the development of a fine grained subaqueous platform.

The relationship between RSL change and barrier evolution may also experience significant change as the post-LIA rebound of the land may reduce RSL rise. Indeed this process may already be underway.

### 8.3.2 The post-LIA evolution of glacial-fed coastal systems

The post-LIA retreat of glaciers has arguably triggered the most dramatic change in the Svalbard landscape since deglaciation at the start of the Holocene. Retreating glaciers have exposed vast areas of fresh and unstable glacial sediments that were easily released, eroded, transported and redistributed by an array of processes: dead-ice melting (e.g. SCHOMAKER and KJÆR 2008), meltwater streams (e.g. ETZELMÜLLER *et al.* 2000), jökulhlaups (e.g. ETIENNE *et al.* 2008), slope processes (e.g. MERCIER *et al.* 2009), wind action (e.g. RACHLEWICZ 2010) and finally coastal processes (e.g. MERCIER and LAFFLY 2005). Intensified operation of those processes was strengthened by warming of the climate that thawed permafrost and destabilised unlithified river banks or fjord shores because of thinner ice cover and/or weaker thermal insulation of slopes and rockwalls by reduced snow cover. The response of the Svalbard coastal zone to the post-LIA paraglaciation, which in theory constitutes 'the ultimate sink' (BALLANTYNE 2002) for paraglacially eroded, reworked and transported sediments before they are moved further offshore, has been observed in several sites along W and S Spitsbergen. Previous studies have linked coastal progradation and rapid development of depositional landforms with uninterrupted periods of sediment supply from glacial rivers (HÉQUETTE 1992; MERCIER and LAFFLY 2005), episodes of dramatic coastal erosion in areas no longer covered or protected by glacier ice (ZIAJA *et al.* 2009), and coastal reworking of glacial landforms (mainly frontal moraines, margins of outwash plains and smaller proglacial features) exposed after the retreat of glaciers (ZAGÓRSKI *et al.* 2012).

It is important to note that despite the enhanced post-LIA sediment supply to the coastal zone in all investigated sites (Sørkappland – ZIAJA *et al.* 2007, 2009; Hornsund - ZAGÓRSKI *et al.* 2012; Bellsund - ZAGÓRSKI 2011), except for the section of Kongsfjorden coast described by MERCIER and LAFFLY (2005), the observed rates of coastal erosion exceeded the rates of coastal progradation (Table 8.1.). These observations confirm the picture of Svalbard's coastal zone as classified on the most recent map of Arctic coast erosion rates as being a 'stable' or 'aggrading' coastline (LANTUIT *et al.* 2011).

The dominance of erosion along those mostly open-type coasts in W and S Spitsbergen (Figure 8.3.) can be explained by:

- the prolonged exposure of coasts to the operation of waves and more frequent storms caused by the earlier disappearance and later formation of sea-ice and ice-foot;
- the increased influx of warmer Atlantic waters that weaken sea-ice cover and disturb the thermal state of coastal permafrost (ZAGÓRSKI *et al.* 2012 b);

- the thickening of the active layer in coastal areas that leads to the destabilisation of coastal sediments and increases their permeability by both groundwater and seepage of seawater, and;
- the rutting of the coastal sediments by heavy machines in the vicinity of research stations (e.g. the Polish Polar Station in Hornsund or bases in Ny-Ålesund).

	Kongsfjorden NW Spitsbergen	Bellsund W Spitsbergen	Hornsund SW Spitsbergen	Sørkappland S Spitsbergen	NW Petuniabukta Central Spitsbergen
<b>Highest observed rates of coastal erosion</b>	up to 30 m (1 m yr <sup>-1</sup> ) [1966-1995]	up to 110 m (1.5 m yr <sup>-1</sup> ) [1936-2007]	up to 46 m (0.9 m yr <sup>-1</sup> ) [1960-2011]	up to 460m (6.7 m yr <sup>-1</sup> ) [1936-2005]	up to 50 m (1.04 m yr <sup>-1</sup> ) [1961-2009]
<b>Highest observed rates coastal seaward progradation</b>	up to 90 m (3 m yr <sup>-1</sup> ) [1966-1995]	up to 65 m (0.9 m yr <sup>-1</sup> ) [1936-2007]	up to 20 m (0.4 m a <sup>-1</sup> ) [1960-2011]	up to 300 m (20 m yr <sup>-1</sup> ) [1990-2005]	up to 48 m (0.96 m yr <sup>-1</sup> ) [1961-2009]
<b>Highest rates of elongation of coastal landforms (spits)</b>	x	up to 85 m (1.8 m yr <sup>-1</sup> ) [1960-2007]	x	x	up to 187 m (9.8 m yr <sup>-1</sup> ) FS3 [1990-2009]
<b>Glacier retreat rates (LT): land-terminated (TW): tide-water and mean distance between snout and coast (SCD)</b>	(LT) Midtre Lovénbreen: (10 m yr <sup>-1</sup> ) • SCD: 1200 m  (TW) Kronebreen (150 m yr <sup>-1</sup> )	(LT) Scottbreen: (16 m yr <sup>-1</sup> ) [1936-2002] • SCD: 2300 m  (TW) Recherchebreen (27 m yr <sup>-1</sup> ) [1960-2008]	(LT) Ariebreen: (10 m yr <sup>-1</sup> ) • SCD: 2200 m  (TW) Hansbreen: (25 m yr <sup>-1</sup> ) [1900-2008]	(LT) Kambreen: (12m yr <sup>-1</sup> ) [1900-2005] • SCD: 600 m  (TW) Hambergbreen: (160 m yr <sup>-1</sup> ) [1900-2000 ]	(LT) Hørbye: (10.6 m yr <sup>-1</sup> ) [1900-2009] • SCD: 3800 m  Sven: (11.7 m yr <sup>-1</sup> ) • SCD: 3500 m  Ferdie: (13.9 m yr <sup>-1</sup> ) • SCD: 3100 m  Elza: (11.3 m yr <sup>-1</sup> ) • SCD: 3200 m  Ragnar: (14.7 m yr <sup>-1</sup> ) • SCD: 5700 m

*Table 8.1. Comparison of coastal change rates and glacier retreat rates between central (study site – Petuniabukta – <PET on Figure 8.3.>, western (Kongsfjorden – MERCIER and LAFFLY (2005) – <NYA>, (Bellsund - ZAGÓRSKI (2011) <CAL> – on Figure 8.3., Hornsund - ZAGÓRSKI et al. (2012) – <HOR> and southern (Sørkappland – Ziaja et al. (2002, 2007, 2009, 2011) – <SOR - on Figure 8.3>, parts of Spitsbergen.*

The general image of the post-LIA paraglacial coasts in Svalbard that can be determined from previous studies suggests a very responsive and unstable system that rapidly reacts to changes in sediment supply delivered from retreating glaciers and climate-driven forcings of coastal erosion (retreat of tide-water glaciers, prolonged open water conditions and influx of warmer waters).

The results of the research presented in this thesis confirms an increase in post-LIA sediment delivery to the coastal zone, but has also shown that the link between coastal evolution, glacier retreat and sediment supply change seen along the W and S coasts of Spitsbergen, have been less dramatic in the protected, inner-fjord environment of Petuniabukta.

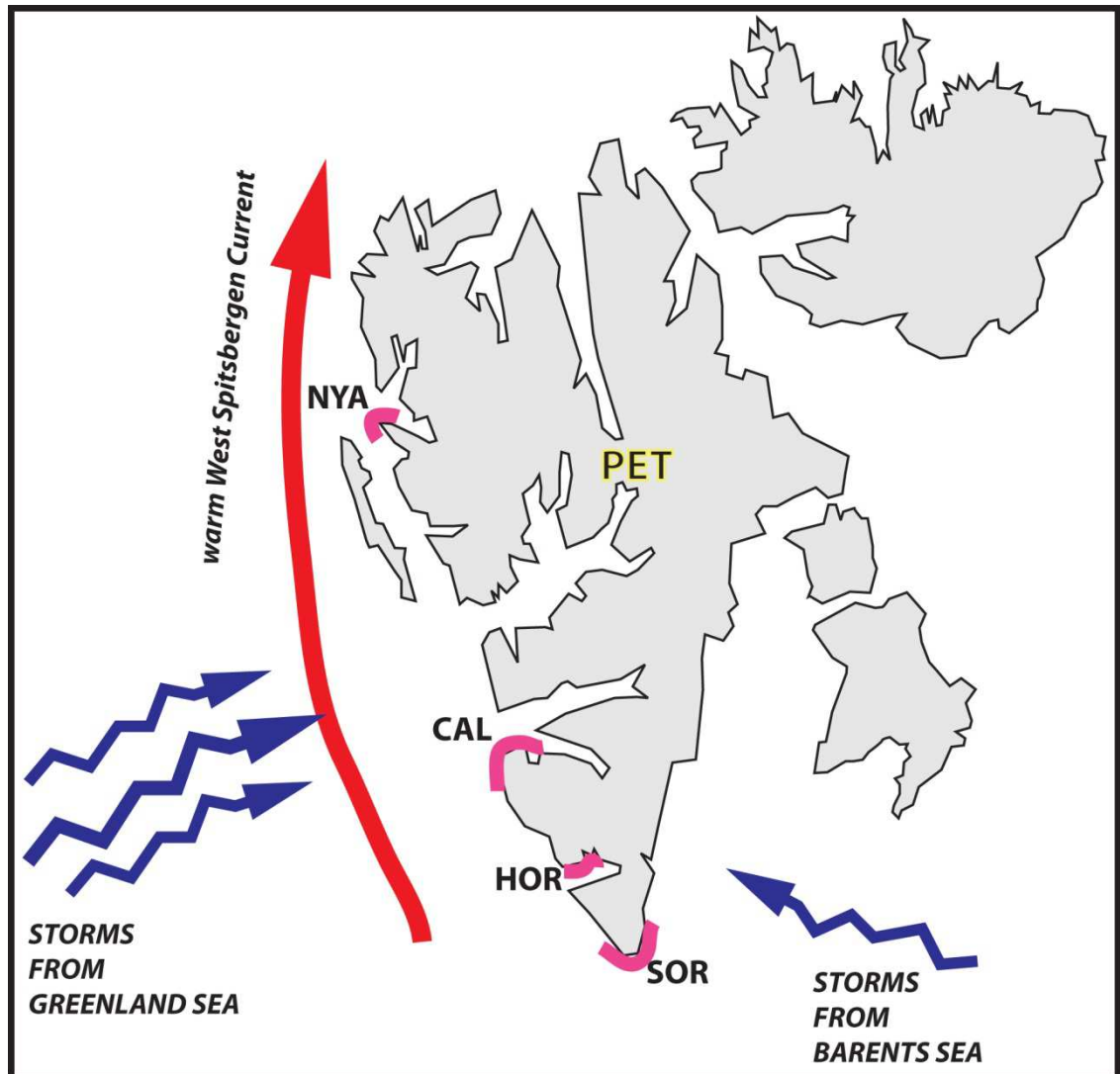


Figure 8.3. Coastal areas of Spitsbergen investigated in previous studies. NYA – Kongsfjorden coast, CAL - Bellsund coasts, HOR – Hornsund coast, SOR - Sørkappland coast, and PET – Petuniabukta coasts – this study.

Geomorphological evidence and information derived from aerial imagery indicate that the post LIA development of the coasts of NW Petuniabukta is strongly influenced by local factors that include local climate, basement topography, the inherited landscape, wave climate, surface waters circulation pattern, and to some extent the pattern of relative sea-level change.

Warmer and drier summers in Petuniabukta related to those experienced along the W and S of the island (see climate conditions on Figure 3.17.) drive glacier



retreat high into their valleys. This, in turn, increases the distance between glacier snouts and the coastal zone (Table 8.1.). On average, glacier rivers draining to the NW Petuniabukta have to overcome almost twice the distance to the coast compared with rivers transporting sediments from comparable proglacial zones of W and S Spitsbergen. This decreases the stream power, reduces sediment transport, and increases the sediment load loss in intermediate sinks such as river banks, river bars, floodplains or proglacial lakes. Therefore, even though glacier retreat rates in Petuniabukta are similar with those observed in the other parts of Spitsbergen (Table 8.1., see also RACHLEWICZ *et al.* (2007), MAŁECKI (2009) coastal responses are less dramatic than in W and S Spitsbergen.

In W and S Spitsbergen, it is common to observe erosional and depositional shorelines that are distributed in time and space according to sediment supply and delivery rates or the appearance of protective sea-ice before the arrival of storms (e.g. Calypsostranda responding to pulses of sediment supply from Scottbreen and Renardbreen as described by ZAGÓRSKI (2011).

In NW Petuniabukta, post-LIA shoreline erosion is limited to a short (300-350 m) section of coastline located between the Elzaelva delta and the FF4 fan delta (Figure 6.20). This occurred despite continuous sediment delivery to the coast by Elzaelva and Ferdinandelva, and continued severe sea-ice conditions throughout the last century. It is difficult to explain this section of eroded coast, although it is possible that the coastline orientation with reference to the prevailing winds and surface water circulation directions in the fjord has been influential. Remotely sensed data and weather observations shows that both erosional and accumulative landforms develop in the opposite direction to the prevailing winds (SSE), the longest wave fetch (S) and the general pattern of surface water circulation driven by the Coriolis effect, which pushes waters towards the SW and entrance to the bay (Figure 8.4.A). However, in the NW Petuniabukta the erosional shorelines and all of the Ferdie Spits develop towards the NE. The sediment plumes released from Elzaelva and the FF4 fan deltas also drift towards the NE, and then travel along the tidal flat edge before they reverse to the SW, together with the main sediment plume from Ebbaelva and tidal channels. The spatial orientation of relict landforms formed earlier during the Holocene (i.e. Ferdie Old Spits and Ferdie Barrier Islands), also indicates that their formation proceeded contrary to the dominant wind direction and oceanographic forcings.

One possible explanation for this pattern is the operation of the 'Ekman spiral effect' in NW Petuniabukta driven by strong NE winds from the Lomonosovfonna ice cap that descends to Ebbadalen (Figure 8.4. B and C). These locally-generated NE winds drive nearshore waves and currents towards the SW and, as a result, waves attack the western coast of Petuniabukta. However, at the same time, as a consequence of the 'Ekman spiral effect' the water layers below the surface commence a clockwise rotation that is opposite to the prevailing wind direction and hence a NE longshore current is initiated (Figure 8.4.C). The bedrock topography plays an important role here by directing winds that originate from Lomonosovfonna to Ebbadalen (orographic forcing) where they hit the water surface over a relatively deep part of the fjord, allowing full development of the spiral.

The basement topography of the fjord basin may further contribute to the formation of the longshore current in NW Petuniabukta. Due to the Billefjorden Fault, which has shattered adjacent rock units, the western submarine slopes of the bay are steeper than along the eastern coast, so the longshore current initiated by these processes can run uninterrupted along the western coast until it reaches the shoals formed by prograding fan deltas and the tidal flat.

Analysis of aerial images of the Svalbard coastal zone available at NPI topographical map portal ([toposvalbard.npolar.no](http://toposvalbard.npolar.no)) suggests that the formation of 'reversed-coastal landforms', such as the Ferdie Spits, may be a characteristic feature of sheltered fjords (e.g. the spits and barrier islands in Dicksonfjorden, Ekmanfjorden, Van Mijenfjorden or Bockfjorden where, during short periods of open water conditions, strong local winds may predominate over general surface water circulation patterns).

Sea ice is another important factor in controlling coastal change. The western and southern coasts of Spitsbergen are generally ice-free for longer periods and exposed to storms originating far away in the Barents and Greenland Seas that define local wind directions and shape coastal geomorphology.

In contrast to Petuniabukta, coastal development at a site like Hornsund (SW Spitsbergen) is strongly influenced by the rapid decay of tide-water glaciers and an associated influx of warm Atlantic waters delivered by West Spitsbergen Current. Due to the 20<sup>th</sup> century retreat of glaciers, the fjord areas there have increased by over 100 km<sup>2</sup> (VIELI *et al.* 2002; PÄLLI *et al.* 2003; OERLEMANS *et al.* 2011). The post-LIA deglaciation not only lengthened fjord shorelines, but also increased the exchange of waters between the

fjord and open sea, leading to the acceleration of tidal currents that might have intensified the coastal erosion (Piotr Głowacki pers. comm.).

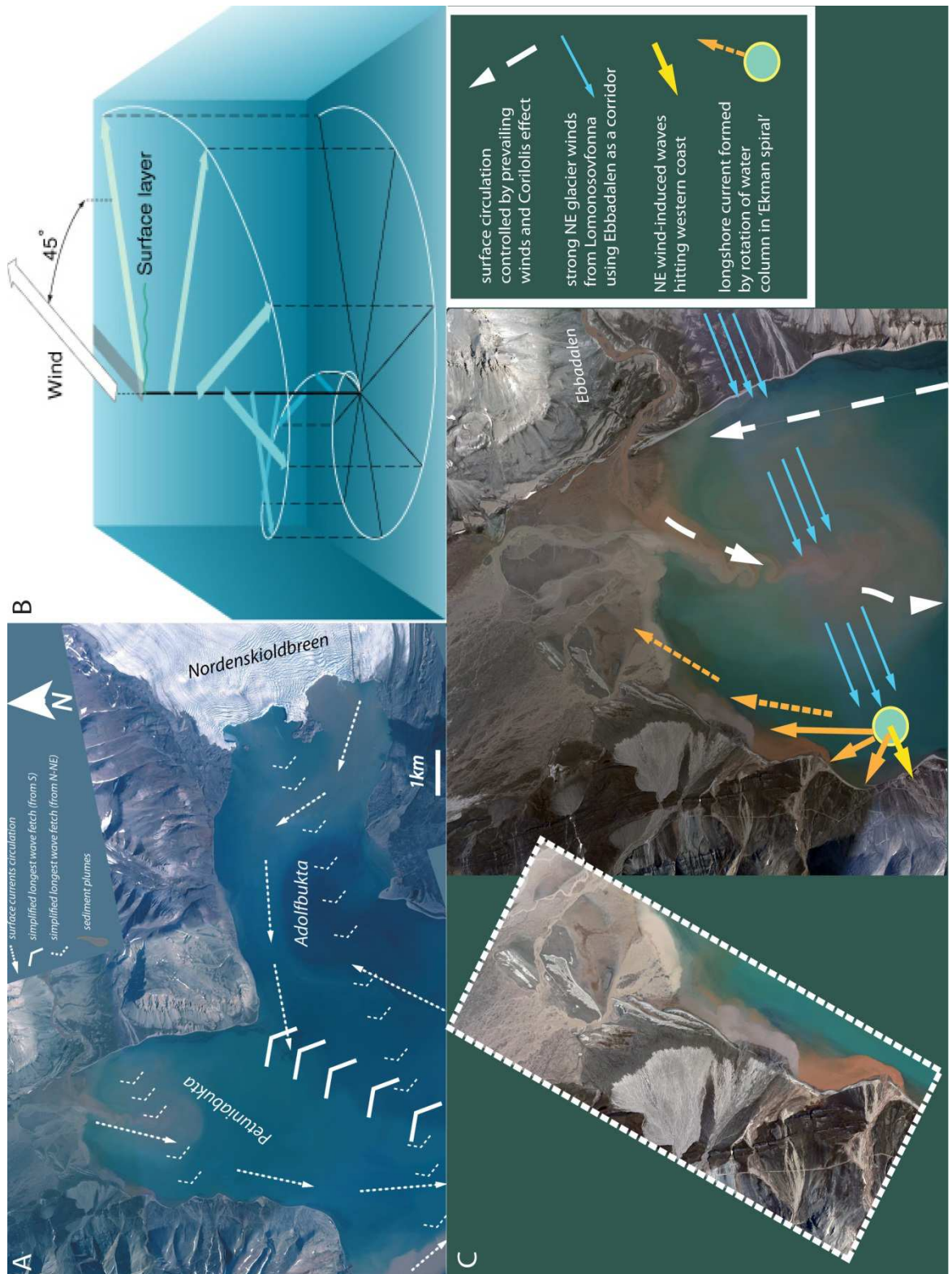


Figure 8.4. A – Simplified water surface circulation and directions of longest wave-fetch development in the study area, B – The operation of Ekman spiral, after NASA oceanmotion.org. As represented by horizontal vectors, the speed and direction of water motion change with increasing depth, C – The functioning of the 'Ekman spiral' in NW Petuniabukta, which generates longshore current in the opposite direction to prevailing winds and surface circulation patterns.

Another important difference between NW Petuniabukta coast and coasts from W and S Spitsbergen is the lack of a direct connection between the coastal zone and glacial landforms (moraines, eskers, kames, crevasse fills etc.). The erosion of landforms left by retreating glaciers by waves and longshore currents constitutes an important source of coarse-clastic sediment delivery to Kongsfjorden, Bellsund, Hornsund and to the bays around Sørkappland. This mode of glacial sediment delivery make them similar to mid-latitude paraglacial coasts supplied with sediment from erosion of drumlins and other landforms left along the coast by last ice sheets e.g. the paraglacial coasts of Ireland and Nova Scotia (TAYLOR *et al.* 1986; SHAW *et al.* 1990; ORFORD *et al.* 1991). Evolution of this type of paraglacial coastal systems is characterised by episodes of rapid reorganisation associated with gaining access to and reworking of glacial landforms. According to FORBES *et al.* (1995), the lifespan of a paraglacial coast is dependent on the volume and endurance of the (glacial) sediment source, so that the phase of intensified growth and migration of paraglacial barriers is often abruptly terminated by the exhaustion of sediment supply that occurs when a glacial landform is fully eroded.

The relatively dry and warm climate of the study area (compared with the W Spitsbergen coast) limits the growth of local glaciers to high elevations. This means that the post-LIA sediment supply to the NW Petuniabukta coast was more distant to that in W Spitsbergen. Therefore, it can be assumed that the shorelines here experienced the decaying phase of paraglacial sedimentation associated with reworking of former glacial sediments already transported and modified by non-glacial fluvial, slope and aeolian processes.

This situation resembles the fourth stage of fjord evolution model proposed by SYVITSKI and SHAW (1995) who determined the following steps of fjord infilling: Stage One - the complete coverage of fjord by glacier ice; Stage Two - the ice-contact sedimentation associated with retreating tide-water glacier; Stage Three - distal proglacial sedimentation after transformation of the glacier into a land-based type; Stage Four - paraglacial sedimentation associated with the reworking of glacial deposits left by a retreating and later a fully disappearing glacier; and Stage Five - complete infilling of the fjord basin. As noted by BALLANTYNE (2002), such a sequence of events can be disturbed, stopped or reversed by a shift of climate conditions, and can be either slowed down or accelerated by sea-level change.

Changes in relative sea-level can exert a fundamental control on coastline change by limiting or facilitating access to glacial landforms in all types of paraglacial coasts. The

case of NW Petuniabukta provides an interesting example of how strongly the Holocene relative sea-level changes determined the recent evolution of the barrier coast in central Spitsbergen. The rapid RSL fall observed in Petuniabukta since the onset of the Holocene resulted in cutting off the direct contact of fjord with glacial landforms as early as 9700 cal yr BP, at which time Petuniabukta was filling the entrances to Ebbadalen and Hørbyedalen, reworking the ice-contact deposits produced by at that time tide-water Ebbabreen and Hørbyebreen. As described in Chapter 7, RSL fell to reach close to present sea level by *ca.* 3100 cal yr BP. This fall in RSL exposed new stretches of coastal lowlands that were gradually infilled by alluvial fans supplied in sediments by glacial rivers along the western coast (two generations of Ferdie Fans) and by the snow-fed Dynamiskbekken along the eastern coast (Chapter 6.3).

In the northern part of the bay, the tidal flat started to develop along the distal margin of an outwash plain supplied from Sven-Hørbye-Ragnarbreen catchments. The trend in the mid Holocene RSL data suggests that after 3100 cal yr BP the RSL may have fallen below present sea-level and then started to rise again to reach the present. This period was probably the most important phase for the Old Ferdie Fan incision and for establishing the foundations for the modern Ferdie Fans and spit evolution.

As RSL serves as the ultimate base-level and controls the river bed level (MUTO (1987) *after* DAVIES (1902)) the proposed Late Holocene fall in RSL could explain the incision of Old Ferdie Fan 2 and the creation of accommodation space for Ferdie Fan 3 and 4 by dissection and removal of older, uplifted marine deposits on the western coastal lowlands that formed during the early and mid-Holocene. Coastline erosion caused by RSL rise would steepen river gradients, promoting incision. Such incision is seen in many areas by the truncated nature of the lower portion of alluvial fans that formerly were graded to a lower-than-present sea level. Such a sequence of events would place the formation of Ferdie Old Spits (FOS) and Ferdie Barrier Islands (FBIs) around the same age as the erosion of a small scarp in NE Petuniabukta that divides the Ebba spit-platform and the last late Holocene beach (Ebba LH-I beach from Chapter 7).

As suggested in Chapter 7, it is also possible that some of the late Holocene RSL rise may be the result of local reloading of the Earth's crust due to a late Holocene increase in ice cover in central Spitsbergen (FEYLING-HANSEN 1955). In his study of Cape Napier development in the adjacent Adolfbukta, FEYLING-HANSEN (1955) correlated the recent rise in sea-level with glacier readvance about 2500 years ago. This is a timing of the first 'glacial maxima' reached by several small valley glaciers and tide-water glaciers in



Isfjorden that started to form around 3000-4000 years ago, after the potential full melt-out that occurred due to the Younger Dryas-Holocene warming (SVENDSEN and MANGERUD 1997). It is, however, widely accepted that Spitsbergen glaciers reached their Holocene maximum extent during the second late Holocene 'glacial maxima' that occurred during the Little Ice Age (e.g. BARANOWSKI and KARLÉN 1976; WERNER 1993; SVENDSEN and MANGERUD 1997; MANGERUD and LANDVIK 2007; RACHLEWICZ 2009; MAJEWSKI *et al.* 2009). The local reloading of the Earth's crust during the LIA would then be potentially greater during the LIA than during the '2500 BP' event.

Under this scenario, it is possible that the formation of the Ferdie Spit I initiated during the LIA when the sea transgressed the Ferdie Fans and used the sediments eroded from the shoreface to build a barrier that subsequently migrated onshore and started to extend laterally. This is consistent with one of the common models of barrier formation during RSL rise that suggests that spit elongation is the main driver of barrier onshore development (ORFORD 2004).

Studies of mid-latitude paraglacial coasts show a general tendency of inland migration of swash-aligned gravel-dominated barriers with rising sea-level (CARTER and ORFORD 1993; FORBES *et al.* 1995). For drift-aligned barriers, development is largely a function of sediment supply. Reworking of updrift portions of spits can release sediment via cannibalisation of older beach deposits, but if sufficient sediment is lacking, then drift aligned barriers may breakdown and be redistributed entirely (ORFORD *et al.* 1991). The planform of FSI provides important support for the suggested LIA timing of spit formation. Figure 6.22 shows that, despite the accumulation of overlapping recurves, the planform of FSI remained rectilinear and, in general, FSI has the straightest shape from among the three Ferdie Spits. According to CARTER and ORFORD (1991), this is a diagnostic feature of a drift-aligned spits formed by high volume but episodic sediment supply. During the LIA, the sediment supply to NW Petuniabukta was limited to high magnitude/low frequency pulses associated with snow-melt and summer discharge. The episodic deposition of spits may also have been linked with prolonged sea-ice conditions during the LIA that bounded the fjord for the most part of the year. This probably limited the period of storm wave operation and shortened the time for sediment transport and deposition by waves.

The geomorphological evidence presented in this study provides some evidence to support post-LIA RSL fall. First, as noted above, RSL fall may have increased the incision of Old Ferdie Fan 2 that allowed the shift of the main channel of Ferdinandelva towards

the second bedrock gorge G2 and the enlargement of Ferdie Fan 4. The incision was also enhanced by an increase in elevation of the retreating glacier snouts which, in turn, increased river length and the stream gradient. The post-LIA lowering of the Ferdinandelva base-level and associated incision of Ferdie fans resulted in the delivery of a large volume of paraglacial sediments stored in ice-marginal, proglacial and alluvial zones – the material that fed Ferdie Spit 2 and Ferdie Spit 3.

Post-LIA rebound could also partly explain the observed height difference between the crests of three Ferdie Spits (crest of FS1 is located *ca.* 0.4 m higher than FS2 and *ca.* 0.8 m the youngest FS3) and the shifting of spits towards the NE. If spits had formed on the submerged Ferdie Fan 3 surface, their formation would be diametrically different to the formation of spits in the mouth of Ebbaelva along the NE Petuniabukta coast.

In Chapter 5.3, the evolution of Ebba spits was associated with the formation of an enlarged submarine spit-platform that developed in pace with tidal flat progradation and the Ebbaelva ebb-tide delta. The deposition of this submarine structure controlled the rate of growth and direction of migration of Ebba spits, whereas the migration of Ferdie Spits could be related to the process of spit adjustment to Ferdie Fan 3 relief. Once spits reached the muddy tidal flat, they behaved similarly to Ebba spits and started a southern migration together in tandem with the prograding tidal flat.

The lowering of river base-levels and accumulation of the Sven-Hørbye-Ragnar outwash plain to the north of the tidal flat may also explain the increase in erosion of tidal islands and the incision of new tidal channels during the last 50 years. This is different to the patterns observed on mid- and low-latitude coasts where changes in creek density, sinuosity, and headward erosion are often linked to RSL rise, high tide frequency or storm surges e.g. tidal network changes in Venice Lagoon (RIZETTO and TOSI 2012), Dyfti Estuary in Wales (SHI *et al.* 1995) or marsh creek changes in Southern Carolina (HUGUES *et al.* 2009). Similar changes to those observed in Petuniabukta (tidal channel migration and erosion) occurred also in the Braganzavågen tidal flat between 1990-2009 (FAUCHERRE 2011), suggesting that the recent evolution of tidal flats in central Spitsbergen fjords is dynamically responding to some of the external controls such as post-LIA land-rebound.

The discussion above has identified a strong link between decadal shifts in climate and coastal evolution in Petuniabukta. Post-Little Ice Age coastal evolution was characterised by dramatic changes in sediment delivery and by the formation of coastal landforms associated with a warming climate, retreating local ice masses, a shortened

winter sea-ice season and melting of permafrost. Figure 8.5. summarises the interactions between climate change and paraglacial coastal evolution during and after the LIA, based on observations from this study.

This model emphasises the role of climate in controlling sediment supply to the coastal zone. Thus, under cooler conditions (blue in Figure 8.4.), sediment supply to the coast falls and coastal erosion occurs, whereas under warmer conditions (red in Figure 8.5.) the opposite occurs.

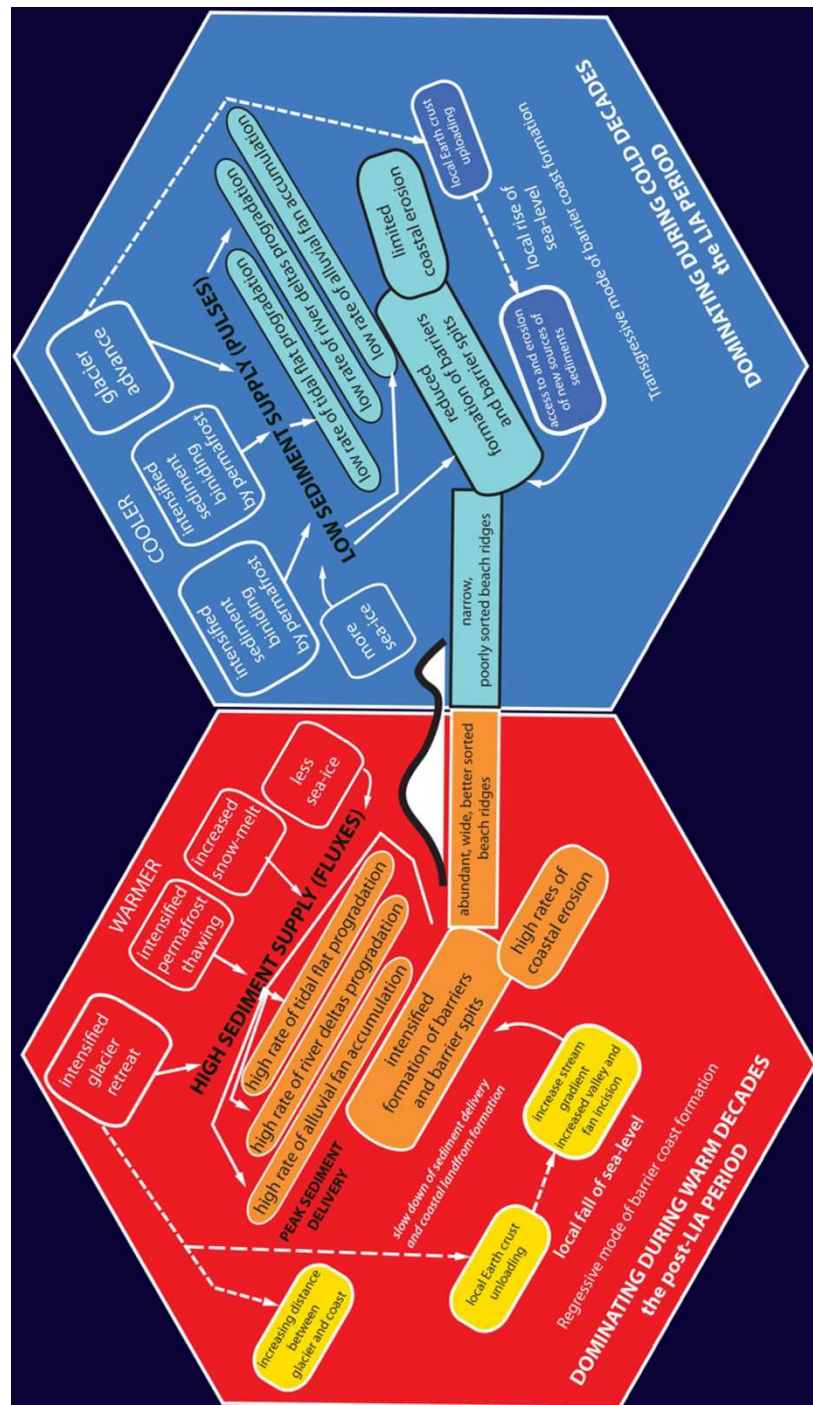


Figure 8.5. Scenarios of High Arctic coastal change over century-timescales. Note the emphasis on climate as a key driver.

As with the model depicting interannual changes in coastal development, it is important to note that variations in the intensity of terrestrial processes may complicate this model by, in particular, causing the erosion and modification (burial, or destruction) of coastal landforms. Thus, structures formed by shoreline progradation may not always persist in the landscape as geomorphologically resilient landforms over timescales of several millennia. Conversely, mantling of coastal deposits by slope deposits may, as observed at the famous site of Kapp Ekholm a short distance from the study site (see Figure 7.9. for location), actually preserve coastal landforms for hundreds of millennia, even when overlain by glaciers.

## 8.4 MILLENNIAL TIMESCALES: MECHANISMS CONTROLLING LATE HOLOCENE RELATIVE SEA-LEVEL CHANGE AND COASTAL EVOLUTION IN PETUNIABUKTA

### 8.4.1 Dating Arctic raised beaches with marine molluscs

Marine molluscs are only one potential source of data for constraining the ages of raised beach deposition and reconstructing RSL records in the High Arctic.

BONDEVIK *et al.* (1995) report 81 radiocarbon dates from mostly driftwood and whalebone with a smaller number of mollusc samples ( $n=10$ ) from Edgeøya and Brentsøya (Svalbard) (Figure 8.6.). They compare paired sample ages derived from driftwood and whalebone from several sites and demonstrate a close agreement. For example, on Humla they report radiocarbon ages of  $9240 \pm 55$  (T-9888) and  $9125 \pm 130$  (T-10803) for samples from the same beach. Their preference for driftwood as the main dating material reflects the fact that it floats and becomes stranded at high tide level, with storm waves throwing it further up and either burying it in the beach or leaving it on the surface.

By dating the youngest, outer part of each sample, BONDEVIK *et al.* (1995, p. 153) generate what they describe as “some of the most precise sea-level curves from the Arctic”. They further argue (p. 164) that because shells live below sea-level and provide a minimum estimate of former sea-level they are “normally not suitable as sea-level indicators in these regions”. This statement is certainly valid when considered in the context of sea-level data derived from mixed shell samples analysed using conventional radiocarbon dating. Both reworking of old material and uncertainties in relating the ages of such deposits to a former sea-level are illustrated by DONNER and JUNGNER (1975) who dated replicate 100-200 g samples of mixed shells from five raised beaches in Disko Bugt (west Greenland). In two instances, the paired samples from a single beach, which were of mid Holocene age, had age differences  $>2400$   $^{14}\text{C}$  years. RSL in west Greenland was falling at  $> 10$  m per thousand years at this time and this age range introduces significant uncertainty when using these data for RSL reconstruction. However, the application of AMS radiocarbon dating in the late 1980s and early 1990s, which enables the dating of individual shells, has significantly reduced (but not eliminated) the potential difficulties associated with dating shells from raised beach deposits.

In northern Spitsbergen, BRÜCKNER *et al.* (2002) find close agreement between AMS-dated paired samples of *Mya truncata* collected in their living position in sub-littoral sands that are overlain by beach sands that yielded ages of  $10079 \pm 81$  (Hd-20790) and



10031±77 (Hd-20822). In the Sisimiut area of central West Greenland, PETERSEN and HOCH (2004) report four AMS dates from samples of *Mytilus edulis* (n = 2), *Hiattella arctica* and *Littorina saxatilis* from a raised beach that range in age between 3020±50 (AAR-3583) and 3570±60 (AAR-3582). This age range is slightly larger than that observed in three samples of *Astarte borealis* from LH-2 (4188±37 (SUERC-33589) to 4314±37 (SUERC-35587).

An important difference to the approach applied here and that proposed by others (e.g. BRÜCKNER *et al.* 2002) is that emphasis was placed not on searching for datable *in situ* shells – but, in fact, to date samples that have been transported from their original subtidal life position onto the beach crest under storm conditions. By focusing on small, delicate, articulated samples that cannot have been reworked or transported long distances, the potential effects of reworking were significantly reduced. Because the samples, like driftwood, are deposited close to the top of the storm beach, they also provide good sea-level indicators.

In order to check its precision, the presented shell-based record from the Ebbadalen was compared with driftwood-based datasets from a site on Humla (Figure 8.6.), one of the four sites studied on Edgeøya by BONDEVİK *et al.* (1995) and selected for comparison because of its excellent Holocene driftwood RSL history. Visual comparison of the data confirm that the *Astarte borealis* data provide RSL data of comparable quality, in terms of age and height scatter, to those from driftwood. BONDEVİK *et al.* (1995) summarise their RSL data using a second or third order polynomial, citing a  $R^2$  of 0.97-0.99 for the four records that they present.

Using a similar approach, the  $R^2$  for a second order polynomial from the Petuniabukta data is 0.99 (Figure 7.8.). It can be assumed that carefully collected samples of *Astarte borealis* have the potential to be as good as driftwood for RSL reconstruction in the High Arctic waters of the Svalbard Archipelago.

There are other advantages and limitations to the approach applied in this study. As with all studies that use marine carbonate for  $^{14}\text{C}$  dating, assumptions must be made about the marine reservoir effect and the appropriate  $\Delta R$ . The latter is based on only four samples and, as noted in the consideration of cod otolith bomb spike comparison, the interpretation would be stronger if an equivalent record using known age 20<sup>th</sup> century samples of *Astarte borealis* was determined. Secondly, the approach will only work elsewhere if shells are present in the beaches under study. For instance, in summer 2012 I had a chance to investigate gravel-barriers in Bellsund (W Spitsbergen) which were almost

completely devoid of shell detritus. Inspection of uplifted beach ridges spanning between 1-3 m above MTL also revealed an absence of datable shell material.

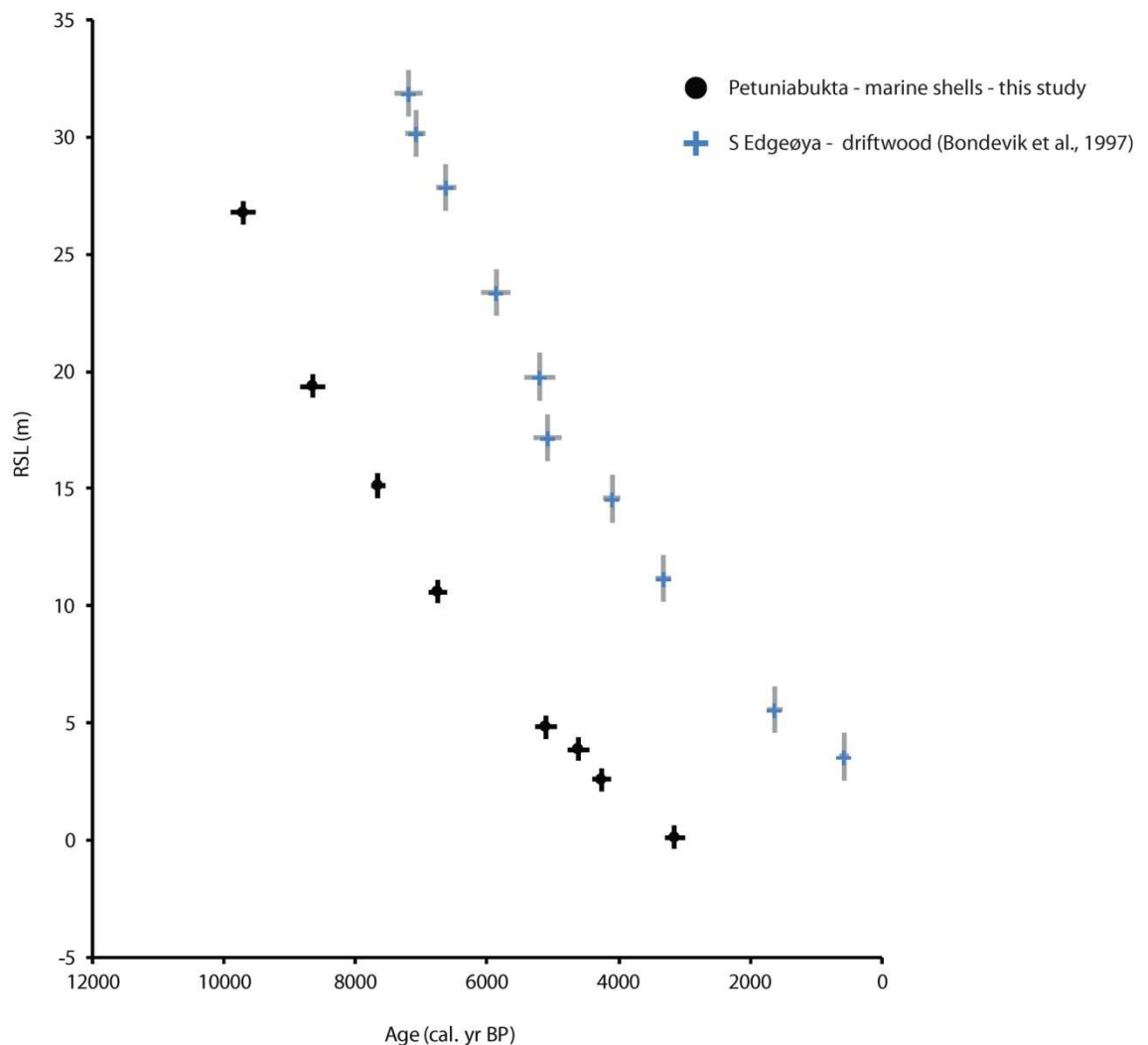


Figure 8.6. A comparison of the relative sea-level records developed from this study, based on marine shells (*Astarte borealis*) and a record from southern Edgeøya based on driftwood (BONDEVIK et al. 1995). Note that the precision of both approaches is similar, demonstrating the potential for shell-based chronologies to perform well when based on carefully collected material.

As described by FEYLING-HANSEN (1955), *Astarte borealis* is dominant in the mid and late Holocene raised beach sequences of Billefjorden, is common in Svalbard (FEYLING-HANSEN 1955), and is recorded elsewhere in the High Arctic (e.g. BLAKE 1976; ENGLAND 1997). However, *Astarte borealis* is only recorded in the Billefjorden area below 34.5 m, which equates to an age of *ca.* 10,000 cal. yr BP, whereas driftwood and whale bone is recorded in higher and older sequences (e.g. SALVIGSEN 1981).

Perhaps the most exciting potential application of the method presented here is to target the collection of *Astarte borealis* specimens from individual beaches within a beach

ridge complex and thus develop detailed chronologies for their formation. The Ebbadalen beaches are remarkably well preserved between LH4 (ca. 5100 cal. yr BP) and LH1 (ca. 3100 cal. yr BP). During this period, over 80 individual storm beaches formed (Figure 8.7.).

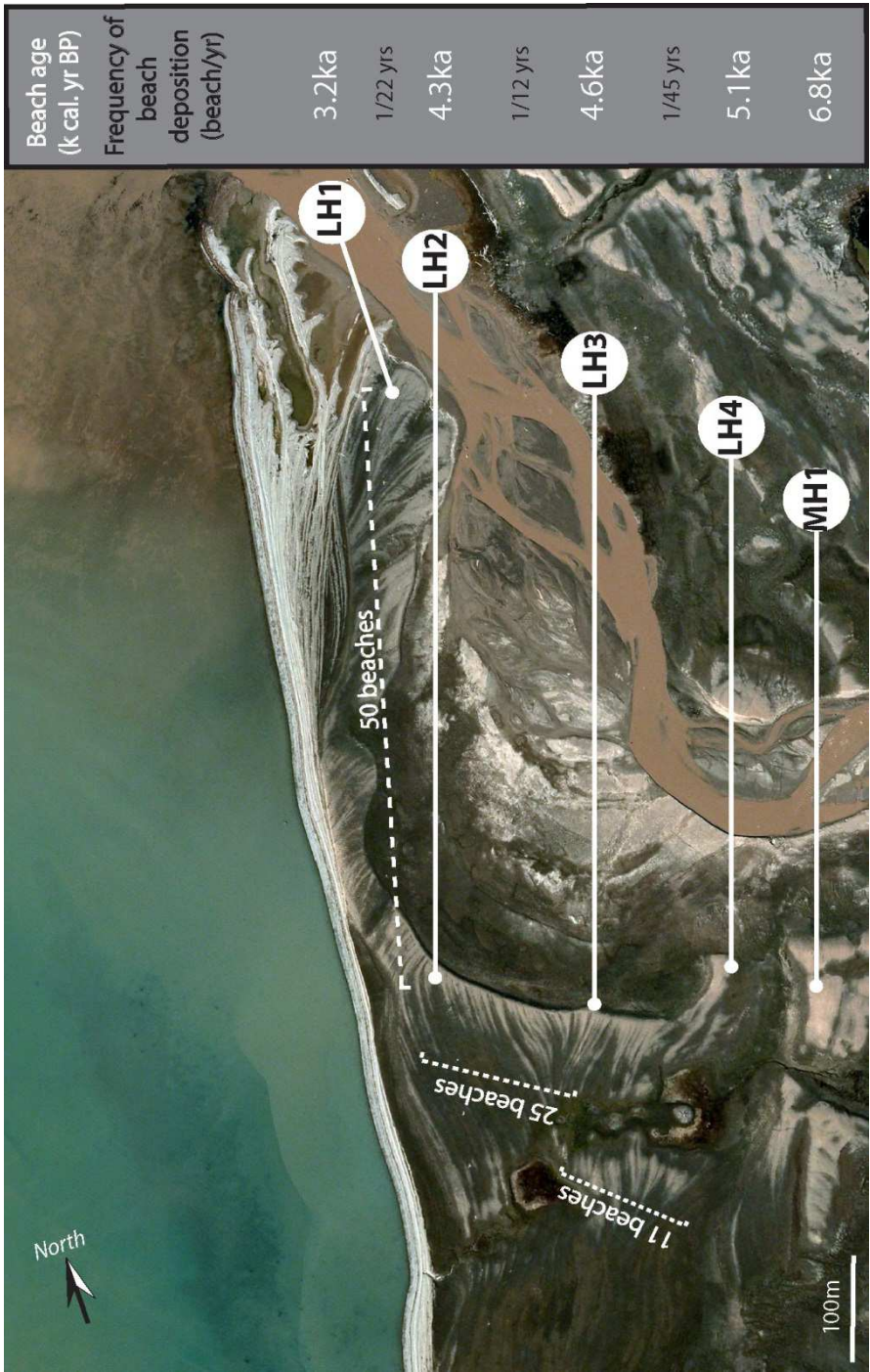


Figure 8.7. Estimated frequency of beach ridges deposited during the last ca. 6000 cal. yr BP based on the chronology provided by samples of *Astarte borealis*.

Taking the mid-point of each of the four calibrated radiocarbon dates from this series, it is clear that the frequency of beach ridge deposition is initially slow, with one forming

every *ca.* 45 years between *ca.* 5100 and 4600 cal. yr BP. However, from this point onwards the rate of beach formation more than doubles, with one beach forming every *ca.* 22-17 yrs between *ca.* 4600 and 3100 cal. yr BP. The cause of this change is not certain, but it likely reflects a change in one or more of: the rate of RSL fall; sediment supply; sea-ice extent and near-shore water depth. Additional, closer-spaced sampling of this and other comparable sequences in Billefjorden are needed to resolve this issue further.'

#### 8.4.2 Implications for the former Svalbard-Barents Sea Ice Sheet

FORMAN *et al.* (2004) summarised the RSL history of Svalbard in 25 individual RSL curves. This analysis concluded that the former centre of the Svalbard-Barents Sea Ice Sheet was probably located in the northwest of the Barents Sea, to the southeast of Kong Karls Land (Figure 8.8.) in agreement with a number of previous studies (SCHYTT *et al.* 1968; BOULTON and RHODES 1974; FORMAN 1990; BONDEVİK *et al.* 1995; SALVIGSEN *et al.* 1995; LAMBECK 1995, 1996). However, recently this model has been challenged and two alternative models proposed that envisage:

- *a major ice dome located on easternmost Spitsbergen or southern Hinlopen Strait (DOWDESWELL et al. 2010);*
- *additional smaller local cold-based ice domes over Nordaustlandet (HORMES et al. 2011) (Figure 8.8.).*

The DOWDESWELL *et al.* (2010) model is based on the interpretation of flow directions inferred from streamlined submarine bedforms. DOWDESWELL *et al.* (2010) also argue that this location is consistent with raised beach data from Kong Karls Land (Figure 8.8.), noting that the highest shorelines in west Kong Karls Land described by SALVIGSEN (1981) are *ca.* 20 m above the highest shorelines in the east of the islands, implying a maximum ice load to the west. The latter, multi-centre ice dome model is based on field evidence and cosmogenic radionuclide dating from Nordaustlandet (glacial striae and erratic boulders with known source regions) (HORMES *et al.* 2011).

In order to compare new RSL record from Billefjorden with records from sites that are close to the different ice domes described above three places were selected: Edgeøya (Humla) (BONDEVİK *et al.* 1995), Kong Karls Land (SALVIGSEN 1981) and south Nordaustlandet (Svartknausflya) (SALVIGSEN 1978). They are chosen over other sites because of the quality of their RSL records which are based on numerous well-dated driftwood samples that have an excellent height relationship to former sea-level (Figure 8.8.a).

As previously explained, the altitudes of the driftwood samples were reduced to MTL by correcting for the current height difference between MTL and the present storm beach (Humla 2.8 m, Kong Karls Land 3 m, south Nordaustlandet 2.7 m – this is an estimate based on the lowest altitude cited by SALVIGSEN (1978) for driftwood above present mean tide level).

The small age and height scatter in the combined RSL data enables the differentiation of distinct RSL trends between sites that are consistent over much of the Holocene and enable testing of the different ice dome models outlined above. The combined RSL data shows that all of the data from sites in eastern Svalbard plot above new observations from Billefjorden (Figure 8.8.a). This indicates a thick Late Weichselian ice load over the east Spitsbergen/north Barents Sea area as previously proposed (e.g. BONDEVIK *et al.* 1995; LANDVIK *et al.* 2005). The Kong Karls Land data plot above comparable data from the other sites. This is contrary to what would be expected with a large ice dome centred over easternmost Spitsbergen or southern Hinlopen Strait.

DOWDESWELL *et al.* (2010) cite the shorelines on Svenskøya (east Kong Karls Land) as additional evidence for their model, but there are only two Holocene dates from these (Figure 8.8.a) (SALVIGSEN 1981). It is hard to be persuaded that these dates and the other undated shorelines can be used to infer greater ice to the west of Kong Karls Land. The trend in the RSL data from south Nordaustlandet suggest that RSL reached close to present during the late Holocene, about a thousand years or so after it did so in Petuniabukta. In contrast, the data from Kong Karls Land and north Edgeøya indicate RSL was above mean tide level throughout the Holocene at these sites. Considered together, the Kong Karls Land RSL data are not compatible with a significant ice dome located over easternmost Spitsbergen or southern Hinlopen Strait. Rather, these and the other RSL data presented in Figure 8.8. are more readily explained by a large ice dome over or close to Kong Karls Land, as proposed previously.

*Figure 8.8. (next page) a) Relative sea-level data from central and eastern Svalbard. Sample elevations are adjusted for the current height difference between MTL and the present storm beach cited in the original publications (Humla 2.8 m (BONDEVIK *et al.* 1995), Kong Karls Land 3 m (SALVIGSEN 1981), south Nordaustlandet 2.5 m (SALVIGSEN 1978). b) Reconstructed Svalbard–Barents Sea Ice Sheet domes and ice flows (LANDVIK *et al.* 1998; DOWDESWELL *et al.* 2010). DOWDESWELL *et al.* (2010) identify two potential ice domes based on the glacio-isostatic rebound modelling of LAMBECK (1995, 1996) (blue dashed circle) and from their own marine geophysical data (red dashed circle). The ice domes proposed by HORMES *et al.* (2011) over Nordaustlandet are also shown (green dashed circles).*



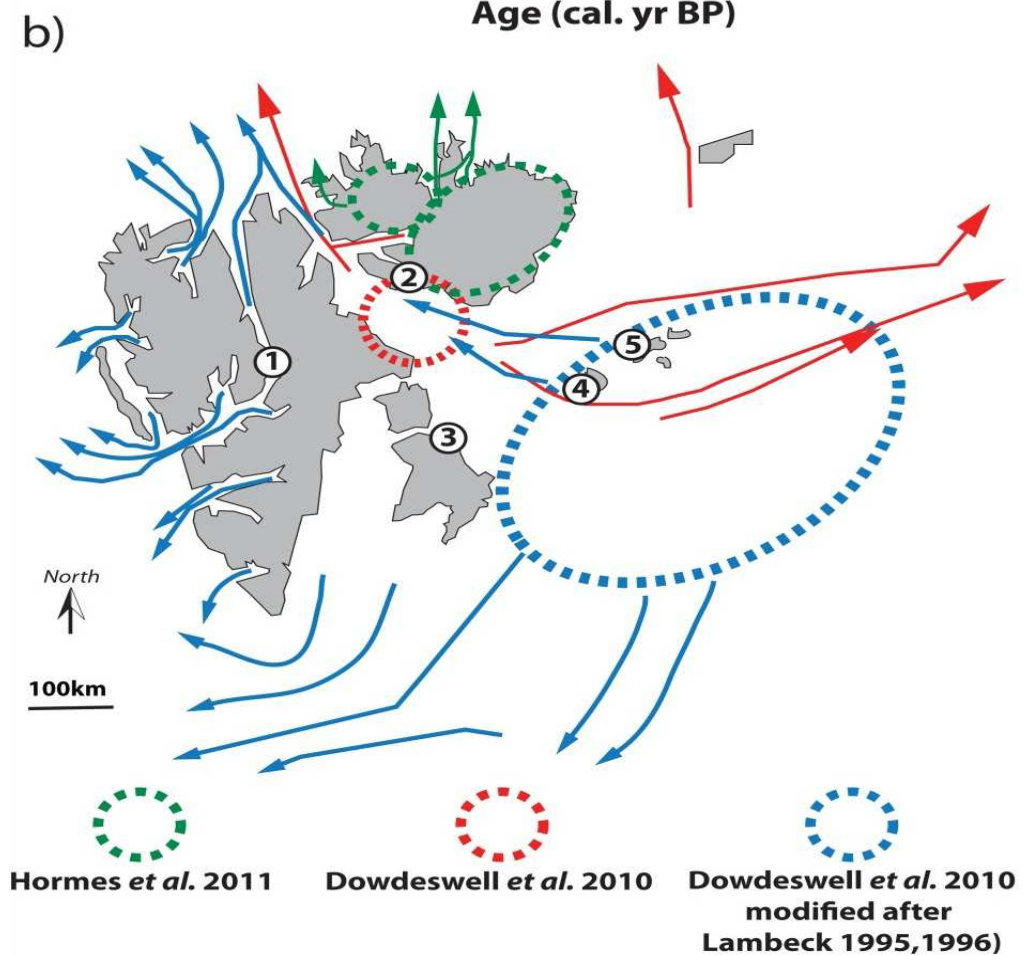
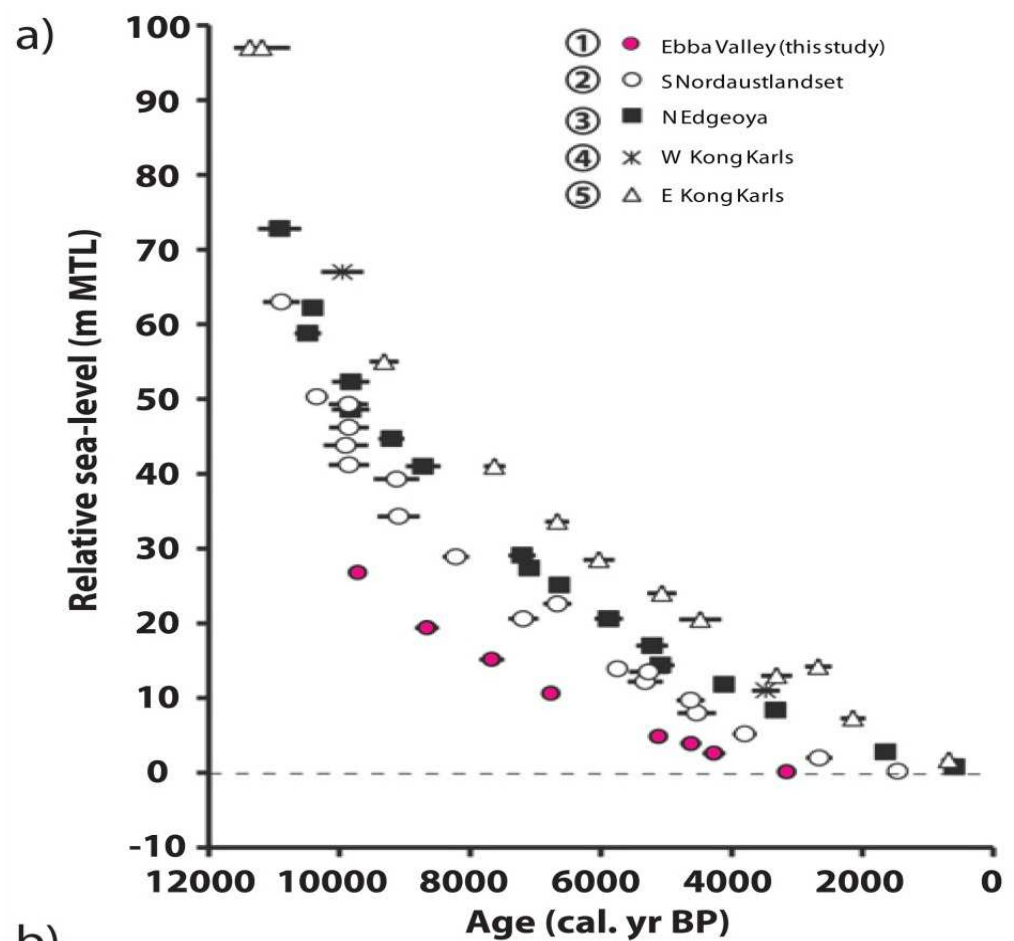


Figure 8.8.

The possibility of several smaller domes remains (HORMES *et al.* 2011), including the potential for topographically-routed warm-based ice associated with these domes shaping the bedforms described by DOWDESWELL *et al.* (2010), but their associated ice loads were too small to modify the regional patterns in RSL described above. Alternatively, it is possible that the bedforms identified by DOWDESWELL *et al.* (2010) originate from a smaller ice dome in Hinlopen that formed at some stage of deglaciation and have been superimposed on the pattern produced by the large ice dome located to the southeast.

This chapter has discussed the late Holocene RSL changes in Petunibukta and explained their implications for the rate and mode of the beach ridge system development. Figure 8.9. summarises the interplay between environmental forcings that control the evolution of High Arctic coasts over these timescales.

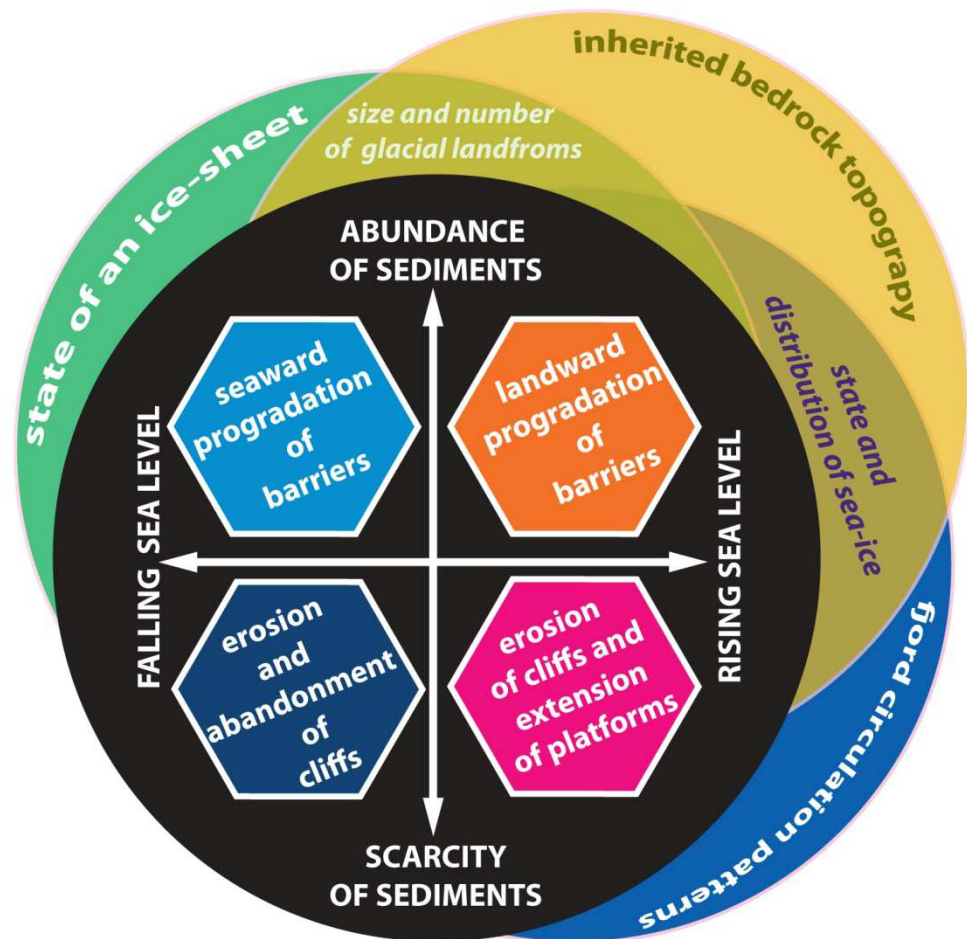


Figure 8.9. Scenarios of High Arctic coastal change over millennial –timescales.

In particular, the model emphasises the key role of sediment supply and RSL, as observed in temperate latitude coastal environments, as key controls on coastal evolution over these timescales. However, in addition, the model shows the importance of other factors

that are peculiar to the High Arctic and which necessitate revision to existing models of paraglacial coastal change, notably the role of bedrock topography in controlling coastal response, as well as the nature and distribution of glacial landforms, the state of the cryosphere in the study area, sea-ice extent, and fjord circulation patterns. As in the previous models discussed above, this summary must also recognise that gravel and sand barriers are inherently unstable landforms in many parts of the study area, liable to reworking by both marine and terrestrial processes in many contexts except those that specifically encourage the deposition and preservation of landforms.

## 8.5 A NEW MODEL FOR PARAGLACIAL COASTAL EVOLUTION IN THE HIGH ARCTIC

The paraglacial concept integrates research on landscape recovery from glaciation and links the high latitude and lower latitude studies on the re-establishment of non-glacial processes as the dominant drivers of landscape inherited after the retreat of ice sheets and glaciers at the end of the last glacial maximum.

BALLANTYNE (2002) claimed that since the wider application of the term in geomorphology and Quaternary science, which began in the mid 1980s, no other aspect of paraglacial research has advanced so fruitfully as the coastal element. Although the first 'paraglacial coast' study was probably provided by JOHNSON (1919), who described the role of reworking of glacial landforms (drumlins) in the development of barriers in Boston Harbour and the Massachusetts Bay, the proliferation in recent paraglacial coastal studies is attributed to DONALD FORBES, JAMES SYVITSKI, RICHARD CARTER, JULIAN ORFORD and their co-workers who have worked extensively along the gravel-dominated coasts of Atlantic Canada, Ireland and on fjord geomorphology in the 1980s and 1990s.

FORBES and SYVITSKI (1994, p. 376) defined paraglacial coasts *'to be those on or adjacent to formerly ice-covered terrain, where glacially excavated landforms or glacigenic sediments have a recognisable influence on the character and evolution of the coast and nearshore deposits'*.

Under this definition, paraglacial coasts encompass a large range of coastal environments previously covered by the last major glaciation and in the northern hemisphere include Greenland, parts of the North American Pacific and Atlantic coasts, Iceland, the majority of High Arctic archipelagos, much of north-western Europe, and the coasts of the Baltic Sea. Another glacial aspect (apart from presence of glacigenic sediments and glacial landforms) linking these regions is the effects of glacio-isostasy which directly controls RSL change and the accessibility of the sea to sediment sources.

FORBES *et al.* (1995) proposed the first evolutionary typology of coasts formed in paraglacial environments and argued that their development is dependent on the following factors: (I) physiographic and geologic setting; (II) RSL change; (III) sediment (glacigenic) supply; (IV) climate, and; (V) tides and river discharge. It is noteworthy that the major developments in our understanding of paraglacial coastal system were achieved along the coasts of Ireland (Figure 8.10.), NE United States and Atlantic Canada (BOYD *et al.* 1987; FORBES and TAYLOR 1987; CARTER *et al.* 1989; CARTER *et al.* 1990; ORFORD *et al.* 1991a, b;

CARTER *et al.* 1992; ORFORD *et al.* 1992; SHAW *et al.* 1990; SHAW and FORBES 1995; FORBES *et al.* 1995 a, b; ORFORD *et al.* 1995 a, b; ORFORD *et al.* 2002).

These are coasts that develop by the reworking of inherited sources of glacialigenic sediments, thus transforming relict glacial landforms into active coastal landforms until their full destruction (Figure 8.11.). Presently, the majority of mid-latitude paraglacial coasts have already adjusted to non-glacial conditions and their evolution is therefore controlled mainly by trends in RSL, the availability of sediments and the energy of the surrounding body of water.

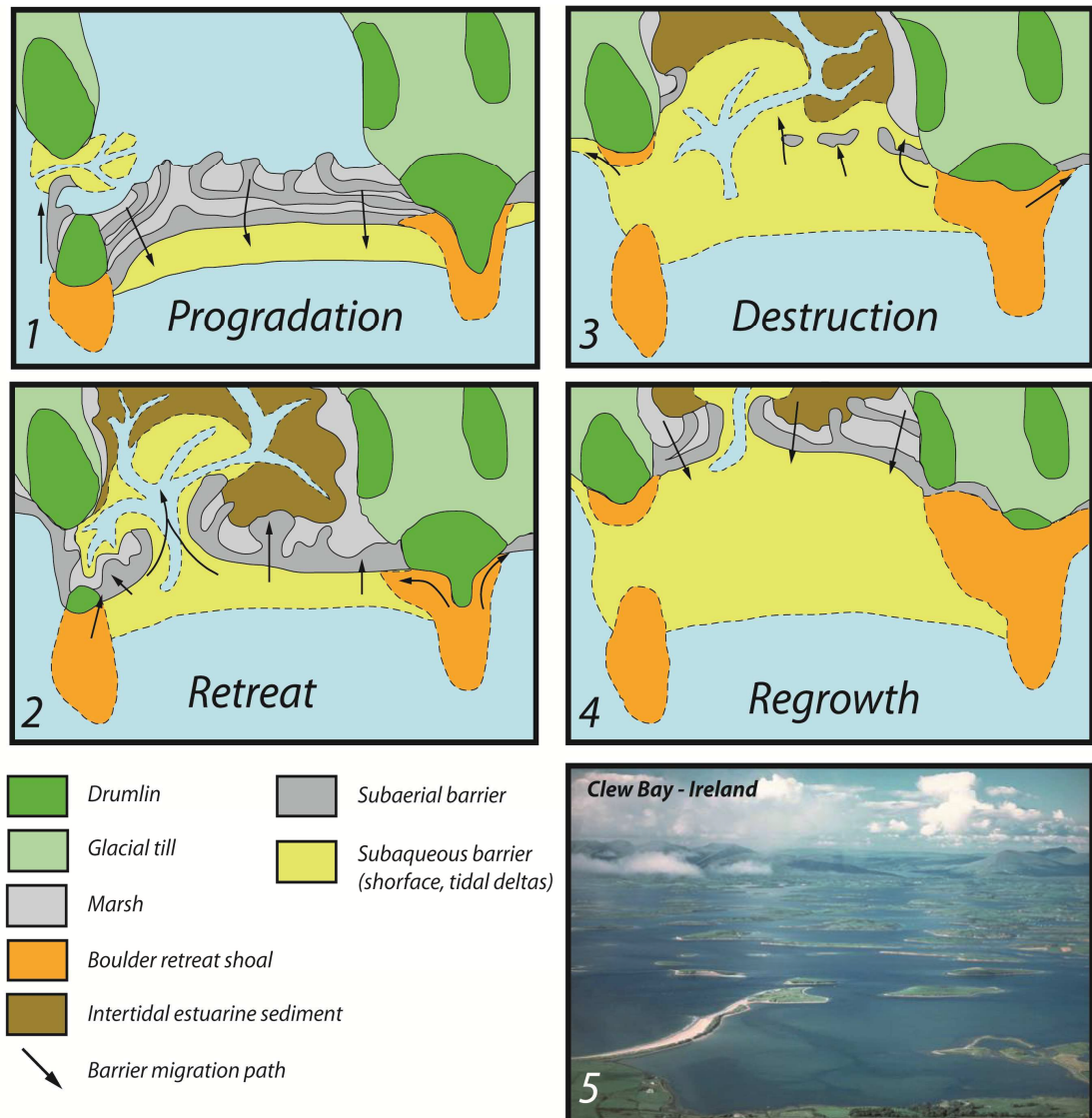


Figure 8.10. Cycle of formation, destruction and re-formation of paraglacial barrier systems according to BOYD *et al.* (1987). Phase 1 - Reworking of glacialigenic deposits by coastal processes and progradation of barrier system. Phase 2 - Retreat of barrier begins after a decrease in sediment supply; sediments are lost due to washover and trapped in dunes and tidal inlets. Phase 3 - Destruction of the initial barrier system. Phase 4 - Regrowth of a new barrier system from reworking of new sediment sources. Image no. 5 is an example of a paraglacial coast formed by reworking of drumlins - Clew Bay, Ireland, photo source <http://number1poet.files.wordpress.com/2011/06/clew-bay.jpg>



In the High Arctic, coastal zone development is strongly linked with climate-driven processes including ongoing deglaciation and sediment fluxes from still actively forming glacial and periglacial landforms e.g. moraine belts, outwash plains, talus slopes, alluvial fans.

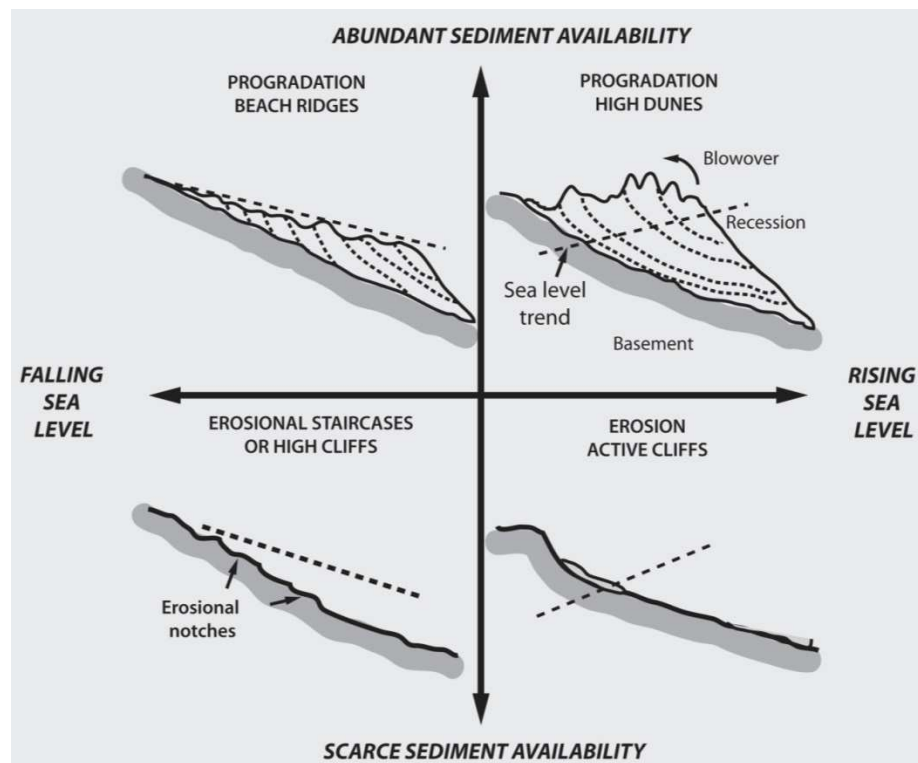


Figure 8.11. Major controls on mid-latitude paraglacial coastal progradation or recession: the rate and direction of sea-level change and the availability of sediments. Modified from CARTER et al. (1987).

A classic example of the strong linkage between High Arctic coastal evolution and climate-driven change of sediment delivery is the study carried out by NIELSEN (1992) in West Greenland. Here, the climate warming intensified the retreat of the tide-water glacier Equip Sermia and led to the formation of new coastal landforms. The reworking of a lateral moraine into a barrier spit and the formation of a lagoon system occurred in just 70 years. NIELSEN (1992) argued that such a rapid landform transformation has serious implications for Holocene landscape interpretation. The retreat of Mitdluagkat Glacier released significant amount of sediments that led to delta progradation and the formation of a range of depositional landforms including spits, barriers, tidal islands and tombolos. Over time, paraglacial sediment delivery fell and wave action under rising RSL rose in importance and delta degradation began. Similar coastal processes have been described along the W and S coasts of Spitsbergen (e.g. MERCIER and LAFFLY 2005; ZIAJA *et al.* 2009; ZAGÓRSKI *et al.* 2012) emphasising the role of continuous glaciofluvial sediment delivery from the proglacial zone to barrier progradation, as well as the influence of tidewater glacier retreat on increased rates of coastal erosion.

Climate warming triggers a complex glacier response and hence sediment delivery to the coastal system. In general, glacial systems produce significant amount of sediments during both advance and retreat phases, but as shown by KOPPEs and HALLET (2002), the erosion and transport of sediment is greater during the latter.

On the one hand, current PhD study showed that the accelerated glacier retreat and increasing precipitation results in enhanced river discharge and associated sediment delivery to the coast. On the other hand, it was also noted that retreating glaciers build-up extensive outwash plains that function as intermediate sediment storage systems that can delay delivery of material to the coast. These outwash plains become an important source of aeolian sediments which are being transported towards the coasts and fjords.

The critical phase of this sediment cascade is the period when the retreating glacier system exceeds the moment of peak sediment production and when glacial-fed rivers, with reduced discharges, lose their high sediment transport capacity. At this moment, the significance of secondary sediment sources (inherited glacial landforms, slope sediments, reworking of previously developed coastal depositional features) come into prominence. The coastal zone starts to be dependent on the rejuvenation of paraglacial sediment delivery caused by extrinsic perturbations (e.g. RSL change, catastrophic landslides etc.) until the non-glacial sink-to-source system adjusts to the new (steady) environmental conditions. This is the case of deglaciaded fjords and catchments of British Columbia, Alaska, New Zealand or Chile (SYVITSKI *et al.* 1987; HOWE *et al.* 2011). In contrast, the High Arctic fjords of Svalbard are still in a phase typified by the overlapping effects of paraglacial adjustment to deglaciation from the Last Glacial Maximum and most recent period of glacial dominance over the landscape – the Little Ice Age (SZCZUCIŃSKI *et al.* 2009; FORWICK and VORREN 2011).

Mid-latitude paraglacial coasts that were often formed by RSL rise and submergence of coastal lowlands are commonly characterised by gentle slopes and shallow nearshore zone, whereas the High Arctic coasts are often dominated by high relief fjord topography. This is an important factor that controls the wave climate and the accommodation space for sediments delivered to the coastal zone. For instance, the barriers formed by ocean waves that approach gentle slopes tend to be wider and thinner than along the coasts with steep slopes where their thickness and height increases (ST-HILAIRE-GRAVEL *et al.* 2010).

The climate amelioration that followed the last glaciation ended periglacial processes that once operated on glacial sediments in mid-latitude sites and led to the

complete melt out of permafrost. In contrast, frozen ground is an essential ‘*sediment binder*’ in the High Arctic today.

High Arctic barrier morphology is also influenced by sea ice processes which are very limited, if not absent, along present-day mid-latitude paraglacial coasts. This said, the research detailed in this thesis demonstrates that the impact of sea-ice processes is rather ephemeral and the preservation of characteristic ‘ice features’ is limited.

Another significant factor controlling the sediment availability along paraglacial coasts is the presence of vegetation cover. The majority of glacial landforms in the mid-latitudes are covered by mature vegetation, whereas freshly exposed moraines, drumlins, or eskers as well as High Arctic coastal landforms (deltas, spits, and barrier islands) are barren and more vulnerable to washout, wind action or mass wasting. Indeed, vast sections of mid-latitude paraglacial coasts are already in the ‘post-paraglacial period’ and their evolution is no longer controlled by their glacial history (i.e. HEIN *et al.* 2012).

The above discussion highlights the profound differences that exist between the ‘paraglacial’ coasts of Ireland and Canada that formed the basis for development of models of gravel-barrier development, and the conditions that operate in the study area (and elsewhere in the High Arctic), especially those recorded in the post-LIA period of rapid glacier retreat and climate warming (Figure 8.12.).

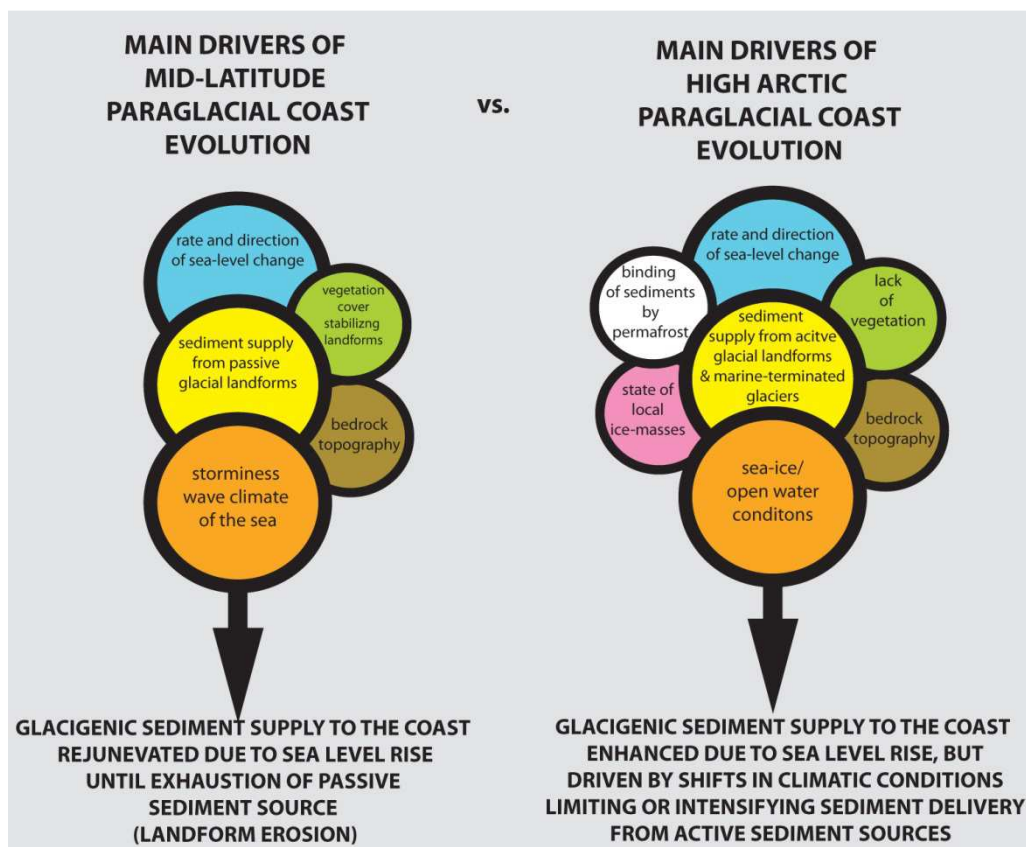


Figure 8.12. Key differences between mi mid-latitude and High Arctic paraglacial coastal evolution.

There are important similarities and differences in the two models proposed above. A common theme that unites the two models is the interplay between sediment supply and the rate of RSL change. It has not been possible in this thesis to quantify the precise relationship between these variables, but it is possible to infer broad relationships based on geomorphological change over different time periods. In particular, in Petuniabukta it is clear that there has been abundant deposition and preservation of raised beaches in the vicinity of the Ebbaelva delta throughout the Holocene, yet elsewhere in Petuniabukta the accumulation of Holocene-age coastal landform complexes is absent. This spatial variability cannot reflect changes in relative sea-level change across such a small area and instead points to local variations in sediment supply (Figure 8.13.).

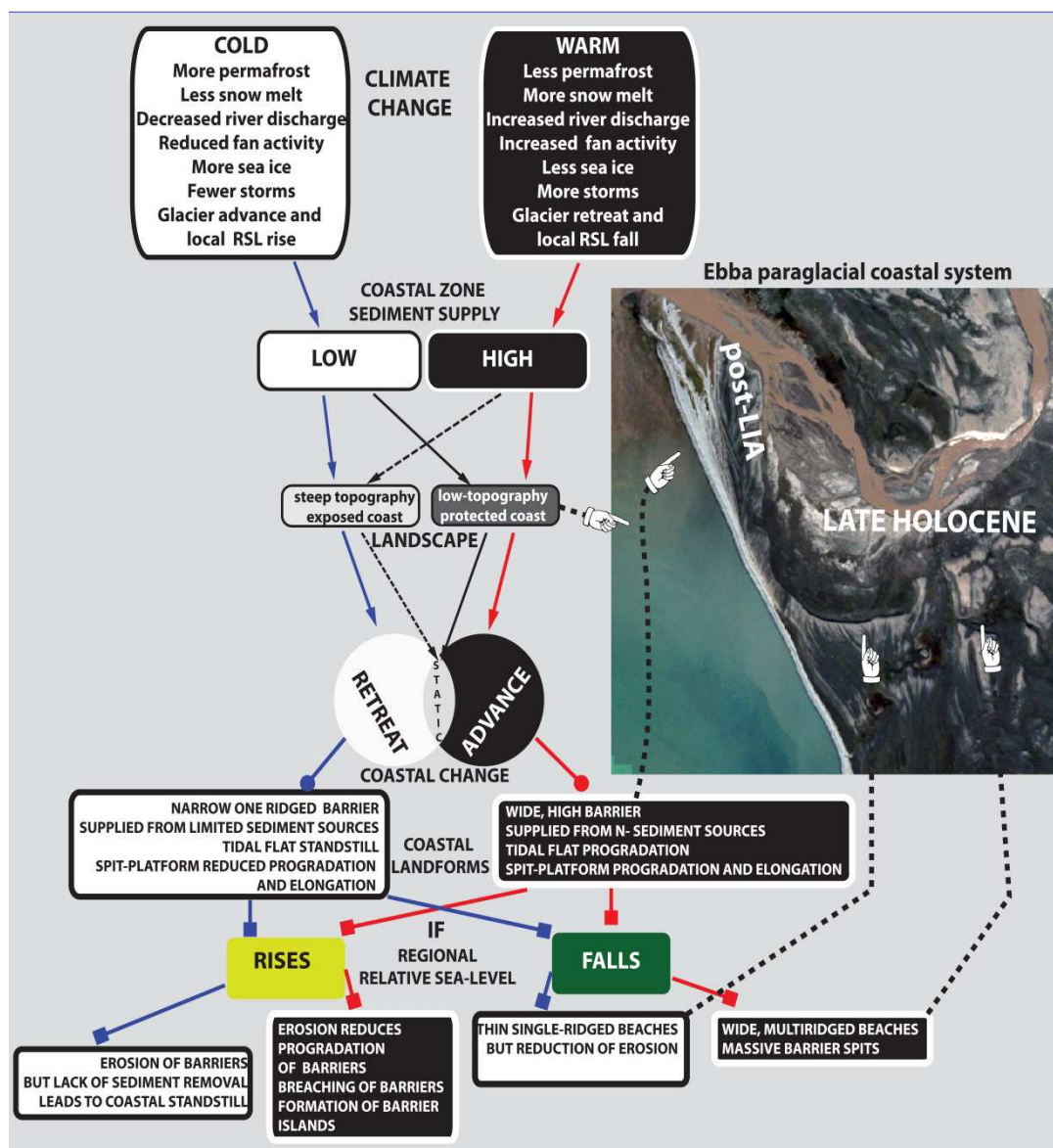


Figure 8.13. Late Holocene evolution of High Arctic paraglacial coastal system at the entrance to Ebbadalen, Eastern Petuniabukta coast – representing a regressive paraglacial coastal system developing in low-angled topography which facilitates the storage of abundant sediments supplied from glacial and non-glacial sources.

In addition, the comparison of the conceptual models above demonstrates that, over time, climate variability is a critical control on sediment delivery to the coastal zone and therefore directly influences local and regional patterns of coastal change. This is less obvious in the mid latitude environments where climate is generally considered as a driver of sea surface variability over different timescales (storms, long term RSL change) rather than a driver of coastal change via terrestrial sediment flux to the coast.

These important differences, as well as the effects of sea ice and permafrost, mean that existing models of paraglacial evolution are not fit for purpose as descriptors of how the beaches in Petunaibukta operate over interannual, century or millennial time-scales. What is proposed here is a model that recognises the primacy of climate change as a key driver of coastal change in the High Arctic. Rather than seen as a means to address issues of coastal management and shoreline response to future sea-level rise, as has been the case in temperate latitude settings. Models of High Arctic coastal evolution provide insights into past climate change as well as lenses through which the interaction of terrestrial and coastal processes can be observed and predicted into the future.



## 8.6 Future research

In this study I have analysed High Arctic coastal zone changes that occurred over three different timescales, looking for their interrelationships and key differences expressed in the formation of landforms and their ability to react to shifts in climate conditions, sediment supply and sea-level.

The research has several wider implications for cold region coastal geomorphology and in particular for work on:

I) Controls on the microrelief of gravel-dominated barriers

*This research has confirmed the relative resilience of Svalbard barriers formed in inner-fjord setting to a lengthening of open water conditions and an increase in storminess detected in other High Arctic settings (St-Hilaire-Gravel et al. 2011). It has highlighted the need for long-term observation of the adjustment of present-day accumulative coasts of Svalbard to continuous decrease in sea-ice cover, thawing of coastal permafrost and intensified sediment supply from unstable slope and deglaciated valley systems.*

II) Controls on rocky cliffs and shore platforms;

*This research has confirmed the existence of “coastal amplification” of rock weathering in High Arctic settings hypothesised in previous studies (Jahn 1961) and has demonstrated the usefulness of Schmidt Hammer Rock Tests in coastal geomorphology investigations in polar regions.*

III) Controls on sediment delivery from glacierised and non-glacierised catchments to the coastal zone;

*This research has estimated the rate of coastal changes that occurred in the northern Billefjorden since the end of the Little Ice Age and has noted the high sensitivity of these systems to fluctuations of air temperature, precipitation and associated shifts in glaciofluvial and fluvial modes of sediment transport. A comparison of coastal changes with those observed along western coast of Spitsbergen has highlighted strong regional contrasts in the response of the coastal zone to the 20<sup>th</sup> century warming and increased storminess.*

IV) Accuracy of RSL reconstructions using uplifted beaches,

*This research has demonstrated a new approach for improving the accuracy of dating uplifted beaches in High Arctic settings using shells of juvenile marine mollusks, especially in those locations where other datable material (driftwood or whale bones) is sparse or have been reworked. This research has also showed that the collection of new RSL data from uplifted*

*beaches is crucial to test different models of ice-sheet configuration based on submarine investigations of ice-streams flow directions or geophysical modelling. This study demonstrates the potential of morphosedimentological properties of gravel barriers to reconstruct past changes in sediment supply and associated climate change.*

Looking ahead, future research in High Arctic coastal geomorphology should:

- 1) Establish a circumpolar coastal monitoring network covering various types of coasts and collecting data according to a common methodology;
- 2) Improve knowledge of permafrost distribution and understand permafrost-related impacts on barrier morphology. Of great interest would be a study of the development of 'young' permafrost on recently deglaciated coasts. This would enable comparative studies of different coastal permafrost properties and their landform impacts across different regions of the Arctic, including NW Canada, Alaska, Siberia and the High Arctic archipelagos;
- 3) Increase efforts to understand the controls on rocky coastal development in lithologies encountered along the varied coasts of Svalbard, Franz Joseph Land, the Canadian Arctic Archipelago and Greenland. It is noteworthy that High Arctic rocky coastlines provide an excellent setting for investigating cliff and shore platform development in periglacial conditions, research that is to date mainly restricted to lake environments, for example in Scotland (SISSONS 1978), Norway (MATTHEWS *et al.* 1986; SHAKESBY and MATTHEWS 1987; AARSETH and FOSGEN 2004) and Canada (TRENHAILE 2004). It is also important to better understand the role of glacial debuitressing on the High Arctic rock cliffs stability as well as the impact of recently delivered paraglacial sediments on erosion and protection of rocky shore platforms;
- 4) Test the different models of paraglacial coastal evolution by observations of barrier coast development along the sections of High Arctic coasts that are characterised by differing rates and directions of RSL change, exposure to storm waves, degree of catchment glacierisation, as well as distance between the coast and the proglacial zone. An ideal area for such a study would be the Canadian Arctic Archipelago where a diversity of coastal landforms and settings exist. Realisation of such a project would allow the testing of scenarios of coastal zone responses to climate change proposed for the Eastern Canadian Arctic by SYVITSKI and ANDREWS (1994);

- 5) Improve our understanding and ability to predict coastal hazards. With growing human interest in the polar regions, and ongoing infrastructure developments concentrated along the coasts, this is a crucial task for Arctic coastal researchers. Among extreme processes that impact directly on the coastal environment and Arctic communities are storms and tsunami waves. Since the second half of 20th century there has been an increase in the number and intensity of storms entering the Arctic (ZHANG *et al.* 2004), particularly in summer months when coastlines are free of their protective ice cover. Recent reports from Greenland on landslide-triggered tsunamis, potentially triggered by warmer air temperatures (PEDERSON *et al.* 2001; DAHL-JENSEN *et al.* 2004), demonstrate that Arctic coasts are vulnerable to such extreme events. Indeed, the unstable nature of polar landscapes in terms of landslides and also the existence of calving glaciers producing icebergs provide abundant potential tsunami sources, especially in fjord-settings where constraining topography can amplify wave heights at the local scale;
- 6) This research and several previous Arctic studies (e.g. FLETCHER *et al.* 1993; RASCH and NIELSEN 1995; MÖLLER *et al.* 2002; BRÜCKNER and SCHELMANN 2002; SANJAUME and TOLGENSBARK 2009; ST-HILLAIRE-GRAVEL *et al.* 2010, FUNDER *et al.* 2011) benefited from dating and interpreting the palaeoenvironmental information recorded in morphosedimentological properties of uplifted beaches. The most common application of High Arctic uplifted beach ridges are reconstructions of RSL change and sea-ice conditions. Future research on relict beach ridges using improved dating methods, such as those presented in this thesis, will help us extract more precise information on past storminess and sediment supply changes and help address the long-standing research question of what processes control beach ridge formation and preservation in High Arctic settings?
- 7) This project has also identified several interesting coastal landforms and processes that to my knowledge have not yet been studied in High Arctic settings:
- a) the development of so-called ‘reversed’ landforms developing in sheltered fjords, in the opposite direction to prevailing wind conditions and surface water circulation patterns (e.g. the Ferdie Spits);
  - b) the mechanisms that control the formation of fetch-limited barrier islands;

- c) the role of seaweed and driftwood incorporation in beach ridge structure;
- d) and the mechanisms responsible for tidal creek network formation and erosion along High Arctic tidal flats.

Aware of the limitations of the research presented in this thesis, and the number of important outstanding research questions listed above, I have been involved in the formation of research teams and the preparation of new research projects during the final stages of this thesis that could further develop some of the issues discussed above. Table A.2 (Appendix 2) summarises the research initiatives that have evolved from my PhD research and provide an indication of the research direction I intend to explore in the future.

## 8.7 Chapter summary

This Chapter has sought to integrate the main results of this thesis in order to explore models of High Arctic coastal evolution over a range of timescales. The key findings are:

- On interannual timescales, sediment supply and sea-ice extent combine to influence whether shorelines in the study area prograde or erode and retreat. The PhD research coincided with a relatively warm period, characterised by a long ice free summer and also increased storm activity. It is no surprise, therefore, that over the period of observation most coastal profiles either retreated landwards or lowered. This pattern indicates a coastal system that, although rich in sediment, is also stressed by high wave energy as well as the strong influence of terrestrial processes that erode and modify coastal landforms over these timescales.
- Over century timescales, encompassing the pre- and post-LIA, coastal development in the study area is dominated by the effects of climate change. Under cooler conditions, reduced run-off, increased permafrost, glacier expansion and associated RSL rise, as well as increased sea-ice extent, all combine to reduce sediment supply to the coast, limit delta progradation and cause coastal stability or erosion. In contrast, under warmer conditions, the opposite patterns occur and coastal progradation occurs.
- Finally, over millennial timescales, changes in the balance of RSL change and the delivery of sediment to the coast emerge as key controls on coastal development. In this regard, the High Arctic coasts are similar to their mid latitude counterparts, although the effects of century-scale climate variability is superimposed on these long-term processes and significantly modifies coastal responses. Over these timescales other factors also emerge as significant in influencing long-term landform preservation. For example, the spatially restricted preservation of Holocene-age beaches in the study area testifies to the locally-restricted combination of circumstances that enable beach ridge deposition *and* their long-term preservation.
- Existing models of paraglacial coastal evolution are not applicable to the study area, or to many other regions of the High Arctic. This is because the terrestrial and marine processes operating in the High Arctic are radically different to those encountered in the mid-latitudes. A new model is therefore proposed that seeks to capture the critical importance of “climate – landscape” interactions that combine with the conventional “RSL / sediment supply” processes to create a unique set of controls on High Arctic coastal development.



# Chapter 9:

# Conclusions

## 9.1 Introduction

This chapter summarises this PhD project by summarising the main findings of the four case studies in the context of the original research questions outlined in Chapter 1. The overall aim of this project was *to develop a comprehensive description and process-based understanding of coastal changes in central Spitsbergen in response to recent climate change and to identify possible linkages between coastal morphodynamics and paraglacial activity in adjacent deglaciated landscapes during the Late Holocene.*

In order to achieve these aims, I have addressed four research objectives:

- to characterise the landforms and processes operating on the modern depositional and rocky coasts of central Spitsbergen;
- to use archival data, photogrammetric analysis of aerial images and GIS techniques to quantify the post-Little Ice Age adjustment of the coastal zone to landscape change during the last century;
- to reconstruct late Holocene coastal morphodynamics and decipher the relative importance of terrestrial and marine processes in controlling landform change, and;
- informed by the above, to develop a new model of paraglacial coastal zone evolution that is characteristic for High Arctic coasts.

In addressing these objectives the PhD has sought to answer the following research questions:

- 1) *What is the interannual morphological variability of the gravel-dominated barriers along Petuniabukta between 2008 and 2010?*
- 2) *What processes operate on recently deglaciated rocky coasts in the study area?*
- 3) *How did glacial and non-glacial-fed, gravel-dominated barriers in Petuniabukta respond to warmer, post-LIA conditions characterised by enhanced paraglacial processes?*
- 4) *How can we improve the accuracy of sea-level reconstructions and long-term coastal evolution studies in the High Arctic?*
- 5) *Can answers to questions 1-4 above enable the formulation of a new conceptual model of paraglacial coastal evolution in the High Arctic?*

In the next sections I will summarise the key conclusions of this project and assess the extent to which they have answered these research questions. The chapter will also consider the wider implications of this study and make recommendations for future research on High Arctic coastal evolution.

## **9.2 WHAT IS THE INTERANNUAL MORPHOLOGICAL VARIABILITY OF THE GRAVEL-DOMINATED BARRIERS ALONG PETUNIABUKTA BETWEEN 2008 AND 2010?**

The starting point of this thesis was to understand the controls and responses of coastal barriers in Petuniabukta over annual timescales, based on repeat observations of coastal processes during summer and winter conditions, as well as repeat survey of established beach profiles between 2008 and 2010. The key question was to assess the spatial and temporal rate of coastal change, and to try and understand what processes were responsible for the pattern seen.

Petuniabukta is ice-bound for long periods and a first question was to assess the impact of sea-ice processes on barrier morphology. This was achieved by using ground-based surveying, interpreting time lapse photography from a camera installed overlooking the study site, and through reference to published sea-ice information from the wider Isfjord area. These data demonstrated that, in Petuniabukta, the direct morphological effects of sea-ice on coastal landforms were very short lived and often significantly modified by factors such as seaweed cover, driftwood displacement or trampling and operation of heavy machines in the coastal zone. Persistent sea-ice features are only preserved locally in the Holocene beach complexes, suggesting that relatively rare combinations of winds and tides are required to enable their preservation over time. However, sea-ice is seen to have an important impact on the longer-term development of the coastlines indirectly, by influencing the duration of ice free conditions in Petuniabukta and the intensity of wave processes. Moreover, sea ice conditions in the wider Isfjord area can also be important, by influencing the fetch of waves that propagate into the inner fjord areas such as Petuniabukta.

Field observation and levelling survey show that the episodic delivery of coarse debris to the barrier surface from terrestrial sources (from rock glaciers, cliffs, mountain slopes, and adjacent alluvial fans) control phases of barrier seaward progradation. The landforms (storm ridges, berms, bars) created from sediments delivered by such events persist over

multiple years. This testifies to the direct connection between terrestrial sediment supply and coastal barrier development over this timescale.

Overall, most of the shoreline surveys indicate lowering of the shoreface over the period of observation. This most likely reflects a longer period of summer ice free conditions in 2010, as well as the largest storm in the three year period also recorded in the summer of 2010. Variations in near-shore wave conditions have an important control on patterns of sediment transport and landform development. In particular, for sites exposed to high waves created by strong glacier winds, especially where there is steep relief in the nearshore topography, storm waves are able to approach and break closer to the barrier face than in more protected, shallower settings. These variations in wave energy are important in controlling areas of barrier retreat along the western coast of Petuniabukta, as observed in the summer storms of 2010.

For each of the studies beach profiles I measured the surficial grain size characteristics. In general, the beaches in the study area are comprised of gravel with variable quantities of sand, and less amounts of silt. In general, interannual changes of barrier morphology occurred regardless of the type of surface sediment cover, although there was a tendency for the seaward migration of storm ridges formed by subangular, rod-shaped pebbles that are typically delivered to the barrier by debris flows, rockfalls and ephemeral snow-melt streams.

Comparing the survey data of this thesis to the landform assemblages visible from remotely sensed data and field survey indicates that the short-term barrier changes observed, often operated in the opposite direction to the land form patterns seen in the late Holocene coastal geomorphology. This suggests that the generally slow pattern of coastal evolution observed in the sheltered bay of Petuniabukta is interrupted by fluxes of sediment supply that occur on a timescale that is longer than 1-3 years.

### **9.3 WHAT PROCESSES OPERATE ON RECENTLY DEGLACIERISED ROCKY COASTS IN THE STUDY AREA?**

A second aspect of the contemporary coastal monitoring work in this thesis involved an assessment of the weathering behaviour of the rocky coasts in Adolfbukta. Several previous studies, in Spitsbergen and elsewhere, have argued that coastal processes in High Arctic settings, notably those related to freeze-thaw cycles and salt hydration, can lead to amplified coastal weathering of rock surfaces. To test for this effect, I completed a study using a Schmidt Hammer that compared rock strength in an area of coastline that

has recently become ice free following glacier retreat after the end of the LIA. The sample design sought to assess spatial variations in rock strength, paying attention to different landforms and their distance from the coast.

The study demonstrates a statistically significant reduction in rock resistance with decreasing distance from the present-day shoreline. Two contrasting explanations for reduced rock resistance in the coastal zone are proposed:

- 1) coastal processes (tidal wetting and drying, salt weathering, wave action, sea ice action) weaken the rock surfaces more efficiently than other subaerial agents operating on rocky landforms in more inland locations, and allow deeper and more efficient rock weathering;
- 2) the low efficiency of coastal processes in sheltered fjord environments leads to preservation of a weathered rock layer along the coast, whereas high intensity of para-periglacial processes across more inland areas removed the weathered material left after post-LIA glacier retreat.

It is important to note that the results of SHRTs should be treated only as a preliminary reconnaissance and the pilot study on the influence of coastal processes on rock breakdown in polar climates should be supported by application of more advanced methods (e.g. Equotip, MEM, Terrestrial Laser Scanning, digital photogrammetry, GIS modelling) to assess results using a range of techniques. The major weakness of this study is, above all, the lack of information regarding the spatial distribution of permafrost and the spatial variations in the nature of the active layer between coastal and inland areas. The Schmidt hammer measurements failed to detect any significant differences in bedrock exposure ages, suggesting that the method should be combined with either lichenometry (e.g. MATTHEWS and SHAKESBY (1984), EVANS *et al.* (1999)), <sup>14</sup>C dating (SHAKESBY *et al.* 2006) or terrestrial cosmogenic nuclide dating (WINKLER 2009).

#### **9.4 HOW DID GLACIAL AND NON-GLACIAL-FED, GRAVEL-DOMINATED BARRIERS IN PETUNIABUKTA RESPOND TO WARMER, POST-LIA CONDITIONS CHARACTERISED BY ENHANCED PARAGLACIAL PROCESSES?**

It is possible to identify two main types of coastal barriers in the Petuniabukta study area on the basis of their connection to terrestrial sediment sources. The first are non-glacial fed systems, that are reliant on sediment delivered by fans, talus slopes, rock glacier melt etc., and the second are glacial-fed systems which derive their sediment from



glacial landforms and processes, often moderated by sediment flux via large outwash plains. In this study I examined the behaviour of both types of coastal landform using a combination of remotely sensed data, using old photographs as well as a set of high quality images specifically flown for this research programme, and also extensive field survey. I analysed these data using GIS software and developed several DEMs that were ground-truthed against geo-referenced points of known location. Coastal landform changes in each coastal system were mapped since the ~1930s and different generations of DEM were compared to assess rates of sediment flux and landscape transformation.

The case study of fan-fed, non-glacial systems, focussed on the Ebba barrier coast and spit-platform in east Petuniabukta. Since the end of LIA, this spit-platform experienced significant seaward progradation (*ca.* 36 m between 1961 and 2009) and lateral extension in the form of three new spits forming (172 to 250 m long). Between 1990 and 2009, the seaward progradation rates slowed down to  $0.4 \text{ m yr}^{-1}$  in comparison with  $1 \text{ m yr}^{-1}$  recorded between 1961 and 1990.

Mapping of the Ebba spit platform topography revealed that beach ridges from the colder decades of the 20<sup>th</sup> century (1960-1980s) were generally more closely spaced and narrower than those of the pre-1960s, and beach ridges that developed in the last 20 years. The height of beach ridge crest above MTL has been gradually decreasing through the 20<sup>th</sup> century, from 60 cm MTL (1900-1961), to 48 cm (1961-1990), and to 30 cm (1990-2009).

The post-LIA development of the Ebba spit-platform and spit systems were largely controlled by the formation of a submarine platform that was dependent on sediment supply to the coast from deglaciating catchments. The uneven delivery of debris from the fan system depended mainly on changes in precipitation, which influenced slope stability and ephemeral stream flow, and the duration of open water conditions.

The future evolution of the Ebba spit-platform will depend on the ability of the landform to adjust to the increasingly delayed delivery of paraglacial sediment from glacier outwash plains and valleys that are increasing in size and storage capacity as a result of glacier retreat up-valley. This, together with factors such as intensified precipitation related to increase in storminess that is predicted in the coming decades, will destabilise permafrost that binds sediments in talus and fan systems, potentially leading to the further reactivation of slope processes and the accelerated delivery of coarse clastic sediment to the coast. Increased sediment delivery to the coast will provide potentially favourable conditions for extension depositional landforms.

Study of the post-LIA development of glacial-fed barrier coasts show that since the end of the LIA, the NW Petuniabukta coast has experienced the largest geomorphic change in the entire bay. Delivery of sediments from retreating glaciers has led to the formation of extensive gravel-dominated barriers, spits and tidal flats. The formation of the barrier coast here was to a large degree dependent of the rate of sediment excavation from relict sediment storage systems, such as alluvial fans and outwash plains, that developed across a wide coastal plain between the glacier valleys and the fjord.

Rates of coastal evolution in these contexts are comparable to or higher than those seen along the W and S coasts of Spitsbergen. This implies that local processes, including basement topography, climate, surface water circulation patterns, and RSL, are all important in controlling geographic patterns of the post-LIA coastal zone development in inner-fjord environments of central Spitsbergen.

The formation of three spits along NW Petuniabukta in the opposite direction to the prevailing wind direction was identified. It is suggested that their development reflects the surface water circulation associated with the functioning of 'Ekman spiral effect' induced by strong eastern winds descending the Ebbadalen.

The migration of modern spits and changes to the orientation of relict coastal barriers and barrier islands suggests the rapid adjustment of landforms to a late Holocene RSL rise associated with local glacier advances around 2500 BP and during the LIA, as well as to RSL fall and land uplift following LIA glacial retreat and unloading. RSL fall and the increased elevation of glacier snouts caused the lowering of river levels and the associated incision of alluvial fans and outwash plains. Sediments eroded from those intermediate sediment storage systems served as the most important source for the development of the NW barrier coast in Petuniabukta.

## **9.5 HOW CAN WE IMPROVE THE ACCURACY OF SEA-LEVEL RECONSTRUCTIONS AND LONG-TERM COASTAL EVOLUTION STUDIES IN THE HIGH ARCTIC?**

A characteristic of the coastal zones of Svalbard and other High Arctic regions is the development of extensive flights of raised beaches that testify to long-term changes in RSL, variations in sediment supply, open water conditions, storminess, as well as basement topography and other local processes. As noted above, the rate and direction of RSL change has not been constant in the Holocene, with an important change from RSL fall to rise in the late Holocene. Existing methods to dating RSL change in Svalbard have relied heavily on either reworked marine shells, which have an uncertain age and

height relationship to a former sea-level, or the driftwood. The latter has the advantage of providing precise age estimates for beaches but can only be used in sites where abundant driftwood exists. In Petuniabukta, human activity in the last century or so has meant that the present beaches have abundant drift wood. However, this is not the case in much of the Holocene, and drift wood cannot be used to date the shorelines here.

This thesis sought to develop a new method to dating the raised beaches in Petuniabukta based on the careful collection of formerly articulated valves of juvenile specimens of the marine bivalve *Astarte borealis*. This taxon is common in the beaches of the study area but has normally been collected by fairly crudely digging into beach sections or simply collecting surface material.

The approach developed here focusses on the fact that, under storm conditions, juvenile specimens of still-articulated specimens of *Astarte borealis* are cast up onto the beach crest, often associated with a soft cushion of seaweed. Over time, the seaweed decomposes or is buried by other sediment, and the paired valves become trapped in the surface levels of the beach. They can be identified by painstaking excavation whereby grain by grain cleaning of shallow surface pits can reveal formerly paired juvenile valves within a few centimetres of the beach crest.

To test whether the method worked, I collected three samples of juvenile, articulated, specimens of *Astarte borealis* from a present storm beach crest in the Ebbadalen. Each was dated using AMS  $^{14}\text{C}$  dating and was shown to contain modern  $^{14}\text{C}$  and therefore lived after 1960. Comparison with a marine bomb spike curve developed using cod otoliths from the Barents Sea region suggests the samples likely died within a decade of their collection (2010). Next, I assessed potential reworking in a late Holocene beach by dating three equivalent samples from a raised beach. The results showed that each sample yielded a  $^{14}\text{C}$  dates that overlapped with the others at the two sigma calibrated age range. These two experiments demonstrate that the careful collection of reworked juvenile *Astarte borealis* from the upper levels of storm beaches can avoid the dating of older reworked shells and provide a reliable chronology for beach deposition.

Radiocarbon dates from a further seven raised beaches provide a chronology for Holocene beach ridge formation in the Ebbadalen. The highest Holocene beaches, at ca. 40 to 45 m a.s.l., formed shortly after local deglaciation at ca. 10,000 cal. yr BP. RSL fell from this level to reach within a meter of present sea-level by ca. 3100 cal. yr BP. The absence of any data points younger than ca. 3000 cal. yr BP, together with the downward

trend in mid and late Holocene RSL, suggest that RSL fell below present and rose again in the last few millennia.

Comparison of this new data with previously published RSL data from eastern Svalbard is compatible with an ice dome located over or close to Kong Karls Land. No evidence was found in these data for a proposed ice dome over easternmost Spitsbergen or southern Hinlopen Strait as proposed by DOWDESWELL *et al.* (2010).

*Astarte borealis* is the dominant mollusc in the Holocene beach sequences of Billefjorden and is common elsewhere in Svalbard and other Arctic regions. In contrast to driftwood and whalebone, the abundance of this mollusc means it has the potential to be used to date specific beach ridges, or complexes of beaches and thus help determine the processes responsible for raised beach ridge formation in Svalbard and elsewhere.

## **9.6 DEVELOPING A NEW CONCEPTUAL MODEL OF PARAGLACIAL COASTAL EVOLUTION IN THE HIGH ARCTIC**

Existing models of paraglacial coastal evolution are developed largely from deglaciated, mature landscapes in the mid-latitudes that have been ice free for much of the Holocene, for example along the coasts of Ireland or Nova Scotia. These models have emphasised the importance of the interaction between RSL and sediment supply, as well as shorter-term events in controlling coastal response. Typically, the models assume three phases comprising an initiation, triggered by initial release of sediment into the coastal zone by, for example, the onset of drumlin erosion. This is followed by a phase of stability, when the barrier extends and consolidates as sediment supply continues to increase. The third phase is often termed 'breakdown' and is characterised by a fall in sediment supply, reworking and cannibalisation of the existing landform and finally by its complete breakdown and redistribution into other landforms or sediment sinks.

This three stage model has been applied to drift-aligned structures, that are especially dependent on sediment supply from up-drift locations and on the prevailing wind / wave direction that drives longshore currents. For swash-aligned coasts, that are generally more stable when faced by reductions in sediment supply, they often change over time by migrating landwards via over-washing or over-topping, when sediment supply falls and / or RSL increases.

The basic landscape settings of the High Arctic are very different to those observed in Ireland or Canada. The single biggest difference is that the hinterland landscape is still geomorphologically active (often still with variable amounts of glacial ice

cover) and is strongly influenced by climate change. This contrasts with the essentially passive coastal landscape of the mid-latitudes which have been essentially stable for centuries or millennia before coastal erosion, largely caused by an upward trend in RSL, triggers a change in sediment supply. The contrast in landscape and climate setting also includes important differences in the nature and extent of ground and sea-ice, which influence sediment stability and also the duration and open water conditions as well as the nature of energy delivery to the coast. It also includes variations in the nature of vegetation cover and soil stability, and also the nature of fluvial sediment delivery to the coastal zone.

For these reasons, existing models of paraglacial coastal evolution require revision if they are to adequately describe the processes that combine to influence the development of High Arctic paraglacial gravel barriers. The key modification is to recognise the dynamic, climatically sensitive nature of terrestrial sediment delivery to the coastal zone. This means that High Arctic models of coastal evolution are not merely a function of RSL change and sediment supply, but also involve a critical climate-landscape element that drives variations in terrestrial sediment delivery via climatically-sensitive assemblages of landforms and processes.

To conclude, this thesis opened with the proposition that High Arctic coasts have received relatively little attention compared to their better studied mid and low latitude counterparts. This position needs rectifying given the rapid pace of change in the impacts on the coastal zones of the High Arctic in response to global warming. Although based on a detailed case study in Petuniabukta, located in the interior of Spitsbergen, the research presented here has, I hope, contributed in a novel way to addressing how and why High Arctic coasts respond to different local to regional processes. Perhaps the most important conclusion from this study is recognition that there is a need to understand the High Arctic coastal zone as part of an integrated set of landscape elements. High Arctic coasts do not depend only on rates of sea-level and sediment supply, but crucially on the functioning and climate sensitivity of terrestrial and marine processes. Given the potential for future climate change in these regions, the coastlines of the High Arctic and their associated landscapes promise to be areas of profound change.



# Chapter 10: Bibliography

## A

- AARSETH I., and FOSGEN H., 2004. A Holocene lacustrine rock platform around Storavatnet, Osterøy, western Norway. *Holocene* 14, 589-596.
- ÅKERMAN J., 1984. Notes on talus morphology and processes in Spitsbergen. *Geografiska Annaler* 66A, 267-284.
- ÅKERMAN J.H., 1987. Periglacial forms of Svalbard: a review. In BOARDMAN J. (Ed.) *Periglacial processes and landforms in Britain and Ireland*. Cambridge University Press, Cambridge, 9-26.
- ÅKERMAN J.H., 2008. Coastal Processes and Their Influence Upon Discharge Characteristics of the Strokdammane Plain, West Spitsbergen, Svalbard. Proceedings of the Ninth International Conference on Permafrost University of Alaska Fairbanks June 29-July 3, 2008, Vol 1, 19-24.
- AMUNDSON J.M., TRUFFER M., LUTHI M.P., FAHNESTOCK M., WEST M., AND MOTYKA R.J., 2008. Glacier, fjord, and seismic response to recent large calving events, Jakobshavn Isbrae, Greenland, *Geophysical Research Letters* 35, L22501, doi:10.1029/2008GL035281.
- AMUNDSON J. M., FAHNESTOCK M., TRUFFER M., BROWN J., LUTHI M.P., and MOTYKA R.J., 2010. Ice melange dynamics and implications for terminus stability, Jakobshavn Isbrae, Greenland. *Journal of Geophysical Research* 115, F01005, doi:10.1029/2009JF001405.
- ANDRÉ M-F., 1990. Frequency of debris flows and slush avalanches in Spitsbergen: a tentative evaluation from lichenometry. *Polish Polar Research* 11, 345-363.
- ANDRÉ M.-F., 1997. Holocene rockwall retreat in Svalbard: a triple-rate evolution. *Earth Surface and Processes and Landforms* 22, 423-440.
- ANDRÉ M-F., 2009. From climatic to global change geomorphology: contemporary shifts in periglacial geomorphology. In KNIGHT J., AND HARRISON S., (Eds.) *Periglacial and Paraglacial Processes and Environments*. *Geological Society, London Special Publications* 320, 5-28.
- ANTHONY E.J., 2008. Gravel Beaches and Barriers. In Anthony E.J. (ed.) *Shore Processes and their Palaeoenvironmental Applications*. 289-324. *Developments in Marine Geology Series*. Amsterdam: Elsevier.
- Arctic Climate Impact Assessment (ACIA) Scientific Report* 2005. Cambridge University Press, Cambridge: 1042pp.
- ARÉ F.E., 1988. Thermal abrasion of sea coasts. *Polar Geography and Geology* 12, 1 157.
- ARÉ F.E., REIMNITZ E., GRIGORIEV M., HUBBERTEN H.-W. and RACHOLD V., 2008. The influence of cryogenic processes on the erosional Arctic shoreface. *Journal of Coastal Research* 24, 110-121.
- ARENDT A., ECHELMAYER K., HARRISON W., LINGLE C. and VALENTINE V., 2002. Rapid wastage of Alaska glaciers and their contribution to rising sea levels. *Science* 297, 382-386.

## B

- BAETEN N. J., FORWICK M., VOGT C. AND VORREN T. O., 2010. Late Weichselian and Holocene sedimentary environments and glacial activity in Billefjorden, Svalbard. In: HOWE J. A., AUSTIN W. E. N., FORWICK M. AND PAETZEL M. (eds) *Fjord Systems and Archives*. *Geological Society, London, Special Publications*, 344, 207-223.
- BALCHIN W.G.V., 1941. The raised features of Billefjord and Sessenfjord west Spitsbergen. *Geographical Journal* 97, 364-376.
- BALLANTYNE C., 2002. Paraglacial geomorphology. *Quaternary Science Reviews* 21, 1935-2017.

- BALLANTYNE C., 2005. Paraglacial landsystems. In EVANS D.J.A (ed.) *Glacial Landsystems*. Hodder Arnold.
- BALLANTYNE C.K., BLACK N.M. and FINLAY D.P., 1989. Enhanced boulder weathering under late-lying snowpatches. *Earth Surface Processes and Landforms* 14, 745-750.
- BARANOWSKI S. and KARLÉN W., 1976 Remnants of Viking Age Tundra in Spitsbergen and Northern Scandinavia. *Geografiska Annaler* 58, 35-40.
- BARNES P.W., RAWLINSON S.E. and REIMNITZ E., 1988. Coastal Geomorphology of Arctic Alaska. In: *Arctic Coastal Proc. and Slope Protection Design, TCCR Practice Rept*, ASCE: 3–30.
- BARNES P.W., KEMPEN E.W., REIMNITZ E., MCCORMICK M., WEBER W.S. and HAYDEN E.C. 1993. Beach profile modification and sediment transport by ice: an overlooked process on Lake Michigan. *Journal of Coastal Research* 9, 65-86.
- BARRAND, N. E., JAMES, T. D. and MURRAY, T. 2010. Spatio-temporal variability in elevation changes of two high-Arctic valley glaciers. *Journal of Glaciology* 56, 771–780.
- BARTRUM, J. A., 1947. The rate of rounding of beach boulders. *Journal of Geology* 55, 514-515.
- BASSFORD, R. P., SIEGERT, M. J., DOWDESWELL, J. A., OERLEMANS, J., GLAZOVSKY, A. F. and MACHERET, Y. Y., 2006. Quantifying the mass balance of ice caps on Severnaya Zemlya, Russian High Arctic. I: Climate and mass balance of the Vavilov Ice Cap. *Arctic, Antarctic, and Alpine Research* 38, 1–12.
- BENESTAD R.E., HANSEN-BAUER I., SKAUGEN T.E. and FØRLAND E.J., 2002. Associations between sea-ice and the local climate on Svalbard. *Norwegian Meteorological Institute Report No. 07/02*, 1-7.
- BENN D., 2006. Clast Form Analysis. In ELIAS S. (ed.) *Encyclopedia of Quaternary Science*. Vol 1. Elsevier, 904-909.
- BENNETT G. and EVANS D.J.A 2012. Glacier retreat and landform production on an overdeepened glacier foreland: the debris-charged glacial landsystem at Kviárjökull, Iceland. *Earth Surface Processes and Landforms* doi: 10.1002/esp.3259
- BENNIKE O., 2004. Holocene sea-ice variations in Greenland: onshore evidence. *The Holocene* 14, 607-613.
- BERTHLING I. and ETZELMÜLLER B., 2007. Holocene rockwall retreat and the estimation of rock glacier age, Prins Karls Forland, Svalbard. *Geografiska Annaler* 89A(1), 83–93.
- BERTHLING I. and ETZELMÜLLER B., 2011. The concept of cryo-conditioning in landscape evolution. *Quaternary Research* 75, 378-384.
- BIRD E., 2008. *Coastal geomorphology*. Wiley, Chichester: 412p.
- BLAKE, W., 1975. Radiocarbon age determinations and postglacial emergence at Cape storm, southern Ellsmere Island, Arctic Canada. *Geografiska Annaler* 57A, 1-71.
- BLANCO-CHAO R., PÉREZ-ALBERTI A., TRENHAILE A.S., COSTA-CASAS M. and VALCÁRCCEL-DÍAZ M., 2007. Shore platform abrasion in a para-periglacial environment, Galicia, northwestern Spain. *Geomorphology* 83, 136–151.
- BLUCK, B. J., 1967. Sedimentation of beach gravels: examples from South Wales. *Journal of Sedimentary Petrology* 37, 128-156.
- BLUCK, B. J., 1969. Particle rounding in beach gravels. *Geological Magazine* 106, 1-14.
- BLĄSZCZYK M., JANIA J.A., HAGEN J.O. 2009. Tidewater glaciers of Svalbard: Recent changes and estimates of calving fluxes. *Polish Polar Research* 30: 85-142.
- BOGEN J., BØNSNES T., 2003. Erosion and sediment transport in High Arctic rivers, Svalbard. *Polar Research* 22, 175-189.
- BONDEVİK, S., MANGERUD, J., RONNERT, L., SALVIGSEN, O., 1995. Postglacial sea-level history of Edgeøya and Barentsøya, eastern Svalbard. *Polar Research* 14, 153-180.
- BOOTH, C.A., WALDEN, J., NEAL, A., SMITH, J.P., 2005. Use of mineral magnetic concentration data as a particle size proxy: a case study using marine, estuarine and fluvial sediments in the

- Carmarthen Bay area. *South Wales, U.K. Science of the Total Environment* 347, 241–253.
- BORÓWKA M., 1989. The development and relief of the Petuniabukta tidal flat, central Spitsbergen. *Polish Polar Research* 10(3), 379–384.
- BOULTON G.S., 1972. Modern Arctic glaciers as depositional models for former ice sheets. *Journal of Geological Society London* 128, 361–393.
- BOULTON G.S., 1972. The role of thermal regime in glacial sedimentation. In: PRICE R.J., SUGDEN D.E., (Eds.) *Polar geomorphology*. Institute of British Geographers' Special Publication 4, 1–19.
- BOULTON G.S., 1976. The origin of glacially fluted surfaces observations and theory. *Journal of Glaciology* 76, 287–309.
- BOULTON G.S., 1979. Glacial history of the Spitsbergen archipelago and the problem of the Barents shelf ice sheet. *Boreas* 8, 1–57.
- BOULTON, G.S. and RHODES, M., 1974. Isostatic uplift and glacial history in northern Spitsbergen. *Geological Magazine* 111, 481–576.
- BOYD R., BOWEN A.J. and HALL R.K., 1987. An evolutionary model for transgressive sedimentation on the eastern shore of Nova Scotia. In: FITZGERALD D.M. AND ROSEN, P.S. (Eds.), *Glaciated Coasts*. Academic Press, San Diego, 87–114 pp.
- BRADLEY R., 2000. 1000 Years of Climate Change. *Science* 288, 1353–1355.
- BRÜCKNER H. and SCHELLMANN G., 2003. Late Pleistocene and Holocene shorelines of Andréeland, Spitsbergen (Svalbard)—geomorphological evidence and palaeo-oceanographic significance. *Journal of Coastal Research* 19, 971–982.
- BRÜCKNER H., SCHELLMANN G. and VAN DER BORG K., 2002. Uplifted beach ridges in northern Spitsbergen as indicators for glacio-isostasy and palaeo-oceanography. *Zeitschrift für Geomorphologie* 46, 309–336.
- BUCHWAŁ A., 2008. Funkcjonowanie dróg w górskim systemie stokowym masywu Pyramiden na Spitsbergenie. *Prace Geograficzne UJ*, 120, 9–17.
- BYRNE M.-L. and DIONNE J.-C., 2002. Typical Aspects of Cold regions Shorelines. In: K. HEWITT, M.-L. BYRNE, M. ENGLISH and G. YOUNG (eds.), *Landscapes in Transition. Landform Assemblages and Transformations in Cold Regions*. Kluwer Academic Publishers, Dordrecht: 141–158 pp.

## C

- CAMPEAU S. and HÉQUETTE A., 1995. Buttes cryogènes saisonnières de plages arctiques, péninsule de Tuktoyaktuk, Territoires du Nord-Ouest. *Géographie physique et Quaternaire* 49, 265–274.
- CARR, A .P., GLEASON, R . and KING, A., 1970. Significance of pebble size and shape sorting by waves. *Sedimentary Geology* 4, 89–101.
- CARTER R.W.G., 1988. *Coastal Environments*. London: Academic Press, 615 pp.
- CARTER R.W.G. and ORFORD J.D., 1991. The sedimentary organization and behaviour of drift-aligned gravel barriers, *Coastal Sediments '91*, American Society of Civil Engineers 1, 934–948.
- CARTER, R. W. G. and ORFORD, J. D. 1993. The morphodynamics of coarse clastic beaches and barriers: a short and long-term perspective, *Journal of Coastal Research*, Special Issue 15, 158–179.
- CARTER R.W.G., JOHNSTON T. W., MCKENNA J. and ORFORD J.D., 1987. Sea-level, sediment supply and coastal changes: examples from the coast of Ireland. *Progress in Oceanography* 18, 79–101.

- CARTER R.W.G., FORBES D.L., JENNINGS S.C., ORFORD J.D., SHAW J. and TAYLOR R.B., 1989. Barrier and lagoon coast evolution under differing sea-level regimes: examples from Ireland and Nova Scotia. *Marine Geology* 88, 221–242.
- CARTER R.W.G., ORFORD J.D., FORBES D.L. and TAYLOR R.B., 1990. Morphosedimentary development of drumlin-flank barriers in a zone of rapidly rising sea level, Story Head, Nova Scotia. *Sedimentary Geology* 69, 117–138.
- CARTER R.W.G., ORFORD J.D., JENNINGS S.C., SHAW J. and SMITH J.P., 1992. Recent evolution of a paraglacial estuary under conditions of rapid sea level rise: Chezzetcook inlet, Nova Scotia. *Proceedings of the Geologists' Association* 103, 167–185.
- CHELLI A., PAPPALARDO M., LLOPIS I.A. and FEDERICI P. B., 2010. The relative influence of lithology and weathering in shaping shore platforms along the coastline of the Gulf of La Spezia (NW Italy) as revealed by rock strength. *Geomorphology* 118, 93–104.
- CHURCH M. and RYDER J.M., 1972. Paraglacial sedimentation: a consideration of fluvial processes conditioned by glaciation. *Bulletin of Geological Society of America* 83, 3059–3071.
- CHRISTIANSEN H.H., 2005. Thermal regime of ice-wedge cracking in Adventdalen, Svalbard. *Permafrost and Periglacial Processes* 16, 87–98.
- CIOPPA M., PORTER N., TRENHAILE A., IGOKWE B., VICKERS J., 2010. Beach Sediment Magnetism and Sources: Lake Erie, Ontario, Canada. *Journal of Great Lakes Research* 36, 674–685.
- CLARK P., DYKE A., SHAKUN J., CARLSON A., CLARK J., WOHLFARTH B., MITROVICA J., HOSTETLER S. and MCCABE A., 2009. The Last Glacial Maximum. *Science* 325 (5941): 710–4.
- COLELLA, A. & PRIOR, D.B. (eds) 1990. *Coarse-grained deltas*. Int. Assoc. Sedimentol. Spec. Publ., 10, 357 pp.
- COMISO, J. C., PARKINSON C. L., GERSTEN R. AND STOCK L., 2008. Accelerated decline in the Arctic sea ice cover. *Geophysical Research Letters* 35, L01703, doi:10.1029/2007GL031972.
- COSTARD F., GAUTIER E., BRUNSTEIN D., HAMMADI J., FEDOROV A., YANG D. AND DUPEYRAT L., 2007. Impact of the global warming on the fluvial thermal erosion over the Lena River in central Siberia. *Geophysical Research Letters* 34: L14501, doi:10.1029/2007GL030212
- COX J.C. AND MONDE M.C., 1985. *Wave erosion of an unprotected frozen gravel berm*. Arctec Engineering Inc., 43 p.
- CRUSLOCK E.M., NAYLOR L.A., FOOTE Y.L. and SWANTESSON J.O., 2010. Geomorphologic equifinality: A comparison between shore platforms in Höga Kusten and Färö, Sweden and the Vale of Glamorgan, South Wales, UK. *Geomorphology* 114, 78–88.
- CZAJKA P., 2010. *The satellite remote sensing database from the years 1973 – 2008 for the vicinity of the Petunia Bay, West Spitsbergen, and example of its applications*. Unpublished Master's Thesis, AMU Poznan, 134pp.
- CZEPPE, Z., 1966. The course of the main morphogenetic processes in the south-west Spitsbergen. *Zesz. Nauk. UJ, Pr. Geogr.*, 13: 15–24.

## D

- DAHL E., 1946. On the origin of the strandflat. *Norsk Geografisk Tidsskrift* 11, 159 – 172.
- DAHL-JENSEN, T., LARSEN, L.M., PEDERSEN, S.A.S., PEDERSEN, J., JEPSEN, H.F., PEDERSEN, G.K., NIELSEN, T., PEDERSEN, A.K., VON PLATEN-HALLERMUND, F. and WENG W. 2004. Landslide and tsunami 21 November 2000 in Paatuut, West Greenland. *Natural Hazards* 31, 277–287.
- DALE J.E., LEECH S., MCCANN B., and SAMUELSON G., 2002. Sedimentary characteristics, biological zonation and physical processes of the tidal flats of Iqaluit, Nunavut. In: K. HEWITT, M-L. BYRNE, M. ENGLISH and G. YOUNG (eds.), *Landscapes in Transition. Landform Assemblages and Transformations in Cold Regions*. Kluwer Academic Publishers, Dordrecht: 205–234.



- DALLMANN W.K., PIPEJOHN K. and BLOMEIER D., 2004. Geological map of Billefjorden, Central Spitsbergen, Svalbard with geological excursion guide 1 : 50,000. Norsk Polarinstitutt Tematkart, No 36.
- DAVIES J.L., 1980. *Geographical Variation in Coastal Development*. Longman, New York: 212p.
- DAVIS W. M., 1902. Base-level, grade, and pene-plain. *Journal of Geology* 10, 77-111.
- DAY M.J. and GOUDIE A.S., 1977. *Field assessment of rock hardness using the Schmidt test hammer*. British Geomorphology Research Group Technical Bulletin 18, 19-29.
- DECAULNE A., SAEMUNDSSON T. and PETURSSON, O., 2005. Debris flow triggered by rapid snowmelt; a case study in the Gleidarhjalli area, northwestern Iceland. *Geografiska Annaler* 87A, 487-500.
- DICKSON R.R., OSBORN T.J., HURRELL J.W., MEINCKE J., BLINDHEIM J. ADLANDSVIK B., VINJE, T., ALEKSEEV G., MASLOWSKI W. AND CATTLE H., 2000. The Arctic Ocean response to the North Atlantic Oscillation. *Journal of Climate* 15, 2671-2696.
- DIONNE J.-C., 1965. Algues et sédimentologie littorale. *Revue de Géographie de Montreal* 19, 91-98.
- DIONNE J.-C., 1968. Morphologie et sedimentologie glacielles, littoral sus du Saint-Laurent, *Zeitschrift fur Geomorphologie Supplement band 7*, 56-84.
- DIONNE J.-C., 1969. Tidal flat erosion by ice at La Pocatière, St. Lawrence Estuary. *Journal of Sedimentary Petrology* 39, 1174-1181.
- DIONNE J.-C., 1973. The notion of Icefoot with special reference to the St Lawrence Estuary. In D.J.A. EVANS (ed.). 1994. *Cold Climate Landforms*. Wiley, Chichester, pp.325-350.
- DIONNE J.-C., 1976. (Ed.) Le Glaciel. *La Revue de Géographie de Montréal* 30, 233pp.
- DIONNE J.-C., 1988. Characteristic features of modern tidal flats in cold regions. In P.L. de Boer *et al.*, (eds.), *Tide influenced sedimentary environments and facies*. Dordrecht: 301-332.
- DIONNE J.-C., 1989. The role of ice and frost in tidal marsh development. A review with particular reference to Quebec, Canada. *Earth Science Reviews* 26, 185-212.
- DIONNE J.-C., 1989. The role of ice and frost in tidal marsh development - a review with particular reference to Québec, Canada. In *Zonality of coastal Geomorphology and Ecology*. In Bird E.C.F. and Kelletat D., (Eds), *Essener Geographische Arbeiten* 18, 171-210.
- DIONNE J.-C. and BRODEUR D., 1988. Frost weathering and ice action in shore platform development, with particular reference to Quebec, Canada. *Zeitschrift fur Geomorphologie Supplement band 71*, 117-130.
- DONNER J. and JUNGNER H., 1975. Radiocarbon dating of shells from marine Holocene deposits in the Disko Bugt area, West Greenland. *Boreas* 4, 25-45.
- DOWDESWELL J. and DOWDESWELL E.-K., 1989. Debris in icebergs and rates of glaci-marine sedimentation; observations from Spitsbergen and a simple model. *Journal of Geology* 92, 221-231.
- DOWDESWELL J.A., HAGEN J.O., BJÖRNSSON H., GLAZOVSKY A.F., HARRISON W.D., HOLMLUND P., JANIA J., KOERNER R.M., LEFAUCONNIER B., OMMANNEY C.S.L. and THOMAS R.H., 1997. The mass balance of circum-Arctic glaciers and recent climate change. *Quaternary Research* 48, 1-14.
- DOWDESWELL J.A., HOGAN K.A., EVANS J., NOORMETS R., O'COFAIGH C.O. and OTTESEN, D., 2010. Past ice-sheet flow east of Svalbard inferred from streamlined subglacial landforms. *Geology* 38, 163-166.
- DRAKE J.J. and MCCANN S.B. 1982. The movement of isolated boulders on tidal flats by ice floes. *Canadian Journal of Earth Sciences* 19: 748-54.

- DYKE A.S. and MORRIS T.F. 1990. Postglacial history of the bowhead whale and of driftwood penetration; implications for paleoclimate, central Canadian Arctic. Geological Survey of Canada, Paper 89-24. 17 p.
- DYKE A.S., MORRIS T.F. and GREEN D.E.C., 1991. Postglacial tectonic and sea level history of the central Canadian Arctic. *Geological Survey of Canada Bulletin* 1, 1-397.
- DYKE A., ENGLAND J., REIMNITZ E. and JETTÉ H. 1997. Changes in driftwood delivery to the Canadian Arctic Archipelago: the hypothesis of Postglacial oscillations of the transpolar drift. *Arctic* 50, 1–16.
- DYURGEROV M. and MCCABE G., 2006. Associations between accelerated glacier mass wastage and increased summer temperature in coastal regions. *Arctic, Antarctic and Alpine Research* 38, 190-197.

## E

- EAMER J.B.R. and WALKER I.J., 2010. Quantifying sand storage capacity of large woody debris on beaches using LiDAR. *Geomorphology* 118, 33-47.
- ECKERSTORFER M. and CHRISTIANSEN H.H., 2011. The “High Arctic Maritime Snow Climate” in Central Svalbard. *Arctic, Antarctic, and Alpine Research* 43, 11–21.
- ECKERSTORFER M., CHRISTIANSEN H.H., VOGEL S. and RUBENSDOTTER L., 2012. Snow cornice dynamics as a control on plateau edge erosion in central Svalbard. *Earth Surface Processes and Landforms* 38, 466-476.
- EGGERTSSON Ó. and LAEYENDECKER D. 1995. A dendrochronological study of the origin of driftwood in Frobisher Bay, Baffin Island, N.W.T., Canada. *Arctic and Alpine Research* 27, 180-186.
- ELVERHØI A., SVENDSEN J.I., SOLHEIM A., ANDERSEN E.S., MILLIMAN J., MANGERUD J. and HOOKE R.L.B., 1995. Late Quaternary sediment yield from the High Arctic Svalbard area. *Journal of Geology* 103, 1-17.
- EMERY K.O., 1955. Transportation of rocks by driftwood. *Journal of Sedimentary Petrology* 25, 51-57.
- ENGLAND J., 1997. Unusual rates and patterns of Holocene emergence, Ellesmere Island, Arctic Canada. *Journal of the Geological Society* 154, 781-792.
- ETIENNE S., MERCIER D. and VOLDOIRE O., 2008. Temporal scales and deglaciation rhythms in a polar glacier margin, Baronbreen, Svalbard'. Norsk Geografisk Tidsskrift - *Norwegian Journal of Geography* 62, 102 — 114.
- ETZELMÜLLER B. and HAGEN J.O. 2005. Glacier-permafrost interaction in Arctic and alpine mountain environments with examples from southern Norway and Svalbard. In HARRIS, C. & MURTON, J.B. (eds.) *Cryospheric Systems: Glaciers and Permafrost*, 11-27. Geological Society Special Publications 242. Geological Society, London.
- ETZELMÜLLER B., ØDEGÅRD R.S., VATNE G., MYSTERUD R.S., TONNING T. and SOLLID J.L., 2000. Glacier characteristics and sediment transfer system of Longyearbreen and Larsbreen, western Spitsbergen. *Norwegian Journal of Geography* 54, 157–168.
- ETZELMÜLLER B., ØDEGÅRD R.S. and SOLLID J.L., 2003. The spatial distribution of coast types on Svalbard. In RACHOLD V., BROWN J, SOLOMON S. and SOLLID J. (eds.) *Arctic Coastal Dynamics Report of the 3rd International Workshop University of Oslo, Oslo (Norway) 2-5 December 2002*, 137 pp. 33-40.
- EVANS D.J.A., ARCHER S. and WILSON D.J.H., 1999. A comparison of the lichenometric and Schmidt Hammer dating techniques based on data from the proglacial areas of some Icelandic glaciers. *Quaternary Science Reviews* 18, 13–41.

- EVANS D.J.A, STRZELECKI M., MILLEDGE D.G. and ORTON C. 2012. Hørbyebreen polythermal glacial landsystem, Svalbard. *Journal of Maps* 8, 1-11.
- EWERTOWSKI M., KASPRZAK L., SZUMAN I. and TOMCZYK A.M., 2010 - Depositional processes within the frontal ice-cored moraine system, Ragnar glacier, Svalbard. *Quaestiones Geographicae* 29, 27-36.
- EWERTOWSKI M., KASPRZAK L., SZUMAN I. and TOMCZYK A., 2012. Controlled, ice-cored moraines: sediments and geomorphology. An example from Ragnarbreen, Svalbard. *Zeitschrift für Geomorphologie* 56(1), 53-74.

## F

- FARBROT H., ISAKSEN K., EIKEN T., KÄÄB A. and SOLLID J.L., 2005. Composition and internal structures of a rock glacier on the strandflat of western Spitsbergen, Svalbard. *Norwegian Journal of Geography* 59, 139 - 148.
- FAUCHERRE S., 2011. *Sediment dynamics in Braganzavågen, western Svalbard, an ITRAX study*. Master thesis. Université Bordeaux I: UMR 5805 "EPOC" and University Centre in Svalbard.
- FEYLING-HANSSSEN R.W., 1955. Stratigraphy of the marine Late-Pleistocene of Billefjorden, Vestspitsbergen. *Norsk Polarinstitutt Skrifter* 107, 1-168.
- FEYLING-HANSSSEN R.W., 1965. Shoreline displacement in central Vestspitsbergen. *Norsk Polarinstitutt Meddelelser* 93, 1-5.
- FEYLING-HANSSSEN R.W. and OLSSON I.U. 1960. Five radiocarbon datings of post-glacial shorelines in central west Spitsbergen. *Norsk Polarinstitutt Meddelelser* 86, 122- 131.
- FORBES D.L. 2005. *Paraglacial coasts*. In SCHWARTZ M.L. (Ed.) *Encyclopedia of Coastal Science*. Springer, Dordrecht, 760-762.
- FORBES D.L. (editor). 2011. *State of the Arctic Coast 2010 – Scientific Review and Outlook*. International Arctic Science Committee, Land-Ocean Interactions in the Coastal Zone, Arctic Monitoring and Assessment Programme, International Permafrost Association. Helmholtz-Zentrum, Geesthacht, Germany, 178 pp. <http://arcticcoasts.org>
- FORBES D.L. and TAYLOR R.B., 1987. Coarse-grained beach sedimentation under paraglacial conditions, Canadian Atlantic Coast. In: D. FITZGERALD AND P. ROSEN (eds.), *Glaciated Coasts*. Academic Press, New York: 51-86.
- FORBES D.L. and TAYLOR R.B., 1994. Ice in the shore zone and the geomorphology of cold coasts. *Progress in Physical Geography* 18, 59-89.
- FORBES D.L., ORFORD J.D., CARTER R.W.G., SHAW J., JENNINGS S.C., 1995a. Morphodynamic evolution, self-organisation, and instability of coarse-clastic barriers on paraglacial coasts. *Marine Geology* 126, 63–85.
- FORBES D.L., SHAW J. and TAYLOR R.B., 1995b. Differential preservation of coastal structures on paraglacial shelves: Holocene deposits of south-eastern Canada. *Marine Geology* 124, 187–201.
- FORMAN S.L., 1990. Postglacial relative sea-level history of northwestern Spitsbergen, Svalbard. *Geological Society of America Bulletin* 102, 1580-1590.
- FORMAN S., LUBINSKI D., INGOLFSSON O., ZEEBERG J., SNYDER J., SIEGERT M. and MATISHOV G., 2004. A review of postglacial emergence on Svalbard, Franz Josef Land and Novaya Zemlya, northern Eurasia. *Quaternary Science Reviews* 23, 1391–1434.
- FORWICK M. and VORREN T.O., 2010. Stratigraphy and deglaciation of the Isfjorden area, Spitsbergen. *Norwegian Journal of Geology* 90, 163-179.

- FOURNIER A. and ALLARD M., 1992. Periglacial shoreline erosion of rocky coast: George River Estuary, Northern Quebec. *Journal of Coastal Research* 8, 926-942.
- FØRLAND E. J., BENESTAD R. E., FLATØY F., HANSEN-BAUER I., HAUGEN J. E., SORTEBERG A. and ADLANDSVIK B., 2009. *Climate development in North Norway and the Svalbard region during 1900-2100*. Tromsø, Norsk polarinstitutt (eds.), 43 s. pp.
- FRENCH M. H., 2007. *The Periglacial Environment*. Third edition. Chichester, U.K. and Hoboken, New Jersey: John Wiley and Sons, 458 pp.
- FUNDER S., GOOSSE H., JEPSEN H., KAAS E., KJÆR K.H., KORSGAARD N.J., LARSEN N.K, LINDERSON H., LYSÅ A., MÖLLER P., OLSEN J. and WILLERSLEV E., 2011. A 10,000-year record of Arctic Ocean sea-ice variability—view from the beach. *Science* 333, 747-750.

## G

- GALE, S.J. 1990. The shape of beach pebbles. *Journal sedimentary petrology* 60,787-789.
- GAWALI, P.B., BASAVAIAH, N. and HANAMGOND, P.T., 2010. Mineral magnetic properties of sediments of beaches, Redi-Vengurla Coast, central west coast of India: a seasonal characterization and provenance study. *Journal of Coastal Research* 26, 569-579.
- GERLAND S. and HALL R., 2006. Variability of fast-ice thickness in Spitsbergen fjords. *Annals of Glaciology* 44, 231-239.
- GIBAS J., RACHLEWICZ G. and SZCZUCIŃSKI W., 2005: Application of DC resistivity soundings and geomorphological surveys in studies of modern Arctic glacier marginal zones, Petuniabukta, Spitsbergen. *Polish Polar Research* 26, 239-258.
- GILBERT R., 1984. The movement of gravel by alga *Fucus Vesiculosus* (L.) on an Arctic intertidal flat. *Journal of Sedimentary Petrology* 54, 463-468.
- GILBERT R., 1990. A distinction between ice-pushed and ice-lifted landforms on lacustrine and marine coasts. *Earth Surface Processes and Landforms* 15, 15-24.
- GIRARDIN P., 1910. Études de cônes de déjections. *Annales de Géographie* 105, 193-207.
- GLASSER N. F. and HAMBREY, M. J. 2003. Ice-marginal terrestrial landsystems: Svalbard polythermal glaciers. In Evans, D. J. A. (ed.): *Glacial Landsystems*, 65-88. Arnold. London
- GREENE H.G., 1970. Microrelief on an arctic beach. *Journal of Sedimentary Petrology* 40: 419-427.
- GORDEEV V., 2006. Fluvial sediment flux to the Arctic Ocean. *Geomorphology* 80, 94-104.
- GOUDIE A., 2006. The Schmidt Hammer in geomorphological research. *Progress in Physical Geography* 30, 703-718.
- GÖKTAN R.M. and AYDAY C., 1993. A suggested improvement to the Schimdt Rebound Hardness ISRM method with particular reference to rock machineability. *International Journal of Rock Mechanics* 30, 321-322.
- GUILCHER A., BODERE J-C., COUDE A., HANSOM J.D, MOIGN A. and PEULVAST J-P., 1986. The Strandflat problem in Five High Latitude Countries. In D.J. EVANS. *Cold Climate Landforms*. Wiley, Chichester: 351-393.

## H

- HAGEN J.O., MELVOLD K., PINGLOT F. and DOWDESWELL J.A., 2003. On the net mass balance of the glaciers and ice caps in Svalbard, Norwegian Arctic. *Arctic, Antarctic and Alpine Research* 35, 264-270.
- HAGEN J.O., EIKEN T., KOHLER J. and MELVOLD K., 2005. Geometry changes on Svalbard glaciers: mass-balance or dynamic response. *Annals of Glaciology* 42, 255-261.
- HÄGGBLUM A., 1982. Driftwood in Svalbard as an indicator of sea ice conditions. *Geografiska Annaler* 64 A, 81-94.

- HALD M., DAHLGREN T., OLSEN T. E. and LEBESBYE E., 2001. Late Holocene paleoceanography in Van Mijenfjorden, Svalbard. *Polar Research* 20, 23–35.
- HALD M., EBBESEN H., FORWICK M., GODTLIEBSEN F., KHOMENKO L., KORSUN S., OLSEN L.R. and VORREN T.O., 2004. Holocene paleoceanography and glacial history of the West Spitsbergen area, Euro-Arctic margin. *Quaternary Science Reviews* 23, 2075–2088.
- HALD M., ANDERSSON C., EBBESEN H., JANSEN E., KLITGAARD-KRISTENSEN D., RISEBROBAKKEN, B., SALAMONSEN G., SARNTHEIN M., SEJRUP H. P. AND TELFORD R. 2007. Variations in temperature and extent of Atlantic Water in the northern North Atlantic during the Holocene. *Quaternary Science Reviews* 26, 3423–3440.
- HALL K., 1993. Enhanced bedrock weathering in association with late-lying snowpatches – evidence from Livingston Island, Antarctica. *Earth Surface Processes and Landforms* 18, 121–29.
- HAMBREY M.J., BENNETT M.R., DOWDESWELL J.A., GLASSER N.F. and HUDDART D., 1999. Debris entrainment and transfer in polythermal valley glaciers, Svalbard. *Journal of Glaciology* 45: 69–86.
- HANSELL D. and CARLSON C. (Eds.), 2002. *Biogeochemistry of Marine Dissolved Organic Matter*. Elsevier Science, San Diego, p. 774.
- HANSEN L., 2004. Deltaic infill of a deglaciated Arctic fjord, East Greenland: Sedimentary facies and sequence stratigraphy. *Journal of Sedimentary Research* 74, 422–437.
- HANSOM J.D. and KIRK R.M., 1989. Ice in the intertidal zone: examples from Antarctica. In: E.C.F. BIRD AND D. KELLETAT (eds.) *Zonality of Coastal Geomorphology and Ecology*. *Essener Geographische Arbeiten* 18, 211–236.
- HARLAND W.B. 1952. The Cambridge Spitsbergen Expedition, 1949. *The Geographical Journal* 118, 309–329.
- HARPER J.R., 1990. Morphology of the Canadian Beaufort Sea coast. *Marine Geology* 91, 75–91.
- HARRIS C. and MURTON J.B., 2005. *Cryospheric systems: glaciers and permafrost*. Geological Society, London, Special Publication 242: 161p.
- HARRY D.G., FRENCH H.M. and CLARK M.J., 1983. Coastal conditions and processes, Sachs Harbour, Banks Island, western Canadian Arctic. *Zeitschrift für Geomorphologie Supplementband* 47, 1–26.
- HARVEY A.M., MATHER A.E. and STOKES M.R. 2005. Alluvial fans: geomorphology, sedimentology, dynamics. A review of alluvial-fan research. *Special Publication of the Geological Society of London vol. 251, 239 pp.*
- HEIN C.J., FITZGERALD D.M., CARRUTHERS E.A., STONE B.D., BARNHARDT W.A., GONTZ A.M., 2012. Refining the model of barrier island formation along a paraglacial coast in the Gulf of Maine. *Marine Geology* 307–310, 40–57.
- HÉQUETTE A. 1992. Morphosedimentological dynamics and coastal evolution in the Kongsfjorden area, Spitsbergen. *Polar Geography and Geology* 16, 321–329.
- HÉQUETTE A. and BARNES, P.W. 1990: Coastal retreat and shoreface profile variations in the Canadian Beaufort Sea. *Marine Geology* 91, 113–32.
- HÉQUETTE, A. and RUZ, M-H., 1986. Migration of offshore bars by a process of overtopping by storms within the framework of a marine transgression (Kvadehuk, Brøggerhalvøya, Spitsbergen). *Géographie physique et Quaternaire* 40, 197–206.
- HÉQUETTE A. and RUZ M-H., 1990. Coastal sedimentation along glacial outwash plain shorelines in northwest Spitsbergen. *Géographie physique et Quaternaire* 44, 77–88.
- HEWITT K., 2002. Introduction: Landscape assemblages and transitions in cold regions. In: HEWITT K. BYRNE M-L., ENGLISH M., YOUNG G., (Eds.), *Landscapes in Transition. Landform*



- Assemblages and Transformations in Cold Regions*. Kluwer Academic Publishers, Dordrecht, pp. 1- 9.
- HILL P.R., BARNES P.W., HÉQUETTE A. and RUZ M-H 1994. Arctic coastal plain shorelines. In Carter, R.W.G. and Woodroffe, C., editors, *Coastal evolution. Late Quaternary shoreline morphodynamics*. Cambridge: Cambridge University Press. 341-372pp.
- HODGKINS R., 1997. Glacier hydrology in Svalbard, Norwegian high Arctic. *Quaternary Science Reviews* 16, 957–973.
- HODSON A.J., TRANTER M., DOWDESWELL J.A., GURNELL A.M. AND HAGEN J.O., 1997. Glacier thermal regime and suspended-sediment yield: a comparison of two high-Arctic glaciers. *Annals of Glaciology* 24, 32-37.
- HOLTEDAHL H., 1998. The Norwegian strandflat – a geomorphic puzzle. *Norsk Geologisk Tidsskrift* 78, 47-66.
- HOLLING C.S., 2001. Understanding the complexity of economic, ecological and social systems. *Ecosystems* 4, 390–405.
- HORMES A., AKCAR N. and KUBIK P.W., 2011. Cosmogenic radionuclide dating indicates ice-sheet configuration during MIS 2 on Nordaustlandet, Svalbard. *Boreas* 40, 636-649.
- HOUNSLOW M.W. and MORTON A.C., 2004. Evaluation of sediment provenance using magnetic mineral inclusions in clastic silicates: comparison with heavy mineral analysis. *Sedimentary Geology* 171, 13–36.
- HOWARD J.L. 1992. An evaluation of shape indices as palaeoenvironmental indicators using quartzite and metavolcanic clasts in Upper Cretaceous to Palaeogene beach, river and submarine fan conglomerates. *Sedimentology* 39, 471-486.
- HUGUES Z., FITZGERALD D., WILSON C., PENNINGS S., WIĘSKI K. and MAHADEVAN A., 2009. Rapid headward erosion of marsh creeks in response to relative sea level rise. *Geophysical Research Letters* 36, doi:10.1029/2008GL036000.
- HUME J. D. and SCHALK M., 1964a. The effects of beach barrow in the Arctic. *Shore and Beach* 32, 37- 41.
- HUME J. D. and SCHALK M., 1964b. The effects of ice-push on Arctic beaches. *American Journal of Science* 262, 267- 273.
- HUME J.D. and SCHALK M., 1967. Shoreline processes near Barrow, Alaska: a comparison of the normal and the catastrophic. *Arctic* 20, 86-103.
- HUME J.D. and SCHALK M., 1976. The effects of ice on the beach and nearshore, Pt Barrow, Arctic Alaska. *La Revue de Géographie de Montréal* 30, 105-14.
- HUMLUM O., 2002. Modelling late 20th century precipitation in Nordenskiöld Land , central Spitsbergen , Svalbard , by geomorphic means. *Norwegian Geographical Journal* 56, 96-103.
- HUMLUM O., INSTANES A. and SOLLID J.L., 2003. Permafrost in Svalbard: a review of research history, climatic background and engineering challenges. *Polar Research* 22, 191-215.
- HUMLUM O., CHRISTIANSEN H. H. and JULIUSSEN, H., 2007: Avalanche derived rock glaciers in Svalbard. *Permafrost and Periglacial Processes* 18, 75–88.
- HURRELL, J.W., 1995. Decadal Trends in the North Atlantic Oscillation: Regional Temperatures and Precipitation. *Science* 269, 676-679
- HURRELL J. W., KUSHNIR Y., OTTERSEN G. and VISBECK M., 2003. *The North Atlantic Oscillation: climatic significance and environmental impact*. Geophysical Monograph Series 134. American Geophysical Union, Washington, D.C., USA.

- INGÓLFSSON Ó., 2011. Fingerprints of Quaternary glaciations on Svalbard. In MARTINI I, FRENCH H. and ALBERTI A. (eds.). *Ice-Marginal and Periglacial Processes and Sediments*. Geological Society, London, Special Publications, 354, 15-31.
- Intergovernmental Panel on Climate Change (IPCC), 2007. Climate Change 2007: The Physical Science Basis. Contribution of Working Group I to the Fourth Assessment Report of the Intergovernmental Panel on Climate Change, edited by S. Solomon *et al.*, Cambridge Univ. Press, Cambridge, 996 pp.
- IRVINE-FYNN, T.D.L., PORTER, P.R., BARRAND, N.E, BENN, D.I., TEMMINGHOFF, M. and LUKAS, S. 2010. **High Arctic glacial-periglacial interactions and the development of terrain morphology on Brøggerhalvøya, Svalbard.** *Proceedings of Geo2010: 63<sup>rd</sup> Canadian Geotechnical and 6<sup>th</sup> Canadian Permafrost Conferences*, Calgary, AB., Canada: 8pp.
- IRVINE-FYNN, T.D.L., BARRAND, N.E., PORTER, P.R., HODSON, A.J. and MURRAY, T., 2011. **Recent High-Arctic proglacial sediment redistribution: a process perspective using airborne lidar.** *Geomorphology* 125, 27-39.
- ISAKSSON E., POHJOLA V., JAUHIAINEN T., MOORE J., PINGLOT J.F., VAIKMÄE R., VAN DE WAL R.S.W., HAGEN J.O., IVASK J., KARLÖF L., MARTMA T., MEIJER H.A.J., MULVANEY R., THOMASSEN M. and VAN DEN BROEKE M., 2001. A new ice-core record from Lomonosovfonna, Svalbard: viewing the 1920-97 data in relation to present climate and environmental conditions. *Journal of Glaciology* 47, 335-345.
- ISAKSSON E., HERMANSON M., HICKS S., IGARASHI M., KAMIYAMA K., MOORE J., MOTOYAMA H., MUIR D., POHJOLA V., VAIKMÄE R., VAN DE WAL R.S.W. and WATANABE O., 2003: Ice cores from Svalbard – useful archives of past climate and pollution history, *Physics and Chemistry of the Earth* 28, 1217-1228.
- ISAKSSON E., DIVINE D., KOHLER J., MARTMA T., POHJOLA V., MOTOYAMA H. and WATANABE O., 2005. Climate oscillations as recorded in Svalbard ice core  $\delta^{18}\text{O}$  records between ad 1200 and 1997. *Geografiska Annaler* 87 A, 203–214.
- ISAKSSON E., KOHLER J., POHJOLA V., MOORE J., IGARASHI M., KARLÖF L., MARTMA T., MEIJER H., MOTOYAMA H., VAIKMÄE R. and VAN DE WAL R. S. W., 2005. Two ice-core  $\delta^{18}\text{O}$  records from Svalbard illustrating climate and sea-ice variability over the last 400 years. *The Holocene* 15, 501–509.

## J

- JACKSON R.M., 1931. A Traverse from Ice Fjord to Wijde Bay, Spitsbergen. *The Geographical Journal* 78 (3), 277-283.
- JAHN A., 1961. Quantitative analysis of some periglacial processes in Spitsbergen. *Zeszyty Naukowe Uniwersytetu Wrocławskiego Seria B, nr 5, Nauka o Ziemi III/ Geophysics, Geography, Geology II*: 3-54.
- JAHN A., 1967. Some features of mass movement on Spitsbergen slopes. *Geografiska Annaler* 49 A, 213-225
- JAKOBSSON M., L. A. MAYER, B. COAKLEY, J. A. DOWDESWELL, S. FORBES, B. FRIDMAN, H. HODNESDAL R. NOORMETS, R. PEDERSEN, M. REBESCO, H.-W. SCHENKE, Y. ZARAYSKAYA A., D. ACCETTELLA, A. ARMSTRONG, R. M. ANDERSON, P. BIENHOFF, A. CAMERLENGHI, I. CHURCH, M. EDWARDS, J. V. GARDNER, J. K. HALL, B. HELL, O. B. HESTVIK, Y. KRISTOFFERSEN, C. MARCUSSEN, R. MOHAMMAD, D. MOSHER, S. V. NGHIEM, M. T. PEDROSA, P. G. TRAVAGLINI, and P. WEATHERALL, The International Bathymetric Chart of the Arctic Ocean (IBCAO) Version 3.0, *Geophysical Research Letters*, doi: 10.1029/2012GL052219.

- JANIA J. and HAGEN J. O. (Eds.), 1996. *Mass balance of arctic glaciers*. Report 5, IASC, Potsdam, Germany. 62 pp.
- JANIA J., VASILENKO E., LAPAZARAN J., GŁOWACKI P., MIGAŁA K., BALUT A., PIWOWAR B.A., 2005. Temporal changes in the radiophysical properties of a polythermal glacier in Spitsbergen. *Annales of Glaciology* 42, 125 – 134.
- JENNINGS R. and SCHULMEISTER J., 2002. A field based classification scheme for gravel beaches. *Marine Geology* 186, 211-228
- JOHN B.S. and SUGDEN D.E., 1975. Coastal geomorphology of high latitudes. *Progress in Geography* 7, 53-132.

## K

- KALISH J.M., NYDAL R., NEDREAAS K.H., BURR G.S. and EINE G.L., 2001. A time history of pre- and post-bomb radiocarbon in the Barents Sea derived from Arcto-Norwegian cod otoliths. *Radiocarbon* 43, 843-855.
- KARCZEWSKI A., 1989. The development of the marginal zone of the Hørbyebreen, central Spitsbergen. *Polish Polar Research* 10(3), 371–377.
- KARCZEWSKI A. and KŁYSZ P., 1994. Lithofacies and structural analysis of crevasse filling deposits of the Svenbreen foreland (Petuniabukta, Spitsbergen). 21st Polar Symposium, Warszawa, 23–24.09.1994, 123–133.
- KARCZEWSKI A., BORÓWKA M., MAĆKOWIAK K., RYGIELSKI W., ULATOWSKI P. and WOJCIECHOWSKI A., 1987. Funkcjonowanie strefy marginalnej lodowca Hørbye oraz udział jego wód proglacialnych w rozwoju równi pływowej zatoki Petunia. Mat. XIV Symp. Pol., Lublin, 80–83.
- KARCZEWSKI A. (ED.), BORÓWKA M., GONERA P., KASPRZAK L., KŁYSZ P., KOSTRZEWSKI A., LINDNER L., MARKS L., RYGIELSKI W., STANKOWSKI W., WOJCIECHOWSKI A. and WYSOKIŃSKI L., 1990: *Geomorphology – Petuniabukta, Billefjorden, Spitsbergen, 1 : 40 000*. Univ. im. A. Mickiewicza, Poznań.
- KASPRZAK L. and EWERTOWSKI M., 2007. Ice-cored moraines in the Petunia Bukta area – examples from Ragnar marginal zone. *Landform Analysis* 5, 37–40.
- KENNEDY D. M., PAULIK R. and DICKSON M. E., 2010. Subaerial weathering versus wave processes in shore platform development: reappraising the Old Hat Island evidence. *Earth Surface Processes and Landforms* 36, 686-694.
- KIENAST F., WETTERICH S., KUZMINA S., SCHIRMEISTER L., ANDREEV A., TARASOV P., NAZAROVA L., KOSSLER A., FROLOVA L. and KUNITSKY V., 2011. Paleontological records indicate the occurrence of open woodlands in a dry inland climate at the present-day Arctic coast in western Beringia during the Last Interglacial. *Quaternary Science Reviews* 30, 2134-2159.
- KIDA, J. 1986. Eolian processes in the Werenskiöld, Nann and Torell glacier forefields (Wedel-Jarlsberg Land, SW Spitsbergen). *Acta Universitatis Wratislaviensis*, Wrocław: VI (1966), 25–43.
- KING C. A. M. and BUCKLEY J. T., 1968. The analysis of stone size and shape in an Arctic environment. *Journal of Sedimentary Petrology* 38, 200-218.
- KLEMSDAL T., 1986. Lagoons along the coast of the Svalbard archipelago and the island of Jan Mayen. *Norsk Geografisk Tidsskrift* 40, 37–44.
- KLEMSDAL T., 2010. Svalbard and Jan Mayen. In: Eric C.F. Bird (ed.) *Encyclopedia of the World's Coastal Landforms*. Springer, Dordrecht: 581 – 588.
- KŁYSZ P., 1983. Uwagi o morfologii doliny Ebba w rejonie Petuniabukta (Spitsbergen). Spr. PTPN, 97–99, 172–173.

- KŁYSZ P., 1985. Glacial forms and deposits of Ebba Glacier and its foreland (Petuniabukta region, Spitsbergen). *Polish Polar Research* 6, 283–299.
- KŁYSZ P., LINDNER L., MAKOWSKA A., MARKS L. and WYSOKIŃSKI L., 1988. Late Quaternary glacial episodes and sea level changes in the northeastern Billefjorden region, Central Spitsbergen. *Acta Geologica Polonica* 38, 107–123.
- KŁYSZ P., LINDNER L., MARKS L. and WYSOKIŃSKI L., 1989: Late Pleistocene and Holocene relief remodelling in the Ebbadalen–Nordenkiöldbreen region in Olav V Land, central Spitsbergen. *Polish Polar Research* 10, 277–301.
- KOENIGK T., MIKOLAJEWICZ U., JUNGCLAUS J.C. and KROLL A., 2009. Sea ice in the Barents Sea: seasonal to interannual variability and climate feedbacks in a global coupled model. *Climate Dynamics* 32, 1119–1138.
- KOPPE M.N. and HALLET B., 2002. Influence of rapid glacial retreat on the rate of erosion by tidewater glaciers. *Geology* 30, 47–50.
- KOSTRZEWSKI A. and ZWOLIŃSKI Z., 2003. Środowisko sedimentacyjne stożków piargowych. Materiały Warsztatów Geomorfologicznych SGP, 49–52.
- KOSTRZEWSKI, A., KAPUŚCIŃSKI, J., KLIMCZAK, R., KANIECKI, A., STACH, A. and ZWOLIŃSKI, Z., 1989. The dynamics and rate of denudation of glaciated and non-glaciated catchments, central Spitsbergen. *Polish Polar Research* 10, 317–367.
- KOWALSKA A. and SROKA W., 2008. Sedimentary environment of the Nottinghambukta delta, SW Spitsbergen. *Polish Polar Research* 29/3: 245–259.
- KWOK R. and ROTHROCK D.A., 2009. Decline in Arctic sea ice thickness from submarine and ICESat records: 1958 – 2008. *Geophysical Research Letters* 36, L15501, doi:10.1029/2009GL039035.

## L

- LAJEUNESSE P. and HANSON M., 2008. Field observations of recent transgression on eastern and northern Melville Island, western Canadian Arctic Archipelago. *Geomorphology* 101, 618–630.
- LAMBECK K., 1995. Constraints on the Late Weichselian ice-sheet over the Barents Sea from observations of raised shorelines. *Quaternary Science Reviews* 14, 1–16.
- LAMBECK K., 1996. Limits on the areal extent of the Barents Sea ice sheet in Late Weichselian time. *Global and Planetary Change* 12, 41–51.
- LAMBRECHT A., MAYER C., HAGG W., POPOVNIK V., REZEPKIN A., LOMIDZE N., and SVANADZE D., 2011. A comparison of glacier melt on debris-covered glaciers in the northern and southern Caucasus. *The Cryosphere* 5, 525–538.
- LANDVIK J.Y., BONDEVİK S., ELVERHØI A., FJELDSKAAR W., MANGERUD J., SALVIGSEN O., SIEGERT M.J., SVENDSEN J.I. and VORREN T.O., 1998. The last glacial maximum of Svalbard and the Barents Sea area: ice sheet extent and configuration. *Quaternary Science Reviews* 17, 43–75.
- LANDVIK J.Y., INGOLFSSON O., MIENERT J., LEHMAN S.J., SOLHEIM A., ELVERHØI A. and OTTESEN D., 2005. Rethinking Late Weichselian ice-sheet dynamics in coastal NW Svalbard. *Boreas* 34, 7–24.
- LANTUIT H. and POLLARD W.H., 2008. Fifty years of coastal erosion and retrogressive thaw slump activity on Herschel Island, southern Beaufort Sea, Yukon Territory, Canada. *Geomorphology* 95, 84 – 102.
- LANTUIT H., RACHOLD V., POLLARD W.H., STEENHUISEN F., ØDEGÅRD R. and HUBBERTEN H.-W., 2009. Towards a calculation of organic carbon release from erosion of Arctic coasts using non-fractal coastline datasets. *Marine Geology* 257, 1–10.

- LANTUIT H., OVERDUIN P., SOLOMON S. and MERCIER D., 2010. Coastline dynamics in polar systems using remote sensing. In MAANAN M. AND ROBIN M (eds.) *Geomatic Solutions For Coastal Environments*. Nova Science Publishers. 163-174 pp.
- LANTUIT H., OVERDUIN P.P., COUTURE N., ARÉ F., ATKINSON D., BROWN J., CHERKASHOV G., DROZDOV D., FORBES D.L., GRAVES-GAYLORD A., GRIGORIEV M., HUBBERTEN H.-W., JORDAN J., JORGENSEN T., ØDEGÅRD R.S., OGORODOV S., POLLARD W., RACHOLD V., SEDENKO S., SOLOMON S., STEENHUISEN F., STRELETSKAYA I., VASILIEV A. and WETTERICH S. 2012. The ACD coastal database: a new classification scheme and statistics on Arctic permafrost coastlines. *Estuaries and Coasts* 35: 383-400.
- LARIO C., ZAZO A.J. and PLATER I., 2001. Particle size and magnetic properties of Holocene estuarine deposits from the Donana National Park (SW Iberia): evidence of gradual and abrupt coastal sedimentation. *Zeitschrift für Geomorphologie* 45, 33–54.
- LARSSON S., 1982. Geomorphological effects on the slopes of Longyear valley, Spitsbergen, after a heavy rainstorm in July 1972. — *Geografiska Annaler* 64 A: 105—125.
- LAWRENCE D. M., SLATER A. G., TOMAS R. A., HOLLAND M. M. and DESER C., 2008. Accelerated Arctic land warming and permafrost degradation during rapid sea ice loss. *Geophysical Research Letters* 35, L11506, doi:10.1029/2008GL033985.
- LEONTIEV I.O., 2006. Forecast of Coastal Changes Based on Morphodynamical Modeling. *Oceanology* 46, 564–572.
- LEVIN I. and KROMER B., 1997. Twenty years of atmospheric (CO<sub>2</sub>)-C-14 observations at Schauinsland station, Germany. *Radiocarbon* 39, 205-218.
- LISS S., SNYDER P. K., and HARDING K. J., 2010. Modeling the Response of Boreal Forest Expansion on the Summer Arctic Frontal Zone. American Geophysical Union, Fall Meeting 2010, abstract #A41D-0121.
- LIM M., ROSSER N.J., ALLISON R.J. and PETLEY D.N., 2010. Erosional processes in the hard rock coastal cliffs at Staithes, North Yorkshire. *Geomorphology* 114, 12-21.
- LIU J., CURRY J.A. and HU Y., 2004. Recent Arctic Sea Ice Variability: Connection to the Arctic Oscillation and the ENSO. *Geophysical Research Letters* 31, L09211, doi:10.1029/2004GL019858
- LONG A.J., WALLER M.P. and STUPPLES P., 2006. Driving mechanisms of coastal change: peat compaction and the destruction of late Holocene coastal wetlands. *Marine Geology* 225, 63–84.
- LONG A.J., STRZELECKI M.C., LLOYD J.M. and BRYANT C., 2012. Dating High Arctic Holocene relative sea level changes using juvenile articulated marine shells in raised beaches. *Quaternary Science Reviews* 48, 61-66.
- LØNNE I. and NEMEC W., 2004. High-arctic fan delta recording deglaciation and environment disequilibrium. *Sedimentology* 51, 553-589.
- LØNNE I. and LYSÅ A., 2005. Deglaciation dynamics following the Little Ice Age on Svalbard: Implications for shaping of landscapes at high latitudes. *Geomorphology* 72, 300-319.
- LUKAS, S., NICHOLSON, L. I., ROSS, F. H. and HUMLUM, O. (2005), Formation, meltout processes and landscape alteration of high-arctic ice-cored moraines - examples from Nordenskiöld land, Central Spitsbergen. *Polar Geography* 29, 157-187.
- LUKYANOVA S. A., SAFYANOV G. A., SOLOVEVA G. D. and SHIPILOVA L. M., 2008. Types of Arctic Coasts of Russia. *Oceanology* 48;: 268–274.
- LUNDBERG J. and LAURITZEN S-E., 2002. The search for an Arctic coastal karren model in Norway and Spitzbergen. In: K. HEWITT, M-L. BYRNE, M. ENGLISH and G. YOUNG (eds.), *Landscapes in Transition. Landform Assemblages and Transformations in Cold Regions*. Kluwer Academic Publishers, Dordrecht:185-203.



## M

- MAJEWSKI W., SZCZUCIŃSKI W. and ZAJĄCZKOWSKI M., 2009. Interactions of Arctic and Atlantic water-masses and associated environmental changes during the last millennium, Hornsund (SW Svalbard). *Boreas* 38, 529–544.
- MAŁECKI K., 2009. *Zmiany zasięgów i geometrii lodowców otoczenia Petuniabukta (Ziemia Dicksona, Spitsbergen) w XX i XI wieku. (Changes in the extent and geometry of glaciers in Petuniabutka region (Dicksonland, Spitsbergen) in 20<sup>th</sup> and 21<sup>st</sup> century)*. Unpublished MSc thesis (in Polish). Faculty of Geographical and Geological Sciences, Adam Mickiewicz University, Poznań. 149 pp.
- MAKOWSKA M., 2008. *Dynamika transportu fluwialnego w zlewni zlodowaczonej Ebbaelva, Spitsbergen środkowy, w sezonach letnich 2005 i 2006*. M. Sc. Thesis, Inst. Paleogeography and Geoecology AMU, 79 p.
- MANGERUD J. and SVENDSEN J.I., 1990. Deglaciation chronology inferred from marine sediments in a proglacial lake basin, western Spitsbergen, Svalbard. *Boreas* 19, 249–272.
- MANGERUD J. and SVENDSEN J.I., 1992. The last interglacial glacial period on Spitsbergen, Svalbard. *Quaternary Science Reviews* 11, 633–664.
- MANGERUD J. and LANDVIK J. Y., 2007. Younger Dryas cirque glaciers in western Spitsbergen: smaller than during the Little Ice Age. *Boreas* 36, 278–285.
- MANGERUD J., BOLSTAD M., ELGERSMA A., HELLIKSEN D., LANDVIK J.Y., LONNE I., LYCKE A.K., SALVIGSEN O., SANDAHL T. and SVENDSEN J.I., 1992. The last glacial maximum on Spitsbergen, Svalbard. *Quaternary Research* 38, 1–31.
- MANGERUD J., DOKKEN T., HEBBELN D., HEGGEN B., INGOLFSSON O., LANDVIK J.Y., MEJDAHL V., SVENDSEN J.I. and VORREN T.O., 1998. Fluctuations of the Svalbard-Barents Sea ice sheet during the last 150 000 years. *Quaternary Science Reviews* 17, 11–42.
- MARSZ A.A., 1995. *Wskaźnik oceanizmu jako miara klimatycznego współdziałania w systemie ocean-atmosfera-kontynenty*. WSM, Gdynia, 110 p.
- MARSZ A., 1996. Processes controlling shore morphology in recently developing fjords (based on examples from Hornsund and Admiralty Bay). *Proceedings of the Department of Navigation Naval Academy in Gdynia* 3, 85–141.
- MARTINS C. (Ed.), 1867. *Les glaciers actuels et leur ancienne extension pendant la période glaciaire*. Imprimerie J. Claye, Paris. 94 pp.
- MARZO M., and PUIGDEFÀBREGAS C., 1993. *Alluvial sedimentation*. Oxford: Basil Blackwell. 585 pp.
- MASON O.K., 2010. Beach ridge geomorphology at Cape Grinnell, northern Greenland: a less icy Arctic in the mid-Holocene. *Danish Journal of Geography* 110, 337–355.
- MATTHEWS E.R., 1983. Measurements of beach pebble attrition in Pallister Bay, southern North Island, New Zealand. *Sedimentology* 30, 787–799.
- MATTHEWS J.A. and SHAKESBY R.A., 1984. The status of the 'Little Ice Age' in southern Norway: relative age dating of Neoglacial moraines with Schmidt Hammer and lichenometry. *Boreas* 13, 333–46.
- MAZUREK M, PALUSZKIEWICZ R, RACHLEWICZ G. and ZWOLIŃSKI Z., 2012. Variability of water chemistry in Tundra Lakes, Petuniabukta Coast, Central Spitsbergen, Svalbard. *Scientific World Journal* doi:10.1100/2012/596516
- MCCANN S.B. and OWENS E.H., 1969. The size and shape of sediments in three Arctic beaches, SW Devon Island, NWT. *Arctic and Alpine Research* 1, 267–78.
- MCCANN S.B. and TAYLOR R.B., 1975. Beach freezeup sequence at Radstock Bay, Devon Island, Arctic Canada. *Arctic and Alpine Research* 7, 379–86.

- MCCANN S.B. and DALE J.E., 1986. Sea ice breakup and tidal flat processes, Forbisher Bay, Baffin Island. *Physical Geography* 7, 168-180.
- MCCANN S.B. and HANNELL F.G., 1971. Depth of the "frost table" on Arctic beaches, Cornwallis and Devon Islands, N. W. T., Canada. *Journal of Glaciology* 10, 155-158.
- MCCANN S.B., DALE J.E. and HALE P.B., 1981. Subarctic tidal flats in areas of large tidal range, southern Baffin Island, Eastern Canada. *Géographie physique et Quaternaire* 35, 183-204.
- MERCIER, D. 2000. Du glaciaire au paraglaciaire: la métamorphose des paysages polaires au Svalbard. *Annales de Géographie* 616, 580-596
- MERCIER D., 2008. Paraglacial and paraperiglacial landsystems: concepts, temporal scales and spatial distribution. *Géomorphologie: relief, processus, environnement* 4, 223-233.
- MERCIER D. and LAFFLY D., 2005. Actual paraglacial progradation of the coastal zone in the Kongsfjorden area, western Spitsbergen (Svalbard). In C. HARRIS and J.B. MURTON (eds.): *Cryospheric systems: glaciers and permafrost*. Geological Society, London, Special Publication 242, 111-117.
- MERCIER D., ÉTIENNE S., SELLIER D. and ANDRÉ M-F., 2009. Paraglacial gullying of sediment-mantled slopes: a case study of Colletthøgda, Kongsfjorden area, West Spitsbergen (Svalbard). *Earth Surface Processes and Landforms* 34, 1772-1789.
- MIGON P., 1997. Post-emergence modification of marine cliffs and associated shore platforms in periglacial environment, SW Spitsbergen: implications for the efficacy of cryoplanation processes. *Quaternary Newsletter* 81, 9-17.
- MILLER D.J., 1960. "Giant Waves in Lituya Bay, Alaska" Geological Survey Professional Paper 354-C, U.S. Government Printing Office, Washington.
- MOIGN A., 1974. Geomorphologie du strandflat au Svalbard: problèmes (age, origine, processus), méthodes de travail. *Inter-Nord* 13-14, 67-72.
- MOIGN A. and GUILCHER A., 1967. A coastal spit in periglacial arctic environment: Sarstangen, Spitsbergen. *Norvège* 14, 5-17.
- MOIGN A. and HÉQUETTE A., 1985. Summertime evolution of an arctic coast, Broggerhalvøya, Spitsbergen. *Norvège* 32, 5-17.
- MOOK W.M. and VAN DER PLICHT J., 1999. Reporting <sup>14</sup>C activities and concentrations. *Radiocarbon* 41, 227-239.
- MORISON J., AAGAARD K. and STEELE M., 2000. Recent Environmental Changes in the Arctic: A Review. *Arctic* 53, 359-371.
- MÖLLER P., STUBDRUP O.P. and KRONBORG C., 1995. Late Weichselian to early Holocene sedimentation in a steep fjord/valley setting, Visdalen, Edgeøya, eastern Svalbard: glacial deposits, alluvial/colluvial-fan deltas and spit-platforms. *Polar Research* 14, 181-203.
- MØLLER J.J., YEVZEROV V.Y., KOLKA V.V. and CORNER C.D., 2002. Holocene raised-beach ridges and sea-ice-pushed boulders on the Kola Peninsula, northwest Russia: indicators of climatic change. *The Holocene* 12, 169-176.
- MUSKETT R., LINGLE C., SAUBER J., POST A., TANGBORN W., RABUS B. and ECHELMAYER K., 2009. Airborne and spaceborne DEM- and laser altimetry-derived surface elevation and volume changes of the Bering Glacier system, Alaska, USA, and Yukon, Canada, 1972-2006. *Journal of Glaciology* 55, 16-26.
- MUTO T., 1987. Coastal Fan Processes Controlled by Sea Level Changes: A Quaternary Example from the Tenryugawa Fan System, Pacific Coast of Central Japan. *Journal of Geology* 95, 716-724.

## N

- NANSEN F., 1922. The strandflat and isostasy. *Videnskapsselskapets Skrifter. I. Mat.-Naturu. Klasse. 1921*. No. 11. 313 pp.
- NEMEC W. and STEEL R.J. 1988. *Fan Deltas – Sedimentology and Tectonic Settings*. Blackie, London, 444 pp.
- NICHOLS R.L. 1961. Characteristics of beaches formed in polar climates. *American Journal of Science* 259, 694-708.
- NICHOLS R.L. 1968. Coastal geomorphology, McMurdo Sound, Antarctica. *Journal of Glaciology* 7 (51), 449-478.
- NIEDZIELSKI T., MIGOŃ P. and PLACEK A., 2009. A minimum sample size required for Schmidt Hammer measurements. *Earth Surface Processes and Landforms* 34, 1713–1725.
- NIELSEN N. 1979. Ice-foot processes. Observations of erosion of the rocky coast, Disko, West Greenland. *Zeitschrift für Geomorphologie* 23, 321-331.
- NIELSEN N., 1992. A boulder beach formed by waves from a calving glacier: Eqip Sermia, West Greenland. *Boreas* 21, 159 – 168.
- NIELSEN N., 1994. Geomorphology of a degrading Arctic delta, Sermilik, South-East Greenland. *Geografisk Tidsskrift* 94, 46-57.
- NIKIFOROV S., PAVLIDIS Y., RACHOLD V., GRIGORYEV M., RIVKIN M, IVANOVA N. and KOREISHA M., 2005. Morphogenetic classification of the Arctic coastal zone. *Geo-Marine Letters* 25, 89-97.
- NORDØY E.S., 1995. Gastroliths in the harp seal *Phoca Groenlandica*. *Polar Research* 14, 335-338.
- Norwegian Arctic Climate Impact Assessment (NorACIA) Report 2011. Climate change in the Norwegian Arctic. Consequences for life in the north. Norwegian Polar Institute Report Series no. 136: 138pp.
- NUTH C., MOHOLDT G., KOHLER J., HAGEN J.O. and KÄÄB A., 2010. Svalbard glacier elevation changes and contribution to sea level rise. *Journal of Geophysical Research* 115: doi:10.1029/2008JF001223.

## O

- ØDEGÅRD R. S. and SOLLID J. L., 1993. Coastal cliff temperatures related to the potential for cryogenic weathering processes, western Spitsbergen, Svalbard. *Polar Research* 12, 95-106.
- ØDEGÅRD R. S, ETZELMÜLLER B., VATNE G. and SOLLID J., 1995. Nearsurface spring temperatures in an Arctic coastal cliff: possible implications of rock breakdown. In O. SLAYMAKER (ed.): *Steepland geomorphology*. Wiley, Chichester: 89–102.
- OERLEMANS J., 2007. Extracting a climate signal from 169 glacier records. *Science* 308, 675–677.
- OERLEMANS J., JANIA J. and KOLONDRÁ L., 2011. Application of a minimal glacier model to Hansbreen, Svalbard. *The Cryosphere* 5, 1-11.
- OGORODOV S.A., 2003. The role of sea ice in the coastal zone dynamics of the arctic seas. *Water Resources* 30, 509-518.
- ORFORD J. D., 1975. Discrimination of particle zonation on a pebble beach. *Sedimentology* 22, 441-463.
- ORFORD J., 2004. Barrier and Barrier Islands. In GOUDIE A., (Ed.). *Encyclopedia of Geomorphology*. London, Routledge, 1202 pp.
- ORFORD J.D., CARTER R.W.G. AND FORBES D.L., 1991a. Gravel barrier migration and sea-level rise: some observations from Nova Scotia. *Journal of Coastal Research* 7, 477–490.

- ORFORD J.D., CARTER R.W.G. and JENNINGS S.C., 1991b. Coarse clastic barrier environments: evolution and implications for Quaternary sea-level interpretation. *Quaternary International* 9, 87– 104.
- ORFORD J.D., HINTON A.C., CARTER R.W.G. and JENNINGS S.C., 1992. A tidal link between sea-level rise and coastal response of a gravel-dominated barrier, Story Head, Nova Scotia. In: Woodworth, P., Pugh, D.T., De Ronde, J., Warrick, R.G., Hannah, J. (Eds.), *Sea-Level Changes: Determination and Effects*. Geophysical Monograph Series, vol. 69. American Geophysical Union, Washington, DC, pp. 71– 79.
- ORFORD J.D., CARTER R.W.G., MCKENNA J. and JENNINGS S.C., 1995a. The relationship between the rate of mesoscale sea-level rise and the retreat rate of swash-aligned gravel-dominated coastal barriers. *Marine Geology* 124, 177– 186.
- ORFORD J.D., CARTER R.W.G., JENNINGS S.C. and HINTON A.C., 1995b. Processes and timescales by which a coastal gravel-dominated barrier responds geomorphologically to sea-level rise: Story Head barrier, Nova Scotia. *Earth Surface Processes and Landforms* 20, 21– 37.
- OSTERKAMP T.E. AND GOSINK J.P., 1984. Observations and analyses of sediment-laden sea ice. In: P.W. BARNES, D.M. SCHELL AND E. REIMNITZ (eds.). *The Alaskan Beaufort Sea: Ecosystems and Environments*. Academic Press, Orlando: 73-93.
- OTTESEN, D., DOWDESWELL, J. A. and RISE, L. 2005. Submarine landforms and the reconstruction of fast-flowing ice streams within a large Quaternary ice sheet: the 2500-km-long Norwegian-Svalbard margin (57°–80°N). *Geological Society of America Bulletin* 117, 1033–1050.
- OVERDUIN P. P., HUBBERTEN H. -W., RACHOLD V., ROMANOVSKII N., GRIGORIEV M. N. and KASYMSKAYA M., 2007. Evolution and degradation of coastal and offshore permafrost in the Laptev and East Siberian Seas during the last climatic cycle, Coastline changes : interrelation of climate and geological processes. In: J. HARFF, W.H. HAY AND D.M. TETZLAFF. *The Geological Society of America special paper* 426, Boulder, Colorado. *Geological Society of America*, 97-111. doi:10.1130/2007.2426(07).
- OVEREEM I. and SYVITSKI J.P.M., 2010. Shifting discharge peaks in Arctic rivers, 1977–2007. *Geografiska Annaler* 92A, 285–296.
- OWENS E.H. AND MCCANN S.B., 1970. The role of ice in the arctic beach environment with special references to Cape Ricketts, south-west Devon Island, Northwest Territories, Canada. *American Journal of Science* 268: 397-414.
- OWENS E.H. AND HARPER J.R., 1983. Arctic coastal processes: a state-of-knowledge review. In: B.J. HOLDEN (ed.) Proc. Can. Coastal Conf. National Research Council Canada (ACROSES), Ottawa: 3-18.

## P

- PALUSZKIEWICZ R., 2003. Zróżnicowanie natężenia transport eolicznego w warunkach polarnych jako efekt zmienności czynników meteorologicznych na przykładzie doliny Ebby (Petuniabukta, Billefjorden, Spitsbergen środkowy). *Mat. XXIX Symp. Pol.*, Kraków, 235–238.
- PÄLLI, A., MOORE, J. C., JANIA, J., KOLONDRÁ, L. and GLOWACKI, P., 2003. The drainage pattern of two polythermal glaciers: Hansbreen and Werenskiöldbreen in Svalbard. *Polar Research* 22(2), 355–371.
- PEDERSEN, S. A. S., DAHL-JENSEN, T., JEPSEN, H., LARSEN, L. M., PEDERSEN, G. K., NIELSEN, T., PEDERSEN, A. K., AND WENG, W. 2001. *Fjeldskred ved Paatuut*. Rep. 2001/99. Geological Survey of Denmark and Greenland, Copenhagen.

- PETERSEN K.S. and HOCH E., 2004. Holocene marine fauna and shoreline studies in the Sisimiut area. In GOTFREDSEN A.B., and MØBJERG T. (Eds.) *Nipisat – a Saqqaq Culture Site in Sisimiut, Central West Greenland. Man and Society* 31/2004 Copenhagen Danish Polar Centre 2004.
- PISARIC M.F.J., THIENPONT J.R., KOKELJ S.V., NESBITT H., LANTZ T.C., SOLOMON S. and SMOL J.P., 2011. Impacts of a recent storm surge on an Arctic delta ecosystem examined in the context of the last millennium. *Proceedings of the National Academy of Sciences* 108, 8960-8965.
- PORTER N.J. and TRENHAILE A.S., 2007. Short-term rock surface expansion and contraction in the intertidal zone. *Earth Surface Processes and Landforms* 32, 1379–1397.
- PORTER N.J., TRENHAILE A.S., PRESTANSKI K.J. and KANYAYA J.I., 2010. Patterns of surface downwearing on shore platforms in eastern Canada. *Earth Surface Processes and Landforms* 35, 1793-1810.
- PRITCHARD H.D., ARTHURN R.J., VAUGHAN D.G. and EDWARDS L.A., 2009. Extensive dynamic thinning on the margins of the Greenland and Antarctic ice sheets. *Nature* 461, 971-975.
- PRZYBYLAK R., 2003. *The Climate of the Arctic*. Atmospheric and Oceanographic Sciences Library 26, Kluwer Academic Publishers, Dordrecht/Boston/London: 288p.
- PRZYBYLAK R., KEJNA M., ARAŻNY A., MASZEWSKI R., GLUZA A., HOJAN M., MIGAŁA K., SIKORA S., SIWEK K. and ZWOLIŃSKI Z., 2007. Porównanie warunków meteorologicznych na zachodnim wybrzeżu Spitsbergenu w sezonie letnim 2006 r. In PRZYBYLAK R., KEJNA M., ARAŻNY A. and GŁOWACKI P., (eds.), *Abiotyczne środowisko Spitsbergenu w latach 2005–2006 w warunkach globalnego ocieplenia*. Wyd. Zakł. Klim. UMK Toruń, 179–194.
- PULINA M. 1982. Karst-related phenomena at the Bertil Glacier, West Spitsbergen. *Kras i Speleologia*, 4, Katowice
- PYÖKÄRI M., 1997. The provenance of beach sediments on Rhodes, southeaster Greece, indicated by sediment texture, composition and roundness. *Geomorphology* 18, 315-332.
- PYÖKÄRI M., 1999. Beach sediments of Crete: texture, composition, roundness, source and transport. *Journal of Coastal Research* 15, 537-553.

## R

- RACHLEWICZ G., 1989. Budowa i klasyfikacja łąch w korytach rzek roztokowych na przedpolu lodowca Hørbye – Spitsbergen Środkowy. *Mat. XVI Symp. Pol.*, Toruń, 122–124.
- RACHLEWICZ G., 2003. Geomorfologia strefy marginalnej lodowca Ebba. *Mat. Warsztatów Spitsbergeńskich SGP*, 40–41.
- RACHLEWICZ G., 2009. River floods in glacier covered catchments of the high Arctic (Billefjorden-Wijdefjorden, Svalbard). *Norsk Geografisk Tidsskrift* 63, 115-122.
- RACHLEWICZ G., 2009. *Contemporary sediment fluxes and relief changes in high Arctic glacierized valley systems (Billefjorden, Central Spitsbergen)*. Wydawnictwo Naukowe UAM, Poznań: 203pp.
- RACHLEWICZ G., 2010. Paraglacial modifications of glacial sediments over millennial to decadal time-scales in the high Arctic (Billefjorden, central Spitsbergen, Svalbard). *Quaestiones Geographicae* 29, 59–67.
- RACHLEWICZ G. and SZCZUCIŃSKI W., 2003. Czwartorzędowe podniesione osady morskie centralnego Spitsbergenu – nowe dane. *Mat. IV Symp. „Geneza, litologia i stratygrafia utworów czwartorzędowych”*, Poznań, 72.



- RACHLEWICZ G. and SZCZUCIŃSKI W., 2008. Changes in permafrost active layer thermal structure in relation to meteorological conditions, Petuniabukta, Svalbard. *Polish Polar Research* 28, 261–278.
- RACHLEWICZ G., SZCZUCIŃSKI W. and EWERTOWSKI M., 2007. Post-“Little Ice Age” retreat rates of glaciers around Billefjorden in central Spitsbergen, Svalbard. *Polish Polar Research* 28, 159–186.
- RACHOCKI A. and CHURCH M.A. (eds) (1990) *Alluvial Fans: a Field Approach*. John Wiley & Sons, Chichester, 301 pp.
- RACHOLD V., ARE F., ATKINSON D., CHERKASHOV G. and SOLOMON S., 2005. Arctic Coastal Dynamics (ACD): an introduction. *Geo-Marine Letters* 25, 63 – 68.
- RAPP A., 1960. *Talus slopes and mountain walls at Tempelfjorden, Spitsbergen—a geomorphological study of the denudation of slopes in an Arctic locality*. Norsk Polarinstitutt Skrifter 119, 96pp.
- REIMER P.J., BAILLIE M.G.L., BARD E., BAYLISS A., BECK J.W., BERTRAND C.J.H., BLACKWELL P.G., BUCK C.E., BURR G.S., CUTLER K.B., DAMON P.E., EDWARDS R.L., FAIRBANKS R.G., FRIEDRICH M., GUILDERSON T.P., HOGG A.G., HUGHEN K.A., KROMER B., MCCORMAC F.G., MANNING S.W., RAMSEY C.B., REIMER R.W., REMMELE S., SOUTHON, J.R., STUIVER M., TALAMO S., TAYLOR F.W., VAN DER PLICHT J. and WEYHENMEYER C.E., 2004. IntCal04 terrestrial radiocarbon age calibration, 26-0 ka BP. *Radiocarbon* 46, 1029-1058.
- REIMER P.J., BAILLIE M.G.L., BARD E., BAYLISS A., BECK J.W., BLACKWELL P.G., BRONK RAMSEY C., BUCK C.E., BURR G.S., EDWARDS R.L., FRIEDRICH M., GROOTES P.M., GUILDERSON T.P., HAJDAS I., HEATON T.J., HOGG A.G., HUGHEN K.A., KAISER K.F., KROMER B., MCCORMAC F.G., MANNING S.W., REIMER R.W., RICHARDS D.A., SOUTHON J.R., TALAMO S., TURNEY C.S.M., VAN DER PLICHT J. and WEYHENMEYER C.E., 2009. Intcal09 and Marine09 radiocarbon age calibration curves, 0-50,000 years cal BP. *Radiocarbon* 51, 1111-1150.
- REIMNITZ E. and MAURER D.K., 1979a. Effects of storm surges on the Beaufort Sea coast, northern Alaska. *Arctic* 32, 329-344.
- REIMNITZ E. and MAURER D.K., 1979b. Eolian sand deflation – a cause of gravel barrier islands in arctic Alaska? *Geology* 7, 507-510.
- REIMNITZ E., BARNES P.W. and HARPER J.R., 1990. A review of beach nourishment from ice transport of shoreface materials, Beaufort Sea, Alaska. *Journal of Coastal Research* 6: 439-470.
- REINSON G.E. and ROSEN P.S., 1982. Preservation of ice-formed features in a sub-Arctic sandy beach sequence: geologic implications. *Journal of Sedimentary Petrology* 52, 463-71.
- REX R. W., 1964. Arctic Beaches, Barrow, Alaska. In R.L MILLER (ed.) *Papers in Marine Geology*. MacMillan, New York: 384- 400.
- RHINE J. and SMITH D., 1988. The late Pleistocene Athabaskan braid delta of northeastern Alberta, Canada: a paraglacial drainage system affected by aeolian san supply. In W. NEMEC AND R. STEEL (eds.) *Fan Deltas: Sedimentology and Tectonic Settings*. Blackie and Son, London: 158-172.
- RIGNOT E., BOX J. E., BURGESS E. AND HANNA E., 2008. Mass balance of the Greenland ice sheet from 1958 to 2007. *Geophysical Research Letters* 35: L20502, doi:10.1029/2008GL035417.
- RIGNOT E., VELICOGNA I., VAN DEN BROEKE M. R., MONAGHAN A. AND LENAERTS J., 2011. Acceleration of the contribution of the Greenland and Antarctic ice sheets to sea level rise. *Geophysical Research Letters* 38: L05503, doi:10.1029/2011GL046583.
- RIZETTO F., and TOSI L., 2012. Rapid response of tidal channel networks to sea-level variations (Venice Lagoon, Italy). *Global and Planetary Change* 92, 191-197.

- ROGERS J. C. and MOSLEY-THOMPSON, E., 1995. Atlantic Arctic cyclones and the mild Siberian winters of the 1980s. *Geophysical Research Letters* 22, 799–802.
- ROTMAN R., NAYLOR L., McDONNELL R. and MACNIOCAILL C., 2008. Sediment transport on the Freiston Shore managed realignment site: an investigation using environmental magnetism. *Geomorphology* 100, 241–255.
- ROMANOVSKII N., HUBBERTEN H.-W., GAVRILOV A., TUMSKOY V. and KHOLODOV A.L., 2004. Permafrost of the east Siberian Arctic shelf and coastal lowlands. *Quaternary Science Reviews* 23, 1359–1369.
- ROMANOVSKY V., SMITH S AND CHRISTIANSEN H., 2010. Permafrost Thermal State in the Polar Northern Hemisphere during the International Polar Year 2007–2009: a Synthesis. *Permafrost and Periglacial Processes* 21: 106–116.
- ROSEN P.S., 1978. Degradation of ice-formed beach deposits. *Maritime Sediments* 14, 63–68.
- ROSEN P.S., 1979. Boulder barricades in Central Labrador. *Journal of Sedimentary Petrology* 49, 1113–1124.
- ROWLAND J. C., JONES C. E., ALTMANN G., BRYAN R., CROSBY B. T., GEERNAERT G. L., HINZMAN L. D., KANE D. L., LAWRENCE D. M., MANCINO A., MARSH P., MCNAMARA J. P., ROMANOVSKY V. E., TONIOLO H., TRAVIS B. J., TROCHIM E. and WILSON C.J., 2010. Arctic landscapes in transition: responses to thawing permafrost, *Eos Trans. AGU*, 91(26), 229, doi:10.1029/2010EO260001.
- RYDER J.M., 1971a. The stratigraphy and morphology of paraglacial alluvial fans in south-central British Columbia. *Canadian Journal of Earth Sciences* 8, 279–298.
- RYDER J.M., 1971b. Some aspects of the morphometry of paraglacial alluvial fans in south-central British Columbia. *Canadian Journal of Earth Sciences* 8, 1252–1264.
- RYGIELSKI W., 1988. Geomorfologia skał gipsowych/anhydrytowych obramowania Petuniabukty, centralny Spitsbergen. *Mat. XV Symp. Pol.*, Wrocław, 38–44.

## S

- SALVIGSEN O., 1978. Holocene emergence and finds of pumice, whalebones, and driftwood at Svartknausflya, Nordaustlandet. *Norsk Polarinstitutt Årbok* 1977, 217–228.
- SALVIGSEN, O., 1981. Radiocarbon dated raised beaches in Kong Karls Land, Svalbard, and their consequences for the glacial history of the Barents Sea area. *Geografiska Annaler Series A-Physical Geography* 63, 283–291.
- SALVIGSEN O., 1984. Occurrence of pumice on raised beaches and Holocene shoreline displacement in the inner Isfjorden area, Svalbard. *Polar Research* 2, 107–113.
- SALVIGSEN O., 2002. Radiocarbon-dated *Mytilus edulis* and *Modiolus modiolus* from northern Svalbard: climatic implications. *Norsk Geografisk Tidsskrift* 56, 56–61.
- SALVIGSEN O., FORMAN S. L. and MILLER G. H., 1992. Thermophilous molluscs on Svalbard during the Holocene and their paleoclimatic implications. *Polar Research* 11, 1–10.
- SAMOŁYK M., 2002. *Odpyw fluwiogłacjalny, transport materiału i wykształcenie osadów strefy przykorytowej w systemie doliny Ragnar, Spitsbergen środkowy, sezon letni 2001*. M. Sc. Thesis, Inst. Paleogeography and Geoecology AMU, 55 p.
- SCHIRRMEISTER L., GROSSE G., KUNITSKY V., FUCHS M., KRBETSCHKE M., ANDREEV A., HERZSCHUH U., BABYI O., SIEGERT C., MEYER H., DEREVYAGIN A. and WETTERICH S., 2010. The mystery of Bunge Land (New Siberian Archipelago): implications for its formation based on palaeoenvironmental records, geomorphology, and remote sensing. *Quaternary Science Reviews* 29, 3598–3614.

- SCHOMACKER A., 2008. What controls dead-ice melting under different climate conditions? A discussion. *Earth Science Reviews* 90, 103–113.
- SCHOMACKER, A. & KJÆR, K.H. 2007. Origin and de-icing of multiple generations of ice-cored moraines at Brúarjökull, Iceland. *Boreas* 36, 411/425.
- SCHOMACKER A. and KJÆR KH. 2008. Quantification of dead-ice melting in ice-cored moraines at the high-Arctic glacier Holmströmbreen, Svalbard. *Boreas* 37, 211–225.
- SCHYTT V., 1969. Some comments on glacier surges in eastern Svalbard. *Canadian Journal of Earth Sciences* 6, 867–873.
- SELBY M.J., 1980. A rock mass strength classification for geomorphic purposes: with test from Antarctica and New Zealand. *Zeitschrift für Geomorphologie* 24, 31–51.
- SEMPELS J.M., 1987. The Coastal Morphology and Sedimentology of Cape Hatt Peninsula. *Arctic* 40, 10-19.
- SERREZE M. C. and FRANCIS J.A., 2006. The Arctic on the fast track of change. *Weather* 61, 65 – 69.
- SERREZE M. C., CARSE F., BARRY R. G. and ROGERS J. C., 1997. Icelandic low cyclone activity: climatological features, linkages with the NAO, and relationships with recent changes in the Northern Hemisphere circulation. *Journal of Climate* 10, 453–464.
- SERREZE M., WELSH J., CHAPIN III F., OSTERKAMP T., DYURGEROV M., ROMANOWVSKY V., OECHEL W., MORISON J., ZHANG T. and BARRY R., 2000. Observational evidence of recent change in the northern high-latitude environment. *Climatic Change* 46, 159-207.
- SISSONS J.B., 1978. The parallel roads of Glen Roy and adjacent glens, Scotland. *Boreas* 7, 229-44.
- SHAKESBY R.A., MATTHEWS J.A., 1987. Frost weathering and rock platform erosion on periglacial lake shorelines: a test of a hypothesis. *Norsk Geologisk Tidsskrift* 67, 197-203
- SHAKESBY R.A., MATTHEWS J.A. and OWEN G., 2006. The Schmidt hammer as a relative-age dating tool and its potential for calibrated age dating in Holocene glaciated environments. *Quaternary Science Reviews* 25, 2846–67.
- SHAW J. and FORBES D.L. 1992. Barriers, barrier platforms, and spillover deposits in St. George's Bay, Newfoundland: paraglacial sedimentation on the flanks of a deep coastal basin. *Marine Geology* 105, 119-140.
- SHAW J. and FORBES D.L., 1995. The postglacial relative sea-level lowstand in Newfoundland. *Canadian Journal of Earth Sciences* 32, 1308– 1330.
- SHAW J., TAYLOR R.B. and FORBES D.L., 1990. Coarse clastic barriers in eastern Canada: patterns of glaciogenic sediment dispersal with rising sea levels. *Journal of Coastal Research Special Issue* 9, 160–200.
- SHI Z., LAMB H. F., and COLLIN R.L., 1995. Geomorphic change of salt marsh tidal creek networks in the Dyfi Estuary, Wales. *Marine Geology* 128, 73– 83.
- SHORT A. 1976. Observations on ice deposited by waves on Alaskan Arctic beaches. *La Revue de Géographie de Montréal* 30, 115-122.
- SHORT A. and WISEMAN JR W., 1974. Freezeup processes on arctic beaches. *Arctic* 27, 216-224.
- SLATER G., 1925: Observations on the Nordenskiöld and neighboring glaciers of Spitsbergen, 1921. *Journal of Geology* 33, 408–446.
- SLAYMAKER O., 2009. Proglacial, periglacial or paraglacial? In Knight J., and Harrison S., (Eds.) *Periglacial and Paraglacial Processes and Environments. Geological Society London Special Publications* 320, 71-84.
- SLAYMAKER O., 2011. Criteria to distinguish between periglacial, proglacial and paraglacial environments. *Quaestiones Geographicae* 30, 85–94.
- SLAYMAKER O. and KELLY E.J., 2007. *The Cryosphere and Global Environmental Change*. Blackwell Publishing, Malden-Oxford-Carlton.

- ŚLUBOWSKA M.A., KOÇ N., RASMUSSEN T.L. and KLITGAARD-KRISTENSEN D., 2005. Changes in the flow of Atlantic water into the Arctic Ocean since the last deglaciation: evidence from the northern Svalbard continental margin, 80 N. *Paleoceanography* 20 PA4014, doi:10.1029/2005PA001141, 2005
- ŚLUBOWSKA-WOLDENG M., RASMUSSEN T.L., KOÇ N., KLITGAARD-KRISTENSEN D., NILSEN F. and SOLHEIM A., 2007. Advection of Atlantic Water to the western and northern Svalbard shelf since 17,500 cal yr BP. *Quaternary Science Reviews* 26, 463–478.
- ŚLUBOWSKA-WOLDENG M., KOÇ N., RASMUSSEN T. L., KLITGAARD-KRISTENSEN D., HALD M. and JENNINGS A.E., 2008. Time-slice reconstructions of ocean circulation changes on the continental shelf in the Nordic and Barents Seas during the last 16,000 cal yr B.P. *Quaternary Science Reviews* 27, 1476–1492.
- SMITH L. C., SHENG Y., MACDONALD G. M. and HINZMAN L.D., 2005. Disappearing Arctic lakes. *Science* 308(5727), 1429, doi:10.1126/science.1108142.
- SNYDER, J.A., WERNER, A. and MILLER, G.H., 2000. Holocene cirque glacier activity in western Spitsbergen, Svalbard: sediment records from proglacial Linnévatnet. *The Holocene* 10, 555–563.
- SOLOMON S.M., 2005. Spatial and temporal variability of shoreline change in the Beaufort–Mackenzie region, northwest territories, Canada. *Geo-Marine Letters* 25, 127–137.
- STANKOWSKI, W., KASPRZAK, L., KOSTRZEWSKI, A. and RYGIELSKI, W., 1989. An outline of the morphogenesis of the region between Horbyedalen and Ebbadalen Petuniabukta, Billefjorden, central Spitsbergen, Norway. *Polish Polar Research* 10, 267–276.
- STÄBLEIN G., 1978. Extent and Regional Differentiation of Glacio-Isostatic Shoreline Variation In Spitsbergen. *Polarforschung* 48 (1/2), 170–180.
- STEPHENSON W.J. and KIRK R.M., 2000a. Development of shore platforms on Kaikoura Peninsula, South Island, New Zealand. Part One: The role of waves. *Geomorphology* 32, 21–41.
- STEPHENSON W.J. and KIRK R.M., 2000b. Development of shore platforms on Kaikoura Peninsula, South Island, New Zealand. Part Two: The role of subaerial weathering. *Geomorphology* 32, 43–56.
- ST-HILAIRE-GRAVEL D., BELL T.J. and FORBES D.L., 2010. Raised gravel beaches as proxy indicators of past sea-ice and wave conditions, Lowther Island, Canadian Arctic Archipelago. *Arctic* 63, 213–226.
- ST-HILAIRE-GRAVEL, D., FORBES, D.L. and BELL, T.J., 2011. Multitemporal analysis of a gravel-dominated coastline in the Central Canadian Arctic Archipelago. *Journal of Coastal Research* 28, 421–441.
- STRELETSKAYA I.D., VASILIEV A.A. and VANSTEIN B.G., 2009. Erosion of sediment and organic carbon from the Kara Sea coast. *Arctic, Antarctic, and Alpine Research* 41, 79–87.
- STROEVE J., HOLLAND M. M., MEIER W., SCAMBOS T. and SERREZE M., 2007. Arctic sea ice decline: Faster than forecast. *Geophysical Research Letters* 34: L09501, doi:10.1029/2007GL029703.
- STRZELECKI M.C., 2009. Suspended and solute transport in a small glaciated catchment Bertram River, Central Spitsbergen, in 2005–2006. *Norsk Geografisk Tidsskrift* 63, 98–106.
- STRZELECKI M.C., 2011. Schmidt hammer tests across a recently deglaciated rocky coastal zone in Spitsbergen - is there a 'coastal amplification' of rock weathering in polar climates? *Polish Polar Research* 32/3, 239–252.
- SUND M., EIKEN T., HAGEN J.O. and KÄÄB A., 2009. Svalbard surge dynamics derived from geometric changes. *Annals of Glaciology* 50, 50–60.
- SUNAMURA T., 1992. *Geomorphology of Rocky Coasts*. Chichester, UK: Wiley.
- SURELL A., 1841. *Étude sur les torrents des Hautes-Alpes*. Carillan- Goeuvry éditeurs, Paris, 283 p.

- SUTHERLAND, R.A., LEE, C.T. (1994). Discrimination between coastal subenvironments using textural characteristics. *Sedimentology* 41, 113-1145.
- SVENDSEN J.I and MANGERUD J., 1997. Holocene glacial and climatic variations on Spitsbergen, Svalbard. *The Holocene* 7, 45-57.
- SVENDSEN J.A., ALEXANDERSON H., ASTAKHOV V.I., DEMIDOV I., DOWDESWELL J.A., FUNDER S., GATAULLIN V., HENRIKSEN M., HJORT C., HOUMARK-NIELSEN M., HUBBERTEN H.W., INGÓLFSSON O., JAKOBSSON M., KJÆR K.H., LARSEN E., LOKRANTZ H., LUNKKA J.P., LYSÅ A., MANGERUD J., MATIOUCHKOV A., MURRAY A., MÖLLER P., NIESSEN F., NIKOLSKAYA O., POLYAK L., SAARNISTO M., SIEGERT C., SIEGERT M.J., SPIELHAGEN R.F. and STEIN R. 2004. Late Quaternary ice sheet history of northern Eurasia. *Quaternary Science Reviews* 23, 1229–1271.
- SVOBODA, J., HENRY, G. H., R., 1987, Succession in marginal arctic environments. *Arctic and Alpine Research* 19(4), 373-384.
- SWIFT J.H., 1986. The Arctic Waters. In: Hurdle B.G. (Ed.), *The Nordic Seas*. Springer, New York, pp. 129–153.
- SYVITSKI J., 2002. *Sediment* discharge variability in *Arctic rivers*: implications for warmer future. *Polar Research* 21: 323-330.
- SYVITSKI J.P.M. and ANDREWS J.T., 1994, Climate change: numerical modelling of sedimentation and coastal processes, eastern Canadian Arctic. *Arctic and Alpine Research* 26 (3), 199–212.
- SYVITSKI J. and SHAW J., 1995. Sedimentology and Geomorphology of Fjords . In Perillo, G.M.E.. *Geomorphology and Sedimentology of Estuaries*. Amsterdam, Elsevier, 113-178 pp.
- SYVITSKI J.P.M., BURRELL D.C. and SKEI J.M., 1987. *Fjords: Processes and Products*. Springer-Verlag, New York: 379p.
- SZCZUCIŃSKA A.M., 2011. Occurrence and temporal variations of groundwater outflows in the Petuniabukta region, Spitsbergen. *Polish Polar Research* 32, 361-374.
- SZCZUCIŃSKI W. and ZAJĄCZKOWSKI M., 2012. Factors controlling downward fluxes of particulate matter in glacier-contact and non-glacier contact settings in a subpolar fjord (Billefjorden, Svalbard). In: Li M., SHERWOOD C. & HILL P.(eds.). '*Sediments, Morphology and Sedimentary Processes on Continental Shelves: Advances in technologies, research and applications*' International Association Sedimentological Special Publication 44, 369–386.
- SZCZUCIŃSKI W., ZAJĄCZKOWSKI M. and SCHOLTEN J., 2009. Sediment accumulation rates in subpolar fjords – Impact of post-Little Ice Age glaciers retreat, Billefjorden, Svalbard. *Estuarine, Coastal and Shelf Science* 85, 345-356.
- SZUMAN I. and KASPRZAK L., 2010. Glacier ice structures influence on moraines development (Hørbye glacier, Central Spitsbergen). *Quaestiones Geographicae* 29, 65/73.

## T

- TAYLOR R.B., 1978. The occurrence of grounded ice ridges and shore ice piling along the northern coast of Somerset Island, N.W.T.. *Arctic* 31, 133-139.
- TAYLOR R.B and MCCANN S.B., 1983. Coastal depositional landforms in northern Canada. In: D.E SMITH and A.G. DAWSON (eds.) *Shorelines and Isostasy*. Institute of British Geographers, Special publication No. 16, London: 54-75.
- TAYLOR R.B., FORBES D.L., CARTER R.W.G. and ORFORD J.D., 1986. Beach sedimentation in Ireland: similarities and contrasts with Atlantic Canada. *Geol. Surv. Can. Pap.*, 86-1B, 55-64.



- THORN C.E. and LOEWENHERZ D.S., 1987. Spatial and temporal trends in alpine periglacial studies: implications for paleo-reconstruction. In: J. BOARDMAN (ed). *Periglacial Processes and Landforms in Britain and Ireland*. Cambridge University Press, Cambridge: 57–65.
- THORNTON L.E. and STEPHENSON W.J., 2006. Rock strength: a control of shore platform elevation. *Journal of Coastal Research* 22, 224–231.
- TRENHAILE A.S., 1983. The development of shore platforms in high latitudes. In: D.E SMITH and A.G. DAWSON (eds.) *Shorelines and Isostasy*. Institute of British Geographers, Special publication No. 16, London: 77-96.
- TRENHAILE A.S., 1997. *Coastal Dynamics and Landforms*. Oxford University Press, Oxford UK. 366pp.
- TRENHAILE A.S., 2001. Modelling the effect of weathering on the evolution and morphology of shore platforms. *Journal of Coastal Research* 17, 398–406.
- TRENHAILE A.S., 2004. Lacustrine shore platforms in southwestern Ontario, Canada. *Zeitschrift für Geomorphologie* 48, 441-459.
- TRENHAILE A.S. and MERCAN D.W., 1984. Frost weathering and the saturation of coastal rocks. *Earth Surface Processes and Landforms* 9, 321–331.
- TRENHAILE A.S., PEPPER D.A., TRENHAILE R.W. and DALIMONTE M., 1998. Stacks and Notches at Hopewell Rocks, New Brunswick, Canada. *Earth Surface Processes and Landforms* 23, 975–988
- TRENHAILE A.S., PORTER N.J. and KANYAYA J.I., 2006. Shore platform processes in eastern Canada. *Géographie Physique et Quaternaire* 60, 19–30.

## U

- URDEA P., 2007. About some geomorphological aspects of the polar beaches. *Revista de geomorfologie* 9: 5-16.

## V

- VAN ANDEL T.H, WIGGERS A.J. and MAARLEVELD G., 1954. Roundness and shape of marine gravels from Urk (Netherlands): a comparison of several methods of investigation. *Journal of sedimentary petrology* 24, 100-116.
- VIELI A., JANIA J. and KOLONDRÁ L., 2002. The retreat of a tidewater glacier: observations and model calculations on Hansbreen, Svalbard. *Journal of Glaciology* 48(163), 592–600.

## W

- WADHAMS P., 1981. The ice cover in the Greenland and Norwegian Seas. *Review Geophysical Space Physics* 19: 345–39.
- WALKER I. J. and BARRIE J. V., 2004. Geomorphology and sea-level rise on one of Canada's most 'sensitive' coasts: Northeast Graham Island, British Columbia. *Journal of Coastal Research, Special Issue* 39.
- WALTON J., 1922. A Spitsbergen salt marsh; with observations on the ecological phenomena attendant on the emergence of land from the sea. *Journal of Ecology* 10, 109-21.

- WANG J, WU B, TANG CCL, WALSH JE and IKEDA M., 2004. Seesaw structure of subsurface temperature anomalies between the Barents Sea and the Labrador Sea. *Geophysical Research Letters* 31:L19301. doi:10.1029/2004GL019981
- WANG M. AND OVERLAND J. E., 2009. A sea ice free summer Arctic within 30 years? *Geophysical Research Letters* 36, L07502, doi:10.1029/2009GL037820.
- WANGENSTEEN, B., GUDMUNSSON, A., EIKEN T., KAAB, A. FARBOT, H. & ETZELMÜLLER, B. 2006. Surface displacements and surface age estimates for creeping slope landforms in Northern and Eastern Iceland using digital photogrammetry. *Geomorphology* 80, 59-79.
- WANGENSTEEN B., EIKEN T., ØDEGÅRD R.S. and SOLLID J.L., 2007. Measuring coastal cliff retreat in the Kongsfjorden area, Svalbard, using terrestrial photogrammetry. *Polar Research* 26, 14–21.
- WERENSKIOLD W., 1952. The Strand Flat of Spitsbergen. *Geografisk Tidsskrift*, 52, 302-309.
- WERNER A., 1993. Holocene moraine chronology, Spitsbergen, Svalbard: lichenometric evidence for multiple neoglacial advances in the Arctic. *The Holocene* 3, 128–137.
- WETTERICH S., KUZMINA S., ANDREEV A., KIENAST F., MEYER H., SCHIRRMEISTER L., KUZNETSOVA T. and SIERRALTA M., 2008. Palaeoenvironmental dynamics inferred from Late Quaternary permafrost deposits on Kurungnakh Island, Lena Delta, Northeast Siberia, Russia. *Quaternary Science Reviews* 27, 1523–1540.
- WETTERICH S., SCHIRRMEISTER L., ANDREEV A., PUDENZ M., PLESSEN B., MEYER H. and KUNITSKY V., 2009. Eemian and Late Glacial/Holocene palaeoenvironmental records from permafrost sequences at the Dimitry Laptev Strait (NE Siberia, Russia). *Paleogeography, Paleoclimatology, Paleoecology* 279, 73–95.
- WINKLER S., 2009. First attempt to combine terrestrial cosmogenic nuclide ( $^{10}\text{Be}$ ) and Schmidt hammer relative-age dating: Strauchon Glacier, Southern Alps, New Zealand. *Central European Journal of Geosciences* 1(3), 274-290.
- WOBUS C., ANDERSON R., OVEREEM I., MATELL N., CLOW G., URBAN F., 2011. Thermal Erosion of a Permafrost Coastline: Improving Process-Based Models Using Time-Lapse Photography. *Arctic, Antarctic, and Alpine Research* 43, 474-484.

## Y

- YAMAMOTO K., TACHIBANA Y., HONDA M. and UKITA J. 2006. Intra-seasonal relationship between the Northern Hemisphere sea ice variability and the North Atlantic Oscillation. *Geophysical Research Letters* 33: L14711. doi:10.1029/2006GL026286

## Z

- ZAGÓRSKI P. 2011. Shoreline dynamics of Calypsostranda (NW Wedel Jarlsberg Land, Svalbard) during the last century. *Polish Polar Research* 32: 67-99.
- ZAGÓRSKI P. GAJEK G. and DEMCZUK P., 2012a. The influence of glacier systems of polar catchments on functioning of the coastal zone (Recherchefjorden, Svalbard). *Zeitschrift für Geomorphologie* 56 Suppl. 1, 101-122.
- ZAGÓRSKI P., MALCZEWSKI A. and ŁĘCZYŃSKI L., 2012b. *Shoreline changes of Isbjørnhamna (Hornsund, Svalbard) in years 1960-2011*. Field report UMCS University, 34 pp.
- ZAJĄCZKOWSKI M., SZCZUCIŃSKI W. and BOJANOWSKI R., 2004. Recent sediment accumulation rates in Adventfjorden, Svalbard. *Oceanologia* 46, 217-231

- ZHANG X., WALSH J.E., ZHANG J., BHATT U.S. and IKEDA M. 2004. Climatology and interannual variability of Arctic cyclone activity: 1948–2002. *Journal of Climatology* 17, 2300–17.
- ZENKOVICH V.P., 1967. *Processes of Coastal Development*. (trans. Fry O.G., Steers J.A. ed.). Oliver and Boyd, Edinburgh: 738 pp.
- ZENKOVICH V.P., 1985. Arctic USSR. In: E.C.F. BIRD AND M.L. SCHWARTZ (eds.). *The World's Coastline*. New York: Van Nostrand Reinhold Co., 863–869 pp.
- ZIAJA W., MACIEJOWSKI P. and OSTAFIN K., 2009. Coastal Landscape Dynamics in NE Sørkapp Land (SE Spitsbergen), 1900–2005. *Ambio* 38, 201–208.
- ZIAJA W., LISOWSKA M., OLECH M., OSYCZKA P., WĘGRZYN M., DUDEK J. and OSTAFIN K., 2011. *Transformation of the natural environment in Western Sørkapp Land (Spitsbergen) since the 1980s*. Jagiellonian University Press. 92 pp.
- ZINGER E., 2006. *Špicbergen : ledovyj archipela*. Moscow: Penta, 303 pp.
- ZINGG T., 1935. Beitrag zur Schotteranalyse. *Schweizer Miner. Petrog. Mitt.* 15, 39–140.
- ZWOLIŃSKI Z., MAZUREK M., PALUSZKIEWICZ R. and RACHLEWICZ G., 2008. The matter fluxes in the geoecosystem of small tundra lakes, Petuniabukta coast, Billefjorden, Central Spitsbergen. *Zeitschrift für Geomorphologie* 52, Suppl. 1, 79–101.

# **APPENDIX I – Research plan and Coastal sections selected for analysis**

## APPENDIX I – Research plan and Coastal sections selected for analysis

### Research schedule

Type of activity	When?	Why?
Field reconnaissance	July 2008	<ul style="list-style-type: none"> <li>• To identify sections of the coast for beach profiling, sampling and seasonal change monitoring.</li> <li>• To delimit needed aerial imaginary coverage in order to produce geomorphological maps and DEMs of study area.</li> </ul>
Weather observations using portable Davies Vantage Pro weather station	July 2008 – August 2010	<ul style="list-style-type: none"> <li>• To record air temperature, humidity, barometric pressure, wind speed and direction, precipitation, incoming shortwave and UV radiation changes to characterise the role of local climate conditions on the development of the coastal zone.</li> </ul>
Deployment of tide gauge station using a sea-bed pressure transducer	July 2008 – August 2010	<ul style="list-style-type: none"> <li>• To define tidal range in Petuniabukta and establish Mean Tidal Level in the study area.</li> </ul>
Differential Global Positioning System Surveying (DGPS) using Leica A500 and I200 systems	July 2008, July 2009, July 2010	<ul style="list-style-type: none"> <li>• To monitor profile and micro-relief changes of gravel-dominated barriers between 2008-2010.</li> <li>• To complete field survey of selected control points in the Petuniabukta landscape including large rocks, boulders, corners of wooden cabins etc., and deploying a network of geofiber squares (2x3 m) to georeference aerial images and improve the precision of constructed orthophotomaps and Digital Elevation Models (DEM).</li> <li>• To ground-truth DEM's and geomorphological maps.</li> </ul>
Measurement of bottom temperatures of snow cover (BTS)	April 2009	<ul style="list-style-type: none"> <li>• To measure the state of permafrost along gravel-dominated barriers.</li> <li>• To quantify snow cover thickness along the coast and over the frozen fjord.</li> </ul>
Deployment of time-lapse camera monitoring system using DigiSnap system manufactured by Harbotronics Inc.	April 2009 – July 2010	<ul style="list-style-type: none"> <li>• To monitor: <ul style="list-style-type: none"> <li>- snow cover changes along selected sections of coast;</li> <li>- sea ice cover changes;</li> <li>- wave activity;</li> <li>- the extent of high tide on the tidal flat;</li> <li>- distribution of sediment plumes;</li> </ul> in order to study environmental forcings on selected coastal zones. </li> </ul>
Schmidt hammer rock tests	July 2009- August 2009	<ul style="list-style-type: none"> <li>• To characterise rock resistance variability across a recently deglaciated coastal zone.</li> </ul>
Sonar sounding of Petuniabukta seabed using EagleFish Elite 480 sonar	July 2009	<ul style="list-style-type: none"> <li>• To map seabed morphology. Particular attention was paid to nearshore areas.</li> <li>• To combine sonar measurements with barrier profiling in order to describe the relationship between barrier and nearshore morphologies.</li> </ul>
Photographing of gravel-dominated	July 2008 July-	<ul style="list-style-type: none"> <li>• To document coastal landscape changes that occur during the fieldwork seasons.</li> </ul>



barriers, spits and other coastal landforms using Nikon D80 Digital SLR camera	August 2009 July-August 2010	<ul style="list-style-type: none"> <li>• To compliment the description of physical properties of sediments that build coastal, glacial and periglacial landforms.</li> </ul>
Laboratory analyses of collected sediments	Autumn 2009, Autumn 2010	<ul style="list-style-type: none"> <li>• To characterise the size, shape and provenance of modern and palaeo- coastal landforms by analyses of: <ul style="list-style-type: none"> <li>- particle size of collected sediments;</li> <li>- magnetic susceptibility of collected sediments.</li> </ul> </li> </ul>
Collection of shell samples from modern and uplifted beaches	August 2010	<ul style="list-style-type: none"> <li>• To collect new datable organic material from the study area in order to reconstruct relative sea-level changes that occurred in last millennia.</li> </ul>
AMS radiocarbon dating of collected shells using the NERC Radiocarbon Facility	December 2010 – May 2011	<ul style="list-style-type: none"> <li>• To produce a new RSL change curve and improve understating of post-glacial emergence in central Spitsbergen.</li> </ul>
Photogrammetric analyses of aerial images and DEMs production using the ERDAS Leica Photogrammetry Suite 2010 (LPS).	December 2009 – December 2011	<ul style="list-style-type: none"> <li>• To analyse landscape changes on aerial photographs taken by the Norwegian Polar Institute (NPI) in 1936, 1960-1961, 1990 and 2009.</li> <li>• To processes selected images in photogrammetric software in order to produce new DEMs of the study area.</li> <li>• To produce orthophotomaps of selected areas for use in geomorphological mappings.</li> </ul>
GIS analyses using ESRI ArcGIS 9.3 software.	February 2010 – February 2012	<ul style="list-style-type: none"> <li>• To analyse coastal zone evolution and quantify sediment volume and area changes in coastal landforms since the end of LIA.</li> <li>• To produce geomorphological maps of selected coastal sections.</li> </ul>
Graphics design using Adobe Illustrator and Photoshop CS.	January 2012- September 2012	<ul style="list-style-type: none"> <li>• To correct graphical layout and aesthetics of maps, Figures and tables produced in various software during the conducted research.</li> </ul>

Table A1 – Research schedule

## Coastal sections selected for analysis

This section describes the coastal sections selected for analysis illustrating seasonal (2008-2010), decadal (1900-2009) and millennial (Late Holocene) coastal zone changes (Figure A.1.).

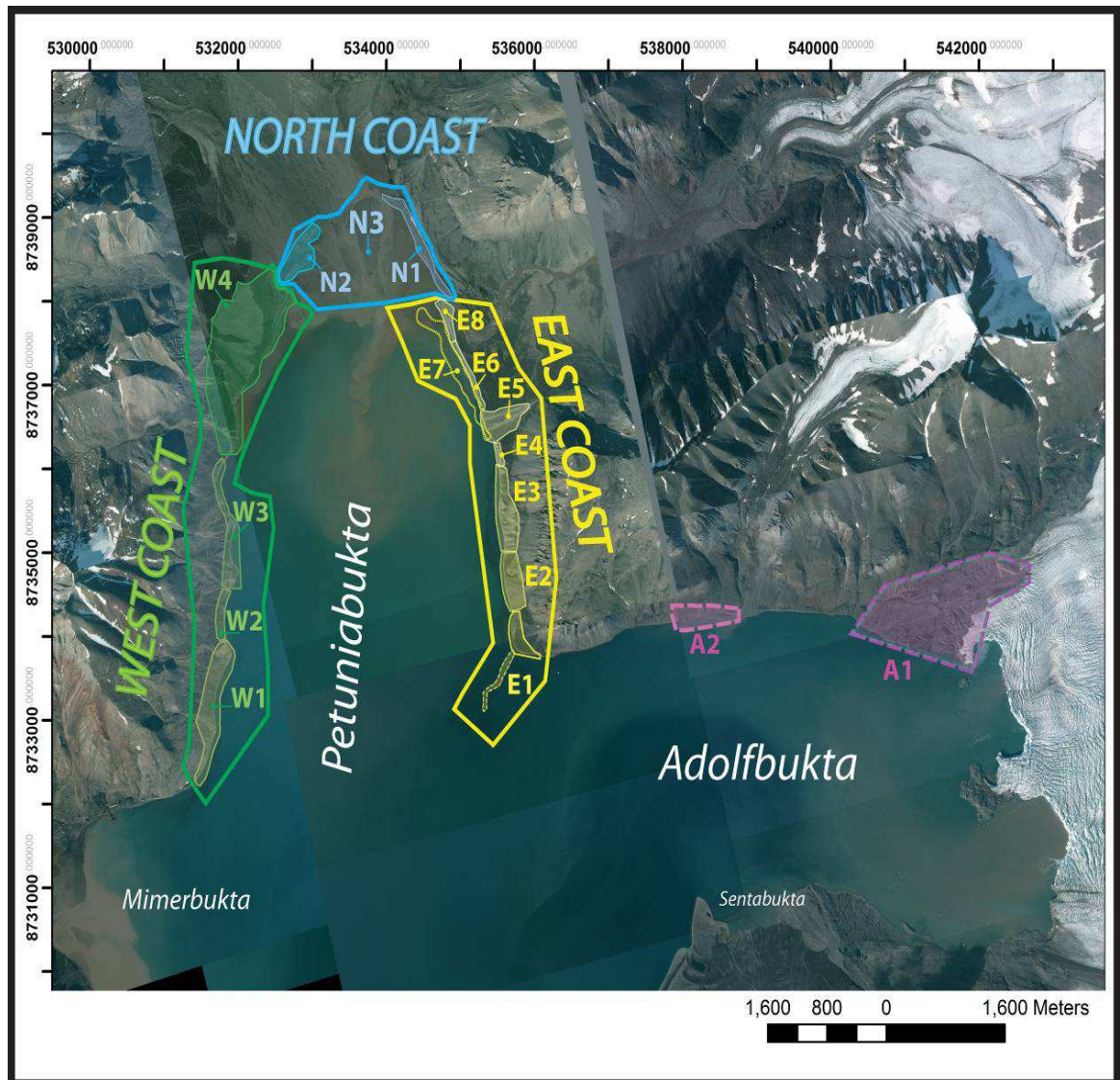


Figure A.1. Coastal sections identified during this doctoral project: Adolfbukta coastal sections: A1 - Northern Adolfbukta – submerged roches moutonnées, plunging cliffs; A2 – Mid-northern Adolfbukta – boulder-strewn coast, sandstone cliff and platform. – not considered for further investigations Petuniabukta coastal sections: EAST COAST: E1 - Raudmospynten; E2- Rock glacier coast; E3 – Anhydrite/Gypsum cliffs and shore platforms; E4 – Palaeospit; E5- Dynamiskbekken delta; E6 - Skottehytta coast; E7 - Skerry islands coast; E8 - Spit platform and Ebba River mouth; NORTH COAST: N1 – northern barrier and lagoon coast; N2 - Fetch limited barrier islands; N3 - Tidal flat; WEST COAST: W1 - barrier coast I; W2 - limestone cliff coast; W3 – barrier coast II; W4 – Ferdinandbreen alluvial fan deltas and barriers.

## A.1 Petuniabukta East Coast sections

### A.1.1 Coastal section E1: Raudmosepynten coast (Figure A.1.1.)

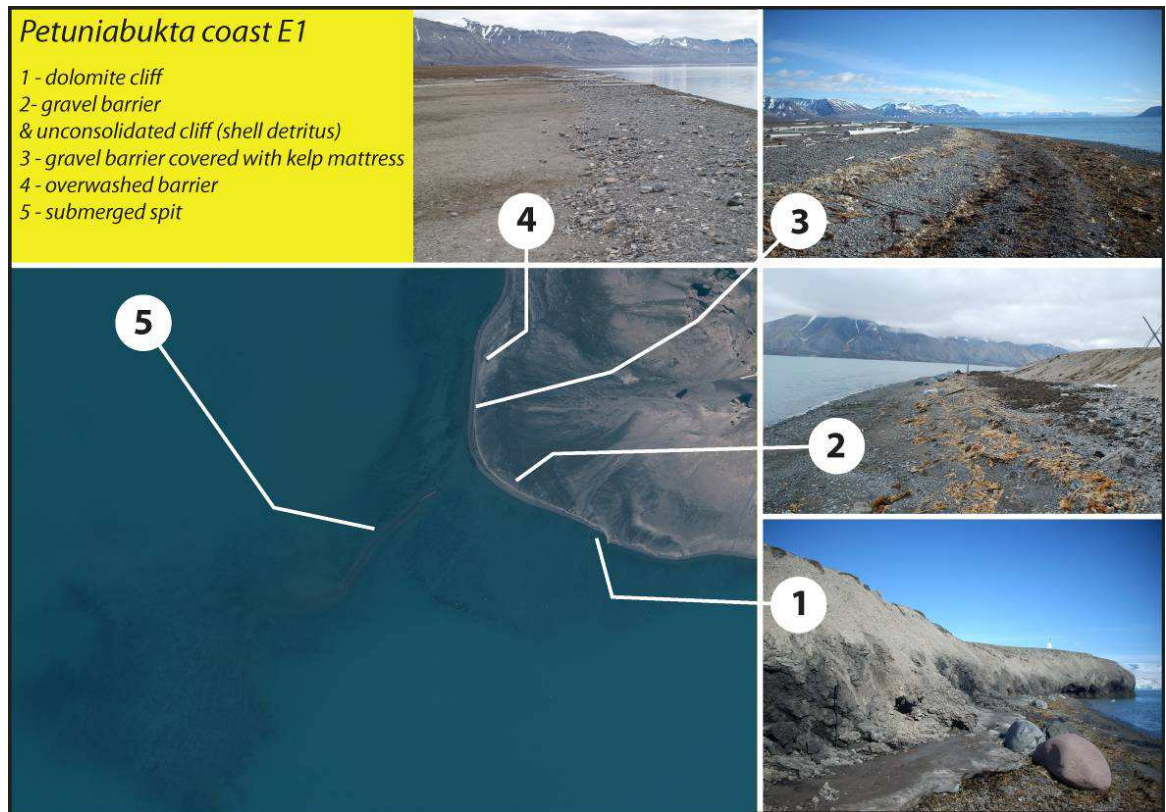


Figure A.1.1. Petuniabukta coast section E1

**Coastal length:** 875 m

**Geomorphological description:** The geomorphology of Raudmosepynten cape, located at the junction between Petuniabukta and Adolfbukta, is influenced by waves of longest fetch in the area (SE, and NE descending Nordenskiöldbreen). This section of the coast is characterised by wide diversity of coastal landforms. The southern coast consists of: dolomite breccia cliff and platform; a low cliff formed in an uplifted marine terrace and composed of unconsolidated sediments (marine sands, gravels and shell detritus), a narrow swash-aligned gravel-dominated barrier spotted with large erratic transported by ice-bergs from the calving Nordenskiöldbreen and largely covered with seaweed mattress. In Petuniabukta the gravel-dominated barriers become drift-aligned and wider. This part of the barrier coast is studded with driftwood and thick seaweed mattresses. There is a characteristic strip of coarse gravel, pebbles and driftwood on the surface of flat marine terraces as well as overwash inlets and washover fans in the back of the barrier, suggest overwashing and barrier seepage during highest tide levels and summer storms. A flat-barrier plain is periodically flooded during the spring melt-out, in the summer all shallow depressions dry out and are covered with desiccation cracks. During spring-melt season and occasional summer downpours, debris and mudflows from the adjacent Fortet massif form small alluvial fans which fill depressions. In the winter season the coastal zone around the cape is scattered with ice floes piling up along submerged spit



and a thick ice-foot frequently extends from the dolomite cliff. However, the preservation of sea-ice micro-relief is very weak due to wave activity and deposition and movement of seaweed cover.

#### Major sediment supplies:

- boulder to pebble fraction: derived from icebergs calving from Nordenskiöldbreen
- gravel to sand fraction: delivered by wave erosion of older barriers and cliffs, and longshore drift
- silt-clay: from spring floodings of depressions, mudflows and aeolian transport from Nordenskiöldbreen foreland and Cape Napier.

#### A.1.2 Coastal section E2: Rock glacier coast (Figure A.1.2.)



Figure 46. Petuniabukta coast section A.1.2.

**Coastal length: 750 m**

**Geomorphological description:** The first part of this section is dominated by a large alluvial fan built by a snow-fed stream that drains the southern part of the Wordiekammen massif. A thick debris fan is covered with thermokarstic depressions suggesting intensified permafrost degradation that has facilitated transport of coarse debris to the coast. Despite an abundance of coarse sediments from scree slope erosion, a relatively narrow, drift-aligned barrier has formed along a steep cliff that blocks the majority of stream outlets draining the fan system. This barrier widens in the northern part of the coastal section. The dominant hinterland landform is an avalanche-derived rock glacier and a solifluction slope covered with tundra tufts. However, the modern

barrier is separated from this source of sediment by a palaeo-lagoon and two wide palaeo-barrier ridges. The last 200 m of this section are characterised by well-preserved sea-ice derived landforms with barrier surface covered by sea-ice kettles, elongated depressions, gravel mounds, ice-push ridges and (uniquely in the study area) a large kaimoo ridge.

**Major sediment supplies:**

- boulders to cobbles: scree cliffs of alluvial fan
- gravel to sand sized fractions: longshore drift, snow-melt streams and reworking of palaeo-ridges
- silt and clay fraction: from aeolian deposition on snow-patches and icefoot.

**A.1.3 Coastal section E3: Anhydrite/gypsum cliff and shore platform coast (Figure A.1.3.)**

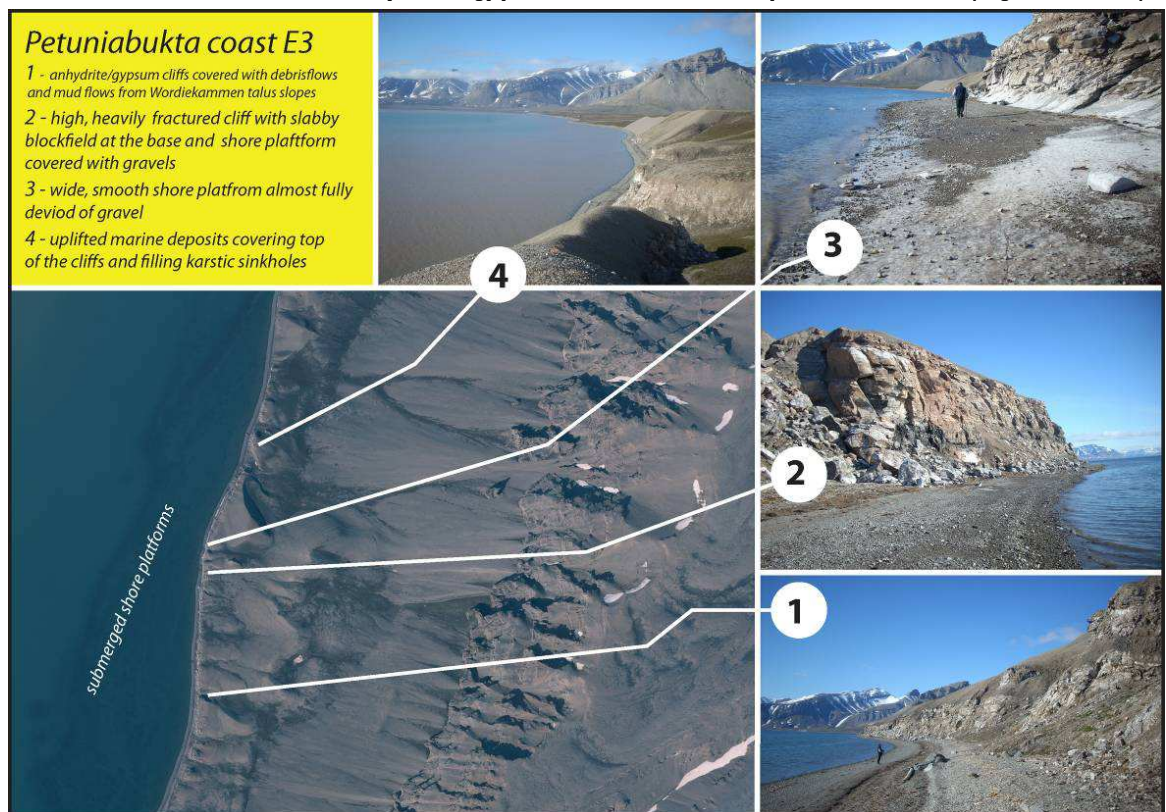


Figure A.1.3. Petuniabukta coast section E3.

**Coastal length:** 1050 m

**Geomorphological description:** A rock coast composed of anhydrite/gypsum bevelled cliffs and abrasion platforms. Cliffs are overlain by periglacially sorted uplifted marine deposits, debris flows and debris avalanches from the steep talus slopes that cover the western slope of the Wordiekammen massif. Wide abrasion platforms formed along the cliffs are partially covered with thin layer of mixed sand and gravel. The main part of the platforms is submerged and extends up to 250 m seaward.

**Major sediment supplies:**



- boulder to cobble fraction: occasional rockfalls from cliff faces and snow avalanches descending from talus slopes
- gravel to sand fraction: limited longshore drift, debris and mudflows from upper part of the cliff
- silt and clay fraction: karstic dissolution of cliff walls and shore platform surface, decay of icefoot, mudflows from cliff.

#### A.1.4 Coastal section E4: Palaeo-spit coast (Figure A.1.4.)

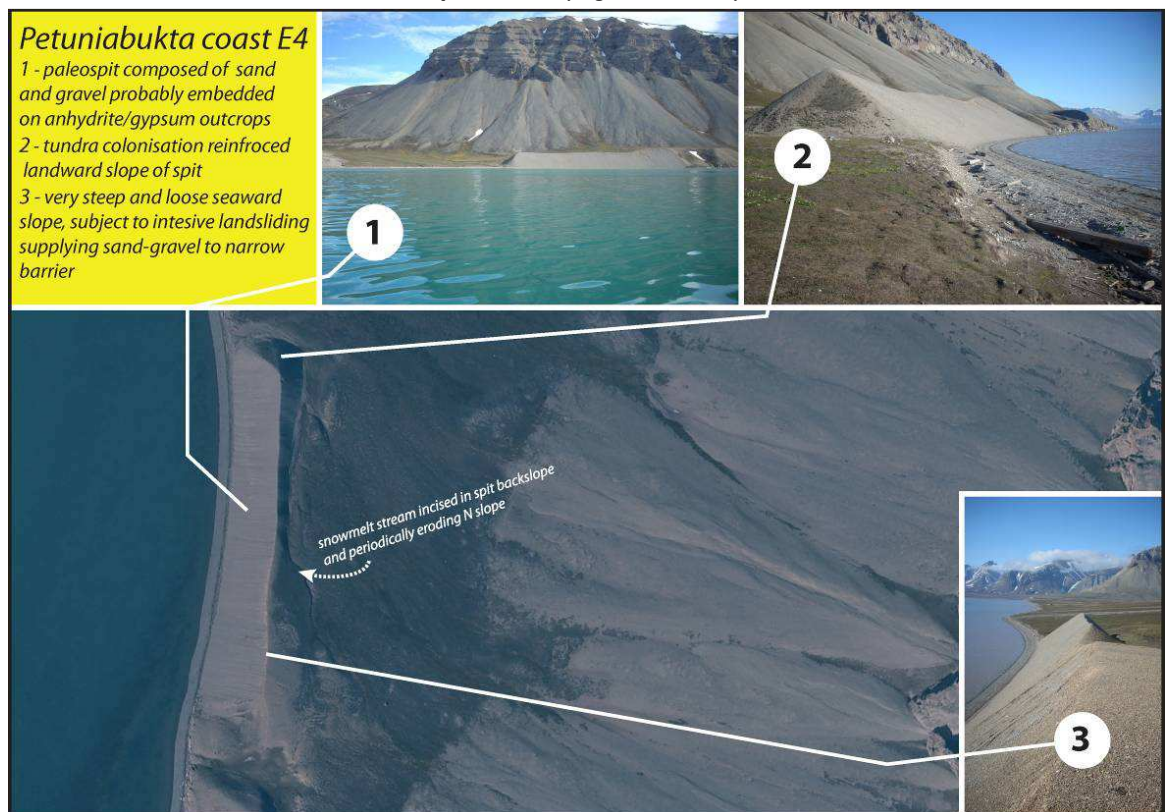


Figure A.1.4. Petuniabukta coast section E4

**Coastal length:** 250 m

**Geomorphological description:** A narrow, gravel-dominated, drift-aligned barrier formed along an uplifted palaeo-spit eroded from the north by a snow-fed stream. Sediments are derived from erosion of the landform together with sediment provided by the Dynamiskbekken stream barrier system supply sections E5, E6 and E8.

#### **Major sediment supplies:**

- boulder to cobble fraction: wave undercutting of the palaeo-spit slope
- gravel to sand: wave undercutting of the palaeo-spit slope
- silt and clay: wave undercutting of the palaeo-spit slope, aeolian transport from Dynamiskbekken delta and the Hørbyebreen outwash plain.



### A.1.5 Coastal section E5: Dynamiskbekken delta coast (Figure A.1.5.)

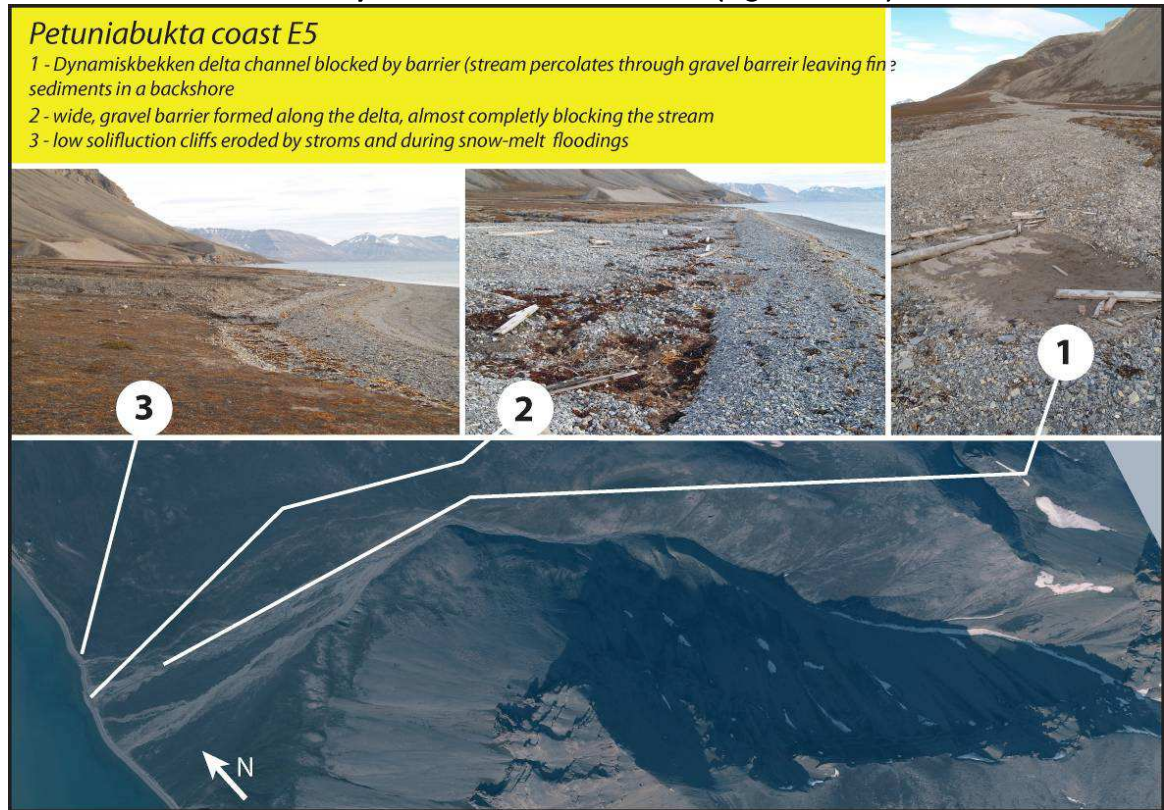


Figure A.1.5 Petuniabukta coast section E5

**Coastal length:** 410 m

**Geomorphological context:** Dynamiskbekken is the largest snow-fed stream along the eastern coast of Petuniabukta. The stream forms a small delta at the coast and delivers a significant amount of sediments to the coastal zone during the snow-melt period. In the last 5 years all stream outlets were blocked by a wide, gravel-dominated barrier. The active channel is incised into a former Holocene delta. This stream was a much more important supplier of sediment to the coastal zone until the early 1990s. In last 5 years, the discharge has diminished earlier in the season. The stream deposits silty sediments in abandoned depressions and channels. Blocking of the main stream outlet by wide storm tide causes accumulation of fine sediments in the back of the barrier. This beach is occasionally eroded during the peak of snow –melt season (May-June)

#### **Major sediment supplies:**

- boulder to cobble fraction: large boulders found in the delta were left by retreating glaciers filling fjord in during last glaciation
- gravel to sand fraction: longshore drift from palaeo-spit from section E4, Dynamiskbekken peak snow-melt discharges
- silt to clay fraction: Dynamiskbekken high discharge, aeolian transport of sediments from bars in abandoned channels and the Hørbyebreen outwash plain, erosion of low solifluction cliffs.

### A.1.6 Coastal section E6: Skottehytta coast (Figure A.1.6.)

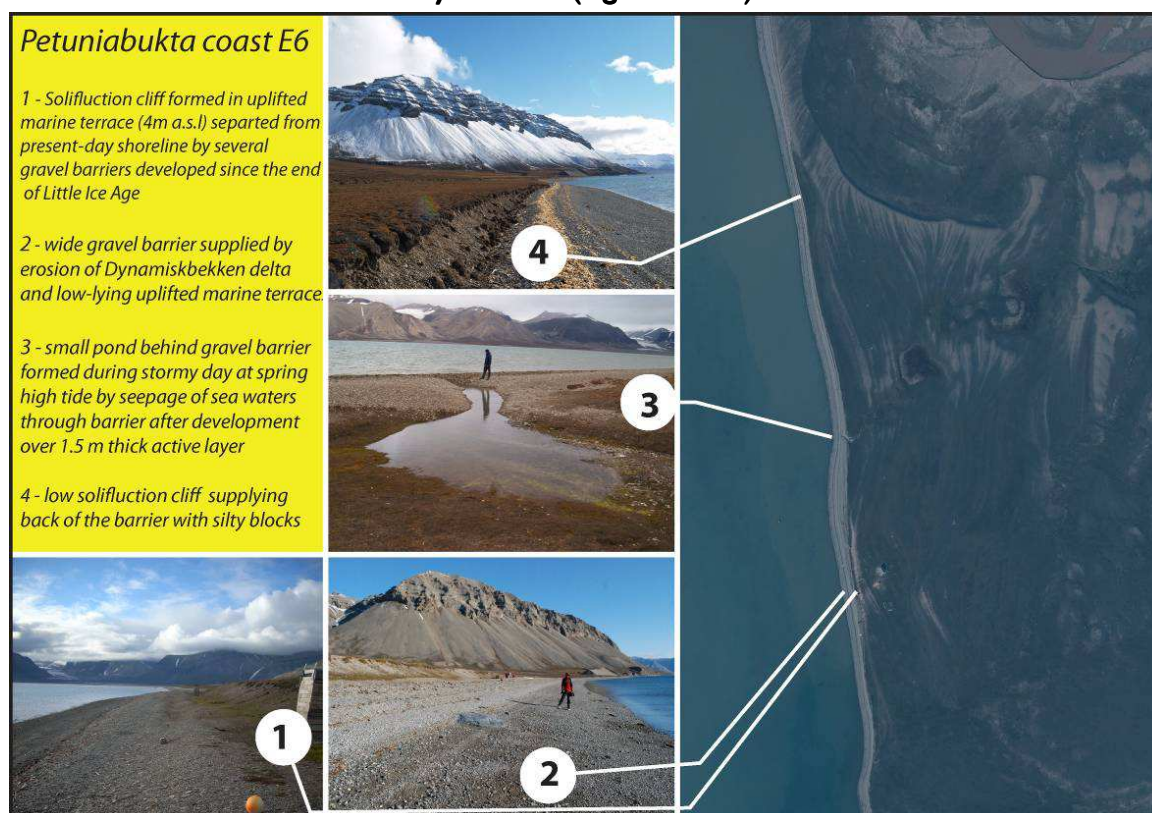


Figure A.1.6. Petuniabukta coast section E6

**Coastal length:** 950 m

**Geomorphological context:** This coast has the longest and best developed gravel-dominated, drift-aligned barriers, fed by longshore drift of sediments deposited in the Dynamiskbekken delta and erosion of low solifluction cliffs formed in uplifted marine terraces. The present-day barrier blocks all ephemeral creeks including a creek that drains a network of snow-fed tundra lakes. During high tides the gravel barriers experience seepage and sea-water floods the lower part of abandoned creeks. Flights of uplifted beaches along E6 section constitute one of the best preserved sequences of Holocene beaches in the Billefjorden region.

#### Major sediment supplies:

- boulder to cobble fraction: large boulders found in the delta were left by retreating glaciers
- gravel to sand fraction: longshore drift from palaeo-spit from section E4, Dynamiskbekken peak snow-melt discharges
- silt to clay fraction: aeolian transport of sediments from Dynamiskbekken abandoned channels and Hørbyebeen outwash plain, solifluction and aeolian transport of sediments from highest solifluction cliff (3 m a.s.l. Skottehytta cliff), wave erosion of low solifluction cliffs.



### A.1.7 Coastal section E7: Skerry islands coast (Figure A.1.7.)

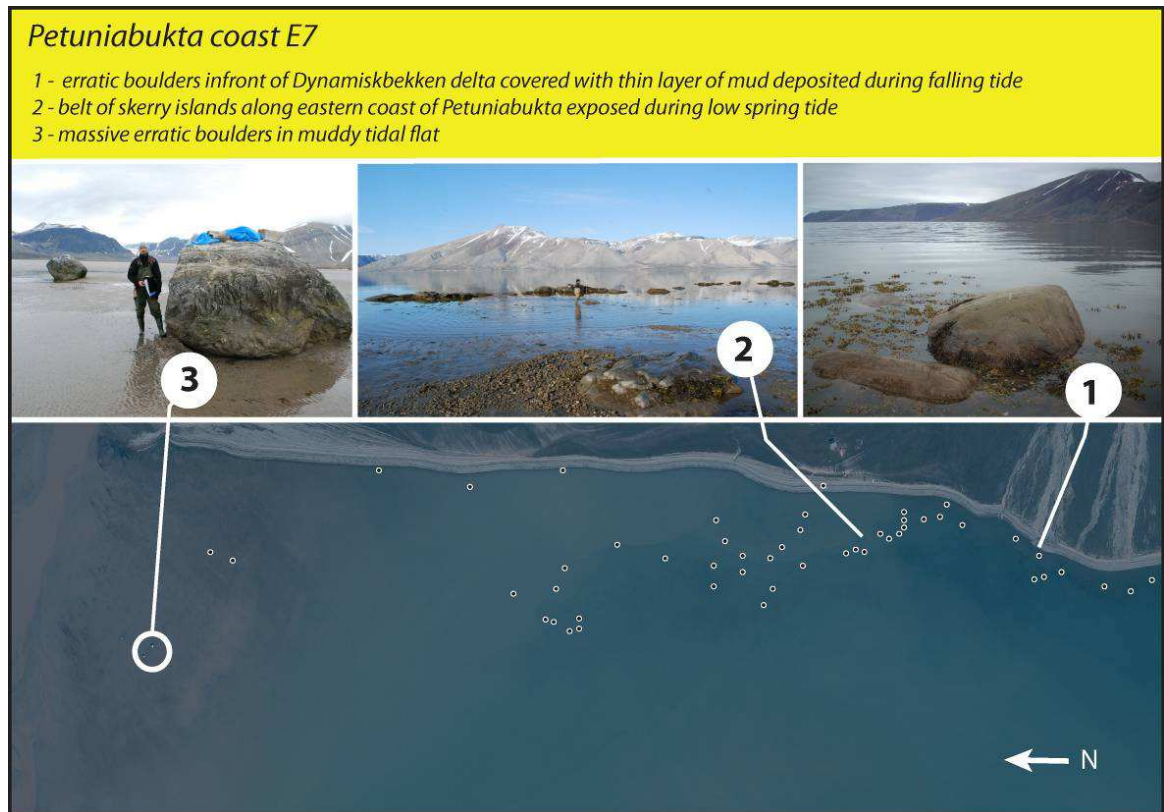


Figure A.1.7. Petuniabukta coast section E7

**Coastal length:** 1600 m

**Geomorphological description:** The intertidal zone and shallows along E4 – E8 are scattered within hundreds of erratic boulders left by glaciers during the last glaciation. The boulders form several skerry islands visible during the low tides and serve as important controls on sea-ice movement (piling of ice-floes on top of boulders), ice-foot formation (sea-ice anchoring to boulders in the intertidal zone) and diffraction of waves.

**Major sediment supplies:**

- boulders: erratics deposited at last glaciation
- gravel to sand fraction: offshore deposition from palaeo-spit and Dynamiskbekken peak snow-melt discharges, Ebbaelva and Hørbyebeen outwash plain.
- silt to clay fraction: aeolian transport of sediments from Dynamiskbekken abandoned channels and Hørbyebeen outwash plain, wave erosion of low solifluction cliffs.

### A.1.8. Coastal section E8: East Petunia spit platform coast (Figure A.1.8.)

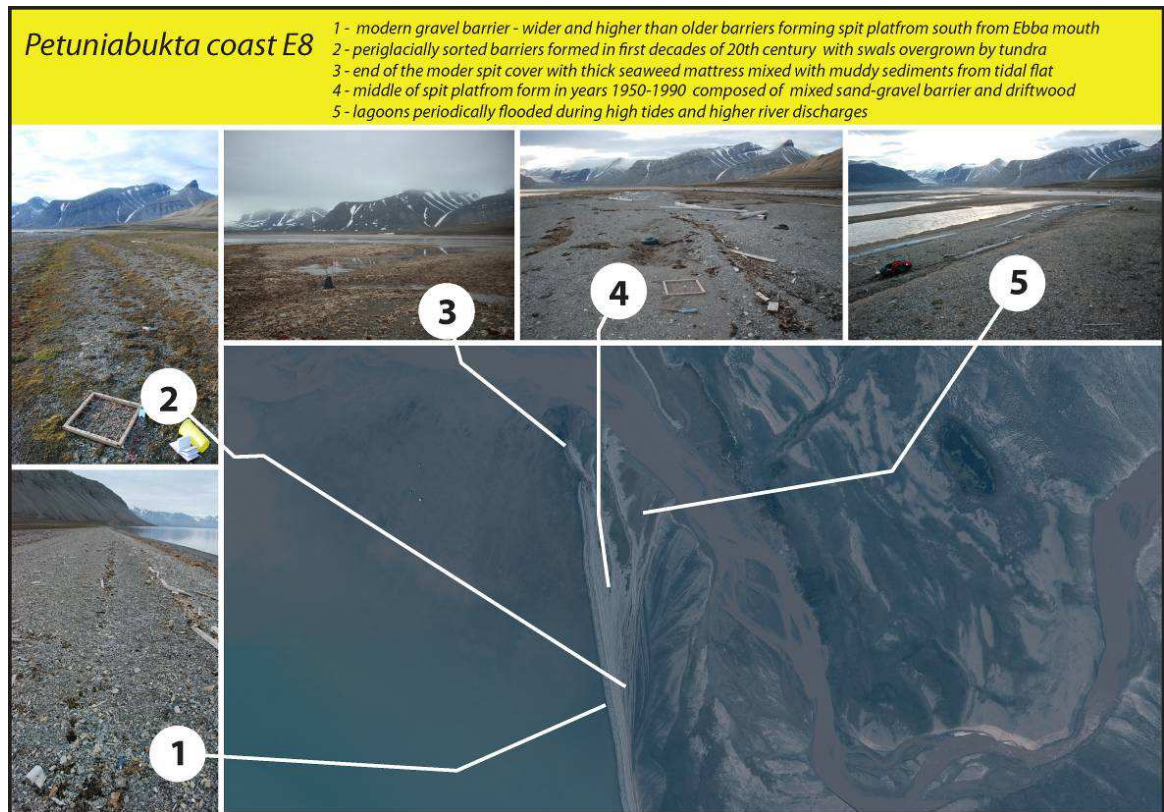


Figure A.1.8. Petuniabukta coast section E8

**Coastal length: 500 m**

**Geomorphological description:** A barrier spit-platform coastline. The spits formed in tandem with the progradation of the barrier platform since at least beginning of the 20<sup>th</sup> century. Four main spits are divided by lagoons filled with mud and decaying seaweed. The platform with 24 beach ridges is likely built on the Ebbaelva ebb-tidal delta. Ebbaelva is the largest glacier river in the study area and second biggest supplier of suspended sediments after Hørbyebreen outwash plain to the tidal flat system of Petuniabukta.

#### **Major sediment supplies:**

- boulder to cobble fraction: large boulders in the Ebbaelva delta were left by retreating glaciers
- gravel to sand fraction: longshore drift from section E7, sediment transport from Ebbaelva
- silt to clay fraction: transported by Ebbaelva, transport by tidal currents from the tidal flat, aeolian transport of fine sediments from Ebbadalen and Hørbyebreen outwash plain.

## A.2 Petuniabukta North Coast sections

### A.2.1. Coastal section N1: Northern Petuniabukta barrier and lagoon coast (Figure A.1.9.)

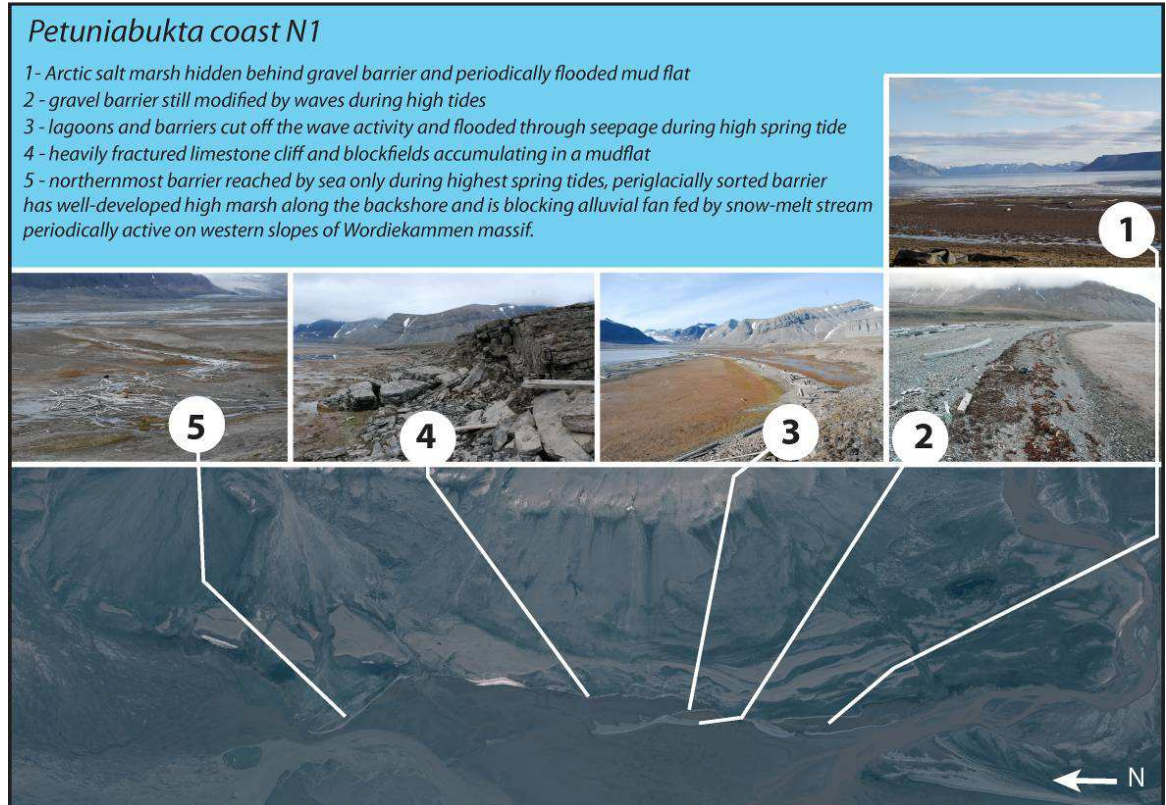


Figure A.1.9. Petuniabukta coast section N1.

**Coastal length:** 2500 m

**Geomorphological description:** Section of the coast composed of the whole mosaic of landforms characteristic for estuarine and tidal flat environments. In the southernmost part Ebbaelva builds ebb-tide delta on prograding tidal flat. In recent years tidal flat progradation supplied by braided rivers draining Hørbyebreen-Ragnarbreen outwash plains led to significant shallowing of the nearshore zone and reduction of the direct influence of coastal processes on the development of barrier islands and lagoons and salt marshes stretching along former cliffed coastline. Lagoons are flooded only during the highest tides mainly by seepage of gravel-dominated barriers. Relict limestone cliffs are cut off the wave action and are currently reshaped by periglacial processes. Surface of cliffs is covered with frost pavements and accumulation of boulders along the base of the cliff suggest operation of effective frost weathering and rock shattering. Rocky rubble sinks in muddy tidal flat and is subject to frost segregation and thrusting. In the intertidal zone is covered with mud-boils suggesting intensive cryoturbation of tidal deposits.

#### Major sediment supplies:

- boulder to cobble fraction: large boulders along the cliff walls and on the tidal flat originate from severe frost weathering of relict limestone cliffs. Some of the boulders are deposited around Ebbaelva mouth during the spring/summer melt



floods, but the massive boulders embedded in the tidal flat were likely deposited by the former Hørbyebreen-Ragnarbreen glacial system.

- gravel to sand fraction: supplied by Ebbaelva and longshore drift of material from adjacent spit-platform (section E8). During high tides that are accompanied by stormy weather, gravel and sand is eroded from and moved along the barrier islands.
- silt to clay fraction: supplied by glacial rivers from the Hørbyebreen-Ragnarbreen outwash plains, aeolian transport of sediments from abandoned channels and Hørbyebreen outwash plain.

### A.2.2 Coastal section N2: North-western Petuniabukta barrier islands (Figure A.I.10.)

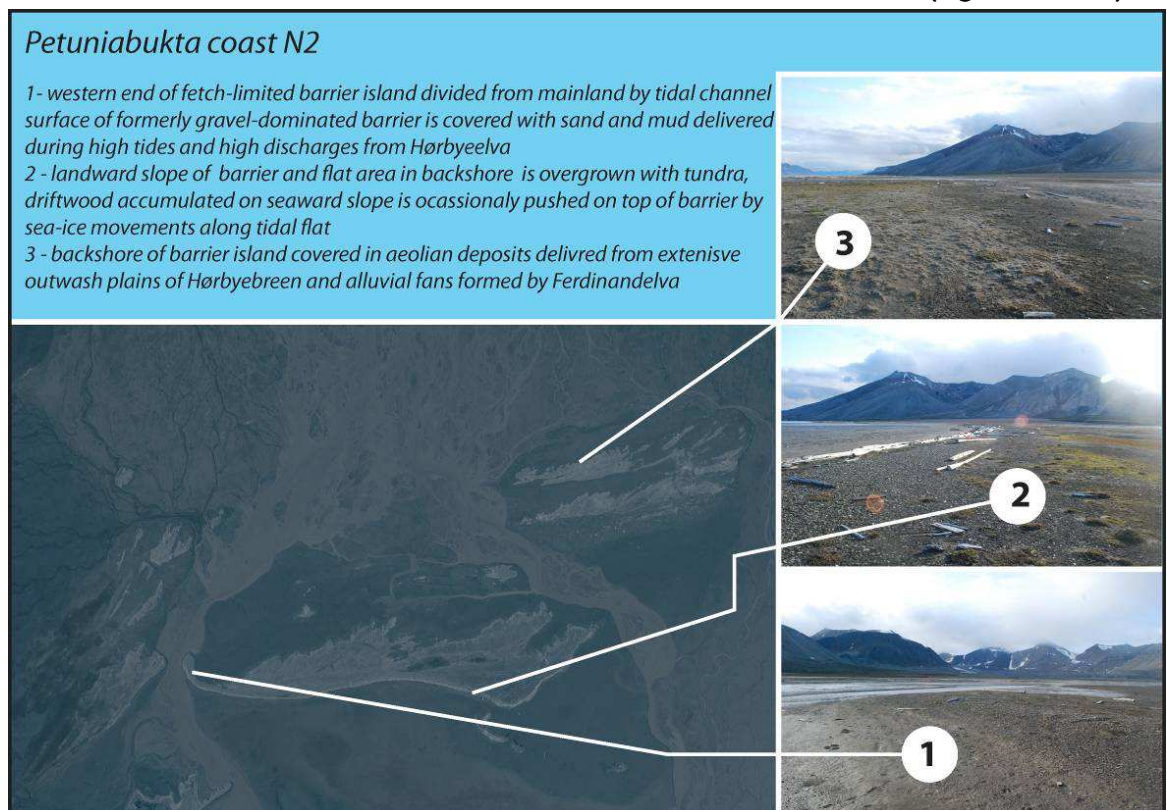


Figure A.I.10. Petuniabukta coast section N2

**Coastal length:** 2300 m

**Geomorphological description:** A group of barrier islands and remnants of relict spits between the Ferdinandbreen fan delta systems and the Petuniabukta tidal flat. Progradation of the tidal flat and shallowing of the water around the barriers leads to progressive isolation of barrier islands from coastal processes. The surfaces of the islands are locally covered with tundra. Tundra vegetation together with driftwood scattered along the barrier surface and shores, helping the accumulation of aeolian deposits from the extensive Hørbyebreen-Ragnarbreen outwash system.



### Major sediment supplies:

- gravel to sand fraction: the supply of gravel and sand is limited to low frequency extreme storms able to reach the barrier crests and overwash the island surfaces. The main source of the sandy deposits is deflation of the adjacent outwash plains and accumulation on wet tundra-vegetated barrier surfaces. Sea-ice movement across the tidal flat and along the western coast of Petuniabukta may also supply coarser fractions during the melting of ice floes on the barrier surfaces.
- silt to clay fraction: deposited around the barrier islands during high tides and occasionally on their surfaces during the spring/summer melt floods of Hørbyeelva and Svenelva.

### A.2.3 Coastal section N3: Petuniabukta Tidal Flat (Figure A.1.11)

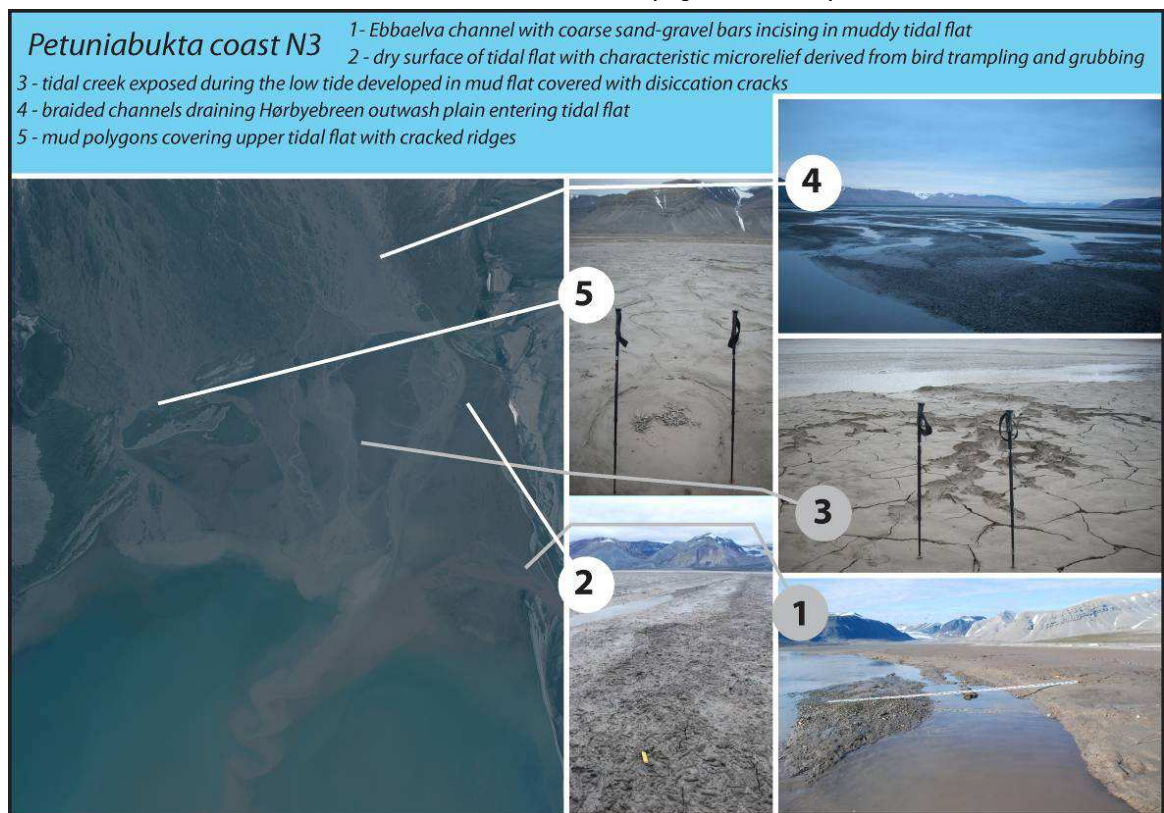


Figure A.1.11. Petuniabukta coast section N3

**Coastal length:** -

**Geomorphological description:** The head of the Petuniabukta is covered with a prograding tidal flat supplied by the Hørbyebreen-Ragnarbreen outwash plain system. A major tidal channel is located in the eastern part of the tidal flat where the main channel of Hørbyeelva and Ragnareelva leave the outwash plain. A large tidal island has also developed in the eastern part of the tidal flat.

### Major sediment supplies:

- gravel to sand fraction: Fluvial supply from the main glacial rivers: Hørbyeelva, Ragnarelva and Ebbaelva. Sea-ice moving across the tidal flat may also contain coarse fractions entrained along the gravel-dominated shores and deposit gravels and sands during melt out.
- silt to clay fraction: supplied by Hørbyeelva, Ragnarelva, Ebbaelva; deposited and redistributed on the surface of the tidal flat during tidal cycle; supplied by melting ice floes.

### A.3. Petuniabukta West Coast sections

#### A.3.1 Coastal section W1: Snow-fed alluvial fan coast I (Figure A.1.12.)

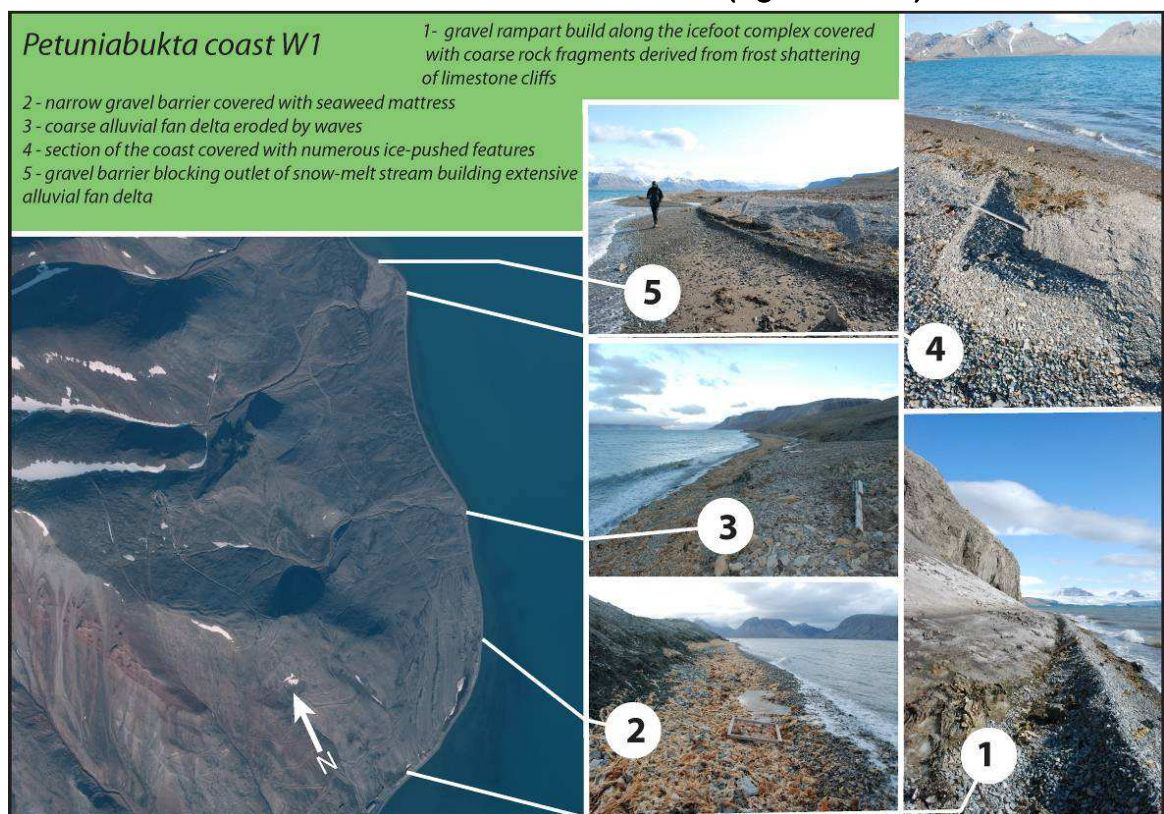


Figure A.1.12. Petuniabukta coast section W1

Coastal length: 2300 m

**Geomorphological description:** Narrow, steep, gravel dominated- barriers and beaches exposed to wave fetch from strong winds descending from Nordenskiöldbreen. Narrow barriers develop on the edge of relatively deep water. The coastal zone is cut by several snow-fed streams. Ephemeral deltas built up by streams are often eroded by wave action and their outlets are blocked by gravel barriers. Barriers formed in the northern part of the W1 coast are covered with ice-made landforms (ridges, grooves, furrows, kettle marks etc).



#### Major sediment supplies:

- boulder to cobble fraction: Large erratics embedded in the barriers were deposited by glaciers filling fjord during the last glaciation, rock rubble occasionally found along the coast is derived from erosion and weathering of small limestone cliffs covered with uplifted marine deposits.
- gravel to sand fraction: fluvial supply from main snow-fed streams and solifluction from uplifted marine terraces.
- silt to clay fraction: supplied by snow-fed streams, solifluction and sea-ice.

#### A.3.2 Coastal section W2: Limestone cliff coast (Figure A.1.13.)

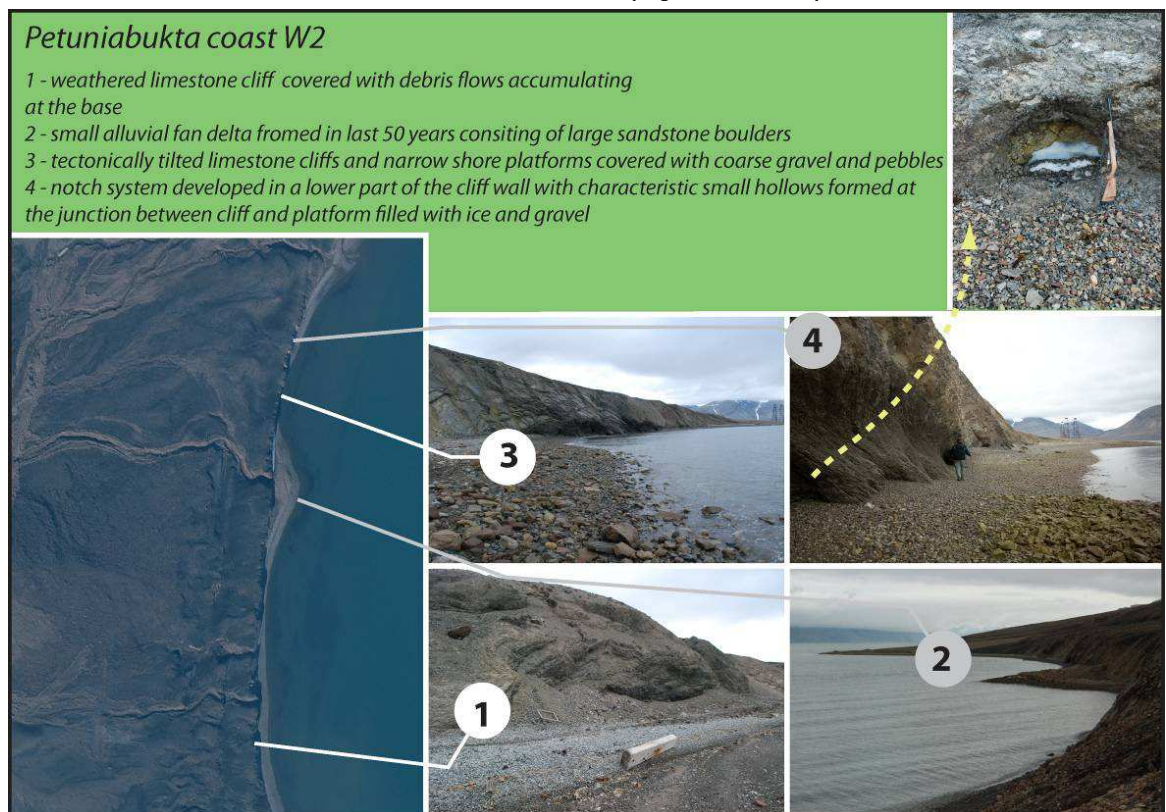


Figure A.1.13. Petuniabukta coast section W2

**Coastal length:** 450 m

**Geomorphological description:** Limestone cliff that divides the western coast of Petuniabukta. Rock cliffs are disturbed by the adjacent fault what explains the characteristic steep dip of the cliff. Cliff walls are heavily weathered and a combination of sea-ice action, icefoot development and snow accumulation along the bottom of the cliff has led to the formation of notches with deep hollows that are often filled with ice, snow and coarse sediments until late summer.

#### Major sediment supplies:

- boulder to cobble fraction: direct rockfalls from the cliff.

- gravel to sand fraction: fluvial supply from snow-fed stream which in last 50 years incised one of the cliff walls and solifluction of uplifted marine sediments that cover the top of the cliffs.
- silt to clay fraction: fluvial supply from a snow-fed stream which in last 50 years incised one of the cliff walls and solifluction of uplifted marine sediments that cover the top of the cliffs.

### A.3.3 Coastal section W3: Alluvial fan coast 2 (Figure A.1.14.)

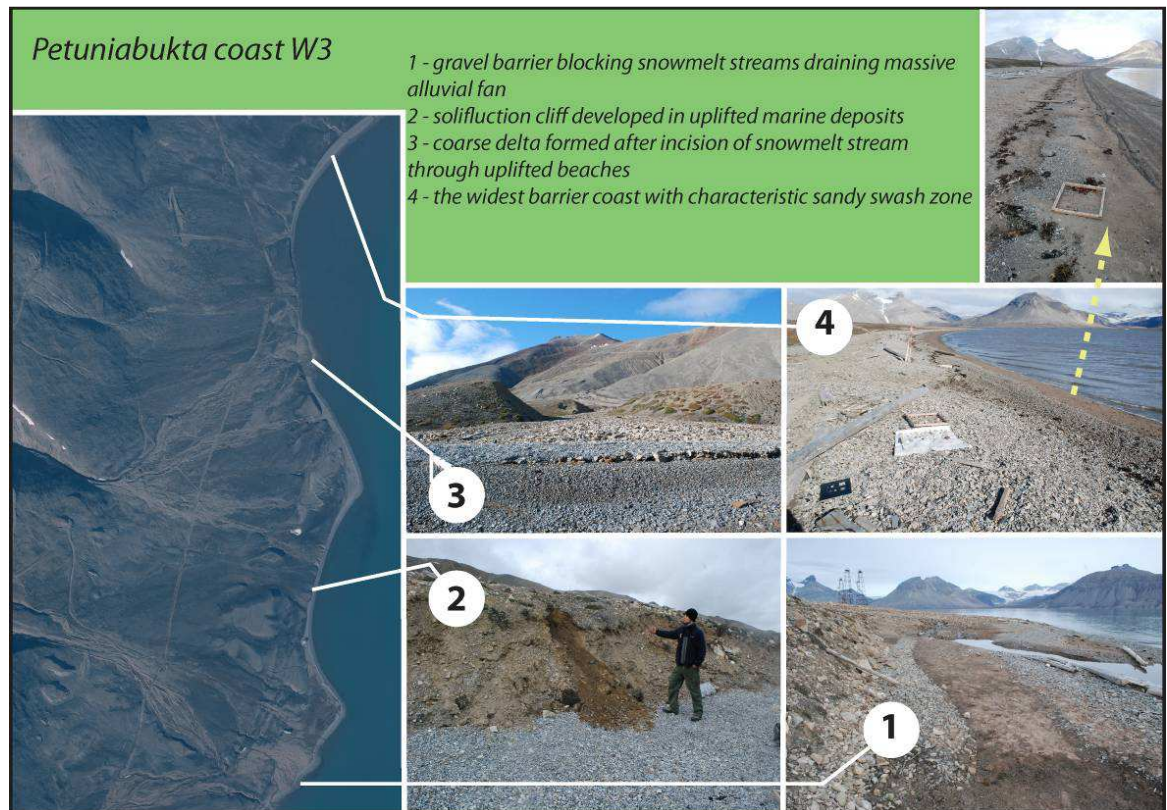


Figure A.1.14. Petuniabukta coast section W3

**Coastal length:** 1900 m

**Geomorphological description:** Supplied by snow-fed streams forming several deltas blocked by gravel-dominated barriers. Barriers are wider, better developed and contain more sand than in W2. Snow-fed streams incise uplifted marine terraces and small solifluction cliffs have formed in unconsolidated sediments.

#### **Major sediment supplies:**

- boulder to cobble fraction: direct rockfalls from the cliff.
- gravel to sand fraction: fluvial supply from snow-fed streams, longshore drift of material forming barriers, solifluction and debris flows from low cliffs.
- silt to clay fraction: fluvial supply from snow-fed streams, deposition from melting sea-ice.



#### A.3.4 Coastal section W4: Ferdinandbreen alluvial fans coast (Figure A.1.15.)

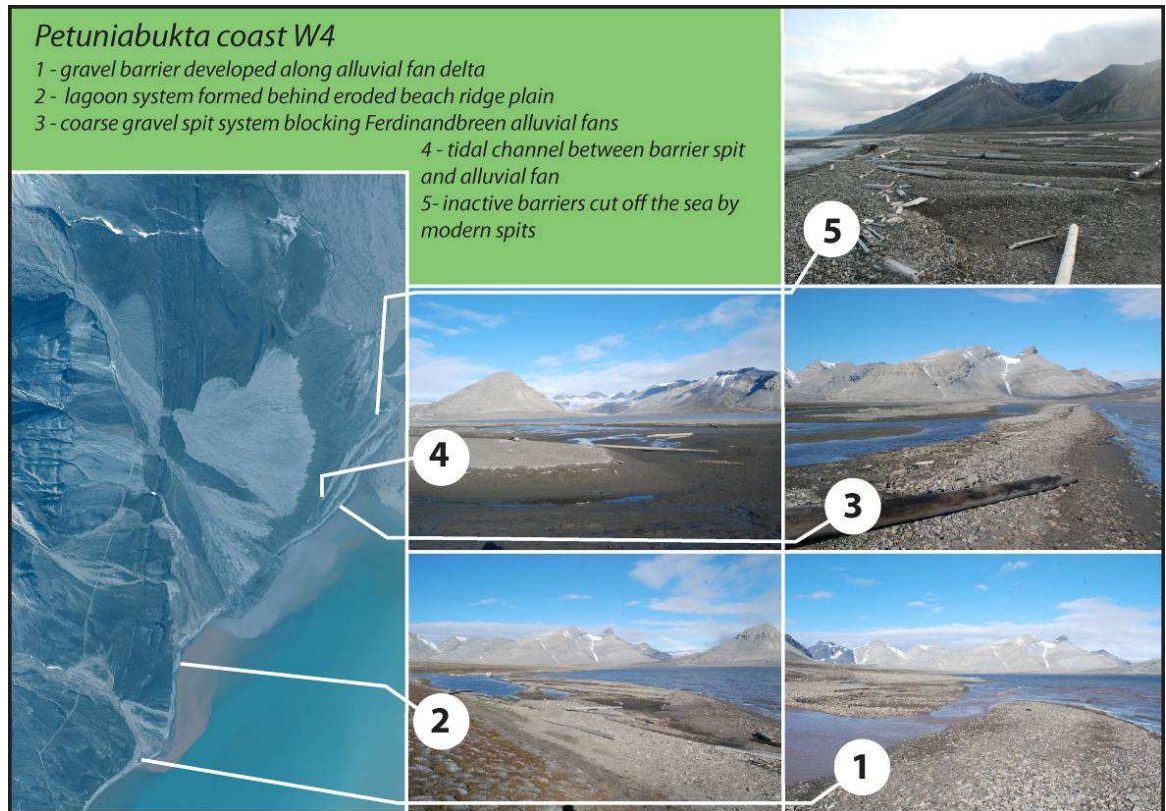


Figure A.1.15. Petuniabukta coast section W4

**Coastal length:** 2500 m

**Geomorphological description:** The coast is dominated by glacial rivers (Elzaelva and Ferdinandelva) that have built extensive alluvial fans and deltas. Glacial-fed fans supply coarse clastic sediments to barrier and spits systems which during last century experienced rapid development and protected a major fan delta from wave action. Barrier spits are also fed by the longshore drift of sediments delivered from erosion of coastal plain between Elzaelva delta and the first Ferdinandelva delta. Abandoned deltas are separated from barriers by small lagoons that are flooded by seepage through barriers. At the head of youngest barrier spit several ice-made features were observed.

**Major sediment supplies:**

- boulder to cobble fraction: most alluvial fans are composed of boulder-cobble fractions but the formation of an extensive barrier and lagoonal system almost completely suppresses the delivery of this material to the coastal zone.
- gravel to sand fraction: fluvial supply from glacial rivers, longshore drift of material eroded from the low coastal plain, longshore drift of sediments eroded from barriers and barrier spits.
- silt to clay fraction: fluvial supply from glacial rivers, aeolian transport from abandoned channels on alluvial fans, and also deposition from melting sea-ice.

#### A.4 Adolfbukta Northern Coast section – A1: Adolfbukta coast (Figure A.1.16.)

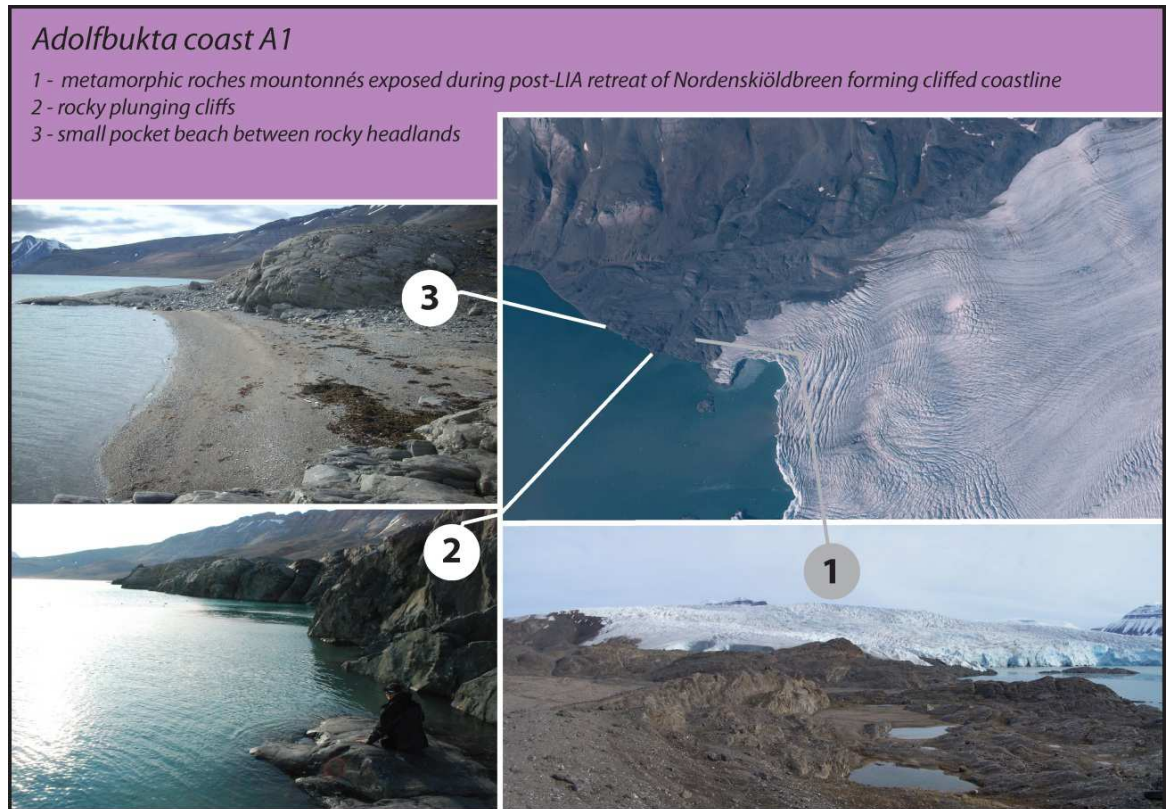


Figure A.1.16. Adolfbukta coast section A1

#### Coastal section A1: Nordenskiöldbreen roches moutonnées cliffed coast (Fig. 63)

**Coastal length:** 1200 m

**Geomorphological description:** Post-LIA retreat of Nordenskiöldbreen led to the exposure of the field of plagiogneiss roches moutonnées. The rocky glacial foreland is covered with a thin cover of glaciofluvial sediments. Fine sediments delivered by Thompsonelva are probably the main source of sediment to a small pocket beach formed in one of the embayments between rocky headlands.

**Major sediment supplies:** This section of the coast (excluding the small pocket beach) is devoid of depositional landforms. Beach sediments are delivered from adjacent glacial Thomsonelva and deposited by ice-bergs from calving tide water glacier. Deposition from melting sea ice plays is also important.



# **APPENDIX II:**

## **Research initiatives and projects**

Research problem	Ongoing or prepared project	Partner institutions	Role in the project
Arctic coastal hazards: Land-slide and ice-berg roll triggered tsunami waves	Tsunami and ice-berg roll events record in coastal lacustrine environments of Greenland - implications for reconstruction of sea-level history, ice-stream dynamics and assessment of natural hazards (2011-2013) National Science Centre NSC research project	Durham University, UK Adam Mickiewicz University in Poznan, Poland	principal investigator
Post-LIA evolution of Svalbard tidal flats	HACOSE (2012-2013) Evolution of Braganzavegen tidal flat in Van Mijenfjorden, central Spitsbergen	University Centre in Svalbard Norwegian Geological Survey, Durham University, UK	Lead author and principal investigator
Comparison of storm dominated and sheltered coasts of Spitsbergen	PET-BELL Comparison of coastal processes operating on the coasts of Bellsund and Petuniabukta	UMCS Lublin, PL Durham University, UK, UNIS, Norway	Co-leader
Development of rock cliffs and shore platforms in polar climates	COROCO Quantifying the processes controlling rock coast evolution in polar climate. (2013-2015) NCS project proposal	Northumbria Uni. UK Windsor University Canada, Wroclaw University. PL Durham University, UK	Lead author and Principal investigator
Mechanisms controlling Holocene evolution of Svalbard barriers	SVALBARRDYN Svalbard Barrier Dynamics (2013-2016) IUVENTUS project proposal for Polish young researchers	AMU Poznan Durham University, UK UNIS, Norway Boston University, USA	Lead author Principal investigator
Sedimentary record of extreme events in Arctic coastal barriers, lakes and lagoons	ATTEMPT - Tracing the record of Arctic Tempests and Tsunamis – pilot study in southern Spitsbergen. (2013) Research Council of Norway project proposal	UNIS Norway, Durham University, UK, AMU Poznan Poland, Lamont Doherty Earth Observatory, USA, Oxford University, UK, Jagiellonian University PL	Lead author and principle investigator
Svalbard coastal research group	SVALCOAST group (active since 2011)	7 Polish research institutions	Group leader

*Table A.2. Research initiatives and projects that have evolved from this PhD research.*

# **APPENDIX III:**

## **Published academic papers**

Academic papers evolved from and published during this PhD project.

1. Long A.J., **Strzelecki M.C.**, Lloyd J.M., Bryant C., 2012. *Dating High Arctic Holocene relative sea level changes using juvenile articulated marine shells in raised beaches. Quaternary Science Reviews* 48 (2012) 61-66.  
IMPACT FACTOR: 3.973
2. Evans D.J., **Strzelecki M.C.**, Milledge D., Orton C., 2012. *Hørbyebreen polythermal glacial landsystem, Svalbard. Journal of Maps* 8(2): 146-156.  
IMPACT FACTOR: 0.296
3. **Strzelecki M.C.**, 2011. *Schmidt hammer tests across a recently deglaciated rocky coastal zone in Spitsbergen - is there a 'coastal amplification' of rock weathering in polar climates? Polish Polar Research* 32/3, 239-252.  
IMPACT FACTOR: 0.875
4. **Strzelecki M.C.**, 2011. *Cold shores in warming times – current state and future challenges in High Arctic coastal geomorphological studies. Quaestiones Geographicae* 30/3, 103-115.
5. **Strzelecki M.**, 2009. *Suspended and solute transport in small glaciated catchment Bertram river, Central Spitsbergen, in 2005-2006. Norwegian Journal of Geography* 63:2, 98-106.  
IMPACT FACTOR: 0.705



# Dating High Arctic Holocene relative sea level changes using juvenile articulated marine shells in raised beaches

Antony J. Long<sup>a,\*</sup>, Mateusz C. Strzelecki<sup>a,b,c</sup>, Jerry M. Lloyd<sup>a</sup>, Charlotte L. Bryant<sup>d</sup>

<sup>a</sup> Department of Geography, Durham University, South Road, Durham DH1 3LE, UK

<sup>b</sup> Department of Cryospheric Research, Adam Mickiewicz University, ul. Dąbrowska 27, 61-680 Poznań, Poland

<sup>c</sup> Alfred Wegener Institute for Polar and Marine Research, Department of Periglacial Research, Telegrafenberg A43, 14473 Potsdam, Germany

<sup>d</sup> NERC Radiocarbon Facility, Scottish Enterprise Technology Park, Rankine Avenue, East Kilbride, Glasgow G75 0QF, UK

## ARTICLE INFO

### Article history:

Received 19 January 2012

Received in revised form

9 June 2012

Accepted 15 June 2012

Available online xxx

### Keywords:

Raised beach

Relative sea-level change

Glacio-isostasy

Svalbard–Barents Sea Ice Sheet

Arctic palaeoclimate

## ABSTRACT

High Arctic raised beaches provide evidence for changes in relative sea-level (RSL), sea-ice extent, storminess, and variations in sediment supply. In many High Arctic areas, driftwood and whale bone are usually the preferred targets for radiocarbon dating, with marine shells a third choice because of their often large age and height uncertainties with respect to former sea level. Here we detail a new approach to sampling marine shells that reduces these problems by targeting juvenile, articulated specimens of *Astarte borealis* that are washed onto the beach under storm conditions and become incorporated into the beach crest. Radiocarbon dates from articulated valves of *A. borealis* from eight raised beaches from Billefjorden, Svalbard, provide a chronology for Holocene beach ridge formation and RSL change that compares favourably to the most precise records developed from elsewhere in Svalbard using driftwood or whale bone. We demonstrate the value of this new approach by comparing our record with previously published RSL data from eastern Svalbard to test different models of Late Weichselian ice load in this region. We find support for a major ice dome centred south and east of Kong Karls Land but no evidence for a significant ice dome located over easternmost Spitsbergen or southern Hinlopen Strait as proposed from recent marine geophysical survey. The approach is potentially applicable elsewhere in Svalbard and the High Arctic to address questions of RSL change and beach ridge chronology, and hence wider questions regarding palaeoclimate and ice load history.

© 2012 Elsevier Ltd. All rights reserved.

## 1. Introduction and aim

Raised beaches are widespread on Arctic coastlines and their geomorphology and sediments contain valuable information about relative sea-level (RSL) change, sea-ice extent and storminess as well as changes in sediment supply. Marine shells are commonly used to date these beaches but they are prone to reworking and may have an uncertain age and height relationship to former sea level. For this reason, in Svalbard and other High Arctic settings, researchers favour alternative material for dating, such as whale bone or driftwood that are considered less vulnerable to reworking (e.g. Dyke et al., 1991; Bondevik et al., 1995; Forman et al., 2004).

In this paper we detail a new approach to the sampling of marine shells from raised beaches in Svalbard that seeks to overcome the potential problems of significant reworking. We target detrital, but still articulated valves of juvenile *Astarte borealis* that

have been transported from their primary fjord-bed habitat and deposited within the upper few decimetres of the storm beach. By sampling juvenile, well-preserved articulated specimens we minimise the potential for reworking and provide tight age constraints on the date of beach formation. We develop a new Holocene RSL record using this approach, compare the results with those obtained from driftwood, and test different models of the configuration of the Late Weichselian Barents Sea Ice Sheet in northern Svalbard. The approach is potentially applicable elsewhere in Svalbard and the High Arctic to address questions of RSL change and beach ridge chronology, and hence wider questions regarding palaeoclimate and ice load history.

## 2. Study area and previous work

The study area is located at the mouth of the Ebba Valley, in the head of Billefjorden (central Spitsbergen) (Fig. 1A, D). The present beach comprises varying quantities of fine gravel and sand, with seaweed and abundant driftwood (Fig. 1B). The bedrock geology here and beneath the adjacent fjord comprises a mixture of

\* Corresponding author. Tel.: +44 191 334 1913; fax: +44 191 334 1801.

E-mail address: [A.J.Long@Durham.ac.uk](mailto:A.J.Long@Durham.ac.uk) (A.J. Long).



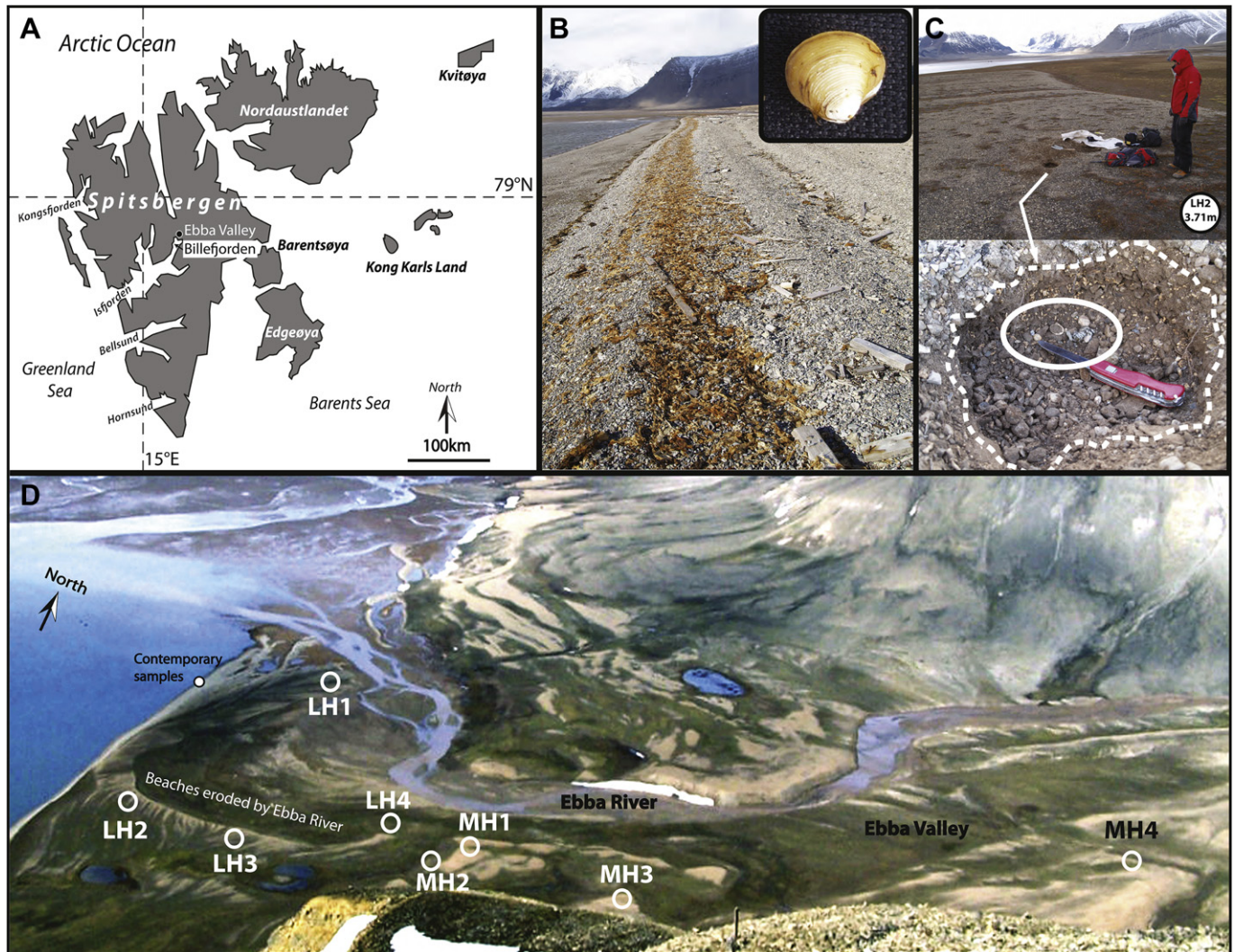


**Fig. 1.** (A) The Svalbard archipelago and the location of the study site. (B) Present-day beach environment at the Ebba Valley showing seaweed and driftwood on the active storm beach. The inset shows a specimen of *Astarte borealis*, c. 10 mm in diameter. (C) Shallow excavation into the crest of a late Holocene beach crest (LH-2) showing two valves of a once-articulated specimen of *A. borealis* targeted for radiocarbon dating. (D) Oblique air photograph showing the raised beaches in the Ebba Valley. Letters (LH1–4, MH1–4) are locations that were dated using samples of *A. borealis*.

Precambrian, Devonian and Carboniferous-Permian outcrops (Dallmann et al., 2004). The spring tidal range is c. 1.5 m and the active storm beach crest to the south of the mouth of the Ebba River has an altitude of between 1.1 and 0.75 m above mean tide level (MTL). The adjacent fjord is normally ice-bound between mid November and mid June. Winds are strongly influenced by the surrounding orography and the presence of a large ice-plateau to the northeast (Lomonosovfonna). The prevailing winds in Petuniabukta are from the S–SSE (along the fjord axis) and also the longest wave fetch potential is from the south.

The Ebbabreen glacier was formerly part of a large ice stream complex that drained the Late Weichselian ice sheet via Billefjorden into Isfjorden (Landvik et al., 1998). Retreat of the Ebbabreen and other tributary glaciers during the Lateglacial meant that by the start of the Holocene their termini were located inland of the present coast (Baeten et al., 2010; Forwick and Vorren, 2010). Marine conditions at this time penetrated into the mouths of the tributary valleys, including the Ebba Valley and, as RSL fell rapidly, staircases of raised beaches developed (Feyling-Hanssen and Olsson, 1960; Feyling-Hanssen, 1965; Salvigsen, 1984; Klyszyk et al., 1988; Stankowski et al., 1989; Mangerud and Svendsen, 1992).

The surface topography of the beach plain close to sea level is characterised by low amplitude (<0.5 m) beach crests that are c. 5 m in width and resemble the fair-weather beaches described by Mason (2010), with no signs of significant overwash or overtopping features. Beach sediment is provided mainly from an alluvial fan that crosses the coast at the south side of the Ebba Valley as well as from eroding cliffs of former raised beaches further to the south.

Marine shells, dominated by the filter-feeder *A. borealis*, are abundant on the present-day beach (Fig. 1B), as elsewhere in the fjords of Spitsbergen (Feyling-Hanssen, 1955). *Astarte* valves observed on the active shoreface are often broken or abraded, whilst better preserved specimens occur higher up the beach, some of which are still articulated and show minimal signs of reworking (e.g. little abrasion on the ventral edge and dorsal margin). All of this shell material is reworked, either directly from the sea bed floor or indirectly by the erosion of Holocene-age raised beach deposits and their associated faunas. Field observations of present day conditions show that during storms reworked shell faunas, including juvenile articulated specimens of *A. borealis*, are cast up onto the beach crest and some are deposited within a cushioning mat of seaweed, either on or near the surface of the storm beach.

When this seaweed decays, the still-articulated specimens of *A. borealis* become incorporated and preserved within the uppermost few decimetres of the beach ridge.

### 3. Methods

We collected small, juvenile (<15 mm diameter) specimens of articulated *A. borealis* for AMS radiocarbon dating that showed minimum signs of surface abrasion to minimise the possibility of reworking effects. We identified specimens by digging shallow (<20 cm deep) pits into the surface of the present and Holocene storm beaches (Fig. 1C). Using a penknife we carefully removed individual grains of gravel to extract suitable specimens. We quote elevation with respect to MTL, established at the study site using a sea-bed pressure transducer deployed between 2008 and 2010. We reconstruct RSL with respect to MTL by correcting our data for the height difference between the present storm beach and MTL. We use a single value of 1.1 m as our estimate of the original beach ridge elevation above contemporaneous MTL, with an uncertainty of  $\pm 0.5$  m that comfortably exceeds the height range in the present-day storm beach crest (0.35 m).

Specimens of *A. borealis* were radiocarbon dated at the NERC Radiocarbon Facility, using the SUERC AMS facility in East Kilbride. Pretreatment involved removal of the outer 20% of the shells by controlled hydrolysis with dilute HCl. We calibrated ages using Calib 6.1.1 (Reimer et al., 2004) using the Marine09 dataset (Reimer et al., 2009) and a  $\Delta R$  of  $100 \pm 39$  years based on four pre-bomb spike ages. We report Holocene samples with a calibrated two standard error age range and modern samples using percent modern carbon.

### 4. Results

We dated three pairs of juvenile *A. borealis* collected from the contemporary storm beach in August 2010 to test for potential reworking (Fig. 1D, Table 1). Each sample contained modern, post-bomb carbon indicating a post-1960 age. Thermonuclear weapons testing in the 1950s and 1960s increased the atmospheric  $\Delta^{14}\text{C}$  signals from c.  $-40$  to  $-50\text{‰}$  to  $850$ – $900\text{‰}$  (Levin and Kromer, 1997). This  $\Delta^{14}\text{C}$  spike was dampened in the marine realm due to mixing of surface and deep ocean waters, diluting the bomb  $^{14}\text{C}$  signal with pre-bomb dissolved inorganic carbon (DIC), but still raised the DIC pool to c.  $200\text{‰}$  by the end of the 1960s (Hansell and Carlson, 2002). Kalish et al. (2001) dated archived pre- and post-bomb (1919–1992) cod otoliths of known age collected from the Barents Sea to develop a marine bomb spike curve (Fig. 2). This

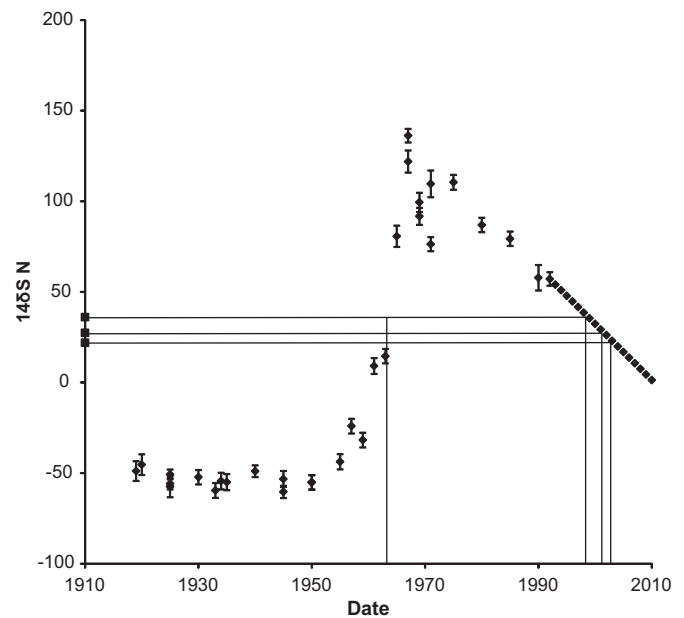


Fig. 2. The marine bomb spike curve of Kalish et al. (2001) based on radiocarbon dates from known-age cod otoliths from the Barents Sea region. The unit  $^{14}\delta\text{SN}\text{‰}$  is equivalent to  $\Delta^{14}\text{C}$  (Mook and van der Plicht, 1999). Our samples (SUERC-33584, SUERC-33585 and SUERC-33586, Table 1) are plotted for comparison and have  $\pm 1$  SD  $\Delta^{14}\text{C}$  values of between 4.74 and 4.81 (this is smaller than the symbol). The youngest otolith sample dated is from 1992 and we extrapolate downwards the trend in  $\Delta^{14}\text{C}$  at a rate of  $3.1\text{‰}$  per year (dashed line, after Kalish et al. (2001)) to estimate the possible age of the samples as being either c. 1962 or, more likely, between 1999 and 2003.

shows that the average pre-bomb (AD 1950)  $\Delta^{14}\text{C}$  was  $-53.8\text{‰}$  and increased to a peak of  $134.2\text{‰}$  in 1967. Between 1973 and 1992 the  $\Delta^{14}\text{C}$  declined linearly ( $n = 5$ ,  $r^2 = 0.97$ ,  $p = 0.002$ ) at a rate of  $3.1\text{‰}$  per year.

Lacking data regarding the  $\text{DI}^{14}\text{C}$  composition of the waters of Petuniabukta we assume that the cod otolith bomb spike is applicable to our samples. Support for this assertion is provided by Kalish et al. (2001) who note that pre-bomb spike  $^{14}\text{C}$  measurements from shells and seawater DIC from several locations in the Barents, Norwegian and Greenland seas provide independent validation of the otolith data, although we recognise that DIC of the fjord waters of our sample site may differ from the Barents Sea because of freshwater dilution as well as potential influences from the local carbonate geology. Noting these caveats, our three samples have two potential ages, one on the rising limb of the

Table 1  
Radiocarbon dates from this study.

Sample code	Code	$^{14}\text{C}$ age $\pm 1$ SD	Calibrated age range $\pm 2$ SD	% Absolute modern $\pm 1$ SD	Altitude above MTL in metres	Carbon content % weight	$\delta^{13}\text{C}$ vPDB $\text{‰}$ $\pm 1$ SD
Ebba contemporary 1	SUERC-33584	Modern	Modern	$102.19 \pm 4.74$	0.80	10.4	1.3
Ebba contemporary 2	SUERC-33585	Modern	Modern	$102.74 \pm 4.74$	0.80	11.0	1.7
Ebba contemporary 3	SUERC-33586	Modern	Modern	$103.60 \pm 4.81$	0.80	9.8	0.9
Ebba LH1	SUERC-35206	$3411 \pm 37$	2995–3317		1.24	10.3	2.2
Ebba LH2–1	SUERC-33587	$4314 \pm 37$			3.71	10.3	1.4
Ebba LH2–2	SUERC-33588	$4382 \pm 38$			3.71	10.5	2.0
Ebba LH2–3	SUERC-33589	$4188 \pm 37$			3.71	9.7	3.0
	Pooled mean of LH2 samples		4127–4416		3.71		
Ebba LH3	SUERC-35209	$4545 \pm 37$	4451–4797		5.01	11.4	1.9
Ebba LH4	SUERC-35210	$4930 \pm 37$	4957–5281		5.97	11.6	3.1
Ebba MH1	SUERC-35211	$6397 \pm 38$	6626–6898		11.73	12.0	2.2
Ebba MH2	SUERC-35212	$7292 \pm 39$	7558–7781		16.26	11.7	2.7
Ebba MH3	SUERC-35213	$8248 \pm 39$	8471–8850		20.50	11.8	2.1
Ebba MH4	SUERC-35214	$9125 \pm 39$	9536–9900		27.90	11.3	2.2



bomb spike at c. 1962 and a second from between c. 1999 and 2003. Due to the excellent shell preservation, we think that the chance of three samples from the modern storm beach all dating from the 1960s is remote and instead consider that the younger age range is more likely. The results demonstrate minimal reworking of the target samples.

We next dated three samples of paired, juvenile *A. borealis* collected from a shallow excavation made into the crest of a late Holocene beach to test for within-beach consistency in dates (LH2, Fig. 1C, D). The age ranges of the samples indicate a close agreement (Table 1), overlapping at the two standard error range, and show that age-mixing of paired specimens of *A. borealis* in late Holocene beaches is small. Finally, we excavated a further seven samples of paired, juvenile specimens of *A. borealis* from shallow pits in beach crests at elevations between 1.24 m (LH1) and 27.9 m (MH4) (Fig. 1D). The results of our dating programme show that all of our radiocarbon dates are in height and age sequence with no age reversals (Table 1).

## 5. Discussion

### 5.1. Using marine molluscs to date High Arctic raised beaches

Our data show RSL fell from c. 27 m MTL at 9.7 k cal yr BP to reach close to present sea level by 3.1 k cal yr BP (Fig. 3). The trend in the mid Holocene RSL data suggests that RSL may have fallen below present during the late Holocene before rising to the present. Elsewhere in Billefjorden, Feyling-Hanssen (1955) notes that at Brucebyen, Kapp Napier and Skansbukta the lowermost beach ridges increase in elevation towards the present storm ridge by about 0.5 m suggesting a recent rise in sea level that he correlates with a glacier readvance about 2500 years ago. In Adventfjorden, late Holocene erosion of a large fan delta is associated with sea-level stabilising close to present (Lønne and Nemec, 2004); similarly in northwest Spitsbergen Forman (1990) suggests RSL rose in the last two millennia. The most likely cause of this rise

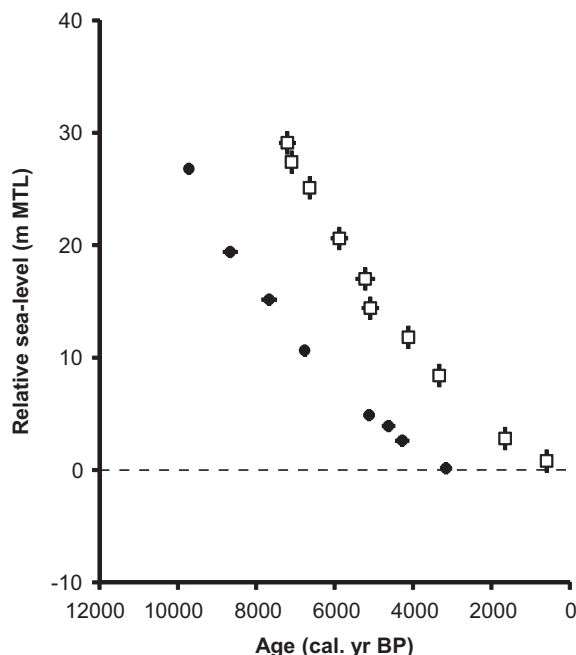


Fig. 3. Relative sea-level graph based on *Astarte borealis* from the Ebba Valley beaches compared with driftwood samples from southern Edgeøya (Bondevik et al., 1995).

is the effect of glacio-isostatic depression due to the collapsing forebulge of the former Svalbard–Barents Sea Ice Sheet (e.g. Lambeck, 1995, 1996).

Marine molluscs are only one potential source of data for constraining the ages of raised beach deposition and reconstructing RSL records in the High Arctic. Bondevik et al. (1995) report 81 radiocarbon dates from mostly driftwood and whale bone with a smaller number of mollusc samples ( $n = 10$ ) from Edgeøya and Brentsøya (eastern Svalbard) (Fig. 1). Their preference for driftwood as the main dating material reflects the fact that it floats and becomes stranded at high tide level, with storm waves throwing it further up and either burying it in the beach or leaving it on the surface in a similar mechanism to that associated with the deposition of the juvenile articulated valves of *A. borealis* targeted in this study. By dating the youngest, outer part of each driftwood sample, Bondevik et al. (1995) generate what they describe as “some of the most precise sea-level curves from the Arctic”. They further argue that because shells live below sea-level and provide a minimum estimate of former sea-level they are “normally not suitable as sea-level indicators in these regions”.

This statement is certainly valid when considered in the context of sea-level data derived from mixed shell samples analysed using conventional radiocarbon dating. However, the application of AMS radiocarbon dating enables the dating of individual shells which can be selected to minimise the possibility of dating mixed age samples and this has significantly reduced (but not eliminated) the potential difficulties associated with dating shells from raised beach deposits. In northern Spitsbergen, for example, Brückner et al. (2002) find close agreement between AMS-dated paired samples of *Mya truncata* collected in their living position in sub-littoral sands that are overlain by beach sands.

We compare our *A. borealis* record from the Ebba Valley with driftwood-only data from Hulma, a site on Edgeøya and chosen because of the excellent chronology from the site (Bondevik et al., 1995) (Fig. 3). The vertical offset between the two datasets records differential uplift between the two study sites (discussed below). This comparison shows that the *A. borealis* data provide RSL data of comparable quality, in terms of age and height scatter, to those from driftwood samples.

There are other advantages and limitations to the approach we present here. As with all studies that use marine carbonate for radiocarbon dating, we must make assumptions about the marine reservoir effect and the appropriate  $\Delta R$ . The latter is based on only four samples and, as we note in our consideration of the cod otolith bomb spike comparison, our interpretation would be strengthened by an equivalent record using known age 20th century samples of *A. borealis*. Secondly, our approach will only work elsewhere if shells are present in the beaches under study. As described by Feyling-Hanssen (1955), *A. borealis* is dominant in the mid and late Holocene raised beach sequences of Billefjorden, and is common in Svalbard (Feyling-Hanssen, 1955) and is recorded elsewhere in the High Arctic (e.g. Blake, 1975; England, 1997). *A. borealis* is only recorded in the Billefjorden area below 34.5 m, which equates to an age of c. 10,000 cal yr BP, whereas driftwood and whale bone are recorded in higher and older sequences (e.g. Salvigsen, 1981).

### 5.2. Implications for Late Weichselian ice sheet loading history

In his review of RSL changes in Svalbard, Forman et al. (2004) concluded that the former centre of the Barents Sea Ice Sheet was probably located to the southeast of Kong Karls Land (Fig. 4B), in agreement with a number of previous studies (Schytt et al., 1968; Boulton and Rhodes, 1974; Bondevik et al., 1995; Lambeck, 1995, 1996; Landvik et al., 1998). Recently, two other reconstructions have been proposed: i) a major ice dome located on easternmost

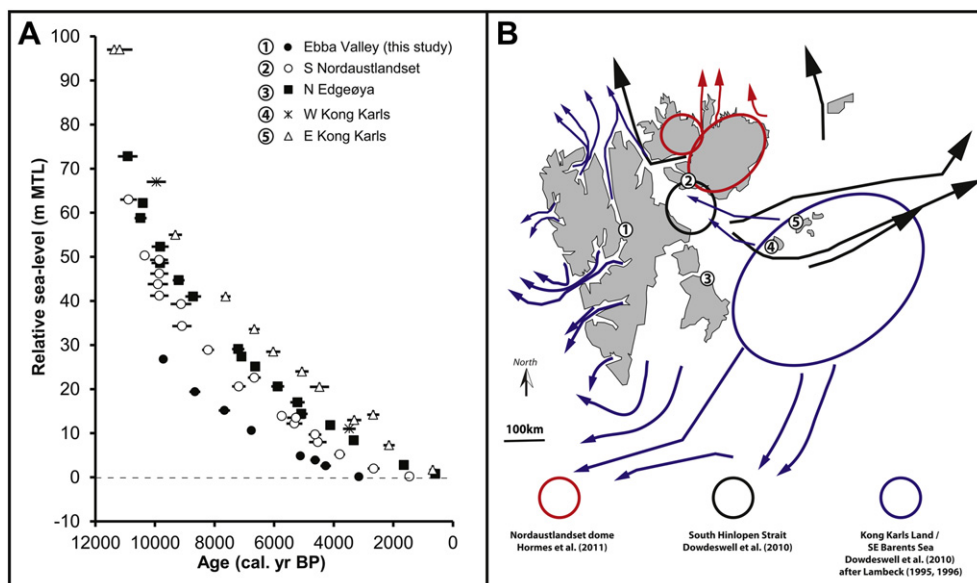


**Fig. 4.** (A) Relative sea-level data from central and eastern Svalbard. Sample elevations are adjusted for the current height difference between MTL and the present storm beach cited in the original publications (Humla 2.8 m (Bondevik et al., 1995), Kong Karls Land 3 m (Salvigsen, 1981), south Nordaustlandet 2.5 m (Salvigsen, 1978)). (B) Reconstructed Svalbard–Barents Sea Ice Sheet domes and ice flows (Landvik et al., 1998; Dowdeswell et al., 2010).

Spitsbergen or southern Hinlopen Strait (Dowdeswell et al., 2010), and ii) additional smaller local cold-based ice domes over Nordaustlandet (Hormes et al., 2011). The former model is based on the interpretation of flow directions inferred from streamlined submarine bedforms and the latter on field evidence and cosmogenic radionuclide dating from Nordaustlandet.

We compare our new RSL record from Billefjorden with published records from sites that are close to the different ice domes described above to test these competing models: Edgeøya (Humla) (Bondevik et al., 1995), Kong Karls Land (Salvigsen, 1981) and south Nordaustlandet (Svartknausflya) (Salvigsen, 1978) (Fig. 4A). The small age and height scatter in the combined RSL data enables the differentiation of distinct RSL trends between sites that are consistent over much of the Holocene.

All data from sites in eastern Svalbard plot above our new observations from Billefjorden. This pattern supports a thick Late Weichselian ice load over the east Spitsbergen/north Barents Sea area as previously proposed (e.g. Bondevik et al., 1995) (Fig. 4B). The Kong Karls Land data plot above same-aged data from the other sites. This is contrary to that expected with a large ice dome centred over easternmost Spitsbergen or southern Hinlopen Strait. Dowdeswell et al. (2010) cite the shorelines on Svenskøya (east Kong Karls Land) as additional evidence for their model, but there are only two Holocene dates from these (Salvigsen, 1981). We are not confident that these two dates and the other undated shorelines can be used to infer greater ice to the west of Kong Karls Land. We further note that the trend in the RSL data from south Nordaustlandet suggests that RSL reached close to present during the late Holocene, about a thousand years or so after it did so in Billefjorden. In contrast, the data from Kong Karls Land and north Edgeøya indicate RSL was above present throughout the Holocene at these sites. This shows increased rebound at these sites compared with south Nordaustlandet.

The RSL data presented in Fig. 4A suggest a large ice dome over or close to Kong Karls Land. However, the possibility of several smaller domes remains (Hormes et al., 2011). This includes the potential for topographically-routed warm-based ice associated with these domes shaping the bedforms described by Dowdeswell et al. (2010), albeit with associated ice loads that were too small to

modify the regional patterns in RSL described here. Such a model is compatible with a relatively thin ice cover over Nordaustlandet and with the development of several secondary domes during ice build up and decay. This discussion highlights the difficulty in inferring the location of ice domes using geomorphological evidence alone and shows the need to reconcile such data with alternative proxies of former ice load wherever possible.

## 6. Conclusions

We draw three conclusions from this study:

1. Marine shells are generally avoided in sea-level studies in Svalbard, and elsewhere in the High Arctic, because of problems associated with dating reworked faunas that can result in unreliable sea-level indicators. We demonstrate that the careful collection of storm deposited, articulated specimens of *A. borealis* from the upper levels of storm beaches can avoid the problem of reworked shells. The approach yields a reliable chronology for beach deposition that is every-bit as precise as alternatives, and establishes a new way to reconstruct High Arctic RSL change.
2. Using this approach we date a suite of raised beaches in the Ebba Valley, central Spitsbergen, and reconstruct a new Holocene RSL record. The highest Holocene beaches, at c. 40–45 m asl, formed shortly after local deglaciation at c. 10,000 cal yr BP. RSL fell from this level to reach within a metre of present sea-level by c. 3100 cal yr BP. The absence of any data points in our study area younger than c. 3000 cal yr BP, together with the downward trend in mid and late Holocene RSL, suggest that RSL fell below present and rose again in the last few millennia.
3. We show the potential of the approach by comparing our new RSL record with previously published RSL data from eastern Svalbard so as to test competing models of Late Weichselian ice load in this region. We find no evidence for a significant ice dome over easternmost Spitsbergen or southern Hinlopen Strait as proposed by Dowdeswell et al. (2010). Instead, our new interpretation supports a significant former ice dome

located over or close to Kong Karls Land in the North-east Barents Sea.

## Acknowledgements

We thank colleagues from the Adam Mickiewicz University in Poznań (Poland) and the NERC Radiocarbon Facility and SUERC AMS for support with the fieldwork and radiocarbon dating, the latter under award number 1520.0910. Fieldwork was partially funded by the Polish Ministry of Science and Higher Education (grant no. N306 284335 and N305098835). Matt Strzelecki is also supported by the Crescendum Est-Polonia Foundation, Adam Mickiewicz University Foundation, AMU programme 'Unique Graduate = Opportunity' funded by EU ESF and German Academic Exchange Service (DAAD) scholarship for young researchers. We thank the anonymous reviewers of this paper and Colm O'Cofaigh, Mike Bentley and Sarah Woodroffe for helpful discussions. This paper is a contribution to the Arctic Palaeo-Gateways Programme, the INQUA Commission on Coastal and Marine Processes, PALSEA and IGCP588.

## References

- Baeten, N.J., Forwick, M., Vogt, C., Vorren, T.O., 2010. Late Weichselian and Holocene sedimentary environments and glacial activity in Billefjorden, Svalbard. In: Howe, J.A., Austin, W.E.N., Forwick, M., Paetzel, M. (Eds.), *Fjord Systems and Archives*. Geological Society, London, Special Publications 344, pp. 207–223.
- Blake, W., 1975. Radiocarbon age determinations and postglacial emergence at Cape storm, southern Ellesmere Island, Arctic Canada. *Geografiska Annaler* 57A, 1–71.
- Bondevik, S., Mangerud, J., Ronnert, L., Salvigsen, O., 1995. Postglacial sea-level history of Edgeøya and Barentsøya, eastern Svalbard. *Polar Research* 14, 153–180.
- Boulton, G.S., Rhodes, M., 1974. Isostatic uplift and glacial history in northern Spitsbergen. *Geological Magazine* 111, 481–576.
- Brückner, H., Schellmann, G., van der Borg, K., 2002. Uplifted beach ridges in northern Spitsbergen as indicators for glacio-isostasy and palaeo-oceanography. *Zeitschrift Für Geomorphologie* 46, 309–336.
- Dallmann, W.K., Pipejohn, K., Blomeier, D., 2004. Geological map of Billefjorden, Central Spitsbergen, Svalbard with geological excursion guide 1: 50,000. Norsk Polarinstitutt Temakart. No 36.
- Dowdeswell, J.A., Hogan, K.A., Evans, J., Noormets, R., O'Cofaigh, C.O., Ottesen, D., 2010. Past ice-sheet flow east of Svalbard inferred from streamlined subglacial landforms. *Geology* 38, 163–166.
- Dyke, A.S., Morris, T.F., Green, D.E.C., 1991. Postglacial tectonic and sea level history of the central Canadian Arctic. *Geological Survey of Canada Bulletin* 1, 1–397.
- England, J., 1997. Unusual rates and patterns of Holocene emergence, Ellesmere Island, Arctic Canada. *Journal of the Geological Society* 154, 781–792.
- Feyling-Hanssen, R.W., Olsson, I.U., 1960. Five radiocarbon datings of post-glacial shorelines in central west Spitsbergen. *Norsk Polarinstitutt Meddelelser* 86, 122–131.
- Feyling-Hanssen, R.W., 1955. Stratigraphy of the marine late-Pleistocene of Billefjorden, Vestspitsbergen. *Norsk Polarinstitutt Skrifter* 107, 1–168.
- Feyling-Hanssen, R.W., 1965. Shoreline displacement in central Vestspitsbergen. *Norsk Polarinstitutt Meddelelser* 93, 1–5.
- Forman, S.L., Lubinski, D.J., Ingolfsson, O., Zeeberg, J.J., Snyder, J.A., Siegert, M.J., Matishov, G.G., 2004. A review of postglacial emergence on Svalbard, Franz Josef Land and Novaya Zemlya, northern Eurasia. *Quaternary Science Reviews* 23, 1391–1434.
- Forman, S.L., 1990. Postglacial relative sea-level history of northwestern Spitsbergen, Svalbard. *Geological Society of America Bulletin* 102, 1580–1590.
- Forwick, M., Vorren, T.O., 2010. Stratigraphy and deglaciation of the Isfjorden area, Spitsbergen. *Norwegian Journal of Geology* 90, 163–179.
- Hansell, D., Carlson, C. (Eds.), 2002. *Biogeochemistry of Marine Dissolved Organic Matter*. Elsevier Science, San Diego, p. 774.
- Hormes, A., Akcar, N., Kubik, P.W., 2011. Cosmogenic radionuclide dating indicates ice-sheet configuration during MIS 2 on Nordaustlandet, Svalbard. *Boreas* 40, 636–649.
- Kalish, J.M., Nydal, R., Nedreaas, K.H., Burr, G.S., Eine, G.L., 2001. A time history of pre- and post-bomb radiocarbon in the Barents Sea derived from Arcto-Norwegian cod otoliths. *Radiocarbon* 43, 843–855.
- Klys, P., Lindner, L., Makowska, A., Marks, L., Wysokiński, L., 1988. Late Quaternary glacial episodes and sea level changes in the northeastern Billefjorden region, Central Spitsbergen. *Acta Geologica Polonica* 38, 107–123.
- Lambeck, K., 1995. Constraints on the Late Weichselian ice-sheet over the Barents Sea from observations of raised shorelines. *Quaternary Science Reviews* 14, 1–16.
- Lambeck, K., 1996. Limits on the areal extent of the Barents Sea ice sheet in Late Weichselian time. *Global and Planetary Change* 12, 41–51.
- Landvik, J.Y., Bondevik, S., Elverhøi, A., Fjeldskaar, W., Mangerud, J., Salvigsen, O., Siegert, M.J., Svendsen, J.I., Vorren, T.O., 1998. The last glacial maximum of Svalbard and the Barents Sea area: ice sheet extent and configuration. *Quaternary Science Reviews* 17, 43–75.
- Levin, I., Kromer, B., 1997. Twenty years of atmospheric (CO<sub>2</sub>)-C-14 observations at Schauinsland station, Germany. *Radiocarbon* 39, 205–218.
- Lønne, I., Nemec, W., 2004. High-arctic fan delta recording deglaciation and environment disequilibrium. *Sedimentology* 51, 553–589.
- Mangerud, J., Svendsen, J.I., 1992. The last interglacial glacial period on Spitsbergen, Svalbard. *Quaternary Science Reviews* 11, 633–664.
- Mason, O.K., 2010. Beach ridge geomorphology at Cape Grinnell, northern Greenland: a less icy Arctic in the mid-Holocene. *Danish Journal of Geography* 110, 337–355.
- Mook, W.M., van der Plicht, J., 1999. Reporting <sup>14</sup>C activities and concentrations. *Radiocarbon* 41, 227–239.
- Reimer, P.J., Baillie, M.G.L., Bard, E., Bayliss, A., Beck, J.W., Bertrand, C.J.H., Blackwell, P.G., Buck, C.E., Burr, G.S., Cutler, K.B., Damon, P.E., Edwards, R.L., Fairbanks, R.G., Friedrich, M., Guilderson, T.P., Hogg, A.G., Hughen, K.A., Kromer, B., McCormac, F.G., Manning, S.W., Ramsey, C.B., Reimer, R.W., Remmele, S., Southon, J.R., Stuiver, M., Talamo, S., Taylor, F.W., van der Plicht, J., Weyhenmeyer, C.E., 2004. IntCal04 terrestrial radiocarbon age calibration, 26–0 ka BP. *Radiocarbon* 46, 1029–1058.
- Reimer, P.J., Baillie, M.G.L., Bard, E., Bayliss, A., Beck, J.W., Blackwell, P.G., Bronk Ramsey, C., Buck, C.E., Burr, G.S., Edwards, R.L., Friedrich, M., Grootes, P.M., Guilderson, T.P., Hajdas, I., Heaton, T.J., Hogg, A.G., Hughen, K.A., Kaiser, K.F., Kromer, B., McCormac, F.G., Manning, S.W., Reimer, R.W., Richards, D.A., Southon, J.R., Talamo, S., Turney, C.S.M., van der Plicht, J., Weyhenmeyer, C.E., 2009. Intcal09 and Marine09 radiocarbon age calibration curves, 0–50,000 years cal BP. *Radiocarbon* 51, 1111–1150.
- Salvigsen, O., 1978. Holocene emergence and finds of pumice, whale bones and driftwood at Svartknausflya, Nordaustlandet. *Norsk Polarinstitutt Arbok* 1977, 217–228.
- Salvigsen, O., 1981. Radiocarbon dated raised beaches in Kong Karls Land, Svalbard, and their consequences for the glacial history of the Barents Sea area. *Geografiska Annaler Series A-Physical Geography* 63, 283–291.
- Salvigsen, O., 1984. Occurrence of pumice on raised beaches and Holocene shoreline displacement in the inner Isfjorden area, Svalbard. *Polar Research* 2, 107–113.
- Schytt, V., Hoppe, G., Blake Jr., W., Grosz, M.G., 1968. The extent of the Würm glaciation in the European Arctic. *Association Internationale des Sciences Hydrologiques* 79, 207–216.
- Stankowski, W., Kasprzak, L., Kostrzewski, A., Rygielski, W., 1989. An outline of the morphogenesis of the region between Horbyedalen and Ebbadalen Petunia-bukta, Billefjorden, central Spitsbergen, Norway. *Polish Polar Research* 10, 267–276.





## Journal of Maps

Publication details, including instructions for authors and subscription information:

<http://www.tandfonline.com/loi/tjom20>

### Hørbyebreen polythermal glacial landsystem, Svalbard

David J.A. Evans<sup>a</sup>, Mateusz Strzelecki<sup>a b</sup>, David G. Milledge<sup>a</sup> & Chris Orton<sup>a</sup>

<sup>a</sup> Department of Geography, Durham University, South Road, Durham, DH1 3LE, UK

<sup>b</sup> Faculty of Geographical and Geological Sciences, Adam Mickiewicz University, Poznan, Poland

Available online: 24 May 2012

To cite this article: David J.A. Evans, Mateusz Strzelecki, David G. Milledge & Chris Orton (2012): Hørbyebreen polythermal glacial landsystem, Svalbard, Journal of Maps, DOI:10.1080/17445647.2012.680776

To link to this article: <http://dx.doi.org/10.1080/17445647.2012.680776>



PLEASE SCROLL DOWN FOR ARTICLE

Full terms and conditions of use: <http://www.tandfonline.com/page/terms-and-conditions>

This article may be used for research, teaching, and private study purposes. Any substantial or systematic reproduction, redistribution, reselling, loan, sub-licensing, systematic supply, or distribution in any form to anyone is expressly forbidden.

The publisher does not give any warranty express or implied or make any representation that the contents will be complete or accurate or up to date. The accuracy of any instructions, formulae, and drug doses should be independently verified with primary sources. The publisher shall not be liable for any loss, actions, claims, proceedings, demand, or costs or damages whatsoever or howsoever caused arising directly or indirectly in connection with or arising out of the use of this material.

## SCIENCE

### Hørbyebreen polythermal glacial landsystem, Svalbard

David J.A. Evans<sup>a\*</sup>, Mateusz Strzelecki<sup>a,b</sup>, David G. Milledge<sup>a</sup> and Chris Orton<sup>a</sup>

<sup>a</sup>Department of Geography, Durham University, South Road, Durham DH1 3LE, UK; <sup>b</sup>Faculty of Geographical and Geological Sciences, Adam Mickiewicz University, Poznan, Poland

(Received 2 November 2011; Resubmitted 12 March 2012; Accepted 14 March 2012)

A contoured surficial geology and geomorphology map of the forelands of the Hørbyebreen, Svenbreen and Ferdinandbreen valley glaciers in Petuniabukta, Svalbard was compiled from an orthophotograph based upon aerial photographs taken in 2009. The map reveals typical polythermal glacial landsystems, comprising ice-cored latero-frontal moraine arcs grading up valley into fluted till surfaces draped by supraglacially-derived longitudinal debris stripes. The additional occurrence on the Hørbyebreen foreland of linear esker and debris ridges arranged in a geometric ridge network is thought to be related to the infilling of densely spaced crevasses, created during a period of elevated meltwater pressures and ice hydrofracturing. These landforms were associated either with a *jökulhlaup* that was blocked by the frozen snout or an historical surge. The Hørbyebreen landform assemblage therefore constitutes an analogue for either: (1) spatial and temporal landsystem overprinting (polythermal and surging activity); or (2) a more refined polythermal landsystem in which the build up and release of meltwater reservoirs in warm-based interiors of polythermal glaciers give rise to a particularly diagnostic landform at the up-ice junction with the cold-based snout.

**Keywords:** glacial landsystem; polythermal glacier; geometric ridge network; ice hydrofracturing; Svalbard

## 1. Introduction

Hørbyebreen and the adjacent glaciers, Svenbreen and Ferdinandbreen are polythermal valley glaciers (Figure 1) located at 78°46'N at the north end of Petuniabukta, in central Svalbard, and have been the subject of previous geomorphological mapping by Karczewski et al. (1990). An early twentieth-century surge has been proposed for Hørbyebreen (Gibas, Rachlewicz, & Szczuciński, 2005; Karczewski, 1989) based upon looped medial moraines that are no longer visible, but otherwise the glaciers in the area have been in continuous recession since the end of the last Little Ice Age Type Event in the early twentieth century (Rachlewicz, Szczuciński, & Ewertowski, 2007). Such glaciological dynamics are typical for many Svalbard glacier snouts and therefore the landform–sediment associations that characterize the Hørbyebreen, Svenbreen and Ferdinandbreen forelands constitute an important modern landsystems analogue for palaeoglaciological reconstruction, not only for warm polythermal glaciers (*sensu* Pettersson, 2004) but also potentially for spatial and temporal landsystem overprinting. Contrasting aspects and radiation receipt in this mountainous terrain have resulted in more pronounced snout thinning on the east side of Hørbyebreen, creating an extensive subglacial landform assemblage that contrasts with the continuous glacier ice and ice-cored end moraine beneath the steep cliffs above the west margin. This has provided a window through to the glacier bed and additionally has recently exposed a network of eskers and associated rectilinear debris ridges, which record deposition in tunnels and fractures in the glacier snout and contrast with the landform assemblages at neighbouring Svenbreen and Ferdinandbreen. The origins and implications of such features in a polythermal glacier are most likely related to a period of hydrofracturing and possible surging activity, making the Hørbyebreen foreland an excellent location to test the concept of landsystem overprinting in Svalbard valley glaciers. The future development of the foreland geomorphology, due largely to ice melt-out, can be quantified through the construction of repeat mapping based upon new aerial photography and utilization of existing

\*Corresponding author. Email: [D.J.A.Evans@durham.ac.uk](mailto:D.J.A.Evans@durham.ac.uk)





Figure 1. Overview of the forelands of Hørbyebreen and Svenbreen from the southwest.

ground survey control initiated for this project (e.g. [Bennett & Evans, in press](#); [Bennett et al., 2010](#); [Schomacker, 2008](#); [Schomacker & Kjær, 2008](#)).

## 2. Map compilation

The Petuniabukta glacier forefields map ([Main Map](#)) was compiled from an orthophotograph constructed from aerial photographs taken by the Norwegian Polar Institute (NPI) on 27 July and 11 August 2009. Images were taken with an UltraCam Xp Large Format Digital Aerial Camera manufactured by Vexcel. In advance of the NPI flights, a network of reference markers ( $2 \times 3$  m white geofibre rectangles) were positioned in the field on suitable, highly visible natural features such as large rocks and rocky outcrops and surveyed with a Leica 1200 Differential Global Positioning Station to improve the precision of the constructed orthophotograph. In addition, 25 further ground control points (massive boulders) were surveyed across the Hørbyebreen proglacial zone in the summer of 2010. The orthophotograph and digital terrain model (DTM) were created in Leica Photogrammetry Suite 2010 by ERDAS and associated contours were extracted digitally from the DTM using ESRI ArcGIS 9.3. Each set of photographs was processed as for a digital camera. The projection used was UTM, with the spheroid WGS 84 for zone 33N.

The proglacial landforms and surficial geology were mapped onto a coloured ink film overlay. Interpretations of surface materials and landforms were made by a combined approach involving stereoscopic mapping directly from the aerial photographs and a reconnaissance level of ground truth fieldwork, undertaken during the summer of 2010.

The map overlay containing the base data was manually digitized on a large format CalComp tablet digitizer using MapData vector digitizing software. The digitized vector files for the base data were converted from MapData format into ArcInfo 'generate' format for importing into Adobe Illustrator, utilizing the Avenza MAPublisher plug-in software to produce a fully editable and structured map file. Final design and production was undertaken in Adobe Illustrator CS5. The raster image used for the glacier surface was created by manipulating the panchromatic orthophotograph in Adobe Photoshop to create the colourized image. Because of the steep mountainous topography, the image reveals areas of shadow, which have been contrast adjusted in order to minimize their impact on the glacier surface features. The digital map needs to be printed on an A0 sheet in order to reproduce the 1:10,000 scale.

## 3. Sediment–landform associations

### 3.1. Surficial geology

There are seven surficial geology units in addition to areas of bedrock and glacier ice. Upland areas and steep valley sides are dominated by bedrock, residuum or weathered bedrock, and paraglacial deposits related to slope processes on recently abandoned glacial features. Additionally, a large rock glacier lies at the base of the steep rock wall on the south margin of the Hørbyebreen forefield; this feature could be either a talus-derived rock glacier or, more likely given its location, a rock-glacierized lateral moraine (cf. [Evans, 1993](#); [Humlum, 1982](#); [Vere & Matthews, 1985](#)). Glacifluvial deposits or complex braidplains predominantly occur as proglacial

outwash fans (sandar), which coalesce to form a 2.2 km wide outwash plain beyond the Little Ice Age ice-cored moraine belts; they also form short ribbon sandar in corridors that have been incised through the ice-cored moraine belts and the subglacial landforms located up valley. Glacimarine sediments of varying thickness lie below the local marine limit of 80 m a.s.l., but only where they have survived reworking by proglacial outwash. Their thin character is best illustrated to the north of the outwash plain where bedrock lineations protrude through the glacimarine veneer. Glacigenic deposits indicative of complete melt-out of buried glacier ice are classified very generally as ‘till and supraglacially-derived debris mounds’. These surfaces may be adorned by flutings, moraine ridges, eskers and crevasse fills, which are discussed in more detail below. Finally, the most significant glacial geomorphological assemblage on the forelands of the Petuniabukta glaciers is the ‘ice-cored moraine’. This forms a high relief latero-frontal moraine arc around each glacier snout and marks the limit of the Little Ice Age advance in the area. It is characterized by controlled moraine (*sensu* Evans, 2009), longitudinal foliae/medial moraines and geometric ridge networks interpreted as crevasse fills and associated eskers (Figures 2–6).

Specific sediment–landform assemblages are instructive in terms of spatial and temporal glacial foreland evolution. They are, therefore, now described and analysed in turn.

### 3.2. Glacial lineations (longitudinal foliae and flutings)

Both the glacier surface and the subglacial till, freshly exposed by glacier thinning, are strongly lineated (Figures 2, 3, 7). The subglacial lineations are less well developed and constitute flutings produced at the ice-bed interface, and thereby indicative of warm-based conditions inside the ice-cored moraine arc. The more prominent supraglacial lineations are longitudinal debris stripes typical of most Svalbard glaciers and explained by Hambrey and Glasser (2003) as englacial debris bands subject to transpression where ice flows from several cirque basins into a major valley. Downwasting of clean ice rather than snout recession has resulted in the emergence of fluted till patches on high points of the bed through the lineated glacier surface (Figure 7). This superimposition and/or juxtaposition of supraglacially-derived debris stripes and subglacial flutings have been reported previously from Svalbard glacier forelands by Glasser and Hambrey (2003).

### 3.3. Ice-cored and controlled moraine

The historical (Little Ice Age) maximum limits of Hørbyebreen and neighbouring glaciers are clearly marked by latero-frontal moraine arcs comprising linear hummocky terrain and more continuous linear ice-cored, transverse ridges or ‘controlled moraine’ (*sensu* Evans, 2009; Figures 3, 5, 6, 8). Melting ice cores are manifest in numerous kettle holes, retrogressive flows and hollows bordered by tension cracks (e.g. Lukas, Nicholson, Ross, & Humlum, 2005; Lyså & Lønne, 2001). Although relief is locally significant (>20 m), areas of advanced melt-out are apparent as low-amplitude, rubble-covered undulations and are mapped separately as ‘till and supraglacially-derived

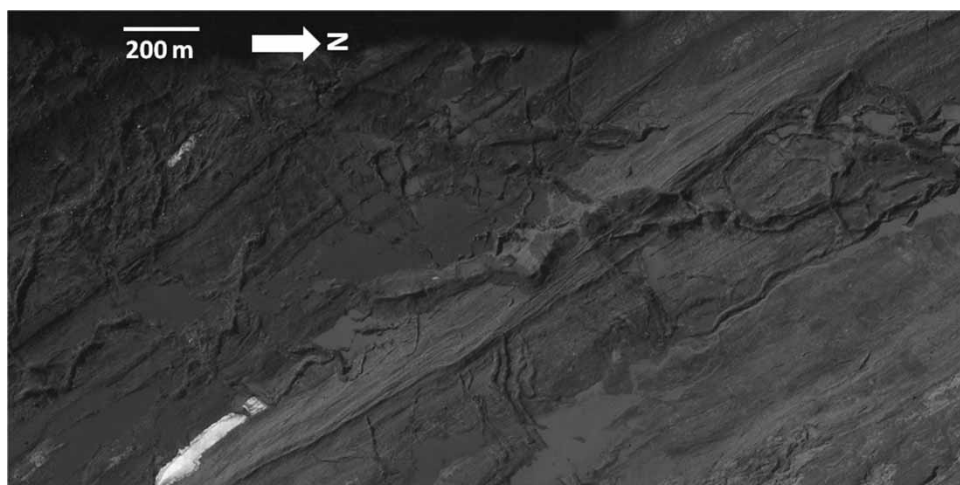


Figure 2. Aerial photograph extract (2009) of geometric ridge network and sinuous ridges emerging through linear debris stripes on the west margin of Hørbyebreen snout, representing esker construction in major tunnels and adjacent crevasses. Centre of image is at 531750/874150.

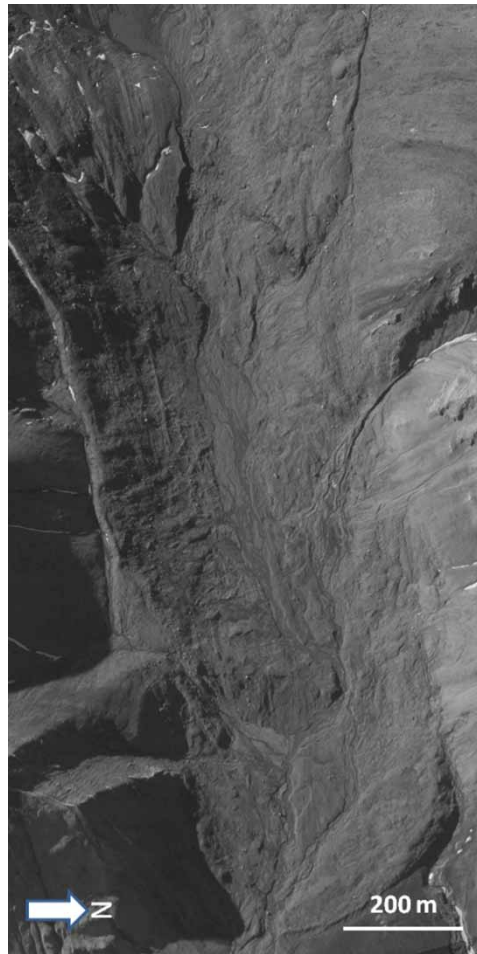


Figure 3. Aerial photograph extract (2009) of the ice-cored latero-frontal moraine arc of Ferdinandbreen. Areas of strongly fluted terrain occur on the foreland and linear debris stripes occur in juxtaposition with crevasse fills ridges in the ice-cored moraine. Centre of image is at 530200/873800.

debris mounds relating to complete melt-out of ice-cored moraine'. The ice-cored latero-frontal moraine arcs have been termed 'moraine-mound complexes' by [Hambrey, Huddart, Bennett, and Glasser \(1997\)](#) and [Bennett, Hambrey, Huddart, and Glasser \(1998\)](#), who relate them to englacial debris transfer along thrusts in the glacier snout. The thrusting concept has remained controversial (cf. [Glasser, Hambrey, Bennett, & Huddart, 2003](#); [Woodward, Murray, & McCaig, 2002, 2003](#)) but regardless of its efficacy in the transfer of debris, a variety of processes, in addition to thrusting, are likely responsible for the production of the remarkable debris-rich ice and controlled moraine around polythermal glacier snouts ([Evans, 2009](#); [Glasser & Hambrey, 2003](#); [Lukas et al., 2005](#); [Sletten, Lyså, & Lønne, 2001](#)).

### 3.4. *Eskers and crevasse fills*

Eskers on the Petuniabukta glacier forelands can be classified into three sub-types: (1) linear esker ridges; (2) sinuous eskers; and (3) localized engorged eskers (Figures 2, 4–8). The former are concentrated on the west side of the snout, are associated with ice-flow transverse and rectilinear debris ridges, and often branch off from major sinuous eskers. Because the linear esker and debris ridges form a rectilinear, cross-cutting pattern with a small range in orientations, it is considered most likely that they were deposited in crevasses created during the surge of the snout reported by [Karczewski \(1989\)](#) and [Gibas et al. \(2005\)](#). This implies compatibility with zig-zag eskers and crevasse-squeeze ridges typical of surging glacier geomorphology ([Evans & Rea, 2003](#); [Rea & Evans, 2011](#); [Sharp, 1985](#)), although the transverse debris ridges at Hørbyebreen have been interpreted as englacial thrust features by [Szuman and Kasprzak \(2010\)](#); cf. [Bennett et al., 1998](#); [Hambrey et al., 1997](#)).



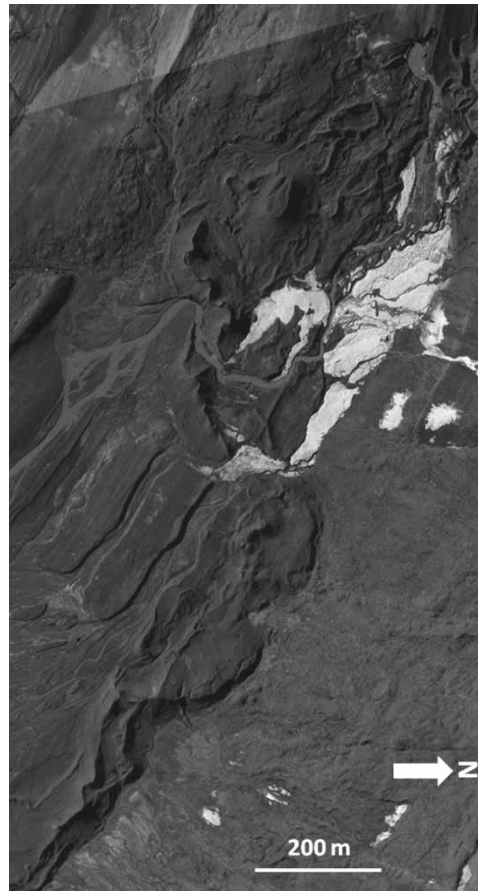


Figure 4. Aerial photograph extract (2009) of the main esker drainage network on the east side of the Hørbyebeen snout, concentrating on the present glacier margin (top) and the occurrence of a braided esker system at the glacier margin which grades down-valley into a simple, single ridge esker. More localized linear ridge segments document crevasse infill due to melt-water leakage from esker tunnels. Centre of image is at 530200/874300.

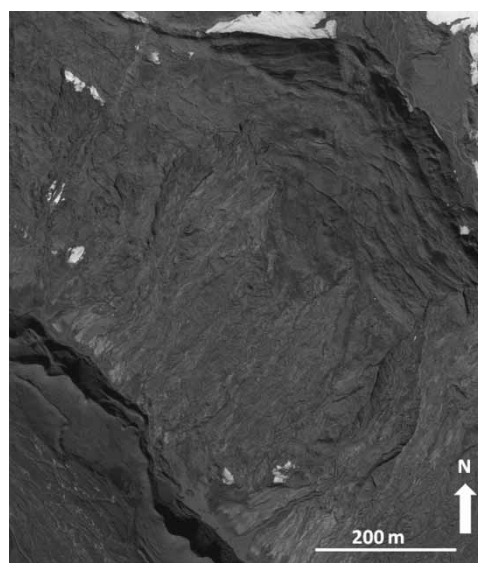


Figure 5. Aerial photograph extract (2009) of the ice-cored moraine belt on the east side of Hørbyebeen, showing controlled ridges and melt-out hollows at the top of the image grading into areas of tension cracks and retrogressive flows on the lower slopes. The main esker ridge of the east margin is visible at the bottom of the image. Centre of image is at 531000/874300.

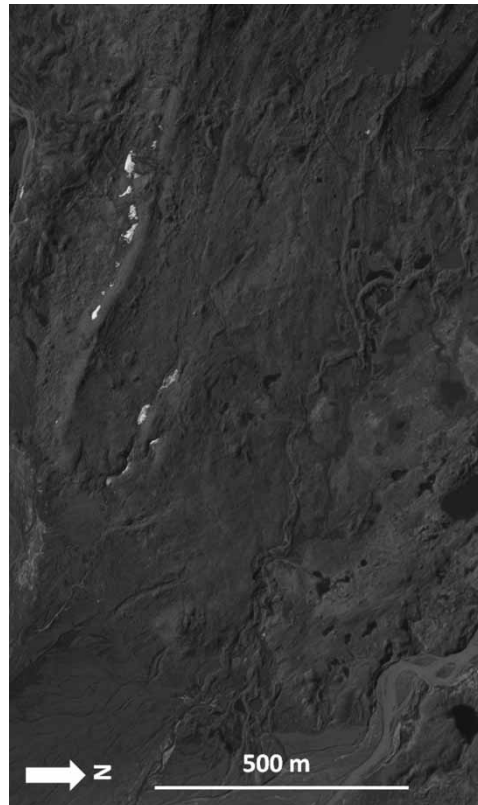


Figure 6. Aerial photograph extract (2009) of controlled ridges, eskers and crevasse fill ridges on the outer ice-cored moraine of Hørbyebreen, where melt-out is at an advanced stage. The prominent ridge towards the left of the image is the former medial moraine between Hørbyebreen and Svenbreen; therefore the eskers at the top left of the image are from Svenbreen drainage. Centre of image is at 531250/874050.

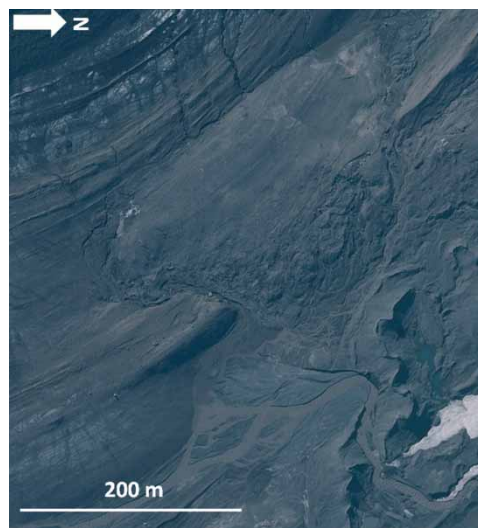


Figure 7. Aerial photograph extract (2009) of fluted subglacial till surface emerging from the downwasting snout of Hørbyebreen. Note that the subglacial flutings are less prominent than the strong lineation created by supraglacial debris stripes. Eskers are emerging from the more contracted margin of the east side of the snout at the top right of the image. Centre of image is at 529800/874280.

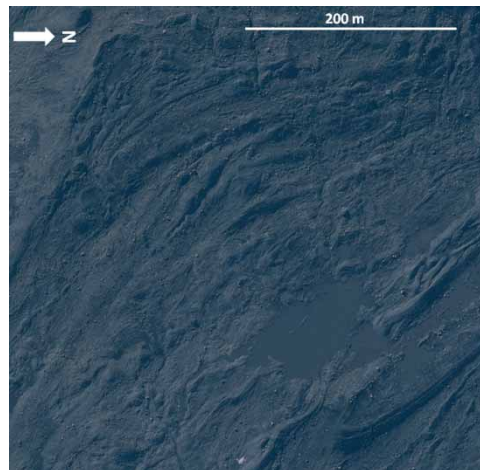


Figure 8. Aerial photograph extract (2009) of the controlled moraine and supraglacial debris stripes on the SW margin of the Hørbyebreen foreland. Esker ridges also occur at the bottom of the image and lie just inside the medial moraine (dark coloured prominent ridge complex) between the main Hørbyebreen trunk ice and the ice debouching from two unnamed cirque glaciers on the west margin of the valley. Centre of image is at 530500/874050.

The branching of linear eskers from a prominent large sinuous esker network indicates that a regular subglacial drainage system was in operation when meltwater and sediment was siphoned off to adjacent crevasses. This suggests a phase of elevated discharge and diversion of meltwater and sediment into the crevasses created by an increasingly fractured snout. Some of the linear esker ridges, as well as some debris ridges, could represent hydrofracture fills similar to those produced during dewatering of the snout of Skeiðararjökull during the *jökulhlaup* of 1996, as described by [Roberts, Russell, Tweed, and Knudsen \(2000, 2001\)](#) and [Bennett, Huddart, and Waller \(2000\)](#). The linear esker and debris ridge assemblages on the Hørbyebreen foreland resemble the ‘geometrical ridge networks’ of [Bennett, Hambrey, Huddart, and Ghienne \(1996\)](#), which are interpreted as super-imposed longitudinal and transverse debris accumulations produced by separate processes but appearing to be cross-cut after melt-out. This explanation does not appear to be applicable to the Hørbyebreen examples, because the linear debris ridges do not parallel the longitudinal debris stripes melting out of the enclosing ice.

Engorged eskers are very short (<50 m long), sinuous ridges presently developing in tunnels in the ice-cored moraine and orientated at right angles to valley slope due to the gravity-driven drainage of water melting from the buried ice. Such features are common in ice-cored moraine arcs on the forelands of both polythermal and surging glaciers ([Evans, Twigg, Rea, & Orton, 2009a](#); [Evans, Twigg, & Orton, 2010](#)) but have been only rarely identified in the ancient landform record where they are often termed ‘valley eskers’ (e.g. [Bird, 1967](#); [Mannerfelt, 1945](#)). Further research on these landforms is warranted, especially as they appear to be closely associated with, and therefore potentially diagnostic of, debris-rich glacier snouts in valley settings.

#### 4. Glacial landsystem classification

Recent identification of modern glacial landsystem analogues for palaeoglaciological reconstruction has demonstrated that dominant landform–sediment assemblages indicative of specific styles of glaciation (e.g. ice stream, surge-type, active temperate, plateau icefield, etc.; [Benn & Evans, 2010](#); [Evans, 2003, 2006, 2007](#)) often contain sub-ordinate landsystem signatures (e.g. sporadic surging during active temperate recession; [Evans & Twigg, 2002](#)) or are overprinted or sequentially replaced (‘intrazonal landsystem change’; [Evans, in press](#)) due to spatial and/or temporal changes in glacier dynamics (e.g. [Evans, 2011](#); [Evans et al., 2010](#); [Krüger, 1994](#)). Such overprinting and intrazonal change has been identified also in ancient glacial landform records (e.g. [Benn, Kirkbride, Owen, & Brazier, 2003](#); [Colgan, Mickelson, & Cutler, 2003](#); [Dyke, Morris, Green, & England, 1992](#); [Evans, 2009](#); [Evans, Clark, & Rea, 2008](#); [Evans, Livingstone, Vieli, & Ó Cofaigh, 2009b](#); [Livingstone, Ó Cofaigh, & Evans, 2008](#); [Ó Cofaigh, Evans, & Smith, 2010](#); [Wilson & Evans, 2000](#)), demonstrating that landsystems have the potential to inform our reconstructions of the complexities of temporal and spatial evolution of ice sheets and glaciers. The landforms on modern Svalbard glacier forelands have been used, somewhat controversially, as analogues for polythermal palaeoglaciers in locations such as upland Britain during the Younger Dryas (cf. [Bennett et al., 1998](#); [Evans, 2009](#); [Graham & Midgley, 2000](#); [Graham, Bennett,](#)

Glasser, Hambrey, Huddart, & Midgley, 2007; Hambrey et al., 1997; Lukas, 2005, 2007; Wilson & Evans, 2000), although the controversy is centred more on the process of debris entrainment than on the landsystem signature of polythermal glaciation. The latter is particularly consistently well developed on Svalbard (Glasser & Hambrey, 2003), but the other prominent style of glacier behaviour on the archipelago, that of surging, gives rise to a very conspicuous landsystem of its own, especially in tidewater systems (e.g. Bennett et al., 1996; Glasser, Hambrey, Crawford, Bennett, & Huddart, 1998; Kristensen, Benn, Hormes, A., & Ottesen, 2009; Ottesen & Dowdeswell, 2006; Ottesen et al., 2008). The impact of surging on landform development in the polythermal valley and extended cirque glaciers may be more difficult to decipher; it likely accounts for at least some of the great complexity in debris entrainment patterns observed in the receding snouts over the last few decades. Short timescale changes in the dynamics of Svalbard valley glaciers have been identified by Glasser and Hambrey (2001) and Hambrey et al. (2005), verifying that landsystem overprinting and intrazonal change may well be a characteristic of these glacial systems.

#### 4.1. *Polythermal glacial landsystem*

Former glacier beds characterized by well-developed subglacial bedforms, such as flutings and eskers, lying up-valley from controlled moraine or ice-cored moraines, have been widely used to infer the existence of temperate or warm-based conditions giving way to a frozen snout zone (Dyke & Evans, 2003; Dyke & Saville, 2000; Evans, 2009, 2011; Evans, Twigg, & Shand, 2006; Evans et al., 2010; Glasser & Hambrey, 2001, 2003; Hambrey, Bennett, Dowdeswell, Glasser, & Huddart, 1999). Such polythermal conditions are common in Svalbard glaciers and give rise to the typical landform assemblage seen of the forelands of Hørbyebreen, Svenbreen and Ferdinandbreen, where large volumes of debris have been frozen on at the warm–cold-based transition zone in the glacier snout. However, the fast flow and accelerated rates of sub-marginal debris entrainment proposed for surging glaciers (Clapperton, 1975; Humphrey & Raymond, 1994; Sharp, Jouzel, Hubbard, & Lawson 1994), could potentially give rise to a similar landsystem signature. Therefore it is important that we begin to develop a conceptual landsystems model for the intermittently surging polythermal glaciers of Svalbard. Similar historical changes in glacier dynamics have been recognized in the landsystem signatures of some Icelandic glaciers; particularly pertinent in this respect is the foreland of Satujökull, on the northern margin of Hofsjökull (Evans, 2011; Evans et al., 2010), where ice-cored moraine arcs and flutings indicative of Little Ice Age advance limits lie beyond two inset sequences of surge-related landforms. A non-surge origin for the ice-cored moraine in such settings is inferred, because the constituent debris is emerging as controlled moraine ridges fed directly by extensive, snout-wide debris-rich foliae that resemble regelation ice. Nevertheless, similar marginal accumulations of debris have been associated with surging by Hambrey, Dowdeswell, Murray, and Porter (1996), Murray, Gooch, and Stuart (1997) and Glasser et al. (1998).

#### 4.2. *Surge signatures*

Diagnostic geomorphological criteria for former glacier surging are summarized in the surge-type glacier landsystem by Evans and Rea (2003). Few of these criteria are visible at Hørbyebreen, being potentially present in the linear esker ridges and crevasse fill landforms, which record deposition into a rectilinear pattern of ice fractures. In the surge landsystem, the emplacement of sediments into crevasse networks is manifest as zig-zag eskers and basal crevasse-squeeze ridges, whose orientations conform to the fracture patterns created in the glacier snout during its surge phase (Rea & Evans, 2011). However, the lack of distortion of the longitudinal debris stripes and their apparent dominance over the transverse ridges, is incompatible with a former surge, because flow lineations of this sort would have been compressed to produce ‘looped medial moraines’. Additionally, the transverse ridges do not cross cut the longitudinal debris stripes, but are emerging instead from areas of lower relief on the downwasting snout, indicating that they were emplaced in the basal ice facies and their enclosing crevasses did not extend to the glacier surface. This pattern of emplacement and its implications for the lack of full depth crevassing, suggest that the emplacement of the transverse ridges could have been by hydrofracture networks induced by elevated meltwater pressures and the overwhelming of the normal englacial and subglacial drainage tunnels. This could have taken place in the absence of a surge, as documented at Skeiðarárjökull during the 1996 *jökulhlaup* (Bennett et al., 2000; Roberts et al., 2000, 2001), whereby a catastrophic subglacial drainage event initiated in the warm-based part of the glacier was blocked by the frozen toe of the snout and forced to escape along pre-existing fractures in the ice. Whether or not this was related to the surge of Hørbyebreen reported by Karczewski (1989) and Gibas et al. (2005) is unknown.

## 5. Conclusions

The surficial geology and geomorphology map of the forefields of the Hørbyebreen, Svenbreen and Ferdinandbreen polythermal valley glaciers reveals a glacial landsystem comprising ice-cored latero-frontal moraine arcs, constructed during the Little Ice Age maximum, that grade up-valley into fluted till surfaces draped by supraglacially-derived longitudinal debris stripes. Such landform associations have been widely associated with polythermal glacier characteristics, but on the Hørbyebreen foreland the additional occurrence of linear eskers and debris ridges arranged in a geometric ridge network are thought to be related to the infilling of densely spaced crevasses, created during a period of elevated meltwater pressures and ice hydrofracturing. A smaller area of such forms occurs also on the Svenbreen foreland. Whether these were associated with a *jökulhlaup* that was blocked by the frozen snout or with an historical surge is unknown, but nonetheless, the landform assemblage depicted in our map constitutes an important modern landsystems analogue for palaeoglaciological reconstruction. In this respect, it is an analogue for either: (1) spatial and temporal landsystem overprinting (polythermal and surging activity); or (2) a more refined polythermal landsystem in which the build up and release of meltwater reservoirs in warm-based interiors of polythermal glaciers give rise to a particularly diagnostic landform at the up-ice junction with the cold-based snout. This is of course not entirely unrelated to surge initiation mechanisms.

## Acknowledgements

This research was partially funded by the Ministry of Science and Higher Education in Poland (Grant NN306 284335). Funds for M.S. were also provided by Crescendum Est-Polonia Foundation and AMU Foundation. Harald Faste Aas from the Norwegian Polar Institute helped us to obtain the aerial photographs. Thanks to Anders Schomacker, Tim Fisher and Bernd Etzelmüller for helpful reviewers' comments.

## References

- Benn, D.I., & Evans, D.J.A. (2010). *Glaciers and glaciation* (2nd ed.). London: Hodder.
- Benn, D.I., Kirkbride, M.P., Owen, L.A., & Brazier, V. (2003). Glaciated valley landsystems. In D.J.A. Evans, (Ed.), *Glacial landsystems* (pp. 372–406). London: Arnold.
- Bennett, G.L., & Evans, D.J.A. (in press). Glacier retreat and landform production on an overdeepened glacier foreland: The debris-charged glacial landsystem at Kviárjökull, Iceland. *Earth Surface Processes and Landforms*.
- Bennett, G.L., Evans, D.J.A., Carbonneau, P., & Twigg, D.R. (2010). Evolution of a debris-charged glacier landsystem, Kviárjökull, Iceland. *Journal of Maps*, 2010, 40–76.
- Bennett, M.R., Hambrey, M.J., Huddart, D., & Ghienne, J.F. (1996). The formation of a geometrical ridge network by the surge-type glacier Kongsvegen, Svalbard. *Journal of Quaternary Science*, 11, 437–449.
- Bennett, M.R., Hambrey, M.J., Huddart, D., & Glasser, N.F. (1998). Glacial thrusting and moraine-mound formation in Svalbard and Britain: The example of Coire a' Cheud chnoic (Valley of a hundred hills), Torridon, Scotland. *Quaternary Proceedings*, 6, 17–34.
- Bennett, M.R., Huddart, D., & Waller, R.I. (2000). Glaciofluvial crevasse and conduit fills as indicators of supraglacial dewatering during a surge, Skeiðarárjökull, Iceland. *Journal of Glaciology*, 46, 25–34.
- Bird, J.B. (1967). *The physiography of Arctic Canada*. Baltimore, MD: Johns Hopkins University Press.
- Clapperton, C.M. (1975). The debris content of surging glaciers in Svalbard and Iceland. *Journal of Glaciology*, 14, 395–406.
- Colgan, P.M., Mickelson, D.M., & Cutler, P.M. (2003). Ice-marginal terrestrial landsystems: Southern Laurentide Ice Sheet margin. In D.J.A. Evans, (Ed.), *Glacial Landsystems* (pp. 111–142). London: Arnold.
- Dyke, A.S., & Evans, D.J.A. (2003). Ice-marginal terrestrial landsystems: Northern Laurentide and Innuite ice sheet margins. In D.J.A. Evans, (Ed.), *Glacial landsystems* (pp. 143–165). London: Arnold.
- Dyke, A.S., Morris, T.F., Green, D.E.C., & England, J. (1992). Quaternary geology of Prince of Wales Island, arctic Canada. *Geological Survey of Canada Memoir*, 433, 1–142.
- Dyke, A.S., & Savelle, J.M. (2000). Major end moraines of Younger Dryas age on Wollaston Peninsula, Victoria Island, Canadian arctic: Implications for palaeoclimate and for formation of hummocky moraine. *Canadian Journal of Earth Sciences* 37 (pp. 601–619).
- Evans, D.J.A. (1993). High latitude rock glaciers: a case study of forms and processes in the Canadian arctic. *Permafrost and Periglacial Processes*, 4, 17–35.
- Evans, D.J.A. (Ed.). (2003). *Glacial landsystems*. London: Edward Arnold.
- Evans, D.J.A. (2006). Glacial landsystems. In P.G. Knight (Ed.), *Glacier science and environmental change* (pp. 83–88). Oxford: Blackwell.
- Evans, D.J.A. (2007). Glacial landsystems. In S.A. Elias, (Ed.), *Encyclopedia of quaternary science* (pp. 808–818). Amsterdam: Elsevier.
- Evans, D.J.A. (2009). Controlled moraines: Origins, characteristics and paleoglaciological implications. *Quaternary Science Reviews*, 28, 183–208.



- Evans, D.J.A. (2011). Glacial landsystems of Satujökull, Iceland: A modern analogue for glacial landsystem overprinting by mountain icecaps. *Geomorphology* (Vol. 129, pp. 225–237).
- Evans, D.J.A. (in press). The glacial and periglacial research – Geomorphology and retreating glaciers. In J. Harbor & R. Giardino (Eds.), *Treatise on geomorphology*. Amsterdam: Elsevier.
- Evans, D.J.A., Clark, C.D., & Rea, B.R. (2008). Landform and sediment imprints of fast glacier flow in the southwest Laurentide Ice Sheet. *Journal of Quaternary Science*, 23, 249–272.
- Evans, D.J.A., Livingstone, S.J., Vieli, A., & Ó Cofaigh, C. (2009b). The palaeoglaciology of the central sector of the British and Irish Ice Sheet: Reconciling glacial geomorphology and preliminary ice sheet modelling. *Quaternary Science Reviews*, 28, 735–757.
- Evans, D.J.A., & Rea, B.R. (2003). Surging glacier landsystem. In D.J.A. Evans, (Ed.), *Glacial landsystems* (pp. 259–288). London: Arnold.
- Evans, D.J.A., & Twigg, D.R. (2002). The active temperate glacial landsystem: A model based on Breiðamerkurjökull and Fjallsjökull, Iceland. *Quaternary Science Reviews*, 21, 2143–2177.
- Evans, D.J.A., Twigg, D.R., & Orton, C. (2010). Satujökull glacial landsystem, Iceland. *Journal of Maps*, 2010, 639–650.
- Evans, D.J.A., Twigg, D.R., Rea, B.R., & Orton, C. (2009a). Surging glacier landsystem of Tungnaárjökull, Iceland. *Journal of Maps*, 2009, 134–151.
- Evans, D.J.A., Twigg, D.R., & Shand, M. (2006). Surficial geology and geomorphology of the Þórisjökull plateau icefield, west-central Iceland. *Journal of Maps*, 2006, 17–29.
- Gibas, J., Rachlewicz, G., & Szczuciński, W. (2005). Application of DC resistivity sounding and geomorphological surveys in studies of modern Arctic glacier marginal zones, Petuniabukta, Spitsbergen. *Polish Polar Research*, 26, 239–258.
- Glasser, N.F., & Hambrey, M.J. (2001). Styles of sedimentation beneath Svalbard valley glaciers under changing dynamic and thermal regimes. *Journal of the Geological Society, London*, 158, 697–707.
- Glasser, N.F., & Hambrey, M.J. (2003). Ice-marginal terrestrial landsystems: Svalbard polythermal glaciers. In D.J.A. Evans, (Ed.), *Glacial landsystems* (pp. 65–88). London: Arnold.
- Glasser, N.F., Hambrey, M.J., Bennett, M.R., & Huddart, D. (2003). Comment: Formation and reorientation of structure in the surge-type glacier Kongsvegen, Svalbard. *Journal of Quaternary Science*, 18, 95–97.
- Glasser, N.F., Hambrey, M.J., Crawford, K.R., Bennett, M.R., & Huddart, D. (1998). The structural glaciology of Kongsvegen, Svalbard and its role in landform genesis. *Journal of Glaciology*, 44, 136–148.
- Graham, D.J., Bennett, M.R., Glasser, N.F., Hambrey, M.J., Huddart, D., & Midgley, N.G. (2007). ‘A test of the englacial thrusting hypothesis of “hummocky” moraine formation: case studies from the northwest Highlands, Scotland’: Comments. *Boreas*, 36, 103–107.
- Graham, D.J., & Midgley, N. (2000). Moraine–mound formation by englacial thrusting: The Younger Dryas moraines of Cwm Idwal, North Wales. In A.J. Maltman, B. Hubbard, & M.J. Hambrey (Eds.), *Deformation of glacial materials*, (Special Publication No. 176, pp. 321–336). London: Geological Society of London.
- Hambrey, M.J., Bennett, M.R., Dowdeswell, J.A., Glasser, N.F., & Huddart, D. (1999). Debris entrainment and transfer in polythermal valley glaciers. *Journal of Glaciology*, 45, 69–86.
- Hambrey, M.J., Dowdeswell, J.A., Murray, T., & Porter, P.R. (1996). Thrusting and debris entrainment in a surging glacier: Bakaninbreen, Svalbard. *Annals of Glaciology*, 22, 241–248.
- Hambrey, M.J., & Glasser, N.F. (2003). The role of folding and foliation development in the genesis of medial moraines: Examples from Svalbard glaciers. *Journal of Geology*, 111, 471–485.
- Hambrey, M.J., Huddart, D., Bennett, M.R., & Glasser, N.F. (1997). Genesis of hummocky moraines by thrusting of glacier ice: Evidence from Svalbard and Britain. *Journal of the Geological Society of London*, 154, 623–632.
- Hambrey, M.J., Murray, T., Glasser, N.F., Hubbard, A., Hubbard, B., Stuart, G., et al. (2005). Structure and changing dynamics of a polythermal valley glacier on a centennial timescale: Midre Lovenbreen, Svalbard. *Journal of Geophysical Research*, 110. DOI:10.1029/2004JF000128.
- Humlum, O. (1982). Rock glacier types on Disko, central west Greenland. *Norsk Geografisk Tidsskrift*, 82, 59–66.
- Humphrey, N.F., & Raymond, C.F. (1994). Hydrology, erosion and sediment production in a surging glacier: Variegated Glacier, Alaska, 1982–83. *Journal of Glaciology*, 40, 539–552.
- Karczewski, A. (1989). The development of the marginal zone of the Hørbyebreen, Petuniabukta, central Spitsbergen. *Polish Polar Research*, 10, 371–377.
- Karczewski, A., Borówka, M., Gonera, P., Kasprzak, L., Kłysz, P., Kostrzewski, A., et al. (1990). *Geomorphology – Petuniabukta, Billefjorden, Spitsbergen, 1:40 000*, Poznań, Poland: Uniwersytet im. A. Mickiewicza.
- Kristensen, L., Benn, D.I., Holmes, A., & Ottesen, D. (2009). Mud aprons in front of Svalbard surge moraines: Evidence of subglacial deforming layers or proglacial tectonics? *Geomorphology*, 111, 206–221.
- Krüger, J. (1994). Glacial processes, sediments, landforms and stratigraphy in the terminus region of Mýrdalsjökull, Iceland. *Folia Geographica Danica*, 21, 1–233.
- Livingstone, S.J., Ó Cofaigh, C., & Evans, D.J.A. (2008). Glacial geomorphology of the central sector of the last British-Irish Ice Sheet. *Journal of Maps*, 2008, 358–377.
- Lyså, A., & Lønne, I. (2001). Moraine development at a small High-Arctic valley glacier: Rieperbreen, Svalbard. *Journal of Quaternary Science*, 16, 519–529.
- Lukas, S. (2005). A test of the englacial thrusting hypothesis of ‘hummocky’ moraine formation: Case studies from the northwest Highlands, Scotland. *Boreas*, 34, 287–307.
- Lukas, S. (2007). ‘A test of the englacial thrusting hypothesis of “hummocky” moraine formation: Case studies from the northwest Highlands, Scotland’: reply to comments. *Boreas*, 36, 108–113.

- Lukas, S., Nicholson, L.I., Ross, F.H., & Humlum, O. (2005). Formation, meltout processes and landscape alteration of High-Arctic ice-cored moraines: Examples from Nordenskiöld Land, Central Spitsbergen. *Polar Geography*, 29, 157–187.
- Mannerfelt, C.M. (1945). Några glacialmorfologiska formelement. *Geografiska Annaler*, 27, 1–239.
- Murray, T., Gooch, D.L., & Stuart, G.W. (1997). Structures within the surge front of Bakaninbreen using ground penetrating radar. *Annals of Glaciology*, 24, 122–129.
- Ó Cofaigh, C., Evans, D.J.A., & Smith, I.R. (2010). Large-scale reorganization and sedimentation of terrestrial ice streams during late Wisconsinan Laurentide Ice Sheet deglaciation. *Geological Society of America Bulletin*, 122, 743–756.
- Ottesen, D., & Dowdeswell, J.A. (2006). Assemblages of submarine landforms produced by tidewater glaciers in Svalbard. *Journal of Geophysical Research*, 111. DOI:10.1029/2005JF000330.
- Ottesen, D., Dowdeswell, J.A., Benn, D.I., Kristensen, L., Christiansen, H.H., Christensen, O., . . . , Vorren, T.O. (2008). Submarine landforms characteristic of glacier surges in two Spitsbergen fjords. *Quaternary Science Reviews*, 27, 1583–1599.
- Pettersson, R. (2004). *Dynamics of the cold surface layer of polythermal Storglaciären, Sweden*. Unpublished PhD thesis, Department of Physical Geography and Quaternary Geology, Stockholm University.
- Rachlewicz, G., Szczuciński, W., & Ewertowski, M. (2007). Post-‘Little Ice Age’ retreat rate of glaciers around Billefjorden in central Spitsbergen, Svalbard. *Polish Polar Research*, 28, 159–186.
- Rea, B.R., & Evans, D.J.A. (2011). An assessment of surge-induced crevassing and the formation of crevasse squeeze ridges. *Journal of Geophysical Research*, 116. F04005, DOI:10.1029/2011JF001970.
- Roberts, M.J., Russell, A.J., Tweed, F.S., & Knudsen, Ó. (2000). Ice fracturing during jökulhlaups: Implications for englacial floodwater routing and outlet development. *Earth Surface Processes and Landforms*, 25, 1429–46.
- Roberts, M.J., Russell, A.J., Tweed, F.S., & Knudsen, Ó. (2001). Controls on englacial sediment deposition during the November 1996 jökulhlaup, Skeiðarárjökull, Iceland. *Earth Surface Processes and Landforms*, 26, 935–952.
- Schomacker, A. (2008). What controls dead-ice melting under different climate conditions? A discussion. *Earth Science Reviews*, 90, 103–113.
- Schomacker, A., & Kjær, K.H. (2008). Quantification of dead-ice melting in ice-cored moraines at the high arctic glacier Holmströmbreen, Svalbard. *Boreas*, 37, 211–225.
- Sharp, M.J. (1985). ‘Crevasse-fill’ ridges – a landform type characteristic of surging glaciers? *Geografiska Annaler*, 67A, 213–220.
- Sharp, M.J., Jouzel, M.J., Hubbard, B., & Lawson, W. (1994). The character, structure and origin of the basal ice layer of a surge-type glacier. *Journal of Glaciology*, 40, 327–340.
- Sletten, K., Lyså, A., & Lønne, I. (2001). Formation and disintegration of a high arctic ice cored moraine complex, Scott Turnerbreen, Svalbard. *Boreas*, 30, 272–284.
- Szuman, I., & Kasprzak, L. (2010). Glacier ice structures influence on moraines development (Hørbye Glacier, central Spitsbergen). *Quaestiones Geographicae*, 29(1), 65–73.
- Vere, D.M., & Matthews, J.A. (1985). Rock glacier formation from a lateral moraine at Bukkeholsbreen, Jotunheimen, Norway: A sedimentological approach. *Zeitschrift für Geomorphologie*, 29 (pp. 397–415).
- Wilson, S.B., & Evans, D.J.A. (2000). Scottish landform example – 24: Coire a’ Cheud-chnoic, the ‘hummocky moraine’ of Glen Torridon. *Scottish Geographical Journal*, 116, 149–158.
- Woodward, J., Murray, T., & McCaig, A. (2002). Formation and reorientation of structure in the surge-type glacier Kongsvegen, Svalbard. *Journal of Quaternary Science*, 17, 201–209.
- Woodward, J., Murray, T., & McCaig, A. (2003). Reply: Formation and reorientation of structure in the surge-type glacier Kongsvegen, Svalbard. *Journal of Quaternary Science*, 18, 99–100.



INTRODUCTION

*Hørbyebreen and the adjacent glaciers, Svenbreen and Ferdinandbreen are polythermal valley glaciers located at 78°46' N at the north end of Petuniabukta, in central Spitsbergen. An early 20th Century surge has been proposed for Hørbyebreen (Karczewski, 1989; Gibas *et al.*, 2005) based upon looped medial moraines that are no longer visible, but otherwise the glaciers have been in continuous recession since the end of the Little Ice Age in the early 20th Century (Rachlewicz *et al.* 2007). Such glaciological dynamics are typical for many Svalbard glacier snouts and therefore the landform-sediment associations that characterize the Hørbyebreen foreland constitute an excellent modern landsystems analogue for palaeoglaciological reconstruction, especially for spatial and temporal landsystem overprinting. Contrasting aspects and radiation receipt in this mountainous terrain have resulted in more pronounced snout thinning on the east side of Hørbyebreen, creating an extensive subglacial landform assemblage in contrasts to the continuous glacier ice and ice-cored end moraine beneath the steep cliffs above the west margin.*

Glacial lineations (longitudinal foliae & flutings)

Both the glacier surface and the subglacial till freshly exposed by glacier thinning are strongly lineated. The subglacial lineations are less well developed and constitute flutings developed at the ice-bed interface, indicative of warm-based conditions inside the ice-cored moraine arc. The more prominent supraglacial lineations are longitudinal debris stripes typical of most Svalbard glaciers and explained by Hambrey and Glasser (2003) as englacial debris bands subject to transpression where ice flows from several cirque basins into a major valley. Downwasting rather than snout recession has resulted in the emergence of fluted till patches on high points of the bed through the lineated glacier surface.

Ice-cored and controlled moraine

The historical (Little Ice Age) maximum limits of Hørbyebreen and neighbouring glaciers are clearly marked by latero-frontal moraine arcs comprising linear hummocky terrain and more continuous linear ice-cored, transverse ridges or “controlled moraine” (sensu Evans 2009). Melting ice cores are manifest in numerous kettle holes, retrogressive flows and hollows bordered by tension cracks (e.g. Lyså & Lønne 2001; Lukas *et al.* 2005). Although relief is locally significant (>20m), areas of advanced melt-out are apparent as low amplitude, rubble-covered undulations and are mapped separately as “mature ice-cored moraine”.

Eskers and crevasse fills

Eskers at Hørbyebreen can be classified into three sub-types: a) linear esker ridges; b) sinuous eskers; and c) localized engorged eskers. The former are concentrated on the west side of the snout, are associated with ice-flow transverse and rectilinear debris ridges, and often branch off from major sinuous eskers. Because the linear esker and debris ridges form a rectilinear, cross-cutting pattern with a small range in orientations, it is considered most likely that they were deposited in crevasses created during the surge of the snout reported by Karczewski (1989) and Gibas *et al.* (2005). This implies compatibility with zig-zag eskers and crevasse-squeeze ridges typical of surging glacier geomorphology (Sharp 1985; Evans & Rea 2003), although the transverse debris ridges at Hørbyebreen have been interpreted as englacial thrust features by Szuman and Kasprzak (2010; cf. Hambrey *et al.* 1997; Bennett *et al.* 1998). The branching of linear eskers from a prominent large sinuous esker network indicates that a regular subglacial drainage system was in operation when meltwater and sediment was siphoned off to adjacent crevasses. This suggests a phase of elevated discharge and diversion of meltwater and sediment into the crevasses created by an increasingly fractured snout. Some of the linear esker ridges, as well as some debris ridges, could represent hydrofracture fills of the type described by Roberts *et al.* (2000, 2001) in relation to the Skeiðarárjökull jokulhlaup of 1996. Engorged eskers are very short, sinuous ridges presently developing in tunnels in the ice-cored moraine and orientated at right angles to valley slope due to the gravity-driven drainage of water melting from the buried ice. Such features are common in ice-cored moraine arcs on the forelands of both polythermal and surging glaciers (Evans *et al.* 2009, 2010).

Polythermal glacial landsystem

Former glacier beds characterized by well developed subglacial bedforms, such as flutings and eskers, lying up-valley from controlled moraine or ice-cored moraines, have been widely used to infer the existence of temperate or warm-based conditions giving way to a frozen snout zone (Hambrey *et al.* 1999; Dyke & Savelle 2000; Hambrey & Hambrey 2001, 2003; Dyke & Evans 2003; Evans *et al.* 2006, 2010; Evans 2009, 2011). Such polythermal conditions are common in Svalbard glaciers and give rise to the typical landform assemblage seen of the forelands of Hørbyebreen, Svenbreen and Ferdinandbreen, where large volumes of debris have been frozen on at the warm–cold based transition zone in the glacier snout.

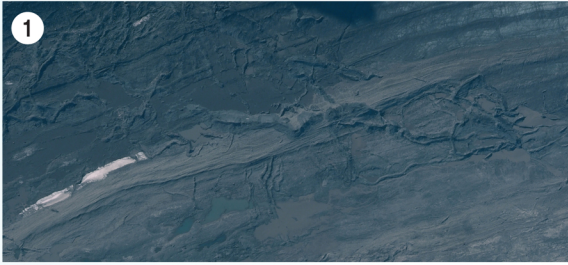
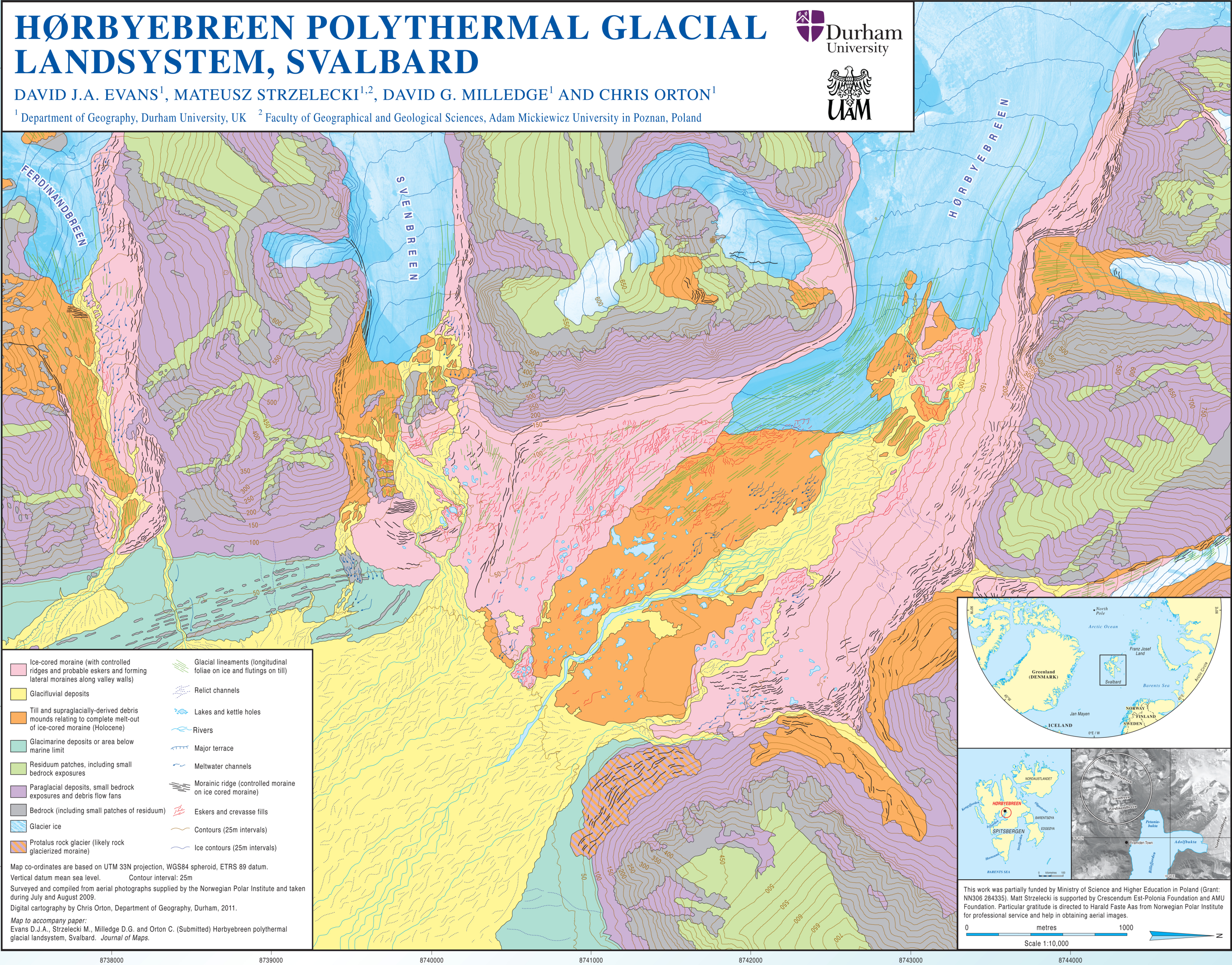


Figure 1: Aerial photograph extract (2009) of the main esker drainage network and sinuous ridges emerging through linear debris stripes on the west margin of Hørbyebreen snout, representing esker construction in major tunnels and adjacent crevasses.

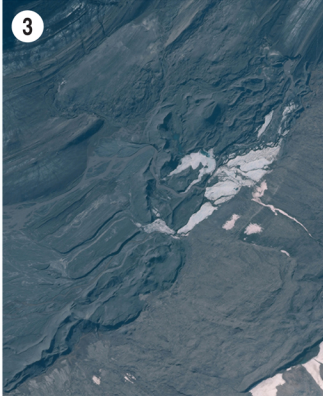


Figure 3: Aerial photograph extract (2009) of the main esker drainage network on the east side of the Hørbyebreen snout, concentrating on the present glacier margin (extreme top) and the occurrence of a braided esker system at the glacier margin which grades down valley into a single, single ridge esker. More localized linear ridge segments document crevasse infill due to meltwater leakage from esker tunnels.



Figure 2: Aerial photograph extract (2009) of the ice-cored latero-frontal moraine arc of Ferdinandbreen. Areas of strongly fluted terrain occur on the foreland and linear debris stripes occur in juxtaposition with crevasse fills ridges in the ice-cored moraine.

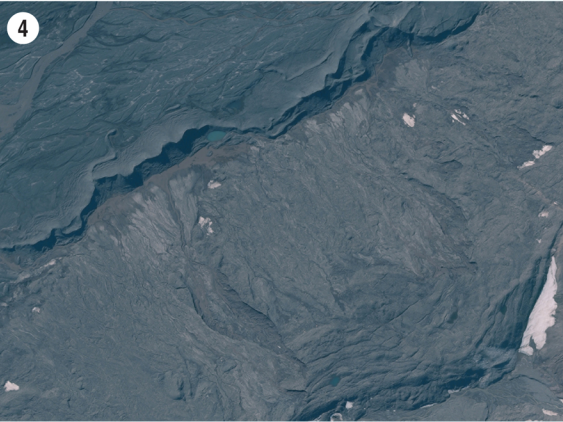


Figure 4: Aerial photograph extract (2009) of the ice-cored moraine belt on the east side of Hørbyebreen, showing controlled ridges and melt-out hollows at the right of the image grading into areas of tension cracks and retrogressive flows on the lower slopes. The main esker ridge of the east margin is visible at the left of the image.



Figure 8: Overview of the forelands of Hørbyebreen and Svenbreen from the southwest.

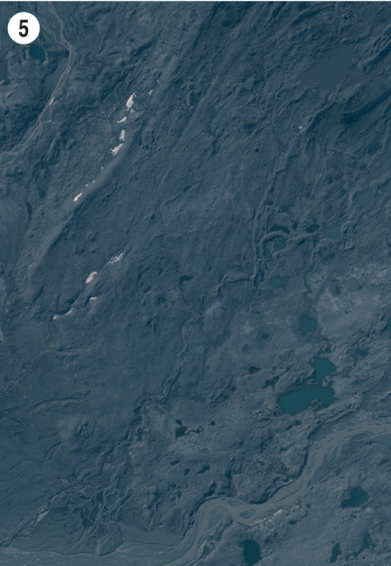


Figure 5: Aerial photograph extract (2009) of controlled ridges, eskers and crevasse fill ridges on the outer ice-cored moraine of Hørbyebreen, where melt-out is at an advanced stage. The prominent ridge towards the left of the image is the former medial moraine between Hørbyebreen and Svenbreen; therefore the eskers at the left of the image are from Svenbreen drainage.

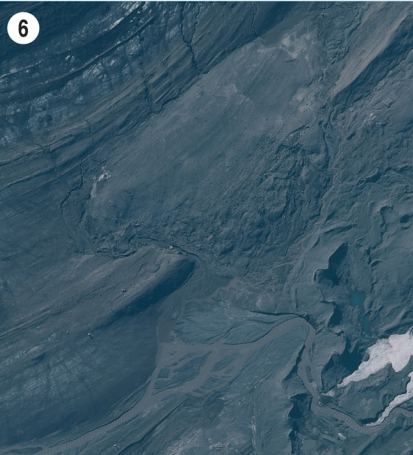


Figure 6: Aerial photograph extract (2009) of fluted subglacial till surface emerging from the downwasting snout of Hørbyebreen. Note that the subglacial flutings are less prominent than the strong lineation created by supraglacial debris stripes. Eskers are emerging from the more contracted margin of the east side of the snout at the top of the image.

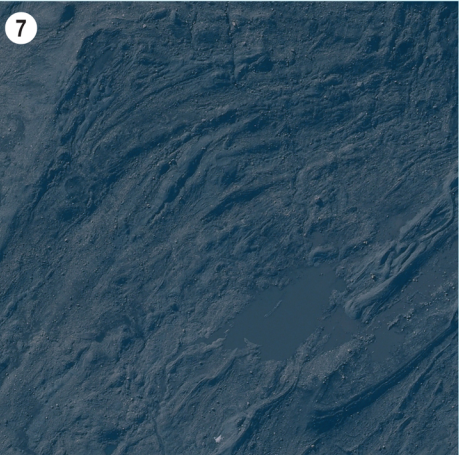


Figure 7: Aerial photograph extract (2009) of the controlled moraine and supraglacial debris stripes on the SW margin of the Hørbyebreen foreland. Esker ridges also occur at the top of the image and lie just inside the medial moraine (dark coloured prominent ridge complex) between the main Hørbyebreen trunk ice and the ice debouching from two unnamed cirque glaciers on the west margin of the valley.

Surge signatures

Diagnostic geomorphological criteria for former glacier surging are summarised in the surge glacier landsystem by Evans and Rea (2003). Few of these criteria are visible at Hørbyebreen, but they are particularly diagnostic nonetheless. They include the linear esker ridges and crevasse fill landforms, which record deposition into a rectilinear pattern of ice fractures. In the surge landsystem, the emplacement of sediments into crevasse networks is manifest as zig-zag eskers and basal crevasse-squeeze ridges, whose orientations conform to the fracture patterns created in the glacier snout during its surge phase. However, the lack of distortion of the longitudinal debris stripes and their apparent dominance over the transverse ridges, is incompatible with a former surge, because flow lineations of this sort would have been compressed to produce “looped medial moraines”. Additionally, the transverse ridge forms do not cross cut the longitudinal debris stripes, but are emerging instead from areas of lower relief on the downwasting snout, indicating that they were emplaced in the basal ice facies and their enclosing crevasses did not extend to the glacier surface. This pattern of emplacement and its implications for the lack of full depth crevasing, suggest that the emplacement of the transverse ridges could have been by hydrofracture networks induced by elevated meltwater pressures and the overwhelming of the normal englacial and subglacial drainage tunnels. This could have taken place in the absence of a surge.

References

Bennett M.R., Hambrey M.J., Huddart D. & Glasser N.F. 1998. Glacial thrusting and moraine-mound formation in Svalbard and Britain: the example of Coire a' Cheud chnoic (Valley of a hundred hills), Torridon, Scotland. *Quaternary Proceedings* 6, 17-34.

Dyke A.S. & Savelle J.M. 2000. Major end moraines of Younger Dryas age on Wollaston Peninsula, Victoria Island, Canadian arctic: implications for palaeoclimate and for formation of hummocky moraine. *Canadian Journal of Earth Sciences* 37, 601–619.

Dyke A.S. & Evans D.J.A. 2003. Ice-marginal terrestrial landsystems: northern Laurentide and Inuitian ice sheet margins. In *Glacial Landsystems*, Evans D.J.A. (ed). Arnold, London, 143–165.

Evans D.J.A. 2009. Controlled moraines: origins, characteristics and paleoglaciological implications. *Quaternary Science Reviews* 28, 183-208.

Evans D.J.A. 2011. Glacial landsystems of Satujökull, Iceland: a modern analogue for glacial landsystem overprinting by mountain icecaps. *Geomorphology* 129, 225-237.

Evans D.J.A. & Rea B.R. 2003. Surging glacier landsystem. In: Evans D.J.A. (ed.), *Glacial Landsystems*. London, Arnold, 259-288.

Evans D.J.A., Twigg D.R. & Orton C. 2010. Satujökull glacial landsystem, Iceland. *Journal of Maps* 2010, 639-650.

Evans D.J.A., Twigg D.R. & Shand M. 2006. Surficial geology and geomorphology of the Þorjökull plateau icefield, west-central Iceland. *Journal of Maps* 2006, 17-29.

Evans D.J.A., Twigg D.R., Rea B.R. & Orton C. 2009. Surging glacier landsystem of Tungnaárjökull, Iceland. *Journal of Maps* 2009, 134-151.

Gibas J., Rachlewicz G. & Szczuciński W. 2005. Application of DC resistivity sounding and geomorphological surveys in studies of modern Arctic glacier marginal zones, Petuniabukta, Spitsbergen. *Polish Polar Research* 26, 239-258.

Glasser N.F. & Hambrey M.J. 2001. Styles of sedimentation beneath Svalbard valley glaciers under changing dynamic and thermal regimes. *Journal of the Geological Society, London* 158, 697–707.

Glasser N.F. & Hambrey M.J. 2003. Ice-marginal terrestrial landsystems: Svalbard polythermal glaciers. In *Glacial Landsystems*, Evans DJA (ed). Arnold, London, 65–88.

Hambrey M.J. & Glasser N.F. 2003. The role of folding and foliation development in the genesis of medial moraines: examples from Svalbard glaciers. *Journal of Geology* 111, 471-485.

Hambrey M.J., Bennett M.R., Dowdeswell J.A., Glasser N.F. & Huddart D. 1999. Debris entrainment and transfer in polythermal valley glaciers. *Journal of Glaciology* 45, 69-86.

Hambrey M.J., Huddart D., Bennett M.R. & Glasser N.F. 1997. Genesis of hummocky moraines by thrusting of glacier ice: evidence from Svalbard and Britain. *Journal of the Geological Society of London* 154, 623-632.

Karczewski A. 1989. The development of the marginal zone of the Hørbyebreen, Petuniabukta, central Spitsbergen. *Polish Polar Research* 10, 371-377.

Lyså I. & Lønne A., 2001. Moraine development at a small High-Arctic valley glacier: Rieperbreen, Svalbard. *Journal of Quaternary Science* 16, 519-529.

Lukas S., Nicholson L.I., Ross F.H. & Humlum O. 2005. Formation, meltout processes and landscape alteration of High-Arctic ice-Cored moraines: examples from Nordenskiöld Land, Central Spitsbergen. *Polar Geography* 29, 157-187.

Rachlewicz G., Szczuciński W. & Ewertowski M. 2007. Post – “Little Ice Age” retreat rate of glaciers around Billefjorden in central Spitsbergen, Svalbard. *Polish Polar Research* 28, 159-186.

Roberts, M.J., Russell, A.J., Tweed, F.S. & Knudsen, O. 2000. Ice fracturing during jokulhlaups: implications for englacial floodwater routing and outlet development. *Earth Surface Processes and Landforms* 25, 1429–46.

Roberts, M.J., Russell, A.J., Tweed, F.S. & Knudsen, O. 2001. Controls on englacial sediment deposition during the November 1996 jokulhlaup, Skeiðarárjökull, Iceland. *EarthSurface Processes and Landforms* 26, 935-52.

Sharp, J.P. 1985. ‘Crevasse-fill’ ridges - a landform type characteristic of surging glaciers?, *Geografiska Annaler* 67A, 213–220.

Szuman I. & Kasprzak L. 2010. Glacier ice structures influence on moraines development (Hørbye Glacier, central Spitsbergen). *Questiones Geographicae* 29/1, 65-73.





## Schmidt hammer tests across a recently deglaciated rocky coastal zone in Spitsbergen – is there a “coastal amplification” of rock weathering in polar climates?

Mateusz Czesław STRZELECKI

*Uniwersytet im. Adama Mickiewicza w Poznaniu, Wydział Nauk Geograficznych i Geologicznych,  
ul. Dziegiełowa 27, 61-680 Poznań, Poland*

and

*Durham University, Department of Geography, Science Site, South Road, Durham DH1 3LE, UK  
<mat.strzelecki@gmail.com>*

**Abstract:** A significant limit to current understanding of cold coast evolution is the paucity of field observations regarding development of rocky coastlines and, in particular, lack of precise recognition of mechanisms controlling rock coast geomorphology in polar climates. Results are presented from a pilot survey of rock resistance using Schmidt Hammer Rock Tests (SHRT) across the recently deglaciated Nordenskiöldbreen forefield and coastal zone, in central Spitsbergen, Svalbard. The aim is to improve understanding of the effects of rock weathering on high latitude coasts. SHRT across a field of roches moutonnées of metamorphic rocks, uncovered from ice over the last century and exposed to the operation of littoral processes, demonstrated significant relationships between rock surface resistance and distance from present shoreline, distance from the ice cliff as well as thickness of the snow cover. Sites closest to the present-day shoreline were characterized by lower resistance in comparison with more inland locations. The result support models that advocate intensification of weathering processes in cold region coastal settings.

Key words: Arctic, Svalbard, rocky coasts; SHRT, coastal evolution.

### Introduction

One of the most controversial problems of cold region coastal geomorphology is the determining of the relative significance of littoral processes and frost weathering in controlling rocky cliff and shore platform morphology. The classic example of this debate is the origin of strandflats which has been a regular topic for discussion in the geomorphological literature for almost a century (Nansen 1922; Dahl 1946; Werenskiöld 1952; Moign 1974; Guilcher *et al.* 1986; Holtedahl 1998). Until the beginning of the 21<sup>st</sup> century world-leading coastal geomorphologists often claimed that it is impossible to obtain a clear agreement on the efficiency of coastal processes in high latitudes (Trenhaile 1983; Byrne and Dionne 2002).

Recent decades have seen major development in Arctic coastal research due to projects of the Arctic Coastal Dynamics (ACD) Group (Rachold *et al.* 2005; Forbes *et al.* 2011) and the reopening of Russian works to the wider scientific community, especially in the field of thermoabrasion (Aré 1988; Nikiforov *et al.* 2005; Aré *et al.* 2008; Streletskaia *et al.* 2009). However, the major focus in these initiatives has been on understanding and modelling ice-rich permafrost coastlines, particularly in Alaska, western Canada, and the Laptev Sea region, which are characterized by some of the most rapid erosion rates in the world (Lantuit *et al.* 2011). The role of ice, snow and frost action on rocky cliffs and shore platforms, specifically in sheltered fjords of polar archipelagos, remains poorly understood (Trenhaile 1997).

Furthermore, the geomorphology of cold region rocky coasts is marked by significant regional contrasts. On the one hand during the last three decades several geomorphological works along Atlantic Canada's rocky shorelines (*e.g.* Dionne and Brodeur 1988; Dionne 1989; Trenhaile and Mercan 1984; Trenhaile *et al.* 1998; Trenhaile 2001; Trenhaile *et al.* 2006; Porter and Trenhaile 2007; Porter *et al.* 2010) have realized fundamental advances in our understanding of ice and frost action on the morphology of intertidal zones as well as "freezing-thawing & wetting-drying" influence on shore platforms and cliffs relief. Relatively few investigations, however, have tested the efficiency of those processes in polar settings.

In the early 1990's Ødegård and Sollid (1993) and Ødegård *et al.* (1995) investigated rocky cliffs in northern Spitsbergen (Kongsfjorden and Liefdefjorden) to understand the thermal regime in frozen rocks beneath a melting snow cover. Their observations identified four periods of differing thermal impacts on coastal cliff breakdown, and postulated processes of thermal stresses related to subzero temperature oscillations. They argued that the formation of segregation ice in fractured rock is one of the leading mechanisms controlling rock coastal morphology in polar environments. The only ACD project carried out on a high latitude rocky coastal zone was a study by Wagensteen *et al.* (2007) in Kongsfjorden (Spitsbergen). Using detailed photogrammetric survey these authors demonstrated that rockwall retreat rates in polar coastal settings are higher relative to the more inland locations studied by Rapp (1960) and André (1997). Interestingly, similar "coastal amplification" of weathering along polar shorelines was previously postulated by Jahn (1961), but the concept has never been sufficiently tested and clarified.

In this paper I explore further the hypothesis of "coastal amplification" of weathering rates on the rocky coasts of Spitsbergen. To do so, I select the recently deglaciated coastline adjacent to the Nordenskiöldbreen glacier, where I report results of Schmidt Hammer Rock Tests across transects that extend from the present coast inland. The work is interesting since the study site is characterised by a relatively dry polar climate and limited fetch, in contrast to the maritime often stormy climate of western coast where majority of previous rocky coastal studies were carried out (Jahn 1961; Moign 1976; Guilcher *et al.* 1986; Ødegård and Sollid 1993; Ødegård *et al.* 1995; Migoń 1997; Wagensteen *et al.* 2007).



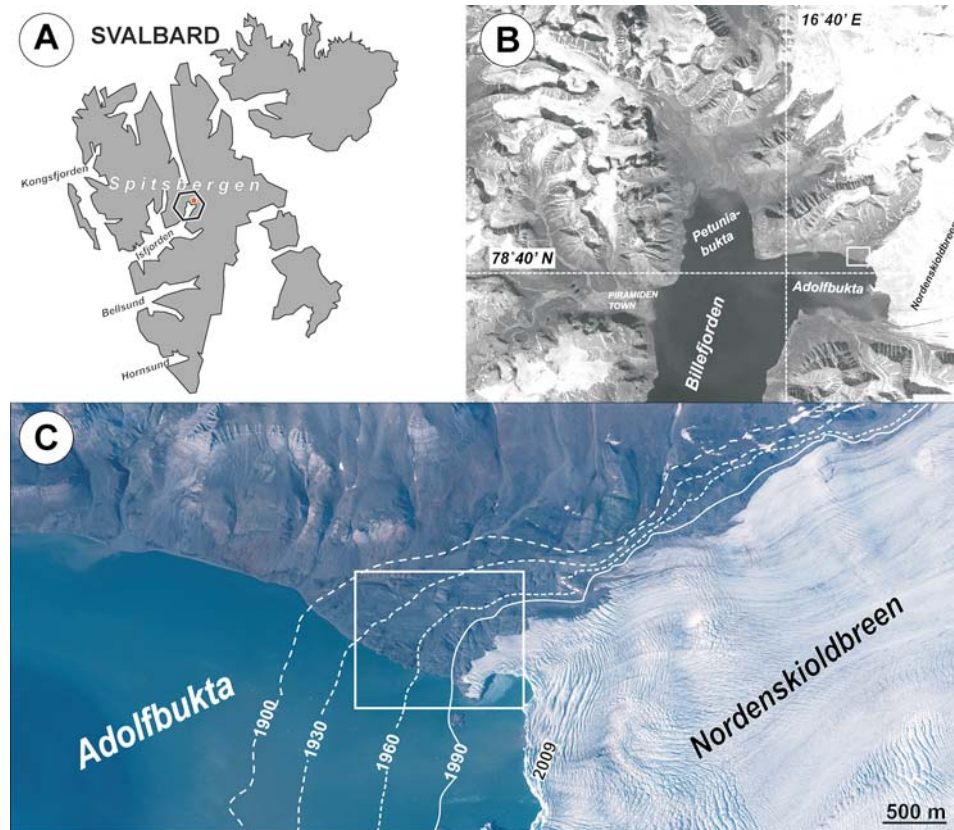


Fig. 1. Location of the study area. **A.** Svalbard Archipelago, map shows main fjords along the western coast of Spitsbergen Island, dot in a polygon marks location of study area. **B.** Main bays of northernmost Billefjorden region – middle branch of Isfjorden largest fjord system of Spitsbergen, white Square indicates section of the rocky coastline selected for study. **C.** Northern Adolfbukta, Central Spitsbergen. Fragment of orthophotomap based on Norwegian Polar Institute aerial photographs taken in 2009. Image shows the current front of Nordenskiöldbreen: the dashed lines indicate former positions of this tide-water glacier, in the years 1900–1930–1960–1990. White square marks the selected roche moutonnée field where SHRTs were carried out in summers 2009–2010 and is zoomed in Fig. 2A.

## Study area

Research was undertaken on the recently exposed rocky forefield of Nordenskiöldbreen, along the northern shores of Adolfbukta, in the central part of Spitsbergen (Fig. 1). Adolfbukta represents a microtidal environment, with a tide range *ca* 1.5m, and is characterized by lengthy periods of winter sea ice (typically 7–8 months). After spring/summer break-up, floating sea ice is normally rapidly removed from the basin under appropriate wind conditions. During the summer, the coastline is influenced by debris-rich growlers which are sourced by calving from Nordenskiöldbreen – the only tidewater glacier in Billefjorden (Szczuciński

*et al.* 2009). Wave energy is limited by a shallow fjord sill (less than 50 m) and narrow entrance, so wave action is restricted to the ice-free summer months, mainly at high tides and under rare storm events. Meteorological conditions in the centre of Spitsbergen differ from the western coast in being colder and less maritime (Przybylak *et al.* 2007). Average annual precipitation is typically less than 200 mm yr<sup>-1</sup>, and mean annual air temperature is *c.* -6.5°C with air temperatures above 0°C occurring between June and the end of September (Rachlewicz and Szczuciński 2008). Frozen ground conditions are extensive and vary from thick and continuous permafrost in the mountain ranges to relatively thin and recently developed permafrost in glacial valleys. Discontinuous and thin permafrost (or even non-frozen ground) occurs in the coastal and seabed area of the fjords (Humlum *et al.* 2003). Snow cover is thin (approx. 0.3 m on the ice-bounded fjord, and 0.6–0.9 m in the valleys), although wind action accumulates snowdrifts 1–2 m deep at the bottom of cliffs (based on author's winter survey in 2009).

Several authors (Rachlewicz *et al.* 2007, Małecki 2009) documented the high rate of retreat of all glaciers in the northern part of the Billefjorden region. Since the end of the Little Ice Age (in Svalbard, at the beginning of 20<sup>th</sup> century) Nordenskiöldbreen retreated approximately 3.5 km (Fig. 1) exposing *ca* 17 km<sup>2</sup> of unstable para-periglacial landscape (following the definition of *para-periglacial* by Mercier 2008) – characteristic of the majority of glacier forelands in the vicinity (Rachlewicz 2010). For coastal studies it is also noteworthy that in the Billefjorden region, the highest Late Weichselian marine limit reaches approx. 90 m a.s.l. and the relative sea-level reached close to present in the mid to late Holocene (Salvigsen 1984; Forman *et al.* 2004).

The local geology is one of the most diverse in the Svalbard Archipelago due to disturbance of geological units associated with the Billefjorden Fault Zone (Dallmann *et al.* 2004). The major bedrock units exposed by post-LIA retreat of Nordenskiöldbreen consist of hard and resistant Precambrian metamorphic rocks (Smutsbreen Unit), including plagiogneisses, garnet-biotite schists, amphibolites, quartzites and marbles. For this study, an approximately 1 km<sup>2</sup> zone was selected, encompassing plagiogneiss *roche moutonnées* and plunging cliffs, between the present-day shoreline, ice-cliff and LIA moraine belt (Fig. 1).

## Methods

Schmidt hammer tests have been used in weathering and dating investigations of glacier forelands and mountainous areas since the 1960's (Goudie 2006), although more recently this inexpensive tool has thrown new light on hard rock coastal geomorphology (*e.g.* Trenhaile *et al.* 1998; Stephenson and Kirk 2000a, b; Dickson *et al.* 2004; Thornton and Stephenson 2006; Cruslock *et al.* 2010; Chelli *et al.* 2010; Kennedy *et al.* 2010). In this pilot study I took 725 Schmidt hammer readings at 29

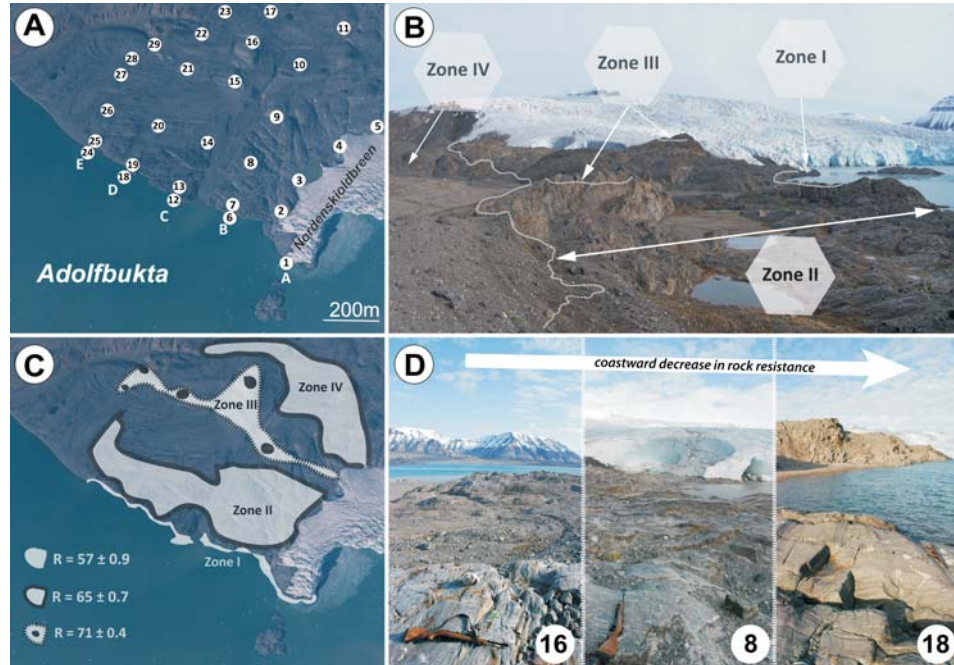


Fig. 2. Location and key findings of SHRT in northern Adolfbukta. **A.** SHRT sites and profiles – white dots with numbers 1–29 indicate locations of rock surfaces hit during tests whereas letters A–E along the coast point the starting point of each of the test profiles. **B.** Oblique image showing the spatial distribution of characteristic zonality in rock resistance along tested rock surfaces. **C.** Map of rock resistance variability: Zone I – coastal zone of lowest rock resistance, Zone II and IV – interior forefield of medium rock resistance, and Zone III – peaks of roches moutonnées of highest rock resistance. **D.** Examples of rock surfaces from different resistance zones, riffle indicates the direction of ice flow, white arrow indicates the general trend of lowering rock resistance. Left image: example from Zone III – peaks of roches moutonnées – highest rock resistance, smooth surfaces, no snow cover; Middle image: example from Zone II & IV – forefield interior – medium rock resistance, debris cover, thick snow cover in winter; Right image: example from Zone I – coastal strip – lowest rock resistance, wandering snowdrifts, wave & tide action. Numbers in white dots (bottom right corner) indicate location of given SHRT site shown on Fig. 2A.

sites (Fig. 2A) following the methodology of Day and Goudie (1977) and Selby (1980), using a classic Proceq N-type tool which provides an arbitrary measure of rock resistance shown on a scale from 10–100 (rebound values – R).

During measurements 25 hits were made at points randomly selected from each of the 29 sites. According to Niedzielski *et al.* (2009) this number of readings provides accurate mean Schmidt hammer test values in the majority of lithologies. Only on several inaccessible surfaces located on the higher parts of cliffs the number of hits was reduced to 10. Each site consisted of *ca* 10×10 cm area of gneissic surface.

The sampling strategy took into consideration distance of the rock surface from the present-day shoreline, and from the current glacier front position (Fig. 2A). The starting point of each of five profile lines was a rock surface at mean

sea-level, approximately 0.5 meters (Profile A: S1–S5), 200 meters (Profile B: S6–S11), 400 meters (Profile C: S12–S17), 600 meters (Profile D: S18–S23) and 800 meters (Profile E: S24–S29) from the present ice cliff position. From each of the starting points the profiles continued inland every 150 meters in line with the Nordenskiöldbreen front. To test if there is a vertical difference in rock resistance up the cliff wall, additional SHRT were taken on the top of the cliffs above the starting points (5–15 meters above mean sea-level) in Profiles B–E.

Prior to statistical analysis all anomalous R-values were removed on the basis of Chauvenet's criterion recommended in the interpretation of SHRT by Gökten and Ayday (1993). To test the significance of differences between R-values measured along coastal and more inland roche moutonnée surfaces, a Cochran and Cox test was applied. Kruskal-Wallis and Dunn's tests were run to compare the R-values variations between zones I, II and III.

## Rock surface resistance

Table 1 summarizes the SHRT results and presents the mean R-values calculated for each tested rock surface. The following zones of rock resistance can be clearly distinguished (Fig. 2):

Zone I – the coastal: strip covering the lower part of plunging cliffs affected by sea ice movement, wave action and sea spray (Sites: S1, S6, S12, S18 and S24), with mean R-values of  $57 \pm 0.89$ .

Zone II – area of intermediate rock resistance – strip of roches moutonnées between the top of the cliffs and Zone III (Sites: S2, S3, S7, S8, S13, S14, S19, S20, S25, S26, S27), with mean R-values of  $66 \pm 0.83$ .

Zone III – summits of roches moutonnées – characterized by the highest rock resistance, with mean R-values of  $71 \pm 0.42$ .

Zone IV – area of intermediate rock resistance – strip of roches moutonnées adjacent to Nordenskiöldbreen lateral moraines (Sites: S5, S11, S17, S23), with mean R-values equal  $64 \pm 0.65$ .

## Discussion

In general, all results of SHRT taken along the present-day shoreline were about 5 units lower compared to R-values on the upper parts of the plunging cliffs, and often over 10 units lower than those from summits of roches moutonnées and more inland sites. In all cases Cochran and Cox tests confirmed differences in R-values between coastal (lower resistance) and inland sites (higher resistance). The analysis of regression proved that R-values from rocks located along the coast were significantly lower than those obtained along inland roches moutonnées (Fig. 3A). No trends exist across profiles perpendicular to glacier front (Fig. 3B–D). In-

**Table 1**  
Schmidt Hammer Rock Tests summary. Statistical parameters for each of the test sites and topographical information regarding their distance from ice front, present shoreline and approximate time of the post-Little Ice Age deglaciation. Sites in grey shading were the starting points of each of five profiles.

Site	Mean R-value	Margin of error (95%CI)	Median	Mode	Min	Max	Skewness	Distance from the shoreline (m)	Distance from the glacier front (m)	Height above mean sea-level (m)	Age of exposure from beneath glacier ice
S1	51	1.17	51	multimodal	45	57	-0.19	0	0.5	0	2008–2009
S2	68	0.58	68	68	65	70	-0.01	150	0.5	23	2008–2009
S3	67	0.68	67.5	69	64.5	69	-0.58	300	0.5	42	2008–2009
S4	68	0.5	68	69	66	70	-0.12	450	0.5	37	2008–2009
S5	68	0.79	69	70	64	70	-0.59	600	0.5	72	2008–2009
S6	57	0.83	57	57	54	61	0.65	0	200	0	1960–1990
S7	65	0.87	66	66	62	68	-0.20	1	200	28	1960–1990
S8	69	0.58	69	70	66.5	71	-0.03	150	200	37	1960–1990
S9	72	0.28	72	73	71	73	-0.62	300	200	33	1960–1990
S10	65	0.47	65	65	63	67	-0.29	450	200	63	1930–1960
S11	62	0.67	62	63	59	64	-0.35	600	200	96	1930–1960
S12	62	0.48	62	61	61	64	0.83	0	400	0	1930–1960
S13	69	0.74	69	70	66	72	-0.20	1	400	13	1930–1960
S14	68	0.79	69	70	64	70	-0.59	150	400	20	1930–1960
S15	68	0.74	68	70	64	70	-0.46	300	400	52	1930–1960
S16	73	0.35	73	73	71	74	-0.68	450	400	78	1900–1930
S17	60	0.88	60	58	55	63	-0.37	600	400	81	1900–1930
S18	59	1.05	59	multimodal	54	64	0.24	0	600	0	1930–1960
S19	63	1.04	63	multimodal	60	68	0.26	1	600	14	1930–1960
S20	68	0.82	69	70	64	70	-0.91	150	600	20	1930–1960
S21	73	0.4	73	73	71	74	-0.45	300	600	40	1930–1960
S22	65	0.56	65	65	62	67	-0.48	450	600	90	1900–1930
S23	63	0.55	63	63	60	65	-0.59	600	600	164	1900–1930
S24	58	0.91	58	58	54	62	-0.08	0	800	0	1900–1930
S25	59	1.16	59	multimodal	54	65	0.14	1	800	14	1900–1930
S26	65	0.73	65	63	62	68	0.19	150	800	17	1900–1930
S27	65	0.7	66	66	62	68	-0.60	300	800	14	1900–1930
S28	70	0.38	70	70	68	71	-0.24	450	800	27	1900–1930
S29	73	0.26	73	73	72	74	-0.30	600	800	40	1900–1930



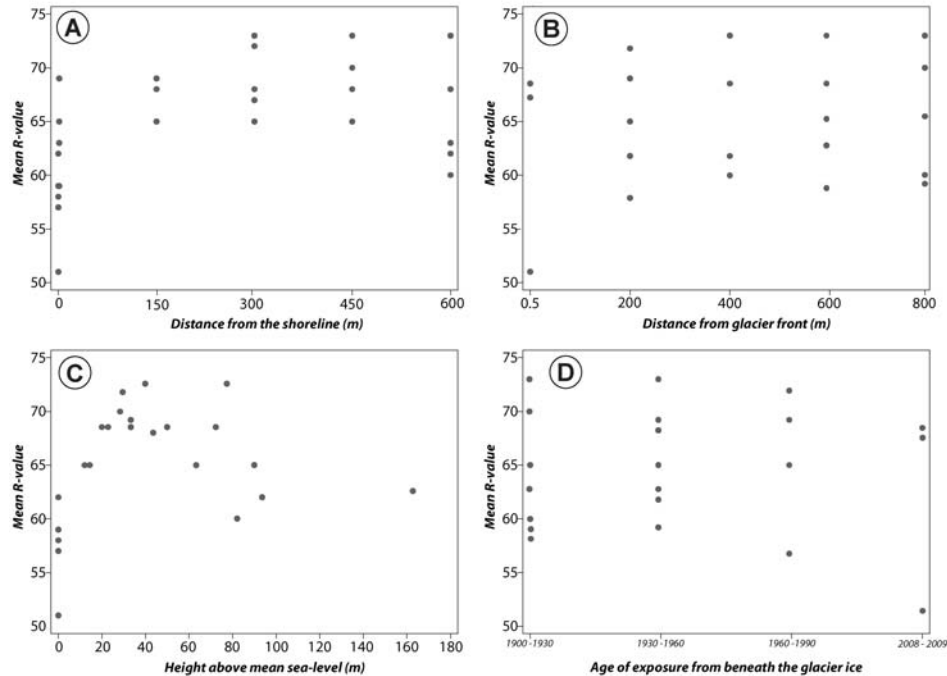


Fig. 3. Mean R-values obtained during SHRT. **A.** Along the coast and more inland locations with a significant trend of seaward rock resistance weakening. **B.** Along lines perpendicular to glacier front – no significant relationship found. **C.** Across roches moutonnées of different height above mean sea-level – no significant relationship found. **D.** Across zones exposed by retreating Norden-skioldbreen since the end of LIA – no significant relationship found.

terestingly the rock surfaces on plunging cliffs do not contain any cracks or signs of ice movement, whereas the roches moutonnées are covered with glacial striations and cracks. However, none of those surficial modifications reduced rock resistance of inland roches moutonnées. On the contrary, it seems that glacial erosion of roche moutonnée surfaces exposed fresh, non-weathered rock, which was hardly modified by para-periglacial processes, whereas rock surfaces deglaciated in the same period, but located in a zone of coastal influence, had been subjected to intensified weathering. Low waves and a lack of beach sediments which could be used in quarrying and polishing the cliff walls appears to have led to the formation of the weak rock layer in the intertidal zone. The lower resistance of coastal rock surfaces in relation to inland outcrops may relate to the low-energy fjord environment. Weak wave activity in such a sheltered fjord as Adolfbukta is unable to erode and remove rock weakened by intertidal wetting-drying and frost shattering. This may be responsible for preservation of a weathered layer in the coastal zone. Moreover, the continuous and intensive operation of para-periglacial processes since the end of the LIA has led to the removal of unstable and weak rock surfaces from the Nordenskioldbreen foreland, exhuming hard resistant outcrops. Similar relation has been discovered by Blanco-Chao et al. (2007) during the study on

shore platform evolution in para-periglacial environment of northern Galicia, Spain. In their survey SHRT indicated lower rock strength along platforms which were continuously influenced by tidally-induced weathering, whereas in areas where weathered material was removed by abrasion exposing fresh outcrops – rocks were more resistant. Galician example highlighted the significance of inherited factors such as glacial deposits and former shoreline configuration which may have a direct influence on the rocky shoreline evolution after deglaciation and during warmer periods associated with intensified sediment removal, abrupt relative sea-level changes and prolonged open water conditions.

Another factor that affects the degree of rock weathering is the effect of snow cover on rock thermal regime (*e.g.* Ødegård and Sollid 1993). Winter observations revealed that the lower parts of the coastal cliffs in the study area are protected by up to 2 meter thick snowdrifts, and an even deeper snow cover could be filling hollows between roches moutonnées in Zones II and IV. However the snow cover along the cliffs is typically uneven, dotted with snow-free rock surfaces and rock bulges. The coastal cliff in Adolfbukta is south-facing and therefore the protruding rock surfaces warm up strongly during polar spring/summer, and the snow cover rapidly melts or sublimates. After sunset or during the polar day when the rockwall is in shadow, the surface temperature cools rapidly, what can lead to freezing of water in rock cracks or crevices: indeed, the surface is always subject to very strong thermal stresses leading to rock disintegration. The results of Hall (1993) on Livingstone Island (Antarctica) emphasized that prolonged wetting of a rock surface by melting snowpatches enhances bedrock weathering, especially on leeward slopes, which appears to be the case on a cliff speckled with snow patches. Differences in snow cover thickness and duration might entail the reduction of rock resistance also in roches moutonnées located far from the coast but affected by late-lying snow cover. The only zones devoid of snow cover or glaciofluvial action were the summits of roches moutonnées and the tops of plunging cliffs, which may imply more stable moisture conditions, and less effective chemical weathering in those zones (*e.g.* Ballantyne *et al.* 1989). The upper parts of the cliffs, however, were often covered with bird guano (a layer up to 2 cm thick), undoubtedly enhancing rock chemical weathering and resulting in slightly weaker resistance (mean R-values for sites 7, 13, 19, 25 are  $64 \pm 0.95$ ) than more inland sites such as 9, 15, 21, 27 (mean R =  $67 \pm 0.53$ ).

Rock surfaces in Zones II and IV were also subject to lichen colonization and there evidence of meltwater overwashing (old stream channels and accumulations of glaciofluvial gravels, which are already covered by tundra). Generally, even though the variety of subaerial processes which may affect the degree of rock fragmentation appeared to be greater in more inland sites, the results of SHRT indicated that rock surfaces there are more resistant than rockwalls near the sea. This suggests the operation of processes, or the existence of specific conditions, responsible for the weakening of rock strength in the lower parts of cliffs. This may be associated with a “coastal amplification” of rock weathering (*e.g.* tidal wetting and drying, rock satu-

ration level, salt weathering, wave action or sea ice action). However the influence of topographic factors (slope height, slope angle, slope aspect), and differences in rock stress release following deglacial debuttressing, cannot be excluded.

The design of the survey also allowed testing of the potential usefulness of SHRT in relative-dating of the Nordenskiöldbreen rocky forefield. While the zonation in rock resistance between coastal and inland sites was quite clear, a similar relation between sites proximal to and distant from the glacier was less apparent. For instance, profile A (S1–S5) across outcrops exposed from Nordenskiöldbreen during 2008–2009, and seemed to represent the area most sensitive to non-glacial conditions, theoretically more prone to weathering processes, demonstrated only slightly lower resistance than bedrock exposed during earlier stages of post-LIA deglaciation (Fig. 3D). However regression analysis did not show any significant differences in R-values for results from sites close to the glacier front in comparison with more distant sites. This suggests that SHRT-dating of Nordenskiöldbreen foreland should be carried out only in conjunction with other dating methods, and it is not clear that any reliable age correlations are to be found.

## Conclusions

This work highlighted the need for a greater understanding of the controls of polar rocky coastal zones. The most important finding in the Adolfbukta pilot study is the clear reduction in rock resistance with decreasing distance from the present-day shoreline. The study suggests two contrasting explanations for reduced rock resistance in the coastal zone:

- coastal processes (tidal wetting and drying, salt weathering, wave action, sea ice action) weaken the rock surfaces more efficiently than other subaerial agents operating on rocky landforms in more inland locations, and allow deeper and more efficient rock weathering;
- the low efficiency of coastal processes in sheltered fjord environments leads to preservation of a weathered rock layer along the coast, whereas high intensity of para-periglacial processes across more inland areas removed the weathered material left after post-LIA glacier retreat.

However SHRT should be treated only as a preliminary reconnaissance and the study on influence of coastal processes on rock breakdown in polar climates should be supported by application of more advanced methods (*e.g.* Equotip, MEM, Terrestrial Laser Scanning, digital photogrammetry, GIS modelling) to reduce the risk of misinterpretation (Lim *et al.* 2005, 2010; Aoki and Matsukura 2007; Viles *et al.* 2011). The major weakness of this study is above all the lack of information regarding the spatial distribution of permafrost and the difference in development of the active layer between coastal and inland outcrops, which could have a significant impact on rock stability and degree of weathering. Schmidt hammer measurements also did not detect any significant differences in bedrock expo-

sure ages, what implies that the method should be combined with either lichenometry (Matthews and Shakesby 1984; Evans *et al.* 1999),  $^{14}\text{C}$  dating (Shakesby *et al.* 2006) or terrestrial cosmogenic nuclide dating (Winkler 2009) for the proper deciphering of Nordenskiöldbreen's deglacial history.

Looking ahead, for further progress in cold region coastal geomorphology, a natural step should be the intensification of research efforts on evolution of rocky coastlines formed in the various lithologies encountered along the coasts of Svalbard, Franz Joseph Land, the Canadian Arctic Archipelago and Greenland. Of particular interest are quantitative studies of typical polar climate-driven factors controlling rocky shoreline landforms and microrelief, and studies of the adjustment of this type of coastal environment to the rapid rate of post-glacial isostatic recovery and to the recent para-periglacial landscape transition, characteristic of many Arctic settings.

**Acknowledgements.** — Research funding was provided by the Ministry of Science and Higher Education in Poland (grants no. N306284335 and N305098835). The author is also supported by a Crescendum Est – Polonia fellowship and the Adam Mickiewicz University Foundation scholarship for the best doctoral students. The author thanks Monika Lutyńska and members of the 14th and 15th AMU Poznań Svalbard Expedition for support during fieldwork, and Piotr Migoń for the inspiration to run Schmidt hammer tests along Spitsbergen coasts. Particular gratitude is directed to Adrian Zwolnicki and Kasia Zmudczyńska from AZB ([www.azb.pl](http://www.azb.pl)) for help with statistical analysis of the data and Ian Evans from the Durham University for interesting comments on a paper draft. David Milledge from the Durham University helped in photogrammetric analysis of aerial images provided by Harald Aas from the Norwegian Polar Institute. Thanks also to friends from Association of Polar Early Career Scientists for shaping together the future of polar research. Critical reviews by Alan Trenhaile and Grzegorz Rachlewicz significantly improved the manuscript.

## References

- ANDRÉ M.-F. 1997. Holocene rockwall retreat in Svalbard: a triple-rate evolution. *Earth Surface and Processes and Landforms* 22: 423–440.
- AOKI H. and MATSUKURA Y. 2007. A new technique for non destructive field measurement of rock-surface strength: an application of the Equotip hardness tester to weathering studies. *Earth Surface Processes and Landforms* 32: 1759–1769.
- ARÉ F.E. 1988. Thermal abrasion of sea coasts. *Polar Geography and Geology* 12: 1–157.
- ARÉ F., REIMNITZ E., GRIGORIEV M., HUBBERTEN H.-W. and RACHOLD V. 2008. The influence of cryogenic processes on the erosional Arctic shoreface. *Journal of Coastal Research* 24: 110–121.
- BALLANTYNE C.K., BLACK N.M. and FINLAY D.P. 1989. Enhanced boulder weathering under late-lying snowpatches. *Earth Surface Processes and Landforms* 14: 745–750.
- BLANCO-CHAO R., PÉREZ-ALBERTI A., TRENHAILE A.S., COSTA-CASAS M. and VALCÁRCEL-DÍAZ M. 2007. Shore platform abrasion in a para-periglacial environment, Galicia, northwestern Spain. *Geomorphology* 83: 136–151.
- BYRNE M.-L. and DIONNE J.-C. 2002. Typical Aspects of Cold regions Shorelines. In: K. Hewitt, M.-L. Byrne, M. English and G. Young (eds) *Landscapes in Transition. Landform Assemblages and Transformations in Cold Regions*. Kluwer Academic Publishers, Dordrecht: 141–158.
- CHELLI A., PAPPALARDO M., LLOPIS I.A. and FEDERICI P.B. 2010. The relative influence of lithology and weathering in shaping shore platforms along the coastline of the Gulf of La Spezia (NW Italy) as revealed by rock strength. *Geomorphology* 118: 93–104.

- CRUSLOCK E.M., NAYLOR L.A., FOOTE Y.L. and Swantesson J.O. 2010. Geomorphologic equifinality: A comparison between shore platforms in Höga Kusten and Flörö, Sweden and the Vale of Glamorgan, South Wales, UK. *Geomorphology* 114: 78–88.
- DAHL E. 1946. On the origin of the strandflat. *Norsk Geografisk Tidsskrift* 11: 159–172.
- DALLMANN W.K., PIPEJOHN K. and BLOMEIER D. 2004. *Geological map of Billefjorden, Central Spitsbergen, Svalbard with geological excursion guide 1:50 000*. Norsk Polarinstitut Tematkart 36.
- DAY M.J. and GOUDIE A.S. 1977. Field assessment of rock hardness using the Schmidt test hammer. *British Geomorphology Research Group Technical Bulletin* 18: 19–29.
- DICKSON M.E., KENNEDY D.M. and WOODROFFE C.D. 2004. The influence of rock resistance on coastal morphology around Lord Howe Island, Southwest Pacific. *Earth Surface Processes and Landforms* 29: 629–643.
- DIONNE J.-C. 1989. The role of ice and frost in tidal marsh development – a review with particular reference to Québec, Canada. In: E.C.F. Bird and D. Kelletat (eds) *Zonality of coastal Geomorphology and Ecology. Essener Geographische Arbeiten* 18: 171–210.
- DIONNE J.-C. and BRODEUR D. 1988. Frost weathering and ice action in shore platform development, with particular reference to Quebec, Canada. *Zeitschrift für Geomorphologie. Supplement Band* 71: 117–30.
- EVANS D.J.A., ARCHER S. and WILSON D.J.H. 1999. A comparison of the lichenometric and Schmidt Hammer dating techniques based on data from the proglacial areas of some Icelandic glaciers. *Quaternary Science Reviews* 18: 13–41.
- FORBES D.L. (ed.). 2011. *State of the Arctic Coast 2010 – Scientific Review and Outlook*. International Arctic Science Committee, Land-Ocean Interactions in the Coastal Zone, Arctic Monitoring and Assessment Programme, International Permafrost Association. Helmholtz-Zentrum, Geesthacht, Germany: 178 pp. <http://arcticcoasts.org>
- FORMAN S., LUBINSKI D., INGOLFSSON O., ZEEBERG J., SNYDER J., SIEGERT M. and MATISHOV G. 2004. A review of postglacial emergence on Svalbard, Franz Josef Land and Novaya Zemlya, northern Eurasia. *Quaternary Science Reviews* 23: 1391–1434.
- GOUDIE A. 2006. The Schmidt Hammer in geomorphological research. *Progress in Physical Geography* 30: 703–718.
- GÖKTAN R.M. and AYDAY C. 1993. A suggested improvement to the Schmidt Rebound Hardness ISRM method with particular reference to rock machineability. *International Journal of Rock Mechanics* 30: 321–322.
- GUILCHER A., BODERE J.-C., COUDE A., HANSOM J.D., MOIGN A. and PEULVAST J.-P. 1986. The Strandflat problem in Five High Latitude Countries. In: D.J.A. Evans (ed.) *Cold Climate Landforms*. Wiley, Chichester: 351–393.
- HALL K. 1993. Enhanced bedrock weathering in association with late-lying snowpatches – evidence from Livingston Island, Antarctica. *Earth Surface Processes and Landforms* 18: 121–29.
- HOLTEDAHL H. 1998. The Norwegian strandflat – a geomorphic puzzle. *Norsk Geologisk Tidsskrift* 78: 47–66.
- HUMLUM O., INSTANES A. and SOLLID J.L. 2003. Permafrost in Svalbard: a review of research history, climatic background and engineering challenges. *Polar Research* 22: 191–215.
- JAHN A. 1961. Quantitative analysis of some periglacial processes in Spitsbergen. *Zeszyty Naukowe Uniwersytetu Wrocławskiego, Seria B, nr 5, Nauki o Ziemi II*: 3–54.
- KENNEDY D.M., PAULIK R. and DICKSON M.E. 2010. Subaerial weathering versus wave processes in shore platform development: reappraising the Old Hat Island evidence. *Earth Surface Processes and Landforms* 36: 686–694.
- LANTUIT H., OVERDUIN P.P., COUTURE N., ARÉ F., ATKINSON D., BROWN J., CHERKASHOV G., DROZDOV D., FORBES D.L., GRAVES-GAYLORD A., GRIGORIEV M., HUBBERTEN H.-W., JORDAN J., JORGENSEN T., ØDEGÅRD R.S., OGORODOV S., POLLARD W., RACHOLD V., SEDENKO S., SOLOMON S., STEENHUISEN F., STRELETSKAYA I., VASILIEV A. and WETTERICH S. 2011. The ACD coastal database: a new classification scheme and statistics on Arctic permafrost coastlines. *Estuaries and Coasts*: doi:10.1007/s12237-010-9362-6.



- LIM M., PETLEY D.N., ROSSER N.J., ALLISON R.J., LONG A.J. and PYBUS D. 2005. Combined digital photogrammetry and time-of-flight laser scanning for monitoring cliff evolution. *The Photogrammetric Record* 20: 109–129.
- LIM M., ROSSER N.J., ALLISON R.J. and PETLEY D.N. 2010. Erosional processes in the hard rock coastal cliffs at Staithes, North Yorkshire. *Geomorphology* 114: 12–21.
- MAŁECKI K. 2009. *Zmiany zasięgów i geometrii lodowców otoczenia Petuniabukta (Ziemia Dicksona, Spitsbergen) w XX i XI wieku. (Changes in the extent and geometry of glaciers in Petuniabukta region (Dicksonland, Spitsbergen) in 20<sup>th</sup> and 21<sup>st</sup> century)*. Unpublished M.Sc. thesis (in Polish). Faculty of Geographical and Geological Sciences, Adam Mickiewicz University, Poznań: 149 pp.
- MATTHEWS J.A. and SHAKESBY R.A. 1984. The status of the “Little Ice Age” in southern Norway: relative age dating of Neoglacial moraines with Schmidt Hammer and lichenometry. *Boreas* 13: 333–46.
- MERCIER D. 2008. Paraglacial and paraperiglacial landsystems: concepts, temporal scales and spatial distribution. *Géomorphologie: Relief, Processus, Environment* 4: 223–234.
- MIGON P. 1997. Post-emergence modification of marine cliffs and associated shore platforms in periglacial environment, SW Spitsbergen: implications for the efficacy of cryoplanation processes. *Quaternary Newsletter* 81: 9–17.
- MOIGN A. 1974. Géomorphologie du strandflat au Svalbard: problèmes (age, origine, processus), méthodes de travail. *Inter-Nord* 13-14: 67–72.
- MOIGN A. 1976. L’Action des glaces flottantes sur le littoral et les fonds marins du Spitsberg central et nord-occidental. *La Revue de la Géographie de Montreal* 30: 51–64.
- NANSEN F. 1922. The strandflat and isostasy. *Videmkapselskapets Skrifter. I. Mat.-Naturu. Klasse*. 1921. No. 11: 313 pp.
- NIEDZIELSKI T., MIGON P. and PLACEK A. 2009. A minimum sample size required for Schmidt Hammer measurements. *Earth Surface Processes and Landforms* 34: 1713–1725.
- NIKIFOROV S., PAVLIDIS Y., RACHOLD V., GRIGORYEV M., RIVKIN M., IVANOVA N. and KOREISHA M. 2005. Morphogenetic classification of the Arctic coastal zone. *Geo-Marine Letters* 25: 89–97.
- ØDEGÅRD R.S. and SOLLID J. L. 1993. Coastal cliff temperatures related to the potential for cryogenic weathering processes, western Spitsbergen, Svalbard. *Polar Research* 12: 95–106.
- ØDEGÅRD R.S., ETZELMÜLLER B., VATNE G. and SOLLID J. 1995. Nearsurface spring temperatures in an Arctic coastal cliff: possible implications of rock breakdown. In: O. Slaymaker (ed.) *Steepland geomorphology*. Wiley, Chichester: 89–102.
- PORTER N.J. and TRENHAILE A.S. 2007. Short-term rock surface expansion and contraction in the intertidal zone. *Earth Surface Processes and Landforms* 32: 1379–1397.
- PORTER N.J., TRENHAILE A.S., PRESTANSKI K.J. and KANYAYA J.I. 2010. Patterns of surface down-wearing on shore platforms in eastern Canada. *Earth Surface Processes and Landforms* 35: 1793–1810.
- PRZYBYŁAK R., KEJNA M., ARAŻNY A., MASZEWSKI R., GLUZA A., HOJAN M., MIGAŁA K., SIKORA S., SIWEK K. and ZWOLIŃSKI Z. 2007. Porównanie warunków meteorologicznych na zachodnim wybrzeżu Spitsbergenu w sezonie letnim 2006 r. In: R. Przybylak, M. Kejna, A. Arażny and P. Głowacki (eds) *Abiotyczne środowisko Spitsbergenu w latach 2005–2006 w warunkach globalnego ocieplenia*. Wydawnictwo Zakładu Klimatologii, UMK, Toruń: 179–194.
- RACHLEWICZ G. 2010. Paraglacial modifications of glacial sediments over millennial to decadal time-scales in the high Arctic (Billefjorden, central Spitsbergen, Svalbard). *Quaestiones Geographicae* 29: 59–67.
- RACHLEWICZ G. and SZCZUCIŃSKI W. 2008. Changes in permafrost active layer thermal structure in relation to meteorological conditions, Petuniabukta, Svalbard. *Polish Polar Research* 28: 261–278.
- RACHLEWICZ G., SZCZUCIŃSKI W. and EWERTOWSKI M. 2007. Post-“Little Ice Age” retreat rates of glaciers around Billefjorden in central Spitsbergen, Svalbard. *Polish Polar Research* 28: 159–186.
- RACHOLD V., ARE F., ATKINSON D., CHERKASHOV G. and SOLOMON S. 2005. Arctic Coastal Dynamics (ACD): an introduction. *Geo-Marine Letters* 25: 63–68.

- RAPP A. 1960. Talus slopes and mountain walls at Tempelfjorden, Spitsbergen – a geomorphological study of the denudation of slopes in an Arctic locality. *Norsk Polarinstitutt Skrifter* 119: 96 pp.
- SALVIGSEN O. 1984. Occurrence of pumice on raised beaches and Holocene shoreline displacement in the inner Isfjorden area, Svalbard. *Polar Research* 2: 107–113.
- SELBY M.J. 1980. A rock mass strength classification for geomorphic purposes: with test from Antarctica and New Zealand. *Zeitschrift für Geomorphologie* 24: 31–51.
- SHAKESBY R.A., MATTHEWS J.A. and OWEN G. 2006. The Schmidt hammer as a relative-age dating tool and its potential for calibrated age dating in Holocene glaciated environments. *Quaternary Science Reviews* 25: 2846–2867.
- STEPHENSON W.J. and KIRK R.M. 2000a. Development of shore platforms on Kaikoura Peninsula, South Island, New Zealand. Part One: The role of waves. *Geomorphology* 32: 21–41.
- STEPHENSON W.J. and KIRK R.M. 2000b. Development of shore platforms on Kaikoura Peninsula, South Island, New Zealand. Part Two: The role of subaerial weathering. *Geomorphology* 32: 43–56.
- STRELETSKAYA I.D., VASILIEV A.A. and VANSTEIN B.G. 2009. Erosion of sediment and organic carbon from the Kara Sea coast. *Arctic, Antarctic, and Alpine Research* 41: 79–87.
- SZCZUCIŃSKI W., ZAJĄCZKOWSKI M. and SCHOLTEN J. 2009. Sediment accumulation rates in sub-polar fjords – Impact of post-Little Ice Age glaciers retreat, Billefjorden, Svalbard. *Estuarine, Coastal and Shelf Science* 85: 345–356.
- THORNTON L.E. and STEPHENSON W.J. 2006. Rock Strength: A Control of Shore Platform Elevation. *Journal of Coastal Research* 22: 224–231.
- TRENHAILE A.S. 1983. The development of shore platforms in high latitudes. In: D.E. Smith and A.G. Dawson (eds) *Shorelines and Isostasy*. Institute of British Geographers, Special publication No. 16, London: 77–96.
- TRENHAILE A.S. 1997. *Coastal Dynamics and Landforms*. Oxford University Press, Oxford: 366 pp.
- TRENHAILE A.S. 2001. Modelling the effect of weathering on the evolution and morphology of shore platforms. *Journal of Coastal Research* 17: 398–406.
- TRENHAILE A.S. and MERCAN D.W. 1984. Frost weathering and the saturation of coastal rocks. *Earth Surface Processes and Landforms* 9: 321–331.
- TRENHAILE A.S., PEPPER D.A., TRENHAILE R.W. and DALIMONTE M. 1998. Stacks and Notches at Hopewell Rocks, New Brunswick, Canada. *Earth Surface Processes and Landforms* 23: 975–988.
- TRENHAILE A.S., PORTER N.J. and KANYAYA J.I. 2006. Shore platform processes in eastern Canada. *Géographie Physique et Quaternaire* 60: 19–30.
- VILES H., GOUDIE A., GRAB S. and LALLEY J. 2011. The use of the Schmidt Hammer and Equotip for rock hardness assessment in geomorphology and heritage science: a comparative analysis. *Earth Surface Processes and Landforms* 36: 320–333.
- WANGENSTEEN B., EIKEN T., ODEGARD R.S. and SOLLID J.L. 2007. Measuring coastal cliff retreat in the Kongsfjorden area, Svalbard, using terrestrial photogrammetry. *Polar Research* 26: 14–21.
- WERENSKIOLD W. 1952. The Strand Flat of Spitsbergen. *Geografisk Tidsskrift* 52: 302–309.
- WINKLER S. 2009. First attempt to combine terrestrial cosmogenic nuclide ( $^{10}\text{Be}$ ) and Schmidt hammer relative-age dating: Strauchon Glacier, Southern Alps, New Zealand. *Central European Journal of Geosciences* 1: 274–290.

Received 30 March 2011

Accepted 24 June 2011

# COLD SHORES IN WARMING TIMES – CURRENT STATE AND FUTURE CHALLENGES IN HIGH ARCTIC COASTAL GEOMORPHOLOGICAL STUDIES

MATEUSZ CZESŁAW STRZELECKI

Adam Mickiewicz University in Poznań, Faculty of Geographical and Geological Sciences, Poland  
& Durham University, Department of Geography, Quaternary Environmental Change Group, UK

Manuscript received:

Revised version:

STRZELECKI M.C., Cold shores in warming times – current state and future challenges in Arctic coastal evolution studies. *Quaestiones Geographicae* 30(3), Bogucki Wydawnictwo Naukowe, Poznań, pp. 103–115, 6 Figs. ISBN 978-83-62662-75-3. ISSN 0137-477X. DOI 10.2478/v10117-011-0030-0

**ABSTRACT.** Many of the existing intellectual paradigms regarding the functioning of the polar coastal zone are now out-dated, based on descriptive geomorphology and a limited process-based understanding. Currently, among many components of Arctic landscape adjusting to global warming, the coastal zone is probably the most critical one both in terms of rapidity of environmental change as well as importance for human communities living in circumpolar regions. This issue was often raised during the 4th International Polar Year 2007–2008 and encouraged the scientific community to focus on the state of cold region coasts in more detail. In this paper I summarize the most recent developments in Arctic coastal geomorphology with a particular focus on the Svalbard Archipelago and draw attention to the research challenges awaiting further investigation. This paper highlights the need for a greater understanding of the controls on High Arctic coastal geoecosystems, especially given the potential for accelerated warming and sea-level rise in the coming decades and centuries. Many of presented views benefited from discussions with Professor Andrzej Kostrzewski – to whom this volume is dedicated.

**KEYWORDS:** cold region coastal geomorphology, global warming, sea-level change, High Arctic landscape dynamics, Svalbard.

Matt Strzelecki, Durham University, Department of Geography, Science Site, South Road, Durham DH1 3LE, UK  
e-mail: mat.strzelecki@gmail.com

## The coasts of neglect

Understanding the transition of Arctic regions, which in recent years have undergone a rapid environmental change in response to climate warming (Serreze *et al.* 2000; ACIA 2005; NorACIA 2011) is of crucial importance for the interpretation of Earth system reaction to former glaciations and climate shifts as well as more ac-

curate prediction of future scenarios of global climate change. The tremendous research efforts undertaken during the 4<sup>th</sup> International Polar Year 2007–2008 have revealed that the Arctic is already experiencing the strongest air and sea temperature rise on Earth. This process directly and indirectly changes the nature of the Arctic coastal zone. Of particular interest is the reaction of Arctic coastal geoecosystems to increased

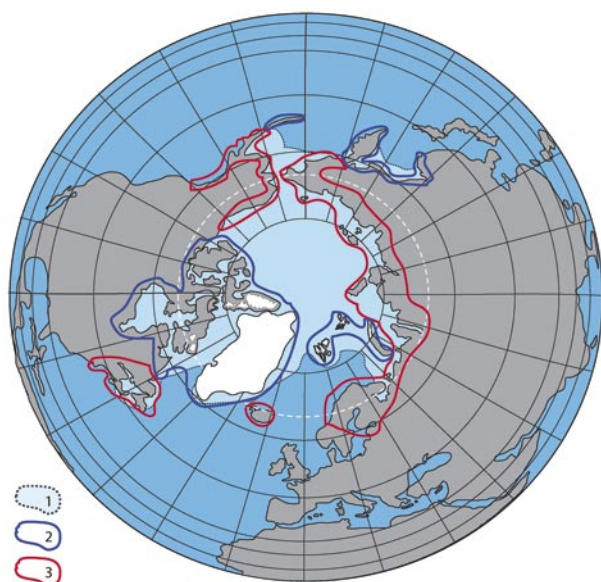


Fig. 1. Simplified map of cold region coasts in the northern hemisphere (modified after Byrne & Dionne 2002).

1 - Extent of winter sea ice cover; 2 - Zone of relatively well-studied cold region coasts with running coastal erosion monitoring programmes, and number of high quality papers published in a last decade. 3 - Zone of still relatively poorly studied cold region coasts where the mechanisms controlling coastal evolution remain unknown.

sediment and nutrient supply from land as well as increasing open-water conditions leading to intensified shoreline erosion and sediment transport. The recently published report 'The State of Arctic Coast 2010 Report' (Forbes *et al.* 2011) suggests that circumpolar coastal zone (Fig.1) is the key interface in the entire Arctic characterized by 'most rapid and severe environmental changes which have serious implications for communities living on coastal resources'. However, many of the existing opinions regarding the functioning of polar coasts based on limited observations are invalid and reduces our ability to understand current mechanisms controlling the present state of this fragile zone and do not deliver any sort of prediction of its future evolution. Not only is the number of academic papers on high latitude coastal environments lower than from temperate and tropical regions, but also their qualitative nature seems to be insufficient to allow numerical modelling and more sophisticated data analyses. In contrast to lower latitude coasts little is known regarding the potential impact of climate and sea-level change on high latitude coastal margins. This relative lack of research advance has persisted for several decades. This is highlighted by the

remark from Trenhaile (1983) that 'there is a lack of even basic agreement on the efficiency of coastal processes in the high latitudes' then almost twenty years later Byrne & Dionne (2002) reviewing the state of high latitude coastal geomorphology still had to admit that coastlines, accounting for at least 30% of the world coasts, have been neglected and studies on their nature are very limited. Most recently Lantuit *et al.* (2011) indicated that only 1% of Arctic coastlines have been investigated in sufficient detail to allow quantitative description of processes operating on them. One of the key messages found in all major papers reviewing the developments in cold region coastal studies is the need for long-term coastal change monitoring and selection of core geo-indicators which could be analyzed in a unified way under the umbrella of a circumpolar observation network (e.g. John & Sugden 1975, Forbes & Taylor 1994, Trenhaile 1997, Byrne & Dionne 2002, Urdea 2007, Forbes *et al.* 2011). Though knowledge of the response of the coastal zone to climate change is fundamental to understanding polar landscape adjustment to global warming, we still cannot precisely measure the rate and scale of changes for vast areas of the Arctic. At the heart of the problem lies a mismatch between out-dated concepts based on short field observations and the lack of the studies linking Arctic coastal evolution with transformation of Arctic landscape occurring during climate shifts on millennial (glacials/interglacial), decadal (e.g. changes in atmospheric circulation patterns such as NAO/AO) and seasonal (i.e. the duration of snow cover, high/low precipitation, high/ low air temperatures, strong/weak winds etc.) timescales.

### 'Known knowns, known unknowns and unknown unknowns'

Cold region coasts are typically defined as 'those areas where frost and ice processes are active during a period of the year which is sufficient to have a significant, if not permanent, impact on the near terrestrial, coastal and marine environments' (Byrne & Dionne 2002). Several authors (e.g. Forbes & Taylor 1994, Trenhaile 1997) noticed that many morphological aspects (cliffs, beaches, barriers, dunes, spits, embayments, lagoons) and proc-





Fig. 2. High Arctic coastal environments in northern Billefjorden:

1 – sandstone boulder-strewn beach in northern Adolfbukta; 2 – plunging metamorphic rock cliffs in northern Adolfbukta; 3 – weathered rock cliffs and mixed sand-gravel barrier in eastern Petuniabukta; 4 – gravel barrier in eastern Petuniabukta; 5 – tidal flat (right), gravel spit (middle) and lagoon (left) in northern Petuniabukta; 6 – spit platform developing at the mouth of Ebbaelva (background), at the front uplifted beach sequences in NE Petuniabukta; 7 – tidal creek in central part of tidal flat (northern Petuniabukta); 8 – High Arctic salt marsh in NE Petuniabukta.



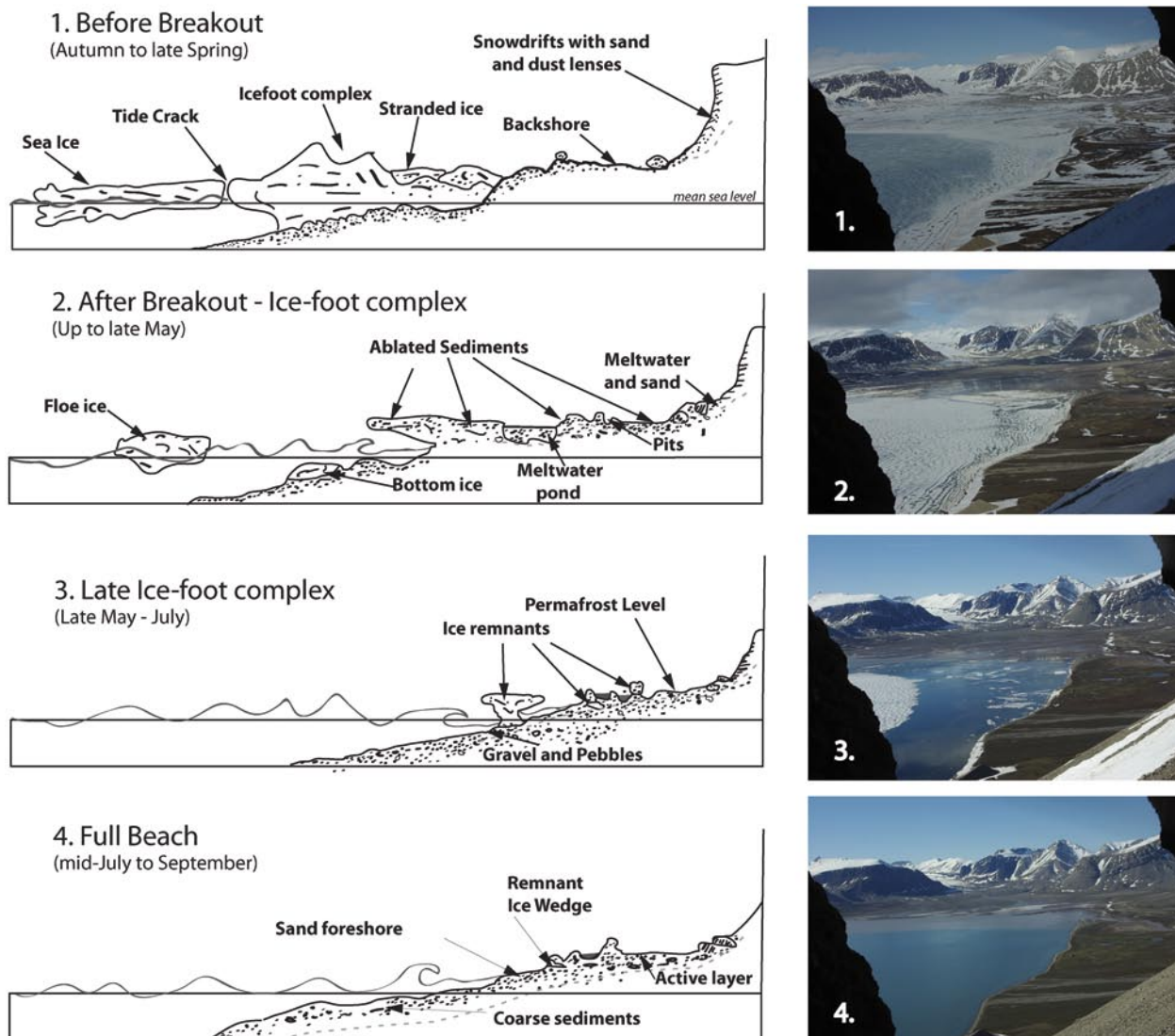


Fig. 3. Seasonal changes in polar beach profiles (sketches after Hansom and Kirk 1989) as they adjust to open water conditions. On the right examples of different stages of beach evolution from Petuniabukta (images taken by time-lapse camera installed on Wordiekammen massif in years 2009–2010)

esses (tides, currents, waves) operating on coasts in cold environments (Fig. 2) are similar to those from lower latitudes. What distinguishes them, however, are the effects of permafrost, ground ice, frost action, sea ice, snow cover, isostasy, glacial history and other zonal factors on coastal morphodynamics. It is important to notice that the scientific description of cold region coastal environments is characterized by many discrepancies. For instance, tremendous effort of Canadian researchers in last 40 years brought a major advance in our understanding of processes controlling Arctic tidal flats and development of the term *glacielto* to describe ice-influenced land-forms, sediments, processes in marine, coastal,

estuarine, lacustrine and fluvial environments (e.g. Dionne 1968, 1969, 1988, 1989; Drake & McCann 1982; McCann *et al.* 1981; McCann & Dale 1986; Dale *et al.* 2002). Also Arctic beach environments (Fig. 3) have been solicitously described in many sites (e.g. Rex 1964; Hume & Schalk 1964a, 1964b, 1967, 1976; Zenkovitch 1967; King & Buckley 1968; McCann & Owens 1969; Green 1970; Owens & McCann 1970; McCann & Taylor 1975; Rosen 1978; Taylor 1978; Reinson & Rosen 1982; Sempels 1987; Reimnitz *et al.* 1990; Barnes *et al.* 1993, Campeau & Héquette 1995) whereas to date there have been relatively few studies investigating Arctic rocky coasts (e.g. Jahn 1961; Nielsen 1979; Dionne & Brodeur 1988, Fournier &

Allard 1992; Ødegård & Sollid 1993; Ødegård *et al.* 1995; Lundberg & Lauritzen 2002; Wagensteen *et al.* 2007; Strzelecki 2011). This gap is even more profound if we take into consideration that up to 35% of Arctic coastlines are rock-dominated (Lantuit *et al.* 2011). The classic example showing the research stagnation in revealing the complexity of high latitude rocky coastal zone is the longstanding controversy regarding the origin of strandflats. This has been a regular topic for discussion in the geomorphological literature for almost a century (Nansen 1922; Guilcher *et al.* 1986; Holtedahl 1998) and a debate on the efficiency of periglacial shoreline evolution, with enthusiasts of slow (Zenkovich 1967) and relatively rapid shore evolution (Jahn, 1961).

Furthermore, the development in Arctic coastal geomorphology is marked by significant regional contrast. The last decade has seen major developments in Arctic coastal research due to research from the Arctic Coastal Dynamics (ACD) Group (Rachold *et al.* 2005; Overduin *et al.* 2007; Lantuit & Pollard 2008, Lantuit *et al.* 2011). Another important step was the reopening of Russian works to the wider scientific community, especially in the field of thermoabrasion and coasts formed in the Yedoma formation (e.g. Aré 1988; Nikiforov *et al.* 2005; Leontiev 2006; Aré *et al.* 2008; Lukyanova *et al.* 2008; Streletskaia *et al.* 2009). The major focus in these initiatives has been the understanding and modelling of ice-rich permafrost along Alaskan and Siberian coastlines. The study by Lantuit *et al.* (2011) indicated that in comparison to Beaufort and Laptev Sea coastlines, the coasts of High Arctic archipelagos such as Svalbard, Franz Josef Land, the Canadian Arctic Archipelago (CAA) and Greenland, whose melting ice masses contribute the most to present-day sea level rise, are still poorly recognized. Nevertheless, thanks to research projects carried out by ACD (Fig. 4) we can consider the beginning of the 21<sup>st</sup> century as a *golden decade* of Arctic coastal studies. Their main findings and predictions from the perspective of coastal geomorphology are:

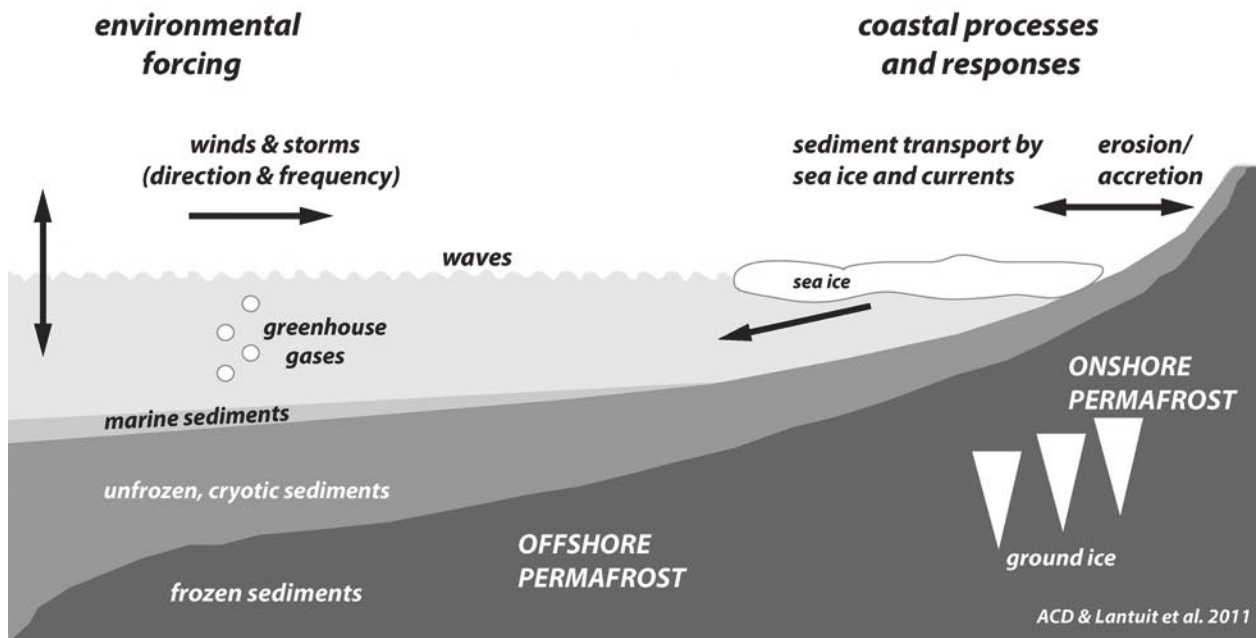
- the expected strong link between Arctic coastal evolution in coming decades and climate warming;
- the duration, intensity and number of storms entering the Arctic has already increased and

the wave influence on the Arctic coasts will continue to intensify with implications for accelerated erosion;

- the changing Arctic sea-ice regime and the timing of ice break-up and freeze-up may result in further reduction of coastal protection from waves (in last decade sea-ice extent reached record minima in extent and perennial ice has been reduced by almost 50% in extent);
- the increased sea-surface temperatures, longer ice-free periods and intensified thawing of subsea, coastal and inland permafrost leads to rapid erosion and retreat of Arctic coasts as it was documented in recent years in Alaska and Siberia. ACD calculations of mean rates of coastal retreat in the last decades are typically in the 1–2 m/year range, but vary up to 10–30 m/year along the Beaufort Sea, the East Siberian Sea, and the Laptev Sea. ACD proved that previous reports underestimated the sediment and carbon supply from Arctic coasts to the ocean;
- the existence of a strong link between sea-level rise in the Arctic coastal zone and warming of the coastal waters as well as increased water freshening;
- the rise in sea level is expected to enhance coastal erosion and affect sediment transport in coastal areas (various IPCC models show higher sea-level rise in the Arctic than mean-global rise);
- glacial legacy (glacioisostatic uplift/subsidence) is a dominant factor controlling the relative sea-level change and is characterized by strong regional contrasts e.g. Canadian Arctic Archipelago with emerging central part and submerging margins;
- climate warming leads to increased Arctic river discharge and sediment supply to the coastal zone. However, in some locations increased terrestrial sediment delivery is not sufficient to balance the negative changes caused by sea-level rise and storm flooding, what leads to submergence and erosion of Arctic deltas, e.g. the second largest Arctic delta, the Mackenzie Delta, is retreating dozens of meters per year.

Currently, the leaders of ACD are planning the organisation of the Arctic Circumpolar Coastal Observatory Network, which should cover more

### A) PROCESSES ACTIVE ON ARCTIC PERMAFROST COASTS (e.g. SIBERIA)



### B) PROCESSES ACTIVE ON HIGH ARCTIC PARAGLACIAL COASTS (e.g. SVALBARD)

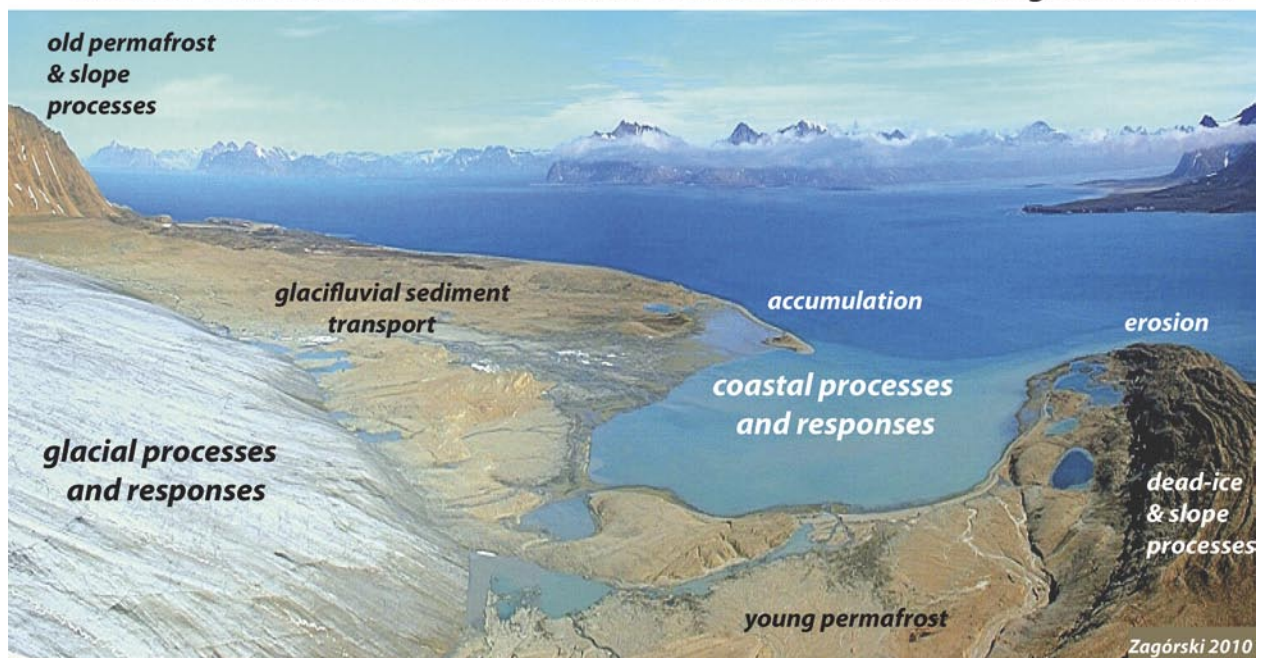


Fig. 4. Functioning of Arctic coastal zone:

A – model developed by Arctic Coastal Dynamics Group for ice-rich permafrost coasts characteristic for Siberian and Alaskan coasts (after Lantuit *et al.* 2011); B – the complexity of High Arctic coastal adjustment to glacier retreat – no model exists (Photo by Piotr Zagórski, 2010, illustrating paraglacial coastal system in Bellsund, Spitsbergen).

sites in the High Arctic and diametrically change the regional disproportion. It is then important to ask what kind of research challenges await the scientific community along the High Arctic coasts.

### High Arctic enigma

To date coastal research in High Arctic settings has been strongly linked to the successful application of the paraglaciation concept (*sensu*

Slaymaker, 2011) in cold region geomorphological studies. During the 1990s French geomorphologists dominated research on High Arctic paraglacial coastal systems. Their research focused on the response of the coastal zone to changes in glacial systems. Héquette & Ruz (1990) and Héquette (1992) suggested that although High Arctic coasts are thought to be low energy in a certain conditions they can transform very rapidly. Their study on coastal margins of glaciofluvial outwash plains in northwest Spitsbergen (Brøgger Peninsula) documented a whole mosaic of abrupt changes in coastal morphology during the short Arctic summer with coexisting episodes of erosion and deposition, formation of new and cannibalization of old barriers, deposition of micro-deltas, landward and seaward migration of coastlines depended on rate of glaciofluvial activity in the surrounding and ability of storm waves to overwash barrier crests.

Mercier & Laffly (2005) linked the periods of intensified sediment supply, associated with the post-Little Ice Age (LIA) retreat of Pedersenbreen, Austre, Midre and Vestre Lovénbreen with coastal progradation. During the last 30 years, the mean annual coastal progradation along studied section of Kongsfjorden was 3 m. It has also been noted that in coastal sections where glaciofluvial sediment delivery was reduced shoreline recession was observed. This study demonstrated the high sensitivity of Svalbard coasts to mechanisms controlling the supply of sediments from deglaciated catchments. In this respect their work confirmed earlier observations from Atlantic Canada, made by Forbes and Taylor (1987) who recorded on-shore migration of gravel barriers during periods of sediment shortage and spit extension after an increase in sediment input. In more sheltered area of Spitsbergen, centrally located – Petuniabukta, characterized by limited fetch and prolonged sea-ice conditions, Strzelecki (2011) reported similar rates of coastal adjustment. This research suggests that High Arctic coasts fed by paraglacially reworked and transported sediments deserve a new model, which will properly reflect the interplay between sediment supply, sea-level change and glacial landscape transition. This is important because many sections of the Svalbard coast are clearly still responding to a combination of ongoing paraglacial and coastal processes.

In recent decades paraglacial processes have become one of the most effective geomorphological processes on Svalbard, reducing the impact of glacial processes to a secondary role in landscape transformation (Laffly & Mercier 2002, Rachlewicz 2010). Also the previous natural shoreline protection in the form of sea-ice, ice-foot complex and snow cover now disappear earlier and form later in the season allowing warmer and stormier sea conditions to access unconsolidated shorelines.

Based on several environmental monitoring case studies on Strokdammane Plain (W Spitsbergen) Akerman (2008) proposed a geoecological model of Svalbard coasts under global warming conditions (Fig. 5). Akerman predicts that prolonged duration of the open waters will be critical to the future impacts of coastal and near-coastal processes and environments in sites such as Svalbard. With frequent storms abrading unprotected shores additionally destabilized by thawing permafrost, flooding of coastal lowlands, high and wide barrier systems blocking stream outlets, Svalbard coastal geoecosystem will change rather abruptly.

On the other hand, Ziaja *et al.* (2009) already documented a whole cycle of coastal landscape transition related to the post-LIA deglaciation of Humbergbukta in SE Sorkapp which highlighted the role of changes in the High Arctic coastal zone as a simulator of polar life expansion. Retreat of Hambergbreen and other surrounding glaciers not only led to formation of new coastlines which quickly become transformed by coastal processes, but also exposed new areas for plant succession and animal colonization.

Another example of Svalbard coastal zone adjustment to climate warming and change in sediment delivery pathways was a study on the decadal-scale shoreline dynamics of Calypsotranda carried by Zagórski (2011). His investigations, combining remote sensing and field-based observations indicated the dominance of coastal erosion over accumulation with maximum coastal retreat upto 100 m, regardless of the retreat of surrounding glaciers and increased sediment supply to the fjord system. In addition, based on a study of post-LIA geosuccession in Recherfjorden region Zagórski *et al.* (in preparation) developed a concept of direct and indirect glacial in-



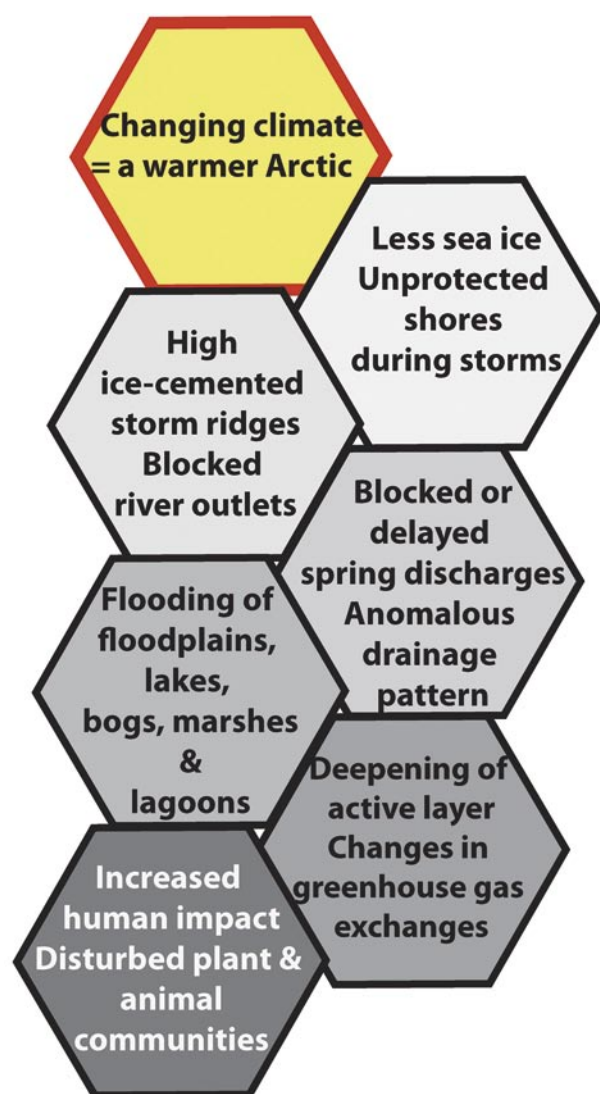


Fig. 5. Scenario of geoeological changes of Svalbard coasts under global warming conditions (modified after Akerman 2008).

fluence on High Arctic coastal evolution which differentiates coasts formed after retreat of tide-water glaciers from coasts formed due to intensification of sediment delivery from valley-glacier systems. The direct influence of glacier systems on the coastal zone was previously documented by Nielsen (1992) in West Greenland. The retreat of the tide-water glacier Equip Sermia after the 1920s advance led to the transformation of a lateral moraine into a barrier spit and formation of a lagoon system in just 70 years. Nielsen argued that such a rapid landform transformation has serious implications for Holocene landscape interpretation, especially in case of landform and sediment assemblages related to tide-water glacier systems.

He also postulated a role of high waves induced by ice-berg roll from calving in over-washing and reshaping High Arctic coastal barriers, leading to the formation of boulder barricades and beaches. It has to be stated that the role of landslide (paraglacial) or ice-berg induced tsunami waves on the Arctic coastal morphology has never been studied in detail. Later on, Nielsen (1994) expanded his concept of glacier/coastal interaction during the study of Arctic delta in Sermilik Fjord. This is a key work documenting the sensitivity of the high latitude coastal zone to post-LIA landscape transition from glacier into paraglacial dominated geoecosystem and the rapidity with which such change can occur. During one century the delta system experienced all stages of evolution from rapid formation after retreat of Mitdluagkat glacier; progradation in response to intensified sediment supply; development of spits, barriers, tidal island and tombolos; finally to a degradation by waves and currents under rising sea-level conditions after reduction of delivery from glacier catchment. More recently Hansen (2004) illustrated the complexity of a High Arctic delta system response (Hall Bredning-Scoresby Sund, East Greenland) to change in topography, sediment supply, rate of deglaciation and shifts in climate on the Holocene timescale. Hansen's model can be adapted to hundreds of small and sheltered Arctic fjords deglaciated during the Holocene; it also proves that High Arctic coastal environments may serve as a useful tool in reconstructing environmental change.

## Stories to be rewritten

One of the classic examples of the application of sedimentological survey of coastal landforms in palaeogeographical reconstruction is a study by Lønne & Nemec (2004) on High Arctic coastal fan delta in Advenfjorden (Spitsbergen). By detailed sedimentological analysis of fan depositional structures they demonstrated the importance of fan deltas as a proxy record of deglaciation history and environmental change in a High Arctic terrain, especially important in regions characterized by low preservation of glacial sediments and landforms. The small fan system developing at the foot of Hiorthfjellet was a very precise re-



corder of the interplay between terrestrial and marine processes adjusting to shifts in sediment delivery from retreating glacier as well as fluctuations of a sea-level. This study, apart from documenting in an unprecedented detail the sedimentology of a polar fan system fed by glacier streams, snow melt and degrading permafrost, also provided the first well-dated onshore proof for a Mid-Holocene transgression in central Spitsbergen. Surprisingly, even after this important research, the significance of cold region coastal fan systems still remains unrecognized.

Another important story can be added to reconstruction of polar landscapes by studying the sedimentology of gravel-dominated storm ridges preserved in many uplifted marine sequences across High Arctic region. In Andr  eland (NW Spitsbergen) Br  ckner *et al.* (2002) and Br  ckner & Schellmann (2003) postulated that uplifted beach ridges may help us decipher the glacio-isostatic and palaeoceanographic changes. They based their hypothesis on the assumption that conditions favourable for formation of beach ridges reflects existence of ice-free conditions associated with retreat of glacier systems and open-water summer season with wave and current activity. In the case of Woodfjorden and Wijdefjorden, formation of hundreds of Holocene beach ridges was possible only due to climate warming which lead to retreat of the glacier, opening of the fjord and entrance of warm waters brought by the West Spitsbergen Current securing removal of sea ice and open water conditions in summer months. More recently St-Hilaire-Gravel *et al.* (2010) studied the topography and sedimentology of uplifted beach ridges on Lowther Island (CAA) in order to test their ability to record past wave intensity and sea-ice conditions. However, reflecting only local conditions they suggested that better-developed beach ridges can be associated with periods of prolonged wave activity (increased duration of ice free periods). One future direction of research might be to compare the onshore record (beach ridges, coastal fan deltas) with the offshore record from ocean cores collected across the High Arctic to shed new light on the history of sea ice and ocean currents.

## Action instead of conclusions

I strongly believe that the described gap in understanding of High Arctic coastal adjustment to global warming conditions represents a great opportunity for the national polar research community. Longstanding history of Polish investigations on Svalbard with environmental monitoring programmes running for decades as well as a network of research stations spread across Spitsbergen constitute a solid basis for an interdisciplinary research project focusing on the functioning of the coastal zone in the heart of the European Arctic. Due to its location at the boundary between oceanic and atmospheric fronts, Svalbard is one of the key areas to study the Arctic sensitivity to climate change. The Svalbard region has, therefore, been an area of many scientific breakthroughs including: palaeo-climate reconstructions (e.g. Isaksson *et al.* 2005); the extent of the last glaciation (e.g. Mangerud *et al.* 1998; Svendsen *et al.* 2004); Holocene sea level changes (e.g. Forman *et al.* 2004); modern and relict glacial systems (e.g. Boulton 1972; L  nne & Lys   2005; Nuth *et al.* 2010); periglacial permafrost processes and mechanisms (e.g. Humlum *et al.*, 2003); ocean water interaction and mixing (e.g.   lubowska-Woldengen *et al.* 2007, Majewski *et al.* 2009). Despite the wealth of research which has been undertaken in Svalbard, there remains a lack of investigation into coastal processes and environments. Previous coastal studies (Mercier & Laffly 2005, Ziaja *et al.* 2009, Strzelecki 2011, Zag  rski 2011) document dramatic changes in sediment flux and coastal response under intervals characterised by a warming climate, retreating local ice masses, a shortened winter sea-ice season and melting permafrost. These terrestrial processes are interacting with glacio-isostatic land emergence and on-going global sea-level rise. The pristine coasts of Svalbard provide a superb opportunity to quantify how High Arctic coasts are responding to rapid climate warming. Nevertheless several crucial research questions are still to be answered including: *What processes control existing Svalbard coasts?; How sensitive is the Svalbard coastal zone to recent increased human impact?; What was the response of the Svalbard coastal zone to intensified glacial recession and sediment supply after the Little Ice Age?; Do coastal processes intensify the*

rate of rock weathering on Svalbard climates?; How did the Svalbard coast and continental shelf respond to climate change, glacier fluctuations and sea ice changes throughout the Holocene?; What is the precision of the morphological and sedimentological records of environmental transformations, climate change and natural disasters along the Svalbard coast?

These research premises and challenges led to the formation of a SVALCOAST research team linking geoscientists from leading national polar research institutions and international scientific partners which in coming years will aim to examine the response of the coastal zone of the Svalbard Archipelago to current climatic warming and multidirectional anthropopression and explore the changes experienced by the coastal landscape during various stages of deglaciation. As well as this, predictions will be made as to the coast's future evolution under scenarios of continuing increases in air temperature and sea-level rise (Strzelecki & Zagórski 2011). Given the diversity of research questions and rapidity of coastal adjustment it seems to be a fascinating challenge!

## Acknowledgements

I would like to thank Professor Andrzej Kostrzewski for many years of excellent supervision, friendship and helping me aim only for the highest goals.



Fig. 6. Prof. Andrzej Kostrzewski and Matt Strzelecki during geomorphological mapping of western coast of Petuniabukta, Spitsbergen August 2007.

Gratitude is directed to Crescendum Est- Polonia Foundation, Adam Mickiewicz University Foundation, Ministry of Science and Higher Education in Poland (grant no. N306284335), National Environmental Research Council in UK and Ustinov College at Durham University supporting my research and career development.

I also thank Jerry Lloyd who gave critical comments on an earlier version of the manuscript. Review by Wiesław Ziaja also improved the manuscript and is highly appreciated.

## References

- AKERMAN J.H., 2008. Coastal Processes and Their Influence Upon Discharge Characteristics of the Strokdammene Plain, West Spitsbergen, *Svalbard. Proceedings of the Ninth International Conference on Permafrost University of Alaska Fairbanks June 29–July 3, 2008* 1: 19–24.
- Arctic Climate Impact Assessment (ACIA) Scientific Report, 2005. Cambridge University Press, Cambridge.
- ARÉ F.E., 1988. Thermal abrasion of sea coasts. *Polar Geography and Geology* 12: 1–157.
- ARÉ F.E., REIMNITZ E., GRIGORIEV M., HUBBERTEN H.-W., RACHOLD V., 2008. The influence of cryogenic processes on the erosional Arctic shoreface. *Journal of Coastal Research* 24: 110–121.
- BARNES P.W., KEMPEN E.W., REIMNITZ E., MCCORMICK M., WEBER W.S., HAYDEN E.C., 1993. Beach profile modification and sediment transport by ice: an overlooked process on Lake Michigan. *Journal of Coastal Research* 9: 65–86.
- BOULTON G.S., 1972. Modern Arctic glaciers as depositional models for former ice sheets. *Journal of Geological Society London* 128: 361–393.
- BRÜCKNER H., SCHELLMANN G., 2003. Late Pleistocene and Holocene shorelines of Andréelund, Spitsbergen (Svalbard) – geomorphological evidence and palaeo-oceanographic significance. *Journal of Coastal Research* 19: 971–982.
- BRÜCKNER H., SCHELLMANN G., VAN DER BORG K., 2002. Uplifted beach ridges in northern Spitsbergen as indicators for glacio-isostasy and palaeo-oceanography. *Zeitschrift für Geomorphologie* 46: 309–336.
- BYRNE M.-L., DIONNE J.-C., 2002. Typical Aspects of Cold regions Shorelines. In: K. Hewitt, M.-L. Byrne, M. English, G. Young (eds.), *Landscapes in Transition. Landform Assemblages and Transformations in Cold Regions*. Kluwer Academic Publishers, Dordrecht: 141–158.
- CAMPEAU S., HÉQUETTE A., 1995. Buttes cryogènes saisonnières de plages arctiques, péninsule de Tuktoyaktuk, Territoires du Nord-Ouest. *Géographie physique et Quaternaire* 49: 265–274.
- DALE J.E., LEECH S., MCCANN B., SAMUELSON G., 2002. Sedimentary characteristics, biological zonation and physical processes of the tidal flats of Iqaluit, Nunavut. In: K. Hewitt, M.-L. Byrne, M. English, G. Young (eds.), *Landscapes in Transition. Landform Assemblages and Transformations in Cold Regions*. Kluwer Academic Publishers, Dordrecht: 205–234.

- DIONNE J.-C., 1968. Morphologie et sédimentologie glacielles, littoral sus du Saint-Laurent. *Zeitschrift für Geomorphologie, Supplement Band 7*: 56–84.
- DIONNE J.-C., 1969. Tidal flat erosion by ice at La Pocatière, St. Lawrence Estuary. *Journal of Sedimentary Petrology* 39: 1174–1181.
- DIONNE J.-C., 1988. Characteristic features of modern tidal flats in cold regions. In: P.L. de Boer et al. (eds.), *Tide influenced sedimentary environments and facies*. Dordrecht: 301–332.
- DIONNE J.-C., 1989. The role of ice and frost in tidal marsh development. A review with particular reference to Quebec, Canada. *Earth Science Reviews* 26: 185–212.
- DIONNE J.-C., BRODEUR D., 1988. Frost weathering and ice action in shore platform development, with particular reference to Quebec, Canada. *Zeitschrift für Geomorphologie, Supplement Band 71*: 117–130.
- DRAKE J.J., MCCANN S.B., 1982. The movement of isolated boulders on tidal flats by ice floes. *Canadian Journal of Earth Sciences* 19: 748–54.
- FORBES D.L. (ed.), 2011. *State of the Arctic Coast 2010 – Scientific Review and Outlook*. International Arctic Science Committee, Land-Ocean Interactions in the Coastal Zone, Arctic Monitoring and Assessment Programme, International Permafrost Association. Helmholtz-Zentrum, Geesthacht, Germany (<http://arcticcoasts.org>).
- FORBES D.L., TAYLOR R.B., 1987. Coarse-grained beach sedimentation under paraglacial conditions, Canadian Atlantic Coast. In: D. Fitzgerald, P. Rosen (eds.), *Glaciated Coasts*. Academic Press, New York: 51–86.
- FORBES D.L., TAYLOR R.B., 1994. Ice in the shore zone and the geomorphology of cold coasts. *Progress in Physical Geography* 18: 59–89.
- FORMAN S., LUBINSKI D., INGOLFSSON O., ZEEBERG J., SNYDER J., SIEGERT M., MATISHOV G., 2004. A review of postglacial emergence on Svalbard, Franz Josef Land and Novaya Zemlya, northern Eurasia. *Quaternary Science Reviews* 23: 1391–1434.
- FOURNIER A., ALLARD M., 1992. Periglacial shoreline erosion of rocky coast: George River Estuary, Northern Quebec. *Journal of Coastal Research* 8: 926–942.
- GREENE H.G., 1970. Microrelief on an arctic beach. *Journal of Sedimentary Petrology* 40: 419–427.
- GUILCHER A., BODERE J.-C., COUDE A., HANSOM J.D., MOIGN A., PEULVAST J.-P., 1986. The Strandflat problem in Five High Latitude Countries. In: D.J. Evans (ed.), *Cold Climate Landforms*. Wiley, Chichester: 351–393.
- HANSEN L., 2004. Deltaic infill of a deglaciated Arctic fjord, East Greenland: Sedimentary facies and sequence stratigraphy. *Journal of Sedimentary Research* 74: 422–437.
- HANSOM J.D., KIRK R.M., 1989. Ice in the intertidal zone: examples from Antarctica. In: E.C.F. Bird, D. Kelletat (eds.), *Zonality of Coastal Geomorphology and Ecology. Essener Geographische Arbeiten* 18: 211–236.
- HÉQUETTE A., 1992. Morphosedimentological dynamics and coastal evolution in the Kongsfjorden area, Spitsbergen. *Polar Geography and Geology* 16: 321–329.
- HÉQUETTE A., RUZ M.-H., 1990. Coastal sedimentation along glacial outwash plain shorelines in northwest Spitsbergen. *Géographie physique et Quaternaire* 44: 77–88.
- HOLTEDAL H., 1998. The Norwegian strandflat – a geomorphic puzzle. *Norsk Geologisk Tidsskrift* 78: 47–66.
- HUME J.D., SCHALK M., 1964a. The effects of beach barrow in the Arctic. *Shore and Beach* 32: 37–41.
- HUME J.D., SCHALK M., 1964b. The effects of ice-push on Arctic beaches. *American Journal of Science* 262: 267–273.
- HUME J.D., SCHALK M., 1967. Shoreline processes near Barrow, Alaska: a comparison of the normal and the catastrophic. *Arctic* 20: 86–103.
- HUME J.D., SCHALK M., 1976. The effects of ice on the beach and nearshore, Pt Barrow, Arctic Alaska. *La Revue de Géographie de Montréal* 30: 105–114.
- HUMLUM O., INSTANES A., SOLLID J.L., 2003. Permafrost in Svalbard: a review of research history, climatic background and engineering challenges. *Polar Research* 22: 191–215.
- ISAKSSON E., DIVINE D., KOHLER J., MARTMA T., POHJOLA V., MOTOMYAMA H., WATANABE O., 2005. Climate oscillations as recorded in Svalbard ice core  $\delta^{18}\text{O}$  records between ad 1200 and 1997. *Geografiska Annaler* 87 A: 203–214.
- JAHN A., 1961. Quantitative analysis of some periglacial processes in Spitsbergen. *Zeszyty Naukowe Uniwersytetu Wrocławskiego, seria B, 5, Nauka o Ziemi II/Geophysics, Geography, Geology II*: 3–54.
- JOHN B.S., SUGDEN D.E., 1975. Coastal geomorphology of high latitudes. *Progress in Geography* 7: 53–132.
- KING C.A.M., BUCKLEY J.T., 1968. The analysis of stone size and shape in an Arctic environment. *Journal of Sedimentary Petrology* 38: 200–218.
- LAFFLY D., MERCIER D., 2002. Global change and paraglacial morphodynamic modification in Svalbard. *International Journal of Remote Sensing* 43: 4743–4760.
- LANTUIT H., OVERDUIN P.P., COUTURE N., ARÉ F., ATKINSON D., BROWN J., CHERKASHOV G., DROZDOV D., FORBES D.L., GRAVES-GAYLORD A., GRIGORIEV M., HUBBERTEN H.-W., JORDAN J., JORGENSEN T., ØDEGÅRD R.S., OGORODOV S., POLLARD W., RACHOLD V., SEDENKO S., SOLOMON S., STEENHUISEN F., STRELETSKAYA I., VASILIEV A., WETTERICH S., 2011. The ACD coastal database: a new classification scheme and statistics on Arctic permafrost coastlines. *Estuaries and Coasts* (Online: DOI: 10.1007/s12237-010-9362-6).
- LANTUIT H., POLLARD W.H., 2008. Fifty years of coastal erosion and retrogressive thaw slump activity on Herschel Island, southern Beaufort Sea, Yukon Territory, Canada. *Geomorphology* 95: 84–102.
- LANTUIT H., RACHOLD V., POLLARD W.H., STEENHUISEN F., ØDEGÅRD R., HUBBERTEN H.-W., 2009. Towards a calculation of organic carbon release from erosion of Arctic coasts using non-fractal coastline datasets. *Marine Geology* 257: 1–10.
- LEONTIEV I.O., 2006. Forecast of Coastal Changes Based on Morphodynamical Modeling. *Oceanology* 46: 564–572.
- LØNNE I., LYSÅ A., 2005. Deglaciation dynamics following the Little Ice Age on Svalbard: Implications for shaping of landscapes at high latitudes. *Geomorphology* 72: 300–319.
- LØNNE I., NEMEC W., 2004. High-arctic fan delta recording deglaciation and environment disequilibrium. *Sedimentology* 51: 553–589.
- LUKANOVA S.A., SAFYANOV G.A., SOLOVEVA G.D., SHILOVA L.M., 2008. Types of Arctic Coasts of Russia. *Oceanology* 48: 268–274.
- LUNDBERG J., LAURITZEN S.-E., 2002. The search for an Arctic coastal karren model in Norway and Spitzbergen. In: K. Hewitt, M.-L. Byrne, M. English, G. Young (eds.), *Landscapes in Transition. Landform Assemblages and Transformations in Cold Regions*. Kluwer Academic Publishers, Dordrecht: 185–203.
- MAJEWSKI W., SZCZUCIŃSKI W., ZAJĄCZKOWSKI M., 2009. Interactions of Arctic and Atlantic water-masses and associ-

- ated environmental changes during the last millennium, Hornsund (SW Svalbard). *Boreas* 38: 529–544.
- MANGERUD J., DOKKEN T., HEBBELN D., HEGGEN B., INGOLFSSON O., LANDVIK J.Y., MEJDAHL V., SVENDSEN J.I., VORREN T.O., 1998. Fluctuations of the Svalbard-Barents Sea ice sheet during the last 150 000 years. *Quaternary Science Reviews* 17: 11–42.
- McCANN S.B., DALE J.E., 1986. Sea ice breakup and tidal flat processes, Forbisher Bay, Baffin Island. *Physical Geography* 7: 168–180.
- McCANN S.B., DALE J.E., HALE P.B., 1981. Subarctic tidal flats in areas of large tidal range, southern Baffin Island, Eastern Canada. *Géographie physique et Quaternaire* 35: 183–204.
- McCANN S.B., OWENS E.H., 1969. The size and shape of sediments in three Arctic beaches, SW Devon Island, NWT. *Arctic and Alpine Research* 1: 267–278.
- McCANN S.B., TAYLOR R.B., 1975. Beach freezeup sequence at Radstock Bay, Devon Island, Arctic Canada. *Arctic and Alpine Research* 7: 379–386.
- MERCIER D., 2008. Paraglacial and paraperiglacial landscapes: concepts, temporal scales and spatial distribution. *Géomorphologie: relief, processus, environnement* 4: 223–233.
- MERCIER D., ÉTIENNE S., SELLIER D., ANDRÉ M.-F., 2009. Paraglacial gullying of sediment-mantled slopes: a case study of Colletthøgda, Kongsfjorden area, West Spitsbergen (Svalbard). *Earth Surface Processes and Landforms* 34: 1772–1789.
- MERCIER D., LAFFLY D., 2005. Actual paraglacial progradation of the coastal zone in the Kongsfjorden area, western Spitsbergen (Svalbard). In: C. Harris, J.B. Murton (eds.), *Cryospheric systems: glaciers and permafrost*. Geological Society, London: 111–117.
- NANSEN F., 1922. The strandflat and isostasy. *Videmkapsselskabet Skrifter. I. Mat.-Naturu. Klasse*. 1921 11.
- NICHOLS R.L., 1961. Characteristics of beaches formed in polar climates. *American Journal of Science* 259: 694–708.
- NIELSEN N., 1979. Ice-foot processes. Observations of erosion of the rocky coast, Disko, West Greenland. *Zeitschrift für Geomorphologie* 23: 321–331.
- NIELSEN N., 1992. A boulder beach formed by waves from a calving glacier: Eqip Sermia, West Greenland. *Boreas* 21: 159–168.
- NIELSEN N., 1994. Geomorphology of a Degrading Arctic Delta, Sermilik, South-East Greenland. *Geografisk Tidsskrift* 94: 46–57.
- NIKIFOROV S., PAVLIDIS Y., RACHOLD V., GRIGORYEV M., RIVKIN M., IVANOVA N., KOREISHA M., 2005. Morphogenetic classification of the Arctic coastal zone. *Geo-Marine Letters* 25: 89–97.
- Norwegian Arctic Climate Impact Assessment (NorACIA) Report 2011. Climate change in the Norwegian Arctic. Consequences for life in the north. *Norwegian Polar Institute Rapport Series* 136.
- NUTH C., MOHOLDT G., KOHLER J., HAGEN J.O., KÄÄB A., 2010. Svalbard glacier elevation changes and contribution to sea level rise. *Journal of Geophysical Research* 115: doi:10.1029/2008JF001223.
- OVERDUIN P.P., HUBBERTEN H.-W., RACHOLD V., ROMANOVSKII N., GRIGORYEV M.N., KASYMSKAYA M., 2007. Evolution and degradation of coastal and offshore permafrost in the Laptev and East Siberian Seas during the last climatic cycle, Coastline changes: interrelation of climate and geological processes. In: J. Harff, W.H. Hay, D.M. Tetzlaff (eds.), *The Geological Society of America special paper* 426, Boulder, Colorado: Geological Society of America, 97–111. doi:10.1130/2007.2426(07).
- OWENS E.H., McCANN S.B., 1970. The role of ice in the arctic beach environment with special references to Cape Ricketts, south-west Devon Island, Northwest Territories, Canada. *American Journal of Science* 268: 397–414.
- ØDEGÅRD R.S., EITZELMÜLLER B., VATNE G., SOLLID J., 1995. Near-surface spring temperatures in an Arctic coastal cliff: possible implications of rock breakdown. In: O. Slaymaker (ed.), *Steepland geomorphology*. Wiley, Chichester: 89–102.
- ØDEGÅRD R.S., SOLLID J.L., 1993. Coastal cliff temperatures related to the potential for cryogenic weathering processes, western Spitsbergen, Svalbard. *Polar Research* 12: 95–106.
- RACHLEWICZ G., 2010. Paraglacial modifications of glacial sediments over millennial to decadal time-scales in the high Arctic (Billefjorden, central Spitsbergen, Svalbard). *Quaestiones Geographicae* 29: 59–67.
- RACHOLD V., ARE F., ATKINSON D., CHERKASHOV G., SOLOMON S., 2005. Arctic Coastal Dynamics (ACD): an introduction. *Geo-Marine Letters* 25: 63–68.
- REIMNITZ E., BARNES P.W., HARPER J.R., 1990. A review of beach nourishment from ice transport of shoreface materials, Beaufort Sea, Alaska. *Journal of Coastal Research* 6: 439–470.
- REINSON G.E., ROSEN P.S., 1982. Preservation of ice-formed features in a sub-Arctic sandy beach sequence: geologic implications. *Journal of Sedimentary Petrology* 52: 463–471.
- REX R.W., 1964. Arctic Beaches, Barrow, Alaska. In: R.L. MILLER (ed.), *Papers in Marine Geology*. MacMillan, New York: 384–400.
- ROMANOVSKII N., HUBBERTEN H.-W., GAVRILOV A., TUMSKOY V., KHOLODOV A.L., 2004. Permafrost of the east Siberian Arctic shelf and coastal lowlands. *Quaternary Science Reviews* 23: 1359–1369.
- ROSEN P.S., 1978. Degradation of ice-formed beach deposits. *Maritime Sediments* 14: 63–68.
- SEMPELS J.M., 1987. The Coastal Morphology and Sedimentology of Cape Hatt Peninsula. *Arctic* 40: 10–19.
- SERREZE M., WELSH J., CHAPIN III F., OSTERKAMP T., DYURGEROV M., ROMANOWSKY V., OECHEL W., MORISON J., ZHANG T., BARRY R., 2000. Observational evidence of recent change in the northern high-latitude environment. *Climatic Change* 46: 159–207.
- SLAYMAKER O., 2011. Criteria to distinguish between periglacial, proglacial and paraglacial environments. *Quaestiones Geographicae* 30: 85–94.
- SOLOMON S.M., 2005. Spatial and temporal variability of shoreline change in the Beaufort–Mackenzie region, northwest territories, Canada. *Geo-Marine Letters* 25: 127–137.
- ST-HILAIRE-GRAVEL D., BELL T., FORBES D., 2010. Raised Gravel Beaches as Proxy Indicators of Past Sea-ice and Wave Conditions, Lowther Island, Canadian Arctic Archipelago. *Arctic* 63: 213–226.
- STRELETSKAYA I.D., VASILIEV A.A., VANSTEIN B.G., 2009. Erosion of sediment and organic carbon from the Kara Sea coast. *Arctic, Antarctic, and Alpine Research* 41: 79–87.
- STRZELECKI M.C., 2011. Paraglacial processes operating on High Arctic coastal margins – recent advances from Svalbard. *Geophysical Research Abstracts* 13: EGU2011-87-1, 2011.
- STRZELECKI M.C., 2011. Schmidt hammer tests across recently deglaciated rocky coastal zone – is there a ‘coastal amplification’ of rock weathering in polar climates? *Polish Polar Research* 32 (in press).

- STRZELECKI M.C., ZAGÓRSKI P., 2011. *SVALCOAST Project – background, aims, impact plan*. SVALCOAST Group meeting, Sosnowiec.
- SVENDSEN J.A., ALEXANDERSON H., ASTAKHOV V.I., DEMIDOV I., DOWDESWELL J.A., FUNDER S., GATAULLIN V., HENRIKSEN M., HJORT C., HOUMARK-NIELSEN M., HUBBERTEN H.W., INGÓLFSSON O., JAKOBSSON M., KJÆR K.H., LARSEN E., LOKRANTZ H., LUNKKA J.P., LYSÅ A., MANGERUD J., MATIOUCHKOV A., MURRAY A., MÖLLER P., NIESSEN F., NIKOLSKAYA O., POLYAK L., SAARNISTO M., SIEGERT C., SIEGERT M.J., SPIELHAGEN R.F., STEIN R., 2004. Late Quaternary ice sheet history of northern Eurasia. *Quaternary Science Reviews* 23: 1229–1271.
- ŚLUBOWSKA-WOLDENGEN M., RASMUSSEN T.L., KOÇ N., KLITGAARD-KRISTENSEN D., NILSEN F., SOLHEIM A., 2007. Advection of Atlantic Water to the western and northern Svalbard shelf since 17,500 cal yr BP. *Quaternary Science Reviews* 26: 463–478.
- TAYLOR R.B., 1978. The occurrence of grounded ice ridges and shore ice piling along the northern coast of Somerset Island, N.W.T. *Arctic* 31: 133–139.
- TRENHAILE A.S., 1983. The development of shore platforms in high latitudes. In: D.E. Smith, A.G. Dawson (eds.), *Shorelines and Isostasy*. Institute of British Geographers, Special Publication 16, London: 77–96.
- TRENHAILE A.S., 1997. *Coastal Dynamics and Landforms*. Oxford University Press, Oxford.
- URDEA P., 2007. About some geomorphological aspects of the polar beaches. *Revista de geomorfologie* 9: 5–16.
- WANGENSTEEN B., EIKEN T., ØDEGÅRD R.S., SOLLID J.L., 2007. Measuring coastal cliff retreat in the Kongsfjorden area, Svalbard, using terrestrial photogrammetry. *Polar Research* 26: 14–21.
- ZAGÓRSKI P., 2011. Shoreline dynamics of Calypsostranda (NW Wedel Jarlsberg Land, Svalbard) during the last century. *Polish Polar Research* 32: 67–99.
- ZAGÓRSKI P., GAJEK G., DEMCZUK P., in prep. The influence of glacier systems of polar catchments on functioning of the coastal zone (Recherchefjorden, Svalbard). Submitted to *Zeitschrift für Geomorphologie*.
- ZENKOVICH V.P., 1967. *Processes of Coastal Development*. Trans. O.G. Fry, J.A. Steers. Oliver and Boyd, Edinburgh.
- ZIAJA W., MACIEJOWSKI P., OSTAFIN K., 2009. Coastal Landscape Dynamics in NE Sørkapp Land (SE Spitsbergen), 1900–2005. *Ambio* 38: 201–208.



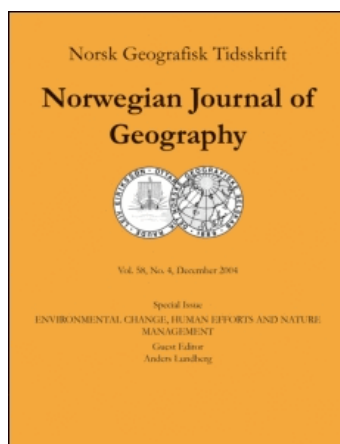
This article was downloaded by: [Swets Content Distribution]

On: 25 June 2009

Access details: Access Details: [subscription number 912280237]

Publisher Routledge

Informa Ltd Registered in England and Wales Registered Number: 1072954 Registered office: Mortimer House, 37-41 Mortimer Street, London W1T 3JH, UK



## Norsk Geografisk Tidsskrift - Norwegian Journal of Geography

Publication details, including instructions for authors and subscription information:

<http://www.informaworld.com/smpp/title~content=t713735796>

### Suspended and solute transport in a small glaciated catchment Bertram River, Central Spitsbergen, in 2005-2006

Mateusz Strzelecki

Online Publication Date: 01 June 2009

**To cite this Article** Strzelecki, Mateusz(2009)'Suspended and solute transport in a small glaciated catchment Bertram River, Central Spitsbergen, in 2005-2006',Norsk Geografisk Tidsskrift - Norwegian Journal of Geography,63:2,98 — 106

**To link to this Article:** DOI: 10.1080/00291950902901002

**URL:** <http://dx.doi.org/10.1080/00291950902901002>

## PLEASE SCROLL DOWN FOR ARTICLE

Full terms and conditions of use: <http://www.informaworld.com/terms-and-conditions-of-access.pdf>

This article may be used for research, teaching and private study purposes. Any substantial or systematic reproduction, re-distribution, re-selling, loan or sub-licensing, systematic supply or distribution in any form to anyone is expressly forbidden.

The publisher does not give any warranty express or implied or make any representation that the contents will be complete or accurate or up to date. The accuracy of any instructions, formulae and drug doses should be independently verified with primary sources. The publisher shall not be liable for any loss, actions, claims, proceedings, demand or costs or damages whatsoever or howsoever caused arising directly or indirectly in connection with or arising out of the use of this material.

# Suspended and solute transport in a small glaciated catchment, Bertram River, Central Spitsbergen, in 2005–2006

MATEUSZ STRZELECKI



Strzelecki, M. 2009. Suspended and solute transport in a small glaciated catchment, Bertram River, Central Spitsbergen, in 2005–2006. *Norsk Geografisk Tidsskrift–Norwegian Journal of Geography* Vol. 63, 98–106, Oslo. ISSN 0029-1951.

The paper presents data on hydrochemistry and suspended sediment dynamics from a small glaciated catchment in Svalbard. Such catchments, formerly omitted and neglected in investigations of polar and high-mountain geo-ecosystems, have become an important subject of environmental research in recent years. High sensitivity to global warming, relative ease of taking measurements, the variety of locations, and further possibilities of modelling, make the catchments important sites for studying glaciological, hydrological and geomorphological processes. Hydrochemical data from seasonal observations and complementary 24-hour measurements, together with detailed geomorphological mapping of river channels and their surroundings, served as a basis for scientific description of the conditioning of seasonal and diurnal variations in suspended and solute matter transport in a small High Arctic catchment. Bertram River is distinguished by a system of waterfalls which divides the 4.9 km<sup>2</sup> catchment in two parts: an upper glaciated part located on mountainous plateau, and a lower part where an abraded plain has been formed within the bottom of the Ebba River valley. On the basis of observations it is concluded that a particular role in the conditioning of glaciofluvial transport was played by an extreme weather event in the form of föhn-type wind, observed in the decline of ablation season and also by waterfalls which diversified the fluvial activity.

**Keywords:** *glaciated catchment, glaciofluvial transport, High Arctic river systems, hydrochemistry, Spitsbergen*

Mateusz Strzelecki, *Institute of Paleogeography and Geocology, Faculty of Geosciences, Adam Mickiewicz University, ul. Dziegielowa 27, 61-680 Poznań, Poland; and Department of Geography, Durham University, Science Laboratories, South Road, Durham DH1 3LE, UK. E-mail: mat.strzelecki@gmail.com*

## Introduction

A major challenge for geoscientists in the 21st century will be to accept that present-day land forming processes shape various geo-ecosystems in a very extreme way and due to increased global warming their response is probably unpredictable. One of the key elements of the Earth's system is polar region rivers and their geomorphic role in the environment, which still need more detailed scientific description. Understanding fluvial transport in cold climate zones of the planet is crucial in every sediment budget study and prediction of landscape evolution. Suspended sediment yields of proglacial rivers are one of the most sensitive indicators of changes in glacial environments revealed in interactions between glaciers, climate and landscape transition (Hodgkins et al. 2003). Additionally, recognition of changes in suspended matter of proglacial streams enables understanding of how active a subglacial abrasion is (Willis et al. 1996) and shows that geomorphological methods can be useful in glaciological investigations. It is known that meltwater runoff from glaciated basins carries a greater volume of suspended sediments than from non-glaciated basins (Hallet et al. 1996). Such highly energetic environments are supplied with sediments from three major sources: namely channel systems, bedrock and glaciers (Benn & Evans 1998), whose thermal types of glacier ice (cold/polythermal/warm) influence the rate of glacier erosion and hence the amount of sediments carried by proglacial rivers. Due to continuous movement on their beds, warm glaciers cause higher rates of erosion than cold ones, which

are more stable. Furthermore, it is important to remember that the amount of water which percolates through glaciers also affects the amount and rate of sediment transport from glacial zones (Drewry 1986).

Many studies of sediment storage have been made in Alpine regions, e.g. several research projects on Haut Glacier d'Arolla (Sharp et al. 1993; Hubbard et al. 1995; Nienow et al. 1998; Mair et al. 2004). However, relatively few studies have been carried out in High Arctic locations. This has resulted in a gap in the understanding of fluvial matter transport in glaciated catchments. Extremely dynamic fluvial systems known from Alpine environments (Swift et al. 2005) have more latent response in Arctic or Antarctic equivalents, and this effect is not fully understood (Warburton 1999). For instance, studies in polar regions have revealed that not all proglacial rivers that have developed braided patterns are characterized by high rates of bedload transport and changes in channel platform (Nicholas & Sambrook Smith 1998).

Important research on glacio-hydrological processes and their impact on cold landscape transformation is being carried out through a number of projects on the Svalbard archipelago. Svalbard is an extremely important gateway to an High Arctic environments and as a result of the work carried out by research centres in Ny-Alesund, Longyearbyen and Hornsund, as well as smaller bases located throughout the island as a whole (Bellsund, Petuniabukta), knowledge of the functioning of glaciated catchment geo-ecosystems has improved significantly (e.g. Kostrzewski et al. 1989; Hodson et al. 1998; 2000; 2002; Wadham et al. 1998; 2000; Krawczyk et al. 2003).

However, during the last thirty years substantial advances in fluvial geomorphology have been made in understanding sediment transfer processes, but the lack of data from Arctic, Subarctic and Antarctic regions complicates the analysis of linkages between glaciers and wider paraglacial environments, and renders the design of precise models practically impossible (Sharp et al. 1998). This situation is now changing, mainly because of the need for basic information about the reaction of glaciers to climate change and the implication for the availability of fresh water. Apart from economic and geopolitical issues, the (glacio-) fluvial domain is a leading factor in reshaping cold region glacier-free landscapes during the present paraglacial period and studies of glacial and proglacial hydrological processes are imperative. Studies of global change rely on data recorded in polar catchments and in the present century there is likely to be increased geoscientific interest in cold region water systems.

For this reason, research was carried out on suspended and dissolved transport in a High Arctic catchment, two years prior to the Fourth International Polar Year, which portends to be a new era for polar science on all fronts. The purpose of the first expedition (16 July – 20 September 2005) was to observe the seasonal changes in river discharge and the concentration of suspended and dissolved matter in meltwaters. Investigations of the chemical composition of glacial meltwaters were carried out simultaneously with observations of suspended particulate matter to estimate the contribution of chemical denudation to the total rate of denudation.

The main purpose of the second season of taking measurements was to observe the diurnal fluctuations of matter concentration and stream discharge during three selected days of the ablation season in 2006 (4 July – 4 September). Around-the-clock hydrological and hydrochemical surveys were carried out as follows:

- (1) at the beginning of July (9th–10th) during the phase of increasing discharge
- (2) at the end of the July (29th–30th) during the phase of the highest summer discharges
- (3) at the end of August (19th–20th) during the early phase of the decay of water flow in Bertram River.

The aim of conducting complementary hydrochemical investigations from 29 July 2006 was to focus on changes in suspended sediments and solute matter concentrations along a longitudinal river profile from glacier gate to river mouth, with reference to the role of the waterfall system in sediment transfer.

## Study site

The study site was located in the central part of Spitsbergen, the biggest island of Svalbard archipelago, where Bertram River flows into Ebba River in Ebbadalen (Ebba valley) (Fig. 1). Ebba River is the major river reaching Petuniabukta, at the head of Billefjorden (Fig. 2). Adam Mickiewicz University (AMU) in Poznań has sent expeditions to the Petuniabukta area for more than twenty years. Information collected in that part of Spitsbergen has proved valuable for studies of environmental changes in the High Arctic, mainly



Fig. 1. Ebbadalen viewed from Wordiekamen (Fig. 2); in the background are two glaciers, Bertramreen (left) and Ebbabreen (right) (Photo: Mateusz Strzelecki, August 2005)

because it is the most ‘inland’ location between other scientific stations, and provides a link between data obtained along the humid western coast and dry eastern coast.

In contrast to the climate at scientific bases located throughout the island and major weather observations from the Polish Academy of Science National Base in Hornsund (southern Spitsbergen), the Petunia Bay station area has the warmest summers, low air humidity (cloud cover in 10 degree scale normally *c.* 6.5) and low precipitation (below 200 mm per year). Fig. 3 shows a comparison of air temperatures from the 2005 and 2006 seasons.

However, an extreme meteorological event disturbed the normal course of ablation during the 2005 season. The event was a strong warm föhn-type wind, which on the 27th and 28th of August blew through Ebbadalen, warmed up decreasing air temperatures and intensified ablation, causing bankfull discharge and extensive flooding in Bertram River, and subsequently in Ebba River. That extreme event, which represents an anomalous event in the seasonal distribution of fluvial transport, served as a basis for detailed measurements recorded in 2006.

The major focus of AMU geoscientific research (Kostrzewski et al. 1989) is Ebbadalen, in which Ebba River carries water and sediments from Ebbabreen (Ebba Glacier) and transforms the bottom of a former glacial valley. The 2 km long Bertram River, the main tributary of Ebba River, was selected for study. The catchment of Bertram River also exhibits some interesting geomorphological characteristics when compared to other proglacial river geo-ecosystems in the area. Bertram River is distinguished by a system of waterfalls (*c.* 250 m high) which divide the catchment into two parts: upper – glaciated and located on mountainous plateau; and lower – a braided plain formed at the bottom of the Ebbadalen (Fig. 4).<sup>1</sup> Approximately 60% (2.9 km<sup>2</sup>) of the catchment is occupied by a small cold-type glacier, Bertramreen, which since the Little Ice Age has been in continuous retreat (Rachlewicz 2004). The glacier's morphology has indirect influence on the amount of sediments

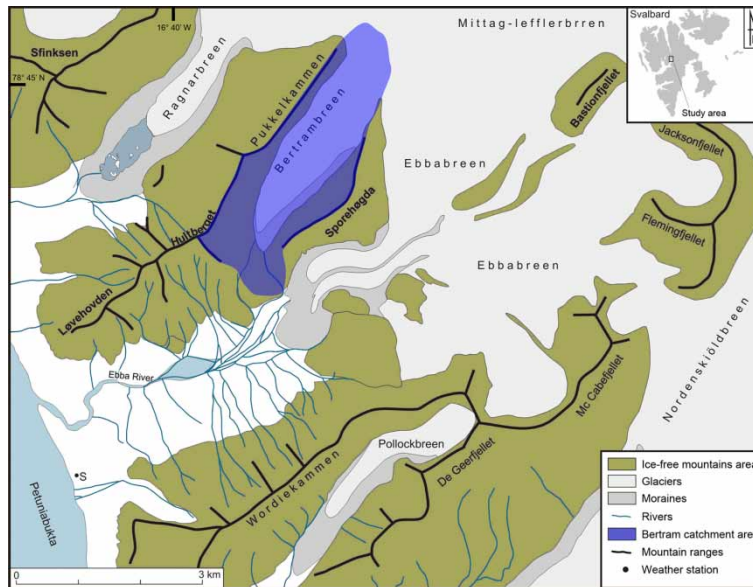


Fig. 2. Map of study area (M. Ewertowski)

incorporated to meltwaters in the upper part of a catchment. The majority of supraglacial streams flow along the south-eastern edge of the glacier, covered by mudflows from Sporehogda massif. In the frontal part of this, dirty glacier streams flow in one channel and plunge into frontal moraine. Very turbid meltwaters leave the glacial system through a portal stream and immediately flow into a straight channel incised into a metamorphic massif. The lithology of the glaciated part of the catchment, where the river runs in a shallow channel, consists of hard Precambrian metamorphic rocks, Palaeozoic dolomites, limestones, shales and sandstones (Szczeniński 2003). The sandstones contain iron oxyhydroxides, which colour the water reddish, resulting in a very distinct catchment feature. The lower part of the catchment is covered with unconsolidated and poorly sorted glaciofluvial deposits which form the outwash plain of Ebbabreen (Fig. 5). There the river cuts through three remnants of ice-cored moraines and during high discharges floods several thermokarst ponds. Hence, two potential sources of sediments can be identified: one glacial and a second one relating to thawing of permafrost and paraglacial activity in the proglacial zone.

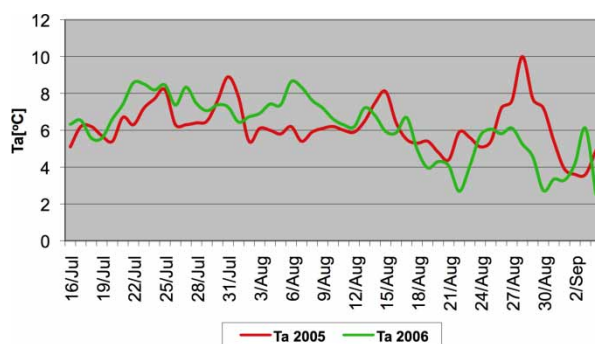


Fig. 3. Comparison of air temperatures measured in 2005 and 2006

## Monitoring and analytical methodology

During both 2005 and 2006 the gauging point was located in the lower part of the catchment, 30 m from an erosion hollow, where streams started to flow in one straight channel. River discharges were calculated by application of the float method. The velocities of floating buoys were measured five times along 5 m long section. After rejecting



Fig. 4. System of waterfalls which divide the Bertram River catchment into an upper rocky part and lower braided part (Photo: Mateusz Strzelecki, July 2005)





Fig. 5. The lower part of the Bertram River catchment, showing a well-developed braided pattern and incision through remnants of ice-cored moraine (Photo: Mateusz Strzelecki, August 2006)

extreme values, the average velocity was estimated. The floating method allowed the calculate river discharge to be calculated very quickly, even during periods of high discharge and in practically all kinds of weather conditions. During 2005, at 14.00 hours daily, water samples were taken by hand using a pre-rinsed 1000 ml polyethylene bottle and immediately vacuum filtered through a 0.45 mm filter membrane (Whatman type: GF/A).<sup>2</sup> After filtration, clear water was poured into two 250 ml polyethylene bottles. At the end of the season, the samples were analysed at UAM Geocological Station in Storkowo, Poland. The water pH and conductivity (SEC) were measured using a multifunctional meter: CX-401 (ELMETRON®). Concentrations of Ca, Mg, Na, and K were detected by use of atomic absorption spectroscopy (Varian Spectra AA 20Plus®), whereas,  $\text{Cl}^-$  and  $\text{SO}_4^{2-}$  were analysed on ion chromatograph (DX-120 Dionex®). Bicarbonate ions were measured in the field by titration.

In 2006 samples were collected from the same place during three 24-hour measurements conducted in different phases of the ablation season. Additionally, on 29 July 2006 samples of water were collected every 50 m in the distinct braided channel. This stage in the Bertram River investigations had one main purpose – to check the effect of the waterfall system on the fluvial transport between the upper and lower parts of the catchment. The second challenge was to capture changes in the chemical composition of river water along the river. Simultaneously with hydrological sampling, geomorphological mapping of the river channel was made to characterize the channel morphology. Table 1 shows the profile symbols used in the survey and the major results of complementary geomorphological mapping.

## Results and discussion

Daily river discharge ( $Q$ ) observations in the 2005 season resulted in the determination of mean seasonal river discharge at  $81 \text{ dm}^3 \text{ s}^{-1}$ . Fig. 6 shows the seasonal course of river discharges plotted against air temperature.

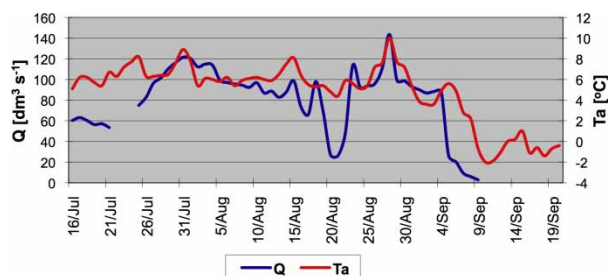


Fig. 6. Changes in river discharge  $Q$  against air temperature  $T_a$  in 2005

The mean unit runoff in Bertram river was  $13.1 \text{ dm}^3 \text{ s}^{-1} \text{ km}^2$ , and varied between  $29.2 \text{ dm}^3 \text{ s}^{-1} \text{ km}^2$ , noted during bankfull discharge, and  $0.6 \text{ dm}^3 \text{ s}^{-1} \text{ km}^2$ , on the last day before freezing. River discharges observed during three 24-hour measurements from the 2006 season showed diurnal fluctuations typical of proglacial rivers (Fig. 7). Between the 9th and 10th of July mean river discharge equalled  $75 \text{ dm}^3 \text{ s}^{-1}$ . Twenty days later, between the 29th and 30th of July it amounted to  $91 \text{ dm}^3 \text{ s}^{-1}$  and when the last measurements were taken in August the mean diurnal discharge was  $13 \text{ dm}^3 \text{ s}^{-1}$ .

In 2005, season data from 64 samples was used to detect changes in suspended sediments concentrations (SSC) and solute matter concentrations (Cd). Obtained values were also related to observed hydro-meteorological variations (Fig. 8a and b).

Average SSC in Bertram River was  $405.41 \text{ mg dm}^{-3}$ . However, on the 27th of August the SSC amounted to  $4040.56 \text{ mg}$  per litre. That extreme value was observed during bankfull discharge, caused by föhn-type wind, which increased the rate of glacier ablation. Temporal distribution of suspended sediments transported by Bertram River confirmed a strong relationship between the occurrence of maximum SSC prior to a peak in river discharge. According to Jania (1997), the largest amount of sediment tears away from a river bottom and banks in a growing phase of river discharge, just before the maximum discharge. The föhn-effect disturbed the normal distribution of SSC, which in the second half of August was decreasing, together with a fall in river discharge. Ten days after this high peak the smallest volume of SSC was measured. The decrease to  $1.53 \text{ mg}$  per litre was caused by the first autumn frost.

Seasonal fluctuations in solute matter, which on average amounted to  $116.59 \text{ mg dm}^{-3}$ , had an inversely proportional course. Namely, the highest values were observed

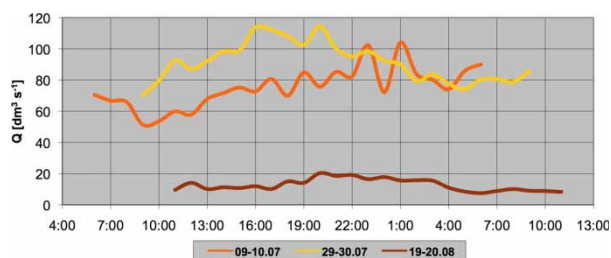


Fig. 7. Changes of discharge  $Q$  [ $\text{dm}^3 \text{ s}^{-1}$ ] during three 24-hour hydrochemical measurements in 2006



Table 1. Characterization of the Bertram River channel features and discharges observed on 29 July 2006 and profile numbers used in the descriptions of hydrochemical changes along Bertram River

Profile number	Distance from glacier gate (m)	Q (dm <sup>3</sup> s <sup>-1</sup> )	Channel description	Comments
<b>BL</b>	–	–	Supraglacial stream channel	Sample of clear glacial water collected in a marginal part of Bertrambreen
<b>BM</b>	–	–	Major supraglacial channel – which drains surface of Bertrambreen	Approximately 40 m from BL – place where glacial streams flow under frontal moraine; common place of mudflows from Sporehogda massif and lateral moraine – sources of high concentrations of sediments in streams
<b>BB</b>	–	–	Straight channel incised in metamorphic rock, bottom covered by pebbles and sharp-edged boulders	Approximately 200 m from BM – collected sample contained mixed waters from supraglacial and subglacial drainage; section where first river channel was formed and river started course on a metamorphic rock
<b>BW</b>	–	–	Channel in waterfall system, incised in hard metamorphic rock	Sample collected from the last rocky threshold accessible without mountaineering equipment, rocky threshold; later river flowed down in 250 m waterfall system
<b>BP1</b>	1170	91.41	Pebbly channel, bottom covered by boulders and small sand-gravel bars	Confluence of streams after waterfall system; many rapids flowing through boulders and rocks scattered near erosion hollow
<b>BP2</b>	1220	112.04	Straight sandy channel with pebbly bars	Sample collected before gorge through ice-cored moraine hills
<b>BP3</b>	1270	108.95	Braided channel, many large boulders on a bottom	Sample collected in a river gorge through ice-cored moraine hills
<b>BP4</b>	1320	71.53	Braided channel	Sample taken from the middle of braided channel part of a catchment, between numerous sand-gravel bars
<b>BP5</b>	1370	123.88	Straight sandy channel	Sample collected beyond the biggest flood plain in the catchment area
<b>BP6</b>	1420	124.42	Pebbly channel with few rapids	Section with the highest banks
<b>BP7</b>	1470	130.03	Pebbly and deep channel with few large sandy bars	Lowering of banks and widening of channel
<b>BP8</b>	1520	99.70	Pebbly channel	Another formation of braided pattern
<b>BP9</b>	1570	81.45	Mixed sandy and pebbly channel	Sample collected between sandy bars; division in two different streams: 'Rapid Bertram' and 'Patient Bertram'
<b>BP10</b>	1620	127.80	Pebbly channel with numerous trims up to 140 cm (mean depth of river channel c.60 cm)	In that section first abstraction of some streams happened; Ebba River took over left-wing channels of Bertram River; major mass of water was flowing in 'Rapid Bertram'
<b>BP11</b>	1670	128.06	Straight pebbly channel	Increased flow velocity and discharge caused by new tributaries from Ebba River
<b>BP12</b>	1720	150.70	Sandy channel with boulder scattered on a bottom	Last sample of water before river mouth
<b>BP13</b>	1800	188.76	Sandy and deep channel (130 cm), in some places very quaggy	Sample taken from the middle of river mouth, in the same place as the highest river discharge was measured; Bertram River ('Rapid') disappeared in currents of Ebba River

during the decreasing phase of river discharge and reached a peak value of 369.46 mg dm<sup>-3</sup> when the river was bounded by ice. A particularly important moment was a sharp increase in the concentration of solute matter observed at the end of August. It is probable that extreme river discharge from the end of August caused the release of 'old waters' accumulated in subglacial drainage. Subglacial waters, which by nature interact with bedrock much longer than supraglacial streams, flowed into Bertram River at the beginning of September and there were still increasing concentrations of dissolved solids during last days of taking measurements. A similar situation was observed on Werenskiöld Glacier in the beginning of the 1990s, when rapid increase of dissolved solids in proglacial waters was caused by the arrival of a föhn-wind (Krawczyk 1992).

Analysis of total dissolved solids (TDS) led to defining the mean chemical composition of Bertram River waters (Fig. 9). The mean seasonal conductivity of Bertram River waters was 177 µS cm<sup>-1</sup>. According to Alekin's water classification scheme (Macioszczyk 1987) the waters of Bertram River can be describe as bicarbonate-calcic, which neatly reflects the chemical composition of surrounding rock formations. The

relation of major ion concentrations was: Ca<sup>2+</sup> > Mg<sup>2+</sup> > Na<sup>+</sup> > K<sup>+</sup>, and SO<sub>4</sub><sup>2-</sup> > HCO<sub>3</sub><sup>-</sup> > Cl<sup>-</sup> > NO<sub>3</sub><sup>-</sup>.

The obtained values of SSC and Cd led directly to the determination of indicators of mechanical and chemical denudation (Dm and Dc). Average Dc in 2005 was 38.06 t km<sup>-2</sup> a<sup>-1</sup> while the Dm indicator was 281.35 t km<sup>-2</sup> a<sup>-1</sup>. However, indicators of mechanical and chemical denudation did not represent real values of matter transported from the catchment. For this reason, suspended sediment (As) and dissolved matter (Ad) fluxes were calculated in the final phase of the research, in order to secure a more detailed description of fluvial activity in the Bertram River catchment (Fig. 10).

Between 16 July and 20 September 2005, 27.07 tons of dissolved matter was removed from the catchment, equal to 12% of the total matter flux from the catchment. Bertram River carried also 200.1 tons of suspended sediment, amounting to 88% of the total matter removed from the catchment.

It is noteworthy that bedload transport was not taken into consideration in the investigations described above, although in certain parts of the ablation season bedload transport is

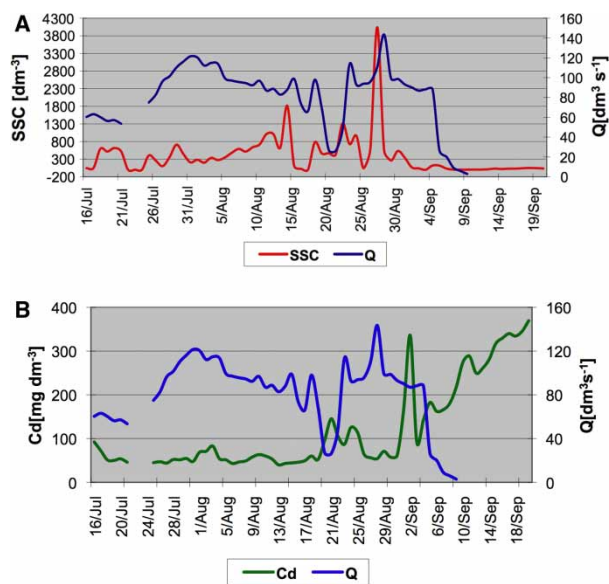


Fig. 8. a) Suspended sediment concentration SSC [ $\text{mg dm}^{-3}$ ] versus river discharge Q [ $\text{dm}^3 \text{s}^{-1}$ ] in the 2005 observation season; b) Solute matter concentration Cd [ $\text{mg dm}^{-3}$ ] versus river discharge Q [ $\text{dm}^3 \text{s}^{-1}$ ] in 2005

the major mechanism of sediment removal from the catchment area (Best & Bristow 1993).

In the 2006 season it was decided to check how the suspended sediment fluxes (As) and solute matter fluxes (Ad) varied in different phases of the ablation season and to trace the hydrochemical changes along Bertram River.

Fig. 11a, b and c show a co-variation of As and Ad in the total matter flux from the Bertram River catchment over 24 hours. Interestingly, the diagram for the middle of the ablation season (Fig. 11b) is similar to the mean of total matter fluxes in the 2005 season. This implies that the main removal of matter from glaciated catchments takes place in the few weeks of Arctic summer, when there are high discharges.

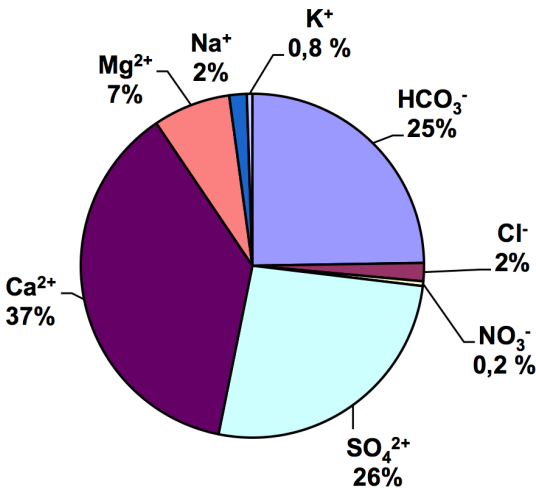


Fig. 9. Average chemical composition of Bertram River waters observed in 2005

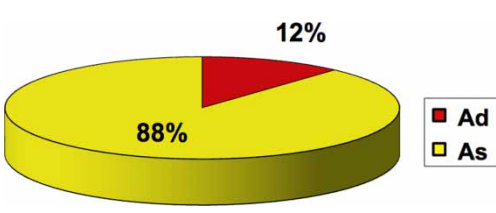


Fig. 10. Proportional participation of suspended sediment fluxes As and solute master fluxes Ad in the total matter flux from the Bertram River catchment observed in 2005

The TDS of river waters as expressed by SEC also varied considerably. During the first measurements taken in July the mean conductivity (SEC) was  $88 \mu\text{S cm}^{-1}$ . When the river experienced the highest water levels the mean SEC decreased to  $60 \mu\text{S cm}^{-1}$ , whereas at the end of August it rose to  $174 \mu\text{S cm}^{-1}$ , while Ad was practically equal to As. The higher TDS during the decline of the ablation season can be attributed to the removal of internal waters from the in- and subglacial drainage system or to the mineralized waters that percolated through the active layer in the peak phase of thawing.

The last stage of the research was probably the most challenging. During the second 24-hour period on 29–30 July (2006), hydrochemical mapping was carried out along the river (Table 1). Given that in the mountains cold glacial waters flows through metamorphic rocks, which are hard and resistant to weathering, the major change in water chemistry was expected to occur in Ebbadalen, where Bertram River flows through unconsolidated deposits of outwash plain and remnants of outwashed frontal moraine material from Ebbabreen. Geomorphological mapping of the surrounding areas showed that in the lower part of the Bertram River catchment there are two different channel

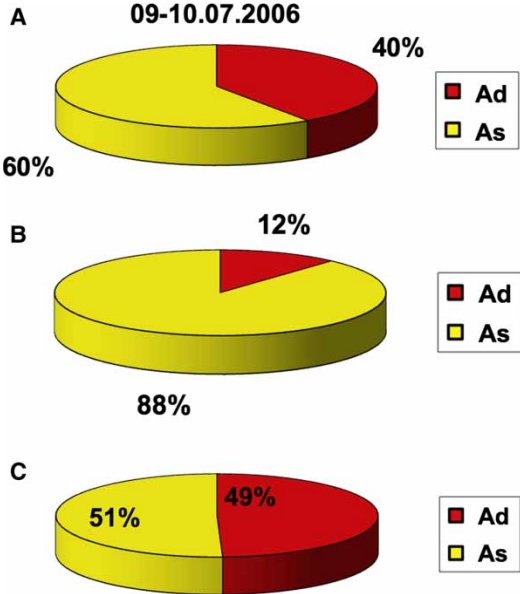


Fig. 11. Proportional participation of As and Ad in the total matter flux from the Bertram River catchment during first 24-hour measurements in 2006; a) 9–10 July 2006; b) 29–30 July 2006; c) 19–20 August 2006

patterns and characteristic flow sections. The first section was labelled the 'Patient Bertram', which formed a braided channel and flowed like a typical sluggish river and formed few backwaters. The second section was named the 'Rapid Bertram', a mainly straight and quite deep channel which carried the major part of the waters and was the first to reach Ebba River (Strzelecki 2008). Hydrochemical mapping started on Bertramreen where the first sample of water was collected. Next, samples were collected up to the last accessible threshold of waterfalls system. The survey continued in the lower part of the catchment, where a transverse river profile was made every 50 m to measure the river discharge. The survey was conducted in the middle of the river channel, and therefore it was possible to detect changes in river bottom morphology and composition. The last sample was taken at the mouth of Bertram River in Ebba River. The changes in suspended sediment are shown on Fig. 12a), and solute matter concentrations on Fig. 12b).

Analysis of the results suggests that the waterfall system formed a natural threshold for suspended matter transport. In clear glacial water, SSC was 0.04 mg per litre. Later Bertram River washed out sediments from Bertramreen moraines and was supplied by mudflows from the Sporehogda massif. That caused rapid increases in SSC to 2596.39 mg dm<sup>-3</sup> in profile BB. Samples collected from the waterfall (profile BW) indicated 1370.56 mg dm<sup>-3</sup>, whereas the first sample collected in the lower part of the catchment contained only 343.45 mg of suspended sediments in one litre of water. In the last sample from river mouth the SSC amounted to 228 mg dm<sup>-3</sup>.

Conversely to suspended sediment transport, solute matter concentrations increased when Bertram River flowed through a system of waterfalls. Changes of Cd can be

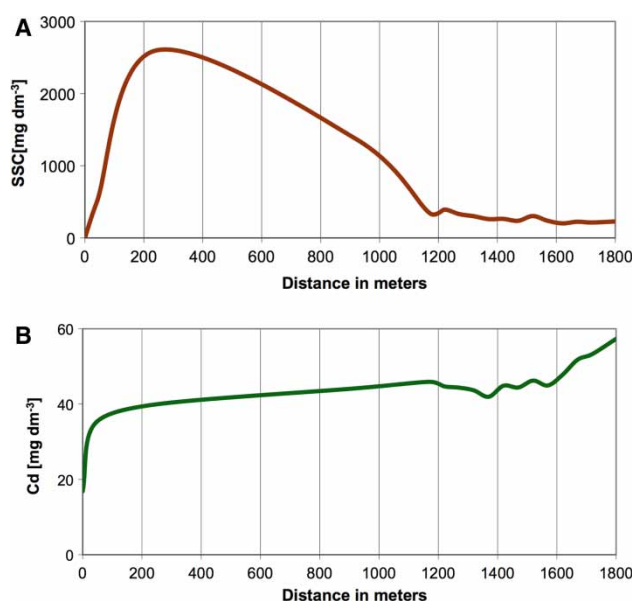


Fig. 12. a) Changes in suspended sediment concentration along the longitudinal profile of Bertram River between the glacier profile BL (0 m) and river mouth profile BP13 (1800 m); b) Changes in dissolved matter concentration along the longitudinal profile of Bertram River between the glacier BL (0 m) and river mouth BP13 (1800 m)

illustrated by using tissue paper as a metaphor. Low-conductivity glacial waters rapidly reflect the chemistry of the surrounding rocks and Bertram River is a very good example of this process. However, in the mountainous section the river flows through a channel incised into hard rock, so the abrupt rise of Cd happened only in the lower part of the catchment where Bertram River washed the surface of the outwash plain and took up the chemical compounds like tissue paper absorbs water from a wet surface.

A sample of clear glacial water had Cd at the level of 16.86 mg dm<sup>-3</sup>, whereas in profile BP1 it was 45.91 mg dm<sup>-3</sup> and in the river mouth (profile BP13) it reached a peak value of 57.33 mg dm<sup>-3</sup>. The average chemical composition of the sample collected on Bertramreen profile BL is shown in Fig. 13a), and in the river mouth, profile BP13, on Fig. 13b).

## Concluding remarks

The dynamics of suspended and solute matter transported in the Bertram River catchment are due to a number of factors, namely the glaciology, hydrometeorological conditions, lithology, and catchment relief. However, the major role in changing the amount of suspended sediments in meltwaters is played by paraglacial activity in a proglacial zone (eroding ice-cored moraines and Ebbabreen outwash plain) and on slopes (several mudflows activated by increased thawing of

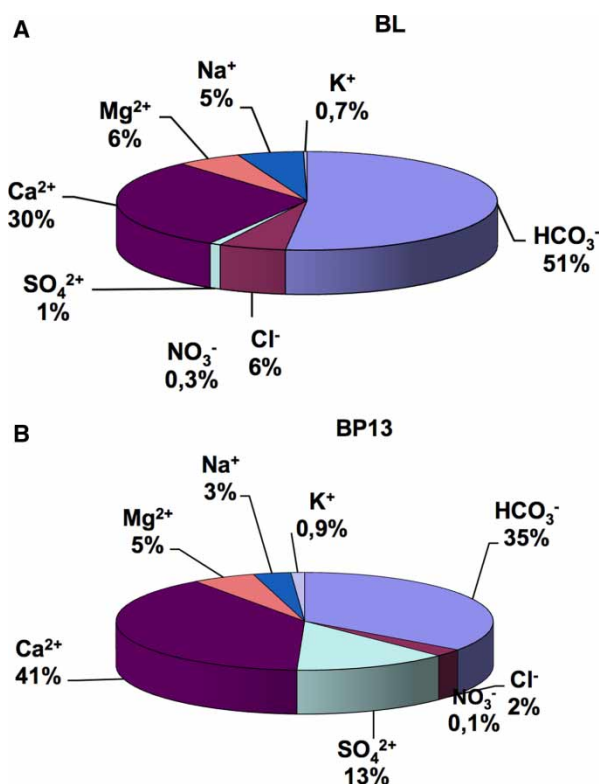


Fig. 13. a) Chemical composition of supraglacial waters – sample taken from a marginal part of Bertramreen profile BL, 29 July 2006; b) Chemical composition of waters of Bertram River in the river mouth profile BP13 – sample collected on 29 July 2006

permafrost), which surround the glacier. Changes in concentrations of dissolved matter along the longitudinal profile suggest the influence of thawing permafrost and release of waters from active layer as well as the mixing of Bertram and Ebba waters beneath the sandur deposits. The example of the föhn-wind phenomenon, which interfered with the normal course of fluvial activity, shows how sensitive glaciated river systems are to weather. Another distinguishing feature of the catchment – the waterfall system – worked as a restraint factor for suspended and probably also bedload transport, and additionally divided the catchment into two parts, each with different water chemistry. It is noteworthy that the Bertram catchment is probably the smallest analysed catchment on the Svalbard archipelago as a whole. Hence, it is quite difficult to compare the obtained results with those of previous studies. In 2005, Irvine-Fynn et al. published data from investigations of suspended sediment transport from the Austre Brøggerbreen catchment. This small glacierized catchment from Oscar II Land (Spitsbergen) occupies  $\approx 9.8 \text{ km}^2$ , of which 71% is a glacier (Hodson 2000). The mean SSC in the ablation season of 2005 was  $170 \text{ mg dm}^{-3}$ , giving a total denudation rate of  $\approx 110 \text{ t km}^{-2} \text{ a}^{-1}$ . In the same season the mean SSC in Bertram River was  $405.89 \text{ mg dm}^{-3}$ , which explains the much higher indicator of denudation ( $319.41 \text{ t km}^{-2} \text{ a}^{-1}$ ). In the beginning of the 1990s, Vatne et al. (1992) investigated glaciofluvial transport in the Erikbreen catchment and calculated sediment and solute matter fluxes from the basin area. The As removed from the catchment between 13 July and 23 August was equal to 3747 t and Ad was 1836 t. The mean SSC during peak discharges amounted to 380 mg per litre and was thus similar to values observed in Bertram River. Researchers have confirmed that the high rate and mass of master fluxes from the glaciated catchments on Svalbard are related to relatively soft sedimentary bedrock with low resistivity to weathering and glaciofluvial erosion.

Investigations of glaciofluvial transport in the Bertram River catchment have enabled a detailed presentation to be made of the geomorphological and hydrological conditions of seasonal and diurnal variations in suspended sediments and solute transport in a High Arctic catchment. However further, more automatic measurements are needed to correlate the obtained data with results from other High Arctic basins.

## Notes

- 1 The analysed area of glaciated catchment, closed by a gauging station, was equal  $4.9 \text{ km}^2$ . The total catchment area was  $\approx 7.0 \text{ km}^2$
- 2 Observations in the 2005 season lasted 67 days. Unfortunately a 3-day break was necessary due to an unexpected visit by a polar bear

**Acknowledgements.** – This work was funded by the Polish Ministry of Science and Higher Education (grant no. PBZ-KBN-108/PO4/2004). Parts of this paper are based on material previously presented in my MSc thesis, which was supervised by Professor Andrzej Kostrzewski. I would like to thank Dr Grzegorz Rachlewicz and Dr Zbigniew Zwoliński for inspiration and support during two seasons of research and preparation for my thesis. I am grateful to Professor Andrzej Kostrzewski for inviting me to become a member of UAM expeditions and for discussions on glaciofluvial matters. I also thank Marlena Makowska, an irreplaceable colleague during long and cold hours of

fieldwork. Thanks also are due to all participants of the I.A.G./A.I.G. Regional Conference on Geomorphology 'Geodiversity of Polar Landforms', Longyearbyen, 1–5 August 2007, for interesting comments, and also one reviewer who provided constructive criticism of the ideas presented in this paper.

Manuscript submitted 1 June 2008; accepted 4 December 2008

## References

- Benn, D. & Evans, D. 1998. *Glaciers and Glaciation*. Arnold, London.
- Best, J.L. & Bristow, C.S. 1993. *Braided Rivers*. Geological Society Special Publication No. 75. Geological Society, London.
- Drewry, D.J. 1986. *Glacial Geological Processes*. Edward Arnold, London.
- Hallet, B., Hunter, L. & Bogen, J. 1996. Rates of erosion and sediment evacuation by glaciers: A review of field data and their implications. *Global and Planetary Change* 12, 213–235.
- Hodgkins, R., Cooper, R., Wadham, J. & Tranter, M. 2003. Suspended sediment fluxes in a high Arctic glacierised catchment: Implications for fluvial sediment storage. *Sedimentary Geology* 162, 105–117.
- Hodson, A., Gurnell, A., Tranter, M., Bogen, J., Hagen, J.O. & Clark, M. 1998. Suspended sediment yield and transfer processes in a small High-Arctic glacier basin, Svalbard. *Hydrological Processes* 12, 73–86.
- Hodson, A.J., Tranter, M. & Vatne, G. 2000. Contemporary rates of chemical denudation and atmospheric  $\text{CO}_2$  sequestration in glacier basin: An arctic perspective. *Earth Surface Processes and Landforms* 25, 1447–1471.
- Hodson, A., Gurnell, A., Tranter, M., Clark, M. & Hagen, J.O. 2002. The hydrochemistry of Bayelva, a high Arctic proglacial stream in Svalbard. *Journal of Hydrology* 257, 91–114.
- Hubbard, B.P., Sharp, M.J., Willis, I.C., Nielsen, M.K. & Smart, C.C. 1995. Borehole water level variations and the structure of the subglacial hydrological system of Haut Glacier d'Arolla, Valais, Switzerland. *Journal of Glaciology* 41, 572–583.
- Irvine-Fynn, T.D.L., Moorman, B.J., Willis, I.C., Sjogre, D.B., Hodson, A.J., Mumford, P.N., Walter, F.S.A. & Williams, J.L.M. 2005. Geocryological processes linked to High-Arctic proglacial stream suspended dynamics: Examples from Bylot Island, Nunavut, and Spitsbergen, Svalbard. *Hydrological Processes* 19, 115–135.
- Jania, J. 1997. *Glaciologia*. Wydawnictwo Naukowe PWN, Warszawa.
- Kostrzewski, A., Kaniecki, A., Kapuściński, J., Klimczak, R., Stach, A. & Zwoliński, Z. 1989. The dynamics and rate of denudation of glaciated and non-glaciated catchments, Central Spitsbergen. *Polish Polar Research* 10, 317–369.
- Krawczyk, W. 1992. Chemical characteristics of water circulating in the Werenskiöld Glacier, (SW Spitzbergen). International Working Group Glacier Caves and Karst in Polar Regions (eds.) *Proceedings of the 2nd International Symposium on Glacier Caves and Karst in Polar Regions, 10–16 February 1992, Miedzygorze-Velká Morava*, 65–80. Silesian University, Sosnowiec.
- Krawczyk, W., Lefauconnier, B. & Pettersson, L. 2003. Chemical denudation rates in the Bayelva Catchment, Svalbard, in the Fall of 2000. *Physics and Chemistry of the Earth Parts A/B/C* 28, 1257–1271.
- Macioszczyk, A. 1987. *Hydrogeochemia*. Wydawnictwo Geologiczne, Warszawa.
- Mair, D., Willis, I., Fischer, U., Hubbard, B., Nienow, P. & Hubbard, A. 2004. Hydrological controls on patterns of surface, internal and basal motion during three spring events, Haut Glacier d'Arolla, Switzerland. *Journal of Glaciology* 49, 555–567.
- Nicholas, A.P. & Sambrook Smith, G.H. 1998. Relationships between flow hydraulics, sediment supply, bedload transport and channel stability in the proglacial Virkisa River, Iceland. *Geografiska Annaler* 80A, 111–122.
- Nienow, P., Sharp, M. & Willis, I. 1998. Seasonal changes in the morphology of the subglacial drainage system, Haut Glacier d'Arolla, Switzerland. *Earth Surface Processes and Landforms* 23, 825–843.
- Rachlewicz, G. 2004. Pomiary ruchów lodowców w otoczeniu Petuniabukta-Billefjorden. Marsz, A. & Styszyńska, A. (eds.) *Materiały XXX Sympozjum Polarnego, 23–25 September 2004, Gdynia*, 149–150. Dział Wydawnictw Akademii Morskiej, Gdynia.

- Sharp, M., Richards, K., Willis, I., Arnold, N., Nienow, P., Lawson, W. & Tison, J.-L. 1993. Geometry, bed topography and drainage system structure of the Haut Glacier d'Arolla, Switzerland. *Earth Surface Processes and Landforms* 18, 557–571.
- Sharp, M., Richards, K.S. & Tranter, M. 1998. *Advances in Hydrological Processes; Glacier Hydrology and Hydrochemistry*. John Wiley and Sons, Chichester.
- Strzelecki, M. 2008. Zmiany koncentracji zawiesiny i materiału rozpuszczonego wzdłuż rzeki Bertram, Spitsbergen Środkowy. Kowalska, A., Latocha, A., Marszałek, H. & Pereyma, J. (eds.) *Środowisko przyrodnicze obszarów polarnych*, 160–170. GAJT, Wrocław.
- Swift, D., Nienow, P., Hoey, T. & Mair, D. 2005. Seasonal evolution of runoff from Haut Glacier d'Arolla, Switzerland and implications for glacial geomorphic processes. *Journal of Hydrology* 309, 133–148.
- Szczuciński, W. 2003. Zarys geologii otoczenia Billefjorden. Kostrzewski, A. & Zwoliński, Zb. (eds.) *Funkcjonowanie dawnych i współczesnych geoekosystemów Spitsbergenu*, 30–31. Warsztaty Geomorfologiczne SGP Spitsbergen 2003. SGP Publications, Poznań–Longyearbyen.
- Vatne, G., Etzelmüller, B. & Sollid, J.L. 1992. Glaciofluvial sediment transfer of subpolar glacier, Erikbreen, Svalbard. *Stuttgart Geographical Studies* 117, 253–266.
- Wadham, J., Hodson, A., Tranter, M. & Dowdeswell, J. 1998. The hydrochemistry of meltwaters draining a polythermal-based high Arctic glacier, south Svalbard. I. The ablation season. *Hydrological Processes* 12, 1825–1849.
- Wadham, J., Tranter, M. & Dowdeswell, J. 2000. Hydrochemistry of meltwaters draining a polythermal-based high-Arctic glacier, south Svalbard. II. Winter and early Spring. *Hydrological Processes* 14, 1767–1786.
- Warburton, J. 1999. Environmental change and sediment yield from glacierised basins: The role of fluvial processes and storage. Brown, A.G. & Quine, T.A. (eds.) *Fluvial Processes and Environmental Change*, 363–384. Wiley, Chichester.
- Willis, I.C., Richards, K. & Sharp, M. 1996. Links between proglacial stream suspended sediment dynamics, glacier hydrology and glacier motion at Midtdalsbreen, Norway. *Hydrological Processes* 10, 629–648.